TOWARDS A COMPREHENSIVE UNDERSTANDING OF TINY STARS IN THE NEAR - INFRARED DOMAIN - DETERMINING STELLAR PARAMETERS OF FGK AND M DWARFS FROM THEIR APOGEE SPECTRA USING THE SPECTRAL SYNTHESIS METHOD

Pedro Sarmento
Doutoramento em Astronomia
Departamento de Física
2020

Orientador
Bárbara Rojas Ayala

Coorientador
Elisa Delgado Mena

Dedication

Esta tese representa uma grande etapa da minha vida. Vê-la finalmente concluída tira-me um enorme peso do peito. Dedico a sua conclusão à minha família, que sempre me apoiou, e aos meus amigos, que me permitiam ir espaireçendo e desanuviando entre capítulos.

Acknowledgements

Over the past 4 1/2 years spent working on this thesis and the Ph.D. itself, I've been lucky to have many collaborators and colleagues that have helped achieve this massive goal. First, among them, I would like to acknowledge the help of my two supervisors, Dr. Bárbara Rojas-Ayala and Dr. Elisa Delgado Mena, who were always available for questions and compelled me to improve my work. I would also like to recognize the support of Dr. Sergi Blanco-Cuaresma, who helped solve every issue with iSpec, and gave important comments for our paper together. Additionally, Dr. Diego Souto and Dr. Katia Cunha were also very helpful and pointed us in the right direction for accurate synthesis of M dwarf spectra. Dr. Bertrand Plez, the creator of Turbospectrum, also provided important assistance regarding the code used for the spectral analysis. Finally, I would like to acknowledge the people behind the institutions of CAUP and IA, who were always available for questions and helped to financially support the costs associated with the research over these past years.

Abstract

Stellar parameters and spectroscopy have been important areas of astronomy for many decades. Like in many other fields of science, technology developments have helped us to gradually improve them. In this thesis, we present our very own contribution towards this field, with the derivation of new atmospheric parameters for both FGK stars and M dwarfs.

We test the usage of previously established software packages, such as *iSpec* and *Turbospectrum*, with the synthetic spectra method for parameter derivation with APOGEE H-band $R \sim 22\,000$ spectra. New line lists and line masks were developed in the context of this project, designed to be optimized for the derivation of spectroscopic parameters of either FGK or M dwarfs, and are made available for general use.

Our main results are the derivation of $T_{\text{eff}} \pm 100\,$K, $[M/H] \pm 0.1\,$dex, and $\log g \pm 0.1\,$dex for around 4000 stars, 3748 FGK stars and 250 M dwarfs. We find some discrepancies in our sample when comparing our results to isochrone predictions, and we propose possible solutions and calibrations for these issues.

Our derived parameters are also compared to several literature sources, including both observations in the visible and the near-infrared, to verify our accuracy and to check for possible discrepancies. We find that the differences between the T_{eff} and $[M/H]$ derived by our method and the APOGEE pipeline (ASPCAP) values for the parameters are within our error margins for both our FGK and M dwarf samples.

For future works and applications, the method itself can be applied to other stellar samples, both with H-band spectra observed by APOGEE, and from other sources and in other wavelength ranges.

Resumo

Parâmetros estelares e a espetroscopia são há muitas décadas áreas fundamentais da astronomia. Tal como em muitos outros ramos da ciência, avanços na tecnologia têm-nos gradualmente ajudado a melhorá-los. Nesta tese, apresentamos a nossa própria contribuição para esta área, através da derivação de novos parâmetros para estrelas FGK e anãs M.

Testámos o uso de pacotes de software já establecidos, tais como o *iSpec* e o *Turbospectrum*, com o método de síntese espetral para derivação de parâmetros atmosféricos estelares com espetro observado pelo APOGEE na banda H com $R \sim 22\,000$. Novas listas de linhas e máscaras de linhas foram desenvolvidas no contexto deste trabalho, desenhadas de forma a estarem optimizadas para a derivação de parâmetros espetroscópicos tanto de estrelas FGK como de Anãs M, e estão disponíveis para uso público.

Os nossos principais resultados são a derivação de $T_{\text{eff}} \pm 100$ K, $[M/H] \pm 0.1$ dex, e $\log g \pm 0.1$ dex de cerca de 4000 estrelas, 3748 estrelas FGK e 250 anãs vermelhas. Encontrámos alguns pontos fora da curva quando comparámos os nossos resultados com previsões das isocronas, e propusémos possíveis soluções e calibrações para resolver estes problemas.

Os nossos parâmetros derivados foram também comparados com diversas fontes de literatura, tanto no visível como no infravermelho próximo, de maneira a verificar a precisão do nosso método e a existência de possíveis discrepâncias. Descobrimos que as diferenças entre a T_{eff} e $[M/H]$ derivadas pelo nosso método e as obtidas pela análise original do APOGEE (ASPCAP) estão dentro das nossas margens de erro estimadas tanto para as estrelas FGK como para as anãs vermelhas.

Para trabalhos e aplicações futuras, o método em si pode ser aplicado a outras amostras estelares, tanto de espetros observados na banda H com o APOGEE, como de outras fontes e noutros comprimentos de onda.

Acronyms

2MASS Two Micron All-Sky Survey.

APOGEE Apache Point Observatory Galactic Evolution Experiment.

ASPCAP APOGEE Stellar Parameter and Chemical Abundances Pipeline.

CARMENES Calar Alto high-Resolution search for M dwarfs with Exoearths with Near-infrared and optical Échelle Spectrographs.

CFHT Canada-France-Hawaii Telescope.

CPS California Planet Survey.

Dec Declination.

ESO European South Observatory.

EW Equivalent Width.

H-R Hertzprung-Russell.

HARPS High Accuracy Radial Velocity Planet Searcher.

HD Henry-Draper Catalog.

IGRINS Immersion GRating INfrared Spectrometer.

LAMOST Large Sky Area Multi-Object Fiber Spectroscopic Telescope.

LSPM Lépine-Shara Proper Motion catalog.

MAD Median Absolute deviation.

MARCS Model Atmospheres in Radiative and Convective Scheme.

NIR Near-Infrared.

RA Right Ascension.

SD Standard deviation.

SDSS Sloan Digital Sky Survey.

SME Spectroscopy Made Easy.

SPIRou SpectroPolarimètre Infra-Rouge.

TESS Transiting Exoplanet Survey Satellite.

UVES Ultraviolet and Visual Echelle Spectrograph.

VALD Vienna Atomic Line Database.

Contents

List of Tables

List of Figures

Chapter 1

Motivation

A star is a sphere of plasma that generates energy from nuclear fusion in its center, and this pressure from the interior keeps it balanced against the force of gravity of its outer layers. Stars have a huge parameter range, and careful study of their light can help us distinguish them. From the M dwarfs to the supergiants, stars can have masses ranging from eight percent to hundreds of times the mass of the Sun. While they are in the main sequence, all stars produce their energy in the same way, by the fusion of four Hydrogen atoms to generate a Helium one. To do this, stars must have a core temperature above $10\,000\,000\,\mathrm{K}$, and objects with masses below $0.07 M_\odot$ and an inferior core temperature are not stars and are called brown dwarfs.

1.1 M dwarf characterization

M dwarfs, also known as red dwarfs, are the dimmest stars in the universe. If the Sun was a light bulb, M dwarfs would be the fireflies of space. The term red dwarf itself was first introduced already in 1915, in Lindemann (1915), distinguishing bigger and hotter blue dwarfs from the smaller and colder red dwarfs. In popular language, the term can include late-K and early/mid-M dwarfs, though it can also just be applied to M dwarf stars.

M dwarfs are main-sequence stars with masses ranging from $0.6\,M_\odot \geq M_* \geq 0.08\,M_\odot$, radii from $0.6\,R_\odot \geq R_* \geq 0.1\,R_\odot$, and T_{eff} from $3800\,K \geq T_{eff} \geq 2300\,K$ (Delfosse et al. 2000). M dwarfs are also characterized by having active chromospheres and coronas (Vilhu & Walter 1987).

Mid and late M dwarfs are fully convective, meaning their convection cycles through the entire star, the Helium created by Hydrogen fusion in its core does not accumulate there. This means that the star can burn a relatively higher amount of its fuel before leaving the main sequence, and therefore will have a much longer estimated lifespan. A $0.1M_{\odot}$ M dwarf may continue burning Hydrogen for up to 10×10^{12} years. Their long lifespans, combined with the fact that low-mass stars are more likely to form than massive ones, leads to M dwarfs being the most abundant stars in the universe. Around 7 in every 10 stars in the Milky Way are M dwarfs (Henry et al. 2006), and they weight heavily on the Galactic mass function (Covey et al. 2008).

M dwarfs have absolute V band visual magnitudes between 7.5 and 20. As a reference, the Sun has a magnitude of 4.83. Even the largest and brightest M dwarfs produce only about 10% of the Sun's luminosity. The peak in emitted flux moves towards longer wavelengths for lower temperature stars. Increased molecular absorption depresses the continuum in optical wavelengths as well. As a result, the total flux emitted below $0.7\,\mu m$ decreases from $\sim 10\%$ for a K7 star to $< 0.5\%$ for an M8 (Reid & Hawley 2005). Later M dwarfs are increasingly redder, having $1.5 < (V - I) < 5$ and $1 < (I - K) < 6$, and most energy emitted by M dwarfs is at infrared wavelengths (between 1 and 2.5 μm) (Reid & Hawley 2005). This fact, combined with the amount of total light emitted by the star (between 0.2 and $5 \times 10^{-4} L_{\odot}$), makes infrared photometry and spectroscopy fundamental for M dwarf science.

Due to their lower effective temperatures, M dwarfs have stronger molecular absorption bands than other FGK stars. Most notably, TiO, VO and metal hydrides (FeH, for example) molecular absorption bands are present at optical wavelengths. H_2O and CO are other molecules with wide absorption bands in the near-infrared. All these contribute to a lower spectral continuum and increased difficulty in performing spectroscopic analysis of these stars.

The spectroscopic study of M dwarfs is more challenging than that of FGK stars due to the molecules present in their atmosphere. Their numerous absorption lines make analyzing their spectra more challenging than those of hotter stars (see works that observed wide band M dwarf spectra, such as Leggett et al. 2000; Terrien et al. 2015), and telluric absorption further limits available wavelength ranges. Therefore, a selection of wavelength ranges (such as the H-band, $1.5 - 1.7\,\mu\mathrm{m}$) that are relatively free of both molecular bands and telluric lines, allows for a better measurement and characterization of atomic lines.

The lower effective temperature of M dwarfs makes them relatively much brighter in the near-infrared than in visible light. These two factors make that wavelength range the one best suited for the analysis of M dwarf spectra. Despite this, there is still an important gap in the available information about stellar spectra, as there have been no large scale studies about the derivation of M-dwarf stellar parameter using high-resolution infrared spectra, (see Chapter 2, containing a general overview of M dwarfs and recent important works on their spectral parameters, detailing important results and innovative methods explored for a more thorough literature revision). The current scientific community lacks a current method that can derive, in a fast, efficient, and precise manner, parameters for large M-dwarf samples using their H-band spectra. That is the problem which we propose to solve with this work.

1.2 Applications for accurate M dwarf atmospheric parameters

Stellar parameters, in general, can be useful for many sub-fields of astronomy. This work, however, focuses not on all stars, but rather M dwarfs in particular. Parameters for FGK-stars are derived as well, but as a test to the method itself and to lay the groundwork for the M dwarf parameter derivation. This begs the question: why M dwarfs? What is so important about these stars? The accurate derivation of M dwarf atmospheric parameters from their near-infrared spectra are needed for:

1.2.1 Galactic Astronomy

M-dwarf stars are one of the main components of the Milky Way and must be considered in any large scale study of the Galaxy. Their long main-sequence lifetimes and large numbers make them useful for tracing the chemical evolution of the Milky Way (e.g, Lépine et al. 2007; Bochanski et al. 2007).

One reason for measuring spectroscopic stellar parameters of M dwarfs is to distinguish between different kinds of galactic stellar populations. The stars in the universe are divided into 3 main populations: Population I (younger and more metal-rich stars), Population II (older and more metal-poor), and Population III (massive old and hot stars, no metallic content). The first two populations were first identified in Baade (1944), and they can be differentiated by both their orbits and their spectral characteristics.

Population I stars are metal-rich and alpha-poor stars that are found mostly in the galactic disk and arms, with the Sun being one of them (Gibson et al. 2003). They were formed at a time in the Galaxy's life where iron and other elements were more abundant compared to the early universe. Their orbits are nearly circular around the galactic center, and they have a wide range of ages, with the oldest ones having formed at around 10×10^9 years ago and new ones still being formed to this day.

Population II stars are older than 10×10^9 years ago and are relatively metal-poorer and with higher alpha content [1] when compared to Population I stars (Kippenhahn 1993). This is due to a lack of iron and relative abundance of Alpha elements at the time they were formed. These stars are mainly in the Milky Way halo and are mostly M dwarfs stars since the more massive Population II stars have already ended their main-sequence and are now white dwarfs, neutron stars or black holes.

Population III was first identified by Bond (1981), and it consists of massive stars, with virtually no metal content, that existed in the early universe. Their existence is inferred from physical cosmology. They have not yet been observed directly, as they would have long been turned into white dwarfs or black holes. If any Population III star is present in the Milky Way, it will be an M-dwarf.

See Fig. 1.1 for a diagram showing the mentioned regions of the Milky Way from an edge-on point of view.

1.2.2 Stellar Astronomy

Despite the considerable advance in the theoretical stellar modeling over the last few decades, there are still disagreements between the observed characteristics of M dwarfs and the values predicted from the current models. Effective temperatures calculated from models, for example, can be up to 200-300 K hotter than observed values, and radii predictions differ from interferometric measurements for up to 25%. Metallicity effects may be related to these observed discrepancies (López-Morales 2007). More accurate measurements of M dwarf parameters can allow for the development of new and improved theoretical models that result in better predictions for atmospheric parameters.

Additionally, recent studies have found significant differences between surface gravity ($\log g$) values measured with spectroscopy and with asteroseismology for FGK stars (Mortier et al. 2014; Delgado Mena et al. 2017, e.g.,). More observations and new data are required for a more complete understanding of this stellar parameter and the calibration of current measurements.

[1] Alpha elements are Ne, Mg, Si, S, Ar, Ca, Ti, and are so-called since their most abundant isotopes are integer multiples of four, the mass of a Helium nucleus (the Alpha particle).

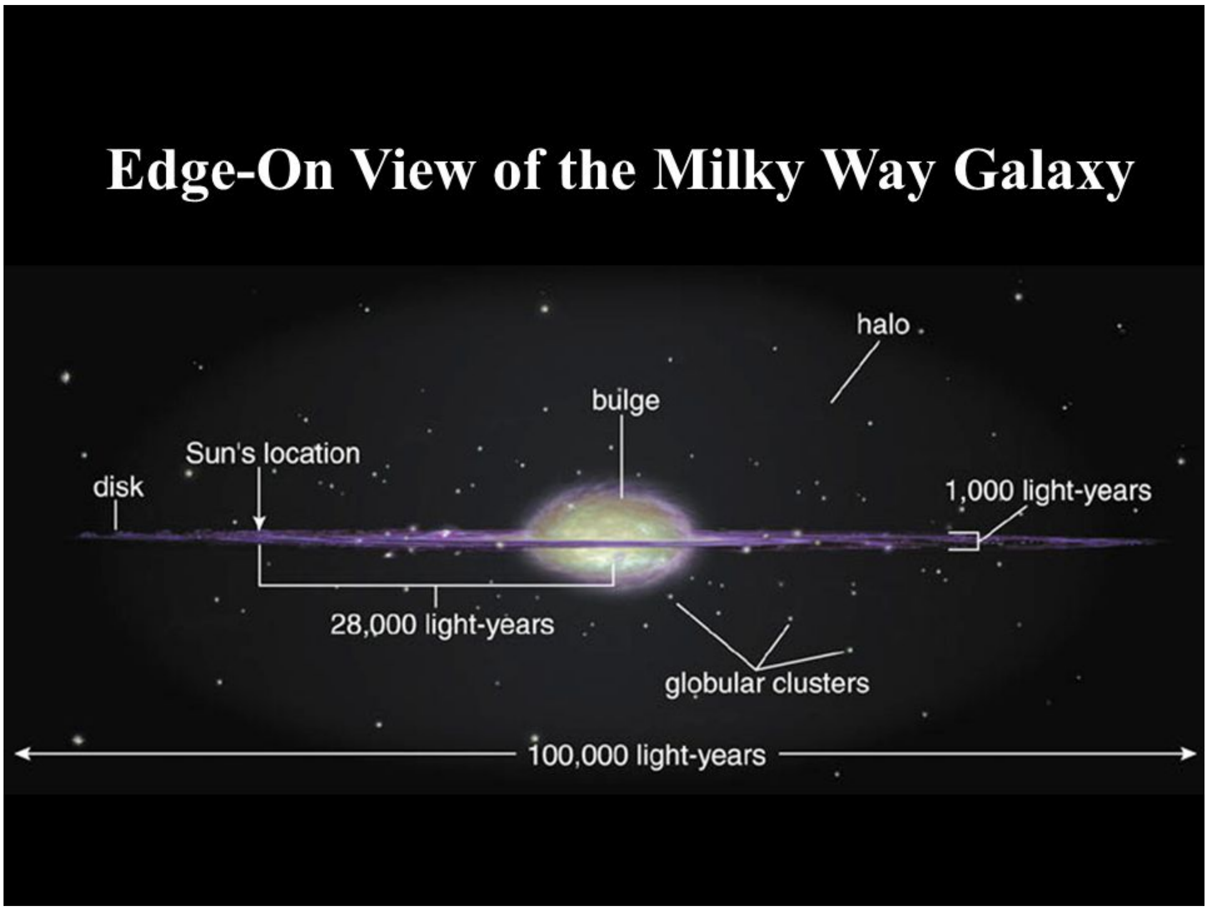

Figure 1.1: Diagram showing an edge-on view of the Milky Way shape and its different stellar regions. Source: Hill (2015)

1.2.3 Planetary Astronomy

The two most successful current methods for planet detection, radial velocity, and transit, are indirect methods. The planet is not directly observed, but rather its effect on the observed light emitted by its parent star. M dwarfs are relatively small and faint stars, much colder than solar-type stars. Due to their faintness, their habitable zone is much closer to the star than it is for solar-type stars, and, due to their small radius and mass, the relative difference in size between any potential exoplanet and the host star is much smaller than for larger stars. This means that detecting exoplanets in the star's habitable zone is orders of magnitude easier for M dwarfs than for solar-type stars.

Several programs focus primarily on finding potentially habitable planets around M dwarfs, such as MEarths (Irwin et al. 2014), and with CARMENES (Alonso-Floriano et al. 2015) or HARPS (Bonfils et al. 2013). There have also been multiple papers detailing how life might be possible in planets around M dwarfs (e.g. Segura et al. 2005; Scalo et al. 2007; France et al. 2013), so this is a very current and debated topic in the prevailing scientific landscape. The characterization of potentially planet-hosting stars is required to advance our understanding of planetary astronomy in general.

1.3 Thesis structure

Our main motivation for this project is, therefore, to provide a new method for the derivation of more accurate spectroscopic parameters for FGK and M dwarfs from their Near-Infrared spectra. We will show how the synthesis of H-band spectra can be used to determine spectroscopic parameters of M dwarfs.

Chapter 2 explains our current understanding of M dwarfs and the available literature analysis (spectroscopy and photometry) on them.

Chapter 3 explains how stellar spectra can be used to derive stellar parameters, and the effects multiple stellar parameters can have on our observed spectra.

Our data is detailed in detail in Chapter 4. The source used for our spectra, APOGEE, is described. We display the sky distribution of our sample stars, as well as available literature analysis on them.

Our method of spectral synthesis and the steps used for the full stellar characterization are explained in Chapter 5. The required line lists and line masks mentioned in this chapter are available upon request. We divide this chapter accordingly to the steps required for the synthesis of FGK stars and M dwarfs.

The chapters regarding our results, and discussion, are divided into FGK stars (Chapter 6) and M dwarfs (Chapter 7).

Our conclusions, as well as possibilities for future work, are laid out in Chapter 8.

Our appendices are in Chapter A. These include all line masks used for parameter determination of both FGK and M dwarfs, as well as our full results for these two samples and a small paragraph describing each individual star characterized by our pipeline.

Chapter 2

Previous M dwarf Analysis

In this chapter, the current landscape of M dwarf science is presented across spectroscopy and photometry, as these fields are complementary and required for a holistic understanding of these stars. Spectroscopy is and has been, an important method for the derivation of M dwarf parameters, but it is not the only one. It is necessary to understand the photometric analysis of these stars as well. This section is dedicated to the recent advances obtained in M dwarf science due to these astrophysical techniques. Results are mentioned in roughly chronological order, with different works by the same author(s) being grouped for readability.

2.1 M dwarf spectroscopy

2.1.1 M dwarf Spectral Classification

Spectral classification of stars is based on the morphology of their spectra, as the appearance and disappearance of particular spectral features indicate the physical properties of the stars themselves. The spectral type of a star can give us a shorthand way to describe the overall physical characteristics of a given star. It should be noted, however, that physical descriptions of stars came afterward, and is independent of, their classification system. The 'type M' code to classify stars had its origin in the system for spectral classification developed in Harvard in 1890, by the hands of Mrs. W. P. Fleming, for the Draper Memorial Catalog. This catalog included 10 351 of the brightest northern stars, and it became the prime astronomical reference system by the 1920s. As these early spectral catalogs were restricted to stars with bright apparent magnitude, most M stars present in them are giants rather than dwarfs. This fact became apparent after Hertzsprung (Hertzsprung 1905) and Russell (Russell 1914) independently created the diagram that now bears their names (Hertzprung-Russell, or H-R for short). When luminosities are plotted against temperature indicators, the distinction between dwarfs and giants (named by Russell) is clear, as well as a main-sequence (defined by Hertzsprung, see Fig. 2.1 for an example of an H-R diagram created with Gaia data). This system provided a way to readily compare the general properties of many stars, and H-R diagrams are still in use to this day.

The presence of the TiO bands, as they dominate the optical spectra of M dwarfs, are the current primary indicators of spectral type. The presence and strength of these molecular bands are used to determine the spectral type of different M dwarfs. TiO bands saturate for later type M dwarfs, and other molecular bands, such as VO, are required for the spectral classification of late-type M dwarfs. These two molecular bands have been proposed for spectral type calibrations by Bessell (1991). Current spectral libraries (e.g., Rayner et al. 2009) still use similar methods for the classification of lower resolution ($R \sim 2000$) stellar spectra for stars of different spectral types.

2.1.2 Optical Wavelength

Although M dwarfs are faint and thus hard to observe, research into them in the visible wavelengths has occurred for over 30 years. Back in the 1970s, Mould (1976) explored TiO and CaH bands in the spectra of both halo and disk M dwarfs. In 1982, Bessell (1982) discovered that the ratio between the oxide and hydride bands in the visible wavelength of an M-dwarf is related to its metallicity content. Later, with Lépine et al. (2007), this was called the Zeta (ζ) index. It quantifies the weakening of the TiO band strength due to metallicity effect, with values ranging from $\zeta_{\mathrm{TiO/CaH}} = 1$ for stars of near-solar metallicity to $\zeta_{\mathrm{TiO/CaH}} \sim 0$ for the most metal-poor (and TiO depleted) subdwarfs. The ζ index has been used to distinguish between dwarfs (K5-M9, or dK5-dM9), metal-poor subdwarfs (sdK5-sdM9), very metal-poor extreme subdwarfs (esdK5-esdM9) and ultra subdwarfs (usd) below the extreme subdwarfs. Later, this index was calibrated by Woolf et al. (2009) to give the actual star's metallicity ($[M/H]$) based on its value for low metallicity stars. This was an important step in M-dwarf parameter determination, as an easy to measure index was now related to a fundamental stellar parameter.

A database including optical spectroscopy on the bright M dwarfs in the northern sky (1564 stars, $R \sim 2000$, Lépine et al. 2013) has also been published. The spectral type, temperature

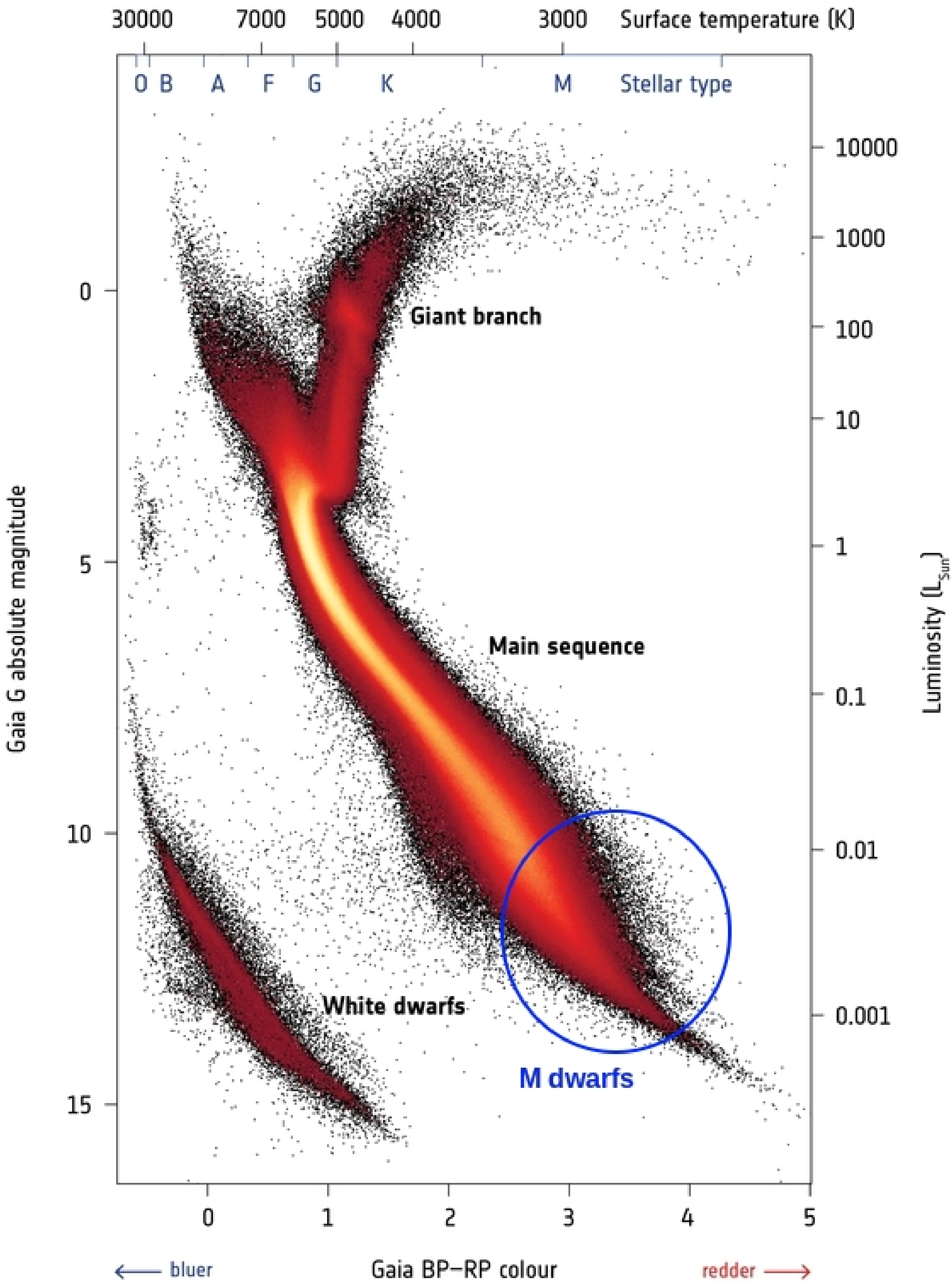

Figure 2.1: H-R diagram created with data published by Gaia DR2 (Prusti et al. 2016; Brown et al. 2018). Notice M dwarf position towards the bottom right of the main sequence, as the coldest and dimmest stars. Source: Gaia Data Processing and Analysis Consortium (DPAC); Carine Babusiaux, IPAG – Université Grenoble Alpes, GEPI – Observatoire de Paris, France.

($\pm 100\,K$) and zeta (ζ) index of these stars were measured within a reasonable margin of error. This was one of the largest M dwarf database with optical spectroscopy constructed in recent years, until the recent publication in 2019 of the parameters of almost 30 000 M dwarfs by Galgano et al. (2019). Using the Large Sky Area Multi-Object Fiber Spectroscopic Telescope (LAMOST, Cui et al. 2012), effective temperatures, radii, masses and luminosities have been determined for many more M dwarfs that had previously been characterized. The observations were made with $R \sim 1800$ and across the optical ($3690 - 9100\,\mathring{A}$). The parameters were derived with supervised machine learning with (Ness et al. 2015, *The Cannon*,) trained with 1388 M dwarfs previously characterized with the Transiting Exoplanet Survey Satellite (Ricker et al. 2010, TESS,) Cool Dwarf Catalog that was also observed by LAMOST with ($S/N > 250$) spectra. The team reported typical uncertainties of 110 K for $T_{\rm eff}$, 0.065 $R_\odot$ for radii, 0.054 $M_\odot$ for masses and 0.012 $L_\odot$ for luminosity. Additionally, the Sloan Digital Sky Survey (Abazajian et al. 2009, SDSS,) has also published five-band photometry for thousands of M dwarfs.

In 2014, Gaidos et al. (2014) published a catalog of optical spectra ($R \sim 1000$) for 2970 nearby ($d < 50\,pc$) and bright ($J < 9$) late K and early M dwarfs, and estimated optical spectroscopic parameters for them. An initial list of stars was selected from the SUPERBLINK proper motion catalog based on their properties, and their $T_{\rm eff}$ was estimated by fitting model spectra to the observed ones. Their estimated errors vary between stars, but are around 100 K for $T_{\rm eff}$ and 0.12 dex for $[Fe/H]$. These values were used in empirical relations to derive estimates for the other parameters.

Hejazi et al. (2019) published chemical properties for 1544 high proper-motion M dwarfs and subdwarfs from low-mid resolution ($\sim 2000 - 4000$) optical spectra. A template-fit method was developed, based on the measurement of TiO and CaH molecular bands near $7000\mathring{A}$. The analysis of 48 binary systems suggests precision levels of ± 0.22 for $[M/H]$, ± 0.08 for $[\alpha/Fe]$, and ± 0.16 for the combined index $[M/H] + [\alpha/Fe]$.

As for higher-resolution studies, we find in 2005 the publication of Woolf & Wallerstein (2005), a study on the Fe and Ti abundances of 35 K and M dwarfs using the Equivalent Width method from $R \sim 33\,000$ spectra. The analyzed stars have 3300 K$<$ $T_{\rm eff} < 4700$ K with reported errors between 20 K and 220 K, and reported errors up to 0.18 dex in their $[Fe/H]$ measurements.

In 2006, Bean et al. (2006) was published. This study presented the spectroscopic metallicity of three M dwarfs with known or candidate planetary-mass companions. This study was made using high resolution ($R \sim 60\,000$) and S/N spectra obtained at the McDonald Observatory, and is one of the first analysis of M dwarf spectra done with this resolution. For their 3 sample stars, they derived $3478 < T_{\text{eff}} < 3498$ K, with adopted uncertainties of 48 K, and $-0.33 < [M/H] < -0.12$ dex, with adopted uncertainties of 0.12 dex.

Neves et al. (2013) published, in 2013, a survey detailing metallicities of planet-hosting M dwarfs using optical spectra. In this case, a photometric estimate of the metallicity and temperature of the star is a starting point for an analysis that makes use of the HARPS (High Accuracy Radial velocity Planet Searcher) high-resolution spectra. The work focuses more on examining relations between metallicity and planet formation. Additionally, and by the same author, there has been some investigation about deriving the effective temperatures and metallicities of M dwarfs using their visible spectra in Neves et al. (2014). This work adopted uncertainties of 0.08 ± 0.01 dex for $[Fe/H]$ and 91 ± 13 K for T_{eff}.

Maldonado et al. (2015), in 2015, used ratios of pseudo-equivalent widths of M dwarf spectral features like a temperature diagnostic. This allowed for a measure of the stellar effective temperature of M dwarfs using their $R \sim 115000$ HARPS spectra. The group identified a total of 112 temperature-sensitive ratios and calibrated them over the range of $3100 - 3950$ K. The typical estimated uncertainties are around $70\,K$ for T_{eff} and between $0.07 - 0.10$ dex for metallicity.

In 2016, Passegger et al. (2016) used the PHOENIX ACES models to derive atmospheric parameters for 4 benchmark stars from their high-resolution ($R \sim 45\,000$ for two stars and $R \sim 100\,000$ for the other two) optical Ultraviolet and Visual Echelle Spectrograph (UVES) spectra. Their inherent uncertainties are $\sigma_{T_{\text{eff}}} = 35\,\text{K}$,$\sigma_{\log g} = 0.14\,\text{dex}$, and $\sigma_{[Fe/H]} = 0.11\,\text{dex}$.

2.1.3 Infrared Wavelength

The studies mentioned in this section have been cross-matched with our observations, with all relevant results compared and analyzed in Section 4.3.2.

As the technology keeps improving, there has been an increasing number of works on M dwarfs using infrared spectra. The observation of M dwarf infrared spectroscopy was already underway in the 1970s with Mould (1978). In 1998, an H-band spectroscopic catalog of 85 stars by Meyer et al. (1998), including M dwarfs, was published. With spectra of $R \sim 1000$ and $S/N > 50$, spectral types within ± 2 sub-classes were derived for late-type stars. This was a breakthrough observation of M dwarf stars in that wavelength, providing the groundwork for future studies in the area.

Afterwards, with Leggett et al. (2000) and Leggett et al. (2001), the infrared spectra (1.0-2.5 micron, $R \sim 600$) of 42 and 14 disk dwarfs, from M1 to L7, was obtained. This was a study limited in scope, with only 56 objects, and all very late-type stars and some brown dwarfs, but it provided uncertainties in the range of $\sim 100-200K$ for the effective temperatures, $\pm 0.25\,\mathrm{dex}$ for the metallicities, and 10% in the radii of these objects. Despite the small samples and low resolution, these studies are groundbreaking in their analysis, providing synthetic model comparison and parameter estimation for these objects, and the precision achieved is still relevant nowadays.

Over the following years, M dwarf results in the infrared barely saw any improvement. The revolution started with Rojas-Ayala et al. (2010), with the publication of $R \sim 2700$ K-band spectra of 17 M dwarfs. All sample stars belonged to binary pairs, and their metallicities were estimated from their FGK companions. The analysis of their spectra showed a new method for measuring metallicities, by using the strength of the spectrum's Na I doublet ($2.206\,\mu m$ and $2.209\,\mu m$) and Ca I triplet ($2.261\,\mu m$, $2.263\,\mu m$, and $2.265\,\mu m$) absorption lines. These results had an accuracy of $\pm 0.15\,\mathrm{dex}$ and the method was also observationally accessible, as it required only a moderate resolution K-band spectrum.

These results were added upon only two years later, with another important K-band (2.0-2.4 micron, $S/N > 200$, $R \sim 2700$) survey by Rojas-Ayala et al. (2012). This paper published studies of 133 M dwarfs, including 18 stars with reliable metallicity estimates and 11 M-dwarf planet hosts. These results were obtained from analyzing both the equivalent widths of the Calcium and Sodium lines mentioned in the previous paragraph and a spectral index quantifying the absorption due to water in the star's atmosphere. In addition to confirming the previous work with a larger sample of stars, this work also provided estimates for stellar effective temperatures and spectral types, based on water absorption. The article, due to its innovative methods, motivated further studies about M dwarfs in the infrared.

In 2013, a series of new methods, and calibrations of previous methods, to determine M-dwarf metallicities from moderate resolution ($1300 < R < 2000$) optical and infrared spectra were published by Mann et al. (2013). A total of 112 wide binary systems containing both a late-type and solar-type stars was analyzed, and metallicities for these stars were derived using either visible, J-, H-, or K- band spectra. 120 features in the spectra of K and M dwarfs that are useful for predicting metallicities were detected. It was also found that the ζ index is correlated with $[Fe/H]$ for super-solar metallicities.

In 2015, a larger survey was published, providing a catalog of 886 M Dwarfs in the full NIR (0.8-2.4 micron) by Terrien et al. (2015). The spectra used had a resolution of about $R \sim 2000$ and $S/N > 100$, and the survey focused on measuring the star's abundances ($[Fe/H]$ and $[M/H]$), using spectroscopic calibrations from different previous publications. These published results have an uncertainty of about $0.1\,\mathrm{dex}$ on both parameters. The T_{eff} of those stars was also estimated using H_2O indices, and their reported precisions are $110\,\mathrm{K}$ (J band), $170\,\mathrm{K}$ (H band), and $78\,\mathrm{K}$ (Ks band). It was also concluded that the best method for $[Fe/H]$ measurement for M1-M5 stars is using the Ks-band spectra, first used in Rojas-Ayala et al. (2010). That year saw the publishing of Mann et al. (2015) as well, which uses both optical and infrared spectra to characterize the properties of 183 nearby M dwarfs.

As for higher-resolution studies, Önehag et al. (2012) was an important publication. This work consisted of high-resolution studies ($R \sim 50000$) in the J band and provided metallicities for a sample of 8 M dwarfs and three wide-binary systems. The authors proposed an analysis of the spectroscopic abundance in the J band as a method to measure metallicities in M dwarfs. Their sample covers a narrow range of both T_{eff} ($3200 - 3400\,\mathrm{K}$, with a single $3900\,\mathrm{K}$ star) and $[M/H]$ ($-0.1\,\mathrm{dex}$ to $+0.2\,\mathrm{dex}$). The group concludes that the method is reliable, having a new metallicity scale for these stars, and proposing new observations in other stars. The method is consistent with previous studies for the analyzed stars, but the small sample size makes its impact limited. This work was expanded over the following years by Lindgren et al. (2015); Lindgren et al. (2016), but the analysis still focused on a small stellar sample. In this case, four binary pairs containing both an M-dwarf and an FGK companion star, and 8 single M dwarfs, were used to infer the M dwarfs' parameters (T_{eff} and $[M/H]$) from an analysis of the stellar pairs and comparisons with previous optical studies of the FGK dwarfs. The results agreed between the two stars of the binary ($\Delta[Fe/H] = 0.01 - 0.04\,\mathrm{dex}$) and also with literary values. However, some of the M dwarfs spectra used have poor S/N (30-70) and would require a better knowledge of their T_{eff} to provide a more accurate and precise estimate of their metallicity. This work was further improved in 2017 with Lindgren & Heiter (2017), expanding the parameter range of both metallicity and effective temperature. A total of 16 targets were analyzed in this work, with $3350 < T_{\mathrm{eff}} < 4550$ K and $-0.5 < [M/H] < +0.4$ dex. Their parameters were determined with synthetic spectra generated on the fly by SME (Piskunov et al. 2017), using a sub-grid of MARCS models for cool dwarfs, and their estimated uncertainties are $100\,\mathrm{K}$ for the

$T_{\rm eff}$, $0.03 - 0.07\,{\rm dex}$ for the $[M/H]$ and $0.1\,{\rm dex}$ for the $\log g$.

Veyette et al. (2017) published an analysis on spectroscopic parameters of 29 M dwarfs using high resolution ($R \sim 25\,000$) Y-band ($\sim 1\mu m$) wavelength spectra, measured with NIRSPEC on Keck II (Veyette et al. 2017). Using PHOENIX models, synthetic spectra were generated and the equivalent width of multiple Fe I and Ti I lines, together with a temperature-sensitive index based on the FeH band head in the spectra, were measured and used to empirically calibrate the spectra and to derive effective temperature, Fe and Ti abundances were determined for their stellar sample.

In 2017, Gilhool et al. (2017), a spectroscopical analysis on the rotational speed ($v \sin i$) of 714 M dwarfs using APOGEE data ($R \sim 22\,000$) was published. This study included the fitting of BT-Settl template spectra calculated from PHOENIX code for the determination of spectroscopical parameters ($T_{\rm eff}$, $\log g$ and $[M/H]$) for these stars. The templates used are limited to a 100 K resolution in $T_{\rm eff}$, values of either -0.5 dex, 0.0 dex, or +0.5 dex for $[M/H]$ and 4.5 dex, 5.0 dex or 5.5 dex for $\log g$.

Two recent studies (Souto et al. 2017; Souto et al. 2018) used APOGEE spectra to perform chemical analysis and to determine spectroscopic parameters of 3 different M dwarfs. Their method used spectral synthesis and a combination of MARCS and PHOENIX model atmospheres to perform their analysis. The detailed analysis, the inclusion of an H-band water line list, and accurate synthetic spectra make these two very important works that helped our research. The analysis was recently expanded to a larger M dwarf sample with Souto et al. (2020), with the characterization of 24 different M dwarfs.

Another study with high-resolution spectra was published in 2018 by Rajpurohit et al. (2018a). This work focused on matching BT-Settl model spectra to CARMENES $R \sim 90\,000$ simultaneous observations in the optical and near-infrared of 292 M dwarf spectra. Since this work determines parameters by matching observed spectra to a grid of previously computed models, the reported uncertainties correspond to the size of the grid, 100 K for $T_{\rm eff}$ and 0.1 dex for both $\log g$ and $[M/H]$. The same authors also published Rajpurohit et al. (2018b), matching the APOGEE observations of 45 M dwarfs with BT-Settl model spectra.

López-Valdivia et al. (2019) determined the $T_{\rm eff}$ of low-mass stars (K and M dwarfs) from their H-band spectra. This work used synthetic spectra and the shapes and depths of specific Fe I, OH and Al I lines in the stellar spectra of 254 stars to derive $T_{\rm eff}$ within $\sim 140\,{\rm K}$. The spectra used was high-resolution ($R \sim 45000$) and observed by Immersion GRating INfrared

Spectrometer (IGRINS, Yuk et al. 2010; Park et al. 2014). Unfortunately, no stars studied by this work are present in the APOGEE sample, so their results cannot be directly compared to this method.

Using CARMENES data, Passegger et al. (2019) published parameters for 282 M dwarfs by fitting PHOENIX models to high-resolution CARMENES spectra in both the visible and infrared wavelength ranges. This work directly compares stellar parameters derived from multi-wavelength range spectra of the same star observed simultaneously and is one of the few available studies that use homogeneous and consistent methods with both optical and near-infrared stellar spectra simultaneously. Their reported uncertainties depend on each star's rotational velocity and, for NIR spectra, are as low as 56 K for T_{eff}, 0.04 for $\log g$, and 0.16 for $[Fe/H]$.

2.2 M dwarf photometry

The surface temperature of a star in its main sequence can be estimated through its spectral type. This can be done using the star's absolute visual magnitude (M_V), which can be measured by photometry, and empirical relations. The M_V values can be estimated through the integration of the total energy emitted by the star across multiple passbands. However, there are significant error margins and limitations to this method, as shown by Fig. 2.2, which shows both the M_V of different single main-sequence stars with accurate trigonometric parallax data, as well as their estimated spectral type. Wide dispersion is present for K-type stars, with possible values for M_V ranging across multiple magnitudes for the same spectral type. The diagram is also coarse-grained, as types are measured to within only 0.5 subclasses and have a ± 0.5 margin of error. This results in a $\sigma(M_V) = \pm 1.5$ magnitudes for early-mid M dwarfs, and also means that distances estimated from spectroscopic type alone are accurate only to a factor of two.

The luminosity determination of stars can be combined with stellar radii measurements to determine effective stellar temperatures through equation $L = 4\pi R^2 \sigma T_{\mathrm{eff}}^4$. Published in 1974, Veeder (1974) was one of the first to obtain a temperature scale for M dwarfs by fitting a black-body curve to optical and near-infrared fluxes. Later, in 1991, Bessell (1991) also published an M dwarf temperature scale. This work differs from Veeder (1974) for up to $180\,\mathrm{K}$ for stars later than M5, but is consistent for earlier ones. Another example of the estimation of effective temperatures, radii, and metallicities calculated through photometry is Casagrande et al. (2008). This work uses the infrared flux method and the multiple optical-infrared technique (first published in Casagrande et al. 2006)) to empirically derive these parameters from high accuracy optical and infrared photometry. The flux ratio across different bands is used as a proxy for both effective temperature and metallicity.

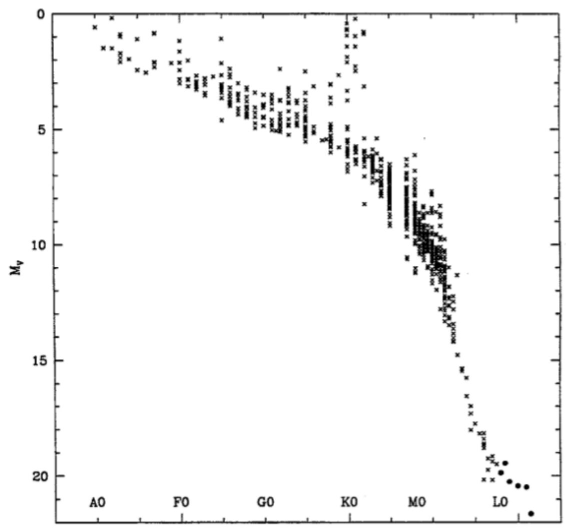

Figure 2.2: Relationship between absolute visual magnitude, M_V, and spectral type, defined by stars with accurate trigonometric parallax data. Source: Reid & Hawley (2005)(Chapter 2, figure 2.14).

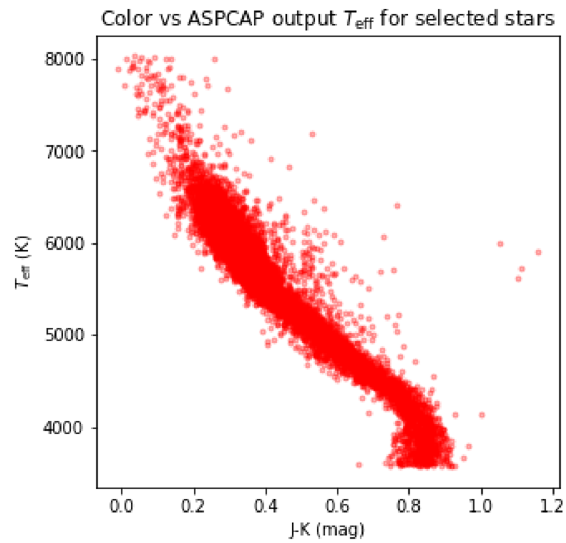

Figure 2.3: Difference in measured magnitude between the infrared J and K bands, as published by APOGEE, and the available ASPCAP spectroscopic $T_{\rm eff}$ for a sample of main-sequence stars with $S/N > 200$ and $v \sin i < 15\,\mathrm{m/s}$.

An alternative method for the estimation of a representative temperature is the black body method. This involves the measurement of flux emitted by the star across multiple photometric bands, and matching them to black-body curves using Planck's law:

$$E(\lambda, T) = \frac{2hc^2}{\lambda^5} \times \frac{1}{\exp^{\frac{hc}{\lambda k T}} - 1} \tag{2.1}$$

, where h is Planck's constant $6.626 * 10^{-34}$ Js; c is the speed of light $2.997925 * 10^8\,\mathrm{m/s}$; λ is the wavelength in meters; k is the Boltzmann constant $1.381 * 10^{-23}$ J/K; and T is the temperature in Kelvin. The usage of this method was pioneered by Greenstein et al. (1970), and later used with photometry up to the K-band ($2.2\,\mu m$) by Reid & Gilmore (1984), Berriman & Reid (1987), and Berriman et al. (1992) as well. Tinney et al. (1993) included the L-band ($3.5\,\mu m$) as well, allowing for a better fit for colder M and L dwarfs.

Other options for M dwarf parameter estimation through photometry involve the usage of empirical color-magnitude diagrams. Akin to the original H-R diagram, plotting the M_V against different optical and infrared colors (flux differences across multiple broadbands) can help us create empirical relations between these parameters and use them to estimate spectral types and temperatures for other stars. The most common and historically used color indices for these purposes were the $B - V$ and $V - I$. However, most passband differences can provide us information about the stellar parameters. Fig. 2.3 shows the relationship between the measured spectroscopic $T_{\rm eff}$ and $J - K$ color, as published by ASPCAP. ASPCAP is the APOGEE spectral parameter determination pipeline and provides parameters for every star observed with APOGEE. See Section 4.1 for more information. It is clear that for the main sequence FGK-star regime this color can provide us with a reasonable guess for the star's effective temperature, and photometric measurements across other passbands can help narrow down the star's possible $T_{\rm eff}$ range even further. Equations and relations established in works such as Mann et al. (2015) can be used to directly estimate $T_{\rm eff}$ and other stellar parameters from photometric colors. Another use of color-magnitude/temperature diagrams is the estimation of photometric parallaxes. The observed colors can be used to infer an absolute magnitude which, coupled with the apparent magnitude measured, allows for distance estimation.

The stellar abundance, or metal content, can have a strong effect on its position in the H-R diagram. Subdwarfs, which have low metal abundance compared to the Sun and other solar neighborhood stars, can be distinguished from other M dwarfs from their color differences. These stars have an abundance distribution that peaks around $[M/H] \sim -1.5\,\mathrm{dex}$, with some reaching $[M/H] = -4.5\,\mathrm{dex}$. Sandage & Eggen (1959) showed that the subdwarf sequence lies below the disk dwarf sequence in the $\log L, T_{\rm eff}$ H-R diagram. Photometric analyses of stars can, therefore, provide us information about their metallicities, by determining whether or not they belong to the subdwarf regime.

In 2011, an all-sky catalog listing bright ($J < 10$) M dwarfs was published by Lépine & Gaidos (2011), identifying 8889 stars based on optical and infrared color cuts, parallax, and proper motion measurements. This catalog allows for a fast reference on a given star's spectral type but, since it is limited to bright stars, it is not very useful for this project.

2.3 Summary

Most current M dwarf analysis in the NIR can be classified in at least one of these 4 categories:

1. Detailed studies on 1-10 individual stars (e.g., Önehag et al. 2012; Lindgren & Heiter

2017; Souto et al. 2017; Souto et al. 2018);

2. Low resolution characterization of mid-sized (100-1000) M dwarf samples (e.g., Meyer et al. 1998; Leggett et al. 2000, 2001; Rojas-Ayala et al. 2010, 2012; Mann et al. 2013; Terrien et al. 2015);

3. Photometric studies using color gradients and empirical relations to infer M dwarf characteristics (e.g., Mann et al. 2015; Lépine & Gaidos 2011);

4. Focus on 1-5 specific spectral lines for parameter derivation (e.g., Veyette et al. 2017; López-Valdivia et al. 2019; Passegger et al. 2019);

5. Matching observations to libraries of synthetic spectra for parameter determination (e.g., Gilhool et al. 2017; Rajpurohit et al. 2018a,b).

Chapter 3

Spectroscopy as a method for stellar characterization

This chapter gives a small rundown on the possible uses of spectroscopy for the characterization of stellar spectra. We include a definition of the method as well as a small summary of recent results obtained with spectroscopy. An explanation for the role synthetic spectra play in spectroscopy is also included. The effects of various stellar parameters on a stellar spectrum are also explored, demonstrating how changes in the stellar $T_{\rm eff}$, $\log g$, $[M/H]$, v_{mic}, v_{mac} or $v \sin i$ can affect the shape of the spectrum and its lines.

3.1 Spectroscopy: definition and relevant uses

A stellar emission spectrum consists of the light we observe as emitted by the star after passing through the stellar atmosphere. Therefore, by studying stellar spectra, we can determine the characteristics of stellar atmospheres, as the atmosphere's behavior is governed by both its density and the energy that flows through it. These parameters depend, in turn, of the star's mass and age, as well as its chemical composition and angular momentum. Therefore, the analysis of stellar light with spectroscopy can provide us with important information about the characteristics of the whole star (Gray 2005).

Spectroscopy consists in the observation, measurement, and study of emission spectra by different objects, be it a stellar, galactic, or even planetary source. Depending on the wavelength and origin of the spectra, they can provide us with different information and characteristics of both their source and the interstellar medium crossed by the light on its journey to Earth. Stars belonging to either Population I or II, since they have different metallicity and alpha-ratios, which can be observed in their spectrum, can be distinguished through spectroscopy, helping to characterize the history of our galaxy.

Spectroscopy can also be used to identify and characterize stellar clusters. Since the stars in a cluster are usually formed at the same time and place, they will have similar chemical properties. However, at the time of observation, stars with different origins may be close together. By measuring stellar parameters for stars in the cluster area, spectroscopy can be used for not only identifying the stars belonging to the cluster but for cluster characterization as well. Several examples of works using spectroscopy to characterize cluster stars can be found in the literature, such as Maxted et al. (2008) and Greene & Meyer (1995).

Binary and other multiple star systems can also be characterized using spectroscopy. Besides spectroscopic binaries, which occur whenever the distance between two stars is smaller than the resolution of individual spectrograph fibers, spectroscopy can be used to characterize in detail the star in the system with the most well understood spectral type and use its parameters as proxies for the parameters of the other star or stars. This is possible because the stars in binary and other multiple star systems share an origin in both time and space, resulting in similar ages and compositions for all of them. This method has been used by Rojas-Ayala et al. (2010) and Önehag et al. (2012), for example, to characterize M dwarfs through the analysis of their more massive parent stars.

Another use for spectroscopy that has become more important in recent years has been the characterization of exoplanet host stars. As most planet detection techniques rely on indirect methods and the observation of the star to discover the presence of a planet, reliable and accurate methods to characterize the stars are fundamental to characterize the planets themselves (Deeg & Belmonte 2018). The transit method, which relies on high-precision comparative photometry of the star over time, can be complemented by a spectroscopic analysis of the star to estimate the size of the planet blocking its light. Only after an accurate characterization of the stellar radius can the planetary radius be inferred, and this can be made possible through spectroscopy. The radial velocity method, using high-resolution stellar spectra to measure the Doppler shifts caused by the presence of an exoplanet, must also include a careful analysis of the star itself to understand its characteristics and infer the ones of the planet.

Additionally, only through spectroscopy would relationships like the giant planet occurrence to stellar metallicity correlation, first published in Gonzalez (1997) and further explored later by Santos et al. (2004), Fischer & Valenti (2005), Johnson et al. (2010), Sousa et al. (2011) and Reffert et al. (2015), be discovered. This correlation shows that the occurrence rates of giant Jupiter-like planets are greater in stars with higher metallicities, and is forever linked to spectroscopic analysis of stars. It shows the important role spectroscopy plays in different astrophysics fields nowadays.

Stellar parameters of large stellar populations, by providing us a glimpse of the galactic conditions at the time of their formation, can also give us a window into the formation stories of these stars, and the history of our galaxy and solar system. Only by knowing and characterizing other stars and solar systems can we truly understand how and why might our own home in the universe be different and special, or if the Sun is a typical star among the many stars present in the Milky Way.

3.2 Modern Spectroscopy methods for parameter determination

The Equivalent Width and the Synthetic Spectra techniques have been developed for the determination of stellar parameters from a given spectrum. This section will go into the details and the workings of them.

3.2.1 Equivalent Width Method

One technique widely used nowadays to derive stellar parameters from an observed spectrum is the Equivalent Width (EW) method. The concept of EW was introduced in the late 1920s as a way to quantitatively measure the total absorption in a spectral line (Minnaert & van Assenbergh 1929; Minnaert 1934). The EW of a line is the width in Åof a completely dark region that has the same area as the one corresponding to the absorption line in the stellar spectrum. This width can be estimated through the fitting of a Gaussian curve across the absorption line of the star, with the parameters of the Gaussian being used to estimate the area of the rectangle. The amount of light absorbed by the stellar atmosphere required to create such a line can be calculated, reducing each line to a single value. These values can then be used to estimate the abundance of a given element, given a set of spectroscopic parameters. This method for spectroscopic parameter determination is called the ionization and excitation balance method, but it is more commonly known as the Equivalent Width Method. Minnaert showed that plotting the EW of a line against the number of absorbers (electrons) resulted in a very similar and universal shape, independently of the line being studied. This relation is illustrated in Fig. 3.1, and can have three different behaviors, depending on the number of absorbers (N). On an optically thin line, more radiation will be absorbed with each atom added to the layer, which translates to a linear increase in the EW of weak lines with the number of absorbers. The flat part of the curve of growth corresponds to a saturation in the center of the line, with every available photon of that wavelength already being absorbed by the layer. The addition of more atoms barely changes the amount of absorption, thus keeping the EW constant as N increases. Finally, with enough absorbers present, the probability of absorption in the wings of the lines becomes significant, and the EW grows with the square root of the number of absorbers. As the number of atoms in a star can't be changed or controlled, the curve of growth can only be estimated by measuring the EW of different lines of the same element (with both low and high transition probabilities).

The equation governing the curve of growth can be simplified as follows (derivation available in Gray 2005, chapter 16), :

$$\log(\frac{w}{\lambda}) = \log C + \log A + \log g_n f\lambda - \theta_{ex}\chi - \log \kappa_\nu \tag{3.1}$$

Where $\frac{w}{\lambda}$ is the EW of the line, A is the species abundance in the star, $\log g_n f\lambda$ is the logarithm of the excitation potential multiplied by statistical weight and wavelength for that line, $\theta_{ex} = \frac{5040}{T}$ is the inverse of the temperature, χ is the excitation potential for the atomic level, κ_ν is the continuous absorption coefficient, and the constant:

$$\log C = \log \frac{\pi e^2}{mc^2} \frac{N_j/N_E}{u(T)} N_H \tag{3.2}$$

This equation shows us that changes in $\log A$ are equivalent to changes in any of the other terms, such as $\log g_n f\lambda$, $\theta_{ex}\chi$, or $\log \kappa_\nu$. For a given specific star, where A is constant, the curves of growth for different lines will vary depending on the other terms, according to their values for $g_n f\lambda$, χ and κ_ν. By understanding the ways spectroscopic parameters influence each of these values, we can understand how the shape and depth of the absorption lines change with them.

Given a specific photospheric model, and choosing a specific line, it will result in a fixed $\log g_n f\lambda$ and χ (which depend on the element and the specific transition considered). The

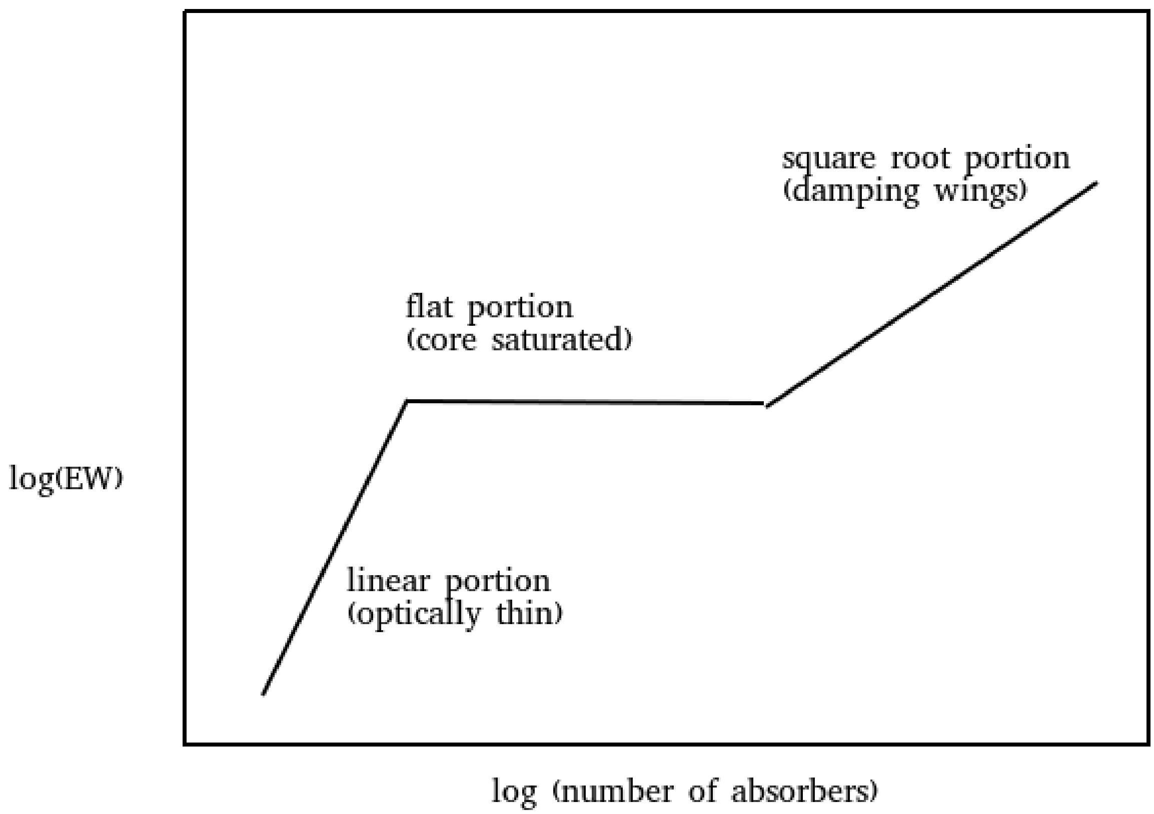

Figure 3.1: A schematic of a curve of growth of a given absorption line. It shows the change in EW as the number of absorbers (A) in the star increase. Created by observing many lines of the same species but with differing strengths. Source: Reid & Hawley (2005) (see Figure 4.4 from that publication).

model itself fixes θ_{ex} (from the temperature) and κ_ν (from the optical characteristics of the photosphere at that wavelength). Varying A, we can create the curve of growth for that line. From an observational point of view, A is constant, depending on the observed star. In this case, different lines of the same species, with different strengths ($\log g_n f\lambda$, χ, and κ_ν), can be studied to determine the abundance of that species. This can be used to construct an empirical curve of growth for that star by plotting the EW - $\log(w/\lambda)$ as a function of $\log(w/\lambda) - \log A$, which can be numerically computed as:

$$\log C + \log A + \log g_n f\lambda - \theta_{ex}\chi - \log \kappa_\nu \tag{3.3}$$

This is the same as adjusting the line-to-line differences present in the $\theta_{ex}\chi$ and $\log \kappa_\nu$ terms, and having only the line strength $\log g_n f\lambda$ as a single variable. By translating the derived curve into the standard curve, the abundance of that species can be derived. This is, in essence, the way EW method can be used for parameter determination.

This method can also be used to determine the surface gravity of a given star by studying the strength of lines given by both neutral and ionized atoms of the same species. $\log g$ can vary the shape and depth of the lines present in a stellar spectrum, as both $\frac{N_j}{N_E}$ and κ_ν can vary with $\log g$. For neutral lines in solar-type stars, however, these two effects tend to cancel out. This is not the case for ionic lines, from Fe II for example, where $\Delta \log A$ and $\Delta \log g$ can have a nearly linear relation. The equivalent width of ionic lines is sensitive to gravity roughly as $g^{-1/3}$. This translates to stronger ionic lines for stars with lower $\log g$ and means that, given a constant EW, the deduced abundance varies as $g^{+1/3}$.

When additional independent measurements for the surface gravity of a star are available, a separate chemical analysis can be performed for the neutral and ionic lines of the same element. As $\log g$ of a given star is a constant, using a consistent technique used must result in the same abundance for both sets of lines. Alternatively, if the surface gravity is unknown, it can be determined by forcing both neutral and ion solutions to give the same abundance.

The EW method can be quite accurate when the spectrum is high-resolution (resulting in separated lines) and an accurate stellar model is available. However, it becomes more inaccurate for spectra with blended lines, which are increasingly common for lower temperature stars, such as M dwarfs.

3.2.2 Synthetic spectra

Another solution for the derivation of stellar parameters from spectra is the synthetic spectra method, which is based on creating synthetic spectra and compare them to an observed one (Gray 2005). If accurate stellar models and complete line lists for a given spectral type and wavelength range are available, spectra can be fully reproduced. These syntheses may be of either the full observed spectrum or of a particular region of interest in the spectrum. Through the use of an iterative code and an algorithm to minimize the difference between the synthetic and the observed spectra, new synthetic spectra can be generated, inching closer and closer to the observed one. When the synthetic spectrum is close enough to the observed one (using a pre-defined threshold), the parameters used to create the synthetic spectrum should also be close to the ones of the observed star. As the full spectrum is created from scratch and includes all lines present in the stellar one, blended lines are less problematic for this method. However, it requires significant computing power, as well as both an accurate stellar atmosphere model and a complete line list.

There are two main methods to use synthetic spectra to derive stellar parameters. One of them is to pre-compute a huge grid of synthetic spectra, and afterward perform a comparison of the observed stellar spectra against the elements of this grid (e.g., Rajpurohit et al. 2018a,b). This method saves some time on the spectral synthesis step per star by having the grid be pre-computed, but loses some flexibility and precision, depending on the size of the grid elements. Another method is to synthesize spectra on-the-fly and compare them individually to each new stellar spectra (e.g., Souto et al. 2017; Souto et al. 2018). This results in a longer computing time per star but results in a more flexible method for synthesizing stars with different characteristics. Due to the characteristics of the stars studied in this project, the syntheses were performed on-the-fly for each star in the sample.

As the spectra analyzed in this project belong to M dwarfs and solar-type stars, we decided to use the synthetic spectra method to derive their parameters.

Radiative Transfer codes

There are many codes publicly available to generate synthetic spectra, each with their particular specifications and characteristics. Choosing the code best suited for a particular task is very important, as many factors can influence it. This section includes an overview of codes to generate a synthetic spectrum available for public use.

MOOG, made available by Sneden et al. (2012), is one of the most widely used codes for generating and studying synthetic spectra. It can perform a variety of Local Thermodynamic Equilibrium (LTE) line analysis and spectrum synthesis tasks. MOOG is written in FORTRAN77, and one of its chief assets is the ability to plot spectra and perform visual analysis.

Spectroscopy Made Easy (SME) is an IDL code to determine spectroscopic parameters by comparing observed and synthetic spectra. It was first developed in Valenti & Piskunov (1996) and has cemented itself as one of the most useful codes for synthesizing and analyzing spectra. It has been recently updated (Piskunov & Valenti 2017) and is available for Mac, Linux, and Windows systems.

Another important code for generating synthetic spectra, historically, has been *SPECTRUM*. *SPECTRUM* was first created by Gray (1999). It works on several different platforms, including UNIX, LINUX, and several windows releases. *SPECTRUM* was written in the C language and is still widely used at present times.

SYNTHE is another good example of a synthetic spectra code. Developed by Sbordone et al. (2004), it was created specifically to complement the ATLAS code (Kurucz 1970; Castelli et al. 1997). ATLAS is used for the production of LTE one-dimensional atmosphere models of stars, and *SYNTHE* creates synthetic spectra from these models.

Finally, *Turbospectrum* is a FORTRAN-based code for spectral synthesis developed by Alvarez & Plez (1998); Plez (2012). Like *SYNTHE*, it is a 1D LTE spectrum synthesis code. It can synthesize 600 different molecules and is very fast at computing spectra, compared to the other codes.

As all codes mentioned above are available on *iSpec*, different comparisons between them were made to assure the one best suited for the project is used. These comparisons are available in section 5.2.2.

Stellar models

All these codes require both a collection of stellar models and a complete line list to function correctly and provide synthetic spectra that match stellar observations. Choosing or creating complete stellar models is thus a fundamental task when generating a synthetic spectrum.

There are two main categories of stellar models: plane-parallel and spherical models. A plane-parallel model rests on the assumption that the stellar atmosphere can be approximated as a series of parallel planes, ranging from the bottom of the atmosphere to its surface. These models are more often used for dwarf (main-sequence) stars. A spherical model takes into consideration the shape of the star as a whole, simulating it as a series of concentric layers. These models are often used for giant stars, where the shape of the star becomes relevant. Stellar models have values for the pressure, temperature, density, sound speed, and opacity for each of these layers/planes, based on astrophysical equations that describe the interior of stars. These models are based on spectroscopic parameters for the star, so that the T_{eff}, $[M/H]$ and $\log g$ at the stellar atmosphere correspond to the values measured when observing the stellar spectrum.

MARCS (Gustafsson et al. 2008) is a source for stellar models and the one used to generate the synthetic spectra used in this thesis. These models were generated for wide ranges of spectroscopic parameters (T_{eff} ranges from $2500 - 8000\,\mathrm{K}$ $[M/H]$ from -5.00 to $+1.00\,\mathrm{dex}$, and $\log g$ from 0.0 to $5.5\,\mathrm{dex}$). The MARCS models used assume plane-parallel 1D stratification, hydrostatic equilibrium, mixing-length convection, and local thermodynamic equilibrium.

Other examples of stellar models include the ones created by ATLAS9 (Kurucz 2005), as mentioned in Section 3.2.2, as well as the PHOENIX models (Husser et al. 2013). ATLAS9 models include large parameter ranges, with T_{eff} values from 3500 to $50000\,\mathrm{K}$, $\log g$ from 0.0 to $5.0\,\mathrm{dex}$, and several different metallicities, depending on the other two parameters. The PHOENIX models are created with the stellar atmosphere code PHOENIX, and range from $500 - 50\,000$ Åwith resolution $R = 500\,000$ in the optical and $R = 100\,000$ in the Infrared. However, since these models are not included in *iSpec*, they are not an option for this project. ATLAS9 models are available within our used *iSpec* distribution, but since they do not include the full M dwarf parameter space, MARCS models were the clear choice for the project.

3.3 The effects of spectroscopic parameters on stellar spectra

The stellar spectrum's shape depends on many spectroscopic parameters affecting the spectrum in different ways. These effects can change which lines are present in the spectrum, as well as their shapes and depths. This section will analyze and compare the effects of these fundamental spectroscopic parameters on the stellar spectrum.

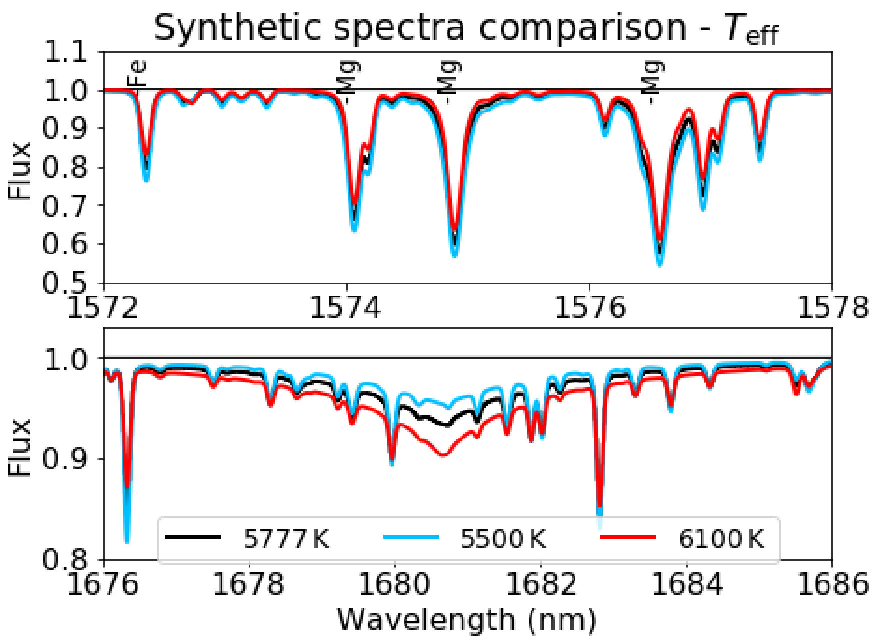

Figure 3.2: Comparison between the shape of 3 different synthetic spectra, changing only $T_{\rm eff}$ between them. Black spectrum has $T_{\rm eff} = 5772\,\rm K$, light blue has $T_{\rm eff} = 5500\,\rm K$, and red has $T_{\rm eff} = 6100\,\rm K$. Other parameters used for the syntheses were $\log g = 4.44\,\rm dex$, $[M/H] = 0.0\,\rm dex$, $v \sin i = 1.6\,\rm km/s$, $v_{mic} = 1.07\,\rm km/s$, $v_{mac} = 4.26\,\rm km/s$ and $R = 22500$.

3.3.1 Effective temperature ($T_{\rm eff}$)

The effective temperature, or $T_{\rm eff}$, cannot be separated from the spectral type of the star itself, and dictates the species (elements or molecules) present in its atmosphere. Large changes in $T_{\rm eff}$ can thus result in large changes in the stellar spectra.

The fact that there are spectral lines very sensitive to temperature, combined with the continuum's sensitivity to temperature, means that a careful analysis of its spectrum can precisely determine the effective temperature of a star. Taking equation 3.1 as a reference, the stellar temperature affects the ionization equilibrium ($\frac{N_j}{N_E}$), κ_ν and θ_{ex} in the determination of each line's shape and EW. This translates to a shift in the $\log A$ coordinate for the curve of growth. The shift will depend on the temperature regime and ionization stage, but it can be very small, even for a $100\rm K$ change in the star's $T_{\rm eff}$.

By changing the number of atoms in a given excitation state for a specific element, changes in $T_{\rm eff}$ can cause spectral lines to become stronger or weaker. This can be observed in Fig. 3.2, which shows the changes in stellar spectra caused by a variation in the star's $T_{\rm eff}$. The top panel shows various elemental lines that are stronger for stars with lower $T_{\rm eff}$. This is explained by Equation 3.1, as a decrease in temperature will increase $\theta_{ex} = 5040/$T, which results in turn in an increase in a given line's EW. The bottom panel shows the line profile of the Hydrogen line around $1681.1\,\mathrm{nm}$ (vacuum wavelength, Brackett series, Wiese & Fuhr 2009). This is a transition line between the 4th and the 11th excitation levels of the H 1 atom. An increase in the star's T_{eff} will result in an increase of the energy of electrons in hydrogen atoms, resulting in an increased probability of transition between the $n = 4$ and $n = 11$ excitation levels. Therefore, the strength of that transition line in the stellar spectrum is increased. As the stellar T_{eff} appears multiple times on a line's curve of growth, changes in that parameter can have different effects on the EW of different lines in the stellar spectrum.

The appendix A.1 and A.2 contain lists with the most and the least sensitive lines to T_{eff} in APOGEE spectra, separated for both FGK and M dwarfs.

Important H-band features for M dwarf T_{eff} determination

H-band spectra at APOGEE resolution ($R \sim 22\,000$) contains several features that can be used to distinguish between different subtypes of M dwarfs. This section contains some examples of these features, and the subtypes (and consequent T_{eff}) their presence usually indicates. Figure 3.3 shows three areas with important features in the H-band that can be used to distinguish M dwarf subtypes and their effective temperature.

First, and most importantly, stars with an effective temperature below 4000 K start to show water lines (H_2O) in their spectrum. These lines form a blanket that lower the continuum across all H-band and they make other elemental and molecular lines harder to measure. The presence of this line “forest” is the most important spectral feature present in M dwarfs that serves as a way to distinguish these stars from hotter ones. These lines are the reason for the continuum depression seen between stars of different temperatures.

Another important feature that can be seen varying between stars of different temperatures is the Mg triplet around 1576 nm (top figure). These lines, very prominent for stars around ~ 4000 K, tend to disappear for colder stars. In the blue spectrum, of a star with $T_{\mathrm{eff}} = 3300$ K, the lines have merged into the water lines decreasing the continuum and cannot be measured. By detecting these lines or their absence, we can make a better estimation of the star's T_{eff}.

The plot in the middle shows another set of complex lines. Most of these lines preserve their shape across multiple stellar effective temperatures, but two of them are stronger at higher T_{eff}. These are the two Fe lines around 1632 nm and the Si line at around 1638 nm. By comparing these two features with the other lines, colder stars can be distinguished from hotter ones.

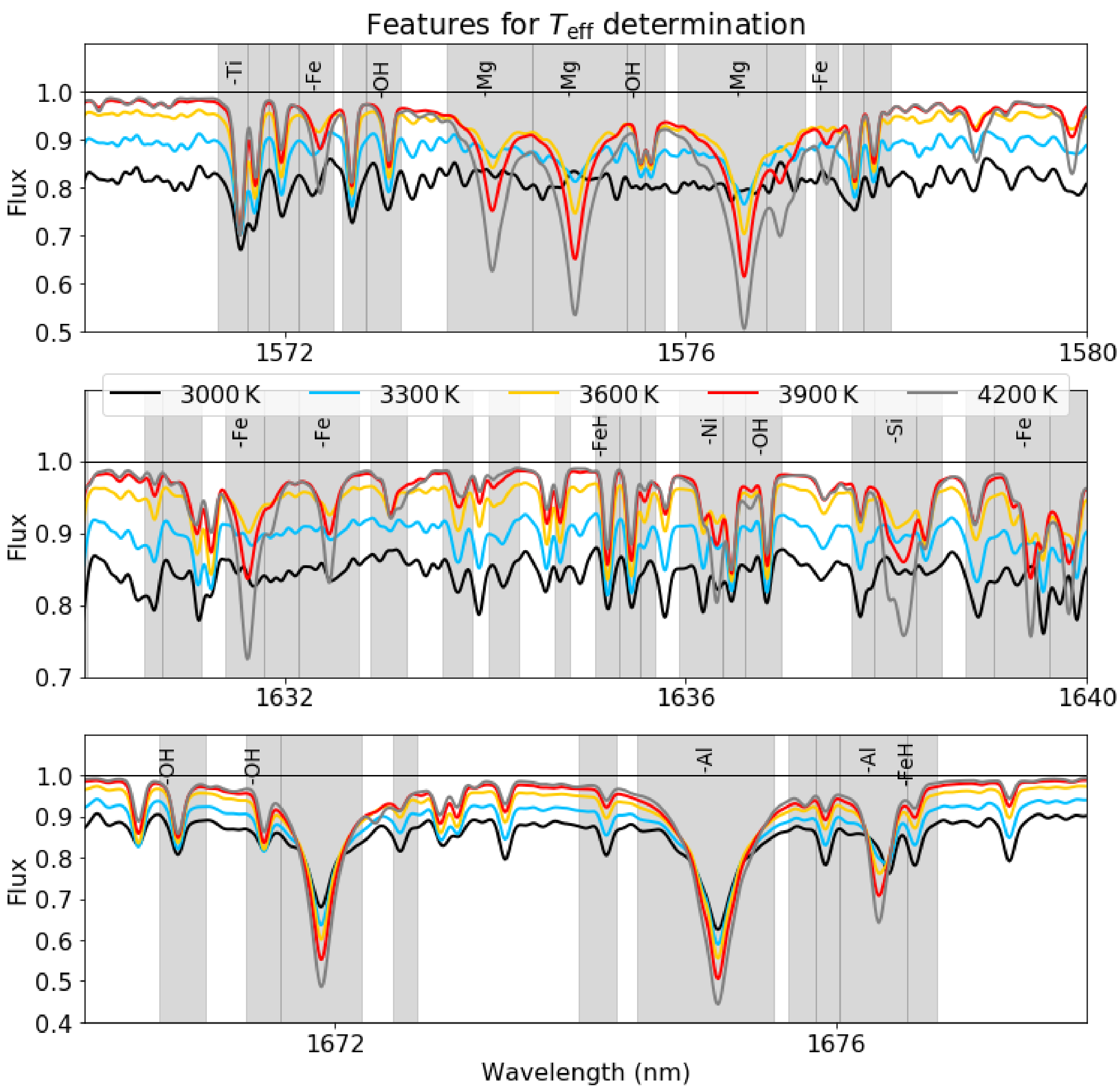

Figure 3.3: Comparison between synthetic spectra made with different T_{eff}. The spectra corresponds to synthesis made with T_{eff} 4200K (gray), 3900K (red), 3600K (orange), 3300K (blue) and 3000K (black). All synthetic spectra shown were created with $[M/H] = 0.0$ dex and $\log g = 5.0$ dex. Areas shown include H-band features that can be used to distinguish T_{eff} of observed stars.

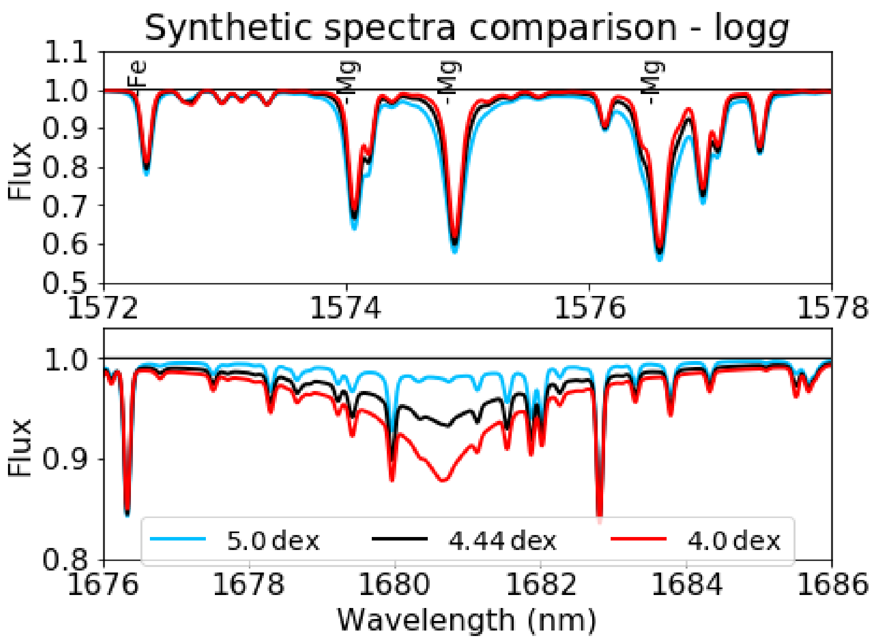

Figure 3.4: Comparison between the shape of 3 different synthetic spectra, changing only $\log g$ between them. Black spectrum has $\log g = 4.44\,\mathrm{dex}$, light blue has $\log g = 5.0\,\mathrm{dex}$, and red has $\log g = 4.0\,\mathrm{dex}$. Other parameters used for the syntheses were $T_{\mathrm{eff}} = 5772\,\mathrm{K}$, $[M/H] = 0.0\,\mathrm{dex}$, $v \sin i = 1.6\,\mathrm{km/s}$, $v_{mic} = 1.07\,\mathrm{km/s}$, $v_{mac} = 4.26\,\mathrm{km/s}$ and $R = 22500$.

The bottom plot shows the two strongest lines that can be observed in APOGEE H-band spectra. The Al doublet around 1672-1676 nm is an unmistakable feature that appears across all spectral types observed. Despite that, this line doublet is not a great T_{eff} indicator, as the shape and depth of these two lines change very little across all the spectra synthesized here. The lines are shallower for colder stars but compared to the other possible lines to use, the difference is not strong enough.

These figures do not show the full available wavelength range but are a representation of some of the strongest features that change with T_{eff}, and they all have one thing in common. All lines shown here are stronger for stars with higher T_{eff} and weaker for colder ones. This factor, associated with the water lines depressing the continuum, makes it very challenging to correctly determine the T_{eff} (and subtype) of the coldest M dwarfs through their H-band spectrum alone, especially if the spectrum is not normalized. These issues will be tackled in Section 5.4.

3.3.2 Surface Gravity ($\log g$)

The Surface Gravity, or g, of a star, represents the gravitational acceleration experienced at its surface at the equator, including the effects of rotation. The surface gravity may be thought of as the acceleration due to gravity experienced by a hypothetical test particle which is very close to the object's surface and which, in order not to disturb the system, has negligible mass.

Surface gravity is measured in units of acceleration ($\mathrm{m/s^2}$ in SI units). In astrophysics, including this thesis, the surface gravity will be expressed as $\log g$, obtained by expressing the gravity in cgs units ($\mathrm{cm/s^2}$), and taking its base-10 logarithm. As an example, the surface gravity of the Earth could be expressed as $980.665\,\mathrm{cm/s^2}$, with a base-10 logarithm ($\log g$) of $2.992\,\mathrm{dex}$. The Sun's surface gravity is $27\,400\,\mathrm{cm/s^2}$, or in $\log g$ units $4.44\,\mathrm{dex}$. Surface gravities of dwarf stars are usually around $4 - 5.5\,\mathrm{dex}$, with giant stars, due to their size, having lower $\log g$ values ($\sim 0 - 3.5\,\mathrm{dex}$).

Fig. 3.4 shows the changes in stellar spectra caused by a variation in the star's $\log g$, comparing synthetic spectra with different values for that parameter. In the top plot, the atomic lines shown are slightly stronger for higher values of $\log g$, with an especially pronounced effect on the wings of the 1574.90 nm Mg line. In the bottom plot, the effects of $\log g$ on the transition lines in a stellar spectrum are visible in the line profile of the weak Hydrogen line around $1681.1\,\mathrm{nm}$ (vacuum wavelength, Brackett series Wiese & Fuhr 2009). Since neutral hydrogen is the dominant species at solar temperatures, its (weak) lines are sensitive to pressure ($\log g$) in the same way as (weak) ionic lines of iron, and nearly disappears at $\log g = 5.0\,\mathrm{dex}$.

The appendix A.1 and A.2 contain lists with the most and the least sensitive lines to $\log g$ in APOGEE spectra, separated for both FGK and M dwarfs.

Important H-band features for M dwarf $\log g$ determination

Figures 3.5 and 3.6 show three areas in the H-band wavelength range observed by APOGEE that can be useful for measuring the $\log g$ of an observed star's spectrum. The highlighted areas are only some of the regions and lines that vary accordingly to the observed star's $\log g$, but the strength and abundance of lines in the regions make them especially important in the determination of the spectroscopic parameter. Despite some effects of the parameter on the shape and depth of the line being minor compared to $[M/H]$ and T_{eff}, they can still be noticed at APOGEE's $R \sim 22\,000$.

The top image displays an area around 1515 nm to 1522 nm. This region of the spectrum contains two strong Potassium lines that are strongly affected by the star's $\log g$, becoming stronger with increasing $\log g$ values. When comparing this image with the other two below it, we can see that this effect is not present in many lines across the spectrum, as lines becoming

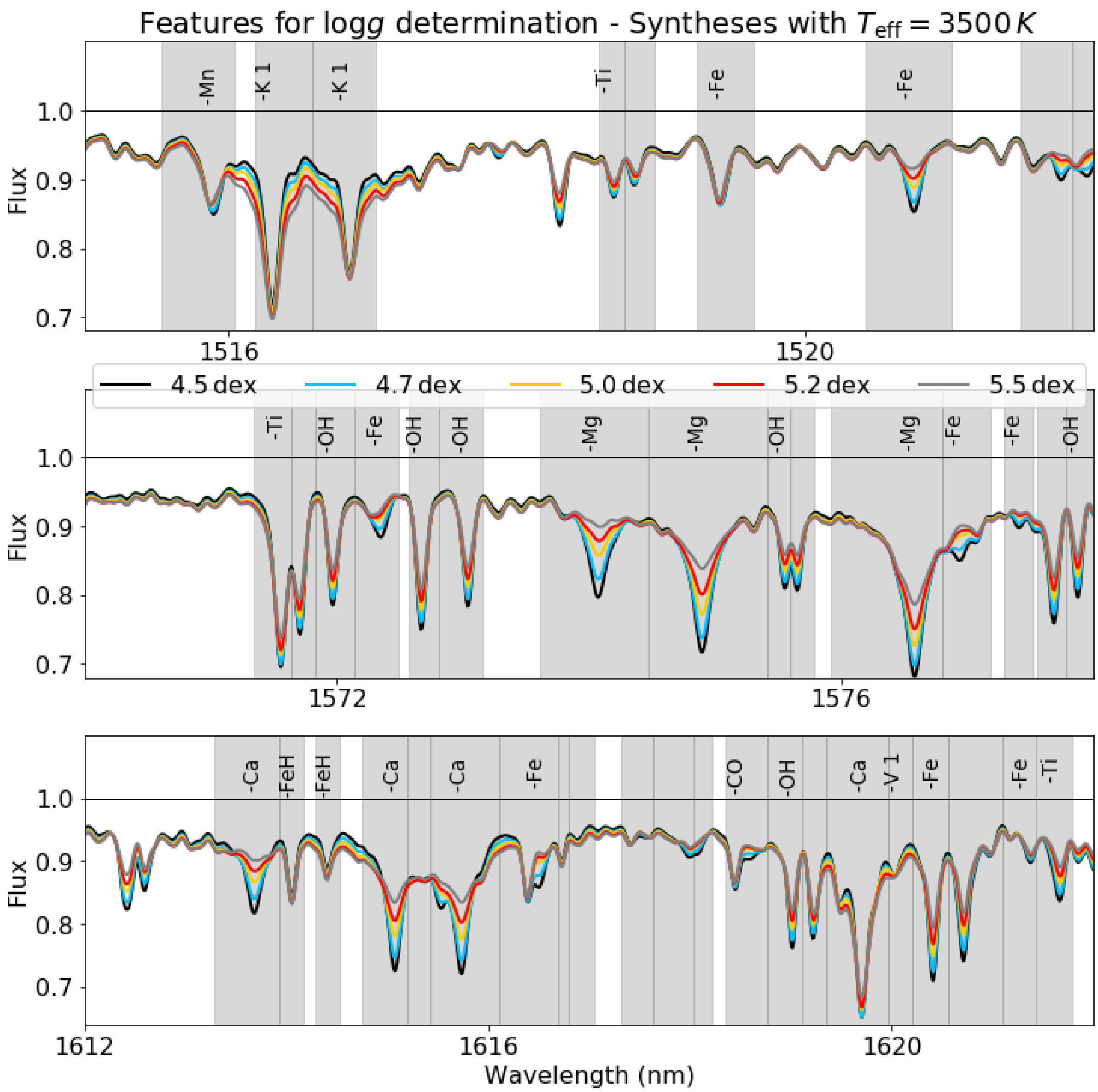

Figure 3.5: Comparison between synthetic spectra made with different $\log g$. The spectra corresponds to synthesis made with $\log g$ 5.5 dex (gray), 5.2 dex (red), 5.0 dex (orange), 4.7 dex (blue) and 4.5 dex (black). All synthetic spectra shown were created with $T_{\rm eff} = 3500$ K and $[M/H] = 0.0$ dex. Areas shown highlight H-band features that can be used to distinguish $\log g$ of observed stars.

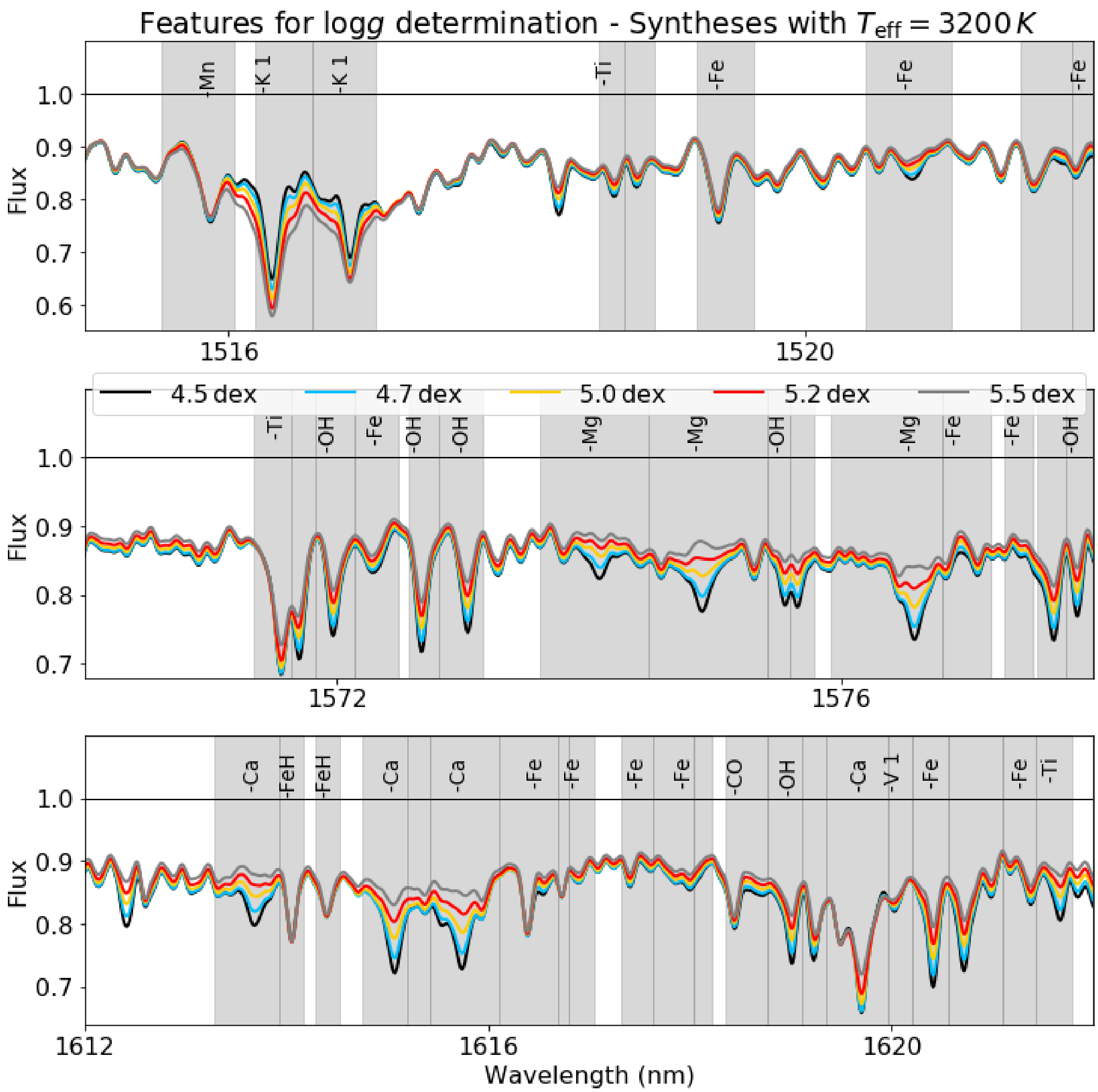

Figure 3.6: Comparison between synthetic spectra made with different $\log g$, made with synthetic spectra for lower temperature stars. The spectra corresponds to synthesis made with $\log g$ 5.5 dex (gray), 5.2 dex (red), 5.0 dex (orange), 4.7 dex (blue) and 4.5 dex (black). All synthetic spectra shown were created with $T_{\rm eff} = 3200$ K and $[M/H] = 0.0$ dex. Areas shown highlight H-band features that can be used to distinguish $\log g$ of observed stars.

stronger with decreasing $\log g$ values are more common. Therefore, the inclusion of this region in a line mask is important for the determination of the $\log g$ of an M dwarf.

The middle image displays the wavelength region between 1570 nm and 1578 nm, containing several strong Magnesium lines that are strongly affected by the observed star's surface gravity. Contrasting the effect shown in the Potassium lines in the top image, the Magnesium lines become stronger for stars with lower $\log g$ values. This region in particular is of increased importance for spectroscopic parameter determination, as it is also strongly affected by the star's T_{eff} (see Fig. 3.3) and $[M/H]$ (see Fig. 3.8).

The bottom image displays a region between 1612 nm and 1622 nm containing several strong Calcium and Iron lines that are affected by the observed star's $\log g$. In this case, the surface gravity affects not only the line depth but its shape as well, with features present at lower $\log g$ disappearing for stars with higher values. This region is also important for the determination of other parameters, such as metallicity (see Fig. 3.8).

3.3.3 Metallicity ($[M/H]$)

Stars are mostly made of Hydrogen ($\sim 90\%$) and Helium ($\sim 10\%$), with the other elements making only a small percentage of the total, like salt for food seasoning. Metallicity is a measure of the amount of these other elements by their abundance relative to the amount present in the Sun. A star with $[M/H] = 0.0\,\text{dex}$ will have the same amount of metals that is present in the Sun, while a star with $[M/H] = -1.0\,\text{dex}$ will have only 10% of that value.

The relative abundance of each element can also differ between stars and be measured individually from the compared strength of each species' lines. By studying lines from a specific element and measuring their EW, the abundances in each star can be estimated. However, and as the abundances of individual elements will not be considered in these syntheses, we will not dwell on them, and rather focus on the overall metallicity of a star.

Looking back to equation 3.1, the abundance of a given element enters only the equation as $\log A$. This means that changing a star's metallicity is the equivalent of moving across the curve of growth in either direction.

Figure 3.7 shows the changes in stellar spectra caused by a variation in the star's $[M/H]$, comparing synthetic spectra with different values for that parameter. As expected, higher metallicities result in deeper and stronger lines all across the whole spectrum, with the specific change being dependent on the element and the line's position in its curve of growth, in either

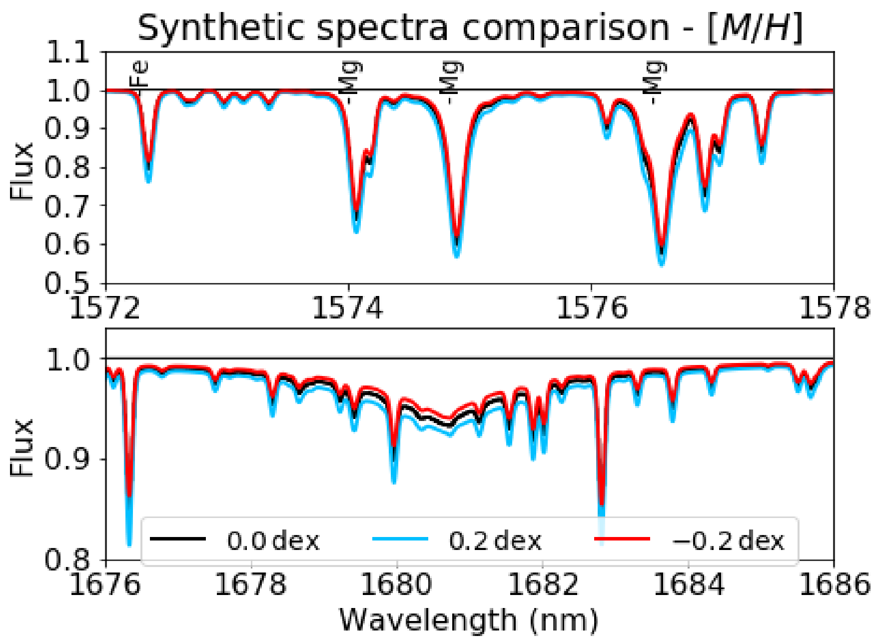

Figure 3.7: Comparison between the shape of 3 different spectra, changing only $[M/H]$ between them. Black spectrum has $[M/H] = 0.0\,\mathrm{dex}$, light blue has $[M/H] = +0.2\,\mathrm{dex}$, and red has $[M/H] = -0.2\,\mathrm{dex}$. Other parameters used for the syntheses were $\log g = 4.44\,\mathrm{dex}$, $T_{\mathrm{eff}} = 5772\,\mathrm{K}$, $v \sin i = 1.6\,\mathrm{km/s}$, $v_{mic} = 1.07\,\mathrm{km/s}$, $v_{mac} = 4.26\,\mathrm{km/s}$ and $R = 22500$.

the linear portion, flat portion or square root portion. As mentioned above in subsection 3.2.1, lines in the linear portion of the curve of growth will have an EW directly proportional to the species' abundance. Lines in the flat portion will have a constant EW with the change in abundance, and the EW of lines in the square root portion will increase proportionally to the square root of the species' abundance.

Important H-band features for M dwarf $[M/H]$ determination

Figure 3.8 contains a selection of three H-band spectral regions of significant importance in the determination of the metallicity of observed M dwarfs. Most lines and features in a spectrum are affected by the metallicity content of the star, but some stronger lines can be more affected than others. The three highlighted areas contain several lines that can be used for the determination of overall stellar metallicity, as they change significantly depending on the metal content of the observed stars. More regions are contained within our selected line masks, but these are particularly important in the determination of stellar metallicity.

The top row of the figure displays the region around the magnesium triplet already highlighted in Fig. 3.3, in a wavelength range from 1570 nm to 1578 nm. This region contains not only three strong Magnesium lines but several OH lines as well, making it a good indicator of

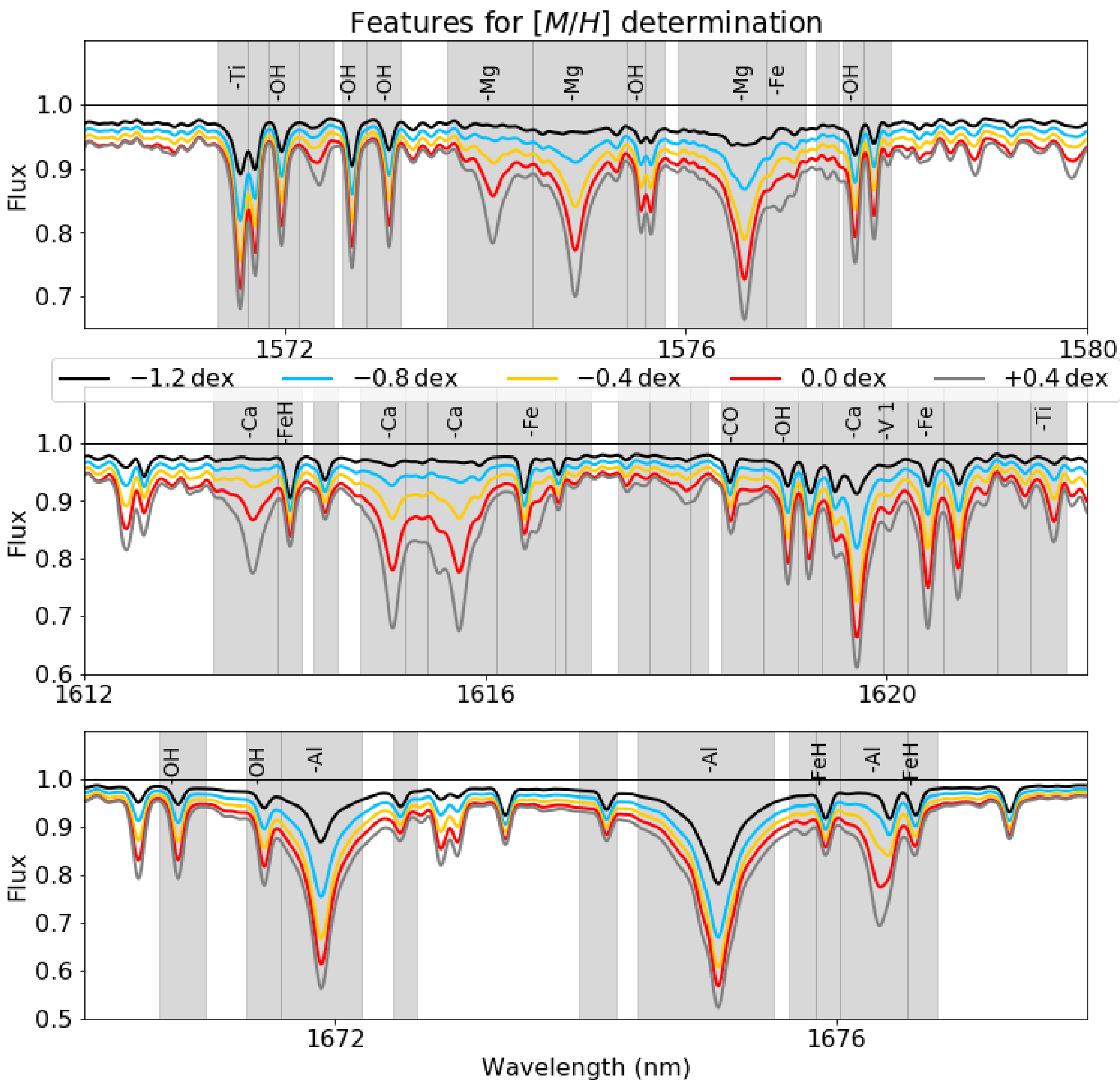

Figure 3.8: Comparison between synthetic spectra made with different $[M/H]$. The spectra corresponds to synthesis made with $[M/H]$ +0.4 dex (gray), +0.0 dex (red), -0.4 dex (orange), -0.8 dex (blue) and -1.2 dex (black). All synthetic spectra shown were created with $T_{\rm eff} = 3500$ K and $\log g = 5.0$ dex. Areas shown highlight H-band features that can be used to distinguish $[M/H]$ of observed stars.

metallicity in the observed star. The fact that the shape and depth of the lines can also change significantly with the stellar effective temperature increases the importance of this region to disentangle the degeneracy between the two parameters. In the case of this particular region, the strong magnesium lines almost disappear both for stars with low overall metallicity and stars with low effective temperature, making it more difficult to distinguish between them.

The middle row displays a region with four important Calcium lines between 1612 nm and 1622 nm that are very strongly affected by the stellar metallicity, as well as some Iron, FeH and OH lines that can also help to measure this stellar parameter. This region is shown in Fig. 3.5 as an important region for $\log g$ determination. It is also mentioned in Section 5.4.1 as one of the regions used for the calculation of the metallicity index used for an approximate determination of the stellar metallicity.

The figure's bottom row displays another region already shown in Fig. 3.3. This region contains three Aluminum lines that correspond to the strongest atomic lines in the full APOGEE H-band wavelength range, present between 1670 nm and 1678 nm. Some additional OH lines in the region are also affected by metallicity and help us determine this parameter in the observed star.

3.3.4 Rotational velocity ($v \sin i$)

The effect of the rotational velocity of a star in its spectrum is measured by its $v \sin i$ parameter. This parameter depends explicitly on the inclination of the star's rotational axis from our point of view. An increase in the rotation of the star does not change the EW of the lines but it results in a widening or broadening of the lines in the spectrum, as well as making the lines more shallow. This is due to the Doppler-shift distribution of the surface of the star, as every element of the surface from which light comes to us is moving relative to the center of mass of the star. These motions can come from photospheric motions, like oscillations or granulations, or from the star's rotation as well.

Figure 3.9 shows the changes in stellar spectra caused by a variation in the star's $v \sin i$, with three synthetic spectra created with different values for that parameter. That figure shows that the sun's rotational velocity of around $1.6\,\mathrm{km/s}$ is too low to be visible in a synthetic spectrum with the resolution of APOGEE's spectra. However, a faster rotating star ($v \sin i = 16$ km/s) will have its lines clearly broadened. Lowering the spectral resolution will result in the observation of some kind of broadening as an increase in the speed of stellar

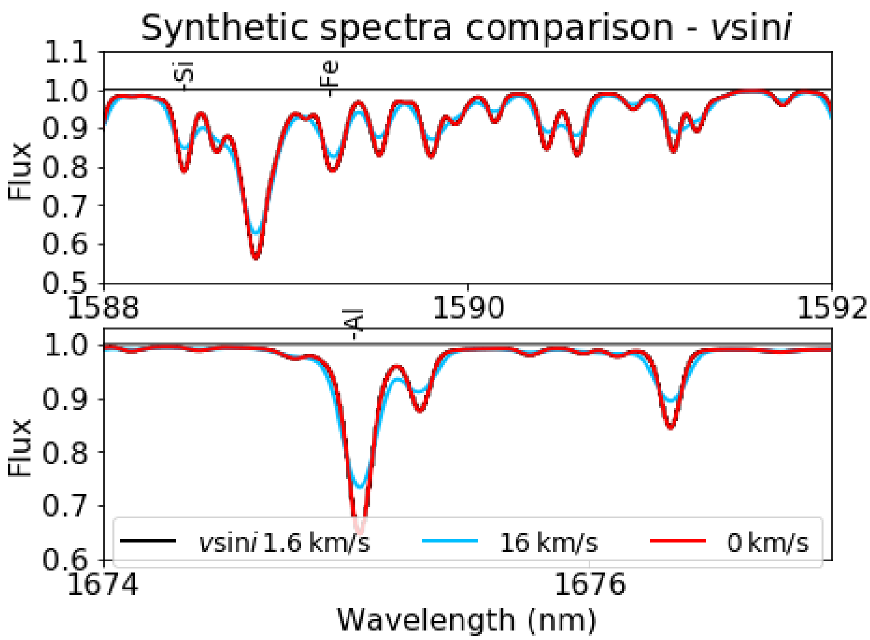

Figure 3.9: Comparison between the shape of 3 different spectra, changing only $v\sin i$ between them. Black spectrum has $v\sin i = 1.6\,\mathrm{km/s}$, light blue has $v\sin i = 16\,\mathrm{km/s}$, and red has $v\sin i = 0.0\,\mathrm{km/s}$. Other parameters used for the syntheses were $\log g = 4.44\,\mathrm{dex}$, $[M/H] = 0.0\,\mathrm{dex}$, $T_{\mathrm{eff}} = 5772\,\mathrm{K}$, $v_{mic} = 1.07\,\mathrm{km/s}$, $v_{mac} = 4.26\,\mathrm{km/s}$ and $R = 22500$.

rotation. This means that, for a given spectral resolution, there will be a minimum rotational velocity that can be measured accurately. It also means that, for a fast-rotating star, there are much more diminishing gains for an increase in the resolution of the observed spectra, compared to a star with a low $v\sin i$, as improvements in spectral resolution will not result in higher-quality spectra.

3.3.5 Turbulent velocities (v_{mic}, v_{mac})

In addition to $v\sin i$, the turbulent velocities v_{mic} (microturbulence) and v_{mac} (macroturbulence) can also result in a broadening of the stellar spectra. Fig. 3.10 shows the changes in stellar spectra caused by a variation in the star's v_{mic}, and Fig. 3.11 shows the changes caused by a variation in the star's v_{mac}.

When our line of sight penetrates through multiple cells of motion in the photosphere, the line profile is molded by the velocity distribution of the particles in the cells. Microturbulence is a measure of this dispersion. The plot shows that an increase in v_{mic} from $1.07\,\mathrm{km/s}$ (Solar Parameters) to $5.0\,\mathrm{km/s}$ and $10.0\,\mathrm{km/s}$ results in deeper lines (more absorption) in cases where the lines are already strong, but weaker lines are not very much affected by this change. This is because the lines have a Gaussian shape. For weak lines, increasing the microturbulence

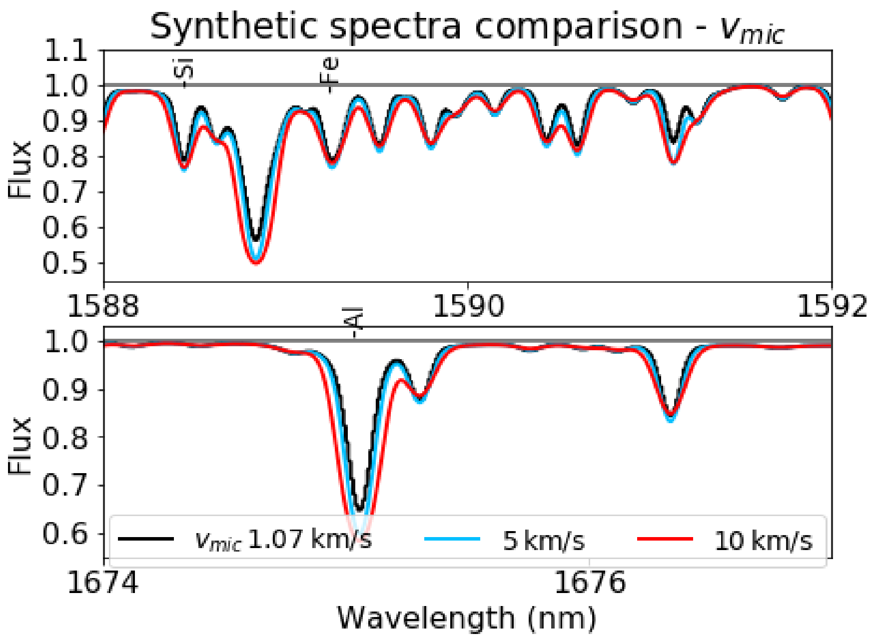

Figure 3.10: Comparison between the shape of 3 different spectra, changing only v_{mic} between them. Black spectrum has $v_{mic} = 1.07\,\mathrm{km/s}$, light blue has $v_{mic} = 5.0\,\mathrm{km/s}$, and red has $v_{mic} = 10.0\,\mathrm{km/s}$. Other parameters used for the syntheses were $T_{\mathrm{eff}} = 5772\,\mathrm{K}$, $\log g = 4.44\,\mathrm{dex}$, $[M/H] = 0.0\,\mathrm{dex}$, $v \sin i = 1.6\,\mathrm{km/s}$, $v_{mac} = 4.26\,\mathrm{km/s}$, and $R = 22500$.

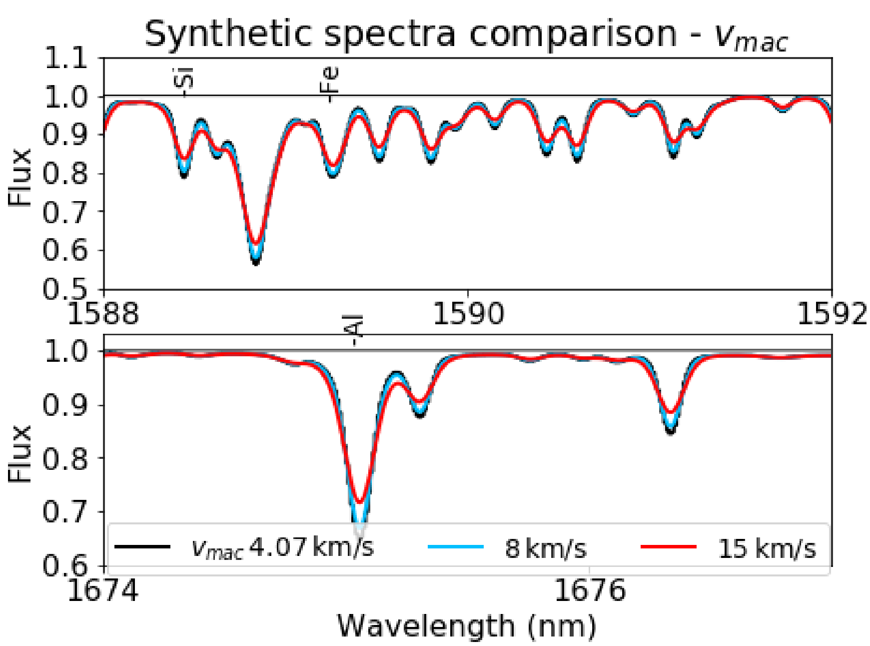

Figure 3.11: Comparison between the shape of 3 different spectra, changing only v_{mac} between them. Black spectrum has $v_{mac} = 4.26\,\mathrm{km/s}$, light blue has $v_{mac} = 8.0\,\mathrm{km/s}$, and red has $v_{mac} = 15.0\,\mathrm{km/s}$. Other parameters used for the syntheses were $T_{\mathrm{eff}} = 5772\,\mathrm{K}$, $\log g = 4.44\,\mathrm{dex}$, $[M/H] = 0.0\,\mathrm{dex}$, $v \sin i = 1.6\,\mathrm{km/s}$, $v_{mic} = 1.07\,\mathrm{km/s}$, and $R = 22500$.

results in a broadening of this Gaussian, and, since the line is not saturated, this produces a wider and shallower absorption line that maintains its Gaussian shape and conserves the Equivalent Width. In the case of stronger, saturated lines (flat portion of the curve of growth equation, 3.1), an increase in microturbulence results in a widening of the wavelength range covered by the absorption and reduces the saturation. This increases the total absorption and the total EW of the line.

When these same turbulence cells are large enough for photons to remain in them from the time they are created until the time they leave the star, we start to have macroturbulence. Viewing the spectra from multiple macro-cells simultaneously results in the observation of this turbulence as line broadening rather than radial-velocity changes. In the case of our plot, a change in macroturbulence from $4.26\,\mathrm{km/s}$ to $16\,\mathrm{km/s}$ resulted in a line broadening similar to the one exemplified before in Fig. 3.9 with a $v\sin i$ of the same value. The most important difference between these two parameters ($v\sin i$ and v_{mac}) is their correlation with other, more distinguishable spectroscopic parameters, such as effective temperature and metallicity. While the star's rotational speed has a dependency on age and the other spectroscopic parameters, it is difficult to accurately estimate it given only these parameters. Conversely, an accurate estimate for v_{mac} can be obtained by measuring the stellar spectroscopic parameters and applying empirical relations based on T_{eff}, $\log g$ and $[M/H]$.

Chapter 4

Data

This chapter includes an extensive characterization of the sources for our data, the software required for our analysis, and characterization of all stars included in the samples used in this project.

We include separate sections detail two different stellar samples, FGK-type stars (see section 4.2) and M dwarf stars (see section 4.3). Magnitude, S/N, sky position, and distance are available for both of the main samples, as well as relevant works in the literature characterizing these stars.

4.1 APOGEE and ASPCAP

The Apache Point Observatory Galactic Evolution Experiment (APOGEE, Albareti et al. 2016) is an H-band (1.51-1.7 micron) Sloan Digital Sky Survey program that focuses on measuring stellar spectra with $R \sim 22500$. It targets mostly red giants and has published spectra for more than 200 000 stars in its latest Data Release (DR14, Holtzman et al. 2018)

APOGEE operates on the Sloan 2.5 m telescope at the Apache Point Observatory in New Mexico (Gunn et al. 2006). It observes spectra with a 300-fiber spectrograph, which means it can observe up to 300 stars at any given time. Nowadays this instrument is called APOGEE-2N (or APOGEE-2 North) as an APOGEE-2S (APOGEE-2 South) has been started in 2.5 m duPont telescope at the Las Campanas Observatory in Chile (Bowen & Vaughan 1973). This telescope uses a $3.5\,\mathrm{deg}^2$ plate to collect light. Fig.4.1 displayes the footprint of the different areas in the sky where APOGEE has made observations of at least 250 stellar spectra.

The main goal of APOGEE is to answer questions about the history, age distribution, and

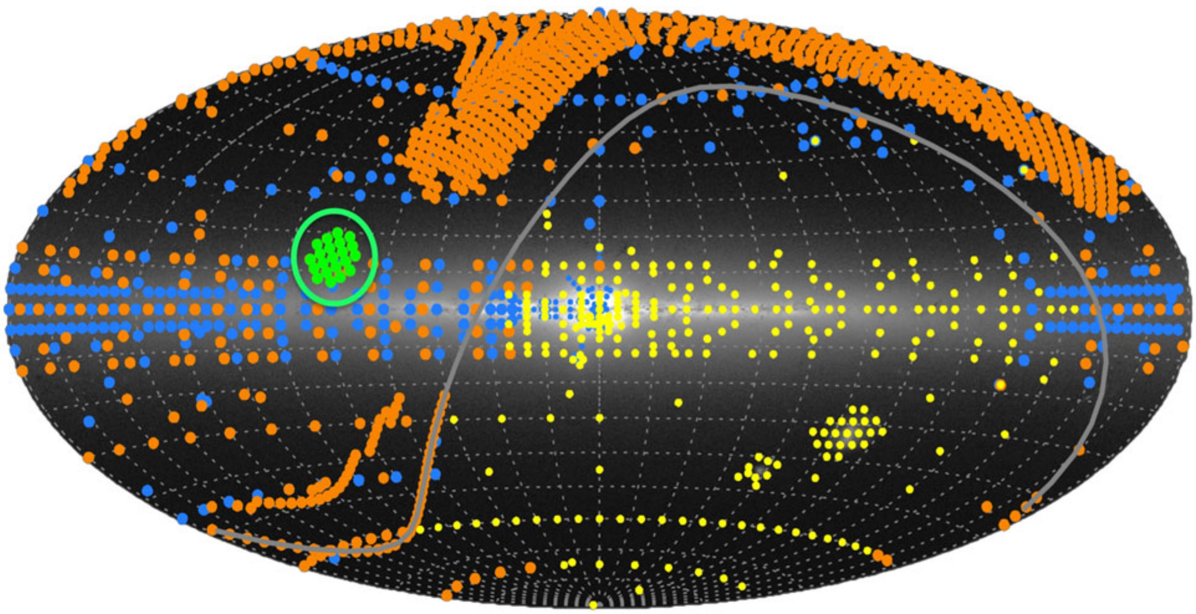

Figure 4.1: The APOGEE-2 survey footprint, overlaid on an infrared image of the Milky Way. Each dot shows a position where APOGEE obtains at least 250 stellar spectra. Source: P. M. Frinchaboy and SDSS/APOGEE, 2MASS

dynamics of the Milky Way, as well as to compare spectral parameters of stars with and without planets. This instrument's observations are in the near-infrared because in that wavelength range it can penetrate regions obscured by interstellar dust and provide us with a better picture of the stars in both the solar neighborhood and the rest of the galaxy.

APOGEE consortia provide parameters for its observed stars with the APOGEE Stellar Parameter and Chemical Abundances Pipeline (ASPCAP Garcia Pérez et al. 2016). The spectroscopic parameters and chemical abundances are determined by ASPCAP in a two-step fashion. First, to derive atmospheric parameters such as $T_{\rm eff}$, $[M/H]$, and $\log g$, APOGEE observations are compared to a large library of synthetic spectra to find the spectra that best matches the observed one by interpolating different synthetic models. This library (Zamora et al. 2015) is separated into five smaller sections, for GK dwarfs, GK giants, M dwarfs, M giants, and F-type stars. Secondly, to derive the abundance of individual elements, the atmospheric parameters obtained from the best fit synthetic spectra are used to fit limited regions of the spectra dominated by spectral features associated with each given element. Afterward, $T_{\rm eff}$ and $[M/H]$ values for dwarf stars are both calibrated using independent methods to ensure their accuracy. $T_{\rm eff}$ values were calibrated by minimization of the differences between ASPCAP and photometric observations by Hernandez & Bonifacio (2009). $[M/H]$ values are internally calibrated as a function of $T_{\rm eff}$. Also, a zero-point shift is adopted to force the mean abundance ratios of all observed stars with solar metallicity to be zero. Despite finding their $\log g$ values for M dwarfs to be too low based on expectations from stellar isochrones, due to a lack of a significant number of asteroseismic calibrators available for dwarf stars, ASPCAP does not calibrate them in any way.[1]

Other available works derived stellar parameters from APOGEE spectra. These include *The Cannon* (Ness et al. 2015), which was created as a python-based method to derive parameters for giant stars. *The Cannon* uses an alternative method to derive stellar parameters, as it requires only the observed spectrum and a training sample with accurate parameters. It learns the labels (parameters) corresponding to these training stars and then determines the labels for the remaining stars after learning how the spectra are affected by each parameter. It is optimized for giant stars, and no stars in our M dwarf sample have parameters published by *The Cannon*, so we cannot compare our results directly with theirs.

There have also been investigations of M dwarf parameters using APOGEE spectra. Works like Souto et al. (2017) and Souto et al. (2018) have provided accurate parameters for small samples of planet-hosting M dwarfs. As these works use the same spectra that were used in this project and are important examples of spectroscopic M dwarf parameters derived with infrared spectra, these 3 stars will be included in the M dwarf sample analyzed in this project (see section 4.3.2).

As mentioned in Chapter 2, Rajpurohit et al. (2018b) also obtained M dwarf spectroscopic parameters by comparing APOGEE observations to BT-Settl model synthetic spectra. Spectroscopic parameters such as $T_{\rm eff}$, $[M/H]$, and $\log g$ were derived for 45 stars. Their reported errors are of 100 K for $T_{\rm eff}$, and vary between 0.2-0.5 dex for $\log g$ and 0.03-0.11 dex for $[M/H]$.

4.2 FGK star sample

Our sample consists of 3748 stars with H-band spectra from the APOGEE survey Data Release 14 (Holtzman et al. 2018). All of these stars have spectroscopic parameters derived with the APOGEE Stellar Parameter and Chemical Abundances Pipeline (ASPCAP Garcia Pérez et al. 2016). Our selection was done by selecting objects with ASPCAP $T_{\rm eff}$ values between $5500 - 6200$ K, $S/N \geq 200$ and -0.5 dex$<$ $[M/H] < 0.5$ dex. This was done to exclude stars

[1] Exact values and calibrations are available in Holtzman et al. (2018), and more information can also be consulted at the APOGEE website https://www.sdss.org/dr14/irspec/aspcap/.

with low-quality spectra and to ensure a sample both homogeneous and with parameters close to solar.

4.2.1 Sample characterization

Parallaxes, positions, and optical photometry for 3645 stars in our sample were found in the Gaia Data Release 2 (Brown et al. 2018). The large majority of the stars are located between 100 pc and 500 pc from us, with only a few reaching distances above 1 Kpc (see Fig. 4.2 (a)). Therefore, our sample, while not entirely composed of solar neighborhood stars ($d < 50\,pc$), consists of local stars. Their magnitudes in the Gaia and H-band filters are shown in Fig. 4.2 (b). Most of these objects exhibit magnitudes in the ranges of $9 < G < 13$ and $8 < H < 11$. The available Gaia distances and magnitudes confirm to us that the sample is composed of FGK dwarf stars, as any giant stars in the sample would either be brighter or further away from us. Fig. 4.2 (c) displays the distribution of the S/N of our FGK sample stars, as estimated by APOGEE. The figure confirms that most stars in our sample have $S/N > 100$. The observed sky positions of our sample stars are displayed in Fig. 4.3. As expected, most of the stars are located in the northern celestial hemisphere, given that most of the observations belong to APOGEE-N. The concentric circles represent the fields chosen by the APOGEE team for follow-up. In red, 449 stars in our sample that are a part of the Kepler Field (Latham et al. 2005) are shown.

We cross-matched our sample of stars with the exoplanet.eu database of discovered exoplanets and found that at least 33 of our stars had companions discovered orbiting around them. Most of these planet detections (30) were made with Kepler, as we analyze a large number of stars in the Kepler field. These stars are listed in table 4.1, as well as some details on the companions orbiting them. All these companions orbit closely to their host star, with periods up to 60 days, and none of them are expected to be in their star's habitable zone. Curiously, one of the companions, MARVELS-11 b, is a brown dwarf with 52 $M_{\rm Jup}$ rather than a planet. We also cross-matched our sample stars with the SWEET-Cat stellar parameter catalog for stars with exoplanets (Santos et al. 2013; Andreasen et al. 2017), finding parameters for 81 different stars. We compare our results to their published parameters in subsection 6.2.2.

Fig. 4.4 shows the distribution of ASPCAP $T_{\rm eff}$ for stars in our FGK star sample, and 4.5 displays a similar plot for the ASPCAP $[M/H]$. Most of these stars were included in the sample by filtering ASPCAP database according to our selection criteria ($5500\,K < T_{\rm eff} <$

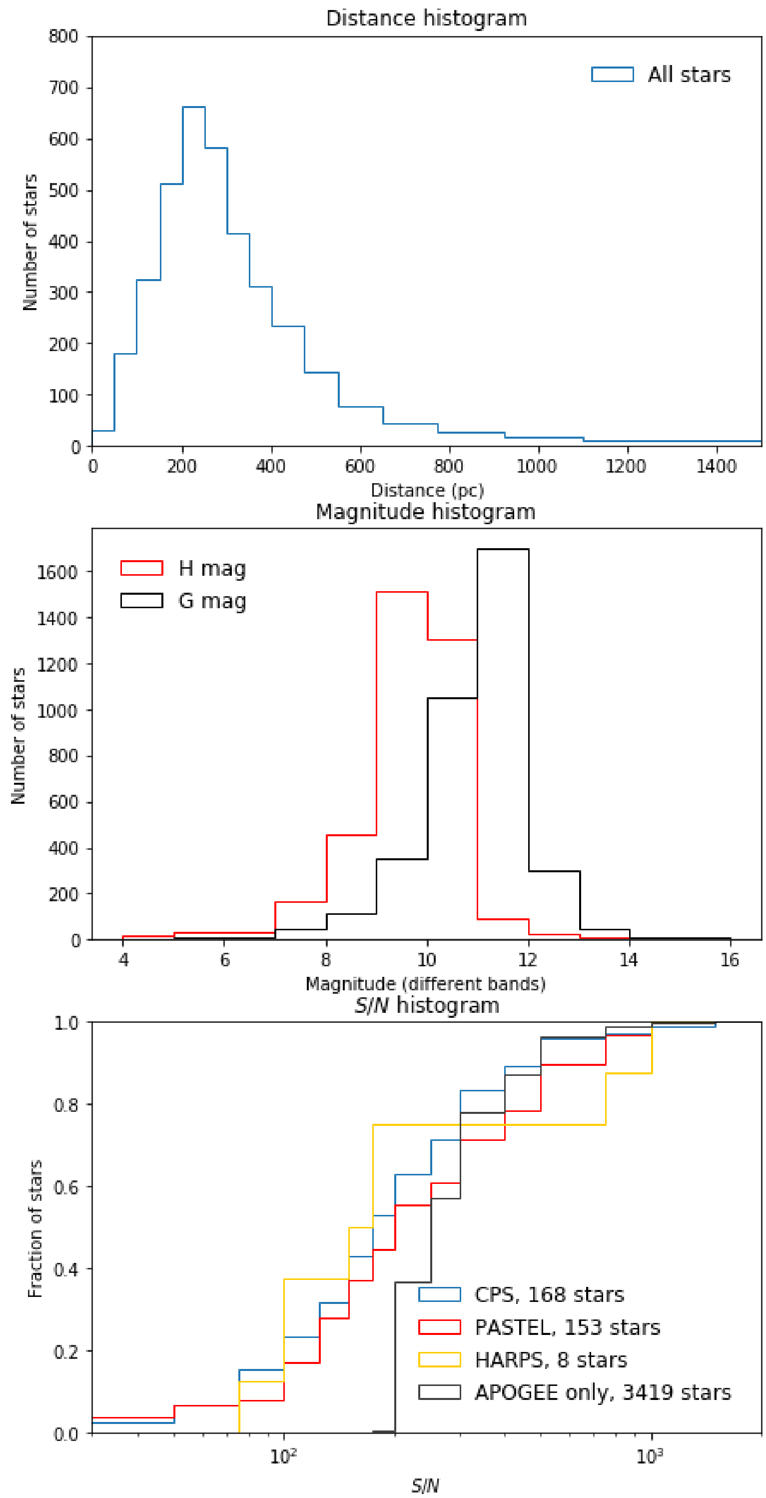

Figure 4.2: TOP (a): Histogram presenting the calculated distances to the sample stars, using Gaia Data Release 2 (Brown et al. 2018) values for the parallax. MIDDLE (b): Histogram presenting the different available magnitudes for stars in the sample. G band data comes from Brown et al. (2018); H band from APOGEE. BOTTOM (c): Cumulative histogram presenting APOGEE-published S/N of our FGK stellar sample.

Table 4.1: Planet-hosting stars in our FGK star sample and characteristics of their planets. All of them have a Confirmed status.

Star	Planet name	M ($M_{\rm Jup}$)	R ($R_{\rm Jup}$)	P (days)	a (AU)
2M13112997+1543190	MARVELS-11 b	52.1	n/a	11.6121	0.1
2M13414903-0007410	WASP-54 b	0.6	1.4	3.7	n/a
2M18575331+3954425	Kepler-1656 b	0.1529	0.4479	31.578659	0.197
2M18590868+4825236	Kepler-408 b	0.02	0.073	2.56502	n/a
2M19024305+5014286	Kepler-10 b	0.01048	0.1311	0.83749026	0.01685
2M19052120+4844387	Kepler-1349 b	n/a	0.062	2.12823928	n/a
2M19064546+3912428	Kepler-1655 b	0.0157	0.19743	11.8728787	0.103
2M19071403+4918590	TrES-2 b	1.253	1.189	2.4706133738	0.03555
2M19103720+3914394	Kepler-510 b	n/a	0.22	19.55659418	n/a
2M19140739+4056322	Kepler-131 b	0.05075	0.215	16.092	n/a
2M19162065+4133465	Kepler-92 b	0.189	0.326	13.748933	n/a
2M19215883+3847437	Kepler-135 b	n/a	0.161	6.00253	0.067
2M19220642+3808347	Kepler-1063 b	n/a	0.133	14.07971466	n/a
2M19224155+3841276	Kepler-198 b	n/a	0.252	17.790037	0.131
2M19233232+3803272	Kepler-773 b	n/a	0.128	3.74910006	n/a
2M19240457+3832440	Kepler-795 b	n/a	0.15	29.6193421	n/a
2M19240775+4902249	Kepler-68 b	0.0188	0.206	5.3987533	0.0617
2M19253173+3807388	Kepler-323 b	n/a	0.128	1.678327	0.028
2M19253263+4159249	Kepler-100 b	0.0231	0.1164	6.887037	n/a
2M19254165+3812597	Kepler-772 b	n/a	0.162	12.99207337	n/a
2M19262571+3824374	Kepler-376 b	n/a	0.095	4.920199	0.057
2M19284793+4202459	Kepler-1365 b	n/a	0.082	7.69993485	n/a
2M19310830+4312575	Kepler-1560 b	n/a	0.079	3.03195744	n/a
2M19312934+4605559	Kepler-1323 b	n/a	0.136	0.92990668	n/a
2M19322256+4253471	Kepler-986 b	n/a	0.211	56.4349938	n/a
2M19324327+4137039	Kepler-520 b	n/a	0.148	19.67416124	n/a
2M19344207+4117432	Kepler-517 b	n/a	0.238	60.92832271	n/a
2M19345420+4714493	Kepler-1199 b	n/a	0.103	15.0447198	n/a
2M19345587+4154030	Kepler-449 b	n/a	0.1834	12.58242	n/a
2M19391944+4639345	Kepler-1391 b	n/a	0.15	54.4092333	n/a
2M19393877+4629292	Kepler-1169 b	n/a	0.084	6.11009134	n/a
2M19395364+4512492	Kepler-215 b	n/a	0.145	9.360672	0.084
2M19481670+4031304	Kepler-96 b	0.027	0.238	16.2385	n/a

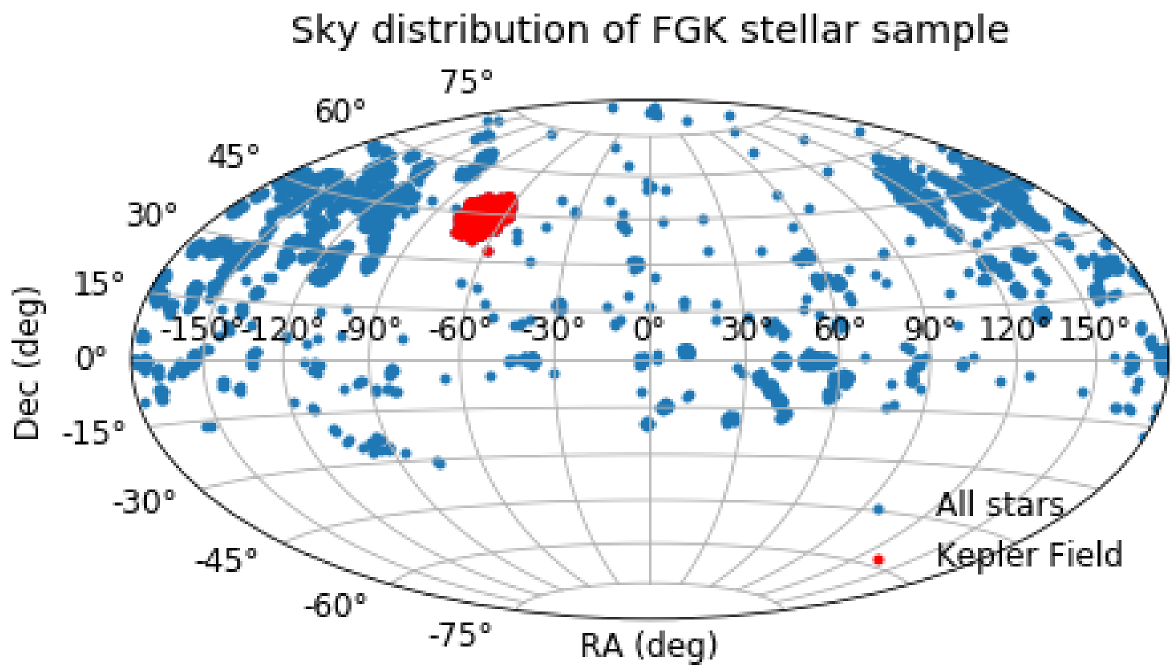

Figure 4.3: Map showing the location in the sky (Right Ascension and Declination) of our sample stars. Kepler target field is highlighted in red.

$6200\,$K, $S/N \geq 200$ and $-0.5\,$dex$< [M/H] < 0.5\,$dex). Therefore, the shape of their parameter distribution is expected. The additional stars found with $T_{\text{eff}} < 5500\,$K or $[M/H] < -0.5\,$dex come from the comparison sub-samples, detailed in section 4.2.2.

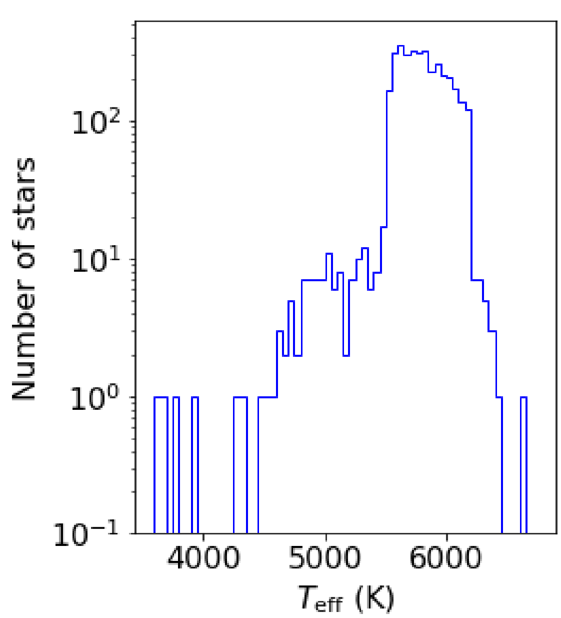

Figure 4.4: Histogram showing the ASPCAP T_{eff} distribution for stars in the sample, in $\log$ scale.

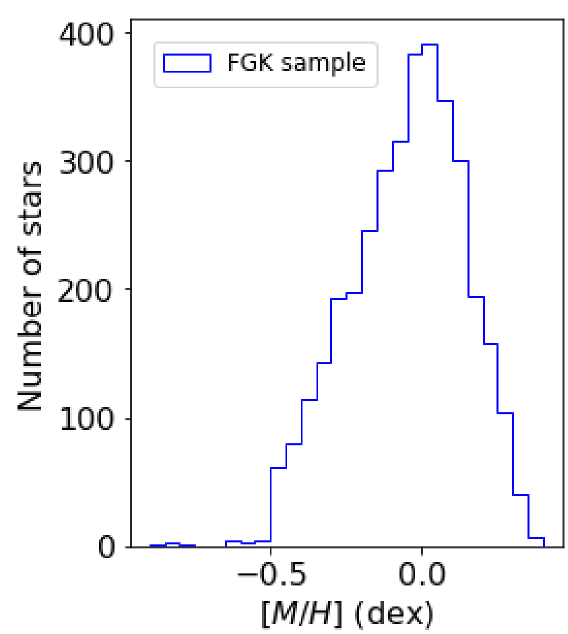

Figure 4.5: Histogram showing the ASPCAP $[M/H]$ distribution for stars in the sample.

4.2.2 Comparison Sub-samples

We selected three works in the literature, with derived stellar parameters of FGK dwarfs from medium to high-resolution spectra, that have analyzed stars in APOGEE. Despite there being other large-scale studies providing parameters for FGK stars from high-resolution optical spectra, such as Guo et al. (2017), these three works had the largest number of stars in common with APOGEE, so they were selected. Stars in common with these surveys were included in our sample, even if they did not meet our initial selection criteria ($5500\,K < T_{\rm eff} < 6200$ K, $S/N \geq 200$ and -0.5 dex$< [M/H] < 0.5$ dex).

The California Planet Survey (Brewer et al. 2016, , hereby referred to as CPS) used data from the HIRES spectrograph ($R \sim 70\,000$) at the Keck Observatory. The stellar parameters were obtained with the semi-automated procedure SME (Valenti & Piskunov 1996), where the observed spectra were fitted iteratively with synthetic spectra from 1D local thermodynamic equilibrium (LTE) plane-parallel MARCS atmosphere models. CPS provides rotational velocities and abundances for 15 elements, as well. The reported precisions are of 25 K for $T_{\rm eff}$, 0.01 dex for $[M/H]$ and 0.028 dex for $\log g$. One-hundred and sixty-eight stars in our sample are found in the CPS catalog.

The PASTEL catalog (Soubiran et al. 2016) is a compilation of spectroscopic parameters from high-resolution ($R \geq 25000$) spectra with $S/N \geq 50$. It contains results from different sources in the literature that derived stellar parameters with model atmospheres, with some examples including studies of low metallicity stars such as Bonifacio et al. (2012) and high-resolution chemical analysis of solar-type stars like Ford et al. (2005). The reported uncertainties vary, with median errors of $\sim 1.1\%$ for the $T_{\rm eff}$ (~ 65 K for a sun-like star), ~ 0.06 dex for $[Fe/H]$ and 0.10 dex for $\log g$. A total of 157 stars in our sample are found in the PASTEL catalog. However, as 4 of these stars are also found in CPS, only 153 stars were considered as the PASTEL comparison sample.

Delgado Mena et al. (2017) revised the spectroscopic parameters and abundances of 1111 FGK dwarf stars of the High Accuracy Radial velocity Planet Searcher Guaranteed Time Observations (HARPS-GTO) Pepe et al. (2000) planet search program (Pepe et al. 2011). The EW method was used on HARPS $R \sim 115\,000$ spectra for parameter and abundance determinations. Their average cited internal errors are 24 K for $T_{\rm eff}$, 0.02 dex for $[M/H]$ and 0.03 dex for $\log g$ for stars close to solar $T_{\rm eff}$. Given that the HARPS-GTO planet survey concentrates on bright inactive stars, only 8 stars of our sample are part of Delgado Mena et al. (2017).

4.3 M dwarf sample

All stars chosen are part of APOGEE's ancillary M dwarf program. Their targets are drawn primarily from two sources, the LSPM-North catalog of nearby stars, Lépine & Shara (2005), and the Lépine & Gaidos (2011) catalog of nearby M dwarfs by Lépine and Gaidos, mentioned in section 2.2. These are both proper-motion selected catalogs, and some of them are known planet hosts and have previous rotational speed, metallicity, or radial velocity estimates. Zasowski et al. (2013) shows the full details of this selection. Although Deshpande et al. (2013) published rotational velocities for these stars, the strong H_2O bands found in the spectra prevented them from providing stellar parameters for all stars in the sample. The stellar sample of over 1200 stars was filtered by S/N to arrive at the final sample shown in this thesis, and the S/N distribution of this final sample (as reported by APOGEE) is available in Fig. 4.6 (c). A total of 250 stellar spectra were synthesized, ranging from early to late M dwarfs. We kept our sample at this size because it both provided us with enough stars to perform a statistical analysis and was not so large that the time for the computational analysis became unpractical.

4.3.1 Sample Characterization

Of the 250 M dwarfs studied, data for 238 of them is available within Gaia Data Release 2 (Brown et al. 2018). In this section, we take a closer look at the available parameters for those stars, such as sky coordinates, distance to the Sun and photometric magnitudes.

Fig. 4.6 (a) shows the estimated distance to our sample stars. As the figure shows, almost all of them are within 100 pc of the Sun, and are therefore part of the solar neighborhood. Comparing with Fig. 4.2 (a), displaying the estimated distances to our FGK star sample, it is clear that the M dwarfs are much closer than them. This is explained by the fact that M dwarfs are intrinsically dimmer than solar-type stars, and therefore must be closer for us to observe them.

In Fig. 4.6 (b) the magnitude distribution of M dwarfs in this sample is plotted. Both G (from Brown et al. 2018) and H magnitudes (from APOGEE data) are shown. This figure, in conjunction with Fig. 4.6 (a), shows how most stars in the sample are rather uniform in both magnitude and distance to the Sun. As our sample selection is done based on S/N, it focuses

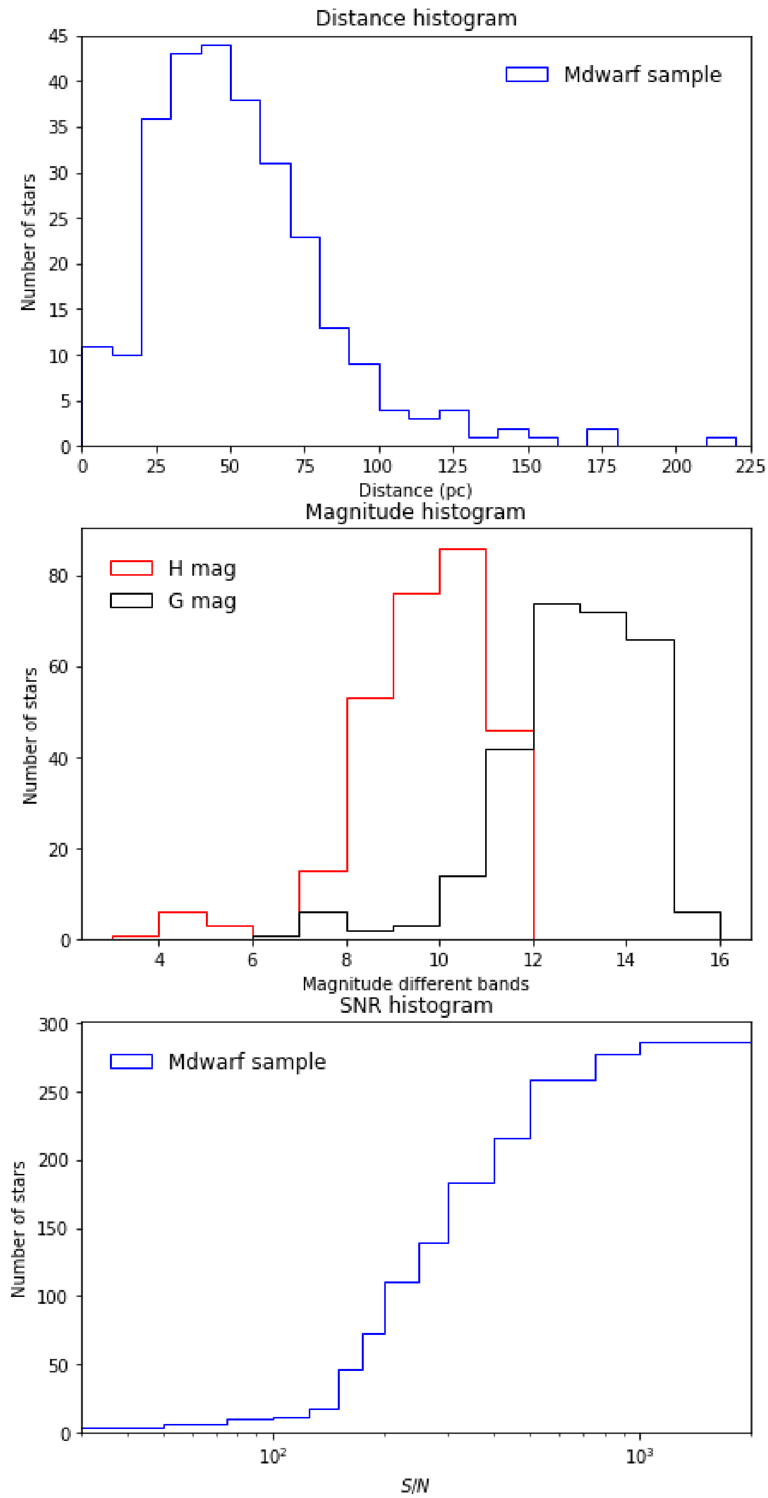

Figure 4.6: TOP (a): Histogram presenting the calculated distances to the M dwarf sample stars, using Bailer Jones et al. (Bailer-Jones et al. 2018) values calculated from Gaia DR2 data for the distance. MIDDLE (b): Histogram presenting the different available magnitudes for stars in the sample. G band data comes from Brown et al. (2018); H band from APOGEE. BOTTOM (c): Cumulative histogram presenting APOGEE-published S/N of our M dwarf stellar sample.

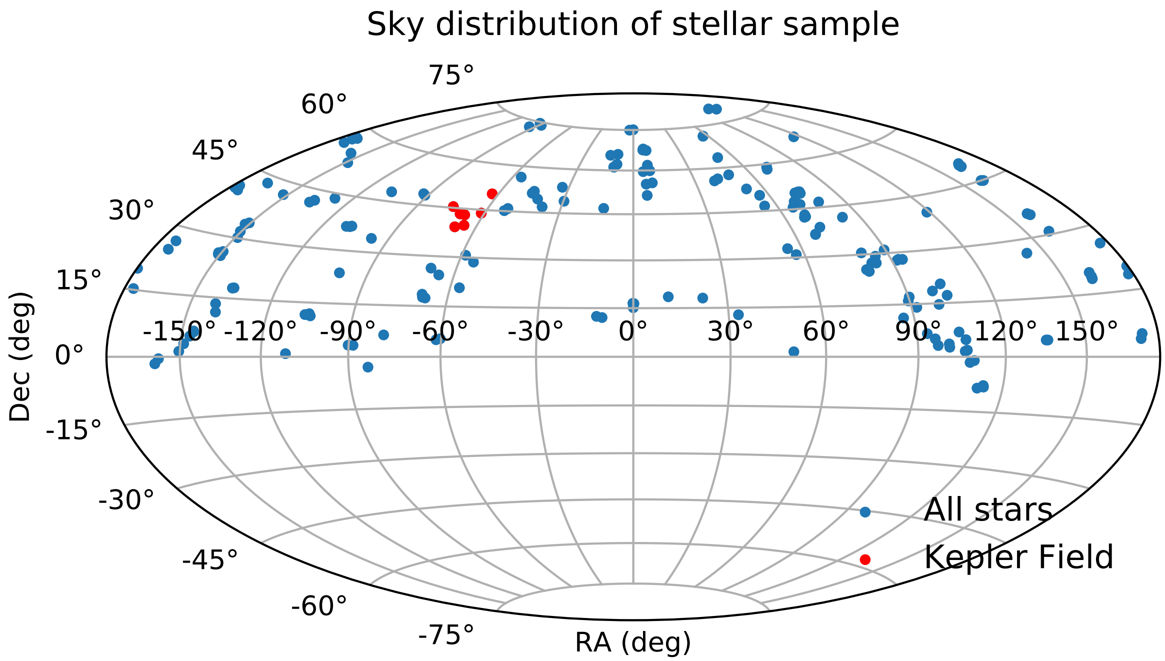

Figure 4.7: Map showing the location in the sky of our sample M dwarfs. Kepler target field is highlighted in red.

on the brightest M dwarfs observed by APOGEE. It is therefore natural that most stars in the sample will be close to the sun, and around the same distance.

Fig. 4.7 maps the location in the sky of all M dwarfs in this sample, showing both Right Ascension (RA) and Declination (Dec). Most of the stars are located in the northern hemisphere ($Dec > 0$ deg), as they were observed by APOGEE-2N. We also highlight 7 stars in our sample that are part of the Kepler field (Latham et al. 2005) and have been observed by the Kepler Space telescope.

4.3.2 Available M dwarf literature parameters

This section is focused on works that have characterized stars in our sample. For other works in the literature that have characterized M dwarfs in general, take a look at Section 2.1.

ASPCAP, the pipeline dedicated to derivation of spectroscopic parameters for stars observed with APOGEE, publishes spectroscopical parameters for stars observed with it. Their parameter ranges don't include all M dwarfs, as its published T_{eff} are all above 3500 K. They only calibrate $\log g$ values below 3.5 dex as well. Nevertheless, their values are an important reference that can be compared to our results. More extensive analysis of ASPCAP parameters and whether or not they are reliable for stars other than giants is available in section

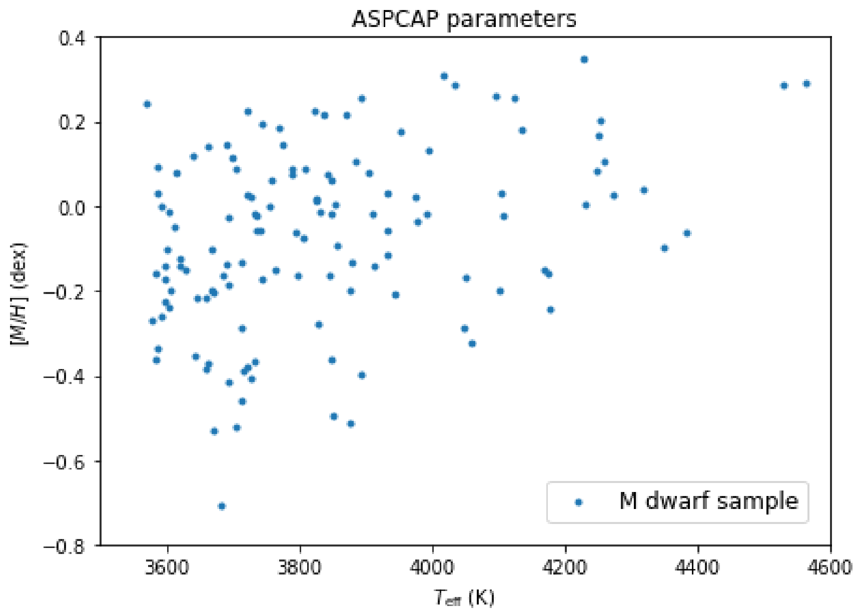

Figure 4.8: ASPCAP $T_{\rm eff}$ and $[M/H]$ values for M dwarfs in sample.

6.2.1. In addition to these results, other works have analyzed and commented on ASPCAP parameters for M dwarfs. Schmidt et al. (2016) performed an extensive analysis on both the $T_{\rm eff}$ and $[M/H]$ values ASPCAP produced for 3834 M dwarfs, comparing them to photometric and interferometric parameters for the same stars, and concluded that the ASPCAP $T_{\rm eff}$ is accurate to about $100\,{\rm K}$ for stars between 3550–4200 K, and $[M/H]$ values are accurate to about $0.18\,{\rm dex}$. This means that, despite ASPCAP's main focus being on giant stars and not M dwarfs, we can take their results as reasonable measures for the parameters of M dwarfs in our sample. Given that, we made a few plots detailing ASPCAP parameters for the M dwarf sample.

Our full stellar sample contains 250 stars. ASPCAP has published calibrated $[M/H]$ for 215 stars, and $T_{\rm eff}$ for 127 stars. They have additional uncalibrated parameters published for the other stars in the sample, but we will consider only calibrated values for comparison here for uniformity reasons. These values are plotted in Fig. 4.8, and displayed in histograms in Figs. 4.9 and 4.10. The figures shows that, for stars in our sample with ASPCAP values, their $T_{\rm eff}$ is concentrated around 3600-4000 K, and $[M/H]$ between -0.4 and +0.4 dex. The metallicity distribution follows an approximately Gaussian shape, with an average value of -0.07 dex and a standard distribution of 0.21 dex. This means that a significant fraction of stars in our sample are early M dwarfs, rather than later, and are, on average, around solar metallicity. It should

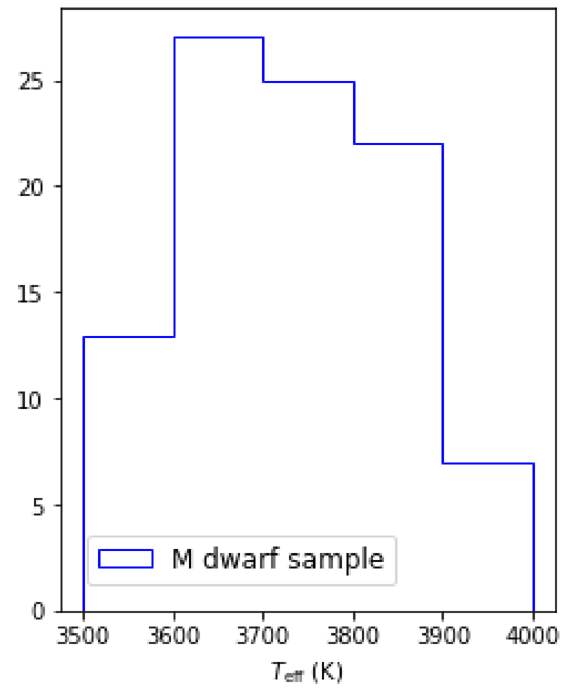

Figure 4.9: Histogram showing the ASPCAP $T_{\rm eff}$ distribution for stars in the M dwarf sample.

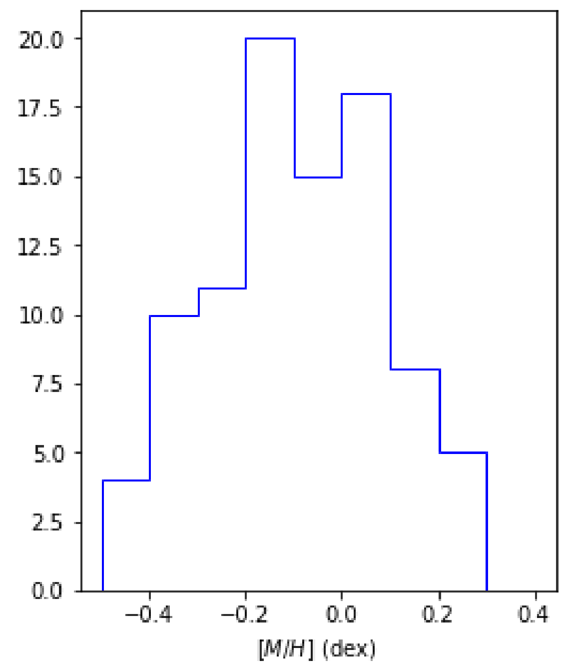

Figure 4.10: Histogram showing the ASPCAP $[M/H]$ distribution for M dwarfs in the sample.

still be noted that ASPCAP provided $T_{\rm eff}$ for less than half the stars in the sample, and the parameter distribution for the full sample could differ from the plotted one.

Compared to solar-type stars, we do not find as much analysis and parameter estimation for our sample M dwarfs in the literature. Nevertheless, independent spectroscopical analysis is available for some M dwarfs observed by APOGEE, and we include it in this section.

Some of the best-characterized stars in our sample are the M dwarfs analyzed by Souto et al. (2017) and Souto et al. (2018). These works use spectral synthesis and a combination of MARCS and PHOENIX model atmospheres to perform their analysis. Both stellar parameters and chemical abundances for 8 different elements were published for 3 different M dwarfs - Kepler 138, Kepler 186 and Ross 128. 2M19213157+4317347 (Kepler-138) has 2 confirmed exoplanet detections by Jontof-Hutter et al. (2015), with one of them being Mars-sized; 2M19543665+4357180 (Kepler-186) has 5 confirmed exoplanets, with one of them being an Earth-sized planet in the star's habitable zone (Quintana et al. 2014); 2M11474440+0048164 (Ross 128) has a confirmed exoplanet in its habitable zone as well Bonfils et al. (2018). The parameters they derived for these stars are included in table 4.2 and will be taken as reference values for our analysis of them.

Table 4.2: Parameters derived by Souto et al. (2017) and Souto et al. (2018) for the stars Kepler-138 (2M19213157+4317347), Kepler-186 (2M19543665+4357180) and Ross 128 (2M11474440+0048164).

Star	$T_{\rm eff} \pm \Delta T_{\rm eff}$	$\log g \pm \Delta \log g$	$[Fe/H] \pm \Delta[Fe/H]$	Source
Kepler-138	3835 ± 64 K	4.64 ± 0.10 dex	-0.09 ± 0.09 dex	Souto et al. (2017)
Kepler-186	3852 ± 64 K	4.73 ± 0.10 dex	-0.08 ± 0.10 dex	Souto et al. (2017)
Ross 128	3231 ± 100 K	4.96 ± 0.11 dex	0.03 ± 0.09 dex	Souto et al. (2018)

In addition to these 3 planet-hosting M dwarfs, an additional star in our stellar sample has had a detected planet orbiting around it. This star is Kepler-210, or 2M19300081+4304593, an M0 dwarf that has been characterized by Muirhead et al. (2012), with measured parameters of $T_{\rm eff} = 3914$ K and $[Fe/H] = -0.12$ dex, and by Frasca et al. (2016) with $T_{\rm eff} = 4933$ K, $\log g = 3.96$ dex $[Fe/H] = -0.23$ dex. LAMOST (Cui et al. 2012) was used to observe optical wavelength spectra with $R \sim 1800$, and ROTFIT to derive parameters from them with the help of Indo US library of real and homogeneous spectra. There are two confirmed exoplanets around this star (Ford et al. 2011) and a third one awaiting confirmation (Ioannidis et al. 2014). No other star in our M dwarf sample has had any detected companions so far.

As mentioned in Section 2, Gaidos et al. (2014), Terrien et al. (2015), and Lindgren & Heiter (2017) observed M dwarf spectra and determined spectroscopic parameters from them. From the 2970 stars observed by Gaidos et al. (2014), 170 have also been observed by APOGEE, meaning that their parameters can be used as a literature comparison against the ones derived by our pipeline. From these 170 stars, 22 are included in our sample, and their parameters are shown in Fig. 4.11. Their parameters were derived using optical spectra with $R \sim 1000$. The reduced number of stars, combined with the lack of $[Fe/H]$ available for half the stars in the sample, does not allow for an extensive statistical analysis of this stellar subsample. Nevertheless, it is possible to notice Gaidos et al. (2014) published $T_{\rm eff}$ values between 3100-3500 K for a greater number of stars in this subsample than in the main ASPCAP one. Gaidos et al. (2014) also published lower metallicity ($-0.6 < [Fe/H] < -0.4$ dex) values for a greater number of stars in our sample than ASPCAP.

One-hundred and seventy-three stars in the 714 M dwarf sample characterized by Gilhool et al. (2017) are present in our sample as well. The remaining stars were excluded due to low S/N. As mentioned in section 2, this study matches template spectra to observed APOGEE spectra before deriving their rotational velocity. The low parameter space resolution limits the output $[M/H]$ and $\log g$ of our sample stars to only three values each (-0.5 dex, 0.0 dex, $+0.5$ dex, and 4.5 dex, 5.0 dex and 5.5 dex for $[M/H]$ and $\log g$, respectively). This severely

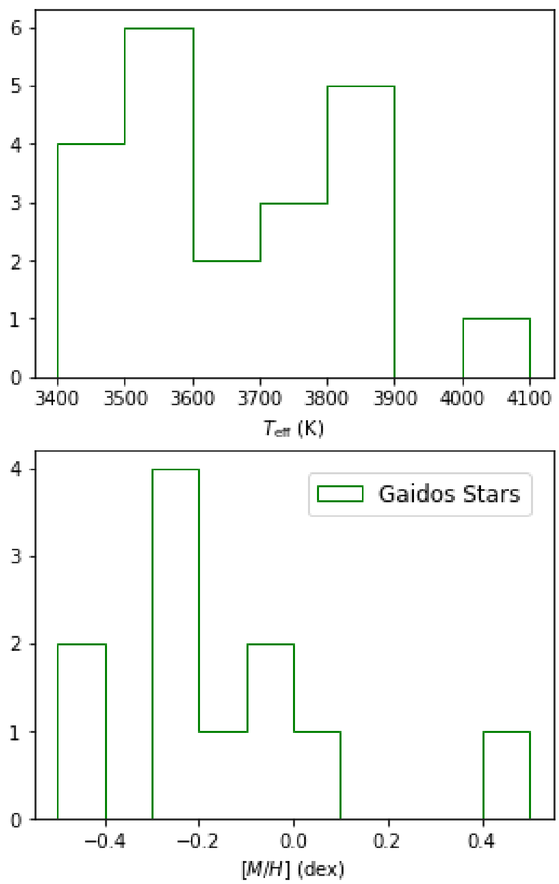

Figure 4.11: $T_{\rm eff}$ and $[M/H]$ values from Gaidos et al. (2014) for M dwarfs in sample. $T_{\rm eff}$ are included for 22 stars, while $[M/H]$ values are only available for 12 stars.

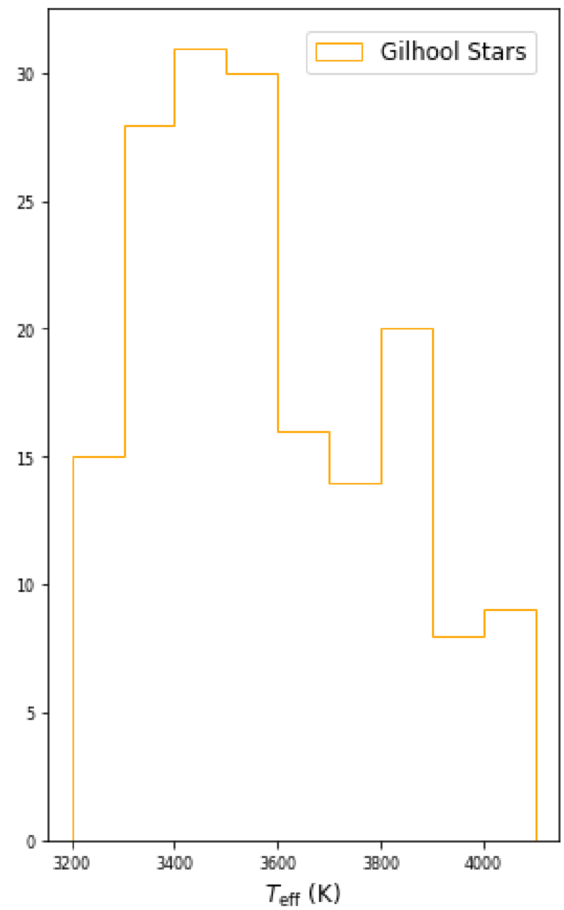

Figure 4.12: $T_{\rm eff}$ values from Gilhool et al. (2017) for 173 M dwarfs in common between our sample and the one studied by them.

limits the usefulness of these values, as they are well below the expected precision of our method. Therefore, we will consider only their output $T_{\rm eff}$, which has a more reasonable 100 K resolution. Fig. 4.12 displays the $T_{\rm eff}$ and $[M/H]$ distribution of all stars in common between both samples. The subsample has more low-temperature stars than the ones characterized only by ASPCAP (Fig. 4.8).

The main goal of Gilhool et al. (2017) was to derive $v \sin i$ for M dwarfs. Their stated detection limit for the measurement of this parameter is $v \sin i = 8$ km/s. This means that the minimum rotational velocity published for any star in their sample is 8 km/s. Among all 173 stars in common between our sample and Gilhool et al. (2017)'s, they estimated $v \sin i = 8$ km/s for 170 of them, and $v \sin i < 9$ km/s for the other 3 stars. Therefore, we can conclude from their results that all stars in our sample rotate slowly, with the exact values for their rotational velocity being below the precision level of Gilhool et al. (2017)'s analysis.

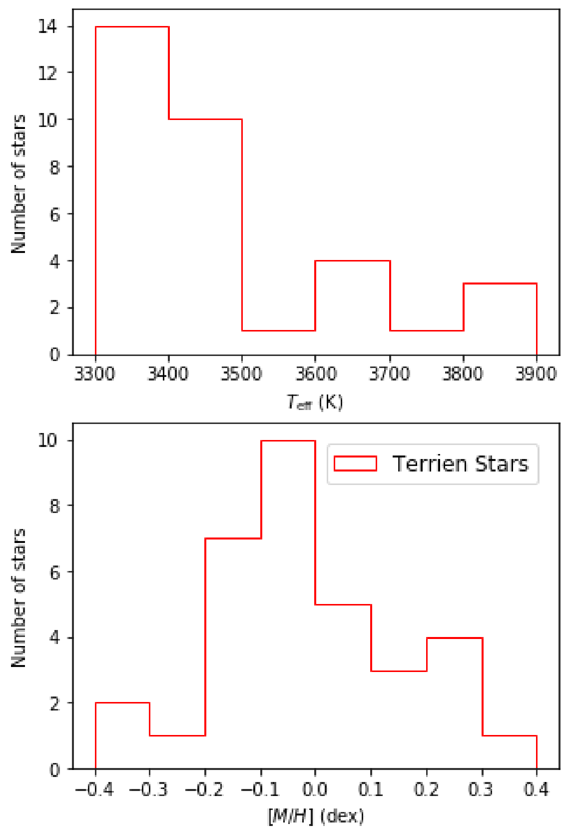

Figure 4.13: $T_{\rm eff}$ and $[M/H]$ values from Terrien et al. (2015) for 33 M dwarfs in sample.

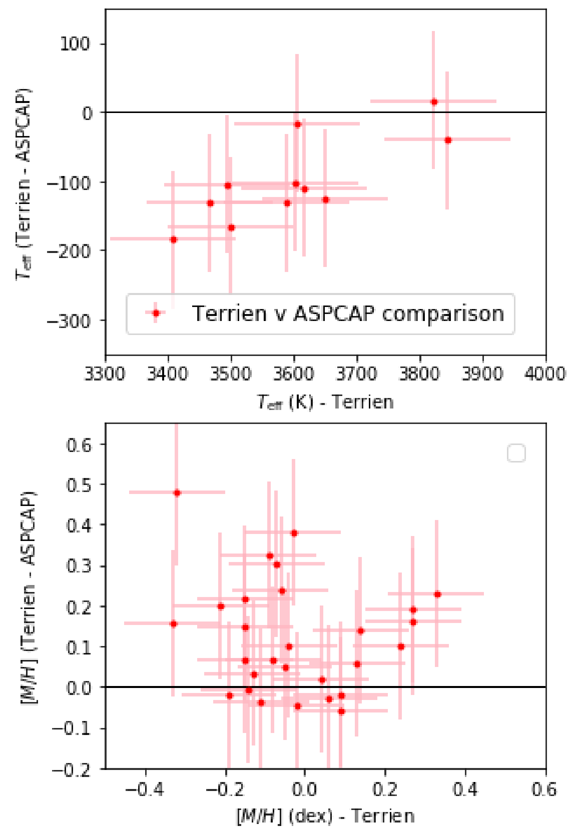

Figure 4.14: Direct comparison of $T_{\rm eff}$ and $[M/H]$ values from Terrien et al. (2015) and from ASPCAP for M dwarfs in sample. Errors included are of 100 K in $T_{\rm eff}$ and 0.18 dex for ASPCAP and 0.12 dex for Terrien (values from Schmidt et al. (2016) and Terrien et al. (2015))

From the 886 stars in Terrien et al. (2015), 200 were also observed by APOGEE, so parameters determined by them can also be used to have an approximate idea on the expected parameters for our sample stars. Their spectra have a wide wavelength coverage $(0.8-2.4\,\mu\mathrm{m})$ but low resolution $(R \sim 2000)$. Their $T_{\rm eff}$ values are determined by analysis of water indices in the K band and have uncertainties above 100 K, and their $[M/H]$ values are measured using empirical spectroscopical calibrations with uncertainties around 0.12 dex. From the 200 stars observed by Terrien et al. (2015) and APOGEE, 39 are included in our sample. We discarded the rest of the sample due to low S/N. The published parameters for the 39 analyzed stars are shown in Fig. 4.13. Comparing their parameter distribution with the full ASPCAP sample, we find that Terrien et al. (2015) published $T_{\rm eff}$ around 3200-3500 K for a significantly higher number of stars. The metallicity distribution of stars in our sample as published by Terrien et al. (2015) is also skewed towards higher values, with a Gaussian fit having an average

Table 4.3: Parameters derived by Rajpurohit et al. (2018b) for stars in common

Star	$T_{\rm eff} \pm \Delta T_{\rm eff}$	$\log g \pm \Delta \log g$	$[Fe/H] \pm \Delta[Fe/H]$
2M00350487+5953079	3100 ± 100 K	5.5 ± 0.3 dex	0.0 ± 0.05 dex
2M03152943+5751330	3200 ± 100 K	5.5 ± 0.3 dex	-0.3 ± 0.05 dex
2M04125880+5236421	3100 ± 100 K	5.5 ± 0.3 dex	0.0 ± 0.05 dex
2M06320207+3431132	3200 ± 100 K	5.5 ± 0.3 dex	-0.4 ± 0.05 dex
2M09301445+2630250	3300 ± 100 K	5.0 ± 0.5 dex	-0.3 ± 0.05 dex
2M11091225-0436249	3900 ± 100 K	4.5 ± 0.5 dex	-0.3 ± 0.04 dex
2M18451027+0620158	3900 ± 100 K	4.5 ± 0.5 dex	-0.4 ± 0.04 dex
2M18562628+4622532	3100 ± 100 K	5.5 ± 0.3 dex	0.0 ± 0.05 dex

Table 4.4: Parameters derived by Rajpurohit et al. (2018a) for stars in common

Star	$T_{\rm eff} \pm \Delta T_{\rm eff}$	$\log g \pm \Delta \log g$	$[Fe/H] \pm \Delta[Fe/H]$
2M03212176+7958022	3500 ± 100 K	5.00 ± 0.10 dex	-0.4 ± 0.10 dex
2M06421118+0334527	3500 ± 100 K	5.1 ± 0.10 dex	0.0 ± 0.10 dex
2M07581269+4118134	3300 ± 100 K	5.0 ± 0.10 dex	$+0.3 \pm 0.10$ dex
2M11474440+0048164	3500 ± 100 K	5.0 ± 0.10 dex	0.0 ± 0.10 dex

of 0.06 dex and a standard deviation of 0.24 dex. Due to these discrepancies, the published values of ASPCAP and (Terrien et al. 2015) for the same stars are directly compared in Fig. 4.14. The comparison shows an approximately constant trend of Terrien et al. (2015)'s work providing values for $T_{\rm eff}$ below ASPCAP, with an average difference of -94 K. In the case of $[M/H]$, Terrien et al. (2015)'s values are above the ones of ASPCAP, with an average difference of 0.11 dex. These two plots show trends that should be taken into consideration when comparing our method's results with either of these literature analyses.

We have 8 stars in common with the previous work Rajpurohit et al. (2018b) that matched APOGEE spectra of 45 M dwarfs with BT-Settl model spectra. The parameters for these stars are listed in Table 4.3. 6 of these stars have $T_{\rm eff} < 3300$ K, being some of the coldest stars in our sample. Despite their high reported precision errors when compared to some other available literature values, especially for $\log g$, it is important to have independent measurements for stars within this region of our parameter space.

We also find 4 stars in common between our sample and the one characterized by Rajpurohit et al. (2018a), matching CARMENES high-resolution spectra with BT-Settl model spectra. These stars are listed in Table 4.4.

Unfortunately, unlike FGK stars, there are no available high-resolution large scale studies of spectroscopical parameters for M dwarfs observed by APOGEE. The best spectroscopic parameters available in the literature for our sample stars are the ones cited in this section and

ASPCAP values. Therefore, comparisons between our results and literature values are made against the works mentioned above.

Chapter 5

Technique

In this chapter, we go over the full methodology used to derive stellar parameters for the samples of stars. The chapter is divided into five sections. The first section contains a description of *iSpec*, the python shell used to control the synthetic spectra generator codes used in this project. The second section contains all steps of the methodology that apply to both FGK and M dwarfs. These include in subsection 5.2.1 the spectra download and format conversion, the choice of code to synthesize spectra in subsection 5.2.2, the solar abundances used in the syntheses in subsection 5.2.3, details on the minimization procedure used by *iSpec* in subsection 5.2.4, and the free parameters included in the syntheses in subsection 5.2.5. The third section contains details about the specific steps of the process (normalization in subsection 5.2.6, the line list creation in subsection 5.2.7 and line mask in subsection 5.2.8) that are applied to FGK stars. The fourth section details the necessary changes and extra steps necessary for the synthesis of M dwarf spectra. Finally, the last section, 5.3, contains an example of the method being used to derive parameters for a solar spectrum, demonstrating possible results it can derive.

5.1 *iSpec*

iSpec is a multi-purpose python-based tool, designed to derive atmospheric parameters from stellar spectra through different methods by Blanco-Cuaresma et al. (2013). It has been used for multiple purposes so far, including analysis of the impact of stellar atmospheric parameter uncertainties on exoplanet studies (Blanco-Cuaresma 2017), to perform spectroscopic analyses of multiple stellar samples (Hełminiak et al. 2019; Polińska et al. 2018), to predict red

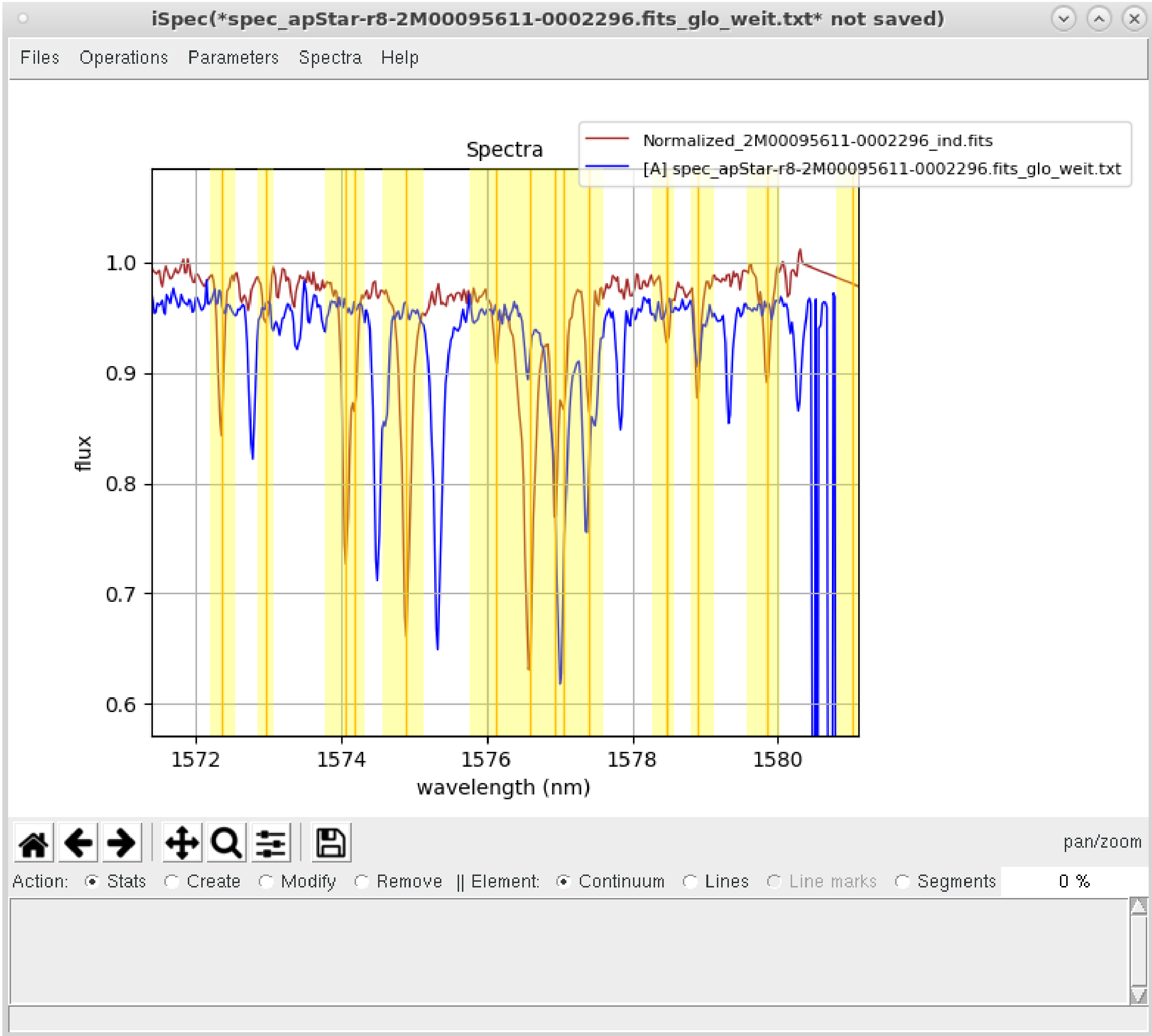

Figure 5.1: An example of *iSpec*'s graphic user interface, showing two spectra of the same star, one normalized and in vacuum wavelength and the other non-normalized and in air wavelength. The yellow areas represent the linemask used in the normalization process for FGK stars.

nova outbursts (Molnar et al. 2017), and to test chemical tagging with open clusters (Blanco-Cuaresma et al. 2015). *iSpec* allows for multiple operations with spectra, including normalizations, divisions, parameter determination, S/N estimation, among others. It has a very versatile graphic user interface (GUI) that allows the user to perform many of these tasks on-the-fly as well (see Fig. 5.1), and it can be fully controlled using python scripts as well.

iSpec has multiple spectrum synthesizing codes integrated within its distribution, including the ones mentioned in section 3.2.2 (*Turbospectrum*, *SPECTRUM*, *SYNTHE*, *MOOG* and *SME*). These codes can provide multiple ways to generate synthetic spectra, and differ in performance and accuracy. These differences and biases have been studied in detail in Blanco-

Cuaresma (2019), where the codes mentioned above were compared for both the EW method and synthetic spectral fitting techniques. These discrepancies can be minimized by selecting the best spectral regions to analyze and having a uniform method for the analysis, which might not be possible for all scientific cases. Blanco-Cuaresma (2019) also concluded that *iSpec* parameters derived using these two methods have large differences that are a result of the intrinsic differences between the methods. Therefore, it is important to know and test the qualities and limitations of each available code before running a spectral synthesis analysis with *iSpec*. *iSpec* also includes multiple stellar models available for the user, such as the ATLAS and MARCS models described in section 3.2.2. Also, multiple solar abundances and line lists are pre-programmed and available for use. This allows for extensive customization of the synthesis and gives the user very high degrees of freedom to optimize their pipeline to obtain the best parameters from their spectra. However, and as shown in the referenced article, careful analysis is needed to confirm the best combination of code, stellar model and line list for each scientific case. These tests and comparisons for our sample stars and spectral region are shown in section 5.2.2.

All these features and customizable options make *iSpec* a great option for synthesizing spectra and deriving parameters, so it was chosen as the primary tool for this project.

5.2 Steps in common for FGKM stars

The steps mentioned in this section are applied for every star analyzed by our pipeline, including both FGK and M dwarfs. The steps and methods specific to FGK dwarfs are noted when necessary.

5.2.1 Spectra Download and format conversion

In all URLs mentioned in this section, to have some brevity, [APOGEE] is a shorthand for `https://data.sdss.org/sas/dr14/apogee/spectro/redux/`. All spectra used in this project and shown in this thesis comes from APOGEE DR 14 unless noted otherwise. In order to obtain it and use it for parameter derivation, our selection is performed using the table "allStar-l31c.2.fits", available for download from `[APOGEE]/r8/allStar-l31c.2.fits` This table contains information about all stars observed by APOGEE so far and is a great resource to have when performing any selection of stars to analyze.

Table 5.1: Example of spectrum in *iSpec* format (excerpt)

waveobs	flux	err
1672.42	4184.44	6.45112
1672.45	4344.43	6.57664
1672.47	4412.36	6.68168
1672.49	4405.05	6.73257
1672.51	4359.27	6.78558
1672.54	4332.2	6.79397

The spectra of the stars themselves can be downloaded individually and directly using URLs such as `[APOGEE]/r8/stars/apo25m/2247/apStar-r8-2M21285852+0023158.fits`, where dr14 is the Data Release used, 2247 is the field the star is in (obtainable through table described above), and the APOGEE ID of the star itself is 2M21285852+0023158. Downloading this object results in a fits file containing up to two combined spectra, created in different ways, as well as the individual visit spectra. The available final spectra are created by combining the spectra observed in the individual visits using two different methods, either a pixel-by-pixel (individual) or a visit-by-visit (global) weighting. We found the individual weighting to produce better results, so all analysis uses these spectra instead of the global weighting.

The individual combined spectra are then extracted from the fits file, and converted into *iSpec* txt format (see example in table 5.1), with columns for wavelength, flux, and error across the whole spectrum. These spectra are not normalized.

5.2.2 Code Choice

Our method relies on using *iSpec* for the creation of synthetic spectra and matching them to observations, over a selection of different chosen areas. The first step needed for this is choosing the best available code for synthetic spectra generation. As mentioned in section 3.2.2, there are several different codes available for this task - *MOOG*, *SYNTHE*, *SPECTRUM*, and *Turbospectrum*. All codes mentioned are available within *iSpec*. To ascertain the code best suited for the parameter determination algorithm, it was necessary to compare the different radiative transfer codes. *MOOG* was excluded, as synthesizing spectra with the available line list lead to *iSpec* repeatedly crashing. This left three codes to be compared, *SYNTHE*, *SPECTRUM*, and *Turbospectrum*.

We decided to test *iSpec* using the various available codes to conclude which one was best suited for the task. This was done by synthesizing a solar spectrum with each of the

Table 5.2: Parameters derived for the sun with 3 different codes, and time required for each code. All syntheses are made using the VALD line list available within the default *iSpec* distribution, and our custom line mask (see section 5.2.8).

Code	$T_{\rm eff}$	$\log g$	$[M/H]$	Time
SYNTHE	$5973\,\mathrm{K}$	$5.33\,\mathrm{dex}$	$-0.08\,\mathrm{dex}$	$52\,\mathrm{min}$
SPECTRUM	$5926\,\mathrm{K}$	$5.27\,\mathrm{dex}$	$-0.15\,\mathrm{dex}$	$27\,\mathrm{min}$
Turbospectrum	$5921\,\mathrm{K}$	$4.54\,\mathrm{dex}$	$-0.09\,\mathrm{dex}$	$31\,\mathrm{min}$

three tested codes and both comparing the output spectra with the available solar one and the output parameters with the reference literature solar parameters.

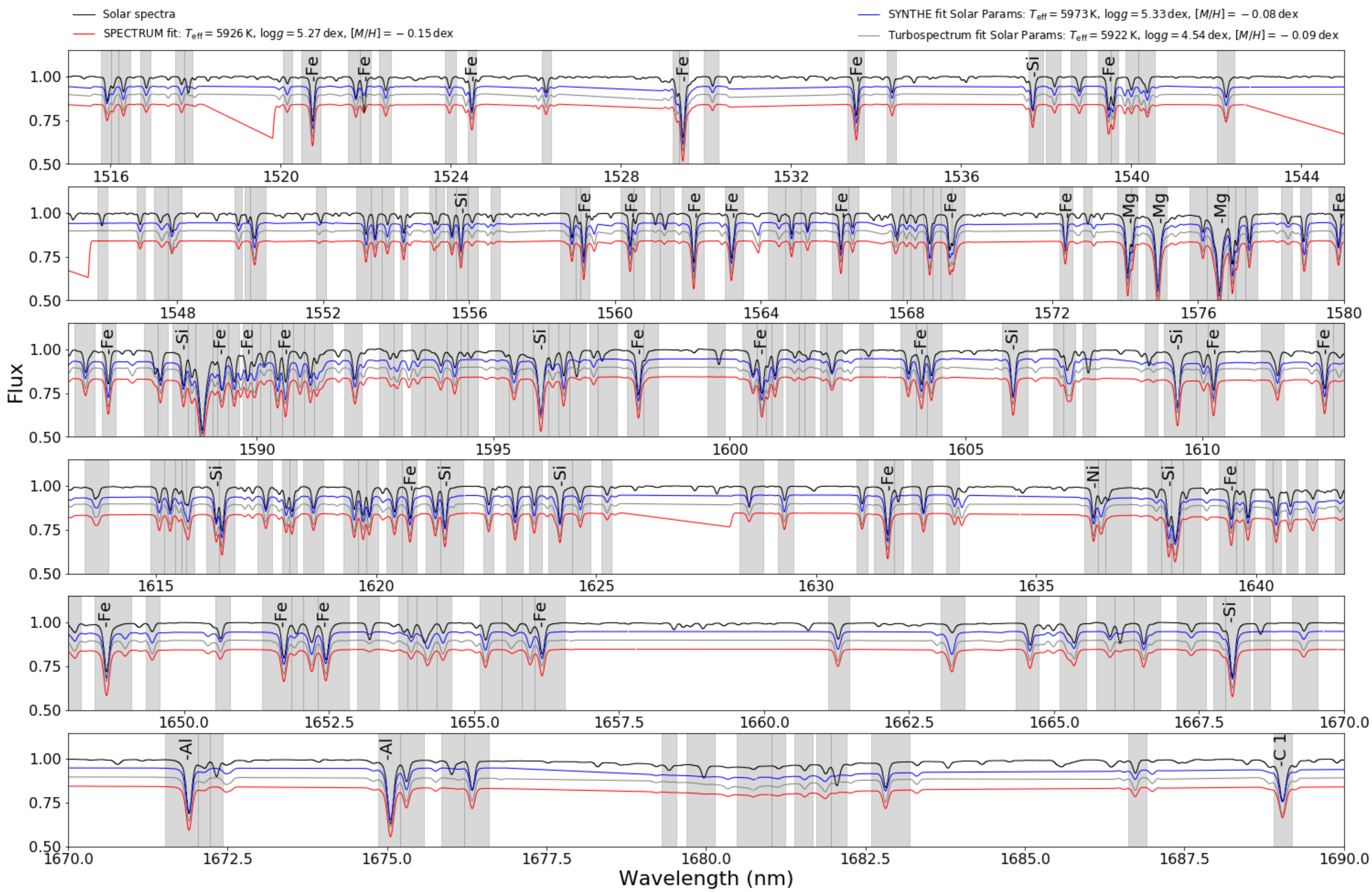

Figure 5.2: Comparison between Solar spectra (black) and the best fits of three different spectral synthesis codes: *SYNTHE* (blue, shifted by -0.05), *Turbospectrum* (gray, shifted by -0.10), and *SPECTRUM* (red, shifted by -0.15). Line list used was the VALD line list (1100-2400 nm) present in the *iSpec* distribution (see section 5.2.7). The parameters derived are summarized in Table 5.2. The gray areas indicate the regions of the spectra included in the line masks (see section 5.2.8).

Figure 5.2 contains the solar spectrum provided by Wallace et al. (1996) (see more details in section 5.3), downgraded to $R = 22\,500$, and three synthetic spectra made to match that observation. These spectra were each generated with a different spectral synthesis code, and the goal of the figure is to make a comparison between *SYNTHE* (blue), *SPECTRUM* (red) and *Turbospectrum* (gray). All synthesis were generated with the VALD linelist available within *iSpec* distribution, and using initial input values of $T_{\rm eff} = 5700\,{\rm K}$, $\log g = 4.5\,{\rm dex}$ and $[M/H] = 0.0\,{\rm dex}$. This line list was used because it is the default line list available within *iSpec*, and it is compatible with all three radiative transfer codes tested. As this line list is not especially optimized for the solar spectrum, the results (summarized in table 5.2) differ slightly from expected literature values. Here, we can conclude that, while all 3 codes calculate values for $T_{\rm eff}$ above and $[M/H]$ below the most commonly accepted solar parameters from Prša et al. (2016) ($T_{\rm eff} = 5772\,{\rm K}$, $\log g = 4.44\,{\rm dex}$ and $[M/H] = 0.0\,{\rm dex}$), *Turbospectrum* has the best overall estimate among the 3 codes ($T_{\rm eff} = 5921\,{\rm K}$, $\log g = 4.54\,{\rm dex}$ and $[M/H] = -0.09\,{\rm dex}$). Additionally, while not the fastest code in this test (31 minutes against 27 minutes for *SPECTRUM*), the difference is not enough to favor *SPECTRUM* over *Turbospectrum*.

Given the quality of the solar synthesized spectrum, the computing speed, and the derived solar parameters, *Turbospectrum* was chosen for all future syntheses required. Additional requirements with the water lines used for M dwarf spectra synthesis also excluded the other codes from being used for this project (see section 5.4.2). Therefore, all other spectra or parameters presented in this thesis are made with *Turbospectrum*, unless otherwise noticed.

5.2.3 Solar Abundances

iSpec has, included in its package, a collection of ready-to-use solar abundances. These come from a variety of sources, including Anders & Grevesse (1989), Grevesse & Sauval (1998), Asplund et al. (2005), Grevesse et al. (2007), and Asplund et al. (2009).

The synthesis of spectra requires the specification of one of these available abundances, and, as we are not synthesizing individual abundances for the stars, the choice of solar abundances becomes very important. The final parameters derived from a given spectrum depend on the choice of solar abundances, as equation 3.1 demonstrates.

From the list of available solar abundances above, two were selected as possibilities for usage in the syntheses: **Grevesse 2007**, published in Grevesse et al. (2007) and **Asplund 2009**, available at Asplund et al. (2009). **Grevesse 2007** is the abundance list used to create

Table 5.3: Parameters derived for the sun with 2 different abundances (**Grevesse 2007**, from Grevesse et al. 2007), and (**Asplund 2009**, first published in Asplund et al. 2009). Syntheses are made using *Turbospectrum*. Syntheses used the line list described in 5.2.7.

Abundance	$T_{\rm eff}$	$\log g$	$[M/H]$
Grevesse 2007	$5739\,\mathrm{K}$	$4.48\,\mathrm{dex}$	$-0.01\,\mathrm{dex}$
Asplund 2009	$5763\,\mathrm{K}$	$4.49\,\mathrm{dex}$	$-0.04\,\mathrm{dex}$

the MARCS stellar models (Gustafsson et al. 2008), which are the ones used in this project. **Asplund 2009** is the most recent abundance list available in *iSpec*. In table 5.3, parameters obtained with syntheses using both of these abundance lists are compared. Taking the most commonly accepted solar parameters from Prša et al. (2016) ($T_{\rm eff} = 5772\,\mathrm{K}$, $\log g = 4.44\,\mathrm{dex}$ and $[M/H] = 0.0\,\mathrm{dex}$) as a reference, it is clear both syntheses are precise and return close values, but there are still small differences. **Grevesse 2007** returns lower $T_{\rm eff}$ than expected (5739 K against 5763 K), while **Asplund 2009** is worse at returning solar metallicity ($-0.04\,\mathrm{dex}$ vs $-0.01\,\mathrm{dex}$). As the $[M/H]$ obtained with the solar abundances of **Grevesse 2007** is more accurate, and this abundance list is the one used to create the MARCS stellar models, **Grevesse 2007** was chosen as the abundance list to use in this project, and all $[M/H]$ values published are scaled by those abundance values.

5.2.4 χ^2 fit and error estimation

iSpec uses a χ^2 minimization procedure based on *mpfit.py* (based on MPFIT, Markwardt 2009) to obtain its results. It uses a Levenberg-Marquardt least-squares minimization to obtain the best fit to a given spectrum considering only the regions that are included in a selected region of the spectrum (line mask, described in sections 5.2.8 and 5.27). All the errors cited for the stellar parameters in this work were calculated by *iSpec* from this code, and correspond to the formal 1σ errors of each parameter, computed from the covariance matrix. The error calculation assumes uncertainties in the observed spectrum equal to the flux divided by the S/N values published by ASPCAP. These are considered as internal errors and are reported in each parameter for all stars in table B.1.

To address our method's capability at recovering the parameters for each star under slightly different conditions, we added random Gaussian noise based on the flux errors to the normalized spectrum for each star. The Gaussian noise added had a zero mean and a standard deviation equal to the estimated flux error for each pixel. To avoid individual points or areas

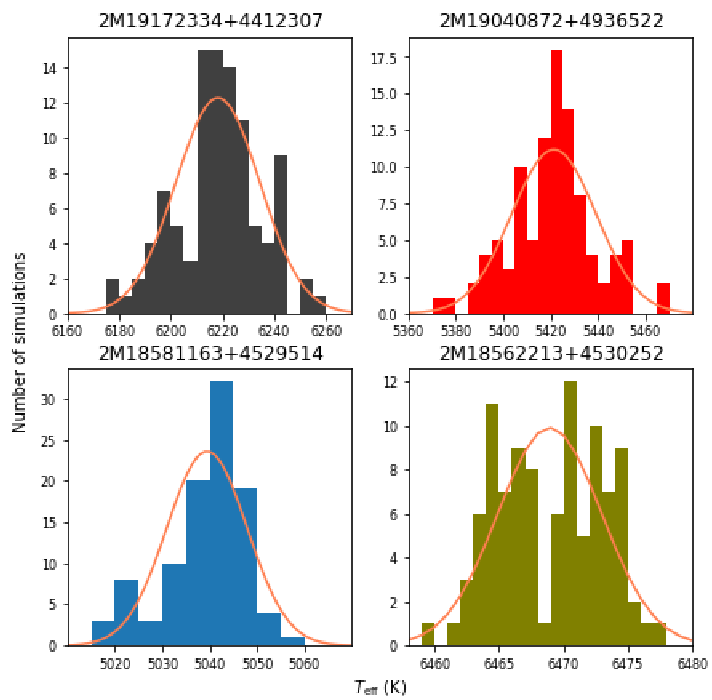

Figure 5.3: Histogram of the output $T_{\rm eff}$ of 4 selected stars over 100 different iterations. Each point in the spectra had random Gaussian noise added to it. Best Gaussian fit overplotted.

with large reported flux errors ($> 1/10$ th of the pixel flux value) that could skew the analysis, we restricted the value of Gaussian noise standard deviation to 1/10th of the flux for those pixels.

We chose 4 stars with different spectral derived parameters from the CPS catalog and different S/N on their APOGEE spectra and added to each spectrum the random Gaussian noise described above 100 times for each star. The derived parameters by *iSpec* from the 100 random Gaussian noise-added spectra are shown in Figs. 5.3 to 5.5. Table 5.4 shows the mean values and standard deviation derived from the 100 iterations for each star. The consistency of our method across multiple syntheses can be confirmed, being able to recover consistent values for all the stars. As expected, the star with the lowest S/N, 2M19172334+4412307, exhibits the largest differences between syntheses, reaching up to $\Delta T_{\rm eff} \sim 100$ K and $\Delta \log g = 0.11$ dex.

5.2.5 Free Parameters

A synthesis done with *iSpec* includes a selection of varying (free) or fixed parameters. The selection of these free or fixed parameters depends on the goal of the synthesis and the

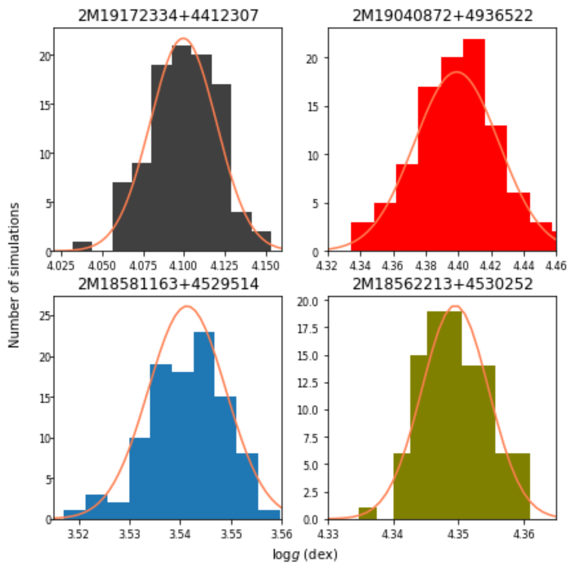

Figure 5.4: Histogram of the output $\log g$ of 4 selected stars over 100 different iterations. Each point in the spectra had random Gaussian noise added to it. Best Gaussian fit overplotted.

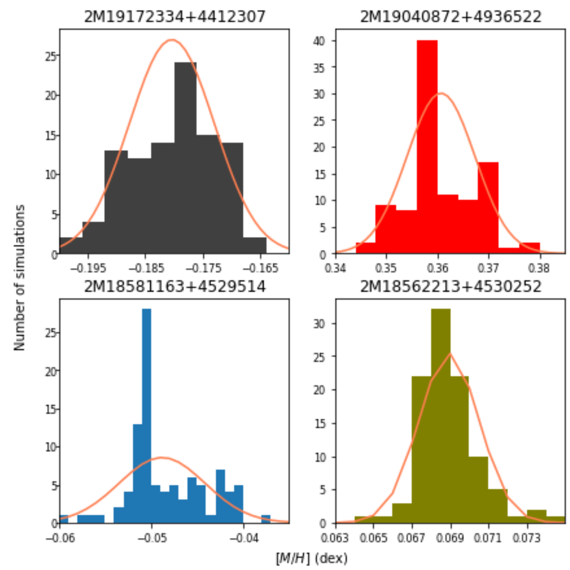

Figure 5.5: Histogram of the output $[M/H]$ of 4 selected stars over 100 different iterations. Each point in the spectra had random Gaussian noise added to it. Best Gaussian fit overplotted.

Table 5.4: Parameters derived in the 4 stars selected. The C indicates the literature (CPS) parameter for that star, and $\overline{parameter}$ and σ indicate the average value and the standard deviation measured across all 100 iterations, respectively. All $T_{\rm eff}$ values are in K, $\log g$ and $[M/H]$ in dex.

APOGEE_ID	S/N	$\overline{T_{\rm eff}} \pm \sigma$	$T_{\rm eff}^C$	$\overline{\log g} \pm \sigma$	$\log g^C$	$\overline{[M/H]} \pm \sigma$	$[M/H]^C$
2M19172334+4412307	121	6218 ± 16	6221	4.10 ± 0.02	4.13	-0.18 ± 0.01	-0.14
2M19040872+4936522	132	5421 ± 18	5487	4.40 ± 0.03	4.31	0.36 ± 0.01	0.34
2M18581163+4529514	216	5039 ± 9	4989	3.54 ± 0.01	3.37	-0.05 ± 0.01	-0.04
2M18562213+4530252	1095	6468 ± 6	6378	4.35 ± 0.01	4.2	0.07 ± 0.01	0.18

relative importance of parameters for later analysis. These are the parameters that can vary during the χ^2 fit and error minimization.

The creator and developer of *iSpec*, Blanco-Cuaresma (private communication) recommended the use of $T_{\rm eff}$, $[M/H]$, and $\log g$, together with v_{mic} and R, as the free parameters for the *iSpec* pipeline, keeping v_{mac} estimated through empirical relations and the other available parameters as fixed. We wanted to test if this combination of free parameters was the best one for parameter derivation, so we ran the pipeline with different combinations of free parameters to analyze the difference between them.

In table 5.5, the results of 12 different synthesis with different free parameters are summarized. In all these cases, $T_{\rm eff}$, $[M/H]$, and $\log g$ were kept as free parameters, with other additional parameters changing from synthesis to synthesis (v_{mic},v_{mac},$v \sin i$, and R). Comparing the output values with the expected solar parameters of $T_{\rm eff} = 5772\,{\rm K}$, $[M/H] = 0.0\,{\rm dex}$,

Table 5.5: Parameters derived for the Sun with varying free parameters. T_{eff}, $[M/H]$, and $\log g$ are always included in the free parameters, with initial guesses of $T_{\text{eff}} = 5772\,\text{K}$, $[M/H] = 0.0\,\text{dex}$, and $\log g = 4.5\,\text{dex}$. The units used were K for T_{eff}, dex for $\log g$ and $[M/H]$, and km/s for v_{mic}, v_{mac}, and $v \sin i$. R means Resolution ($\lambda/\Delta\lambda$)

Free Par.	T_{eff}	$\log g$	$[M/H]$	v_{mic}	v_{mac}	$v \sin i$	R	Reduced χ^2
R	5763	4.49	-0.04	1.05	4.20	1.6	23987	0.0012
v_{mic}	5671	4.29	-0.08	1.39	3.92	1.6	22000	0.0012
$v \sin i$	5663	4.33	-0.08	1.05	3.89	0	22000	0.0012
v_{mac}	5747	4.46	-0.05	1.05	0.00	1.6	22000	0.0012
v_{mic}, R	5771	4.50	-0.04	1.03	4.23	1.6	24034	0.0012
$v \sin i$, R	5764	4.49	-0.04	1.05	4.21	0	23770	0.0012
$v_{mic}, v \sin i$	5668	4.31	-0.09	1.34	3.91	0	22000	0.0012
v_{mic}, v_{mac}	5756	4.47	-0.05	1.14	0.00	1.6	22000	0.0012
$v_{mac}, v \sin i$	5759	4.48	-0.04	1.05	0.00	0	22000	0.0012
$v_{mic}, v \sin i$, R	5764	4.49	-0.04	1.08	4.21	0	23750	0.0012
v_{mac}, v_{mic}, R	5766	4.49	-0.04	1.06	1.60	1.6	22528	0.0012
$v_{mac}, v \sin i, v_{mic}$	5774	4.51	-0.04	0.99	2.30	0	22000	0.0012

and $\log g = 4.44\,\text{dex}$, some conclusions can be drawn about the best output parameter combination to use for the pipeline.

First, we notice that the reduced χ^2 remains constant across all parameter combinations for the syntheses, so the shape of the synthetic spectra and the quality of the fit does not vary significantly between them. Therefore, we must analyze the output parameters instead. Any syntheses without resolution or v_{mac} as a free parameter tends to derive significantly lower values for both the T_{eff}, $\log g$ and $[M/H]$, showing that the inclusion of at least one of these parameters is critical for the pipeline to derive accurate parameters. All other syntheses, excluding the one with both $v \sin i$ and v_{mic}, produce rather similar output parameters, being very close to both the real T_{eff} and $[M/H]$. All parameter combinations still result in values for the $[M/H]$ below expected, ranging from -0.09 to -0.04 dex. This discrepancy seems to be associated with the code and the line list/line mask itself and must be considered for other stellar samples. We considered keeping R as a fixed parameter, as we know its value. However, since having it as a free parameter results in better output parameters overall, and the output R is also very close to the value expected of $R \sim 22000$, we kept it as a free parameter. While the recommended combination of v_{mic} and R as free parameters did not perform significantly better than the other ones, the fact that it was one of the best ones, in addition to Blanco-Cuaresma's recommendation, made us want to choose it as the one to use for the pipeline. Synthesis of $v \sin i$ is important as well, as it is to control for changes in resolution, as both R and $v \sin i$ have similar effects on the spectrum itself (see section 3.3). Additionally, $v \sin i$ is an important stellar parameter that can give us information about the stellar rotation rate. The table shows very little difference in output when adding $v \sin i$ as a free parameter, compared to only v_{mic} and R ($T_{\rm eff} = 5764\,{\rm K}$, $[M/H] = -0.04\,{\rm dex}$, and $\log g = 4.49\,{\rm dex}$ vs $T_{\rm eff} = 5771\,{\rm K}$, $[M/H] = -0.04\,{\rm dex}$, and $\log g = 4.50\,{\rm dex}$). However, this is because the Sun is a slow rotator. We must keep the rotational velocity as free for other observed stars unless we know an approximate value for the parameter.

The limb darkening parameter represents the observed change in the color of the stellar surface from a face view towards its limb. Limb darkening exists because the continuum source function decreases outward (towards the limb). This means that, as we look towards the limb, we see systematically higher photospheric layers that are less bright. *iSpec* allows its users to customize their limb darkening parameter, either by fixing it at a given value or by keeping it as a free parameter. For our method, we tried synthesis with limb darkening fixed to different values, across the range of values measured in Claret & Bloemen (2011) for limb darkening as a function of wavelength. Figure 5.6 shows how fixing this parameter to different values can affect the other output parameters, for the cases of 3 different test stars (2M05373344+7441194, HD 176377, and HD 22879). As shown in that figure, these changes in the limb darkening parameter do not result in a large change in the output parameters. Therefore, we chose to keep the limb darkening as 0.6, as it was the default value for a solar-type star and can represent our stellar sample.

Therefore, the final list of free parameters for the syntheses includes the effective temperature, surface gravity, and metallicity, as well as the microturbulence velocity (v_{mic}), resolution ($\lambda/\Delta\lambda$) and rotational velocity ($v \sin i$). For the synthesis of FGK stars, the initial input values for these parameters were kept at $5800\,{\rm K}$ for the $T_{\rm eff}$, $0.0\,{\rm dex}$ for the $[M/H]$ and, for the $\log g$, $4.5\,{\rm dex}$. The macroturbulent velocity (v_{mac}) is calculated automatically by *iSpec* using empirical relations based on the $T_{\rm eff}$.

5.2.6 Spectra Normalization

APOGEE DR14 spectra include both normalized spectra and multiple stages of spectrum processing for its stars [1]. The normalized spectra are processed by ASPCAP to derive parameters and could, in principle, be used to fit individual lines and determine abundances and parameters using the EW method, for example. However, the normalization done for APOGEE DR14

[1] https://www.sdss.org/dr14/data_access/

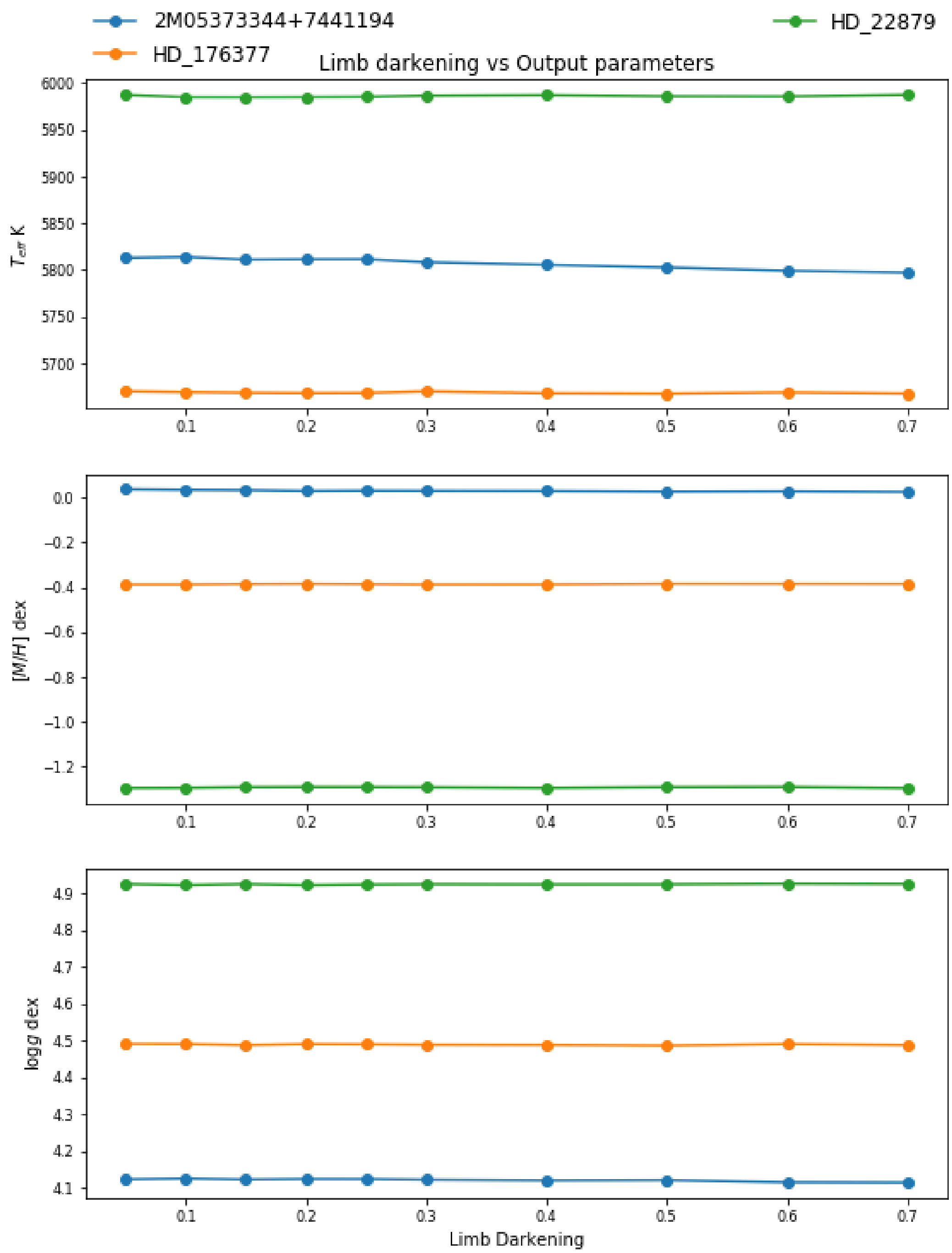

Figure 5.6: 3 plots showing how the output $T_{\rm eff}$, $[M/H]$ and $\log g$ of 3 test stars (2M05373344+7441194, HD 176377, and HD 22879) change with different fixed values for limb darkening (0.05, 0.1, 0.15, 0.2, 0.25, 0.3, 0.4, 0.5, 0.6, 0.7).

spectra is not precise enough to compare the normalized spectrum to our full synthetic spectrum. Normalization issues were particularly noticeable in M dwarfs (see example in Fig. 5.7), but a good and uniform normalization is also very important for FGK stars (see example in Fig. 5.8). Therefore, we had to perform our normalization on the combined spectra [2] of each star in our sample.

[2]https://data.sdss.org/sas/dr14/apogee/spectro/redux/r8/stars/

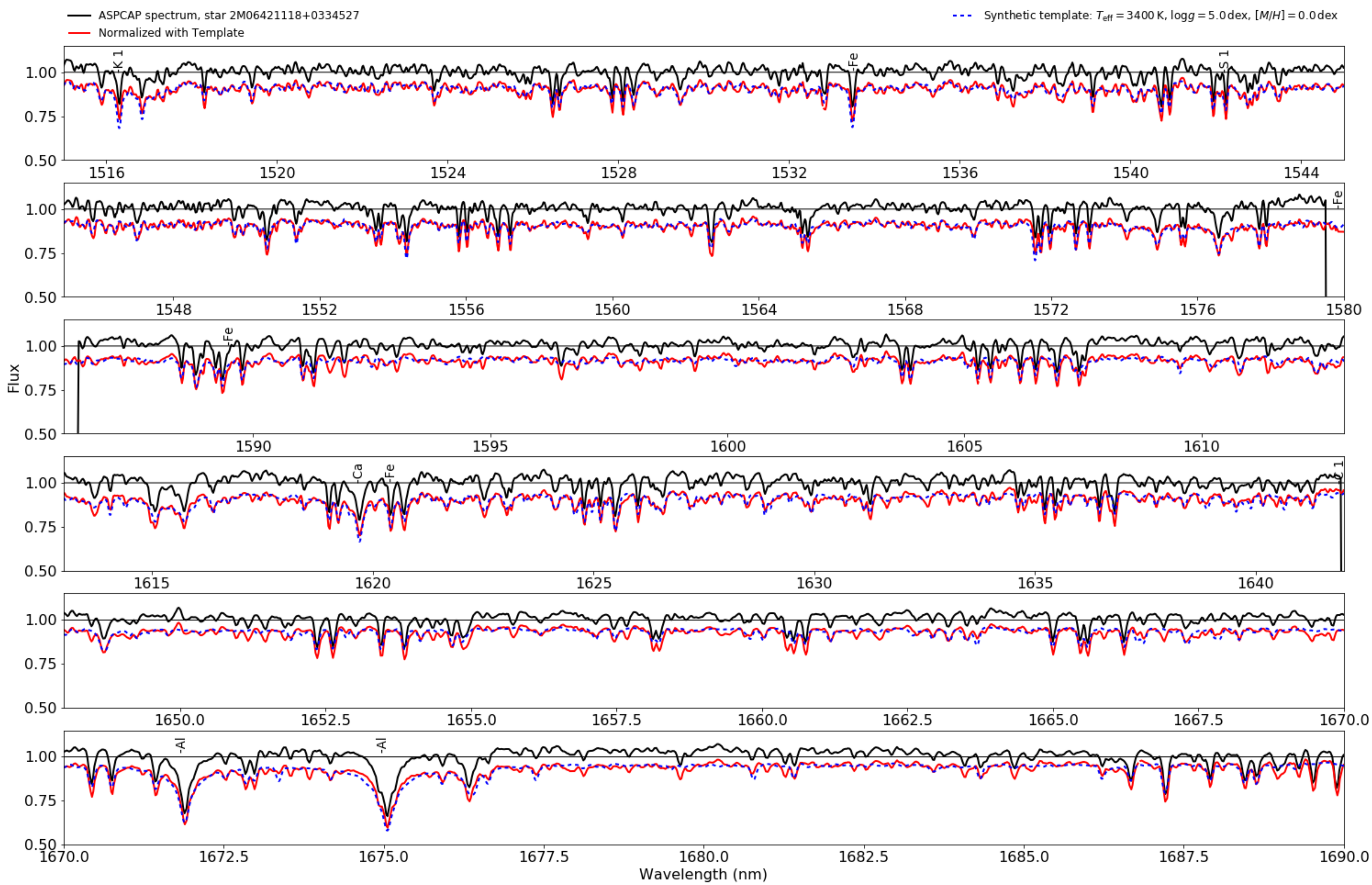

Figure 5.7: Comparison between ASPCAP spectrum (black) and both the template used to normalize the spectrum (blue, dots) and the final normalized spectrum of star 2M06421118+0334527. The parameters used to generate the synthetic spectrum were $T_{\rm eff} = 3400\,{\rm K}$,$\log g = 5.0\,{\rm dex}$, $[M/H] = 0.0\,{\rm dex}$.

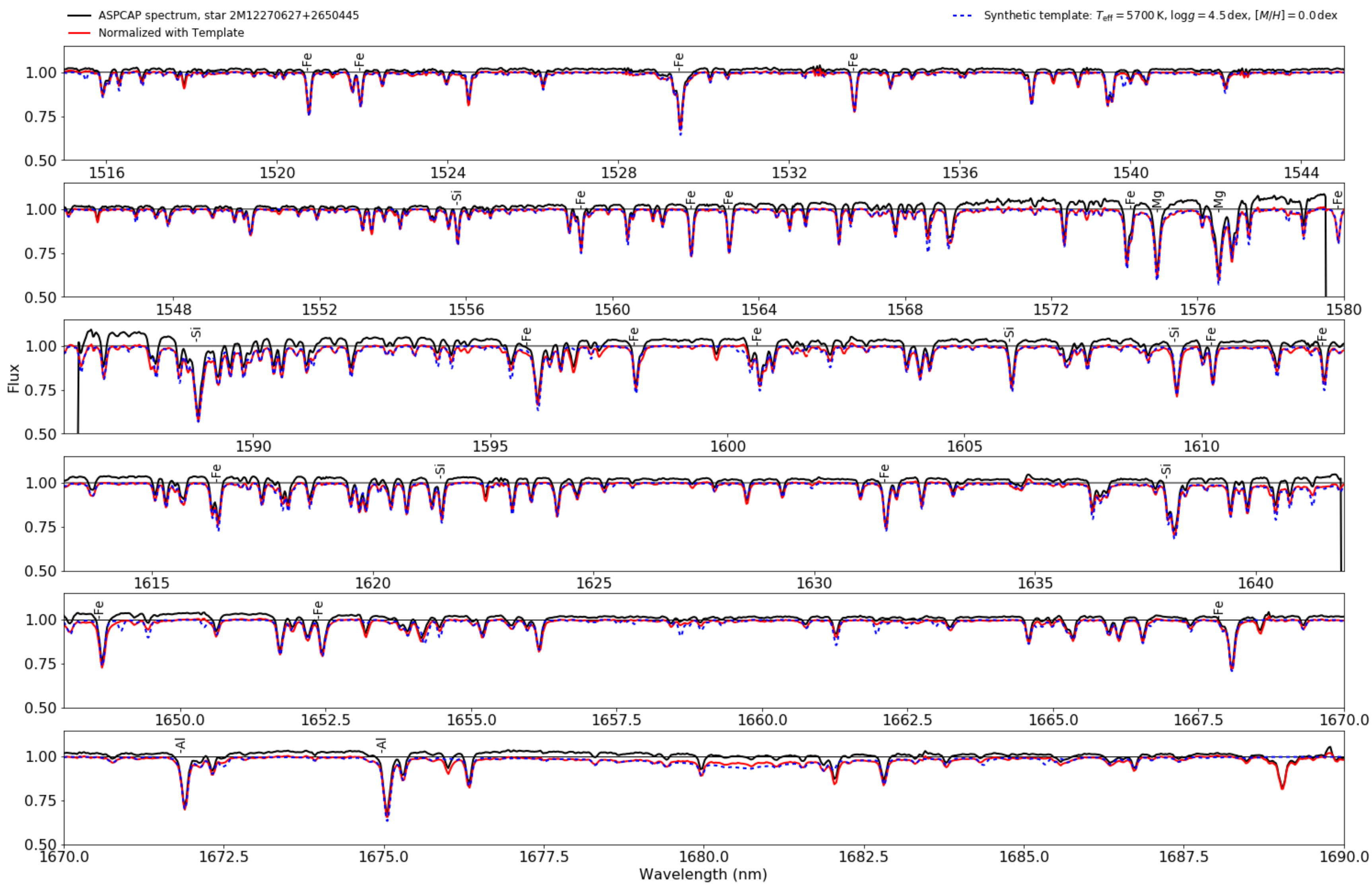

Figure 5.8: Comparison between ASPCAP spectrum (black) and both the template used to normalize the spectrum (blue, dots) and the final normalized spectrum of star 2M12270627+2650445. The parameters used to generate the synthetic spectrum were $T_{\rm eff} = 5700\,\mathrm{K}$,$\log g = 4.5\,\mathrm{dex}$, $[M/H] = 0.0\,\mathrm{dex}$.

iSpec has many normalization techniques programmed and available within its distribution. Among others, *iSpec* allows the user to normalize a spectrum using a fixed value continuum, different customizable splines, or just an optimized polynomial. All these methods were tried before we decided the one to use: the template method.

This method requires the use of a synthetic spectrum with the approximate parameters of the spectrum we want to normalize, which can be created using our pipeline. The template method for normalizing spectra works by dividing the observed spectrum by the synthetic spectrum appropriate for it. Then, the median is calculated for this divided spectrum, with *iSpec* having the possibility of choice of window for the median calculation. This averaged spectrum is taken as the continuum fit for the originally observed spectrum, and that original spectrum is divided by this fit to obtain the final normalized spectrum.

The template method has a clear flaw of requiring an estimate or approximation for the parameters of the observed star to normalize its spectrum. When this estimate is unavailable or of poor quality, it may result in a poor or inaccurate normalization for that star. This is especially important for the normalization of M dwarf spectra because the wide molecular (mostly H_2O) lines make the correct normalization more important than for FGK stars. For the FGK stars, literature values for the spectroscopic parameters are used when available, either from ASPCAP or from studies in optical wavelengths. Solar values are used for stars with no other available parameters. This choice does not strongly affect our results, as the overall spectral shape doesn't vary strongly across our parameter space for FGK stars. M dwarfs require a different method, detailed in section 5.4.1.

5.2.7 Line list

The line-list used in the synthesis in this work is a compilation of lines from different sources. The first line-list used is the VALD (Vienna Atomic Line Database, Piskunov et al. 1995) line list (1100-2400 nm) present in the *iSpec* distribution. The line-list available from APOGEE (Shetrone et al. 2015) is also used to create the final compilation. These line-lists contain all relevant elemental lines as well as the molecular lines for CO, OH, C_2, CN, CH, and FeH. To create the final line-list, a sample of well-characterized stars, like the sun (see Fig. 5.14), was selected. Two different synthetic spectra, each made with a different line list, were created for each of these stars. Then, each 0.2 nm region of each spectrum was compared with APOGEE-resolution spectra from these stars, and one of the two line lists was selected as the one providing the best fit for that region. A final line list was created, using the best-fitting lines from each of the two original line lists. An example of synthetic spectra generated with each of these line lists is available in Fig. 5.9, with a zoom in on relevant areas in Fig. 5.10.

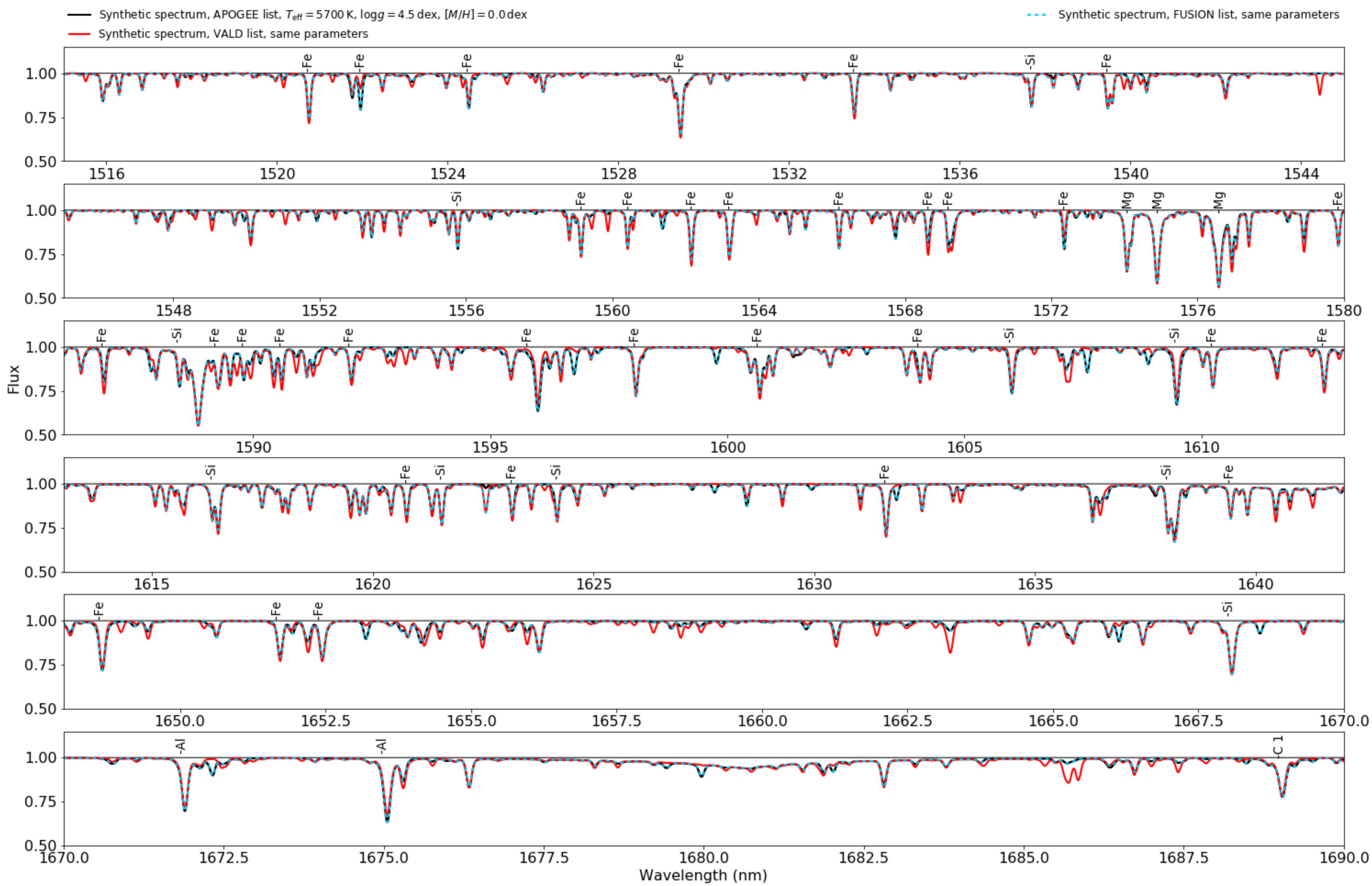

Figure 5.9: Comparison between a synthetic spectrum generated with the APOGEE line list (black), the VALD linelist (red) and a combination of both (FUSION, blue dots). The parameters used to generate the synthetic spectrum were $T_{\rm eff} = 5700\,\mathrm{K}$,$\log g = 4.5\,\mathrm{dex}$, $[M/H] = 0.0\,\mathrm{dex}$.

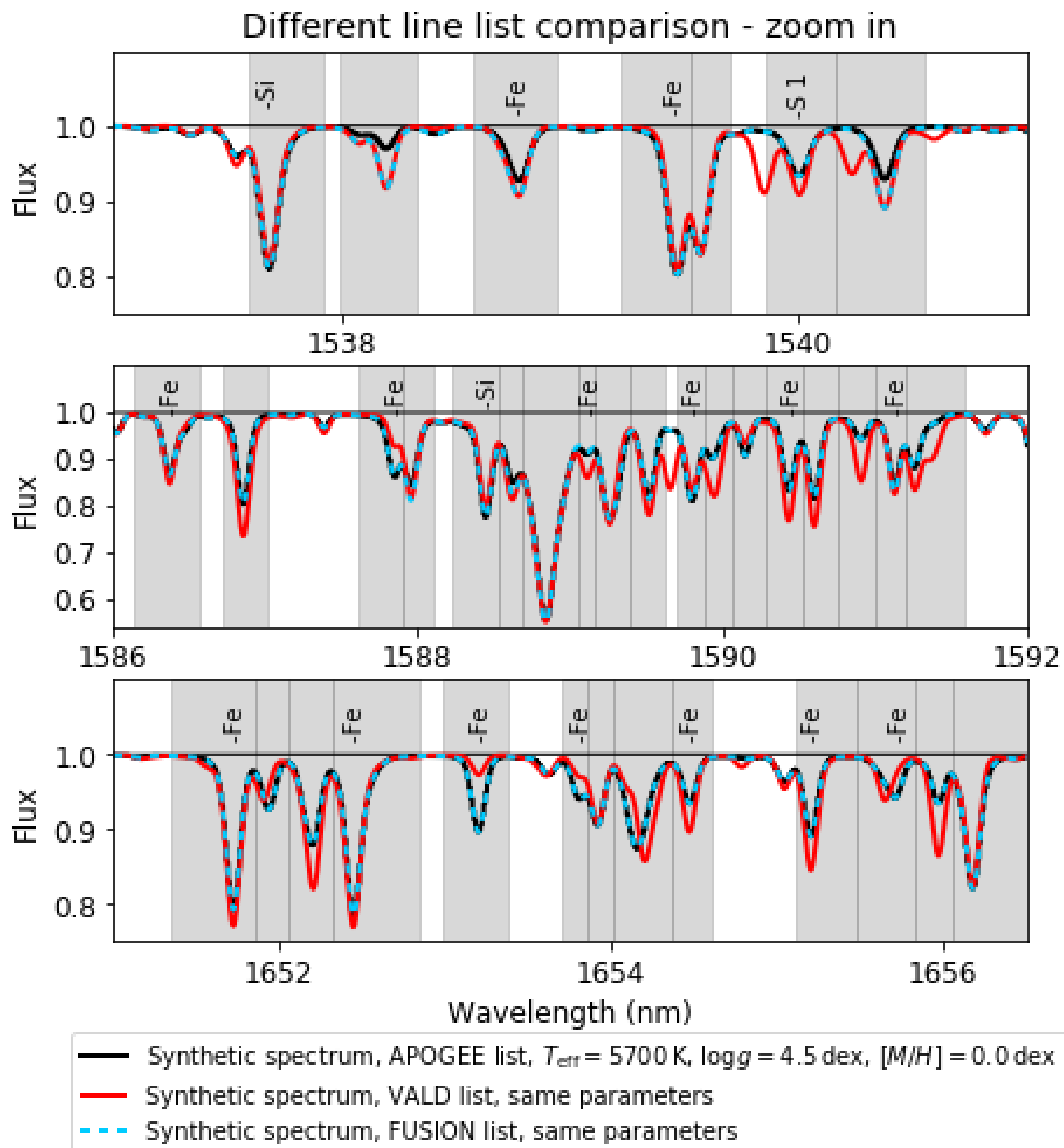

Figure 5.10: Zoom in on three chosen areas of the comparison between a synthetic spectrum generated with the APOGEE line list (black), the VALD line list (red) and a combination of both (FUSION, blue dots), shown in Fig. 5.9. The parameters used to generate the synthetic spectrum were $T_{\rm eff} = 5700\,{\rm K}$,$\log g = 4.5\,{\rm dex}$, $[M/H] = 0.0\,{\rm dex}$.

5.2.8 Line mask

The lines synthesized by *iSpec* are defined by a line mask. A line mask is a selection of regions within the full wavelength that are considered by the code when matching the synthetic and the observed spectra. This is made so lines with poor or unavailable laboratory data are not considered when calculating χ^2. The line selection for the line mask for FGK stars is done based on the solar spectra (see chapter 5.3). In order to create the line mask, a synthetic solar spectrum with standard parameters ($T_{\text{eff}} 5772\,\text{K}$, $[M/H]$ 0.0 and $\log g = 4.44\,\text{dex}$) was created and compared to the solar spectra. Lines that did not match the solar spectra were discarded, and the remaining matching lines make up the line mask used in the synthesis. This comparison is made visually, inspecting each synthesized line and comparing it with the observed solar spectra (see figure 5.14). The final selection is the line mask used for the syntheses with solar-type stars.

5.3 Solar spectrum

The Sun is the closest and best-characterized star available and any reliable synthesis-based method should recover its spectral characteristics. Therefore, one of the most important stars in our sample is the Sun, and this section is dedicated to demonstrate the methodology and to use it as a test to the synthesis itself.

To calibrate and test *iSpec* with *Turbospectrum* in the NIR, a solar spectrum was synthesized using the methodology described above. For comparison, the solar spectrum by Wallace et al. (1996), observed with the Fourier transform spectrometer at the Math-Pierce solar telescope on Kitt Peak, with a resolution of $300\,000$ and high S/N, was used. The spectrum was degraded down to $R = 22\,500$ to match APOGEE's resolution. It was normalized using the template method described in section 5.2.6 with a reference spectrum of $T_{\text{eff}} = 5700$ K, $[M/H] = 0.0$ dex and $\log g = 4.5$ dex.

The observed and synthetic solar spectra are shown in Figure 5.14. We took as the accepted solar parameters $T_{\text{eff}} = 5772$ K, $\log g = 4.44$ dex and $[M/H] = 0.0$ dex (Prša et al. 2016). The synthesis done with our methodology provides a synthetic spectrum that matches the solar spectrum and derives just slightly lower values for the solar spectra at APOGEE's resolution: $T_{\text{eff}} = 5764 \pm 35$ K,$\log g = 4.49 \pm 0.07$ dex, $[M/H] = -0.04 \pm 0.02$ dex. Given the Wallace et al. (1996) solar spectrum did not provide flux errors, we estimated errors from the parameters from 100 syntheses of the solar spectrum with injected Gaussian noise of 1/1000th of the flux at each pixel of the spectra (similar to the process described in section 5.2.4). The average values for T_{eff}, $\log g$, and $[M/H]$ from the 100 syntheses are shown in Table 5.6. As expected, the parameters obtained in each synthesis are not independent from each other.

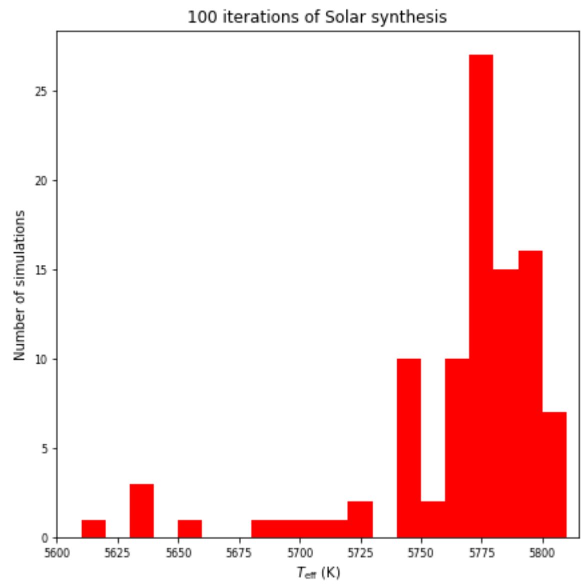

Figure 5.11: Histogram of the output $T_{\rm eff}$ of the Sun over 100 different iterations, with each point in the spectra having random Gaussian noise added to it.

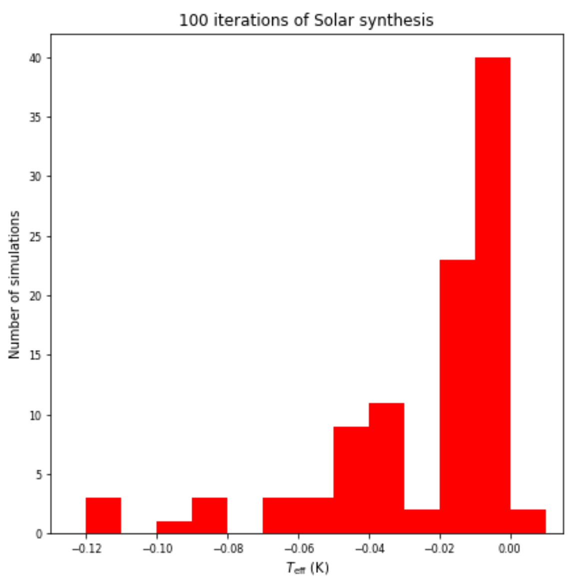

Figure 5.12: Histogram of the output $[M/H]$ of the Sun over 100 different iterations. Each point in the spectra had random Gaussian noise added to it.

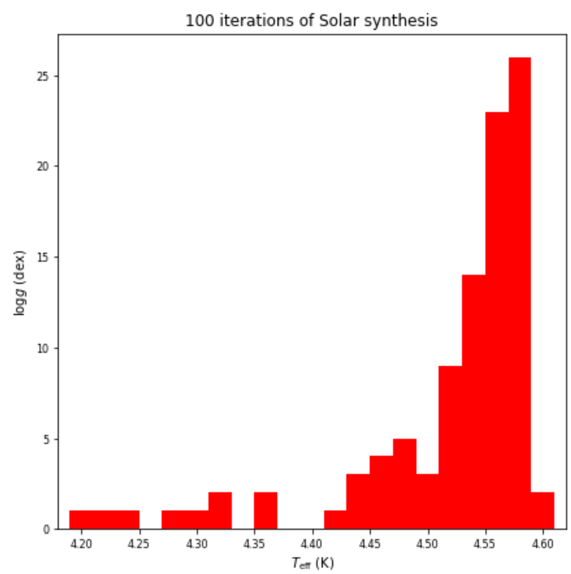

Figure 5.13: Histogram of the output $\log g$ of the Sun over 100 different iterations. Each point in the spectra had random Gaussian noise added to it.

There are multiple degeneracies between them, as shown by the $T_{\rm eff}$, $[M/H]$, and $\log g$ histograms in Figures 5.11, 5.12, and 5.13. 87 out of 100 syntheses have estimated $T_{\rm eff}$ values within 5772 ± 50 K and 65 of them have $[M/H]$ within 0.0 ± 0.02 dex, while only 32 syntheses have estimated $\log g$ values within 4.44 ± 0.1 dex. These results also show standard deviations of 45 K for $T_{\rm eff}$, 0.09 dex for $\log g$, and 0.03 dex for $[M/H]$. This distribution of output parame-

Table 5.6: Solar parameters derived from Wallace et al. (1996) solar spectrum, and average results across 100 iterations with injected errors.

Parameter	Output	Average $\pm\sigma$
$T_{\rm eff}$ (K)	5764	5763 ± 45
$\log g$ (dex)	4.49	4.5 ± 0.09
$[M/H]$ (dex)	–0.04	-0.02 ± 0.03

ters shows, therefore, a tendency for an overestimation of the solar surface gravity, as well as a larger dispersion for this parameter. The parameter analysis indicates a high degree of consistency between the iterations of our pipeline. However, in some cases, the retrieved parameters diverge significantly from the expected. In particular, we registered unusual differences in $T_{\rm eff}$ of -150 K, -0.10 dex for $[M/H]$, and up to -0.2 dex for $\log g$.

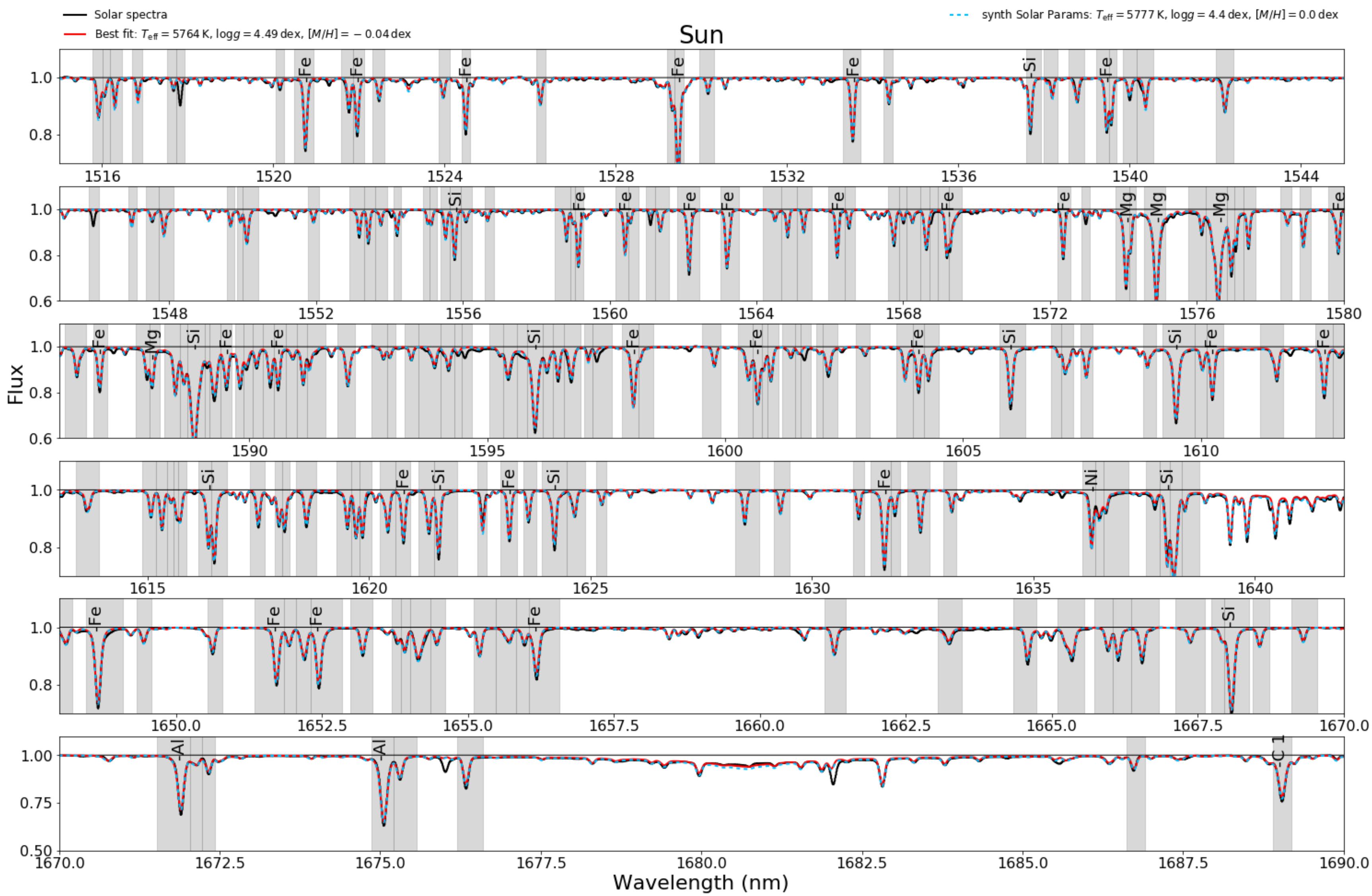

Figure 5.14: Comparison between Solar spectra (black), the best fit from our pipeline synthetic spectra (red), and a second synthetic spectrum made with the standard solar parameters (blue) for APOGEE wavelength range. The parameters derived were $T_{\rm eff} = 5764 \pm 45$ K, $\log g = 4.49 \pm 0.09$ dex, $[M/H] = -0.04 \pm 0.03$ dex, compared to the standard ones of $T_{\rm eff} = 5772$ K, $\log g = 4.4$ dex, $[M/H] = 0.0$ dex. The gray areas indicate the regions of the spectra included in the line masks (see section 5.2.8).

5.4 Specific steps for M Dwarf spectral synthesis

This section includes only steps in our pipeline that are specific for M dwarfs. The full rundown of our pipeline is available in Section 5.2. That chapter should be read before understanding the specific changes required for M dwarf parameter determination.

5.4.1 Spectra Normalization

A good continuum normalization is important for an accurate parameter determination, as shifting continuum values can result in wrong measures for a given line's EW or the fit of synthetic spectra with different stellar parameters. Fig. 5.15 illustrates how a $300\,\mathrm{K}$ difference in T_{eff} can mean a 0.05 difference in the continuum flux for a star, which is enough to turn an accurate fit into a terrible one. Therefore, when using the template method for spectra normalization described in Chapter 5.2.6 to normalize an M dwarf's H-band spectrum, we require an accurate initial input stellar effective temperature for the normalization template. Normalizations with templates synthesized with effective temperatures closer to the star's expected effective temperatures will result in more accurate continuum values, which means that the generated synthetic spectra will better match the observed ones. Therefore, having good estimates on each M dwarf's effective temperature before beginning the normalization process is an important step in deriving its atmospheric parameters. Multiple attempts were explored before finding one that worked for our sample stars, and this section will detail attempts that did not work, as well as the final method used for parameter determination.

Temperature Estimation

The first attempt for parameter determination we tried consisted of estimating the M dwarf temperature through different methods, including using parameters derived by ASPCAP to obtain an initial guess for that value. As mentioned in section 4.3, Schmidt et al. (2016) confirmed the accuracy of ASPCAP's parameters for M dwarfs, stating their T_{eff} to be accurate to about $100\,\mathrm{K}$ for stars between 3550–4200 K, and their $[M/H]$ values accurate to about $0.18\,\mathrm{dex}$. This means that ASPCAP values can be taken as reasonable initial guesses for the parameters of these stars, and can serve as a baseline from which better approximations can be obtained.

The first step of this method consisted of a visual inspection of each spectrum and a comparison between it and synthetic spectra created with different parameters. The most important

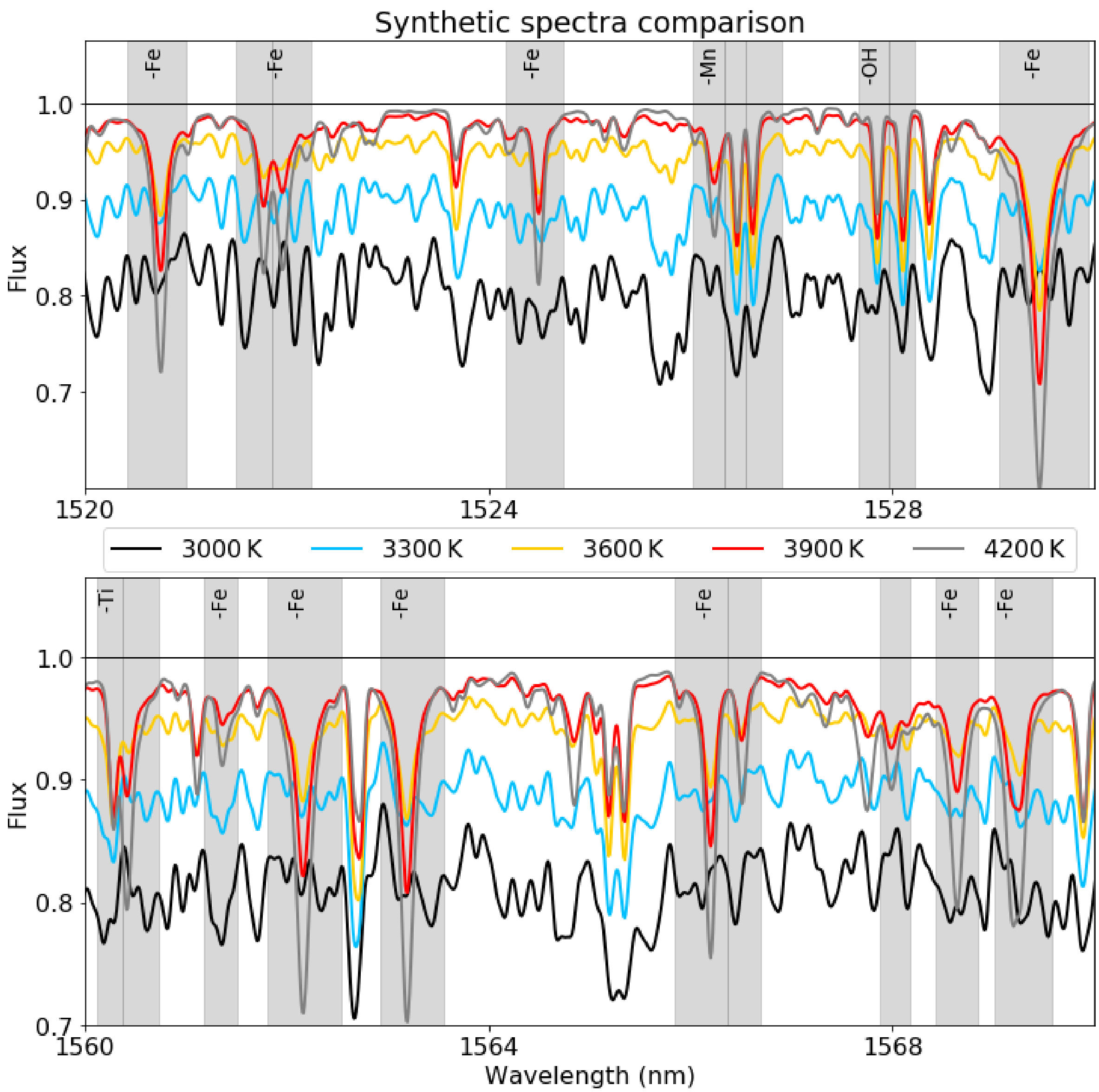

Figure 5.15: Comparison between synthetic spectra made with different $T_{\rm eff}$. The spectra corresponds to synthesis made with $T_{\rm eff}$ 4200 K (gray), 3900 K (red), 3600 K (yellow), 3300 K (blue) and 3000 K (black).

Table 5.7: T_{eff} relation coefficients from Mann et al. (2015) used

Parameters	Value
a	3.172
b	-2.475
c	1.082
d	-0.2231
e	0.01738
f	0.08776
g	0.04355

features for these visual inspections were the areas between 1520 nm and 1530 nm and between 1560 nm and 1570 nm. These areas were chosen as they have lines that are especially sensitive to T_{eff} changes, as shown in Fig. 5.15. These include Fe lines that become weaker for stars with lower T_{eff} and other features that become stronger for those stars. From visual inspections, an approximate T_{eff} was obtained for each star in the sample.

Secondly, to double-check the T_{eff} obtained by visual inspection, photometric relations were used. For these, we cross-matched our M dwarfs with the Gaia DR2 (Brown et al. 2018), to obtain their B_p and Rp photometric indices. These values can be used with equation (7) from Mann et al. (2015) (reproduced here as Equation 5.1, with the coefficients in table 5.7, where B_p and Rp come from Gaia, and J and H available in APOGEE DR 14) to derive an approximate value for M dwarf $T_{\text{eff}} \pm 60$ K. The cited equation was derived from low resolution ($R \sim 1000$) visible and infrared spectra of 183 nearby late K and M dwarfs. See Fig. 5.16 for a comparison between the T_{eff} determined with a visual inspection and the one obtained with Equation 5.1. The median difference (Visual - Photometric) between both distributions is -24 K, with a Standard Deviation (SD) of 188 K and Median Absolute Deviation (MAD) of 156 K.

$$T_{\text{eff}} = a + b(B_p - Rp) + c(B_p - Rp)^2 + d(B_p - Rp)^3 + e(B_p - Rp)^4 + f(J - H) + g(J - H)^2 \quad (5.1)$$

We calculate the average between these two estimates and use it to choose the T_{eff} of the template star for the normalization. The average value is used to minimize possible biases present in either T_{eff} estimate. The normalization is then made through the use of a grid with different possible synthetic spectra. All spectra are then normalized using synthetic spectra made with the chosen T_{eff}, $\log g = 5.0$ dex and $[M/H] = 0.0$ dex as template. The method used for the normalization itself is described in detail in Section 5.2.6, and the results obtained

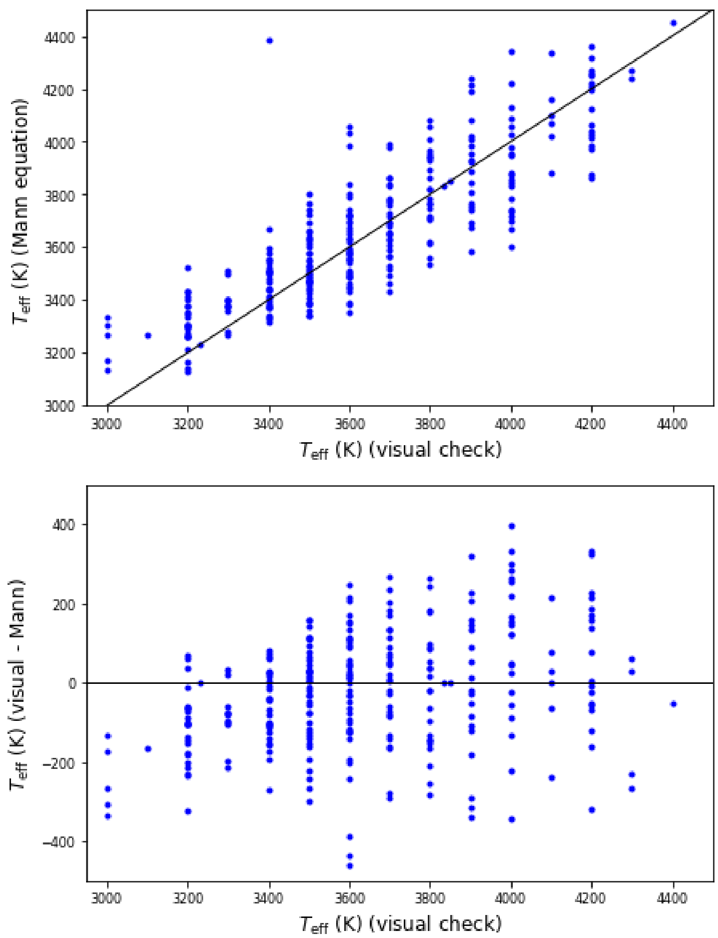

Figure 5.16: Comparison between our visual $T_{\rm eff}$ estimate and the values predicted by Equation 7 from Mann et al. (2015). TOP (a) shows the absolute values while BOTTOM (b) shows $\Delta T_{\rm eff}$.

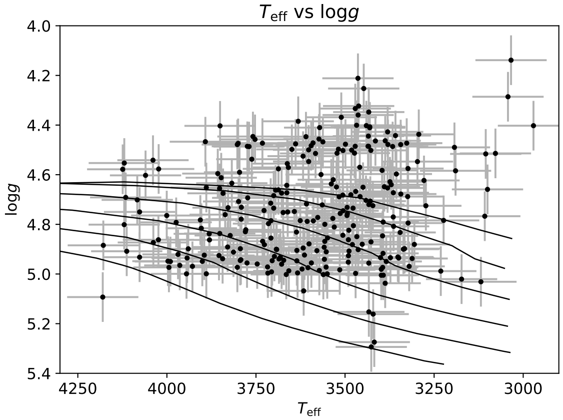

Figure 5.17: HR diagram with $T_{\rm eff}$ and $\log g$ values from *iSpec* output parameter distribution, using the temperature estimation method for the normalization. Overplotted are PARSEC isochrones created with ages of 1 Gyr and different metallicity values.

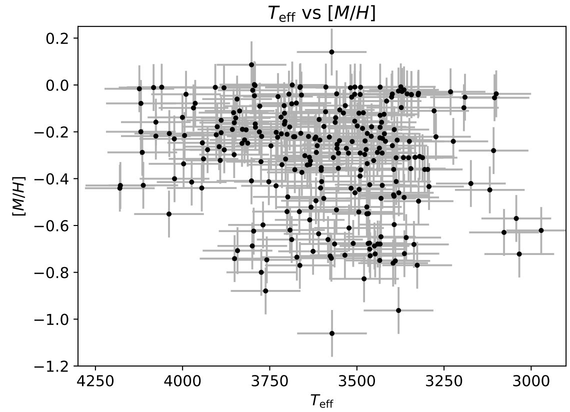

Figure 5.18: $T_{\rm eff}$ and $[M/H]$ from *iSpec* parameter distribution for stars in M dwarf sample, using the temperature estimation method for the normalization.

using this normalization method for our full sample of 289 M dwarfs are in Figs. 5.17 and 5.18. Some biases are clear across the results, with trends across $T_{\rm eff}$ and $[M/H]$ output parameters. A very small number of stars have estimated metallicity values above 0.0 dex as well, and only one of those has $T_{\rm eff} < 4000$ K. When comparing this distribution with the literature values in Figs. 4.8,4.11, 4.13, for example, it is clear that the method has a strong tendency towards underestimating metallicity and the values have an invisible ceiling at $[M/H] = 0.0$ dex. Additionally, a trend with the output $T_{\rm eff}$ for stars below 3750 K also seems to be present. This overall trend in the data results in thin columns of stars with very similar effective temperatures but changing metallicity values. We would expect a more even output parameter distribution instead of results clustered like these. The appearance of these trends seem to suggest that the code itself tends towards specific values for $T_{\rm eff}$ and $[M/H]$ for stars below 3750 K, and will give these values as output for the stars even if they are not the real ones.

Multiple Normalizations

As a result of these trends across the output parameters, we decided to try a second, different method for the normalization of our M dwarf sample. In order to minimize the effect of the choice of our visual $T_{\rm eff}$ on the normalized spectra, we normalized every star in our sample using 6 different synthetic spectra as templates, each created with a different $T_{\rm eff}$ - 3000 K, 3200 K, 3400 K, 3600 K, 3800 K, 4000 K and 4200 K, and fixed values of $\log g = 5.0$ dex and $[M/H] = 0.0$ dex. We chose these values so that both the whole effective temperature parameter range was covered and no extraneous computations were done. This step results in 6 potential normalized spectra for each star in our sample.

Afterward, we apply our pipeline to every possible normalization done for all stars in our sample, and use the resulting χ^2 values to compare every synthesis made for each star. By selecting the output spectra with the smallest χ^2 values, we can find the best fit and normalization $T_{\rm eff}$ for each star in our sample. Table 5.8 shows the output parameters derived for a chosen subsample of stars in common with Terrien et al. (2015), while Figs. 5.19 and 5.20 shows a comparison between template input, output temperature, and $T_{\rm eff}$ taken from Terrien et al. (2015) for some of these stars. We note here that stars like 2M14050849+0312186 are not M dwarfs, but rather late K dwarfs. We also note that the estimated $\log g$ value for 2M19412775+3239512 is lower than expected for a star of that effective temperature and metallicity. The table and plots show how changes in the normalization template can have a pronounced effect on the output values for spectroscopic parameters, as the χ^2 for the fits can vary depending on the quality of the fit.

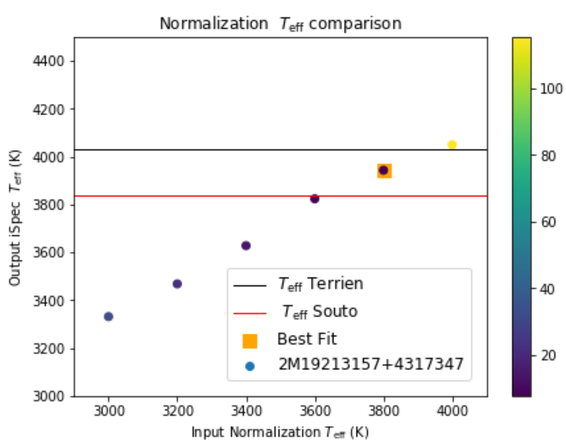

Figure 5.19: Comparison between the input normalization template temperatures (x-axis) and output *iSpec* $T_{\rm eff}$ (y-axis) for star 2M19213157+4317347. Color is given by χ^2. Horizontal lines denotes $T_{\rm eff}$ for this star taken from Terrien et al. (2015) and Souto et al. (2017).

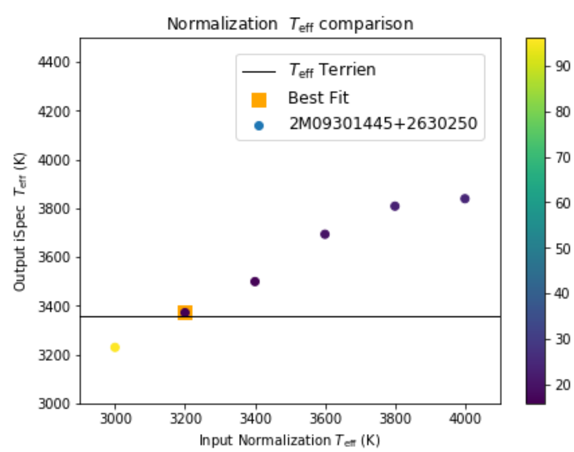

Figure 5.20: Comparison between the input normalization template temperatures (x-axis) and output *iSpec* $T_{\rm eff}$ (y-axis) for star 2M09301445+2630250. Color is given by χ^2. Horizontal lines denotes $T_{\rm eff}$ for this star taken from Terrien et al. (2015)

Figs. 5.21 and 5.22 show, as an example, two normalizations of the spectrum of star 2M09301445+2630250, with templates using either $T_{\rm eff} = 3200$ K and $T_{\rm eff} = 3800$ K. A comparison between the two shows the effect the choice of temperature for the normalization template can have on the output parameters and quality of the synthetic spectrum. Spectra with smaller χ^2, which in this case corresponds to the normalization using a template of $T_{\rm eff} = 3200$ K, corresponds to the best fit for each star.

Table 5.8: Parameters derived for multiple test M dwarfs with different templates used for the normalization. Subscript 'L' indicates the values were taken from the literature (Terrien et al. 2015), and subscript 'T' indicated the temperature for the normalization template. Boldface indicates the best match for each star in the test sample.

Apogee ID	$T_{\rm eff}$	$T_{\rm eff,L}$	$\log g$	$[M/H]$	$[M/H]_L$	Red. χ^2 ($\times 10^3$)	$T_{\rm eff,T}$
2M04310001+3647548	3212	3424	4.24	0.17	0.02	1.63	3000
2M04310001+3647548	**3361**	**3424**	**4.68**	**0.00**	**0.02**	**0.26**	**3200**
2M04310001+3647548	3511	3424	4.81	-0.04	0.02	0.29	3400
2M04310001+3647548	3722	3424	5.40	-0.19	0.02	0.34	3600
2M04310001+3647548	3869	3424	5.40	-0.36	0.02	0.44	3800
2M04310001+3647548	3893	3424	5.40	-0.34	0.02	0.47	4000
2M06412818+1545482	3242	3347	4.71	0.32	0.27	0.38	3000
2M06412818+1545482	3369	3347	4.83	0.14	0.27	0.30	3200
2M06412818+1545482	**3508**	**3347**	**4.98**	**0.01**	**0.27**	**0.29**	**3400**
2M06412818+1545482	3687	3347	5.40	-0.05	0.27	0.38	3600
2M06412818+1545482	3819	3347	5.40	-0.19	0.27	0.48	3800
2M06412818+1545482	3858	3347	5.40	-0.22	0.27	0.52	4000
2M09301445+2630250	3229	3359	4.13	0.21	0.13	2.21	3000
2M09301445+2630250	**3372**	**3359**	**4.66**	**0.12**	**0.13**	**0.37**	**3200**
2M09301445+2630250	3499	3359	4.55	-0.02	0.13	0.39	3400
2M09301445+2630250	3693	3359	5.26	-0.09	0.13	0.46	3600
2M09301445+2630250	3809	3359	5.40	-0.19	0.13	0.54	3800
2M09301445+2630250	3839	3359	5.40	-0.21	0.13	0.56	4000
2M11474440+0048164	**3199**	**3288**	**5.13**	**-0.24**	**-0.09**	**1.09**	**3000**
2M11474440+0048164	3363	3288	5.40	-0.25	-0.09	1.27	3200
2M11474440+0048164	3534	3288	5.40	-0.21	-0.09	0.59	3400
2M11474440+0048164	3500	3288	4.50	0.00	-0.09	3.05	3600
2M11474440+0048164	3503	3288	4.51	-0.01	-0.09	4.48	3800
2M11474440+0048164	3503	3288	4.51	-0.01	-0.09	3.51	4000
2M12212146+5745089	3242	3590	3.99	0.23	-0.02	1.84	3000
2M12212146+5745089	3400	3590	4.60	0.25	-0.02	0.34	3200
2M12212146+5745089	3538	3590	4.59	0.03	-0.02	0.23	3400
2M12212146+5745089	**3701**	**3590**	**4.97**	**-0.02**	**-0.02**	**0.21**	**3600**
2M12212146+5745089	3831	3590	5.00	-0.16	-0.02	0.25	3800
2M12212146+5745089	3864	3590	5.00	-0.16	-0.02	0.28	4000
2M13315838+5443452	3265	3617	4.19	0.36	0.04	2.38	3000
2M13315838+5443452	3411	3617	4.63	0.27	0.04	0.70	3200
2M13315838+5443452	3555	3617	4.66	0.06	0.04	0.54	3400
2M13315838+5443452	**3711**	**3617**	**4.92**	**-0.01**	**0.04**	**0.43**	**3600**
2M13315838+5443452	3832	3617	5.00	-0.10	0.04	0.45	3800
2M13315838+5443452	3899	3617	5.12	-0.11	0.04	0.45	4000
2M14050849+0312186	3413	4087	4.09	0.68	0.40	2.21	3000
2M14050849+0312186	3544	4087	4.03	0.46	0.40	1.81	3200
2M14050849+0312186	3930	4087	4.23	0.40	0.40	1.20	3400
2M14050849+0312186	4235	4087	4.17	0.24	0.40	0.63	3600
2M14050849+0312186	**4312**	**4087**	**4.25**	**0.09**	**0.40**	**0.49**	**3800**
2M14050849+0312186	3574	4087	4.42	-0.01	0.40	4.25	4000
2M19213157+4317347	3331	4030	4.08	0.28	-0.16	0.88	3000
2M19213157+4317347	3468	4030	4.19	0.14	-0.16	0.60	3200
2M19213157+4317347	3628	4030	4.28	-0.04	-0.16	0.38	3400
2M19213157+4317347	3823	4030	4.65	-0.14	-0.16	0.24	3600
2M19213157+4317347	**3943**	**4030**	**4.91**	**-0.19**	**-0.16**	**0.21**	**3800**
2M19213157+4317347	4049	4030	5.18	0.18	-0.16	3.05	4000
2M19412775+3239512	3211	3403	3.99	0.17	-0.33	2.19	3000

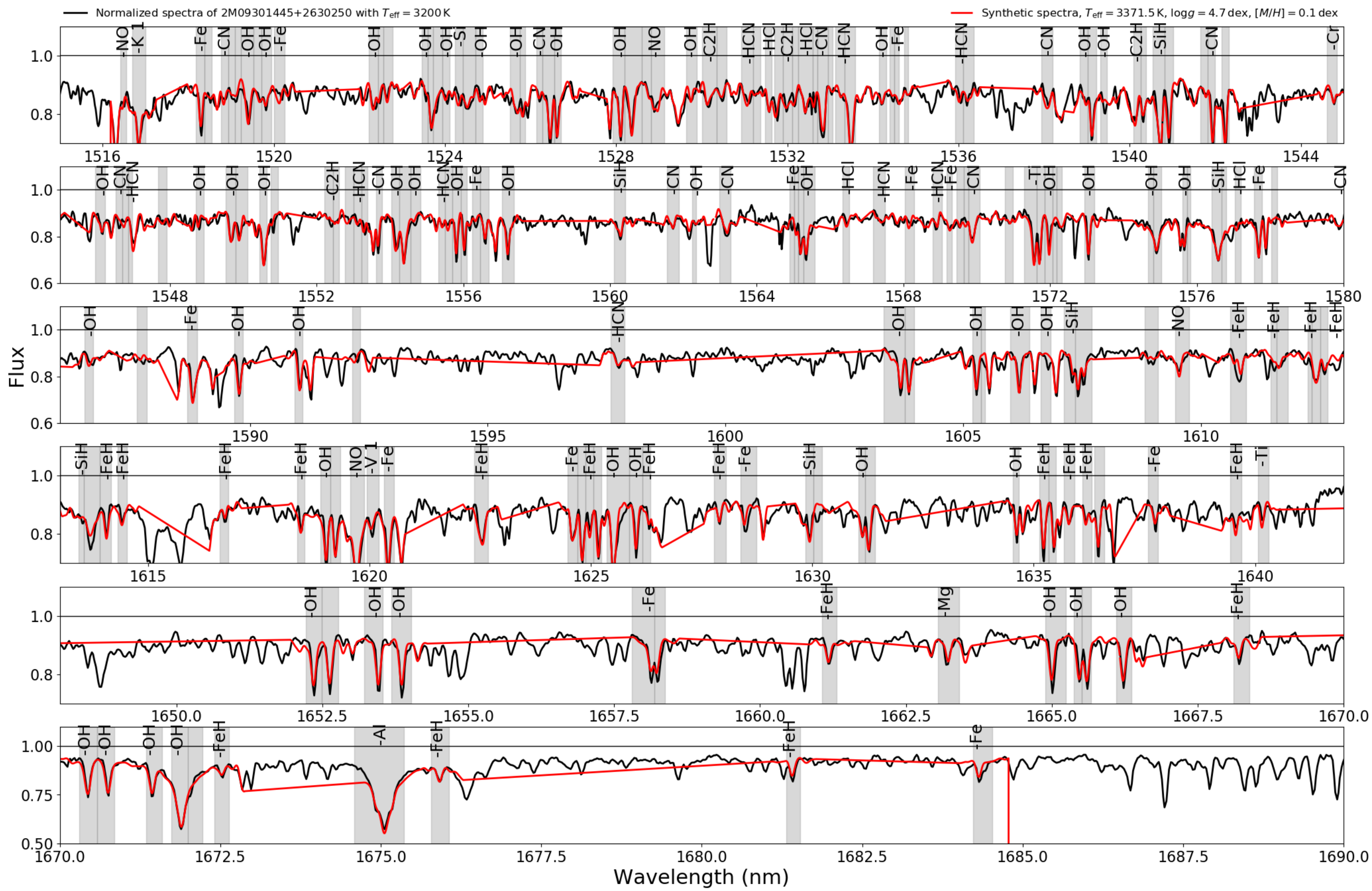

Figure 5.21: Comparison between the observed spectrum of 2M09301445+2630250, normalized using the template method (black) with $T_{\rm eff} = 3200\,$K, and the best match synthetic spectrum for that star (red). The parameters derived with *iSpec* for this spectrum were $T_{\rm eff} = 3371\,$K, $\log g = 4.66\,$dex, $[M/H] = +0.12\,$dex, with $\chi^2 = 15.96$. The areas in grey represent the ones included in the line mask created from these spectra.

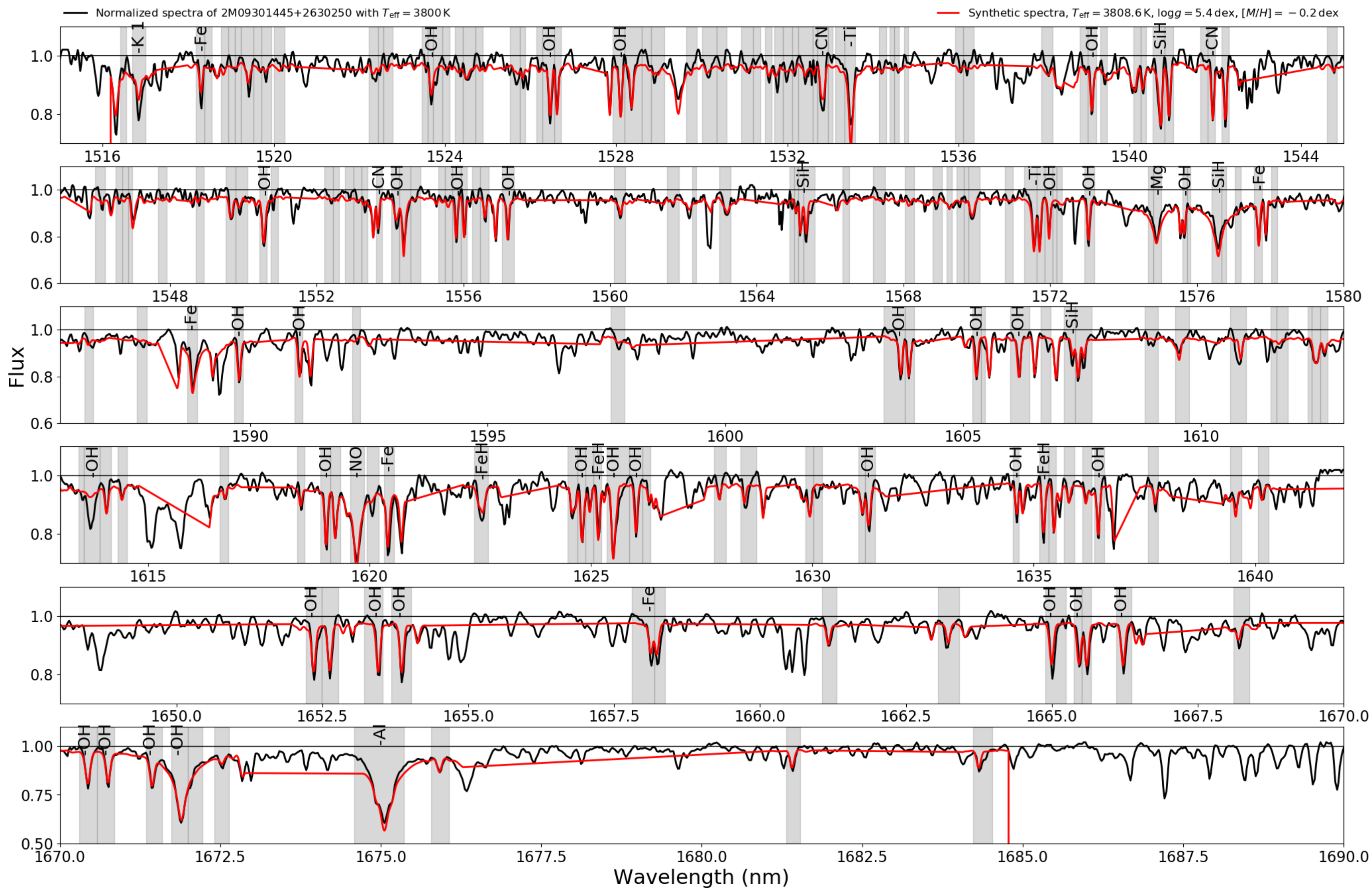

Figure 5.22: Comparison between the observed spectrum of 2M09301445+2630250, normalized using the template method (black) with $T_{\rm eff} = 3800\,{\rm K}$, and the best match synthetic spectrum for that star (red). The parameters derived with *iSpec* for this spectrum were $T_{\rm eff} = 3809\,{\rm K}, \log g = 5.40\,{\rm dex}$, $[M/H] = -0.19\,{\rm dex}$, with $\chi^2 = 23.23$. The areas in grey represent the ones included in the line mask created from these spectra.

The step described above can derive the stellar effective temperature for our sample stars, but an additional step is required to reduce the trends across our $[M/H]$ output parameters. After discovering the $T_{\rm eff}$ resulting in the best normalization template for each star, the normalization process was repeated, using synthetic spectra created using that $T_{\rm eff}$ and different possible metallicities - -1.0 dex, -0.4 dex, -0.2 dex, 0.0 dex, +0.2 dex and +0.4 dex. Surface gravity values were again fixed at $\log g = 4.5$ dex. These $[M/H]$ values were chosen so the parameter space around $[M/H] = 0.0$ dex was best characterized. This was done because we expect, based on $[M/H]$ found on literature, most M dwarfs in our sample have metallicities close to solar (see Figs. 4.8,4.11, 4.13 for examples). Table 5.9 shows a comparison between output parameters derived for the same subsample of stars shown above, this time using different $[M/H]$ for the normalization template. Parameters derived across multiple syntheses of the same star with similar templates are close, indicating the consistency of the method. Parameters synthesized for the test subsample are all close to literature values, and the χ^2 values indicate that the fits are close to the observed spectra. For any star with possible issues or large differences across multiple syntheses, further visual inspections of all matches can give us more confidence in the output spectra and its corresponding stellar parameters.

Using the combination of these two normalization steps, consistent and accurate parameters can be obtained for every individual star in the sample. The disadvantage of this method for normalization is the computational resources required for the synthesis of the whole sample. After dividing the whole sample and parallelization of the process, it would take over two months of full-time computation to derive parameters for our sample of 250 stars. To optimize our usage of computer time, we used spectral indices to narrow the metallicity possibilities for each star in our sample. This was done by testing multiple spectral regions containing either strong lines or an approximate continuum and dividing one of them by the other, then comparing the values of these indices with ASPCAP values for metallicity.

By deriving a trend between the two parameters and extrapolating to our full stellar sample, we can obtain metallicity approximations for all stars in our sample, instead of the limited subsample with available ASPCAP parameters. The chosen metallicity indicator index is:

$$I_{[M/H]} = \frac{f_{1608-1609}/f_{1619.4-1619.9}}{f_{1614.8-1615.8}/f_{1608-1609}} \tag{5.2}$$

, where $f_{w_1-w_2}$ denotes the average flux between the initial and final wavelength for a given

Table 5.9: Parameters derived for multiple test M dwarfs with templates using different $[M/H]$ for the normalization. Subscript 'L' indicates the values were taken from the literature (Terrien et al. 2015), and subscript 'T' indicated the values used for the normalization template. Boldface indicates the best match for each star in the test sample.

Apogee ID	$T_{\rm eff}$	$T_{\rm eff,L}$	$\log g$	$[M/H]$	$[M/H]_L$	Red. $\chi^2 \times 10^3$	$T_{\rm eff,T}$	$[M/H]_T$
2M04310001+3647548	3503	3424	4.50	-0.01	0.02	6.94	3200	-2
2M04310001+3647548	3566	3424	5.11	-0.19	0.02	0.30	3200	-0.6
2M04310001+3647548	**3389**	**3424**	**4.72**	**-0.02**	**0.02**	**0.26**	**3200**	**-0.2**
2M04310001+3647548	3351	3424	4.68	0.04	0.02	0.27	3200	0
2M04310001+3647548	3331	3424	4.72	0.12	0.02	0.28	3200	0.2
2M04310001+3647548	3362	3424	4.67	0.00	0.02	0.26	3200	0.4
2M06412818+1545482	3504	3347	4.50	-0.01	0.27	6.86	3200	-2
2M06412818+1545482	3513	3347	4.82	-0.05	0.27	0.37	3200	-0.6
2M06412818+1545482	**3395**	**3347**	**4.80**	**0.06**	**0.27**	**0.29**	**3200**	**-0.2**
2M06412818+1545482	3360	3347	4.88	0.20	0.27	0.30	3200	0
2M06412818+1545482	3343	3347	4.92	0.29	0.27	0.31	3200	0.2
2M06412818+1545482	3370	3347	4.83	0.14	0.27	0.30	3200	0.4
2M09301445+2630250	3504	3359	4.50	-0.01	0.13	6.24	3200	-2
2M09301445+2630250	3500	3359	4.51	-0.01	0.13	0.46	3200	-0.6
2M09301445+2630250	**3392**	**3359**	**4.62**	**0.05**	**0.13**	**0.36**	**3200**	**-0.2**
2M09301445+2630250	3361	3359	4.65	0.15	0.13	0.37	3200	0
2M09301445+2630250	3343	3359	4.71	0.24	0.13	0.38	3200	0.2
2M09301445+2630250	3370	3359	4.63	0.11	0.13	0.37	3200	0.4
2M11474440+0048164	3547	3288	4.54	-0.04	-0.09	7.72	3000	-2
2M11474440+0048164	3466	3288	5.40	-0.51	-0.09	0.50	3000	-0.6
2M11474440+0048164	3242	3288	5.26	-0.28	-0.09	0.33	3000	-0.2
2M11474440+0048164	3175	3288	5.04	-0.19	-0.09	0.32	3000	0
2M11474440+0048164	**3121**	**3288**	**4.79**	**-0.05**	**-0.09**	**0.32**	**3000**	**0.2**
2M11474440+0048164	3201	3288	5.16	-0.23	-0.09	0.34	3000	0.4
2M12212146+5745089	3505	3590	4.49	-0.01	-0.02	6.68	3600	-2
2M12212146+5745089	3799	3590	4.98	-0.21	-0.02	0.26	3600	-0.6
2M12212146+5745089	3731	3590	4.95	-0.09	-0.02	0.22	3600	-0.2
2M12212146+5745089	**3699**	**3590**	**4.91**	**-0.03**	**-0.02**	**0.20**	**3600**	**0**
2M12212146+5745089	3675	3590	4.81	0.00	-0.02	0.21	3600	0.2
2M12212146+5745089	3703	3590	4.95	-0.03	-0.02	0.21	3600	0.4
2M13315838+5443452	3524	3617	4.48	-0.04	0.04	6.62	3600	-2
2M13315838+5443452	3808	3617	5.00	-0.18	0.04	0.49	3600	-0.6
2M13315838+5443452	**3737**	**3617**	**4.98**	**-0.02**	**0.04**	**0.43**	**3600**	**-0.2**
2M13315838+5443452	3702	3617	4.86	-0.02	0.04	0.44	3600	0
2M13315838+5443452	3690	3617	4.82	0.02	0.04	0.46	3600	0.2
2M13315838+5443452	3719	3617	4.94	-0.02	0.04	0.44	3600	0.4
2M14050849+0312186	4500	4087	4.12	-0.25	0.40	1.01	4000	-2
2M14050849+0312186	4385	4087	4.33	-0.03	0.40	0.58	4000	-0.6
2M14050849+0312186	4340	4087	4.33	0.05	0.40	0.57	4000	-0.2
2M14050849+0312186	4312	4087	4.48	0.13	0.40	0.39	4000	0
2M14050849+0312186	**4300**	**4087**	**4.55**	**0.25**	**0.40**	**0.37**	**4000**	**0.2**
2M14050849+0312186	4327	4087	4.35	0.09	0.40	0.41	4000	0.4
2M19213157+4317347	4081	4030	5.40	-0.36	-0.16	0.57	3800	-2
2M19213157+4317347	4001	4030	5.05	-0.28	-0.16	0.28	3800	-0.6
2M19213157+4317347	3961	4030	4.95	-0.20	-0.16	0.21	3800	-0.2
2M19213157+4317347	**3929**	**4030**	**4.84**	**-0.17**	**-0.16**	**0.20**	**3800**	**0**
2M19213157+4317347	3860	4030	4.68	-0.09	-0.16	0.23	3800	0.2
2M19213157+4317347	3945	4030	4.92	-0.18	-0.16	0.21	3800	0.4
2M19412775+3239512	3504	3403	4.50	-0.01	-0.33	6.86	3200	-2

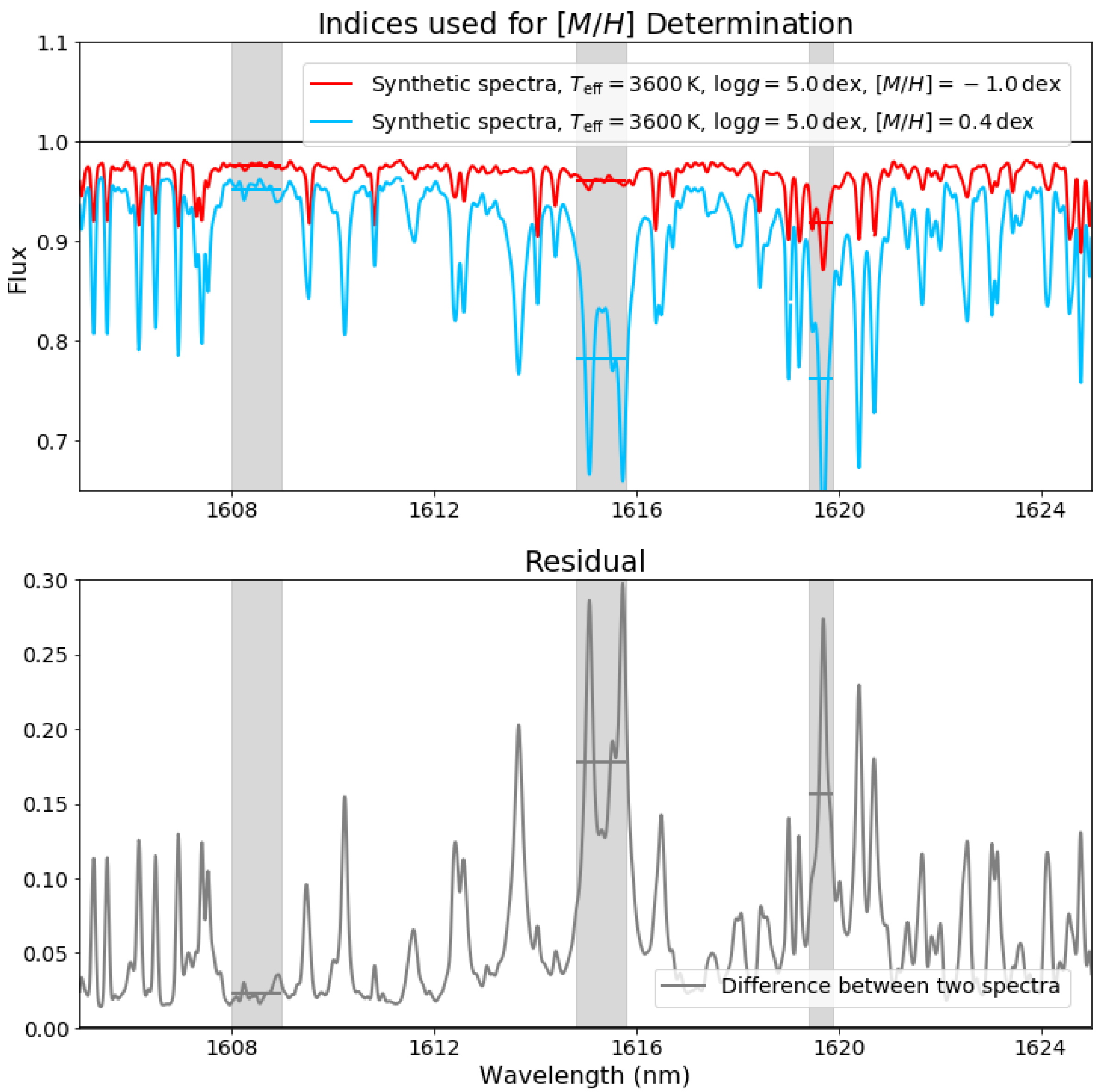

Figure 5.23: Three wavelength areas taken into account to create our metallicity index. Greyed areas the ones used for computing $I_{[M/H]}$ - 1608-1609 nm (approximate continuum), 1614.8-1615.8 nm (Ca doublet) and 1619.4-1619.9 (Ca line). Figure shows two different synthetic spectra, created with $T_{\rm eff} = 3600\,\mathrm{K}$,$\log g = 5.0\,\mathrm{dex}$, and $[M/H] = -1.0\,\mathrm{dex}$ and $[M/H] = +0.4\,\mathrm{dex}$.

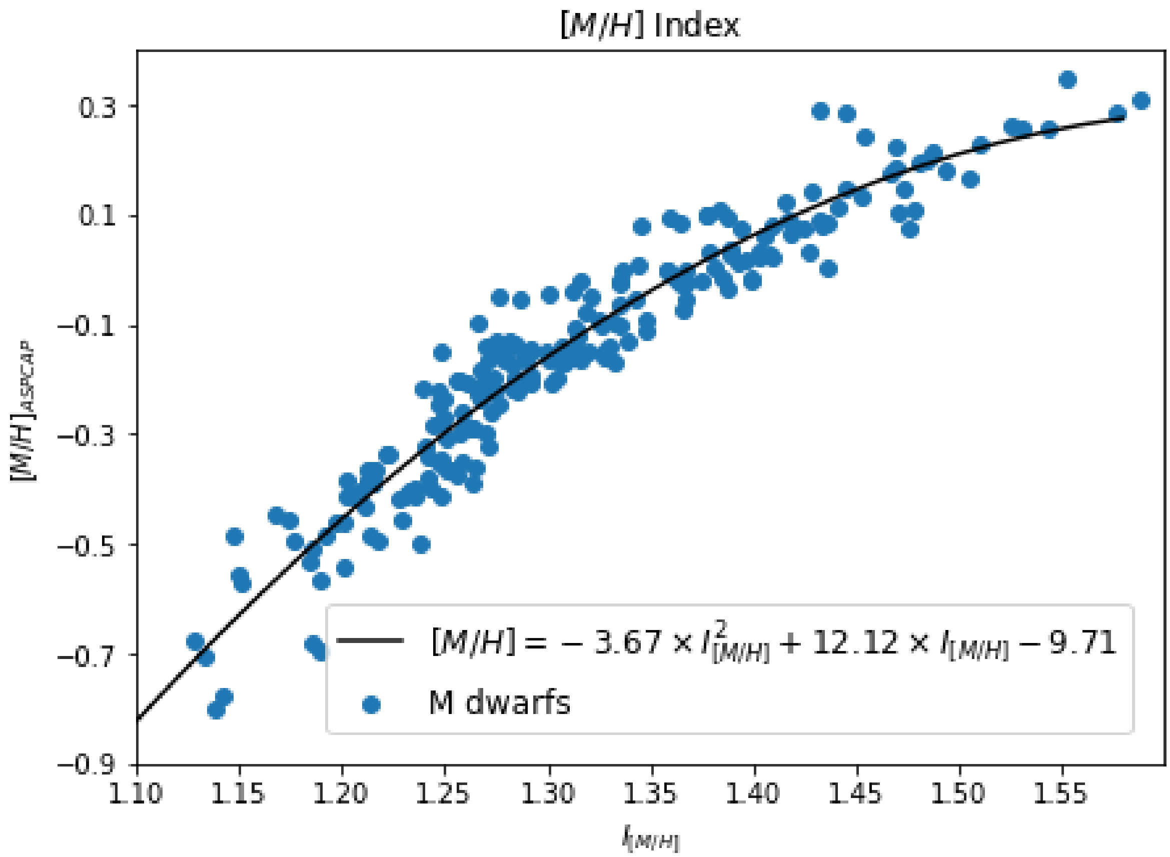

Figure 5.24: Correlation between our calculated index and ASPCAP values for the stellar metallicity, for our sample M dwarfs. The black line shows a second degree polynomial best approximating the relation between the two variables.

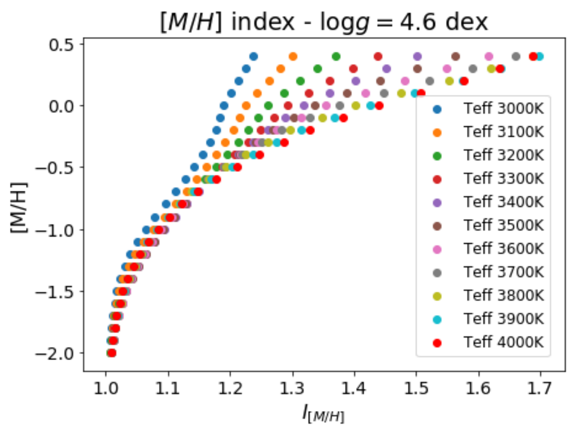

Figure 5.25: $I_{[M/H]}$ and $[M/H]$ for synthesized spectra with $\log g = 4.6$ dex.

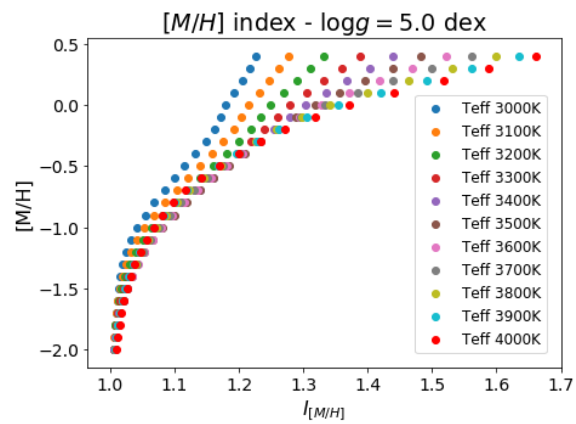

Figure 5.26: $I_{[M/H]}$ and $[M/H]$ for synthesized spectra with $\log g = 5.0$ dex.

star. This index combination was chosen empirically as it had the best correlation with ASPCAP metallicity values out of over 20 tested indices and index combinations. Fig. 5.23 shows the region chosen for this index calculation on two different synthetic spectra, and Fig. 5.24 shows the relation between the calculated index and the ASPCAP metallicity values available, with a second-degree polynomial indicating the relation between the two variables:

$$[M/H] = -3.67 \times I^2_{[M/H]} + 12.12 \times I_{[M/H]} - 9.71 \tag{5.3}$$

The final results table (see Table B.2 in the appendix) contains the $[M/H]$ value used for the final normalization for each star in our M dwarf sample.

Figures 5.25 and 5.26 show a side-by-side comparison for $I_{[M/H]}$ for synthesized stars with $\log g = 4.6$ dex and $\log g = 5.0$ dex, respectively. These figures were included to demonstrate the effects that changes in temperature and surface gravity can have on the relationship between $I_{[M/H]}$ and $[M/H]$.

Each star was then normalized with 3 different metallicity values depending on the approximate $[M/H]$ determined from their $I_{[M/H]}$. These are summarized in Table 5.10. By normalizing each M dwarf spectra with 3 different metallicity values instead of 6, we reduce the time taken for the synthetic spectra matching in half. The final results table (see Table B.2 in the appendix) contains the $[M/H]$ value used for the final normalization for each star in our M dwarf sample.

Table 5.10: Metallicity values used for the normalization of M dwarfs.

$[M/H]$ (from index)	Values used for Normalization
$[M/H] < -0.4$ dex	-1.2 dex; -0.8 dex; -0.4 dex
-0.4 dex< $[M/H] < -0.2$ dex	-0.6 dex; -0.4 dex; -0.2 dex
-0.2 dex< $[M/H] < -0.1$ dex	-0.4 dex; -0.2 dex; 0.0 dex
-0.1 dex< $[M/H] < 0.0$ dex	-0.2 dex; 0.0 dex; 0.2 dex
0.0 dex< $[M/H] < 0.1$ dex	-0.2 dex; 0.0 dex; 0.2 dex
$[M/H] > 0.1$ dex	0.0 dex; 0.2 dex; 0.4 dex

5.4.2 Line list

The M dwarf line-list required special attention as these stars have water (H_2O) lines that are not visible in hotter stars. These water lines form a thick blanket that makes the flux continuum harder to identify, as shown in Figure 5.15. The line list was originally published in Barber et al. (2006), and it was retrieved from Bertrand Plez's website [3]. A total of 1 263 825 water lines were included in the M dwarf line list, along with 85334 lines from other molecules and atoms that come from the fusion list described in Section 5.2.7. This resulted in a final list of 1 349 159 lines. These added water lines were only compatible with syntheses made using *Turbospectrum*, confirming it as our code of choice for this project.

5.4.3 Line mask

M dwarf spectra have relevant lines for parameter determination in the H-band different than those of FGK stars. Therefore, for M dwarf syntheses, a separate line mask had to be constructed. The star Ross128 (2M11474440+0048164), as an APOGEE M-dwarf with $S/N \sim 229$ that has previously been characterized by Souto et al. (2018), was chosen as the basis for this line mask. This star was chosen as it is one of the best-characterized stars in the literature, its observations have a good S/N, and is among the mid-late, and therefore harder to characterize, part of the stellar sample. A synthetic spectrum was generated using the parameters found for the star by Souto et al. (2018) (T_{eff} $3231\,\text{K}$, $[Fe/H]$ 0.03 and $\log g = 4.96\,\text{dex}$). This synthetic spectrum was overplotted on the observed one (normalized) and matching lines and areas were selected for the line mask displayed in Fig. 5.27. The areas where the synthesis did not match the spectrum were discarded to create the final line mask shown. The final compiled line mask is available for consultation in the appendix in Table A.2.

[3] http://www.pages-perso-bertrand-plez.univ-montp2.fr/

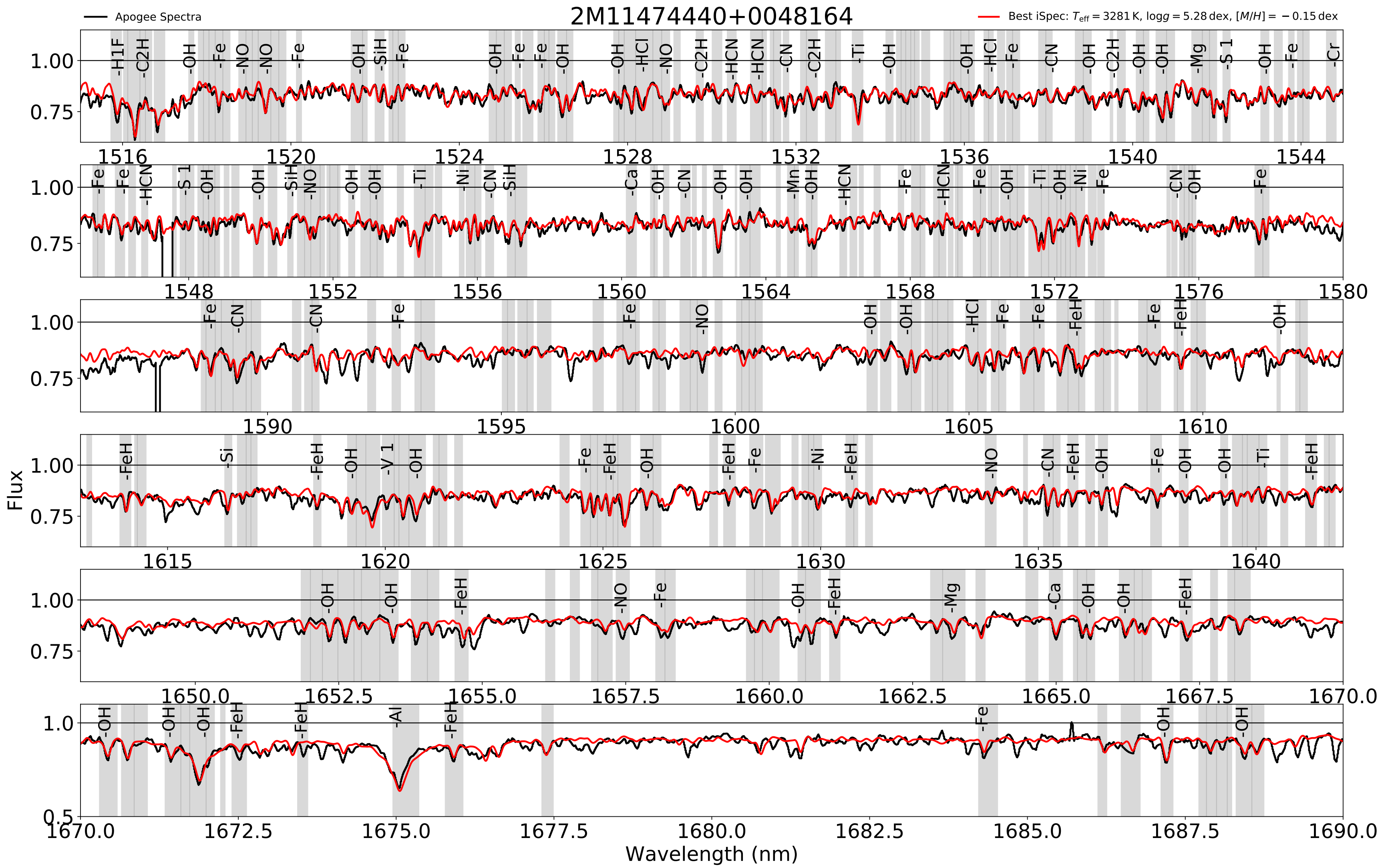

Figure 5.27: Comparison between the observed spectrum of Ross 128 (2MASS J11474440+0048164), normalized using the template method (black), and a synthetic spectrum created using the literature (Souto et al. 2018) parameters for that star (red). The parameters used to generate the synthetic spectrum were $T_{\rm eff} = 3231\,\mathrm{K}$,$\log g = 4.96\,\mathrm{dex}$, $[M/H] = +0.03\,\mathrm{dex}$. The areas in grey represent the ones included in the line mask created from these spectra.

Chapter 6

Synthesis of APOGEE FGK stellar spectra

This Chapter is dedicated to the derivation of stellar parameters for FGK stars. It includes every step necessary for the synthesis of their spectra, as well as the results obtained with our pipeline. Its main results, as well as some of the text, have been published as **?** and is reproduced here with permission from Astronomy & Astrophysics, © ESO.

6.1 Results

The 3748 stars in our sample were synthesized using the methodology described in Chapter 5. Fig. 6.1 shows the distribution of their $\log g$ vs $T_{\rm eff}$ values, color-coded by subset and with overplotted isochrones from PARSEC (Bressan et al. 2012). As expected from our selection of objects described in Section 4.2, the large majority of the stars synthesized fall within a rather small range of parameters, corresponding to FGK main-sequence stars. A small number of stars exhibit lower temperatures than 5 000 K, which are subgiants from the CPS sample ($\log g < 3.9$ dex) and cooler dwarf stars in the PASTEL sample. The $\log g$ for these colder dwarf stars seems to be slightly underestimated, as they are outside the range of the isochrones. Moreover, the $\log g$ of the hottest stars in the sample seems to be overestimated [1]. Therefore, we decided to check in the literature for available $\log g$ sources to better calibrate our values, so they would be more accurate and realistic.

[1] This is a common result when deriving spectroscopic $\log g$, see for example Delgado Mena et al. (2017) or Molenda-Żakowicz et al. (2013)

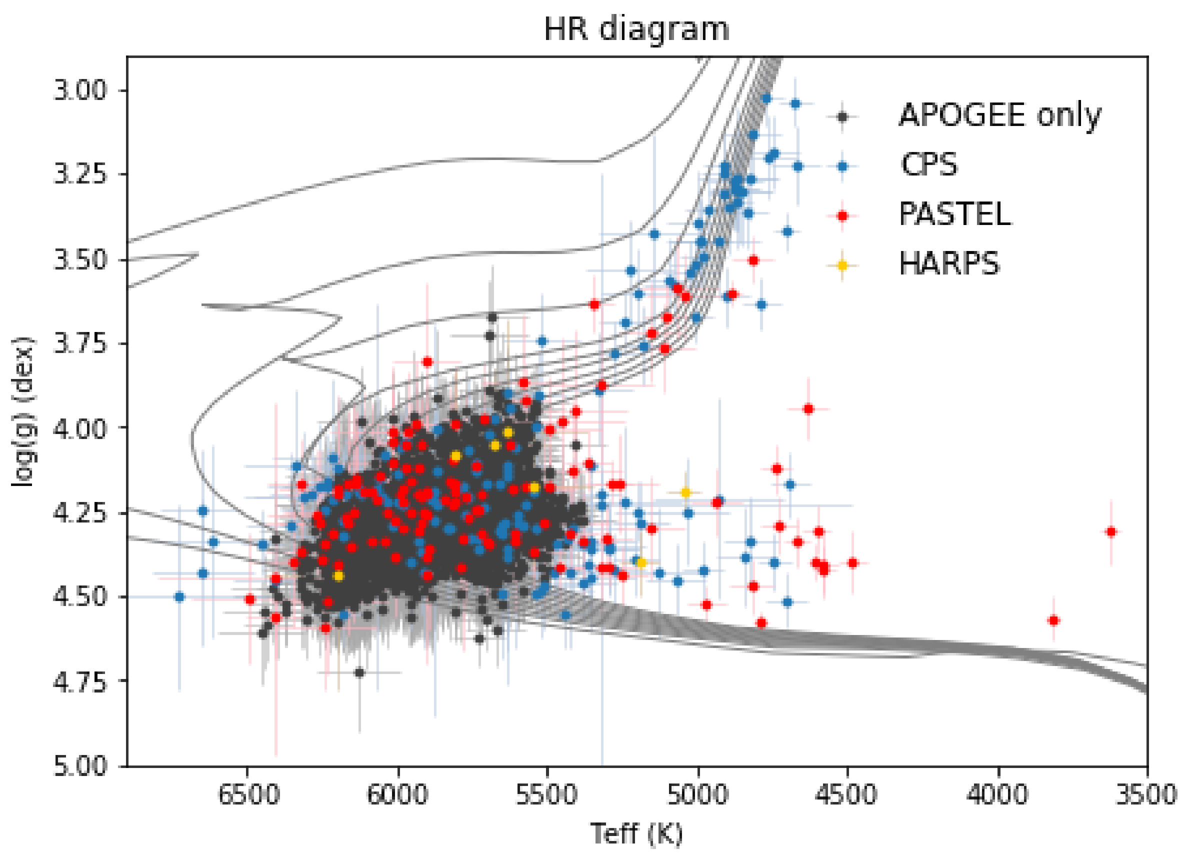

Figure 6.1: Pseudo-HR diagram of our results with the full sample, plotting both the derived $T_{\rm eff}$ and the $\log g$ for all the stars in the sample. Stars are color-coded to indicate their common source (if any). Worst outlier stars are excluded from this plot. PARSEC isochrones from Bressan et al. (2012) are overplotted.

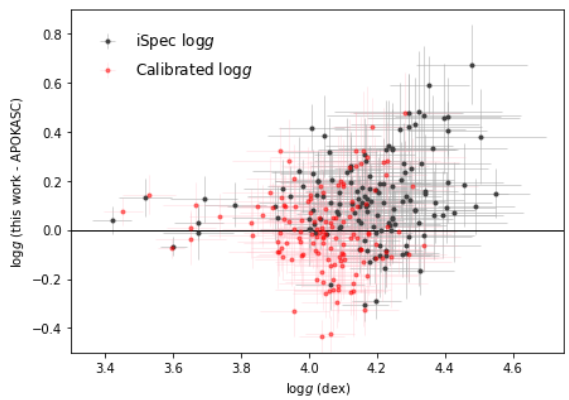

Figure 6.2: Comparison between our pipeline's $\log g$ output values and the ones published by Serenelli et al. (2017), before (black) and after (red) calibration.

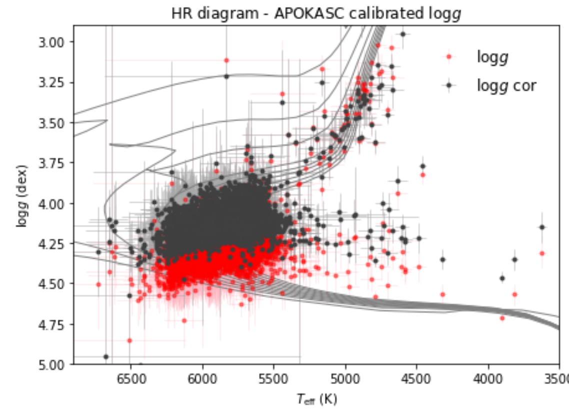

Figure 6.3: Pseudo-HR diagram showing $T_{\rm eff}$ as derived by our pipeline and $\log g$ values after calibration using APOKASC calibration.

We found three available sources that provide either surface gravity values for FGK dwarf stars or equations to calibrate spectroscopic $\log g$. The first paper found was Serenelli et al. (2017). This work uses Kepler and APOGEE data to derive spectroscopic and asteroseismic parameters for 415 FGK dwarfs in the Kepler sample. In particular, $T_{\rm eff}$ and $[M/H]$ values from ASPCAP and asteroseismic frequencies determined with Kepler observations are used together to determine stellar mass, radius and surface gravity using scaling relations and grid-based modeling. By cross-matching their sample with ours, we found 135 stars in common between them, and, by comparing our $\log g$ values with theirs, we could derive equations to calibrate our values. Fig. 6.2 shows a comparison between our derived $\log g$ values and the ones in Serenelli et al. (2017), as well as calibrated $\log g$ values. The calibrated values were obtained using Equation 6.1, and they are plotted gray in an HR-diagram in Fig. 6.3. In red we plot our original $\log g$ values for reference.

$$\log g_{cor} = \log g \times 0.784 + 0.77129 \tag{6.1}$$

The resulting calibrated values have a very poor agreement with the overplotted isochrones for most of the stars in our sample, especially ones around 5000-4500 K. A comparison between the calibrated and uncalibrated $\log g$ values shows that this calibration does not improve the fit with the isochrones. Therefore, we decided to test other possible calibrations for $\log g$ in the literature.

Mortier et al. (2014) describes corrections to stellar surface gravity using transits and asteroseismology. This paper includes an extensive comparison between asteroseismic, transit and spectroscopic methods to derive surface gravity. It also proposes two empirical equations for corrections of spectroscopic $\log g$ with the $T_{\rm eff}$ based on either transit (equation 3) or asteroseismic surface gravities (equation 4). We decided to test these two empirical equations with our data, to assess which one best calibrates our results to approach the isochrones available.

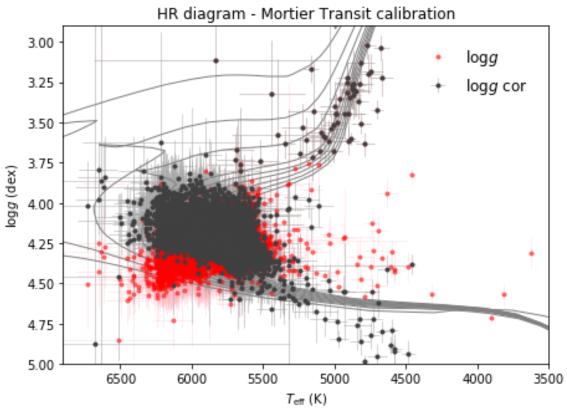

Figure 6.4: Pseudo-HR diagram showing $T_{\rm eff}$ as derived by our pipeline and $\log g$ values after calibration using equation 3 (transit-method) from Mortier et al. (2014).

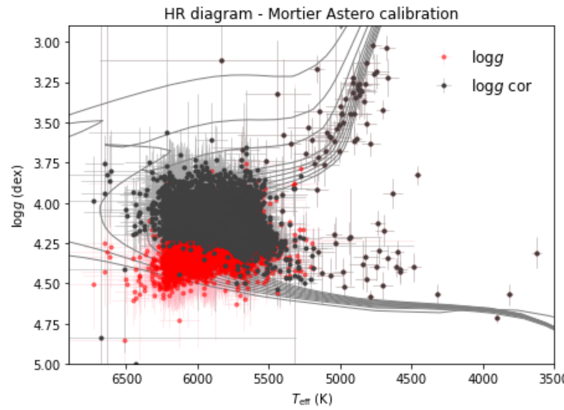

Figure 6.5: Pseudo-HR diagram showing $T_{\rm eff}$ as derived by our pipeline and $\log g$ values after calibration using equation 4 (asteroseismology-method) from Mortier et al. (2014).

We show in Figs. 6.4 and 6.5, in gray, the two possible $\log g$ calibrations from equations in Mortier et al. (2014). In red we also plot our original $\log g$ values for reference. The main problem with the 'transit' calibration (Fig. 6.4) is that it overestimates surface gravities for stars below 5700 K, with them having values around $\log g = 4.75$ dex instead of 4.3 dex, and the fit to the isochrones looks worse than for $\log g$ values derived by our pipeline. The calibration with asteroseismic values (Fig. 6.5) presents the opposite problem, with an underestimation of $\log g$ values for the whole sample, as most stars fall within the subgiants branch rather than main-sequence as expected. Both calibrations are inadequate, and we decided to test other possible $\log g$ calibrations.

Similar behavior for $\log g$ values of FGK dwarfs in the HR diagram has been observed after using the ionization method to derive $\log g$. Therefore, we decided to apply the corrections based on the trigonometric $\log g$ derived in Delgado Mena et al. (2017). We considered using a similar method to derive trigonometric $\log g$ values for our stellar sample, but the stars in our sample are further away from the solar system when compared to their sample (200 pc vs 60 pc). This means that parallaxes are less accurate and extinction in the interstellar medium becomes an important factor in the calculation of trigonometric $\log g$ and making the method itself less reliable. Therefore, we decided to use equations 1,2 and 3 from Delgado Mena et al.

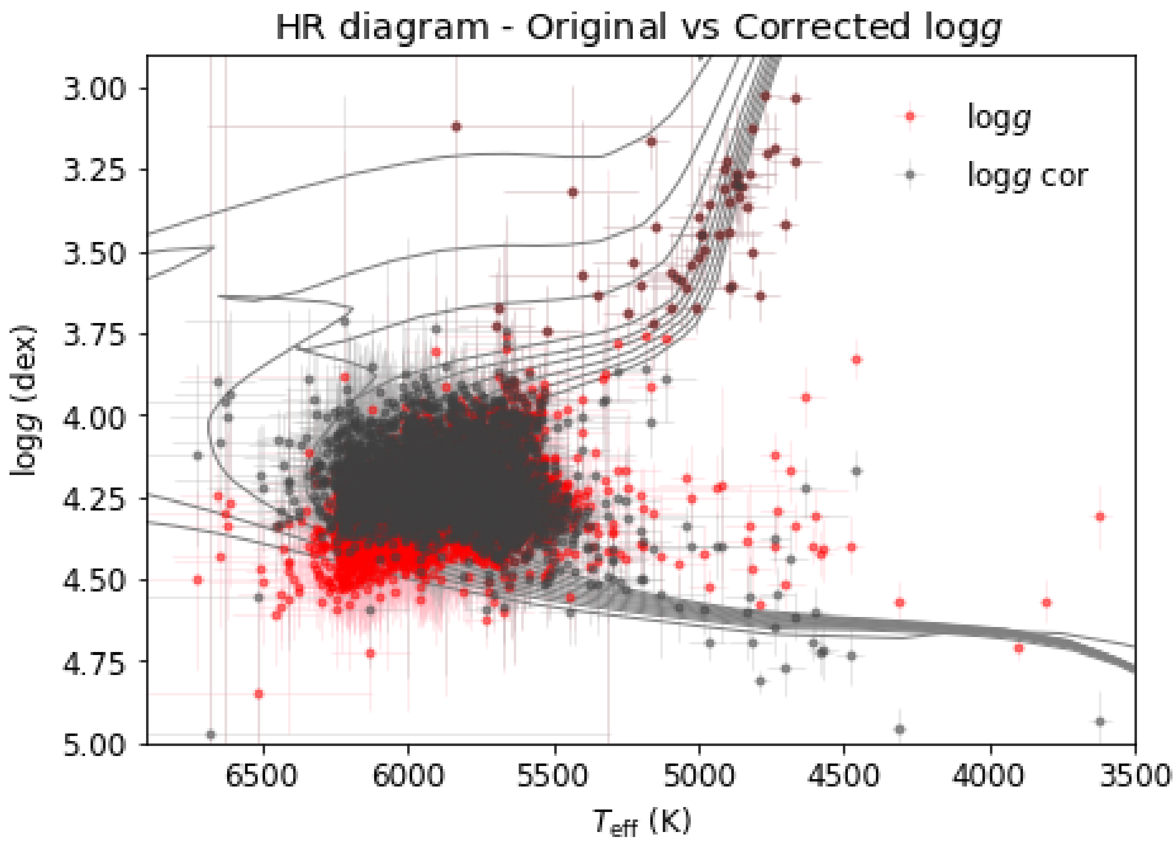

Figure 6.6: Pseudo-HR diagram of our results with the full sample, plotting both the derived $\log g$ and $\log g$ after corrections based on trigonometric $\log g$ from Delgado Mena et al. (2017) against $T_{\rm eff}$ for all the stars in the sample. Worst outlier stars are excluded from this plot. PARSEC isochrones from Bressan et al. (2012) are overplotted.

(2017) as they are published to calibrate our $\log g$ values. Fig. 6.6 shows in red the distribution of both our derived (red) and corrected (gray) $\log g$ against $T_{\rm eff}$. Despite the presence of a $\log g$ underestimation for the hottest stars in our sample, the calibration using these equations proved to be the one resulting in values closer to the ones predicted by the isochrones. They are therefore included as $\log g_{cor}$ in Table B.1.

The $[M/H]$ histograms for each significant subsample are shown in Fig. 6.7. The $[M/H]$ values by *iSpec* follow a Gaussian distribution that peaks around 0.0 dex, the expected average metallicity for stars in the solar neighborhood, but our sample exhibits fewer lower metallicity stars when compared to the solar neighborhood sample (as seen, for example, in Delgado Mena et al. 2017), and plotted in Fig. 6.8. This was expected for our APOGEE-only subsample, since we restricted the sample by metallicity ($-0.5 < [M/H] < +0.5$ dex only).

To reveal the challenges of synthesizing APOGEE spectra, both the observed APOGEE and synthesized spectra for eight distinct stars are shown in Figs. 6.9 to 6.16. For each star,

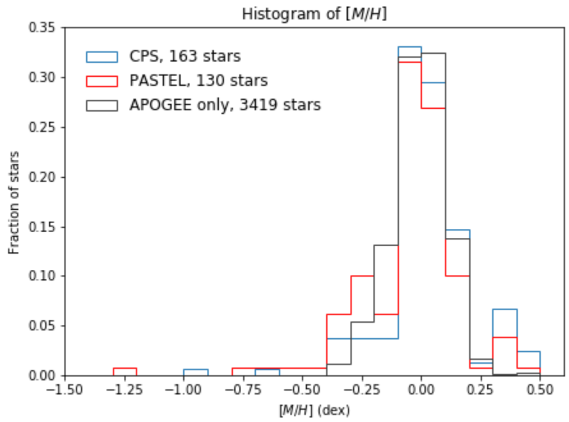

Figure 6.7: Histogram with the metallicity distribution of the final sample, divided by subsamples of stars in common with other catalogs. Values plotted are the output of our pipeline. Worst outlier stars are excluded from this histogram.

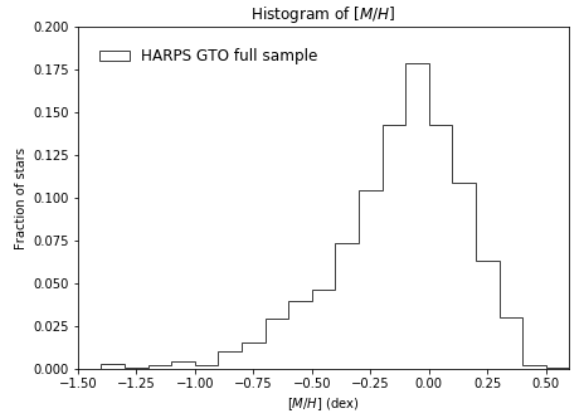

Figure 6.8: Histogram with the metallicity distribution published by Delgado Mena et al. (2017) for 1059 stars in the HARPS GTO sample.

the APOGEE spectrum is shown in black, the 'Best fit' spectrum (synthetic spectrum created with the parameters found by our methodology) is shown in red, and the synthetic spectrum created with the full line-list and using the literature parameters is shown in blue. Therefore, in each figure, the blue spectrum represents the expected spectrum of each star considering its derived parameters from high-res optical spectra.

The spectrum of star 2M19505021+4804508 (BD+47 2936[2], part of PASTEL sub-sample) is shown in Fig. 6.9. The best match parameters derived were $T_{\rm eff} = 4788 \pm 29$ K,$\log g = 4.58 \pm 0.03$ dex, $[M/H] = +0.41 \pm 0.01$ dex, and the ones published by PASTEL were $T_{\rm eff} = 4792 \pm 12$ K,$\log g = 4.59 \pm 0.02$ dex, $[M/H] = +0.33 \pm 0.01$ dex. The available ASPCAP parameters for this star are $T_{\rm eff} = 4797$ K and $[M/H] = +0.38$ dex and $\log g = 4.47$ dex . This is a star significantly colder ($T_{\rm eff} \sim 4800$ K) and more metal-rich than the Sun ($[M/H] \sim +0.4$ dex), so analyzing synthetic spectra for this star can show the flexibility of our method for stars that are not solar-type. The figure shows that the differences between the pipeline's best fit and a synthetic spectrum created with PASTEL parameters are very small, with these two spectra overlapping for almost the full wavelength range. As for the observed spectrum, some regions suggest possible continuum normalization problems (1615-1625 nm), with the observed spectrum being consistently below the synthetic spectra. Despite the synthesized lines having accurate shapes and depths, the normalization might be a reason for the metallicity overestimation (compared with literature values).

[2]http://simbad.u-strasbg.fr/simbad/sim-id?Ident=2Mass+j19505021%2B4804508

In Fig. 6.10 we show the star 2M01081597+5455148 (HD 6582 [3]), member of the CPS sample and one of APOGEE's calibration stars. The best match parameters derived were $T_{\rm eff} = 5639 \pm 163$ K,$\log g = 4.46 \pm 0.20$ dex, $[M/H] = -0.66 \pm 0.07$ dex, and the ones published in CPS were $T_{\rm eff} = 5316 \pm 25$ K,$\log g = 4.66 \pm 0.028$ dex, $[M/H] = -0.73 \pm 0.01$ dex. The available ASPCAP parameters for this star are $T_{\rm eff} = 5246$ K and $[M/H] = -0.73$ dex and $\log g = 4.15$ dex . Our values for $T_{\rm eff}$ and $[M/H]$ using the H-band spectrum for this star are higher than the ones derived from its optical spectra, while our $\log g$ value is lower. We remind the reader that for our synthesis only the gray-shaded areas are considered (line-mask, see Section 5.2.7). It can be seen from the figure that while our method and values can synthesize several lines successfully (e.g. 1587-1600 nm), others are better parametrized using the optical-derived CPS values (e.g 1671-1676 nm).

The spectrum of star 2M16410822-0251258 (HD 150433 [4]) is shown in Fig. 6.11. The star has a confirmed substellar companion detected (Mayor et al. 2011). The best match parameters derived were $T_{\rm eff} = 5547 \pm 201$ K,$\log g = 4.17 \pm 0.23$ dex, $[M/H] = -0.26 \pm 0.09$ dex, and the ones published by the HARPS GTO were $T_{\rm eff} = 5665 \pm 12$ K,$\log g = 4.43 \pm 0.02$ dex, $[M/H] = -0.36 \pm 0.01$ dex. The available ASPCAP parameters for this star are $T_{\rm eff} = 5548$ K and $[M/H] = -0.28$ dex and $\log g = 4.22$ dex . For this star, and despite there being a 100 K and 0.1 dex difference between the best fit and the literature parameters, both synthetic spectra are good fits for the observed one. There are some lines well-fitted by them (Mg triplet from 1575 to 1577 nm, Si at 1637 nm) but several lines are underestimated as well (Al doublet at 1671 and 1675 nm). Adjustments in alpha levels and individual elemental abundances may be necessary to derive more precise synthetic spectra for this star.

In Fig. 6.12, the spectrum of star 2M19302763+4245513 (KOI-2687 [5]) is shown. This star, according to Huang et al. (2012), has a planetary companion candidate, and, parameter-wise, is one of the stars most similar to the Sun found in the sample. The best match parameters derived were $T_{\rm eff} = 5653 \pm 47$ K,$\log g = 4.31 \pm 0.06$ dex, $[M/H] = -0.01 \pm 0.02$ dex, and the ones published in CPS were $T_{\rm eff} = 5770 \pm 25$ K,$\log g = 4.5 \pm 0.028$ dex, $[M/H] = +0.02 \pm 0.01$ dex. The available ASPCAP parameters for this star are $T_{\rm eff} = 5671$ K and $[M/H] = +0.04$ dex and $\log g = 4.47$ dex . A comparison with the solar spectrum in Fig. 5.14 will show that both star's spectra are extremely similar, and so are the synthetics. Most lines are correctly

[3] http://simbad.u-strasbg.fr/simbad/sim-id?Ident=HD+6582
[4] http://simbad.u-strasbg.fr/simbad/sim-id?Ident=HD+150433
[5] http://simbad.u-strasbg.fr/simbad/sim-id?Ident=KOI-2687

synthesized, with accurate shapes and depths, and the synthesis with CPS parameters is very close to the method's best fit for the star. There is a slight difference between the observed and synthetic spectrum around 1617 nm, but this seems to be caused by an issue with the observed spectrum and not by any problem in the method. There are some small differences in lines across the whole spectrum (at 1561 and 1573 nm, for example) but the overall fit is very accurate and close to the observed spectrum. Despite this, there is a difference of over 110 K in $T_{\rm eff}$ between the CPS literature values and the ones derived by this pipeline. Since the synthetic spectra with both sets of parameters are very similar, the difference can be explained by degeneracies in the parameter space causing both parameter combinations to produce similar synthetic spectra. In the case of both this star and the previous one, we find that our best matching parameters are closer to the ones derived by ASPCAP than the ones derived using observations in the optical wavelength range. This suggests differences in the spectra itself caused by the analyzed wavelength range.

In Fig. 6.13, the spectrum of star 2M12192484+3937289 (HD 107211 [6]) is shown. This is a star with a $T_{\rm eff}$ very close to the Sun but with significantly higher metallicity. The best match parameters derived were $T_{\rm eff} = 5771 \pm 55$ K,$\log g = 4.26 \pm 0.06$ dex, $[M/H] = +0.22 \pm 0.02$ dex, and the ones published in CPS were $T_{\rm eff} = 5792 \pm 25$ K,$\log g = 4.23 \pm 0.028$ dex, $[M/H] = +0.33 \pm 0.01$ dex. The available ASPCAP parameters for this star are $T_{\rm eff} = 5575$ K and $[M/H] = +0.27$ dex and $\log g = 4.22$ dex . The synthetic spectrum with our best fit parameters follows the observed one closely across the full wavelength range, and is an accurate match for the observed one, as evidenced by differences in the Mg lines around 1576 nm and 1638 nm. Overall, the synthetic spectrum seems to be a good match for the observed one, and it shows how the method can provide accurate spectrum for metal-rich stars.

The star 2M19250004+4913545 (Kepler-36 [7], Fig. 6.14) has two sub-stellar companions detected (Ford et al. 2011; Rowe et al. 2014). The best match parameters derived were $T_{\rm eff} = 6127 \pm 213$ K,$\log g = 4.21 \pm 0.31$ dex, $[M/H] = -0.07 \pm 0.09$ dex, and the ones published in CPS were $T_{\rm eff} = 6006 \pm 25$ K,$\log g = 4.05 \pm 0.028$ dex, $[M/H] = -0.17 \pm 0.01$ dex. The available ASPCAP parameters for this star are $T_{\rm eff} = 6009$ K and $[M/H] = -0.21$ dex and $\log g = 4.18$ dex . Our derived values are higher than the ones from CPS. However, considering our relatively larger errors (due to its APOGEE spectrum's $S/N \sim 122$), $T_{\rm eff}$ and $\log g$ are still

[6] http://simbad.u-strasbg.fr/simbad/sim-id?Ident=HD+107211
[7] http://simbad.u-strasbg.fr/simbad/sim-id?Ident=Kepler-36

consistent with the CPS values. As for the spectra, the depth of many lines also clearly varies between both synthetic spectra, with the CPS results spectrum being deeper in many cases (e.g Iron line at 1529 nm or Silicon line at 1668 nm). Other spectral features are similar between both spectra (e.g. Aluminum lines at 1671 and 1675 nm) and match the observed spectrum as well.

The star 2M19144528+4109042 (KOI-85 [8], Fig. 6.15) has 3 sub-stellar companions detected (Borucki et al. 2011; Rowe et al. 2014). The best match parameters derived were $T_{\mathrm{eff}} = 6195 \pm 164\,$K,$\log g = 4.28 \pm 0.21\,$dex, $[M/H] = +0.11 \pm 0.06\,$dex, and the ones published in CPS were $T_{\mathrm{eff}} = 6149 \pm 25\,$K,$\log g = 4.13 \pm 0.028\,$dex, $[M/H] = +0.15 \pm 0.01\,$dex. The available ASPCAP parameters for this star are $T_{\mathrm{eff}} = 6240\,$K and $[M/H] = +0.12\,$dex and $\log g = 4.45\,$dex . Like the previous example star, our temperature and surface gravity values for this star are above the ones measured using optical spectra and published in the CPS catalog. For the metallicity, the values are slighter lower. For all 3 parameters, however, the derived values are within each other's error margins. Both synthetic spectra are rather similar between themselves and are accurate matches to the observed spectrum; the most significant differences appear around the strong Hydrogen line about 1681.1 nm and continuum around 1640 nm. There are also differences in line depths across the spectrum, most noticeably the Silicon line at wavelength 1596 nm. This can be explained by the differences in metallicity between the two synthetic spectra.

The spectrum for star 2M06504983-0032270 (HD 49933) is shown in Fig. 6.16. The best match parameters derived were $T_{\mathrm{eff}} = 6727 \pm 293\,$K,$\log g = 4.5 \pm 0.28\,$dex, $[M/H] = -0.38 \pm 0.11\,$dex, and the ones published in CPS were $T_{\mathrm{eff}} = 6674 \pm 25\,$K,$\log g = 4.27 \pm 0.028\,$dex, $[M/H] = -0.27 \pm 0.01\,$dex. The available ASPCAP parameters for this star are $T_{\mathrm{eff}} = 6607\,$K and $\log g = 4.35\,$dex and and $[M/H] = -0.42\,$dex . This is one of the hottest stars in our sample, and it belongs to a multiple star system. This star was chosen to demonstrate that the pipeline works for stars that are both hot and metal-poor ($[M/H] \sim -0.35\,$dex). The combination of parameters leads to a relative lack of lines to match and increases the difficulty for the pipeline, but the synthesis seems to match the observed spectrum regardless. The spectrum synthesized with CPS parameters is different from the best fit, with most lines being deeper and further from the observed spectrum (see the Mg lines nearby 1576 nm and Si around 1585 nm). This discrepancy can be explained by the difference in metallicity estimation

[8] `http://simbad.u-strasbg.fr/simbad/sim-id?Ident=KOI-85`

by *iSpec* and CPS, with a -0.11 dex difference in metallicity between both syntheses.

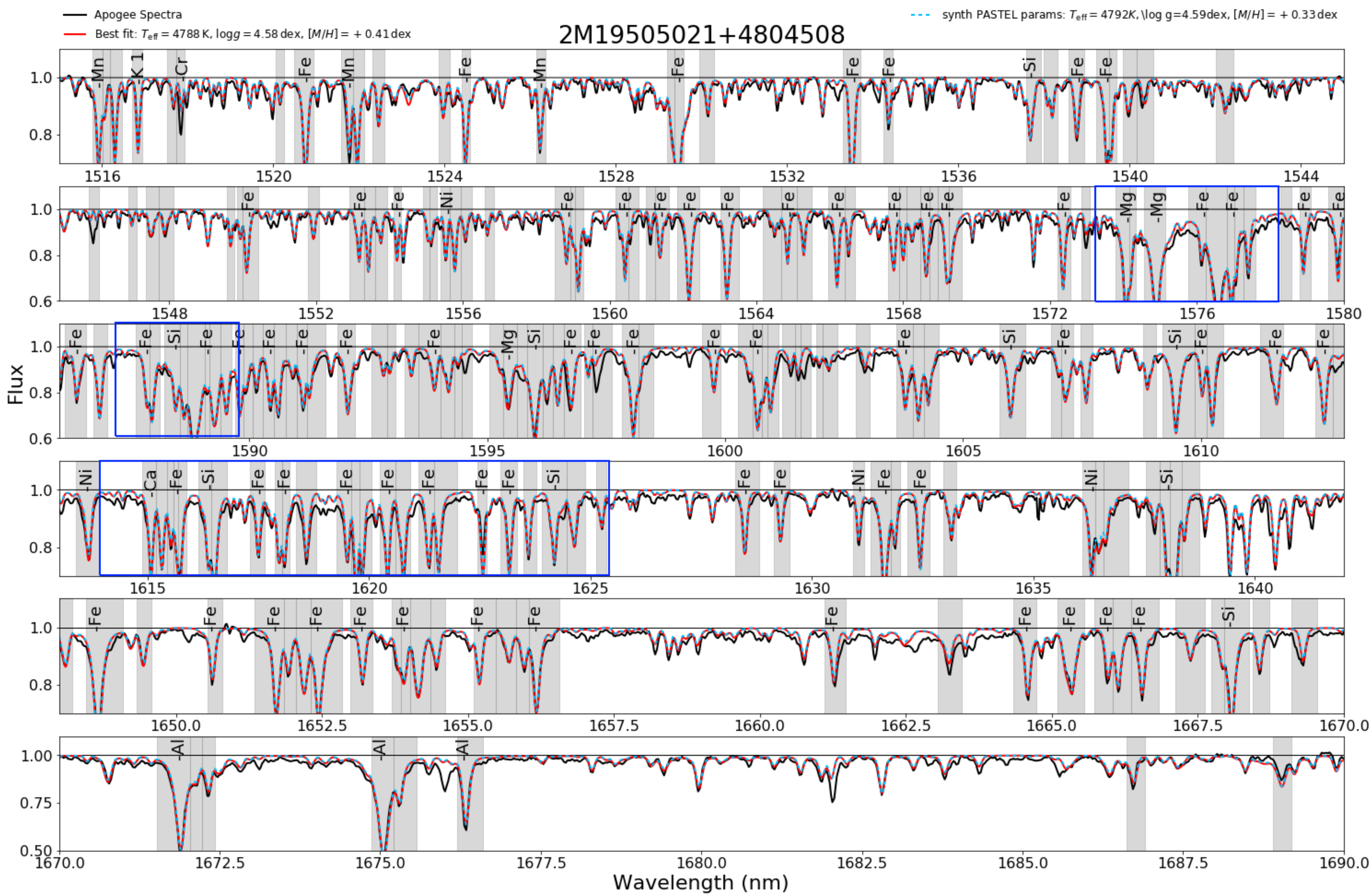

Figure 6.9: Comparison between APOGEE spectra of the star 2M19505021+4804508 (BD+47 2936, black) and two synthetic spectra (red, straight line, with the our pipeline's best match parameters and blue, dashed, with the CPS parameters for this star) for APOGEE wavelength range. In gray highlight are the areas used for χ^2 minimization by our pipeline's algorithm. Highlighted in blue are the relevant areas mentioned in our results discussion. The best match parameters derived were $T_{\rm eff} = 4788 \pm 29$ K, $\log g = 4.58 \pm 0.03$ dex, $[M/H] = +0.41 \pm 0.01$ dex, and the ones published by PASTEL were $T_{\rm eff} = 4792 \pm 12$ K, $\log g = 4.59 \pm 0.02$ dex, $[M/H] = +0.33 \pm 0.01$ dex.

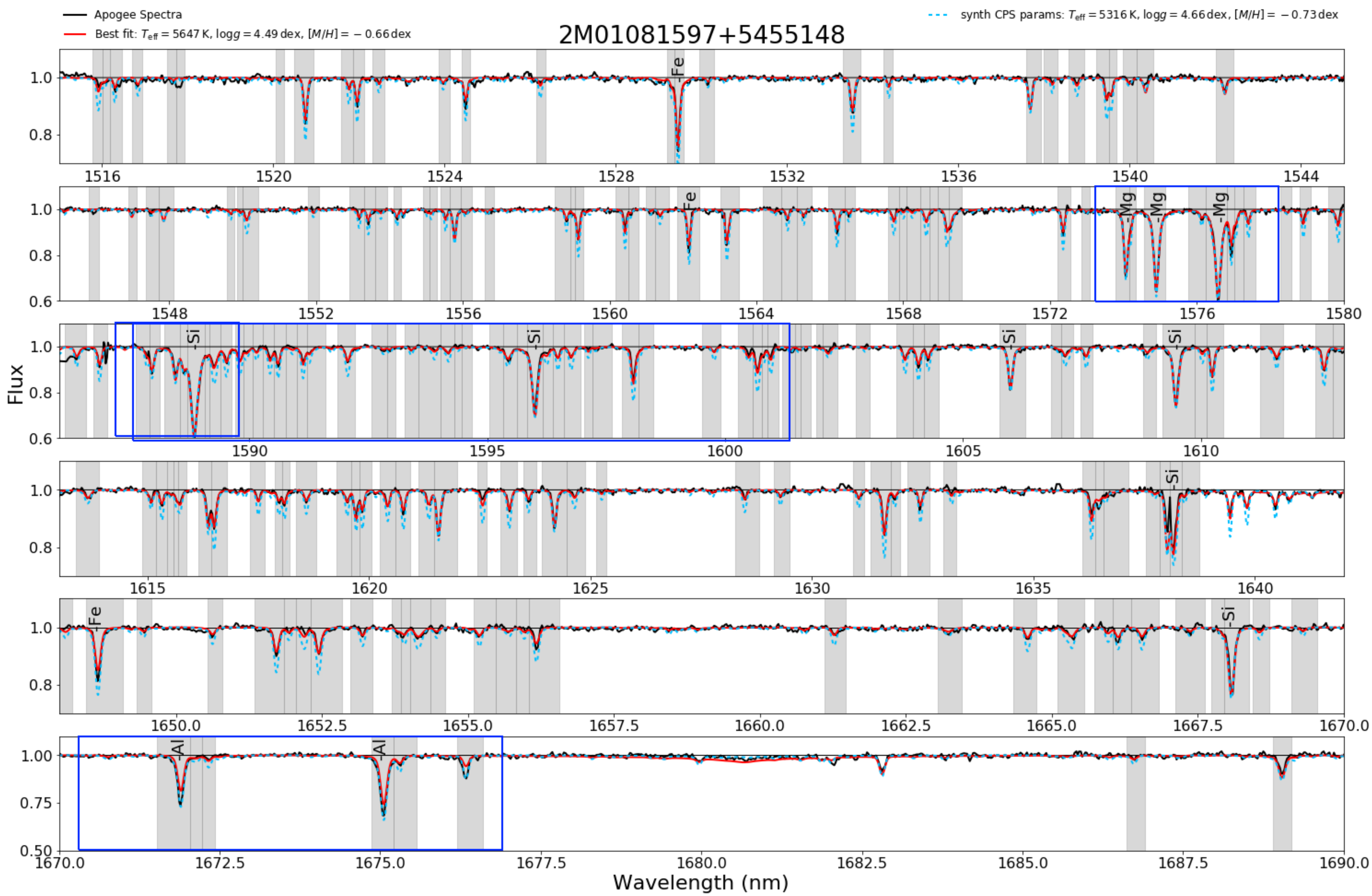

Figure 6.10: Comparison between APOGEE spectra of the star 2M01081597+5455148 (HD 6582, black) and two synthetic spectra (red, straight line, with our pipeline's best match parameters and blue, dashed, with the CPS parameters for this star) for APOGEE wavelength range. In gray highlight are the areas used for χ^2 minimization by our pipeline's algorithm. The best match parameters derived were $T_{\rm eff} = 5639 \pm 163$ K, $\log g = 4.46 \pm 0.20$ dex, $[M/H] = -0.66 \pm 0.07$ dex, and the ones published in CPS were $T_{\rm eff} = 5316 \pm 25$ K, $\log g = 4.66 \pm 0.028$ dex, $[M/H] = -0.73 \pm 0.01$ dex.

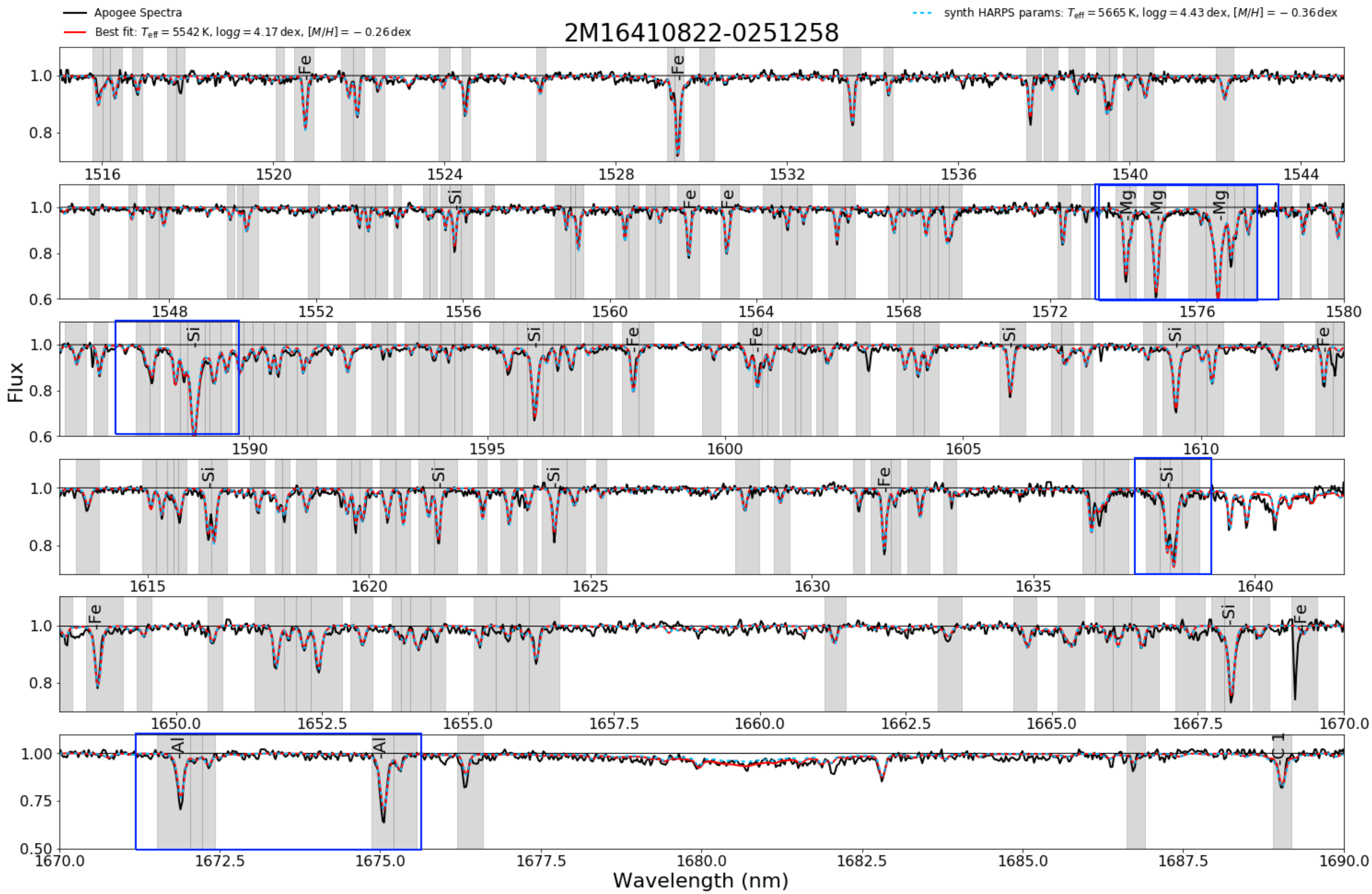

Figure 6.11: Comparison between APOGEE spectra of the star 2M16410822-0251258 (HD 150433, black) and two synthetic spectra (red, straight line, with our pipeline's best match parameters and blue, dashed, with the CPS parameters for this star) for APOGEE wavelength range. In gray highlight are the areas used for χ^2 minimization by our pipeline's algorithm. The best match parameters derived were $T_{\rm eff} = 5547 \pm 201$ K, $\log g = 4.17 \pm 0.23$ dex, $[M/H] = -0.26 \pm 0.09$ dex, and the ones published by the HARPS GTO were $T_{\rm eff} = 5665 \pm 12$ K, $\log g = 4.43 \pm 0.02$ dex, $[M/H] = -0.36 \pm 0.01$ dex.

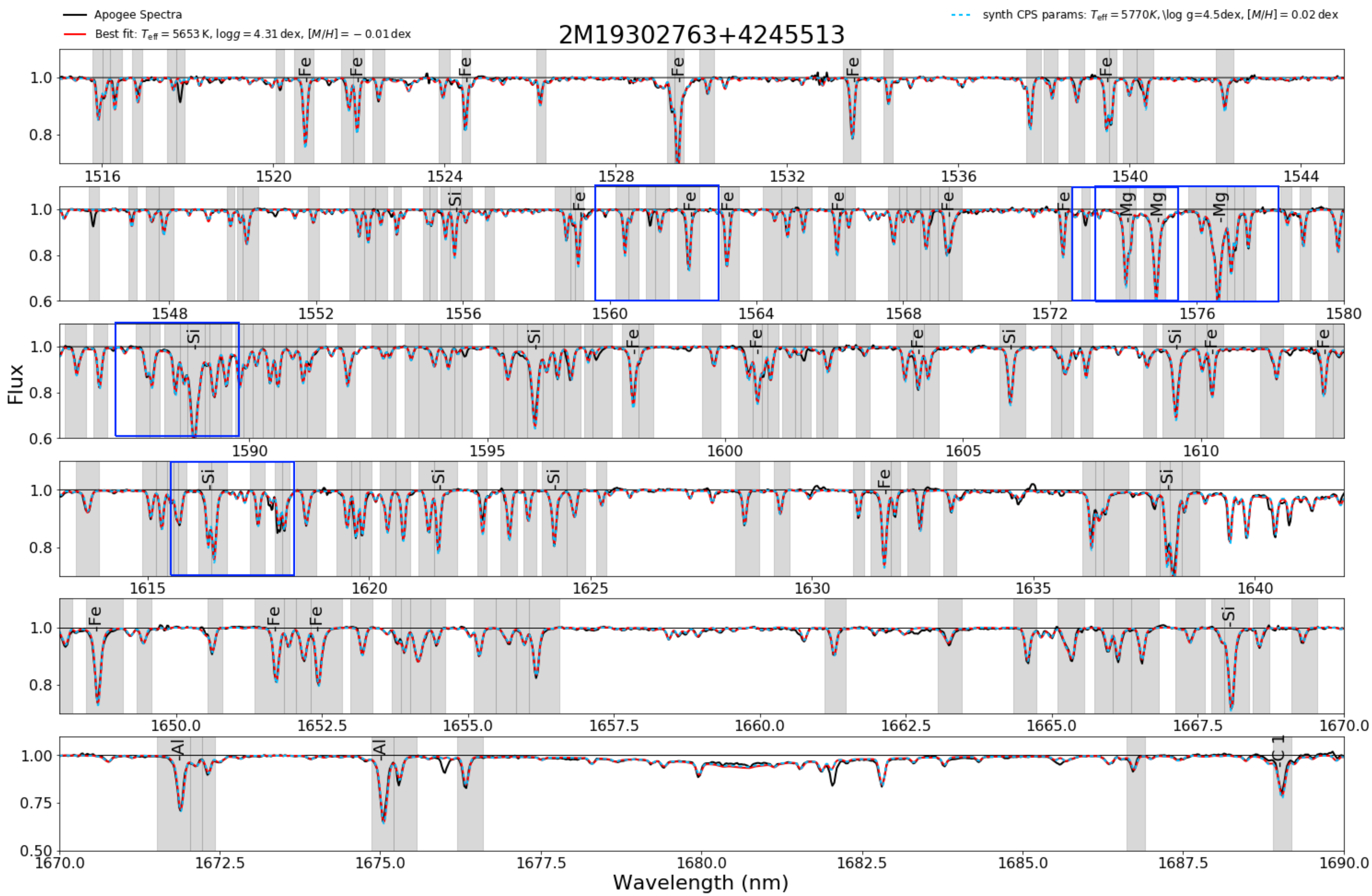

Figure 6.12: Comparison between APOGEE spectra of the star 2M19302763+4245513 (KOI-2687, black) and two synthetic spectra (red, straight line, with our pipeline's best match parameters and blue, dashed, with the CPS parameters for this star) for APOGEE wavelength range. In gray highlight are the areas used for χ^2 minimization by our pipeline's algorithm. The best match parameters derived were $T_{\rm eff} = 5653 \pm 47$ K, $\log g = 4.31 \pm 0.06$ dex, $[M/H] = -0.01 \pm 0.02$ dex, and the ones published in CPS were $T_{\rm eff} = 5770 \pm 25$ K, $\log g = 4.5 \pm 0.028$ dex, $[M/H] = +0.02 \pm 0.01$ dex.

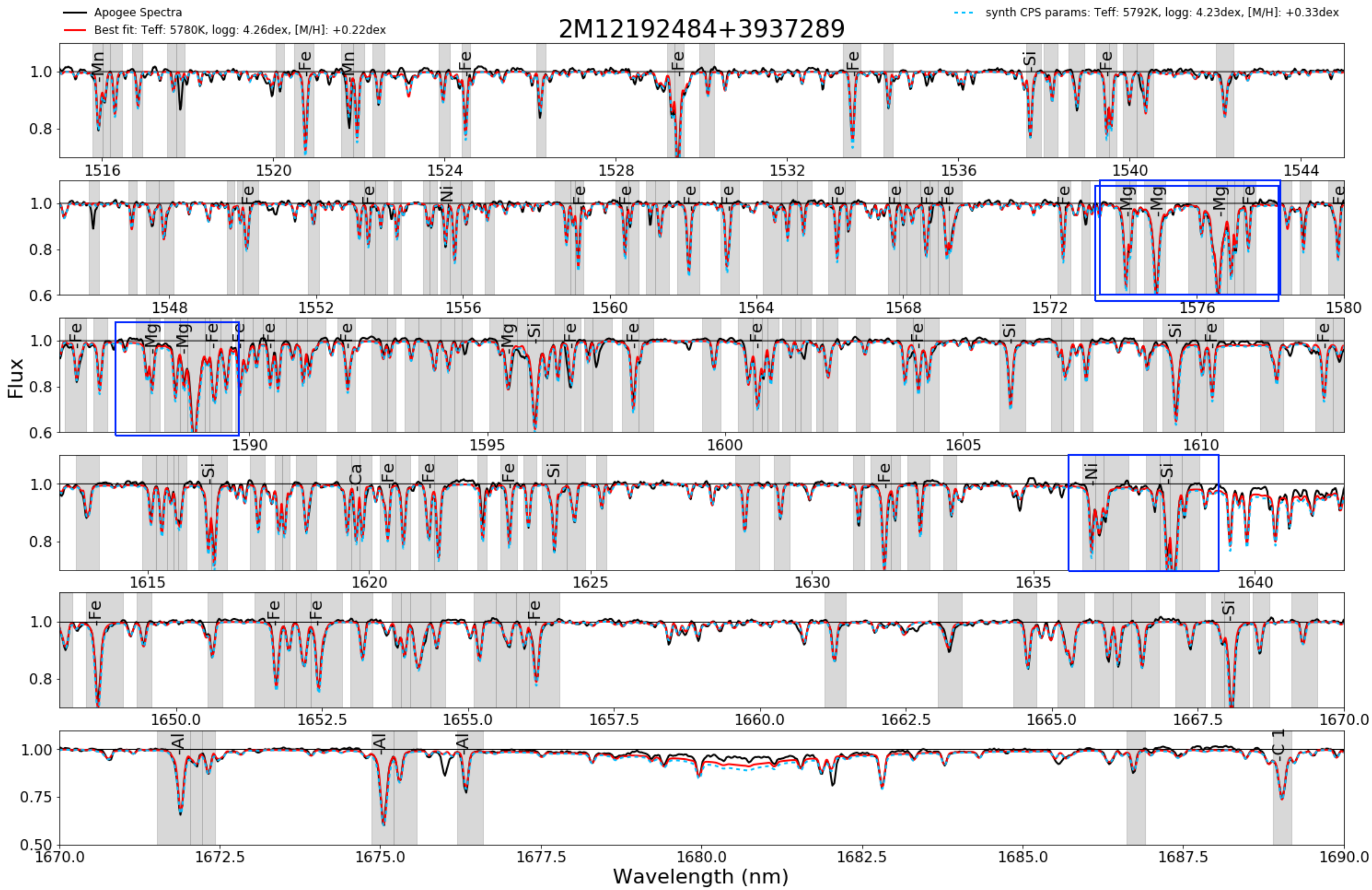

Figure 6.13: Comparison between APOGEE spectra of the star 2M12192484+3937289 (HD 107211, black) and two synthetic spectra (red, straight line, with our pipeline's best match parameters and blue, dashed, with the CPS parameters for this star) for APOGEE wavelength range. In gray highlight are the areas used for χ^2 minimization by our pipeline's algorithm. The best match parameters derived were $T_{\text{eff}} = 5771 \pm 55\,$K, $\log g = 4.26 \pm 0.06\,$dex, $[M/H] = +0.22 \pm 0.02\,$dex, and the ones published in CPS were $T_{\text{eff}} = 5792 \pm 25\,$K, $\log g = 4.23 \pm 0.028\,$dex, $[M/H] = +0.33 \pm 0.01\,$dex.

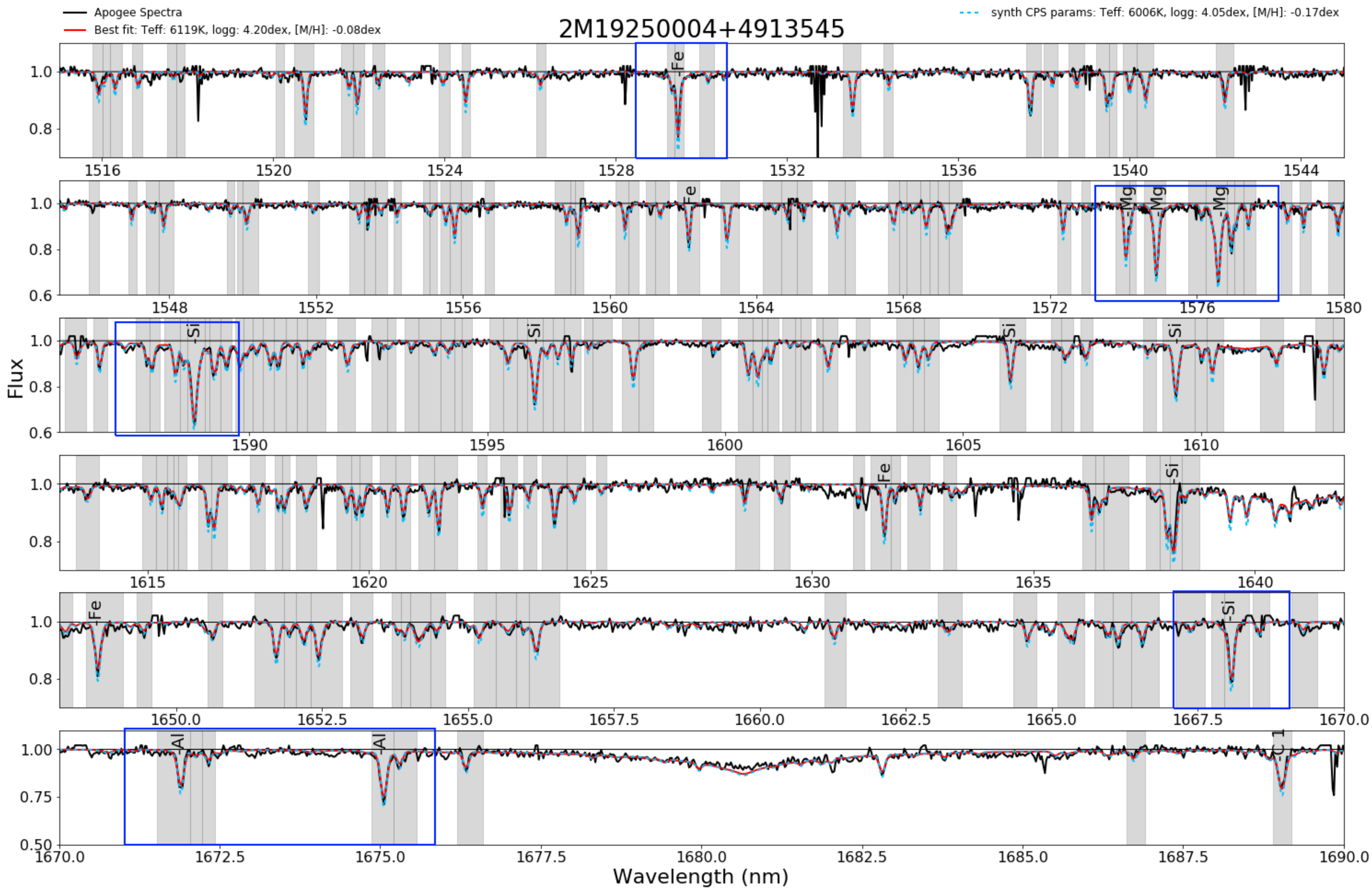

Figure 6.14: Comparison between APOGEE spectra of the star 2M19250004+4913545 (Kepler-36, black) and two synthetic spectra (red, straight line, with our pipeline's best match parameters and blue, dashed, with the CPS parameters for this star) for APOGEE wavelength range. In gray highlight are the areas used for χ^2 minimization by our pipeline's algorithm. The best match parameters derived were $T_{\rm eff} = 6127 \pm 213\,$K, $\log g = 4.21 \pm 0.31\,$dex, $[M/H] = -0.07 \pm 0.09\,$dex, and the ones published in CPS were $T_{\rm eff} = 6006 \pm 25\,$K, $\log g = 4.05 \pm 0.028\,$dex, $[M/H] = -0.17 \pm 0.01\,$dex.

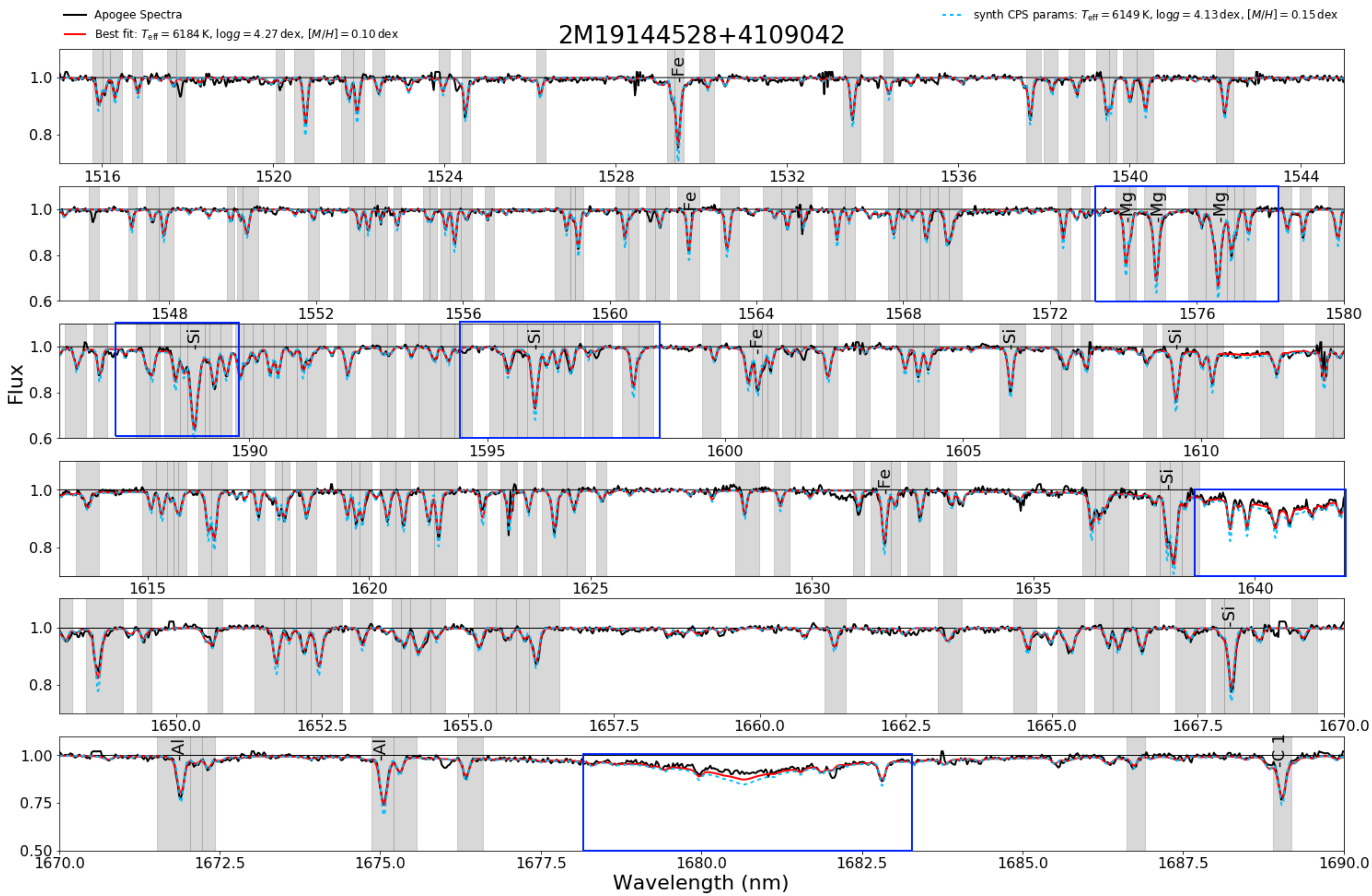

Figure 6.15: Comparison between APOGEE spectra of the star 2M19144528+4109042 (KOI-85, black) and two synthetic spectra (red, straight line, with our pipeline's best match parameters and blue, dashed, with the CPS parameters for this star) for APOGEE wavelength range. In gray highlight are the areas used for χ^2 minimization by our pipeline's algorithm. The best match parameters derived were $T_{\rm eff} = 6195 \pm 164$ K, $\log g = 4.28 \pm 0.21$ dex, $[M/H] = +0.11 \pm 0.06$ dex, and the ones published in CPS were $T_{\rm eff} = 6149 \pm 25$ K, $\log g = 4.13 \pm 0.028$ dex, $[M/H] = +0.15 \pm 0.01$ dex.

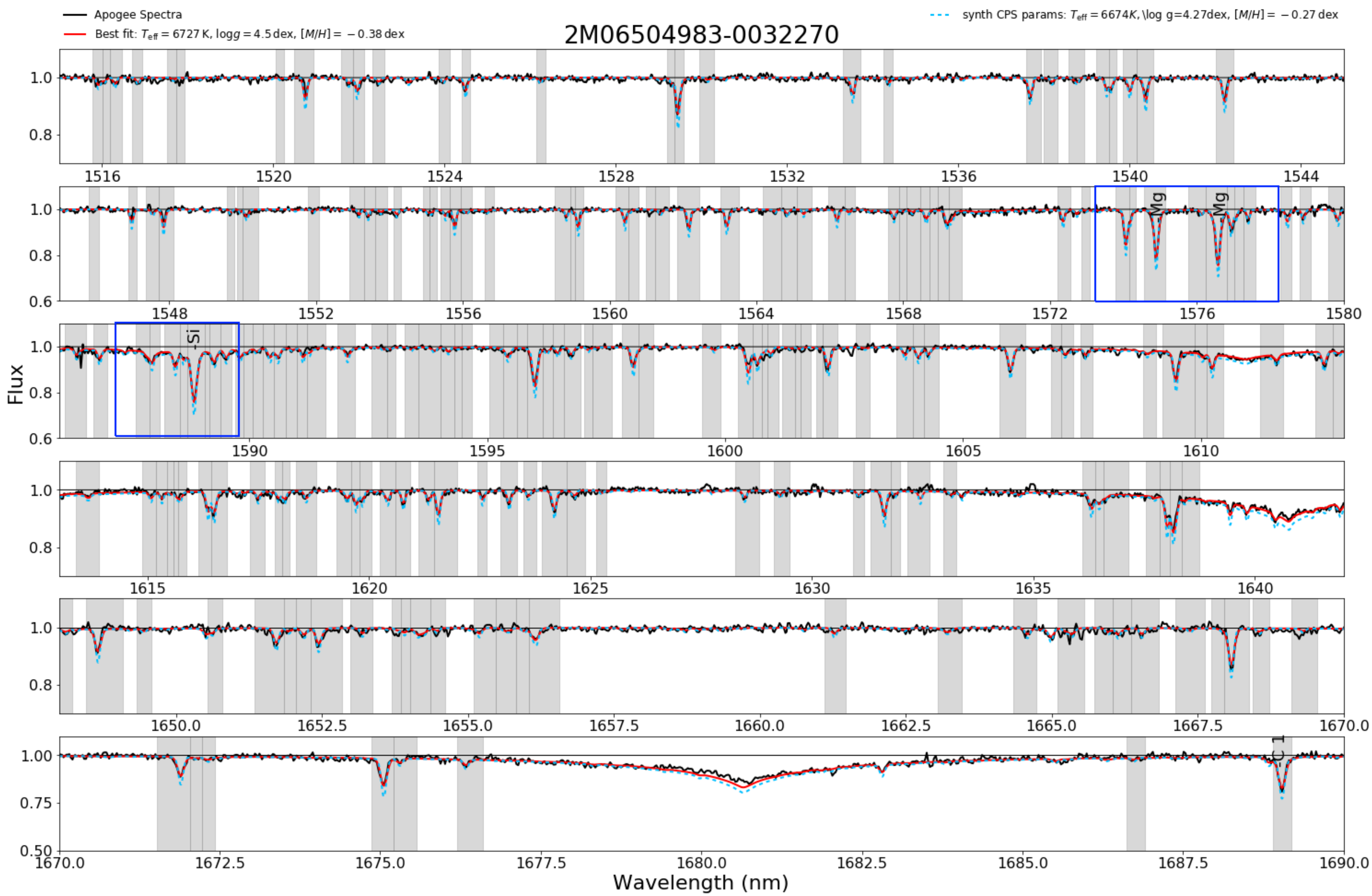

Figure 6.16: Comparison between APOGEE spectra of the star 2M06504983-0032270 (HD 49933, black) and two synthetic spectra (red, straight line, with the our pipeline's best match parameters and blue, dashed, with the CPS parameters for this star) for APOGEE wavelength range. In gray highlight are the areas used for χ^2 minimization by our pipeline's algorithm. The best match parameters derived were $T_{\rm eff} = 6727 \pm 293$ K, $\log g = 4.5 \pm 0.28$ dex, $[M/H] = -0.38 \pm 0.11$ dex, and the ones published in CPS were $T_{\rm eff} = 6674 \pm 25$ K, $\log g = 4.27 \pm 0.028$ dex, $[M/H] = -0.27 \pm 0.01$ dex.

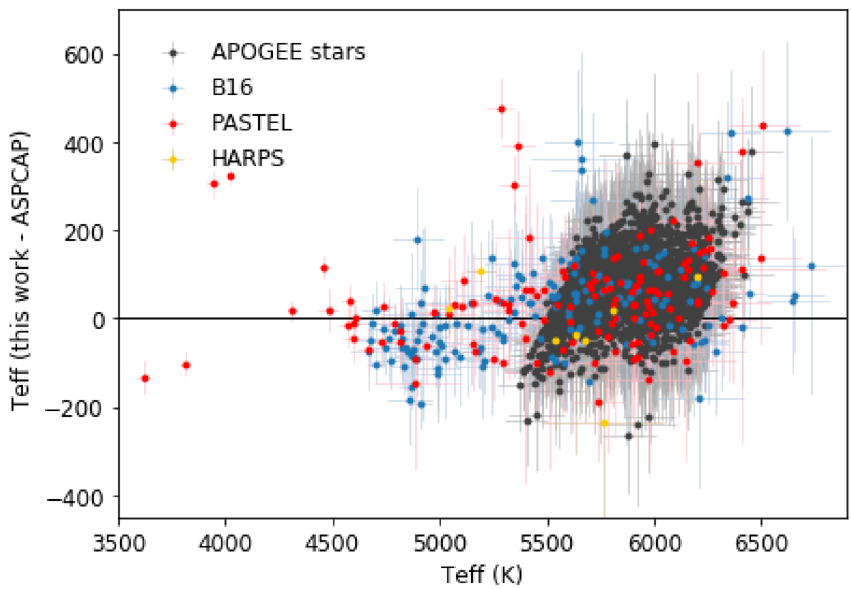

Figure 6.17: Diagram representing the output $T_{\rm eff}$ of our pipeline and the difference between it and the calibrated values published by ASPCAP for that star. Only ASPCAP values are being compared and the different colors are used to distinguish between stellar subsamples. Errors included are our pipeline's estimates using the covariance matrix.

6.2 Discussion

6.2.1 ASPCAP comparison

As the data we are using comes from APOGEE and ASPCAP is the official method to derive parameters for it, a comparison was made between our results and the ASPCAP parameters calibrated with asteroseismology for our sample stars. It is presented in Figs. 6.17 and 6.18. This includes both the subsamples characterized in optical wavelengths and the 3419 stars from only ASPCAP parameters are available. As mentioned in Section 4.1, $[M/H]$, $T_{\rm eff}$, and $\log g$ are provided for all stars in the sample. ASPCAP values for $[M/H]$ and $T_{\rm eff}$ for all stars are calibrated using independent methods, but the $\log g$ values for dwarf stars are not independently calibrated and differ from isochrone values. We decided to compare our values for $T_{\rm eff}$ and $[M/H]$ with the calibrated ones provided by ASPCAP for our sample of stars. We also compare our raw values for $\log g$ with the available ASPCAP $\log g$ values.

Table 6.1: Statistics on the differences between our output results and ASPCAP parameters. The 'Stars' column represents the number of stars with this ASPCAP parameter between the two original samples. SD stands for standard deviation and MAD for Median Absolute Deviation.

Parameter	Stars	Median (This - ASPCAP)	SD	MAD
$T_{\rm eff}$	3670	+62 K	80 K	100 K
$[M/H]$	3668	+0.04 dex	0.10 dex	0.11 dex

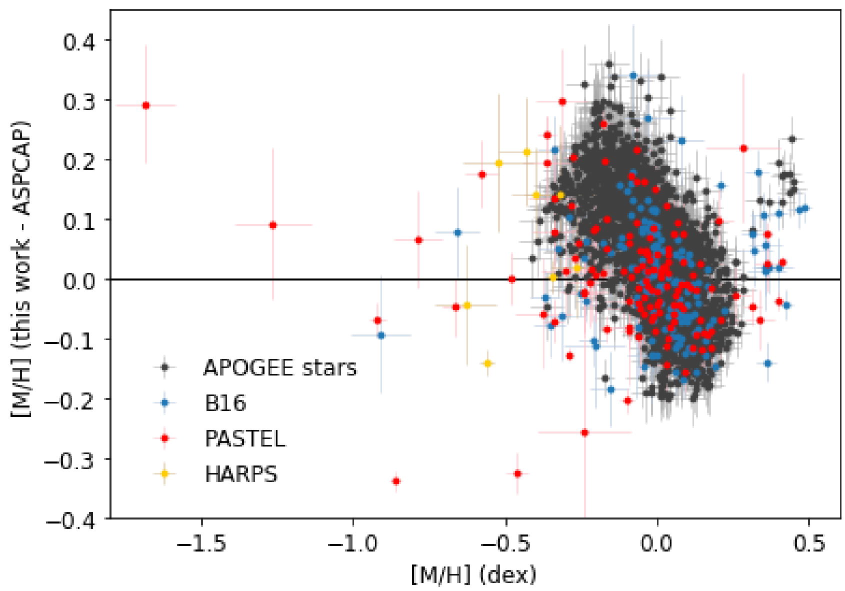

Figure 6.18: Diagram representing the output $[M/H]$ of our pipeline and the difference between it and the calibrated values published by ASPCAP for that star. Only ASPCAP values are being compared and the different colors are used to distinguish between stellar subsamples. Errors included are our pipeline's estimates using the covariance matrix.

We also display a comparison between all published raw ASPCAP values and our raw output in Fig. 6.19. The plot shows that the distributions of both our $\log g$ values and the ASPCAP ones are quite similar, with a median difference of -0.007 dex between them. The difference between both $\log g$ values is also around or below 0.4 dex for most stars in the sample, showing that the values obtained with our method are consistent with the available ASPCAP ones. However, several studies comparing asteroseismic and spectroscopic $\log g$ have demonstrated that later values need to be calibrated (e.g Holtzman et al. 2015; Mortier et al. 2014). Also, the comparison with stellar isochrones points to the inaccuracy of spectroscopic $\log g$ values. Therefore, we decided to apply the correction as shown in Fig. 6.1 and explained in section 6.1.

Despite only ASPCAP values being compared, we distinguish the subsamples characterized in the optical by color (CPS - blue; PASTEL - red; HARPS-GTO - yellow), while the stars in black have only been characterized by ASPCAP and our pipeline. This is done for visual clarity and consistency reasons. In table 6.1, the average differences between our output and the ASPCAP values are presented. With a sample of 3670 stars being so large when compared to our subsamples of stars observed in the optical, the fact that the measured differences between our pipeline's values and ASPCAP's parameters are still within one standard deviation indicates that our method can provide consistent parameters for solar-type stars in the NIR.

For the T_{eff}, the average estimated parameter is 62 K above than the published ASPCAP results, with a standard deviation of 80 K although differences are found with values between –150 K and +300 K. This difference is slightly larger than the ones measured against observations in the optical wavelength for the same stars (+62 K for ASPCAP and -12 K for CPS, +44 K for PASTEL, -8 K for HARPS), but it is still at the level of the uncertainties present in both ASPCAP and this method. The dispersion found is also within our expected uncertainty levels. This difference, coupled with the fact that ASPCAP is optimized for the measurement of giant star parameters and not FGK dwarfs, does not seem to be a critical problem with the pipeline.

With the metallicities, a small difference is present as well. This can be seen in Fig. 6.18 and in table 6.1. Our values are systematically above the average ASPCAP $[M/H]$ for each star by +0.04 dex, which is slightly larger than the average difference when comparing the output $[M/H]$ with the CPS parameter (+0.01 dex) and about the same as the PASTEL comparison (+0.05 dex), while being below the HARPS difference of +0.16 dex. We also find that the difference has a standard deviation of around 0.1 dex, meaning that it reaches our estimated uncertainty levels for the parameter. Also, and as seen in Fig. 6.18, there is a trend that results in smaller $\Delta[M/H]$ values for stars with higher $[M/H]$, with a small number of high $[M/H]$ outliers. A larger sample size of both low and high-$[M/H]$ stars seems necessary to better characterize the behavior of the pipeline for that extended parameter space.

As mentioned in section 4.1, ASPCAP is optimized towards the derivation of parameters for giant stars. That fact combined with the issues in ASPCAP's synthesis of $\log g$ for dwarf stars could result in discrepancies in other spectroscopic parameters. Syntheses with lower values for $\log g$ can result in lower values as well for T_{eff} and $[M/H]$ across a sample of stars, as the line broadening due to low surface gravity must be compensated by a corresponding decrease in both T_{eff} and $[M/H]$. ASPCAP's calibrations correct some of these effects, increasing T_{eff} by around $+90$ K (exact values are not available as ASPCAP's methods for APOGEE DR14 are not yet published) and $[M/H]$ by $+0.027$ dex for stars with $[M/H] > -0.5$ dex. However, considering the difference between our values and ASPCAP ($\Delta T_{\text{eff}} = +62$ K and $\Delta[M/H] = +0.04$ dex, larger than differences against parameters derived from observations in the optical wavelength), some of the differences observed can be associated with further discrepancies associated with ASPCAP's $\log g$ determination for these stars.

To measure the effect ASPCAP parameter calibrations can have on their final results, we decided to show an additional comparison between our results and the uncalibrated ASPCAP

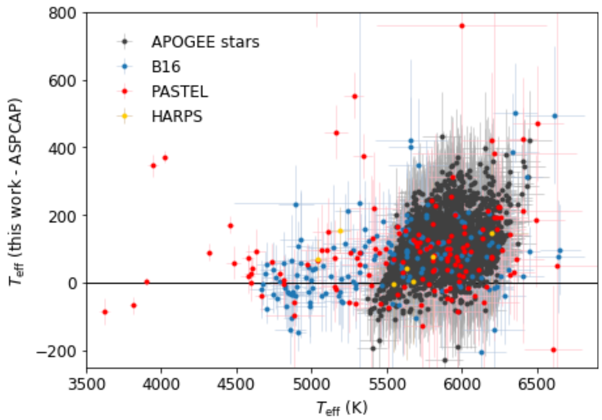

(a)

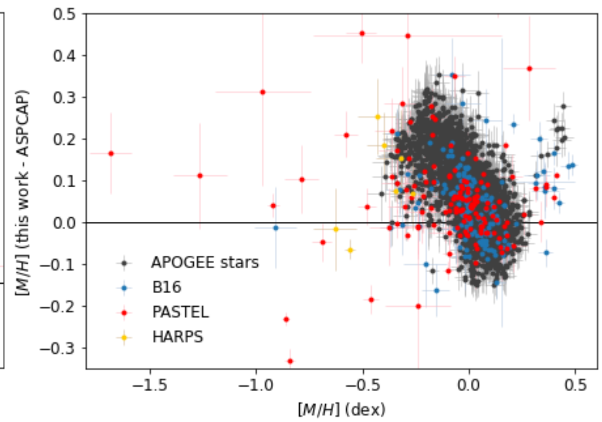

(b)

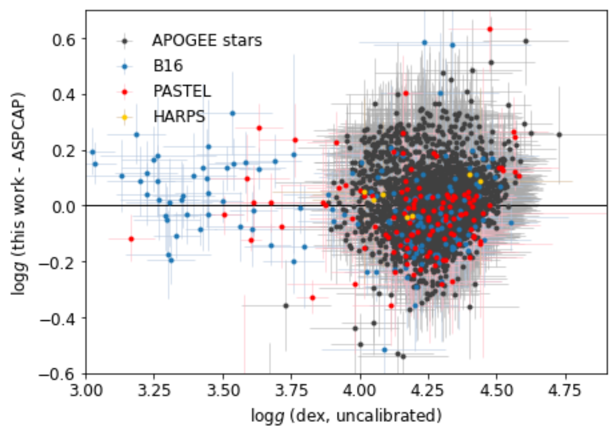

(c)

Figure 6.19: Diagrams showing comparisons between this work's results and uncalibrated ASPCAP parameters. 6.19a shows $T_{\rm eff}$, 6.19b shows $[M/H]$ and 6.19c shows $\log g$. Errors included are our pipeline's estimates using the covariance matrix.

Table 6.2: Statistics on the differences between our output results and uncalibrated ASPCAP parameters. SD stands for standard deviation and MAD for Median Absolute Deviation.

Parameter	Stars	Median (This - ASPCAP)	SD	MAD
$T_{\rm eff}$	3622	+101 K	90 K	150 K
$[M/H]$	3622	+0.08 dex	0.10 dex	0.12 K
$\log g$	3622	-0.01 dex	0.14 dex	0.10 K

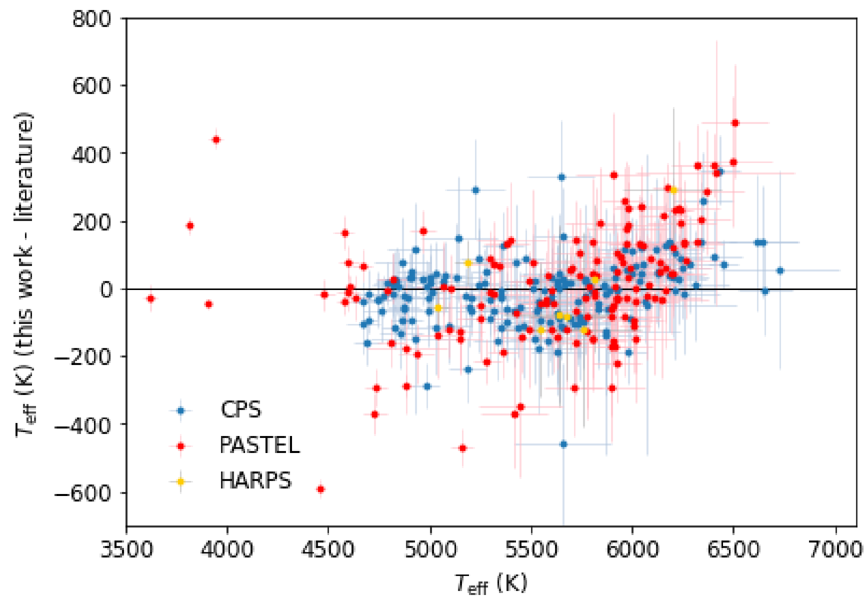

Figure 6.20: Diagram representing the output $T_{\rm eff}$ of our pipeline and the difference between it and the values published by CPS, PASTEL, and the HARPS GTO program. Errors included are our pipeline's estimates using the co-variance matrix.

Table 6.3: Average differences in derived parameters between our method and CPS parameters. Sample size is 168 stars. Median is shown to decrease effect of outliers. SD stands for standard deviation and MAD for Median Absolute Deviation.

Parameter	Median (Pipeline - CPS)	SD	MAD
$T_{\rm eff}$	-7 K	101 K	82 K
$\log g$	+0.01 dex	0.15 dex	0.17 dex
$[M/H]$	-0.02 dex	0.09 dex	0.09 dex

results. This comparison shows how the calibrations shape the overall parameter distribution and also help us conclude on the validity of their parameters as a whole. The results of these tests are presented in Fig. 6.19 and Table 6.2. When comparing tables 6.1 and 6.2, it is clear that the calibrations of $T_{\rm eff}$ and $[M/H]$ derived with ASPCAP for dwarf stars resulted in parameters closer to ours and to other literature values (+62 K vs +104 K in $T_{\rm eff}$ and +0.04 dex vs +0.08 dex for $[M/H]$). In the case of surface gravity, the results are more difficult to interpret. Our pipeline's values for this parameter are within 0.01 dex of uncalibrated values derived by ASPCAP, which are significantly different from ones obtained with asteroseismology (see Figure 4 in Holtzman et al. 2015).

6.2.2 Literature comparisons

In addition to the comparison with ASPCAP parameters in Section 6.2.1, we also compare our output parameters to ones obtained by studying optical spectra, published by the CPS,

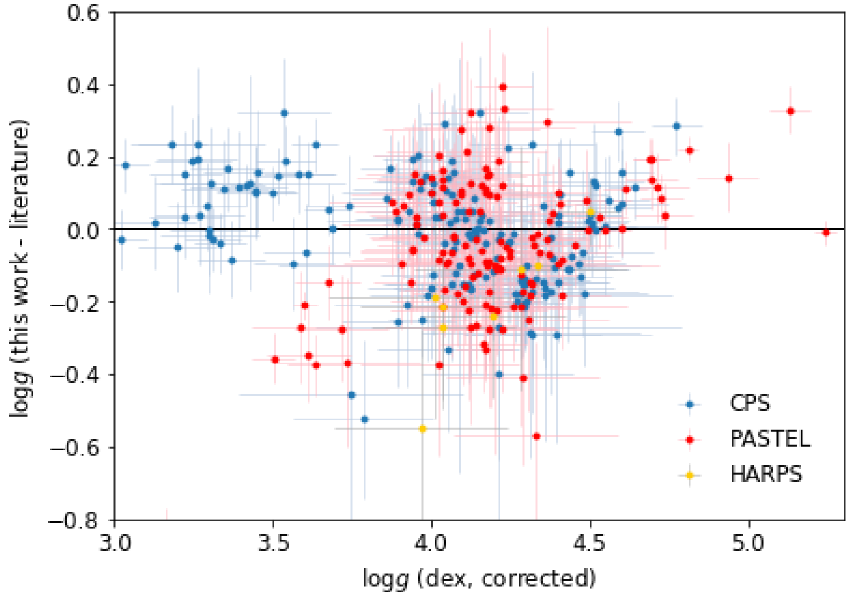

Figure 6.21: Diagram representing the output $\log g$ of our pipeline and the difference between it and the values published by CPS, PASTEL, and the HARPS GTO program. Errors included are our pipeline's estimates using the co-variance matrix.

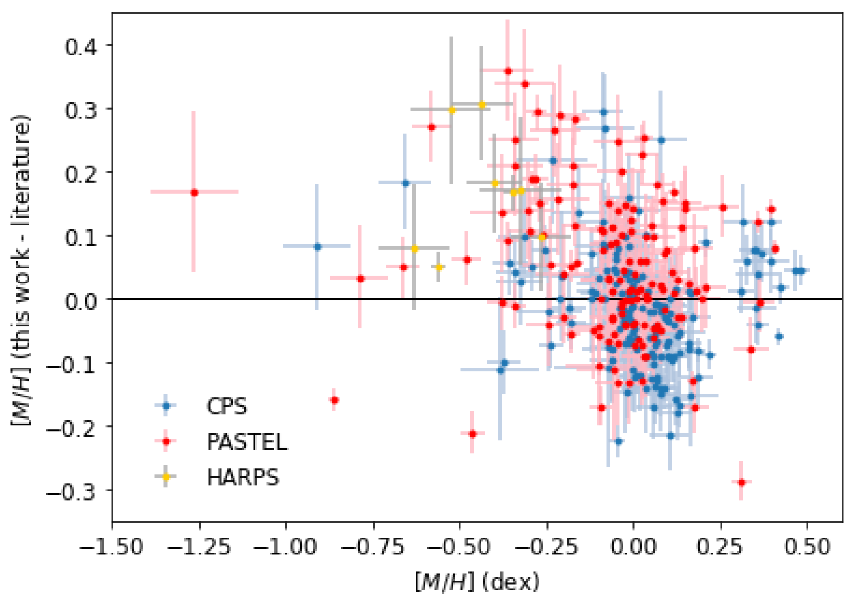

Figure 6.22: Diagram representing the output $[M/H]$ of our pipeline and the difference between it and the values published by CPS, PASTEL, and the HARPS GTO program. Errors included are our pipeline's estimates using the co-variance matrix.

Table 6.4: Average differences in derived parameters between our method and PASTEL parameters. Sample size is 153 stars. Median is shown to decrease effect of outliers. SD stands for standard deviation and MAD for Median Absolute Deviation.

Parameter	Median (Pipeline - PASTEL)	SD	MAD
T_{eff}	-2 K	173 K	148 K
$\log g$	-0.04 dex	0.34 dex	0.17 dex
$[M/H]$	+0.03 dex	0.11 dex	0.11 dex

Table 6.5: Differences in derived parameters between our method and HARPS (our pipeline - literature). The H denotes the literature value for the parameter.

ID (2mass)	$T_{\rm eff}$ (K)	$T_{\rm eff}^H$	$\log g$ (dex)	$\log g^H$ (dex)	$[M/H]$ (dex)	$[M/H]^H$ (dex)
2M03402202-0313005	5762	5884	4.01	4.52	-0.52	-0.82
2M04042029-0439185	5192	5116	4.40	4.45	-0.34	-0.51
2M07385132-0527558	5635	5716	4.01	4.20	-0.32	-0.49
2M08172935-0359221	5678	5762	4.05	4.31	-0.40	-0.58
2M15074648+0852472	5811	5782	4.09	4.25	-0.43	-0.74
2M15124763-0109577	5043	5096	4.19	4.44	-0.56	-0.61
2M16302844+0410411	6200	5908	4.44	4.39	-0.63	-0.71
2M16410822-0251258	5542	5665	4.17	4.43	-0.26	-0.36

HARPS, or in PASTEL.

The derived parameters for the stars in common with optical surveys are plotted in Figs. 6.20-6.22, and are listed in the appendix in Table B.1. The calculated differences between our method's parameters and the ones published in CPS, PASTEL, and HARPS are presented in tables 6.3-6.5, as well as the standard deviations measured across the parameter distributions. In HARPS' case, and since there are only 8 stars in the sample, each result is included.

The spectra displayed in Figs. 6.10-6.15 shows that our pipeline can do a good job minimizing χ^2 and matching the APOGEE observed spectra with a synthesized one. From the figures 6.20-6.22 and the tables 6.3 and 6.4, the method might have some systematic errors in the calculation of $[M/H]$, but not in the case of the other parameters ($T_{\rm eff}$ and $\log g$), as the error margins for our parameter estimates are within the optical measurements.

In the case of the PASTEL stars, some of the small discrepancies can be explained by the fact that PASTEL presents $[Fe/H]$ and not $[M/H]$, and that their values for the $T_{\rm eff}$ come from different sources. This is not true for the CPS parameters, as they are uniformly calculated and have better precision than PASTEL's. We also find that our differences, when compared to PASTEL parameters, have increased standard deviation when compared to the CPS parameter difference standard deviation, which can be explained by the fact that their parameters are not uniformly calculated and are rather a collection of parameters from different optical sources.

The largest difference between our derived parameters and literature is found for the $[M/H]$ measurements in the HARPS sample (average +0.16 dex). This difference may be caused by either an issue with the small sample, as neither the larger PASTEL and CPS samples show these differences, or just a systematic error caused by the method used, as the HARPS parameters were measured using the EW method. All the HARPS sample stars are relatively metal-poor, having $[M/H]$ ranging from -0.82 to -0.36 dex, which means they are in relatively small parameter space and may not represent a real distribution of stars like the other studied samples. In section 6.2.2, we present a comparison with other literature sources using similar methods but a larger $[M/H]$ parameter space to test this hypothesis.

There is also an issue in some PASTEL stars, resulting in a relatively high number of outlier stars (33 out of 153), with poor predictions in either $T_{\rm eff}$, $\log g$, and $[M/H]$. Of these reported outlier stars, and excluding stars with $S/N < 100$, we calculate a value for $\Delta[M/H]$ over 0.35 dex above the one published by PASTEL for 5 of them, with the worst outliers being either very metal-poor stars ($[M/H] < -1.5$ dex) or cold K and M dwarfs ($T_{\rm eff} < 4000\,K$). Although our pipeline is not optimized for these stars, the fact that these outliers exist must be taken into account when synthesizing large samples of stars.

An additional explanation for any discrepancies can be the fact that APOGEE spectra are in the H-band (infrared) and CPS, PASTEL and HARPS results were calculated using spectra in the visible wavelengths. This possibility is explored by comparing our parameters with the ones published by ASPCAP, as explained in the next subsection.

Comparison of parameters obtained for confirmed planet host stars

As mentioned above in Section 4.2.1, exoplanets have been detected orbiting around stars in our sample and parameters for 81 of them are available within SWEET-Cat (Santos et al. 2013; Andreasen et al. 2017). SWEET-Cat is an online catalog compiling spectroscopical parameters for stars with exoplanets. We display a comparison between the results published by them and ours in Figs. 6.23, 6.24, and 6.25. Since SWEET-Cat itself is a compilation of results from multiple sources, we use colors to distinguish the most representative source for stars in our sample. It is (11), with 54 stars in common, while Mortier et al. (2013b) with 6 stars, and Sousa et al. (2018) with 3 stars, are the other two most represented ones. 12 other literature sources provide parameters for the remaining 18 stars in our sample. Full results are provided in Table 6.6.

Analyzing the distribution of the parameters themselves, in the case of $T_{\rm eff}$, we find a high-degree of agreement between our results and the ones compiled by SWEET-Cat. There are a couple of outlier stars, but the overall trend is of $\Delta T_{\rm eff} \leq 200$ K. We also find that our estimates for the precision (error bars in the x-axis) tend to be larger than the ones available in SWEET-

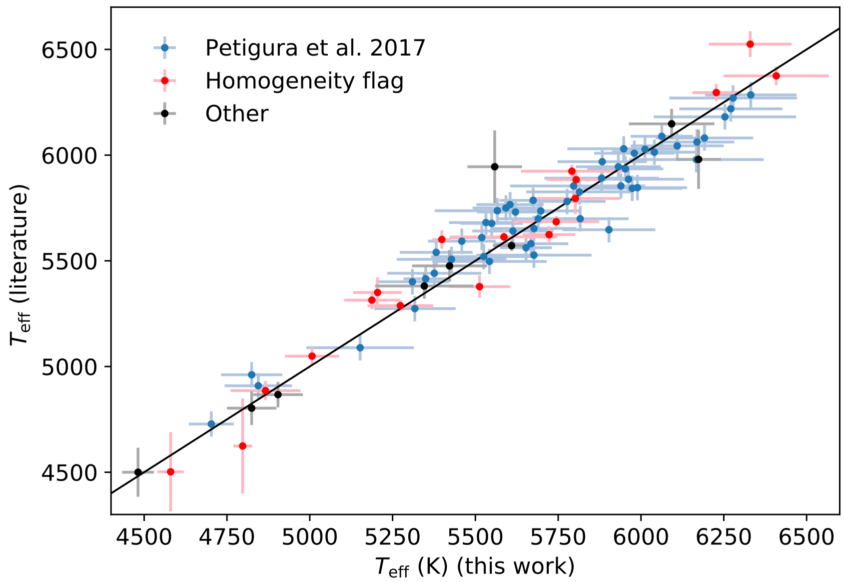

Figure 6.23: Diagram representing the output $T_{\rm eff}$ of our pipeline and the difference between it and the values compiled by SWEET-Cat for planet-host stars in our sample. As (11) was our comparison catalog with the most stars in common (54), we highlight them for easier identification (blue). We also highlight stars with the homogeneity flag in SWEET-Cat, indicating stars characterized using the EW method (red). In black are all other stars. Errors included in the x-axis are our pipeline's estimates using the covariance matrix, and available SWEET-Cat errors in the y-axis.

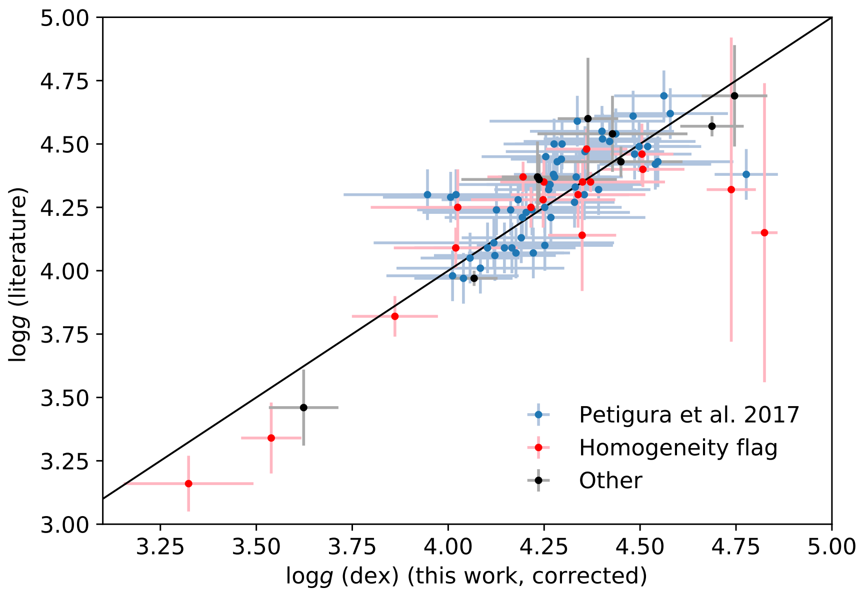

Figure 6.24: Diagram representing the output $\log g$ of our pipeline and the difference between it and the values compiled by SWEET-Cat for planet-host stars in our sample. As (11) was our comparison catalog with the most stars in common (54), we highlight them for easier identification (blue). We also highlight stars with the homogeneity flag in SWEET-Cat, indicating stars characterized using the EW method (red). In black are all other stars. Errors included in the x-axis are our pipeline's estimates using the covariance matrix, and available SWEET-Cat errors in the y-axis.

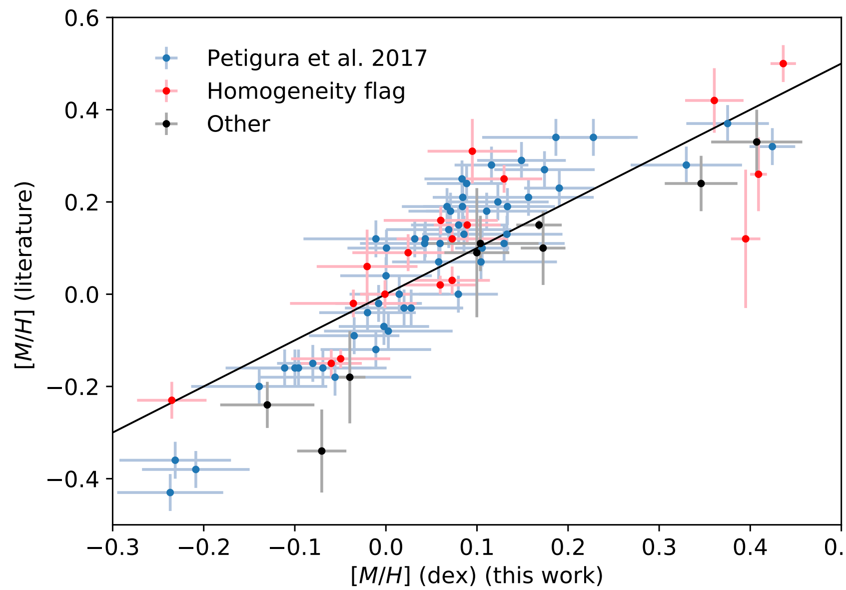

Figure 6.25: Diagram representing the output $[M/H]$ of our pipeline and the difference between it and the $[Fe/H]$ values compiled by SWEET-Cat for planet-host stars in our sample. As (11) was our comparison catalog with the most stars in common (54), we highlight them for easier identification (blue). We also highlight stars with the homogeneity flag in SWEET-Cat, indicating stars characterized using the EW method (red). In black are all other stars. Errors included in the x-axis are our pipeline's estimates using the covariance matrix, and available SWEET-Cat errors in the y-axis.

Cat. Looking at Table 6.7, we find differences very similar to our previous comparisons with optical data (see Tables 6.3 and 6.4), with slightly larger median differences but comparable standard deviation (SD) and median absolute deviation (MAD).

In the case of $\log g$, we find a great concentration of stars within a small parameter space. This is similar to Fig.6.21, but to a greater extent, as we find only 4 stars with $\log g < 4.0$ dex. We expected a similar distribution, as our sample is comprised mostly of solar-type stars with surface gravity values distributed within a small parameter space. Additionally, known planet-hosts tend to be dwarf stars, eliminating many of the sub-giant stars in our sample as possible cross-matches. As for the accuracy of the parameters themselves, we find a larger dispersion than with T_{eff}, with $\Delta \log g \leq 0.4$ dex for some stars in our sample. We also find the median differences to be very close to zero, with SD (0.16 dex) and MAD (0.14 dex) below the values obtained for the CPS comparison (0.15 dex and 0.17 dex).

As for the $[M/H]$, we first have to notice that SWEET-Cat displays $[Fe/H]$ and not $[M/H]$, so some discrepancies could be explained by that. Nevertheless, we find that all stars we have in common with SWEET-Cat fall within a very small metallicity range (-0.3 dex to 0.5 dex), reducing the available parameter space from Fig. 6.22. We find a small trend towards underestimating metallicity for stars with $[M/H] < 0.0$ dex, while the values seem to be overestimated for stars with metallicities above that value. These effects are not very strong, with the maximum $\Delta[M/H]$ being around 0.25 dex, and the overall SD and MAD each being 0.1 dex.

Comparing the metallicity distribution of our 18 flagged stars, we find that the new median differences are much smaller for the new sample of stars characterized by EW (-0.03 dex vs -0.16 dex). This suggests that there is no inherent bias caused by the difference in analysis method between this work and the one published by HARPS, and the measured $\Delta[M/H]$ is more likely caused by the small analyzed sample size or the low metallicity of the analyzed star sample when compared to our overall distribution. Additionally, we also find slightly larger SD and MAD for all three spectroscopic parameters for the flagged star subsample, when compared to all SWEET-Cat stars. The values are all still close to our output, our error margins, and to the overall sample distribution, so we attribute the difference to statistical variation and the increased presence of outlier stars in this subsample.

Table 6.6: SWEET-Cat parameters available for our sample stars. Included are the literature sources and homogeneity flag, which denotes stars analyzed using EW method. (1) indicates Ammler-v. E. et al. (2009), (2) indicates Andreasen et al. (2017), (3) indicates Brewer et al. (2016), (4) indicates Grieves et al. (2017), (5) indicates Hartman et al. (2011), (6) indicates Haywood et al. (2018), (7) indicates Marcy et al. (2014), (8) indicates Mortier et al. (2013a), (9) indicates Mortier et al. (2013b), (10) indicates Morton et al. (2016), (11) indicates Petigura et al. (2017), (12) indicates Rowe et al. (2014), (13) indicates Santos et al. (2013), (14) indicates Sousa et al. (2015), (15) indicates Sousa et al. (2018), and (16) indicates Tsantaki et al. (2014).

ID (2mass)	$T_{\rm eff} \pm \Delta T_{\rm eff}$	$\log g \pm \Delta \log g$	$[Fe/H] \pm \Delta[Fe/H]$	Reference	Flag
2M19071403+4918590	5795 ± 73 K	4.3 ± 0.13 dex	0.06 ± 0.08 dex	(1)	1
2M19285935+4758102	6525 ± 61 K	4.09 ± 0.08 dex	0.31 ± 0.07 dex	(1)	1
2M18561431+4431052	5378 ± 53 K	4.46 ± 0.12 dex	-0.23 ± 0.04 dex	(2)	1
2M08522396+1314005	4867 ± 60 K	3.46 ± 0.15 dex	0.24 ± 0.06 dex	(3)	0
2M19392772+4617090	5381 ± 60 K	4.54 ± 0.15 dex	0.11 ± 0.06 dex	(3)	0
2M16254841+3015545	5572 ± 25 K	3.97 ± 0.03 dex	0.15 ± 0.01 dex	(3)	0
2M13112997+1543190	5980 ± 140 K	4.6 ± 0.24 dex	-0.34 ± 0.09 dex	(4)	0
2M17052315+3300450	4803 ± 80 K	4.57 ± 0.04 dex	0.1 ± 0.08 dex	(5)	0
2M19064546+3912428	6148 ± 71 K	4.36 ± 0.1 dex	-0.24 ± 0.05 dex	(6)	0
2M19040872+4936522	5476 ± 75 K	4.43 ± 0.06 dex	0.33 ± 0.07 dex	(7)	0
2M05073553-1359113	5049 ± 41 K	3.34 ± 0.14 dex	0.03 ± 0.03 dex	(8)	1
2M05475919-0819396	5314 ± 43 K	3.82 ± 0.08 dex	0.25 ± 0.03 dex	(8)	1
2M06434947-0103468	5288 ± 27 K	4.4 ± 0.07 dex	0.02 ± 0.02 dex	(9)	1
2M07480647+5013328	5350 ± 72 K	4.14 ± 0.22 dex	0.42 ± 0.07 dex	(9)	1
2M07273995+2420118	4502 ± 188 K	4.32 ± 0.6 dex	0.12 ± 0.15 dex	(9)	1

ID (2mass)	$T_{\rm eff} \pm \Delta T_{\rm eff}$	$\log g \pm \Delta \log g$	$[Fe/H] \pm \Delta[Fe/H]$	Reference	Flag
2M18430881+0612150	5613 ± 36 K	4.35 ± 0.09 dex	-0.02 ± 0.03 dex	(9)	1
2M19505021+4804508	4624 ± 225 K	4.15 ± 0.59 dex	0.26 ± 0.08 dex	(9)	1
2M13414903-0007410	6296 ± 40 K	4.37 ± 0.06 dex	0 ± 0.03 dex	(9)	1
2M19220642+3808347	5945 ± 172 K	4.37 ± 0.14 dex	0.09 ± 0.14 dex	(10)	0
2M18444674+4729496	4728 ± 60 K	4.38 ± 0.1 dex	0.32 ± 0.04 dex	(11)	0
2M18455585+4712289	4909 ± 60 K	4.62 ± 0.1 dex	0.11 ± 0.04 dex	(11)	0
2M18495813+4358487	6081 ± 60 K	4.09 ± 0.1 dex	-0.03 ± 0.04 dex	(11)	0
2M18503111+4619240	5891 ± 60 K	4.21 ± 0.1 dex	0.21 ± 0.04 dex	(11)	0
2M18575331+3954425	5731 ± 60 K	4.37 ± 0.1 dex	0.19 ± 0.04 dex	(11)	0
2M18575579+4423529	5653 ± 60 K	4.09 ± 0.1 dex	0.27 ± 0.04 dex	(11)	0
2M18590868+4825236	6089 ± 60 K	4.3 ± 0.1 dex	-0.15 ± 0.04 dex	(11)	0
2M19004979+4523036	5401 ± 60 K	4.54 ± 0.1 dex	0.18 ± 0.04 dex	(11)	0
2M19022767+5008087	5826 ± 60 K	4.09 ± 0.1 dex	0.18 ± 0.04 dex	(11)	0
2M19063321+3929164	6285 ± 60 K	4.29 ± 0.1 dex	-0.04 ± 0.04 dex	(11)	0
2M19095484+3813438	5677 ± 60 K	4.24 ± 0.1 dex	0.28 ± 0.04 dex	(11)	0
2M19102533+4931237	4961 ± 60 K	4.69 ± 0.1 dex	0.21 ± 0.04 dex	(11)	0
2M19104752+4220194	5507 ± 60 K	4.47 ± 0.1 dex	0.11 ± 0.04 dex	(11)	0
2M19140739+4056322	5786 ± 60 K	4.44 ± 0.1 dex	0.19 ± 0.04 dex	(11)	0
2M19144528+4109042	6219 ± 60 K	4.21 ± 0.1 dex	0.13 ± 0.04 dex	(11)	0
2M19165219+4753040	5527 ± 60 K	4.51 ± 0.1 dex	-0.2 ± 0.04 dex	(11)	0
2M19172334+4412307	6270 ± 60 K	4.3 ± 0.1 dex	-0.16 ± 0.04 dex	(11)	0
2M19214099+3751064	5520 ± 60 K	4.49 ± 0.1 dex	-0.03 ± 0.04 dex	(11)	0
2M19250004+4913545	5979 ± 60 K	4.11 ± 0.1 dex	-0.18 ± 0.04 dex	(11)	0
2M19253263+4159249	5854 ± 60 K	4.07 ± 0.1 dex	0.1 ± 0.04 dex	(11)	0
2M19253585+3847159	5089 ± 60 K	4.43 ± 0.1 dex	0.11 ± 0.04 dex	(11)	0
2M19294147+3815587	6044 ± 60 K	3.98 ± 0.1 dex	0 ± 0.04 dex	(11)	0
2M19344300+4651099	5415 ± 60 K	4.43 ± 0.1 dex	0.12 ± 0.04 dex	(11)	0
2M19370743+4217274	5854 ± 60 K	4.01 ± 0.1 dex	0.34 ± 0.04 dex	(11)	0
2M19412225+4636081	5737 ± 60 K	4.59 ± 0.1 dex	0.12 ± 0.04 dex	(11)	0

ID (2mass)	$T_{\text{eff}} \pm \Delta T_{\text{eff}}$	$\log g \pm \Delta \log g$	$[Fe/H] \pm \Delta[Fe/H]$	Reference	Flag
2M19480452+5024323	6030 ± 60 K	4.24 ± 0.1 dex	0.14 ± 0.04 dex	(11)	0
2M19481670+4031304	5750 ± 60 K	4.5 ± 0.1 dex	0.1 ± 0.04 dex	(11)	0
2M19495685+4937244	5497 ± 60 K	4.49 ± 0.1 dex	-0.08 ± 0.04 dex	(11)	0
2M19521906+4444467	5441 ± 60 K	4.42 ± 0.1 dex	0.28 ± 0.04 dex	(11)	0
2M19134816+4014431	5886 ± 60 K	4.34 ± 0.1 dex	-0.16 ± 0.04 dex	(11)	0
2M19274223+3800508	5540 ± 60 K	4.52 ± 0.1 dex	0.29 ± 0.04 dex	(11)	0
2M19322962+4056051	5274 ± 60 K	4.46 ± 0.1 dex	0.07 ± 0.04 dex	(11)	0
2M19413907+4615592	5593 ± 60 K	4.32 ± 0.1 dex	0.37 ± 0.04 dex	(11)	0
2M19491993+4153280	6181 ± 60 K	4.23 ± 0.1 dex	0.07 ± 0.04 dex	(11)	0
2M19052120+4844387	5969 ± 60 K	4.24 ± 0.1 dex	0.2 ± 0.04 dex	(11)	0
2M19103720+3914394	5699 ± 60 K	4.28 ± 0.1 dex	-0.36 ± 0.04 dex	(11)	0
2M19162065+4133465	5945 ± 60 K	4.06 ± 0.1 dex	0.19 ± 0.04 dex	(11)	0
2M19215883+3847437	6014 ± 60 K	4.13 ± 0.1 dex	-0.07 ± 0.04 dex	(11)	0
2M19224155+3841276	5681 ± 60 K	4.61 ± 0.1 dex	0.13 ± 0.04 dex	(11)	0
2M19233232+3803272	5736 ± 60 K	4.32 ± 0.1 dex	0.04 ± 0.04 dex	(11)	0
2M19240457+3832440	5581 ± 60 K	4.33 ± 0.1 dex	-0.02 ± 0.04 dex	(11)	0
2M19253173+3807388	5935 ± 60 K	4.34 ± 0.1 dex	-0.16 ± 0.04 dex	(11)	0
2M19254165+3812597	5641 ± 60 K	3.97 ± 0.1 dex	0.12 ± 0.04 dex	(11)	0
2M19262571+3824374	5846 ± 60 K	4.1 ± 0.1 dex	-0.12 ± 0.04 dex	(11)	0
2M19284793+4202459	5699 ± 60 K	4.05 ± 0.1 dex	0.15 ± 0.04 dex	(11)	0
2M19310830+4312575	5766 ± 60 K	4.5 ± 0.1 dex	0.24 ± 0.04 dex	(11)	0
2M19312934+4605559	6062 ± 60 K	4.3 ± 0.1 dex	0 ± 0.04 dex	(11)	0
2M19322256+4253471	5610 ± 60 K	4.38 ± 0.1 dex	0.25 ± 0.04 dex	(11)	0
2M19324327+4137039	6009 ± 60 K	4.45 ± 0.1 dex	-0.09 ± 0.04 dex	(11)	0
2M19344207+4117432	5562 ± 60 K	4.37 ± 0.1 dex	-0.16 ± 0.04 dex	(11)	0
2M19345420+4714493	5843 ± 60 K	4.25 ± 0.1 dex	-0.38 ± 0.04 dex	(11)	0
2M19391944+4639345	5781 ± 60 K	4.07 ± 0.1 dex	0.34 ± 0.04 dex	(11)	0
2M19393877+4629292	6028 ± 60 K	4.27 ± 0.1 dex	0.23 ± 0.04 dex	(11)	0
2M19395364+4512492	5647 ± 60 K	4.55 ± 0.1 dex	-0.43 ± 0.04 dex	(11)	0

Table 6.7: Average differences in derived parameters between our method and SWEET-Cat parameters. Full sample size is 81 stars, with statistics for 18 flagged stars included for reference. Median is shown to decrease effect of outliers. SD stands for standard deviation and MAD for Median Absolute Deviation.

Parameter	Sample	Median (Pipeline - SWEET-Cat)	SD	MAD
$T_{\rm eff}$	All Stars	-15 K	106 K	102 K
$\log g$	All Stars	+0.00 dex	0.16 dex	0.14 dex
$[M/H]$	All Stars	+0.00 dex	0.10 dex	0.10 dex
$T_{\rm eff}$	Flagged	-23 K	107 K	117 K
$\log g$	Flagged	+0.03 dex	0.21 dex	0.15 dex
$[M/H]$	Flagged	-0.03 dex	0.11 dex	0.10 dex

ID (2mass)	$T_{\rm eff} \pm \Delta T_{\rm eff}$	$\log g \pm \Delta \log g$	$[Fe/H] \pm \Delta[Fe/H]$	Reference	Flag
2M19343286+4249298	4500 ± 116 K	4.69 ± 0.2 dex	-0.18 ± 0.1 dex	(12)	0
2M14264827-0510400	5601 ± 44 K	4.25 ± 0.08 dex	0.5 ± 0.04 dex	(13)	1
2M14532303+1814074	4886 ± 45 K	3.16 ± 0.11 dex	0.12 ± 0.03 dex	(14)	1
2M19254039+3840204	5624 ± 40 K	4.48 ± 0.08 dex	-0.15 ± 0.03 dex	(15)	1
2M19024305+5014286	5685 ± 27 K	4.35 ± 0.04 dex	-0.14 ± 0.02 dex	(15)	1
2M19240775+4902249	5884 ± 45 K	4.35 ± 0.09 dex	0.15 ± 0.04 dex	(15)	1
2M18523616+4508233	6375 ± 44 K	4.25 ± 0.15 dex	0.09 ± 0.04 dex	(16)	1
2M20242972+1645437	5924 ± 30 K	4.28 ± 0.11 dex	0.16 ± 0.03 dex	(16)	1

6.2.3 Further Discussion

Tables 6.1-6.3 show that there are some small discrepancies between our values and the ones in the literature, comparing both observations in the optical and in the NIR for our sample stars. This section proposes and analyzes some explanations for these differences, as well as providing additional tests on the method and its capabilities.

Errors in the line-list and/or the models used for the synthesis might be one reason for these discrepancies. The synthetic spectra match the observed one with a very high degree of accuracy (see figures 5.14 and 6.9-6.16), so it is unlikely this is the case. Tests with solar spectra show that our pipeline can provide accurate parameters for a solar-type star with APOGEE resolution (see section 5.3), so it is unlikely that this is the explanation for all discrepancies found between this method's parameters and the ones previously derived in the literature.

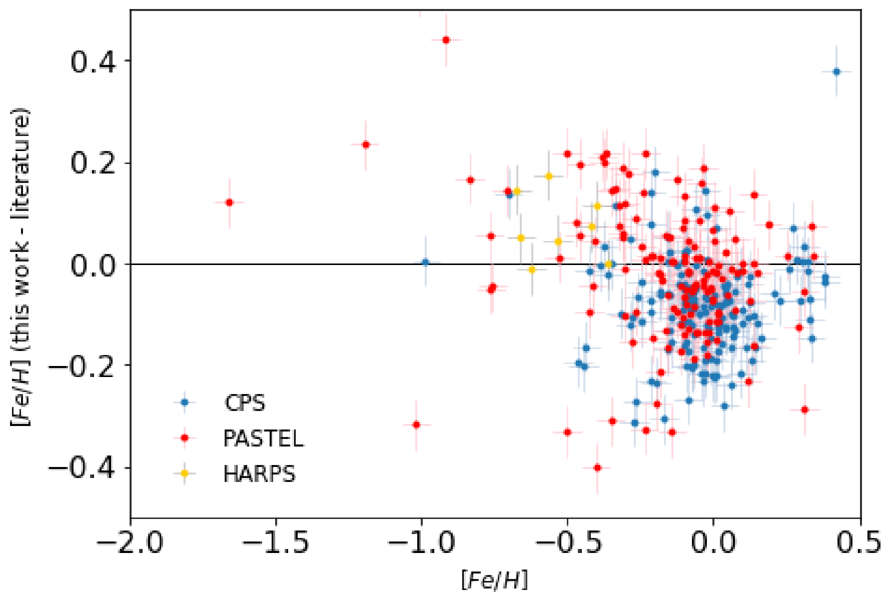

Figure 6.26: Comparison between Iron abundance derived by our pipeline and literature values.

[Fe/H] calculation

Another additional hypothesis can be the difference between $[M/H]$ and $[Fe/H]$ (iron abundances) for these stars. Taking the overall metallicity for each star can lead to a greater disparity in measurements than if the iron abundances are compared. We used our pipeline to determine the [Fe/H] for each star in the sample and compared them to values in literature. These syntheses were done having only the Fe abundance as a free parameter and fixing the other parameters to the results previously derived by our pipeline. The abundances derived are summarized in Fig. 6.26 and are available in a table format in the appendix.

Among our reference optical analysis, CPS provides both $[M/H]$ and $[Fe/H]$ for its characterized stars, while HARPS and PASTEL provide only $[Fe/H]$.

In table 6.8, it is still clear that the $[Fe/H]$ value given by our pipeline is very close to the literature values. The largest measured differences are found when comparing our values with CPS ($\Delta[Fe/H] = -0.08$ dex), while the average difference in the PASTEL sample comparison is -0.01 dex. These results show us that the method is robust and can provide not only $[M/H]$ but $[Fe/H]$ as well for the analyzed stars.

Another possible explanation for any discrepancies in the parameters could be just a difference in the way the parameters are minimized in our pipeline and other codes. We investigated previous works using synthetic spectra and discovered examples in the literature

Table 6.8: Average differences between $[Fe/H]$ derived with this method and literature values for $[Fe/H]$ (all values in dex). Median is shown to decrease effect of outliers. SD stands for standard deviation and MAD for Median Absolute Deviation.

Sample	Stars	Median (Pipeline - Literature)	SD	MAD
CPS	168	-0.08 dex	0.10 dex	0.14 dex
PASTEL	153	-0.02 dex	0.22 dex	0.13 dex
HARPS-GTO	8	+0.06 dex	0.06 dex	0.09 dex

of lower metallicities derived with *Turbospectrum* versus other methods/codes, such as Jofré et al. (2014). The recent work of Blanco-Cuaresma (2019) has shown how different spectral synthesis codes can derive different parameters in the optical with *iSpec*, but there have been no investigations regarding the same thing in the NIR. Further explorations of the output parameter space of *Turbospectrum* and other codes in the NIR are needed to know exactly what the explanation for these discrepancies might be.

Finally, even though our synthetic spectra provide a good match for the observed ones, it does not mean we can fully trust the parameters or that they are better or worse than the ones published before in the literature. Since the observations are different from the ones in the optical, and the normalization is different from the one used by ASPCAP as well, there is no way to conclusively determine the set of parameters that better characterize a particular star. The only thing we can state for certain is that all the parameters shown in this paper were derived with a uniform method and pipeline, so any systematic error or bias will be present across the full sample.

We can also analyze the results by themselves and compare them to previously measured parameters for solar neighborhood stars. Fig. 6.27 shows a histogram with the metallicity and iron abundances found in the full sample. Taking into account a selection bias due to our sampling method (see section 4.2), where we select only stars with APOGEE $-0.5 < [M/H] < 0.5$ dex, we expect a slight bias in our sample towards stars with higher metallicities. This is due to the exclusion of stars with $[M/H] < -0.5$ dex from our sample.

Rotational Velocity ($v \sin i$)

Since our syntheses included rotational velocity $v \sin i$ as a free parameter, we can also analyze those results to check the shape of their distribution. Fig. 6.28 shows a histogram with the distribution of rotational velocities of our stellar sample. 9 stars were also found to have $v \sin i > 20$ km/s, and are included in Table 6.9. We found that all 9 of these stars are in the

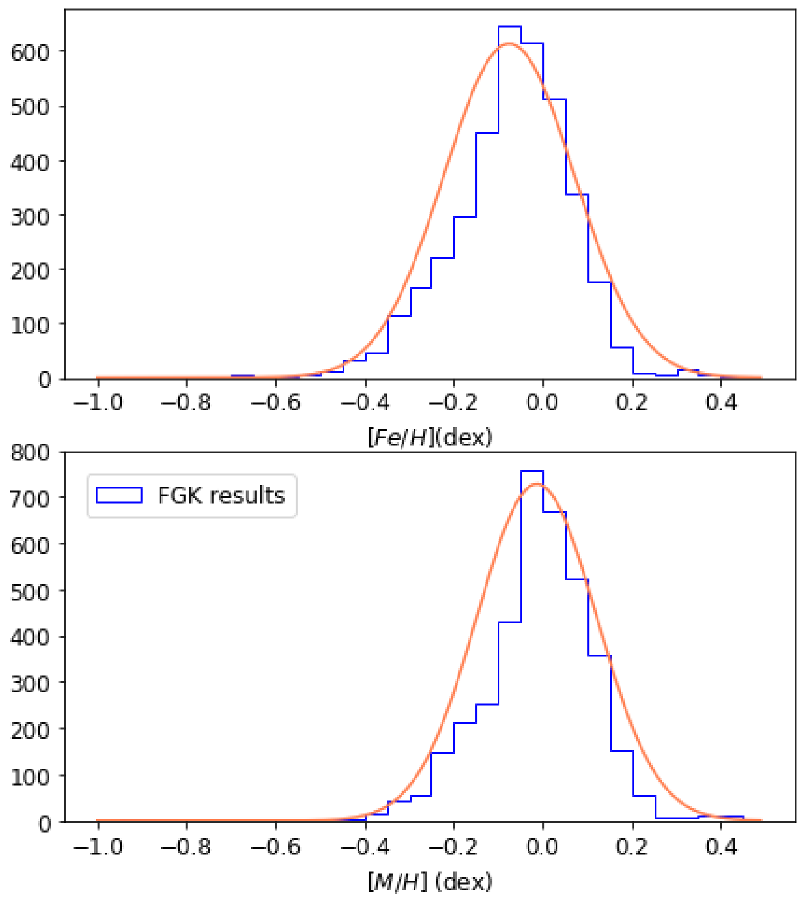

Figure 6.27: Histogram showing the distribution of both our $[M/H]$ and $[Fe/H]$ values across the FGK star sample. Fitting the histogram are Gaussian distributions with the parameters $\mu_{[M/H]} = -0.01$ and $\sigma_{[M/H]} = 0.13$, $\mu_{[Fe/H]} = -0.08$ and $\sigma_{[Fe/H]} = 0.15$

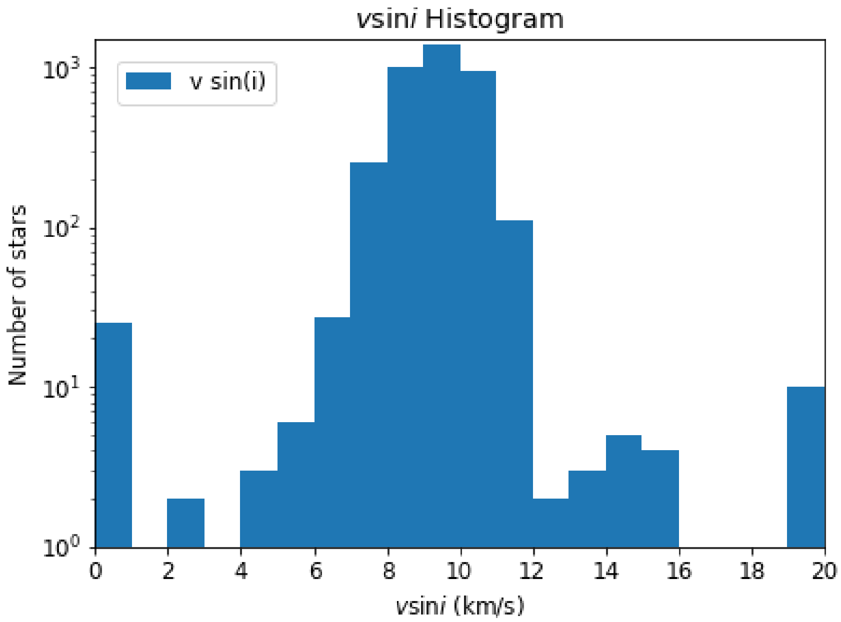

Figure 6.28: Histogram showing the distribution of our $v \sin i$ values across the stellar sample.

Table 6.9: Stars with high $v \sin i$, not included in Fig. 6.28

Apogee ID	$T_{\rm eff}$ (K)	$\log g$ (dex)	$[M/H]$ (dex)	$v \sin i$ (km/s)
2M08510576+1143469	5396	3.58	-0.24	21.5
2M21321194+0013180	4459	3.83	-0.86	22.6
BD-13:3834	6681	5.34	-0.69	23.1
2M19004297+3834248	6364	4.32	0.15	24.3
2M03082560+2619532	5835	3.11	-0.32	27.3
2M06583851-0028490	5029	2.34	0.13	31.4
2M19500857+3954488	6505	4.47	0.21	35.6
2M19250201+4429508	4737	4.12	-0.10	36.2
2M23315208+1956142	5439	3.32	0.28	42.9

PASTEL sample, and they correspond to stars with poor fits overall.

Syntheses with fixed $\log g$

In addition to the previous tests with uncalibrated results, we decided to perform another test related to parameter calibration and our results. To accurately evaluate the possible ranges of errors related to the $\log g$ estimates, we decided to run new syntheses with our method for three selected test stars, fixing surface gravity to different values between $\log g = 3.5$ dex and $\log g = 5.0$ dex. Since both our pipeline and ASPCAP's use similar methods for spectroscopic parameter derivation, by evaluating the magnitude of the differences, we can conclude how problems in the derivation of $\log g$ by both our method and ASPCAP affect other parameters.

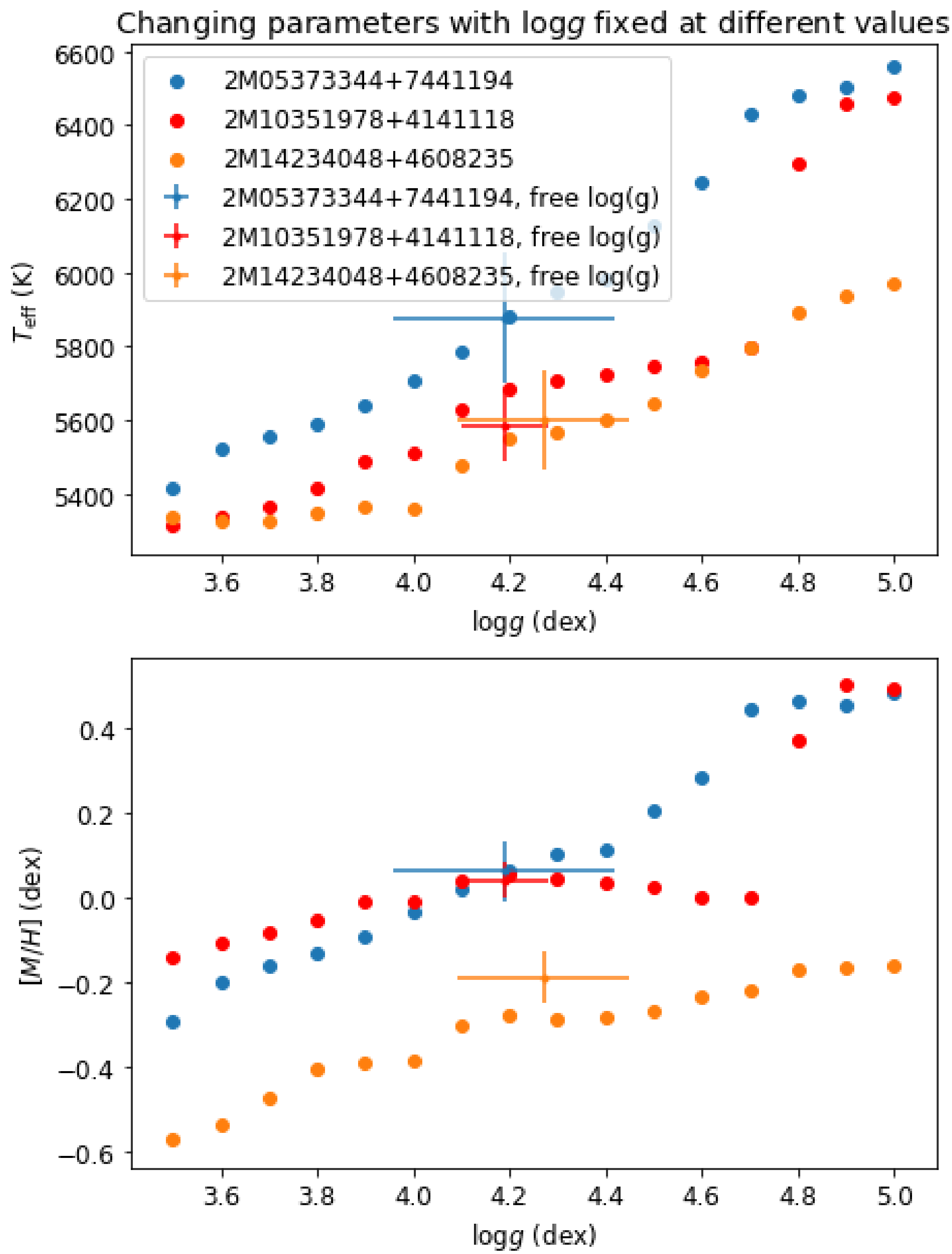

Figure 6.29: Diagram representing the output parameters with fixed surface gravity at different values between $\log g = 3.5$ dex and $\log g = 5.0$ dex. The data for 3 different stars is presented, 2M05373344+7441194 (blue), HD_176377 (orange), and 2M10351978+4141118 (red), with the measured values for each of them indicated by an error bar of the same color.

The results obtained for the 3 test stars are presented in Fig. 6.29. Comparing our test to a similar one with fixed $\log g$ values published in Tsantaki et al. (2018), we find that our results are similar to theirs, although with a larger dispersion in both T_{eff} and $[M/H]$. The derived T_{eff} can vary by up to 1000 K, with a strong dependence on $\log g$. There is also a strong dependence on the output for $[M/H]$ as $\log g$ is fixed at different values, with differences varying up to 0.75 dex. This test shows that performing syntheses with wrong values for the surface gravity can result in errors across other parameters and that fixing the $\log g$ can result in different parameters for the same star. Despite the strong effect changing the $\log g$ can have on the other parameters, such as T_{eff} and $[M/H]$, the fact that our uncorrected $\log g$ are not very different from ASPCAP and optical values, and that our T_{eff} and $[M/H]$ are also comparable, increases our confidence in our final set of parameters. See also Mortier et al. (2013) and Mortier et al. (2014) for a further exploration of the effects fixing $\log g$ values can have on other spectroscopical parameters using the EW method.

We also decided to run a new test for all CPS stars, fixing the $\log g$ to our derived corrected values. By comparing the output parameters between the syntheses with the fixed and the free $\log g$, we improve our knowledge on the precision of our method and the derived parameters. The results are displayed in Fig. 6.30. We find that both the derived metallicity and effective temperatures can change significantly when fixing the surface gravity of the star. There is also a complex interdependency between all three parameters, as stars with high metallicity values tend towards an increase in temperature when compared with lower metallicity stars. A trend towards decreasing metallicity values for syntheses with fixed $\log g$ is also present, with some stars having differences up to around 1.0 dex between the derived $[M/H]$ values with fixed and free $\log g$. This effect seems to be more pronounced for stars with higher T_{eff}, compared to stars with lower T_{eff}.

Given these figures, we can conclude that syntheses with fixed surface gravity values can result in misleading and differing values when compared to syntheses obtained with $\log g$ as a free parameter. The complex degeneracies between the three main spectroscopical atmospheric parameters, $[M/H]$, $\log g$ and T_{eff}, mean that changes in one of them can result in unintended changes to the other two, especially when using the spectral synthesis method for stellar parameter determination. When compared with the previously cited works on fixed vs free $\log g$ with the EW method, the synthetic spectra resulted in a much larger amplitude in the variations of other spectroscopic parameters.

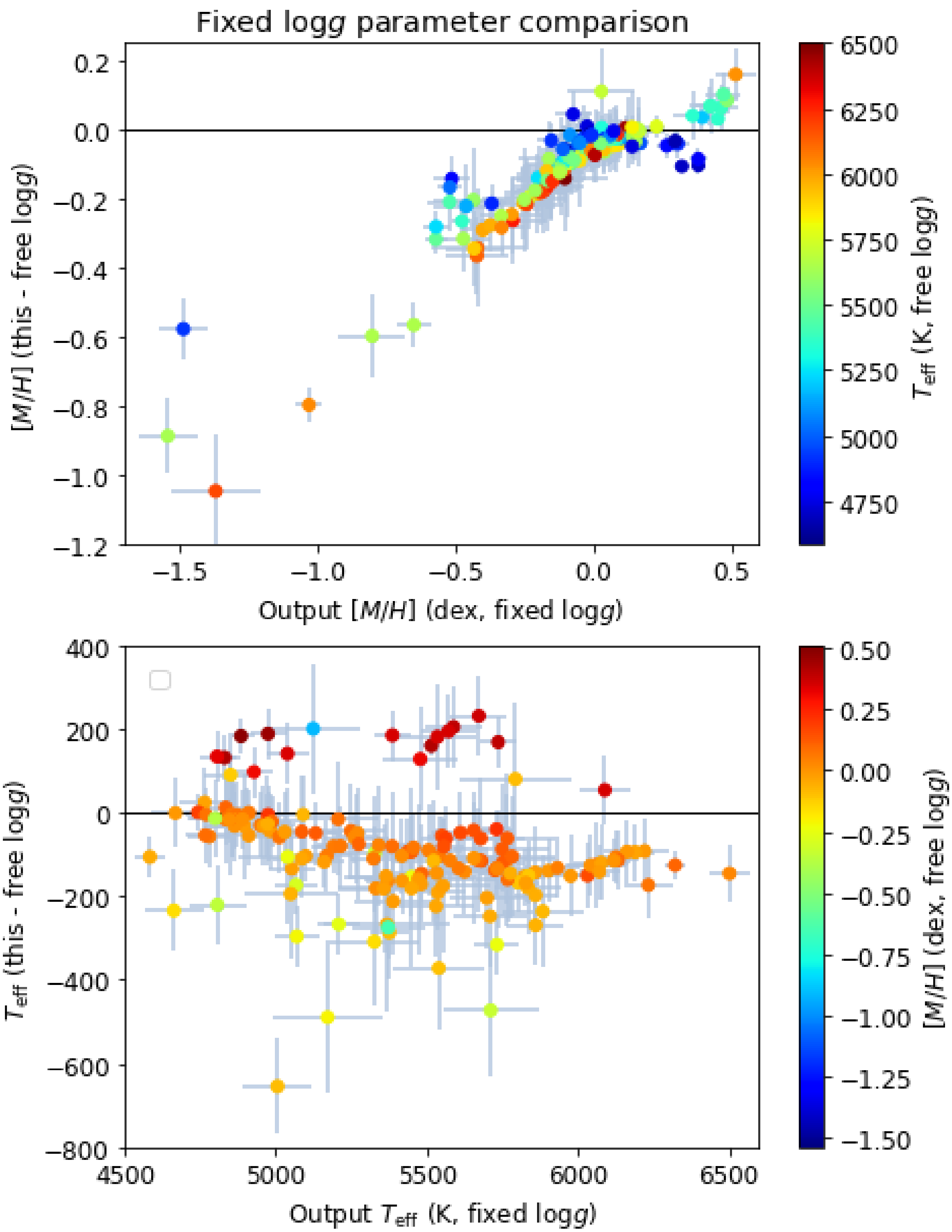

Figure 6.30: Diagram displaying the difference between the output parameters obtained with $\log g$ as a free parameter and the parameters derived with $\log g$ fixed at the final corrected values (see Fig. 6.6). Top plot displays the $[M/H]$ difference with the colors indicating the original T_{eff} values measured for each star with free $\log g$, and the bottom one the T_{eff} difference, with the colors indicating the original $[M/H]$ values measured for each star with free $\log g$. Displayed error bars are our pipeline's estimates using the covariance matrix.

6.3 Final Thoughts

Over the course of this chapter, we have characterized 3748 FGK stars. The synthetic spectra of stars with varying spectral types were compared to observations using *iSpec* and *Turbospectrum* and shown to match observations for most lines and spectral regions. By displaying multiple comparisons with both ASPCAP and other literature parameters, we have also shown that our output results are accurate within our uncertainty margins. Therefore, we conclude that our method is capable of synthesizing FGK star spectra and deriving atmospheric parameters from them. The results shown in this chapter have been accepted by a peer-reviewed journal, showing that our work is recognized by the community.

However, the syntheses of FGK stellar spectra is not the main goal of our project. We intend to tackle the challenge of synthesizing the spectra of M dwarfs and to derive accurate parameters for those stars. In the following pages, we will use the method demonstrated in this chapter to analyze and characterize the spectra of M dwarfs, determining their atmospheric parameters and comparing our results to available literature values.

Chapter 7

Synthesis of APOGEE M dwarf spectra

This Chapter is dedicated to the derivation of stellar parameters for M dwarfs. It includes every result obtained from the synthesis of their spectra with our pipeline, as well as the analysis and comparisons between the results and available literature values.

7.1 Results

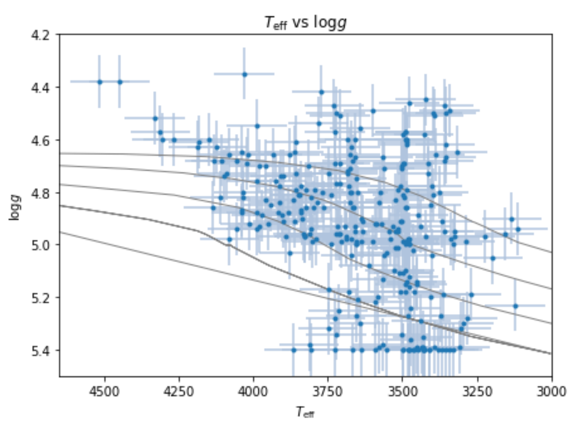

Figure 7.1: HR diagram with T_{eff} and $\log g$ values from *iSpec* output parameter distribution, with overplotted PARSEC isochrones (Bressan et al. 2012).

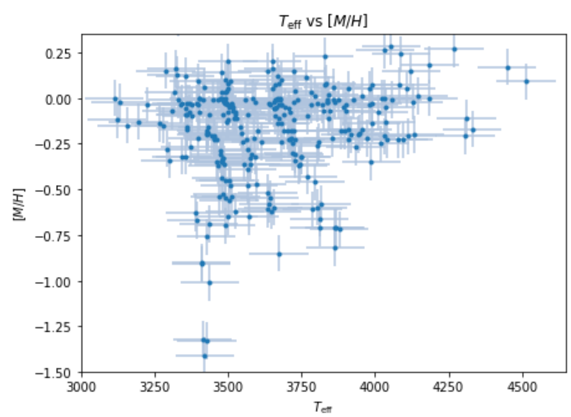

Figure 7.2: T_{eff} and $[M/H]$ from *iSpec* parameter distribution for stars in M dwarf sample.

The 250 M dwarfs in our sample were synthesized with the method detailed in Sections 5.2 and 5.4, and the results for T_{eff}, $\log g$ and $[M/H]$ are summarized in Figs. 7.1 and 7.2. The full results are available in the appendix, in Table B.2. We considered displaying the *iSpec* estimated errors, as we do for the FGK stellar sample, but the high atomic lines/wavelength range ratio causes problems with that estimate, giving approximate errors of around 5-10 K for $T_{\rm eff}$, and below 0.03 dex for both $\log g$ and $[M/H]$. Given that, the errors included in the plots are ± 100 K for the $T_{\rm eff}$, ± 0.1 dex for $\log g$ ± 0.1 dex for $[M/H]$. These values were estimated by taking into account our normalization procedure, which separated stars into 100 K bins, and are only precision errors. These errors may be overestimated, as they are above most differences between our results and available literature (see Section 7.2.1).

The isochrone comparisons presented in Fig. 7.1 show that, for most of the sample, our methodology's output $T_{\rm eff}$ and $\log g$ agree with the values predicted by models for M dwarfs. Despite this, a small number of stars has a seemingly underestimated $\log g$. Some weak trends are present across the results for the full sample in Fig. 5.18, with thin columns of stars with very similar effective temperatures but changing metallicity values. This may indicate the presence of biases in the minimization code or the construction of the line list and line masks.

We display five synthetic spectra in this chapter, separated accordingly to their metallicity and effective temperature. A full table with all derived parameters is available at the appendix B.2. A summary of each of the 250 sample M dwarfs parameters' and available literature is also displayed in Section B.2.1.

7.1.1 Fully convective M dwarfs($T_{\rm eff} < 3400$ K)

The spectra of stars with $T_{\rm eff} < 3400$ K is very challenging to synthetically reproduce due to the degeneracy in continuum depression between multiple spectral parameters such as temperature, metallicity, and surface gravity (see section 3.3). Depressions in the continuum can be caused by any of these parameters, with the pipeline estimating lower metallicity and higher temperature values than the star has in reality. We minimized these effects by repeating the syntheses with multiple normalizations and choosing the best matches across all iterations. The following displayed figures demonstrate how the synthetic spectrum matches the observations, increasing the plausibility of our derived parameters. However, it is impossible to confirm whether the derived parameters correspond to the stellar ones for either of these stars.

Fig. 7.3 displays the observed and best match synthetic spectra for star 2M08050361+4121251 (G 111-52 [1]). ASPCAP's available parameters are $T_{\rm eff} = 3215$ K ,$\log g = 4.34$ dex, $[M/H] = -0.66$ dex. We did not find any other literature parameters for this star. The displayed spec-

[1] http://simbad.u-strasbg.fr/simbad/sim-id?Ident=2Mass+j08050361%2B4121251

trum of the star is the APOGEE observed spectrum normalized using a synthetic spectrum with $T_{\text{eff}} = 3000$ K, $\log g = 4.5$ dex and $[M/H] = -0.4$ dex. This is one of the more metal-poor M dwarfs in the sample, with derived parameters of $T_{\text{eff}} = 3412 \pm 100$ K,$\log g = 4.7 \pm 0.1$ dex, $[M/H] = -1.32 \pm 0.1$ dex. We find that our determined temperature and metallicity are above the ones made available by ASPCAP, but the lack of any other literature values for the star and the correct match between our synthesized spectrum and the observed one makes us trust our derived parameters for it.

In Fig. 7.4, we display the observed and best match synthetic spectra for star 2M18562628+4622532 (G 205-47 [2]). This star was characterized in Gilhool et al. (2017), matching its spectra with a template with $T_{\text{eff}} = 3200$ K,$\log g = 5.0$ dex, $[M/H] = 0.0$ dex. The available ASPCAP parameters for this star are $T_{\text{eff}} = 3287$ K and $\log g = 4.47$ dex, with a $[M/H] = -0.41$ dex. The displayed spectrum for the star has been obtained by normalizing the APOGEE observed one with a synthetic spectrum with $T_{\text{eff}} = 3000$ K, $\log g = 4.5$ dex and $[M/H] = -0.2$ dex, and the derived spectroscopical parameters for this star are $T_{\text{eff}} = 3302 \pm 100$ K,$\log g = 5.3 \pm 0.1$ dex, $[M/H] = -0.34 \pm 0.1$ dex. We find a very good agreement between our derived temperature and metallicity and the ones published by ASPCAP, while Gilhool et al. (2017) estimates different values for these parameters.

The following Fig. 7.5 contains the spectra of star 2M14130286+0506321 (NLTT 36587 [3]), displaying both the observed (black) and best matching spectra (red). This star was characterized in Gilhool et al. (2017), matching its spectra with a template with $T_{\text{eff}} = 3400$ K,$\log g = 5.5$ dex, $[M/H] = 0.5$ dex. The available uncalibrated ASPCAP parameters for this star are $T_{\text{eff}} = 3431$ K and $\log g = 4.65$ dex, with a calibrated $[M/H] = +0.08$ dex. The displayed spectrum for the star has been obtained by normalizing the APOGEE observed one with a synthetic spectrum with $T_{\text{eff}} = 3200$ K, $\log g = 4.5$ dex and $[M/H] = +0.2$ dex, and the derived spectroscopical parameters for this star are $T_{\text{eff}} = 3324 \pm 100$ K,$\log g = 4.95 \pm 0.1$ dex, $[M/H] = +0.16 \pm 0.1$ dex. For this star, we find a greater agreement between the results of Gilhool et al. (2017), ASPCAP, and ours.

The presence of wide water line bands across the full first order of the spectrum (two top rows) results in a jagged and depressed continuum down to around 0.8 instead of the expected 1.0. As stated before, the modeling of these water lines is fundamental for the creation of

[2] http://simbad.u-strasbg.fr/simbad/sim-id?Ident=2Mass+j18562628%2B4622532
[3] http://simbad.u-strasbg.fr/simbad/sim-id?Ident=%404011701&Name=NLTT+36587

accurate synthetic spectra of M dwarfs with $T_{\rm eff} < 3400\,$K. The spectra displayed in Fig. 7.4 corresponds to a much more metal-rich star than the one displayed in Fig. 7.3, resulting in more pronounced and easier to characterize molecular and elemental lines. The synthesized spectrum, therefore, matches the observed one across the full wavelength range, with lines of multiple elements and molecules being correctly synthesized. This fact, combined with the relative agreement of our pipeline's derived parameter with available literature analysis, increases our confidence in the derived parameters for this star.

The increase in metallicity for the spectra displayed in Fig. 7.5 compared with the previous examples is clear across the spectrum, with more pronounced and clear lines across the full wavelength range despite the low stellar effective temperature. The effect can be noticed in the strong Al line around 1675 nm, a line that is accurately matched by the synthetic spectrum. The full observed spectrum is matched by the synthetic one, showing the power of our method and increasing our confidence in the derived parameters for this star.

7.1.2 $3400\,$K $< T_{\rm eff} < 4000\,$K

The spectra of stars with $3400\,$K $< T_{\rm eff} < 4000\,$K is less challenging to accurately synthesize, as the wide water line bands are less deep, and the atomic lines stand out more as a consequence. We show two example spectra in Figs.7.6 and 7.7 of low and high metallicity stars with similar effective temperatures, demonstrating the effect metallicity can have on the stellar spectra.

Fig. 7.6 shows a comparison between 2M10441137+4500152's normalized APOGEE observed spectrum (LSPM J1044+4500 [4], black) and the best matching spectrum derived with our pipeline (red). The star has been characterized by Gilhool et al. (2017), matching its APOGEE spectra with a template spectrum with $T_{\rm eff} = 3800\,$K,$\log g = 4.5\,$dex, $[M/H] = -0.5\,$dex. The available ASPCAP parameters for this star are $T_{\rm eff} = 3876\,$K and $[M/H] = -0.51\,$dex, as well as $\log g = 4.32\,$dex. The displayed spectrum for the star has been obtained by normalizing the APOGEE observed one with a synthetic spectrum with $T_{\rm eff} = 3600\,$K, $\log g = 4.5\,$dex and $[M/H] = -0.1\,$dex, and the derived spectroscopical parameters for this star are $T_{\rm eff} = 3816{\pm}100\,$K,$\log g = 4.7{\pm}0.1\,$dex, $[M/H] = -0.58{\pm}0.1\,$dex. We find very small differences between our output parameters and the available literature values which, when coupled with the strong agreement between our synthesized spectra and the observations increase our

[4] http://simbad.u-strasbg.fr/simbad/sim-id?Ident=2Mass+j10441137%2B4500152

confidence on our results for this star.

In Fig. 7.7, we present the normalized observed spectrum of star 2M02073745+1354497 (G 3-40 [5], black) as well as the best matching spectrum derived by our pipeline (red). This star was characterized in Gilhool et al. (2017) by matching its APOGEE spectra with a template spectrum with $T_{\rm eff} = 3900\,$K,$\log g = 5.0\,$dex, $[M/H] = +0.5\,$dex. The available ASPCAP parameters for this star are $T_{\rm eff} = 3824\,$K and $[M/H] = +0.23\,$dex, with $\log g = 4.48\,$dex. The displayed spectrum for the star has been obtained by normalizing the APOGEE observed one with a synthetic spectrum with $T_{\rm eff} = 3900\,$K, $\log g = 4.5\,$dex and $[M/H] = +0.4\,$dex, and the derived spectroscopical parameters for this star are $T_{\rm eff} = 3827 \pm 100\,$K,$\log g = 4.97 \pm 0.1\,$dex, $[M/H] = +0.23 \pm 0.1\,$dex.

As a star with considerably higher effective temperature than the ones in our first three examples, the spectra displayed in Fig. 7.6 has a significantly different shape than theirs. The continuum depression due to water lines is much less pronounced, resulting in a decrease of around 0.05, and the lines are very well defined and traced by the synthetic spectrum. The only region of the spectrum in the line mask that may have been poorly matched by the synthetic spectra, other than small errors in the first order, seems to be around 1640 nm, where the synthetic and the observed spectra have a different shape. Otherwise, the synthetic spectra match the observations.

The spectra displayed in Fig. 7.7 demonstrates the potential issues the pipeline may have with higher metallicity stars, as some of the deeper lines are not accurately matched by the synthetic spectrum, with the OH line around 1614 nm being a prime example. Another problem with hotter and more metal-rich stars can come in the selection of the parameters used for creating the template spectra applied to the normalization, as normalizations with different templates can result in different output parameters and the choice of the best match can be subjective. The spectra displayed here correspond to the author's selection of best-matching spectra, and bias might be present in that choice.

[5] http://simbad.u-strasbg.fr/simbad/sim-id?Ident=2Mass+j02073745%2B1354497

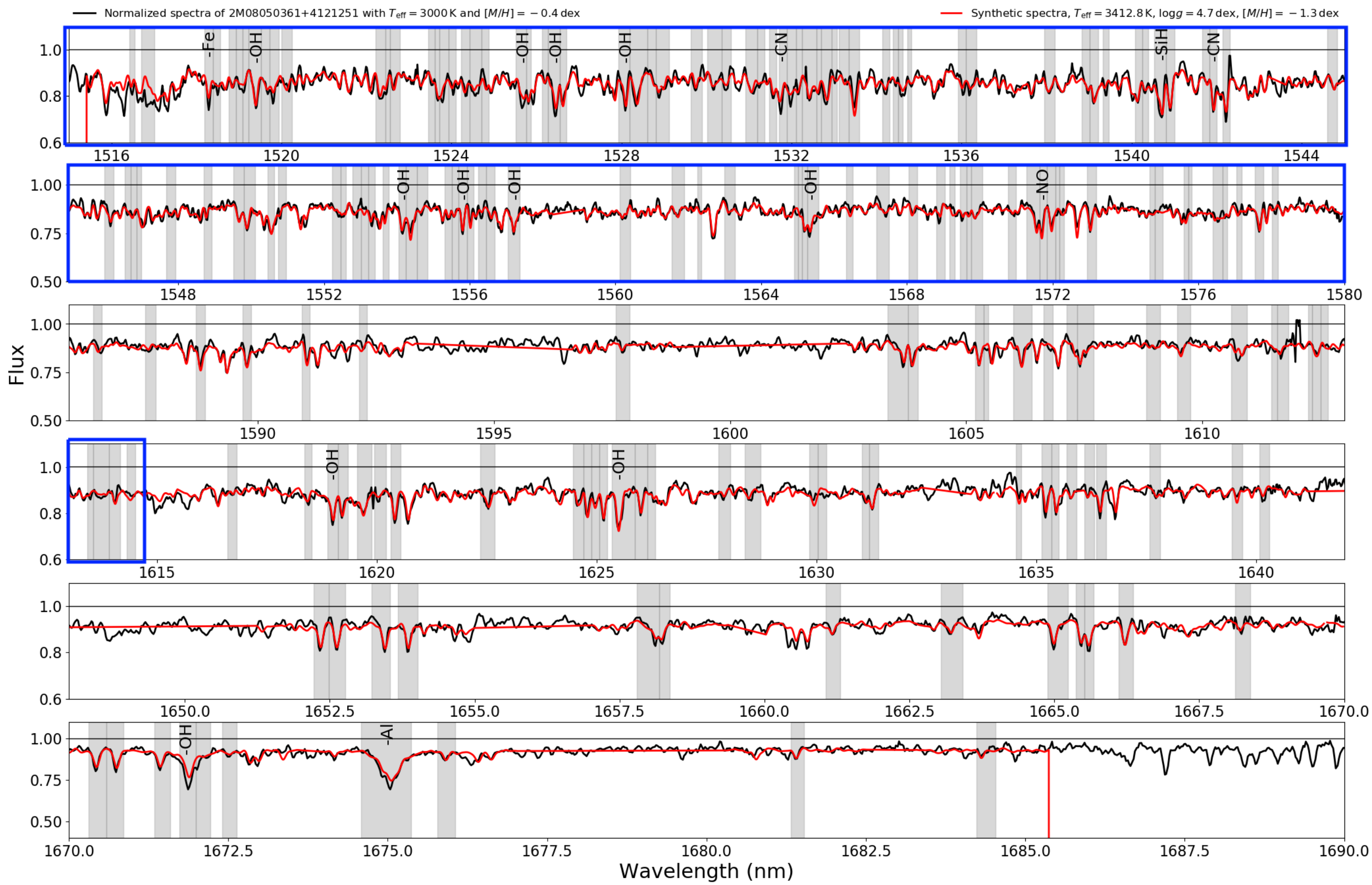

Figure 7.3: Comparison between APOGEE spectra of the star 2M08050361+4121251 (G 111-52, black, normalized using a synthetic spectra with $T_{\rm eff} = 3000$ K, $\log g = 5.0$ dex and $[M/H] = -0.4$ dex) and the best match synthetic spectra (red, straight line) for APOGEE wavelength range. In gray highlight are the areas used for χ^2 minimization by our pipeline's algorithm. Highlighted in blue are the relevant areas mentioned in our results discussion. The best match parameters derived were $T_{\rm eff} = 3412 \pm 100$ K, $\log g = 4.7 \pm 0.1$ dex, $[M/H] = -1.32 \pm 0.1$ dex.

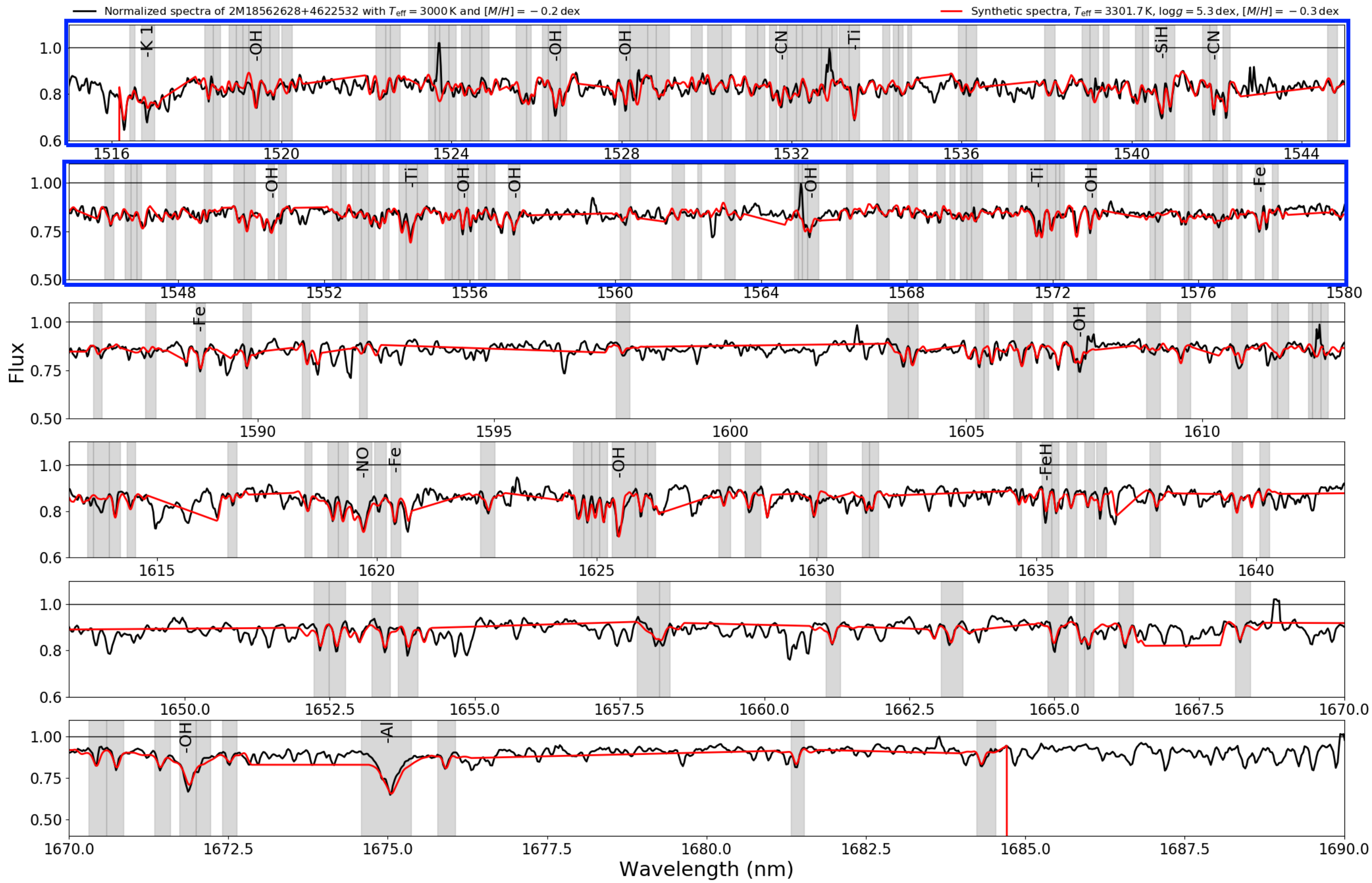

Figure 7.4: Comparison between APOGEE spectra of the star 2M18562628+4622532 (black, normalized using a synthetic spectra with $T_{\rm eff} = 3000\,$K, $\log g = 5.0\,$dex and $[M/H] = -0.2\,$dex) and the best match synthetic spectra (red, straight line) for APOGEE wavelength range. In gray highlight are the areas used for χ^2 minimization by our pipeline's algorithm. Highlighted in blue are the relevant areas mentioned in our results discussion. The best match parameters derived were $T_{\rm eff} = 3302 \pm 100\,$K,$\log g = 5.3 \pm 0.1\,$dex, $[M/H] = -0.34 \pm 0.1\,$dex.

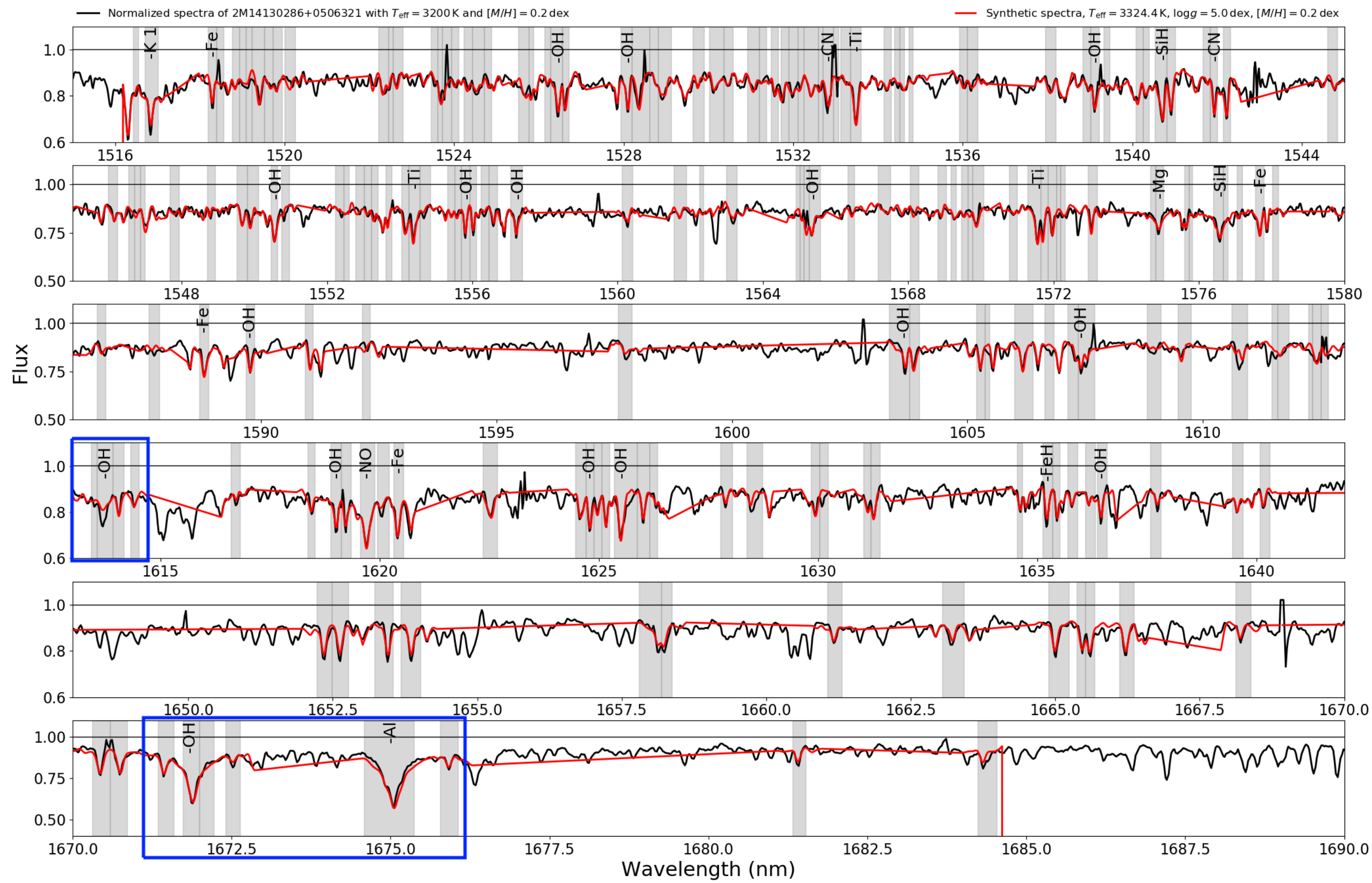

Figure 7.5: Comparison between APOGEE spectra of the star 2M14130286+0506321 (black, normalized using a synthetic spectra with $T_{\rm eff} = 3200\,$K, $\log g = 5.0\,$dex and $[M/H] = +0.2\,$dex) and the best match synthetic spectra (red, straight line) for APOGEE wavelength range. Highlighted in blue are the relevant areas mentioned in our results discussion. In gray highlight are the areas used for χ^2 minimization by our pipeline's algorithm. The best match parameters derived were $T_{\rm eff} = 3324{\pm}100\,$K,$\log g = 4.95{\pm}0.1\,$dex, $[M/H] = +0.16{\pm}0.1\,$dex.

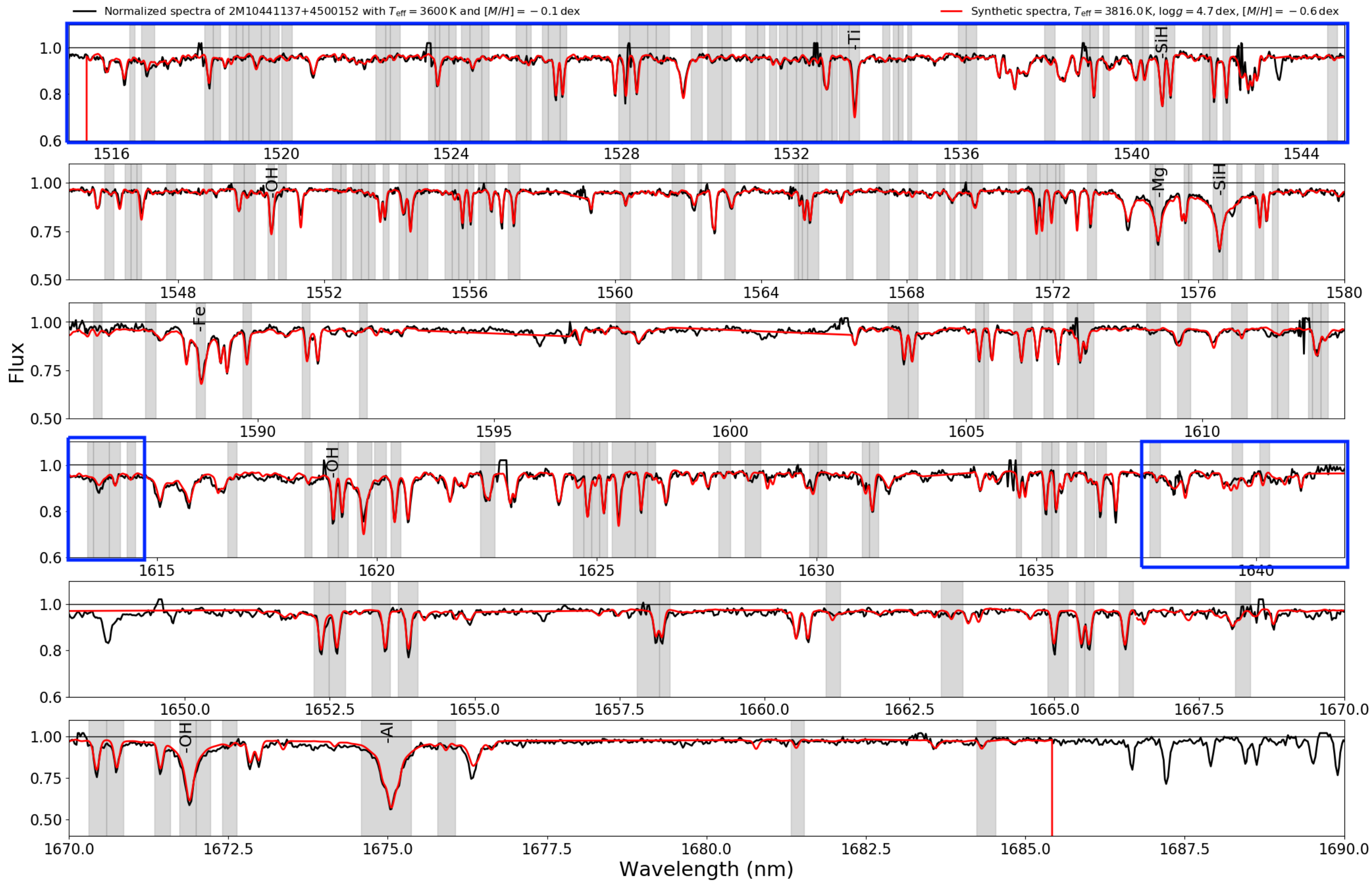

Figure 7.6: Comparison between APOGEE spectra of the star 2M10441137+4500152 (black, normalized using a synthetic spectra with $T_{\rm eff} = 3600\,$K, $\log g = 5.0\,$dex and $[M/H] = -0.1\,$dex) and the best match synthetic spectra (red, straight line) for APOGEE wavelength range. Highlighted in blue are the relevant areas mentioned in our results discussion. In gray highlight are the areas used for χ^2 minimization by our pipeline's algorithm. The best match parameters derived were $T_{\rm eff} = 3816 \pm 100\,$K, $\log g = 4.7 \pm 0.1\,$dex, $[M/H] = -0.58 \pm 0.1\,$dex.

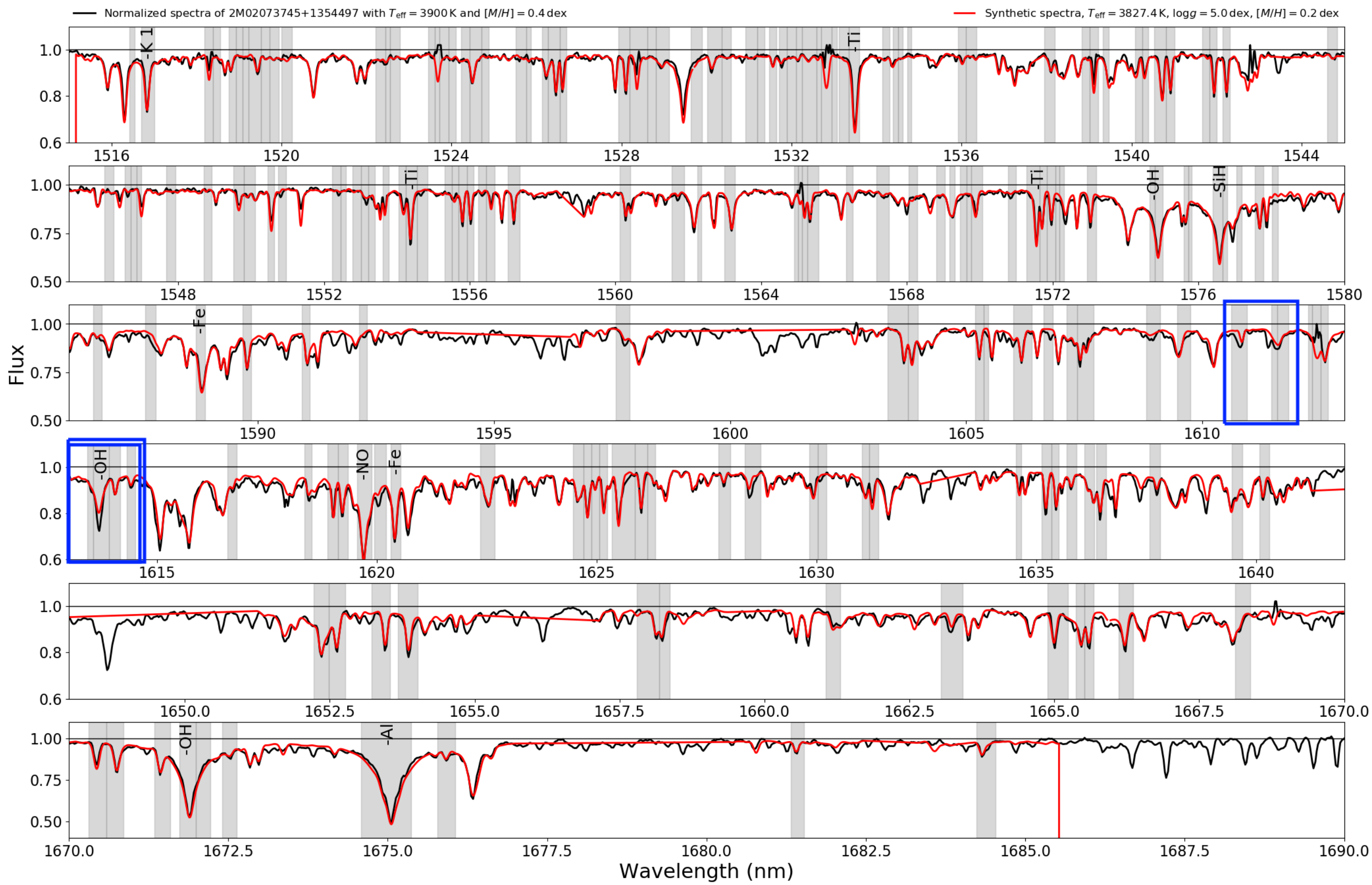

Figure 7.7: Comparison between APOGEE spectra of the star 2M02073745+1354497 (black, normalized using a synthetic spectra with $T_{\mathrm{eff}} = 3900\,\mathrm{K}$, $\log g = 5.0\,\mathrm{dex}$ and $[M/H] = +0.4\,\mathrm{dex}$) and the best match synthetic spectra (red, straight line) for APOGEE wavelength range. Highlighted in blue are the relevant areas mentioned in our results discussion. In gray highlight are the areas used for χ^2 minimization by our pipeline's algorithm. The best match parameters derived were $T_{\mathrm{eff}} = 3827 \pm 100\,\mathrm{K}$, $\log g = 4.97 \pm 0.1\,\mathrm{dex}$, $[M/H] = +0.23 \pm 0.1\,\mathrm{dex}$.

Table 7.1: T_{eff}, $[M/H]$, and $\log g$ comparison between our results and ASPCAP parameters. Median differences, Standard deviation (SD) and Median Absolute deviation (MAD) are presented.

Parameter	Stars	Median (This - ASPCAP)	SD	MAD
T_{eff}	127	-29 K	75 K	76 K
$[M/H]$	214	-0.02 dex	0.14 dex	0.09 dex
$\log g$	250	+0.47 dex	0.28 dex	0.70 dex

7.2 Discussion

7.2.1 Literature comparison

ASPCAP comparison

As mentioned in Section 4.3.2, ASPCAP did not publish calibrated spectroscopic parameters for all stars in our M dwarf sample. From the full 250 star sample, only 127 have ASPCAP values for T_{eff}, and 214 for $[M/H]$. We will limit our comparison to these parameters for consistency reasons. Keeping that in mind, Fig. 7.8 (a) shows a comparison between the $\log g$ values derived with our pipeline and the uncalibrated ones published by ASPCAP, (b) the same comparison for ASPCAP $[M/H]$ values, and (c) a comparison between the T_{eff} values for our sample M dwarfs as derived by *iSpec* and the values published by ASPCAP for the same stars. Errors included are ± 100 K for the T_{eff}, ± 0.1 dex for $[M/H]$ and ± 0.1 dex for $\log g$. As mentioned in Section 7.1, these errors were estimated by taking into account our normalization procedure, which separated stars into 100 K bins, and are only precision errors.

Fig. 7.8 (b) and (c) demonstrate a strong agreement between both the T_{eff} and $[M/H]$ parameters derived by our pipeline and the ones published by them. The differences in 7.1 show median differences for these two spectroscopic parameters within our error margins, increasing the confidence in our pipeline's parameters.

For $\log g$, Fig. 7.8 (a) shows that a trend is present in the data, resulting in median differences of +0.47 dex between our parameters and the ones published by ASPCAP. We find these differences to increase with our $\log g$ estimate, up to around a +1.00 dex difference for the stars with the highest $\log g$ values. Comparisons with the isochrones in Fig. 7.1 show that our values for this parameter are within the expectations for main-sequence stars around these temperatures. The compared values from ASPCAP are also uncalibrated and recognized by their publishers to be unreliable, so these discrepancies will not be taken as evidence against our parameters.

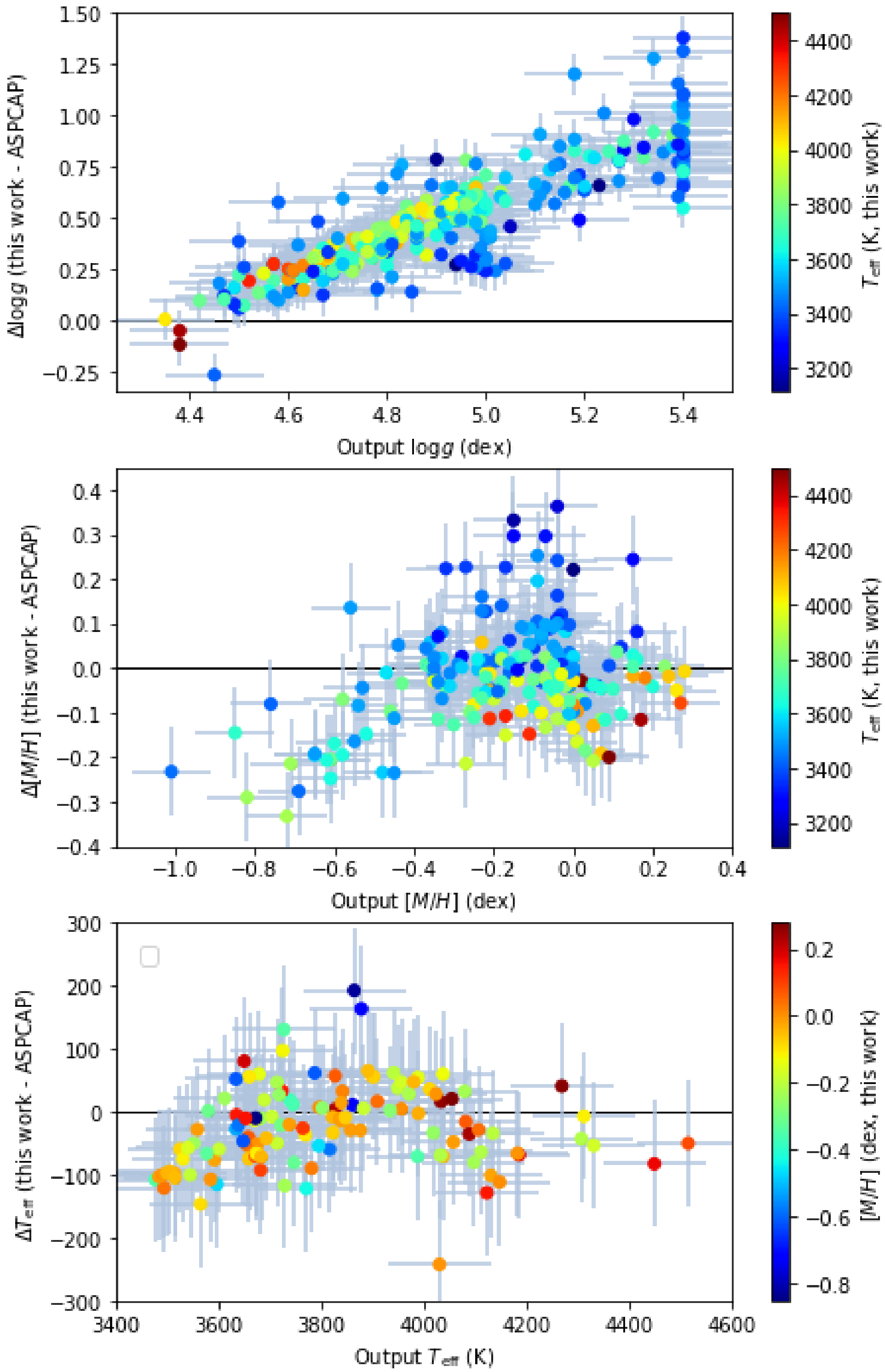

Figure 7.8: TOP (a): Comparison between $\log g$ derived by our pipeline and uncalibrated ASPCAP values, colored accordingly to our method's measured $T_{\rm eff}$ for each star. MIDDLE (b): Comparison between $[M/H]$ derived by our pipeline and ASPCAP values, colored accordingly to our method's measured $T_{\rm eff}$ for each star. BOTTOM (c): Comparison between $T_{\rm eff}$ derived by our pipeline and ASPCAP values, colored accordingly to our method's measured $[M/H]$ for each star.

Table 7.2: $T_{\rm eff}$ and $[M/H]$ comparison between our results and Terrien et al. (2015) parameters for 39 stars in common. Median differences, Standard deviation (SD) and Median Absolute deviation (MAD) are presented.

Parameter	Median (This - Terrien et al. (2015))	SD	MAD
$T_{\rm eff}$	+58 K	81 K	108 K
$[M/H]$	-0.06 dex	0.14 dex	0.15 dex

The points are colored accordingly to other parameters measured by our method to find any correlation or trend between errors across multiple output parameters. In particular, we can observe in Figure (a) that the $\Delta \log g$ is smaller for hotter stars. This can be explained by the fact that ASPCAP's $\log g \leq\sim 4.5$. As we find a correlation between our $\log g$ values and $T_{\rm eff}$, shown in Fig. 7.1, this $\Delta \log g$ therefore increases for colder stars.

As for (b) and $[M/H]$, a trend with $T_{\rm eff}$ is present here, as we find a negative $\Delta[M/H]$ for the hotter stars in our sample and a positive one for the coldest stars. This translates to an overestimation of metallicity for the colder stars in our sample, when compared to ASPCAP values. Both lower $T_{\rm eff}$ and increasing $[M/H]$ can have a similar effect on the spectral shape, lowering the continuum position due to increased strength of the water molecular lines. Therefore, metallicity overestimations can be caused by normalization errors and/or correspond to effective temperature underestimations. We have to note that we are using the $T_{\rm eff}$ values determined by our pipeline to color the points, as ASPCAP does not provide effective temperatures for stars colder than 3500 K. This means that we are comparing parameters determined for the same spectra but with different methods, so the effects may be caused by inherent biases in the methods.

In (c), and relative to the $\Delta T_{\rm eff}$, we find no trend or correlation with metallicity values of the sample stars. We also find this parameter to have a very good agreement with ASPCAP parameters, with the median difference, SD and MAD all being within our error margins. However, since ASPCAP published only effective temperatures for stars above 3500 K, the plot displayed is not necessarily representative of our entire sample.

Comparison with Terrien et al. (2015)

As mentioned in Chapter 2, Terrien et al. (2015) Terrien et al. (2015) published a catalog of ~ 2000 NIR ($0.8 - 2.4\mu$m) spectra and parameters ($T_{\rm eff}$ and $[M/H]$) for 886 nearby M dwarfs, using both photometric and H-band spectral features.

Fig. 7.9 shows a reasonable agreement between our derived parameters and the ones

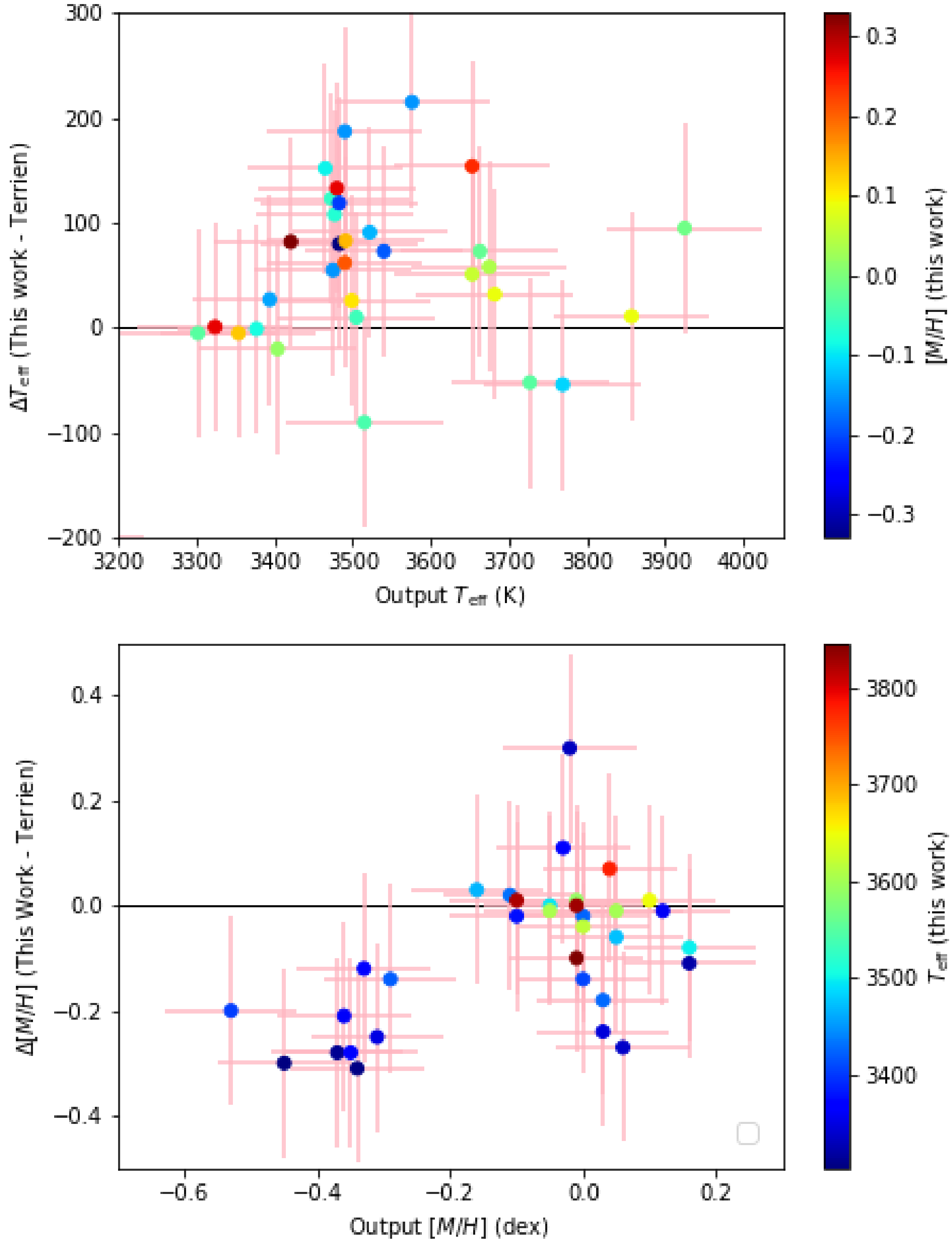

Figure 7.9: TOP (a): Comparison between $T_{\rm eff}$ derived by our pipeline and values published by Terrien et al. (2015), colored accordingly to our method's measured $[M/H]$ for each star. Terrien et al. (2015). BOTTOM (b): Similar comparison for $[M/H]$, colored accordingly to our method's measured $T_{\rm eff}$ for each star.

published in Terrien et al. (2015) for the 33 stars in common between the samples. Table 7.2 shows the median difference between the two parameter distributions. Both the figures and the table demonstrate that the differences are within the error margin for both $T_{\rm eff}$ and $[M/H]$, and show no apparent trend with the parameters themselves.

The fact that Terrien et al. (2015) publishes effective temperatures for M dwarfs colder than the ones characterized with ASPCAP ($T_{\rm eff} > 3288$ K for Terrien et al. (2015) and only 3500 K for ASPCAP) allows for a further analysis of that area of our parameter space. We find that all of our low-temperature ($T_{\rm eff} < 3400$ K) have parameters that agree very strongly with the ones published by Terrien et al. (2015). This fact, combined with the matching synthetic spectra for stars of these temperatures (see Figs. 7.3, 7.4, and 7.5), indicate us that our parameters are likely to be accurate for them.

The data points are colored accordingly to our measured parameters for each star, but we find no correlation or trend in these two figures between either $[M/H]$ and $\Delta T_{\rm eff}$ or $T_{\rm eff}$ and $\Delta[M/H]$.

Comparison with Gaidos et al. (2014)

As mentioned in Section 2, Gaidos et al. (2014) published a catalog of 2970 nearby cool dwarf stars. The sample was selected based on the SUPERBLINK proper motion catalog, based on the stellar properties available. Their parameters for these stars were determined using a least-squares fitting of the spectra to model predictions calibrated by fits to stars with established bolometric temperatures. Metallicities were estimated using the method detailed in Mann et al. (2013), with FGK+M wide binaries being used to identify metal-sensitive features in M dwarf spectra, and deriving an empirical calibration from them. Metallicities are only available for some of the stars in the sample.

Fig. 7.10 and Table 7.3 contain a summary of the differences measured between the parameters derived by our methodology and the ones published in Gaidos et al. (2014) for the same sample of 22 stars (see section 4.3.2). The parameters are very similar across the full stellar sample, with $\Delta T_{\rm eff} < 200$ K and $\Delta[M/H] < 0.2$ dex for almost all stars considered. We find one outlier star for each of the two parameters considered for comparison. They are summarized, together with their derived parameters, in Table 7.4.

Considering the median differences between both parameter distributions, they are within our estimated uncertainty levels, and there seems to be no trend for these differences across

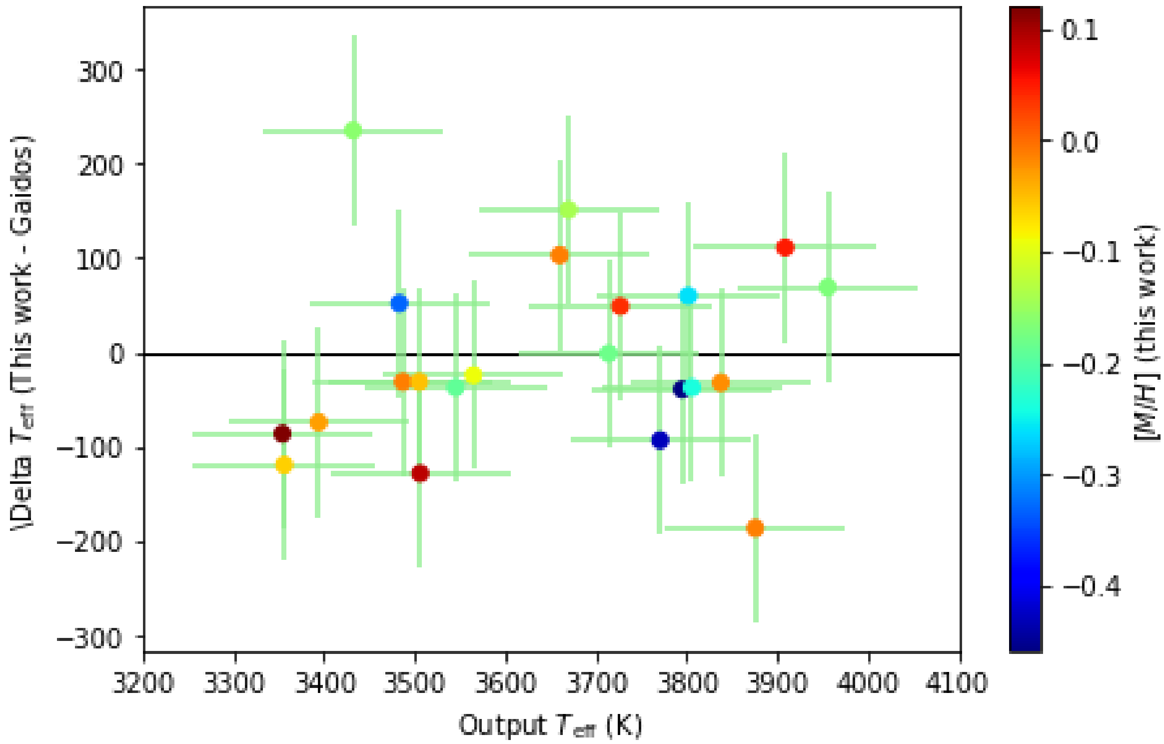

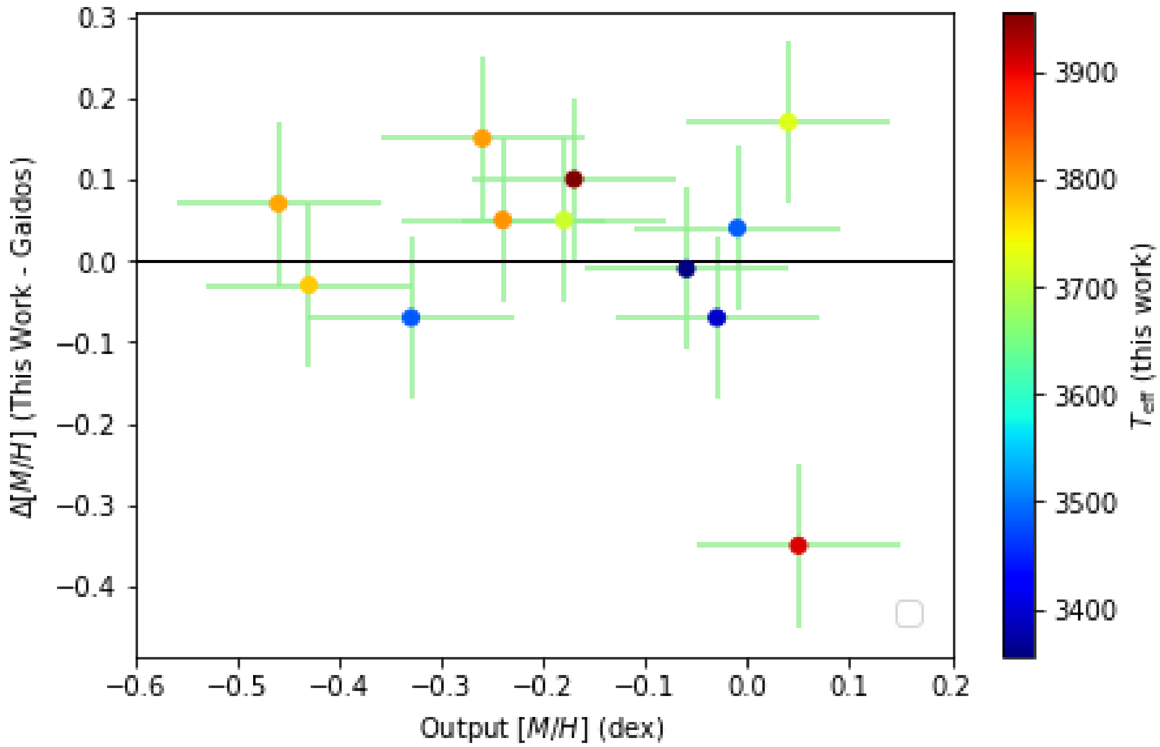

Figure 7.10: TOP (a): Comparison between $T_{\rm eff}$ derived by our pipeline and values published by Gaidos et al. (2014) for 22 stars, colored accordingly to our method's measured $[M/H]$ for each star. BOTTOM (b): Similar comparison for $[M/H]$, colored accordingly to our method's measured $T_{\rm eff}$ for each star.

Table 7.3: $T_{\rm eff}$, $[M/H]$, and $\log g$ comparison between our results and Gaidos et al. (2014) parameters. Median differences, Standard deviation (SD) and Median Absolute deviation (MAD) are presented.

Parameter	Stars	Median (This - Gaidos)		
$T_{\rm eff}$	22	-31 K	97 K	96 K
$[M/H]$	12	+0.04 dex	0.13 dex	0.10 dex

Table 7.4: Stars with outlier parameters when compared to Gaidos et al. (2014) results. T subscript indicates parameter derived using this method, while G indicates Gaidos et al. (2014) parameter.

Star	$T_{\rm eff,T}$	$T_{\rm eff,G}$	$[M/H]_T$	$[M/H]_G$
2M06234645+0502411	3909 K	3798 K	0.05 dex	0.4 dex
2M22010861+4901108	3989 K	4532 K	-0.03 dex	-

either parameter. This agreement of output parameters with literature values contributes to our confidence levels in the method and the results.

The data points are colored accordingly to our measured parameters for each star, but we find no correlation or trend in these two figures between either $[M/H]$ and $\Delta T_{\rm eff}$ or $T_{\rm eff}$ and $\Delta[M/H]$. There are too few points to draw any conclusion based on them.

Comparison with Hejazi et al. (2019)

This subsection presents a comparison between our derived parameters and the ones published in Hejazi et al. (2019). As mentioned in section 2, Hejazi et al. (2019) published parameters for 1544 M dwarfs and subdwarfs based on the comparison of template spectra to low-mid resolution ($R \sim 2000-4000$) observations of TiO and CaH bands in the optical spectra of those stars. We find 16 stars in common between our observed sample and their study.

Fig. 7.11 shows a comparison between our output results and the ones published in that paper, and Table 7.5 displays the median differences found between our values and theirs. The data points themselves are colored accordingly to our measured parameters for each star.

The median $T_{\rm eff}$ differences between both our results and Hejazi et al. (2019) are within uncertainties for most of our sample stars. The biggest outlier is the star 2M07404603+3758253, for which our pipeline resulted in an effective temperature of 3437 K and their analysis es-

Table 7.5: $T_{\rm eff}$, $[M/H]$, and $\log g$ comparison between our results and Hejazi et al. (2019) parameters. Median differences, Standard deviation (SD) and Median Absolute deviation (MAD) are presented.

Parameter	Median (This - Hejazi et al. (2019))	SD	MAD
$T_{\rm eff}$	+41 K	91 K	101 K
$[M/H]$	-0.36 dex	0.44 dex	0.55 dex
$\log g$	+0.06 dex	0.21 dex	0.24 dex

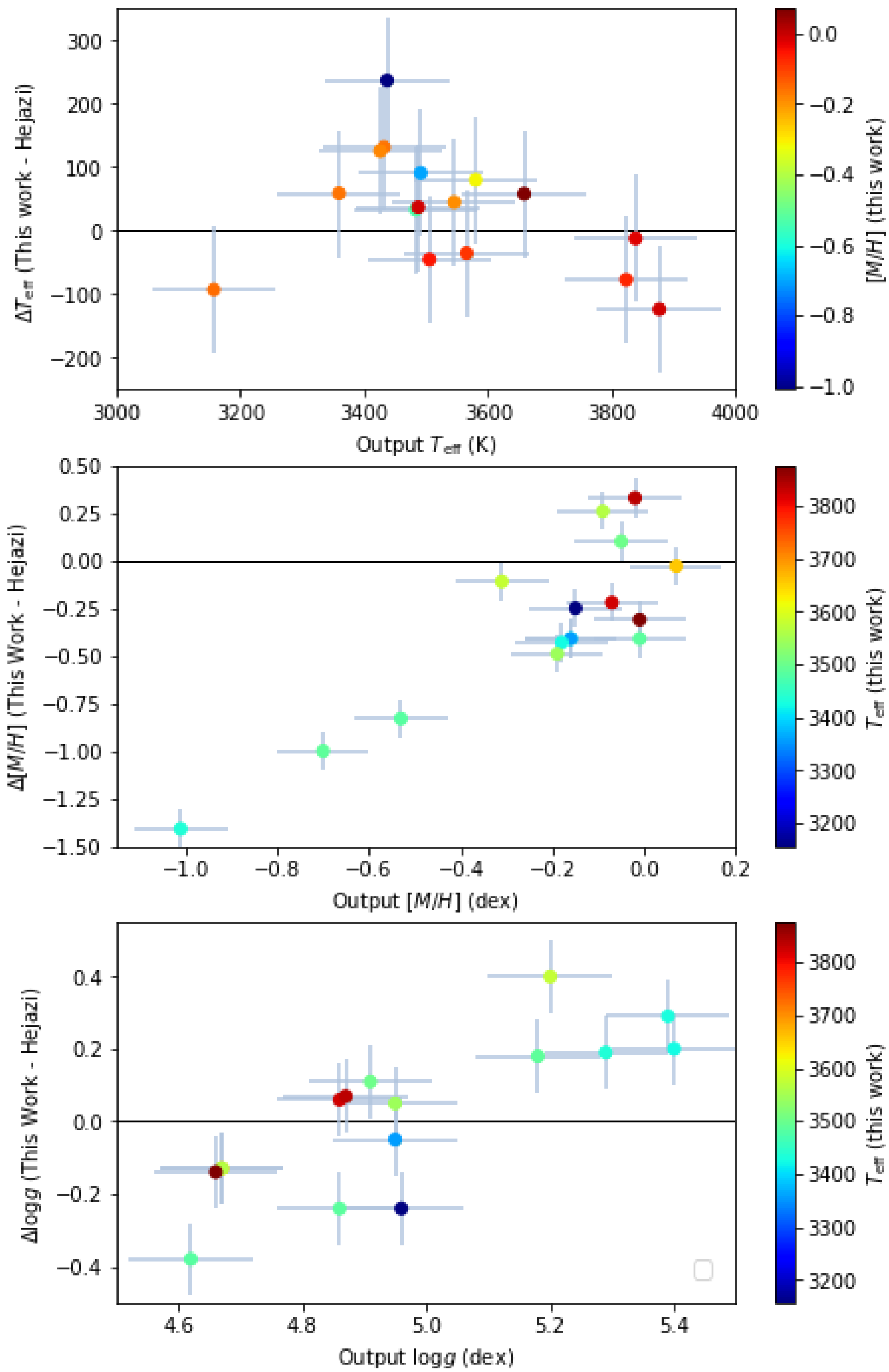

Figure 7.11: TOP (a): Comparison between $T_{\rm eff}$ derived by our pipeline and values published by Hejazi et al. (2019) for 16 stars in common between both samples, colored accordingly to our method's measured $[M/H]$ for each star. MIDDLE (b): Similar comparison for $[M/H]$, colored accordingly to our method's measured $T_{\rm eff}$ for each star. BOTTOM (c): Similar comparison for $\log g$, colored accordingly to our method's measured $T_{\rm eff}$ for each star.

timated 3200 K. This is one of the most metal-poor stars in our sample, as we estimate a metallicity of -1.01 dex, with Hejazi et al. (2019) having a value of $+0.4$ dex, and the huge differences in both parameters may explain each other. Lowering the effective temperature has similar effects on the continuum as decreasing the metallicity, and this degeneracy may be resolved by our pipeline in one way and another by theirs. More independent analysis is needed to differentiate between the two possible parameter combinations.

There are some other clear outliers and trends for both $[M/H]$ and $\log g$. We find three outlier stars with $\Delta[M/H] < -0.5$ dex, one of them already mentioned in the above paragraph. Excluding them, there seems to be no trend across $\Delta[M/H]$ and $[M/H]$, with most other stars having similar output $[M/H]$ across both analyses.

As for surface gravity, we find that stars with higher $\log g$ values tend to have higher $\Delta \log g$, and stars with lower $\log g$ values tend to have lower $\Delta \log g$. This means that our pipeline predicts a larger spread in possible $\log g$ values for different M dwarfs, while Hejazi et al. (2019) estimates a more uniform distribution across their sample stars. In conjunction with the HR-diagrams displayed in Fig. 7.1, we conclude that some of our results for $\log g$ may be biased. Therefore, in Section 7.2.2, we include a new synthesis focused on these stars with outlier $\log g$ values.

Other literature values

As cited above, we find some stars in common with the works of Souto et al. (2017); Souto et al. (2018); Rajpurohit et al. (2018b,a). Unfortunately, we have only analyzed a few stars in common with these works, and large scale comparisons between the methods and results are impossible. Therefore, no special or specific attention will be given to comparisons with them, and any dedicated analysis must be done on a star-by-star basis. Nevertheless, we include Table 7.6 with both our method's derived parameters and the ones available in the literature for stars in common with these works, for future reference.

Comparison with Passegger et al. (2019)

As stated in section 4.3, our sample selection was made based on the characterization of stars as part of APOGEE's ancillary M dwarf program and the S/N of APOGEE observations. The original target selection is therefore not necessarily extensive and representative of the

Table 7.6: Stars in common with other works. T subscript indicates parameter derived using this method, while L indicates Literature parameter. All $T_{\rm eff}$ values are in Kelvin, $[M/H]$ in dex and $\log g$ in dex. The correspondence of the letters in Sources is A - Rajpurohit et al. (2018a), B - Rajpurohit et al. (2018b), C - Souto et al. (2017), D - Souto et al. (2018).

Star	$T_{\rm eff,T}$	$T_{\rm eff,L}$	$\log g_T$	$\log g_L$	$[M/H]_T$	$[M/H]_L$	Source
2M03212176+7958022	3545	3500 ± 100	4.95	5.00 ± 0.10	-0.19	-0.4 ± 0.10	A
2M06421118+0334527	3356	3500 ± 100	4.62	5.1 ± 0.10	-0.06	0.0 ± 0.10	A
2M07581269+4118134	3432	3300 ± 100	5.39	5.0 ± 0.10	-0.16	$+0.3 \pm 0.10$	A
2M11474440+0048164	3281	3500 ± 100	5.28	5.0 ± 0.10	-0.15	0.0 ± 0.10	A
2M00350487+5953079	3196	3100 ± 100	5.05	5.5 ± 0.3	-0.13	0.0 ± 0.05	B
2M03152943+5751330	3361	3200 ± 100	5.19	5.5 ± 0.3	-0.17	-0.3 ± 0.05	B
2M04125880+5236421	3294	3100 ± 100	5.3	5.5 ± 0.3	-0.28	0.0 ± 0.05	B
2M06320207+3431132	3465	3200 ± 100	5.4	5.5 ± 0.3	-0.37	-0.4 ± 0.05	B
2M09301445+2630250	3354	3300 ± 100	4.67	5.0 ± 0.5	0.12	-0.3 ± 0.05	B
2M11091225-0436249	3847	3900 ± 100	4.81	4.5 ± 0.5	-0.07	-0.3 ± 0.04	B
2M18451027+0620158	3727	3900 ± 100	4.69	4.5 ± 0.5	0.04	-0.4 ± 0.04	B
2M18562628+4622532	3302	3100 ± 100	5.32	5.5 ± 0.3	-0.34	0.0 ± 0.05	B
2M19213157+4317347	3910	3835 ± 64	4.84	4.64 ± 0.10	-0.17	-0.09 ± 0.09	C
2M19543665+4357180	3856	3852 ± 64	4.73	4.73 ± 0.10	-0.22	-0.08 ± 0.10	C
2M11474440+0048164	3281	3231 ± 100	5.28	4.96 ± 0.11	-0.15	0.03 ± 0.09	D

full population of Milky Way M dwarfs, and our S/N filtering can introduce an additional bias towards closer, lower magnitude stars. Nevertheless, a comparison between the overall parameter distribution in our sample and other available larger-scale studies of M dwarfs can highlight the presence of larger trends in both ours and their methods and parameters.

One possibility for parameter comparison is Passegger et al. (2019), already mentioned in Section 2. Their pipeline derived stellar parameters using either visible wavelength spectra, near-infrared wavelength spectra, or multiwavelength range spectra. Specific lines were matched to PHOENIX models using the χ^2 minimization method. Despite the lack of stars in common between our analysis and Passegger et al. (2019), we selected this study as a baseline to compare our results due to the high resolution of the analyzed spectra ($R \sim 80500$), similarities in the method used, and large M dwarf sample size (282 stars). Fig. 7.12 shows the spatial distribution of both our stellar sample (a) and the one analyzed in Passegger et al. (2019) (b). The position displayed is in galactic coordinates, with each point colored according to the distances published in (Bailer-Jones et al. 2018) and calculated from Gaia DR2 parallaxes. These two figures serve as an illustration for the differences between both distributions, as our stellar sample is located either in the galactic equator or at even latitude values towards the galactic north and south poles, and distances around $100 - 150$ pc from the earth. In contrasting fashion, Passegger's sample is evenly distributed across the sky and at distances below 50 pc. Both figures also show the lack of observations in the southern direction, as both CARMENES and APOGEE are located in the northern hemisphere.

Fig. 7.13 shows, therefore, a comparison between the parameters derived with our method and the ones published in Passegger et al. (2019). As our method uses H-band spectra, the comparison is made between our parameters and the ones derived there using spectra from $0.96 - 1.71\,\mu m$. Figure (a) shows the wider $\log g$ distribution found across stars in our sample when compared to Passegger et al.'s analysis of CARMENES data. Their values match the overplotted isochrones for high metallicity stars and are highly consistent across the full stellar sample, while the parameters derived using our method have a larger dispersion towards higher values and the other isochrones.

Figure (b) shows a trend in Passegger's metallicity towards much higher and unrealistic values, especially for earlier M dwarfs ($T_{\rm eff} > 3500$ K), with some stars having $[M/H] > 0.5$ dex. Our distribution is more centered around solar metallicity values, with broader distribution and the inclusion of lower metallicity stars. Stars with $T_{\rm eff} > 3500$ K and $[M/H] < -0.5$ dex are also missing from the CARMENES sample, possibly indicating either a selection bias in their sample or a strong trend in the methodology towards the prediction of higher metallicity values for their sample stars. Our sample does have a lack of stars with $T_{\rm eff} < 3350$ K and $[M/H] < -0.5$ dex. However, only 20 stars in our sample of 250 have those effective temperatures, so the lack of stars in this parameter range is not as important in the global sample. The overall $T_{\rm eff}$ distribution is similar between both samples, with ours having a larger population of earlier-type stars and theirs having a larger proportion of later-type ones.

7.2.2 Further Discussion

It is important to remind the reader that no previous large-scale survey of M dwarfs using high-resolution H-band spectra and this method has been published. This is a groundbreaking work in that sense, as the main goal of the project is the publication of a method for the derivation of M dwarf atmospheric parameters using synthetic spectra. We knew from the beginning that our intended analysis of M dwarf spectra was subtle and difficult, as the presence of water lines obfuscating the continuum made the spectra normalization both challenging and time-consuming. The fact that the method provided accurate parameters for FGK-type stars was encouraging, but not a guarantee that it would perform as well for the M dwarf sample.

However, as shown in section 7.1, the results seem very promising, as the synthetic spectra

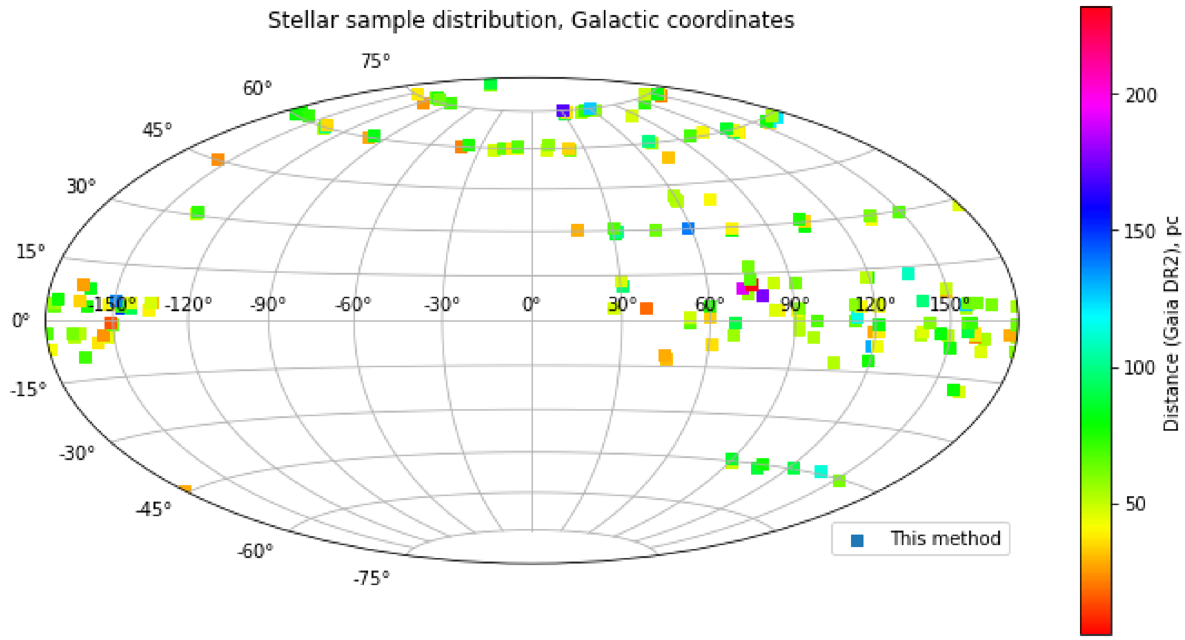

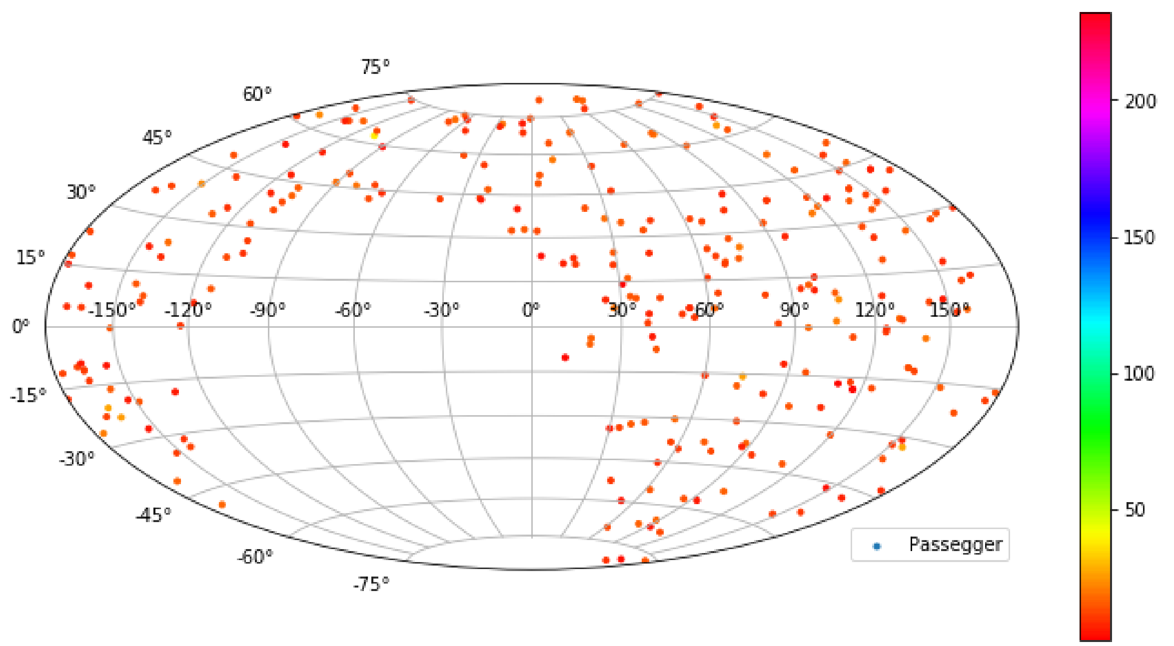

Figure 7.12: TOP (a): Spatial distribution of our stellar sample. Position is indicated in galactic coordinates and each star's position is colored according to measured distance as calculated in (Bailer-Jones et al. 2018) from Gaia DR2 data, in parsec. BOTTOM (b): Similar plot for the stellar sample of Passegger et al. (2019).

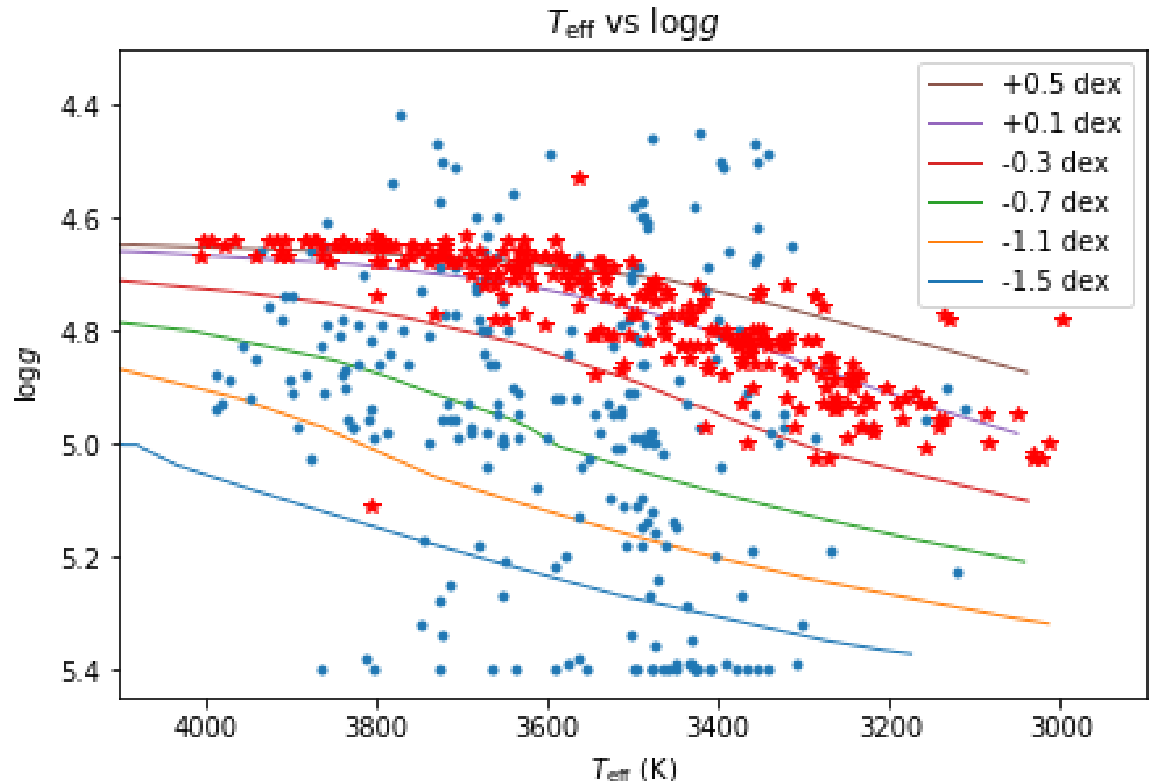

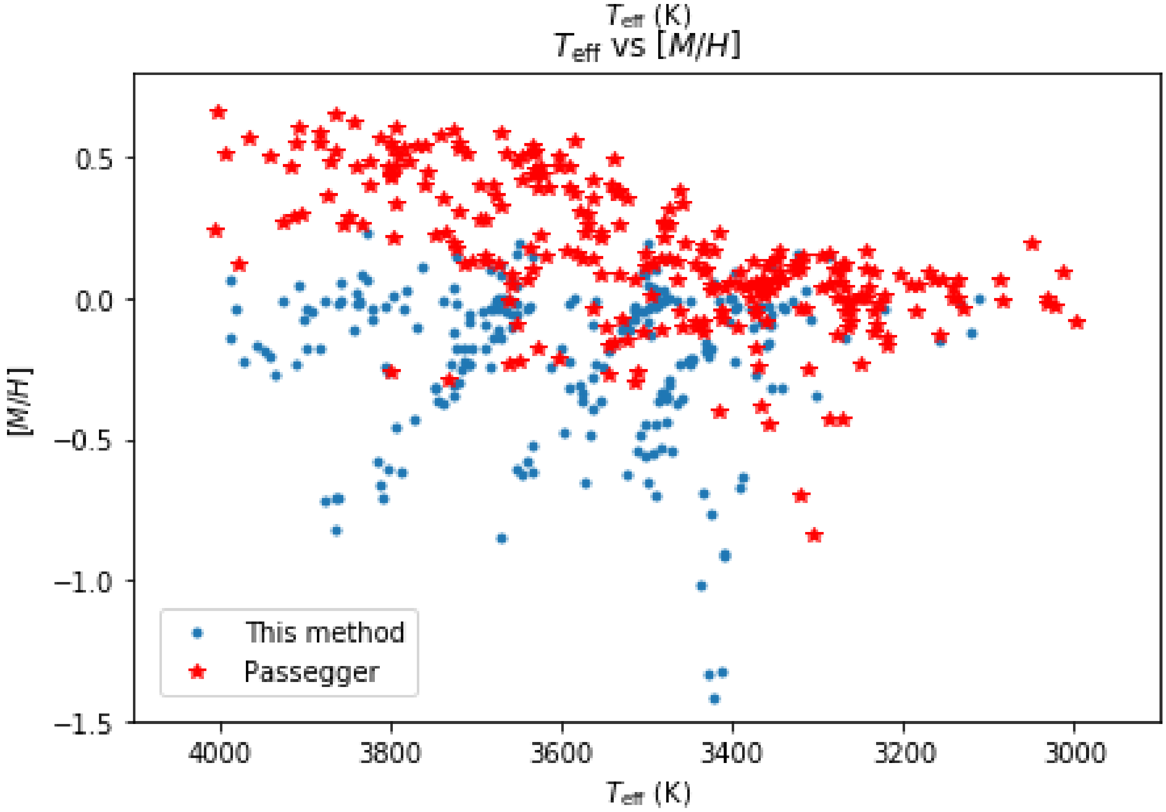

Figure 7.13: TOP (a): Comparison between the full sample of $T_{\rm eff}$ and $\log g$ derived by our pipeline and values published by Passegger et al. (2019). Overplotted are PARSEC isochrones (Bressan et al. 2012) created for stars 10^9 years old and with different $[M/H]$ values. BOTTOM (b): Similar comparison for $T_{\rm eff}$ and $[M/H]$.

match the observed ones across most of the selected lines, and the parameter distribution is centered around PARSEC isochrone (Bressan et al. 2012) values. Section 7.2.1 shows that our method's results agree with the available literature values.

Outlier $\log g$

All results displayed in Section 7.1 were obtained by normalizing the spectra with a template with $\log g = 5.0$ dex. Some of the syntheses resulted in outlier and nonphysical parameters when compared to the PARSEC isochrones (see Fig. 7.1). These outliers include both stars with $\log g < 4.5$ dex, which may not be M dwarfs, and ones with $\log g = 5.4$ dex, which is the edge of our surface gravity grid and the highest possible value attributed to an analyzed star. Therefore, and to improve the results on these stars, we decided to repeat the syntheses of the stellar spectra with different $\log g$ value for the normalization templates. The full list of these 30 outlier stars, their original output parameters, and the new $\log g$ value used in the syntheses are summarized in Table 7.7.

Table 7.7: Stars with outlier $\log g$ values. The O subscript indicates the original value for the parameter, while N indicates the values with the new normalization. T indicates parameters used to generate the synthetic spectra for the template normalization. All stars with $\log g_O = 5.4$ dex were normalized with $\log g_{N,T} = 5.2$ dex, and the rest of the sample was normalized with $\log g_{N,T} = 4.8$ dex.

Apogee ID	$T_{\rm eff,N}$	$T_{\rm eff,O}$	$\log g_N$	$\log g_O$	$[M/H]_N$	$[M/H]_O$	χ^2_N	χ^2_O	$T_{\rm eff,N,T}$	$T_{\rm eff,O,T}$	$[M/H]_{N,T}$	$[M/H]_{O,T}$
2M12105688+4103275	3776	3771	4.4	4.42	-0.46	-0.43	0.1357	0.138	3600	3600	-0.2	0.1
2M06025298+3129415	3318	3421	4.74	4.45	-0.76	-1.41	0.068	0.073	3000	3000	0	-0.4
2M05580690+1557564	3404	3477	4.35	4.46	-0.31	-0.35	0.1029	0.096	3200	3200	-0.2	-0.2
2M20053276+3039324	3729	3729	4.44	4.47	-0.23	-0.23	0.0467	0.046	3600	3600	0	0
2M03400164+4638456	3540	3597	4.5	4.49	-0.07	-0.47	0.7922	0.937	3400	3400	-0.4	-0.1
2M00243855+5119224	3865	3727	5.4	5.4	-0.52	-0.34	0.0895	0.088	4000	3600	0.4	0.1
2M03190939+0130543	3151	3410	5.15	5.4	-0.19	-0.91	0.0905	0.113	3000	3000	-0.2	-0.4
2M03431519+5006558	3343	3637	5.02	5.4	-0.01	-0.03	0.2214	0.269	3200	3600	0.4	0.3
2M03481149+3054134	3135	3554	4.49	5.4	0	-0.36	0.1034	0.104	3000	3400	-0.2	0.1
2M04334819+4227070	3482	3449	5.4	5.4	-0.03	-0.01	0.1035	0.099	3400	3400	0.4	0.3
2M06320207+3431132	3147	3465	4.66	5.4	-0.04	-0.37	0.0977	0.103	3000	3200	-0.2	-0.2
2M06362535+1830520	3315	3478	4.99	5.4	-0.15	-0.44	0.1508	0.151	3200	3200	-0.2	-0.2
2M06375540+0858594	3125	3379	4.79	5.4	-0.01	-0.04	0.0835	0.095	3000	3200	-0.2	-0.2
2M06423361+0239388	3798	3804	5.4	5.4	-0.57	-0.6	0.0886	0.09	3600	3600	0.4	-0.1
2M07421457+7949418	3156	3368	4.97	5.4	0.01	-0.03	0.0899	0.093	3000	3200	0.4	-0.2
2M10330667+2837490	3473	3499	5.31	5.4	-0.04	-0.08	0.0841	0.081	3400	3400	0.4	0.1
2M11021557+4941485	3323	3482	5.25	5.4	-0.14	-0.09	0.0741	0.09	3200	3400	-0.2	0.2
2M11294200+0405175	3648	3410	5.4	5.4	-1.31	-0.9	0.1932	0.13	3600	3000	-0.2	-0.4
2M11353571+0414146	3790	3864	5.4	5.4	-0.64	-0.82	0.0627	0.063	3600	3600	-0.2	-0.4
2M14035430+3008026	3326	3330	4.82	5.4	0.07	0.44	0.1008	0.475	3200	3200	-0.2	0.2
2M14173915+0624144	3521	3590	5.4	5.4	-0.17	-0.22	0.1008	0.108	3400	3400	-0.2	-0.2
2M14180725+0611519	3298	3429	4.99	5.4	-0.02	-0.19	0.0891	0.097	3200	3200	0.4	-0.2
2M15281240+4340086	3366	3477	5.08	5.4	-0.22	-0.35	0.1705	0.16	3200	3200	0.4	-0.2
2M16383835+3700273	3326	3428	5.13	5.4	-0.1	-0.2	0.1857	0.192	3200	3200	-0.2	-0.2
2M16440030+3721597	3729	3355	5.4	5.4	-0.84	-0.32	0.2297	0.363	3600	3000	0.4	-0.4
2M16565961+1133582	3726	3343	5.4	5.4	-0.89	-0.32	0.1344	0.341	3600	3000	-0.2	-0.4
2M17480236+7436562	3750	3460	5.4	5.4	-0.82	-0.35	0.2386	0.171	3600	3200	-0.2	-0.2
2M19485718+5015245	3576	3497	5.4	5.4	-0.29	-0.13	0.1109	0.105	3400	3400	0.4	0.3
2M19541829+1738289	3207	3426	4.96	5.4	-0.32	-0.76	0.1514	0.157	3000	3000	-0.2	-0.4
2M20015056+4500500	3724	3666	5.4	5.4	-0.19	-0.05	0.1439	0.131	3600	3600	-0.6	0.2

Fig. 7.14 is a more visual display of the parameters listed in Table 7.7, to help compare the old and new parameter distribution, as well as the changes in the stellar population parameters. The figures show us that many of the stars that previously tended towards $\log g = 5.4$ dex have now lower estimated surface gravity values, combined with lower $T_{\rm eff}$ and higher $[M/H]$ values. The shifts are present across multiple parameters as expected, as the degeneracy between $T_{\rm eff}$, $[M/H]$, and $\log g$ mean that changes in one of the parameters must be compensated by changes in the other parameters as well. Despite the new parameters being more physical and reasonable, and within the expected isochrone ranges for many of these previously outlier stars, we still find new outliers with both too low and too high $\log g$ values.

Regarding the low $\log g$ values outlier sample stars, we find that they do not significantly change parameters with the new normalization template, with their $T_{\rm eff}$, $[M/H]$, and $\log g$ remaining approximately constant. Despite their synthesized parameters not being realistic and falling outside the expected isochrone values for M dwarfs, we include the derived values in this thesis as they were all derived with a consistent methodology.

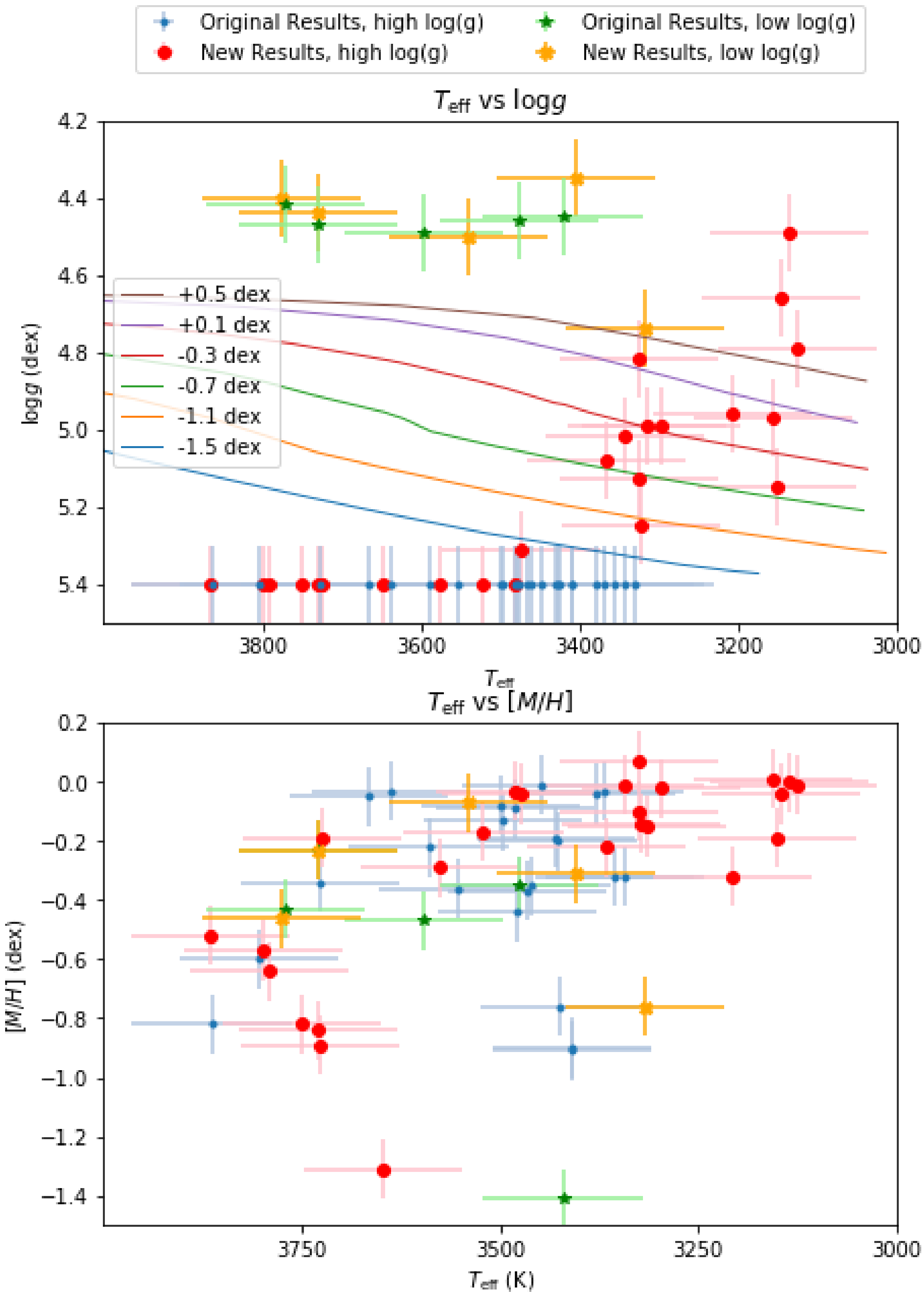

Figure 7.14: TOP (a): HR diagram displaying both the original and the newly derived parameters for the $\log g$ outlier subsample stars analyzed. Color and symbol shape is used to distinguish between stars with low and high $\log g$ values (stars vs points), and original and new parameters for each star. Overplotted are PARSEC isochrones (Bressan et al. 2012) created for stars 10^9 years old, with different $[M/H]$ values. BOTTOM (b): Similar comparison for the $T_{\rm eff}$ and $[M/H]$ of the sample stars.

Chapter 8

Conclusions

The stellar atmospheric parameters of 3748 FGK main-sequence and subgiant stars and 250 M dwarf stars have been determined by matching synthetic spectra to observations made by APOGEE. The synthetic spectra were created using *Turbospectrum*, controlled by *iSpec* with a python shell. To correctly and accurately match the synthesized spectra to the observed ones, a complete line list was created, as well as a line mask distinguishing the lines synthesized by the method. These are both important steps for the method and are made available for use together with all the output parameters determined using the pipeline.

Analyzing both the synthesized spectra and the resulting output parameters, it can be concluded that this pipeline can serve as a precise method for the determination of stellar atmospheric parameters from $R \sim 22\,000$ H-band spectra. The spectra of both FGK (see Chapter 6) and M dwarfs (see Chapter 7) has been accurately synthesized, and the resulting parameters agree within the error margins with available literature values for both cases.

It is important to re-state the systematic differences found when comparing the results derived using this method and the ones published by ASPCAP, as there is $\Delta T_{\rm eff} = 62$ K and $\Delta[M/H] = +0.04$ dex between our values and theirs for our FGK star sample. While these differences are within our margins of error for individual stars, their presence across the full sample indicates potential biases in either our method or ASPCAP.

Regarding our M dwarf analysis, we demonstrate in Chapter 7 that we can create synthetic spectra that accurately match the observed ones across our full sample of 290 stars. The template normalization method and the choice of best matching spectra are still dependent on a visual inspection and possible biased human decisions. This step of the parameter determination pipeline could be improved by turning the process into a more automated and objective one.

The lack of wide-scale M dwarf analysis available for parameter comparison may raise some concerns about the accuracy of our derived parameters. However, both the high quality of the matching spectra (with examples in Figs. 7.3 to 7.7) and the different literature sub-sample parameter comparisons included in section 7.2.1 are good arguments for the accuracy of our derived parameters. As for a comparison with Terrien et al. (2015)'s analysis , we find median differences across 39 stars of $T_{\rm eff} = +62\,$K and $[M/H] = -0.08\,$dex, close to the previously mentioned values and also within our uncertainty levels.

8.1 Future improvements for FGK star analysis

First, we have to note that our sample stars do not cover the full parameter space for FGK stars. Most of our sample stars fall within a small range of the parameter space, as they have temperatures between 5500 K and 6200 K. Expanding this study, we could include stars with both lower and higher $T_{\rm eff}$ values, better populating our parameter space. Further studies with this method could probe a more metal-poor stellar sample, as our sample is limited to stars above $[M/H] \sim -0.75\,$dex.

Another possibility for further exploration of this method could reside in the study of higher resolution NIR spectra, such as the ones observed by CARMENES (Quirrenbach et al. 2014). Characterization of spectra with $R \geq 50\,000$ could help us determine more accurate stellar parameters and better understand the limitations of the method itself. Improvements on both the line lists and line masks, as well as expanding them across larger wavelength ranges, could also be future possibilities for the next steps with the method.

Regarding the analysis of FGK stars in general, one of our issues resided in the relation between our output $\log g$ and the expected $\log g$ values given by isochrones values for stars with a given $T_{\rm eff}$ (see Fig. 6.6). This discrepancy between spectroscopic, asteroseismic, and isochrone $\log g$ values has been observed in previous works in the optical and the near-infrared (Mortier et al. 2014; Delgado Mena et al. 2017; Holtzman et al. 2018, e.g.). Many possible corrections being proposed to solve this issue, from simply multiplying the determined $\log g$ values by a constant, to linear equations based on other observable spectroscopic parameters such as $T_{\rm eff}$ or $[M/H]$, or by fixing $\log g$ to values measured using alternative methods, such as asteroseismology, and just determining other spectroscopic parameters for a given star. Some other works, such as ASPCAP, give no corrections to their output $\log g$ values for dwarf stars and recommend against using them in the first place. None of these solutions is perfect or is effective for all spectroscopic works. Fixing this issue with stellar surface gravity values could be a great advancement in the field, unifying different fields of stellar characterization, such as asteroseismology and spectroscopy, and allowing us to have a more holistic understanding of stars as a whole.

8.2 Future improvements for M dwarf analysis

One possibility for further exploration of the method is an expansion of the explored parameter space, with a larger sample including more metal-poor stars. Our initial sample selection was focused on the S/N limitation as an attempt to both minimize computational time and to optimize our pipeline's chances for the retrieval of accurate spectra. However, increasing the sample size and expanding it to a larger parameter space could help filling out empty regions in Fig. 7.2, and to characterize M dwarfs with different stellar parameters. Despite the current sample size already being 250 stars, the number of available M dwarfs known is orders of magnitude above that. The M dwarf sample could also be improved with the addition of late-type stars, around or below $T_{\text{eff}} = 3300$ K, as they seem to be sub-represented in our sample. Increasing and varying the size and parameter distribution of our M dwarf sample could, therefore, help to shed more light on M dwarf population in the Milky Way as a whole. Adding more stars already characterized by Terrien et al. (2015) and Gaidos et al. (2014), or by recent works such as Birky et al. (2020) and Souto et al. (2020), is also a possibility, as we can verify on how the literature comparison evolves with increasing sample size.

Other future improvements to the method can be on the line list and line masks part of the process. An improvement on the study of molecular and atomic lines in both stellar spectra and laboratory analysis could mean the compilation of a more complete and accurate line list, or a different selection of lines in the line mask. A new solution to the problem of M dwarf spectra normalization could also improve the speed and accuracy of the method, as the current normalization method is dependent on the available ASPCAP parameters for metallicity calibration. The automation of more steps of the method is possible as well. However, a human element is always required to confirm the accuracy of synthetic spectra matching and the possibility of outliers. More computing power could also improve the application of the method to a new and larger sample of stars, as it currently takes over 1 hour to synthesize the spectrum for a single star.

Another possible improvement for the M dwarf analysis could reside on the initial approximate determination of spectroscopic parameters and the consequent spectrum normalization method. A more accurate and easier to apply method for the determination of the initial test parameters could decrease the computational time required for the full parameter determination and analysis, as the current method requires multiple normalizations and iterations of the process before the final parameter set is determined. By optimizing the process, more stars could be analyzed in the same amount of time.

The APOGEE DR16 has been submitted by December 2019 and is at the moment awaiting publication (Ahumada et al. 2019). As this new Data Release includes thousands of new stars observed by APOGEE-S, as well as new calibrations for the $\log g$ of dwarf stars. Any future work should also include the wealth of information from this new Data Release, as soon as it is officially published.

8.3 Applications for other near-infrared spectroscopic observations

Several near-infrared instruments and surveys have either recently been finished or are currently being built. Our method could, in principle, be applied to any new high-resolution observation of FGKM dwarfs. This section details the current panorama of spectroscopic instruments in the near-infrared, as their observations could be analyzed by our method.

In infrared spectroscopy, the identification of infrared stellar lines was already common in the 1960's and the newer generations of telescopes, with improved resolutions and mirror size, have only increased the amount of detail that can be observed in a stellar spectrum. We have arrived at the era of instruments that provide high-resolution spectra in the NIR, such as CARMENES ($R = 80\,000 - 100\,000$, Quirrenbach et al. 2014), GIANO ($R \sim 50\,000$, Origlia et al. 2014), SPIROU ($R \sim 75\,000$, Artigau et al. 2014), and NIRPS ($R \sim 90\,000 - 100\,000$ Wildi et al. 2017).

The Calar Alto high-Resolution search for M dwarfs with Exoearths with Near-infrared and optical Échelle Spectrographs (CARMENES) is an instrument built at the 3.5 m telescope at the Calar Alto Observatory by a consortium of both German and Spanish institutions. It is one of the most advanced instruments of its kind in the world, and it consists of two separate spectrographs that together cover the wavelength ranges from $0.52{-}0.96\mu m$ and $0.96{-}1.71\mu m$, with a spectral resolution of $R \approx 80\,000 - 100\,000$ each. CARMENES can thus perform high-accuracy radial velocity measurements up to $1\,\mathrm{m/s}$ with long-term stability, promising to be an instrument for the near future, as it started observations in Jan 2016.

GIANO is an optimized near-infrared echelle spectrograph that observes spectra in the wavelength range of $0.9 - 2.5\mu m$ at $R = 50\,000$. GIANO is part of the Second Generation Instrumentation Plan of the Italian Telescopio Nazionale Galileo (TNG) and is located in La Palma, Spain, in the Roque de Los Muchachos Observatory (ORM). This instrument is installed in its 3.58 m TNG Alt-Azimutal telescope together with High Accuracy Radial velocity Planet Searcher in North hemisphere (HARPS-N), which is designed for the optical wavelength range. GIANO can thus provide high-resolution spectra for both radial velocity measurements of exo-planets and chemical and dynamical studies of stellar or extragalactic objects.

SpectroPolarimètre Infra-Rouge (Near-InfraRed Spectropolarimeter, SPIRou) is an instrument optimized for high-precision radial velocity measurements. The spectrograph can provide spectra from $0.9 - 2.5\mu m$ in a single shot and with a $R = 75\,000$. It was shipped to the 3.58 m Canada-France-Hawaii Telescope (CFHT) on Maunakea, Hawaii in January 2018, and, at the time of this writing, is still not in full operation mode.

NIRPS (Near Infra Red Planet Searcher) instrument will be another planet-hunter instrument installed at the ESO 3.6-m telescope at the La Silla Observatory in Chile. This instrument already had its first light in 2019 and is expected to start providing spectra very soon. It will work simultaneously with HARPS, the current optical spectrograph working in the same telescope.

8.4 Final Personal Thoughts

We have worked on this method for over four years, suffering some setbacks along the way, but never missing sight from the main goal of M dwarf characterization. We believe this goal has been achieved, as the spectroscopic parameters of 250 M dwarfs have been determined and will be published soon, while our results for the parameters of 3748 FGK stars have already been accepted for publication by Astronomy and Astrophysics. The method itself has proven itself to be very useful in the determination of stellar parameters from NIR spectra and could be expanded in the future to other observed spectra and a larger stellar sample.

Working for four years with this computational method and APOGEE spectra has given me the required experience, knowledge and skills necessary to understand the details and subtleties required to properly characterize stellar spectra using computational methods. It took a lot of work to finally complete the thesis, but I believe it was worth it, as the method stands for itself as another possibility for the spectroscopic parameter determination of both FGK stars and M dwarfs.

Bibliography

Appendix A

Linemasks

A.1 FGK stars linemask, sensitivity to $T_{\rm eff}$ and $\log g$

This section contains the lines included in the linemask for FGK stars, as well as the effects of changing both $T_{\rm eff}$ and $\log g$ for each of the lines.

Table A.1: Effects of changing both $T_{\rm eff}$ and $\log g$ on lines included in the linemask used for parameter estimation in the FGK stars in the sample. Dec means the line strength decreases with increasing spectroscopic parameter, and inc means the line strength increases with increasing spectroscopic parameter.

Element	Wavelength (nm)	$T_{\rm eff}$ effect ($\log g$ = 4.5 dex)	$\log g$ effect ($T_{\rm eff}$ = 5800 K)
Mn 1	1515.9233	EW dec with $T_{\rm eff}$	No variation with $\log g$
Fe 1	1516.05333	EW dec with $T_{\rm eff}$	No variation with $\log g$
K 1	1516.30507	EW dec with $T_{\rm eff}$	EW inc with $\log g$
Fe 1	1520.753	EW dec with $T_{\rm eff}$	EW inc with $\log g$
Mn 1	1521.7709	EW dec with $T_{\rm eff}$	EW inc with $\log g$
Fe 1	1521.9611	EW dec with $T_{\rm eff}$	EW inc with $\log g$
Fe 1	1522.47226	EW dec with $T_{\rm eff}$	EW dec with $\log g$
Fe 1	1523.97062	EW dec with $T_{\rm eff}$	EW dec with $\log g$
Fe 1	1524.49703	EW dec with $T_{\rm eff}$	EW inc with $\log g$
Mn 1	1526.24073	EW dec with $T_{\rm eff}$	No variation with $\log g$
SiH	1529.32466	EW dec with $T_{\rm eff}$	EW inc with $\log g$
Fe 1	1529.45738	EW dec with $T_{\rm eff}$	EW inc with $\log g$
Fe 1	1530.15594	EW dec with $T_{\rm eff}$	No variation with $\log g$
Fe 1	1533.53371	EW dec with $T_{\rm eff}$	EW inc with $\log g$

Element	Wavelength (nm)	T_{eff} effect ($\log g$ = 4.5 dex)	$\log g$ effect (T_{eff} = 5800 K)
Fe 1	1534.37898	EW dec with T_{eff}	No variation with $\log g$
Si 1	1537.6831	EW dec with T_{eff}	Line widens at lower $\log g$
Fe 1	1538.19455	EW dec with T_{eff}	No variation with $\log g$
OH 1	1538.77178	EW dec with T_{eff}	No variation with $\log g$
CN 1	1539.47323	EW dec with T_{eff}	EW inc with $\log g$
S 1	1540.00208	EW inc with T_{eff}	EW dec with $\log g$
S 1	1540.37731	EW dec with T_{eff}	EW dec with $\log g$
S 1	1542.22698	EW inc with T_{eff}	EW dec with $\log g$
S 1	1546.98178	EW inc with T_{eff}	EW dec with $\log g$
Fe 1	1549.67349	EW dec with T_{eff}	EW dec with $\log g$
Fe 1	1549.93854	EW dec with T_{eff}	EW dec with $\log g$
Fe 1	1553.17688	EW dec with T_{eff}	Line widens at lower $\log g$
Fe 1	1553.42521	EW dec with T_{eff}	Line widens at lower $\log g$
Fe 1	1553.76704	EW dec with T_{eff}	Line widens at lower $\log g$
Fe 1	1554.20742	EW dec with T_{eff}	EW dec with $\log g$
Fe 1	1555.05296	EW dec with T_{eff}	EW dec with $\log g$
Ni 1	1555.53288	EW dec with T_{eff}	No variation with $\log g$
Si 1	1555.77817	EW dec with T_{eff}	Line widens at lower $\log g$
Fe 1	1558.82626	EW dec with T_{eff}	Line widens at lower $\log g$
SiH	1559.01294	EW dec with T_{eff}	EW inc with $\log g$
Fe 1	1559.14881	EW dec with T_{eff}	EW inc with $\log g$
Fe 1	1560.42248	EW dec with T_{eff}	EW inc with $\log g$
Ni 1	1560.56574	EW dec with T_{eff}	No variation with $\log g$
Fe 1	1562.16407	EW dec with T_{eff}	EW inc with $\log g$
Fe 1	1564.85084	EW dec with T_{eff}	No variation with $\log g$
Fe 1	1565.28765	EW dec with T_{eff}	No variation with $\log g$
Fe 1	1566.20108	EW dec with T_{eff}	EW inc with $\log g$
Fe 1	1566.52081	EW dec with T_{eff}	EW dec with $\log g$
Cr 1	1568.00357	EW dec with T_{eff}	Line widens at lower $\log g$

Element	Wavelength (nm)	T_{eff} effect ($\log g$ = 4.5 dex)	$\log g$ effect (T_{eff} = 5800 K)
Fe 1	1568.24897	EW dec with T_{eff}	No variation with $\log g$
OH 1	1569.19743	EW dec with T_{eff}	EW inc with $\log g$
Mn 1	1569.25903	EW dec with T_{eff}	EW inc with $\log g$
Fe 1	1572.35863	EW dec with T_{eff}	EW inc with $\log g$
Mg 1	1574.07359	EW dec with T_{eff}	EW inc with $\log g$
OH 1	1574.18033	EW dec with T_{eff}	EW inc with $\log g$
Mg 1	1574.89606	EW dec with T_{eff}	EW inc with $\log g$
Fe 1	1576.13369	EW dec with T_{eff}	EW inc with $\log g$
Mg 1	1576.58044	EW dec with T_{eff}	EW inc with $\log g$
Fe 1	1576.9388	EW dec with T_{eff}	EW inc with $\log g$
Fe 1	1577.40661	EW dec with T_{eff}	EW inc with $\log g$
OH 1	1578.90544	EW dec with T_{eff}	EW inc with $\log g$
Fe 1	1581.01826	EW dec with T_{eff}	EW dec with $\log g$
Fe 1	1582.27725	EW dec with T_{eff}	EW inc with $\log g$
Si 1	1583.36326	EW dec with T_{eff}	EW inc with $\log g$
Fe 1	1583.51391	EW dec with T_{eff}	EW inc with $\log g$
Fe 1	1583.76281	EW dec with T_{eff}	No variation with $\log g$
Fe 1	1584.01769	EW dec with T_{eff}	No variation with $\log g$
Fe 1	1586.37366	EW dec with T_{eff}	No variation with $\log g$
Fe 1	1586.85321	EW dec with T_{eff}	EW inc with $\log g$
Mg 1	1587.95105	EW dec with T_{eff}	EW inc with $\log g$
Si 1	1588.44681	EW dec with T_{eff}	EW inc with $\log g$
Mg 1	1588.63043	EW dec with T_{eff}	EW inc with $\log g$
Si 1	1588.83988	EW dec with T_{eff}	EW inc with $\log g$
Fe 1	1589.11383	EW dec with T_{eff}	No variation with $\log g$
Fe 1	1589.26372	EW dec with T_{eff}	No variation with $\log g$
Fe 1	1589.80097	EW dec with T_{eff}	No variation with $\log g$
Fe 1	1590.15103	EW dec with T_{eff}	Line widens at lower $\log g$
Fe 1	1590.43727	EW dec with T_{eff}	Line widens at lower $\log g$

Element	Wavelength (nm)	$T_{\rm eff}$ effect ($\log g$ = 4.5 dex)	$\log g$ effect ($T_{\rm eff}$ = 5800 K)
Fe 1	1590.60186	EW dec with $T_{\rm eff}$	Line widens at lower $\log g$
Fe 1	1590.91009	EW dec with $T_{\rm eff}$	EW inc with $\log g$
Fe 1	1591.13175	EW dec with $T_{\rm eff}$	EW dec with $\log g$
Fe 1	1591.25811	EW dec with $T_{\rm eff}$	Line widens at lower $\log g$
Fe 1	1592.06795	EW dec with $T_{\rm eff}$	Line widens at lower $\log g$
Fe 1	1593.40202	EW dec with $T_{\rm eff}$	No variation with $\log g$
Fe 1	1593.88776	EW dec with $T_{\rm eff}$	EW dec with $\log g$
Fe 1	1594.18329	EW dec with $T_{\rm eff}$	Line widens at lower $\log g$
SiH	1595.43349	EW dec with $T_{\rm eff}$	EW dec with $\log g$
Si 1	1596.00585	EW dec with $T_{\rm eff}$	EW inc with $\log g$
Fe 1	1596.48634	EW dec with $T_{\rm eff}$	EW inc with $\log g$
Fe 1	1596.76653	EW dec with $T_{\rm eff}$	EW dec with $\log g$
Fe 1	1597.12508	EW dec with $T_{\rm eff}$	No variation with $\log g$
Fe 1	1598.07289	EW dec with $T_{\rm eff}$	EW inc with $\log g$
Fe 1	1599.77181	EW dec with $T_{\rm eff}$	EW dec with $\log g$
C 1	1600.49328	EW inc with $T_{\rm eff}$	EW dec with $\log g$
Fe 1	1600.9605	EW dec with $T_{\rm eff}$	EW inc with $\log g$
C 1	1602.16678	EW inc with $T_{\rm eff}$	EW dec with $\log g$
Fe 1	1603.78295	EW dec with $T_{\rm eff}$	EW inc with $\log g$
Fe 1	1604.06495	EW dec with $T_{\rm eff}$	EW inc with $\log g$
Fe 1	1604.26958	EW dec with $T_{\rm eff}$	EW inc with $\log g$
Si 1	1606.00103	EW dec with $T_{\rm eff}$	EW inc with $\log g$
Fe 1	1607.15807	EW dec with $T_{\rm eff}$	No variation with $\log g$
Fe 1	1607.59145	EW dec with $T_{\rm eff}$	No variation with $\log g$
Si 1	1609.47862	EW dec with $T_{\rm eff}$	EW inc with $\log g$
Fe 1	1610.03131	EW dec with $T_{\rm eff}$	EW dec with $\log g$
Fe 1	1610.24087	EW dec with $T_{\rm eff}$	EW inc with $\log g$
Fe 1	1611.59247	EW dec with $T_{\rm eff}$	No variation with $\log g$
Fe 1	1612.58966	EW dec with $T_{\rm eff}$	EW inc with $\log g$

Element	Wavelength (nm)	$T_{\rm eff}$ effect ($\log g$ = 4.5 dex)	$\log g$ effect ($T_{\rm eff}$ = 5800 K)
Ca 1	1615.0764	EW dec with $T_{\rm eff}$	EW dec with $\log g$
Fe 1	1615.32229	EW dec with $T_{\rm eff}$	No variation with $\log g$
Mg 1	1616.37448	EW dec with $T_{\rm eff}$	EW inc with $\log g$
Fe 1	1616.50089	EW dec with $T_{\rm eff}$	EW inc with $\log g$
Fe 1	1617.49765	EW dec with $T_{\rm eff}$	No variation with $\log g$
Fe 1	1617.96288	EW dec with $T_{\rm eff}$	Line widens at lower $\log g$
Fe 1	1618.08722	EW dec with $T_{\rm eff}$	EW inc with $\log g$
Fe 1	1618.58487	EW dec with $T_{\rm eff}$	EW dec with $\log g$
Fe 1	1619.50655	EW dec with $T_{\rm eff}$	Line widens at lower $\log g$
Ca 1	1619.70936	EW dec with $T_{\rm eff}$	EW inc with $\log g$
Fe 1	1619.84885	EW dec with $T_{\rm eff}$	EW inc with $\log g$
OH 1	1620.41775	EW dec with $T_{\rm eff}$	No variation with $\log g$
Fe 1	1620.77334	EW dec with $T_{\rm eff}$	EW inc with $\log g$
Si 1	1621.56701	EW dec with $T_{\rm eff}$	EW inc with $\log g$
Fe 1	1622.56444	EW dec with $T_{\rm eff}$	EW inc with $\log g$
Fe 1	1623.16481	EW dec with $T_{\rm eff}$	EW inc with $\log g$
Fe 1	1623.59716	EW dec with $T_{\rm eff}$	EW dec with $\log g$
Si 1	1624.18226	EW dec with $T_{\rm eff}$	EW inc with $\log g$
Fe 1	1625.25161	EW dec with $T_{\rm eff}$	No variation with $\log g$
Fe 1	1628.4797	EW dec with $T_{\rm eff}$	EW dec with $\log g$
Fe 1	1629.28553	EW dec with $T_{\rm eff}$	EW dec with $\log g$
Ni 1	1631.05067	EW dec with $T_{\rm eff}$	EW dec with $\log g$
Fe 1	1631.63255	EW dec with $T_{\rm eff}$	EW inc with $\log g$
Fe 1	1631.86741	EW dec with $T_{\rm eff}$	No variation with $\log g$
Fe 1	1632.44589	EW dec with $T_{\rm eff}$	EW inc with $\log g$
Fe 1	1633.15302	EW dec with $T_{\rm eff}$	Line widens at lower $\log g$
Ni 1	1636.31232	EW dec with $T_{\rm eff}$	EW inc with $\log g$
Mg 1	1636.47695	EW dec with $T_{\rm eff}$	EW dec with $\log g$
Fe 1	1637.73679	EW dec with $T_{\rm eff}$	Line widens at lower $\log g$

Element	Wavelength (nm)	$T_{\rm eff}$ effect ($\log g$ = 4.5 dex)	$\log g$ effect ($T_{\rm eff}$ = 5800 K)
Fe 1	1638.40991	EW dec with $T_{\rm eff}$	EW dec with $\log g$
Fe 1	1639.43927	EW dec with $T_{\rm eff}$	EW inc with $\log g$
Fe 1	1639.81861	EW dec with $T_{\rm eff}$	EW dec with $\log g$
Fe 1	1640.46124	EW dec with $T_{\rm eff}$	No variation with $\log g$
Fe 1	1640.77976	EW dec with $T_{\rm eff}$	No variation with $\log g$
C 1	1641.9316	EW inc with $T_{\rm eff}$	EW dec with $\log g$
Si 1	1643.49319	EW dec with $T_{\rm eff}$	No variation with $\log g$
Fe 1	1643.6607	EW dec with $T_{\rm eff}$	EW dec with $\log g$
Fe 1	1644.03945	EW dec with $T_{\rm eff}$	No variation with $\log g$
Fe 1	1644.48271	EW dec with $T_{\rm eff}$	EW inc with $\log g$
Fe 1	1645.48873	EW dec with $T_{\rm eff}$	Line widens at lower $\log g$
Fe 1	1646.69259	EW dec with $T_{\rm eff}$	Line widens at lower $\log g$
Fe 1	1647.40698	EW dec with $T_{\rm eff}$	Line widens at lower $\log g$
Fe 1	1648.6669	EW dec with $T_{\rm eff}$	EW inc with $\log g$
Fe 1	1649.4478	EW dec with $T_{\rm eff}$	Line widens at lower $\log g$
Fe 1	1651.72207	EW dec with $T_{\rm eff}$	EW inc with $\log g$
Fe 1	1652.44727	EW dec with $T_{\rm eff}$	EW inc with $\log g$
Fe 1	1653.19777	EW dec with $T_{\rm eff}$	Line widens at lower $\log g$
Fe 1	1654.46913	EW dec with $T_{\rm eff}$	Line widens at lower $\log g$
Fe 1	1655.19946	EW dec with $T_{\rm eff}$	Line widens at lower $\log g$
Fe 1	1655.96915	EW dec with $T_{\rm eff}$	No variation with $\log g$
Fe 1	1656.17339	EW dec with $T_{\rm eff}$	EW dec with $\log g$
Fe 1	1661.27726	EW dec with $T_{\rm eff}$	Line widens at lower $\log g$
Fe 1	1664.58862	EW dec with $T_{\rm eff}$	Line widens at lower $\log g$
OH 1	1665.33023	EW dec with $T_{\rm eff}$	EW dec with $\log g$
HCl	1665.96879	EW dec with $T_{\rm eff}$	Line widens at lower $\log g$
Fe 1	1666.13807	EW dec with $T_{\rm eff}$	No variation with $\log g$
Fe 1	1666.54724	EW dec with $T_{\rm eff}$	Line widens at lower $\log g$
Ni 1	1667.37196	EW dec with $T_{\rm eff}$	Line widens at lower $\log g$

Element	Wavelength (nm)	T_{eff} effect ($\log g$ = 4.5 dex)	$\log g$ effect (T_{eff} = 5800 K)
Si 1	1668.07719	EW dec with T_{eff}	EW inc with $\log g$
Fe 1	1669.30748	EW dec with T_{eff}	EW dec with $\log g$
Al 1	1671.89551	EW dec with T_{eff}	EW inc with $\log g$
Fe 1	1672.32671	EW dec with T_{eff}	No variation with $\log g$
Al 1	1675.05663	EW dec with T_{eff}	EW inc with $\log g$
Fe 1	1675.3029	EW dec with T_{eff}	No variation with $\log g$
Al 1	1676.33601	EW dec with T_{eff}	No variation with $\log g$
Fe 1	1679.42394	EW dec with T_{eff}	No variation with $\log g$
Fe 1	1679.96728	EW dec with T_{eff}	No variation with $\log g$
Ni 1	1681.54499	EW dec with T_{eff}	No variation with $\log g$
Ni 1	1681.87654	EW dec with T_{eff}	No variation with $\log g$
Fe 1	1682.02162	EW dec with T_{eff}	No variation with $\log g$
Si 1	1682.81576	EW dec with T_{eff}	No variation with $\log g$
Ni 1	1686.7357	EW dec with T_{eff}	EW dec with $\log g$
C 1	1689.04103	EW inc with T_{eff}	EW dec with $\log g$

A.2 M dwarf linemask, sensitivity to T_{eff} and $\log g$

This section contains the lines included in the linemask for M dwarfs, as well as the effects of changing both T_{eff} and $\log g$ for each of the lines.

Table A.2: Effects of changing both T_{eff} and $\log g$ on lines included in the linemask used for parameter estimation for the M dwarfs in the sample. Dec means the line strength decreases with increasing spectroscopic parameter, and inc means the line strength increases with increasing spectroscopic parameter.

Element	Wavelength (nm)	$\log g$ effect (T_{eff} = 3800 K)	$\log g$ effect (T_{eff} = 4200 K)	T_{eff} effect ($\log g$ = 4.5 dex)
K 1	1516.3067	EW dec with $\log g$	EW dec with $\log g$	EW conserved, continuum rises with T_{eff}
K 1	1516.8376	EW dec with $\log g$	EW dec with $\log g$	EW conserved, continuum rises with T_{eff}
Fe 1	1518.2927	EW dec with $\log g$	EW dec with $\log g$	EW inc with T_{eff}
Fe 1	1520.753	EW dec with $\log g$	EW dec with $\log g$	EW inc with T_{eff}
OH 1	1523.6622	EW dec with $\log g$	EW dec with $\log g$	Line width dec with T_{eff}
Fe 1	1526.4191	EW dec with $\log g$	EW dec with $\log g$	Line width dec with T_{eff}
OH 1	1526.6029	EW dec with $\log g$	EW dec with $\log g$	Line width dec with T_{eff}
SiH	1527.8157	EW dec with $\log g$	EW dec with $\log g$	EW conserved, continuum rises with T_{eff}
OH 1	1528.0884	EW dec with $\log g$	EW dec with $\log g$	EW conserved, continuum rises with T_{eff}
Fe 1	1528.3646	EW dec with $\log g$	EW dec with $\log g$	Line width dec with T_{eff}
Fe 1	1529.4562	EW dec with $\log g$	EW dec with $\log g$	EW inc with T_{eff}
Fe 1	1532.8343	EW dec with $\log g$	EW dec with $\log g$	EW conserved, continuum rises with T_{eff}
Fe 1	1533.5387	EW dec with $\log g$	EW dec with $\log g$	EW inc with T_{eff}
OH 1	1536.8555	EW dec with $\log g$	EW dec with $\log g$	EW conserved, continuum rises with T_{eff}
OH 1	1537.1992	EW dec with $\log g$	EW dec with $\log g$	EW conserved, continuum rises with T_{eff}

Element	Wavelength (nm)	$\log g$ effect ($T_{\rm eff}$ = 3800 K)	$\log g$ effect ($T_{\rm eff}$ = 4200 K)	$T_{\rm eff}$ effect ($\log g$ = 4.5 dex)
Fe 1	1538.411	EW dec with $\log g$	EW dec with $\log g$	EW conserved, continuum rises with $T_{\rm eff}$
OH 1	1539.0897	EW dec with $\log g$	EW dec with $\log g$	Line width dec with $T_{\rm eff}$
OH 1	1540.0621	EW dec with $\log g$	EW dec with $\log g$	EW conserved, continuum rises with $T_{\rm eff}$
S 1	1540.3724	EW dec with $\log g$	EW dec with $\log g$	EW conserved, continuum rises with $T_{\rm eff}$
CN 1	1540.7203	EW dec with $\log g$	EW dec with $\log g$	Line width dec with $T_{\rm eff}$
OH 1	1540.9086	EW dec with $\log g$	EW dec with $\log g$	Line width dec with $T_{\rm eff}$
CN 1	1541.9279	EW dec with $\log g$	EW dec with $\log g$	EW conserved, continuum rises with $T_{\rm eff}$
S 1	1542.2276	EW dec with $\log g$	EW dec with $\log g$	EW conserved, continuum rises with $T_{\rm eff}$
Fe 1	1542.7621	EW dec with $\log g$	EW dec with $\log g$	EW conserved, continuum rises with $T_{\rm eff}$
OH 1	1542.84	EW dec with $\log g$	EW dec with $\log g$	EW conserved, continuum rises with $T_{\rm eff}$
SiH	1542.9138	EW dec with $\log g$	EW dec with $\log g$	EW conserved, continuum rises with $T_{\rm eff}$
OH 1	1543.4304	EW dec with $\log g$	EW dec with $\log g$	EW conserved, continuum rises with $T_{\rm eff}$
OH 1	1545.7583	EW dec with $\log g$	EW dec with $\log g$	EW conserved, continuum rises with $T_{\rm eff}$
S 1	1546.9816	EW dec with $\log g$	EW dec with $\log g$	Line width dec with $T_{\rm eff}$
Fe 1	1549.67	EW dec with $\log g$	EW dec with $\log g$	EW conserved, continuum rises with $T_{\rm eff}$
OH 1	1550.5326	EW dec with $\log g$	EW dec with $\log g$	Line width dec with $T_{\rm eff}$
CN 1	1551.3663	EW dec with $\log g$	EW dec with $\log g$	Line width dec with $T_{\rm eff}$
OH 1	1553.5462	EW dec with $\log g$	EW dec with $\log g$	EW conserved, continuum rises with $T_{\rm eff}$
CN 1	1553.6637	EW dec with $\log g$	EW dec with $\log g$	EW conserved, continuum rises with $T_{\rm eff}$
Fe 1	1554.2079	EW dec with $\log g$	EW dec with $\log g$	EW inc with lower $T_{\rm eff}$

Element	Wavelength (nm)	$\log g$ effect ($T_{\rm eff}$ = 3800 K)	$\log g$ effect ($T_{\rm eff}$ = 4200 K)	$T_{\rm eff}$ effect ($\log g$ = 4.5 dex)
Ti 1	1554.3756	EW dec with $\log g$	EW dec with $\log g$	EW conserved, continuum rises with $T_{\rm eff}$
Si 1	1555.7779	EW dec with $\log g$	EW dec with $\log g$	EW conserved, continuum rises with $T_{\rm eff}$
Fe 1	1556.0786	EW dec with $\log g$	EW dec with $\log g$	EW conserved, continuum rises with $T_{\rm eff}$
Fe 1	1556.9236	EW dec with $\log g$	EW dec with $\log g$	EW conserved, continuum rises with $T_{\rm eff}$
Fe 1	1557.1751	EW dec with $\log g$	EW dec with $\log g$	EW conserved, continuum rises with $T_{\rm eff}$
Fe 1	1559.375	EW dec with $\log g$	EW dec with $\log g$	EW inc with $T_{\rm eff}$
Fe 1	1562.1654	EW dec with $\log g$	EW dec with $\log g$	EW inc with $T_{\rm eff}$
OH 1	1562.6659	EW dec with $\log g$	EW dec with $\log g$	EW conserved, continuum rises with $T_{\rm eff}$
Fe 1	1563.195	EW dec with $\log g$	EW dec with $\log g$	EW inc with $T_{\rm eff}$
OH 1	1565.1896	EW dec with $\log g$	EW dec with $\log g$	EW conserved, continuum rises with $T_{\rm eff}$
OH 1	1565.348	EW dec with $\log g$	EW dec with $\log g$	EW conserved, continuum rises with $T_{\rm eff}$
Fe 1	1569.8513	EW dec with $\log g$	EW dec with $\log g$	EW conserved, continuum rises with $T_{\rm eff}$
Ti 1	1571.5573	EW dec with $\log g$	EW dec with $\log g$	EW inc with $T_{\rm eff}$
CN 1	1571.7332	EW dec with $\log g$	EW dec with $\log g$	EW conserved, continuum rises with $T_{\rm eff}$
OH 1	1571.9696	EW dec with $\log g$	EW dec and continuum rises with $\log g$	EW conserved, continuum rises with $T_{\rm eff}$
Ni 1	1572.6636	EW dec with $\log g$	EW dec and continuum rises with $\log g$	EW conserved, continuum rises with $T_{\rm eff}$
OH 1	1573.044	EW dec with $\log g$	EW dec and continuum rises with $\log g$	EW conserved, continuum rises with $T_{\rm eff}$
Mg 1	1574.0706	EW dec with $\log g$	EW dec and continuum rises with $\log g$	EW inc with $T_{\rm eff}$
Mg 1	1574.8988	EW dec with $\log g$	EW dec and continuum rises with $\log g$	EW inc with $T_{\rm eff}$
Fe 1	1575.6037	EW dec with $\log g$	EW dec and continuum rises with $\log g$	Line width dec with $T_{\rm eff}$

Element	Wavelength (nm)	$\log g$ effect ($T_{\rm eff}$ = 3800 K)	$\log g$ effect ($T_{\rm eff}$ = 4200 K)	$T_{\rm eff}$ effect ($\log g$ = 4.5 dex)
Fe 1	1575.6037	EW dec with $\log g$	EW dec and continuum rises with $\log g$	EW inc with $T_{\rm eff}$
Mg 1	1576.5839	EW dec with $\log g$	EW dec and continuum rises with $\log g$	Line width dec with $T_{\rm eff}$
OH 1	1577.6847	EW dec with $\log g$	EW dec and continuum rises with $\log g$	Line width dec with $T_{\rm eff}$
SiH	1577.8448	EW dec with $\log g$	EW dec and continuum rises with $\log g$	Line width dec with $T_{\rm eff}$
OH 1	1588.4898	EW dec with $\log g$	EW dec with $\log g$	Line width dec with $T_{\rm eff}$
Si 1	1588.8409	EW dec with $\log g$	EW dec with $\log g$	EW inc with $T_{\rm eff}$
Fe 1	1589.2398	EW dec with $\log g$	EW dec with $\log g$	EW inc with $T_{\rm eff}$
CN 1	1589.3442	EW dec with $\log g$	EW dec with $\log g$	No change with $T_{\rm eff}$
Fe 1	1589.8018	EW dec with $\log g$	EW dec with $\log g$	Line width dec with $T_{\rm eff}$
OH 1	1591.0432	EW dec with $\log g$	EW dec with $\log g$	Line width dec with $T_{\rm eff}$
Fe 1	1591.2594	EW dec with $\log g$	EW dec with $\log g$	Line width dec with $T_{\rm eff}$
H1F	1591.6003	EW dec with $\log g$	EW dec with $\log g$	EW conserved, continuum rises with $T_{\rm eff}$
OH 1	1602.6283	EW dec with $\log g$	EW dec with $\log g$	EW conserved, continuum rises with $T_{\rm eff}$
HCN	1603.645	EW dec with $\log g$	EW dec with $\log g$	EW conserved, continuum rises with $T_{\rm eff}$
CN 1	1603.8902	EW dec with $\log g$	EW dec with $\log g$	EW conserved, continuum rises with $T_{\rm eff}$
OH 1	1605.2765	EW dec with $\log g$	EW dec with $\log g$	EW conserved, continuum rises with $T_{\rm eff}$
Si 1	1605.5655	EW dec with $\log g$	EW dec with $\log g$	EW conserved, continuum rises with $T_{\rm eff}$
CN 1	1606.1939	EW dec with $\log g$	EW dec with $\log g$	EW conserved, continuum rises with $T_{\rm eff}$
Fe 1	1606.4729	EW dec with $\log g$	EW dec with $\log g$	EW conserved, continuum rises with $T_{\rm eff}$
OH 1	1606.9205	EW dec with $\log g$	EW dec with $\log g$	EW conserved, continuum rises with $T_{\rm eff}$

Element	Wavelength (nm)	$\log g$ effect (T_{eff} = 3800 K)	$\log g$ effect (T_{eff} = 4200 K)	T_{eff} effect ($\log g$ = 4.5 dex)
Fe 1	1607.3872	EW dec with $\log g$	EW dec with $\log g$	EW conserved, continuum rises with T_{eff}
Fe 1	1607.5462	EW dec with $\log g$	EW dec with $\log g$	EW conserved, continuum rises with T_{eff}
Fe 1	1610.2408	EW dec with $\log g$	EW dec with $\log g$	EW inc with T_{eff}
OH 1	1612.3889	EW dec with $\log g$	EW dec with $\log g$	Line width dec with T_{eff}
Ca 1	1613.6823	EW dec with $\log g$	EW dec with $\log g$	EW conserved, continuum rises with T_{eff}
Ca 1	1615.0763	EW dec with $\log g$	EW dec and line width rises with $\log g$	Line width dec with T_{eff}
Fe 1	1615.3249	EW dec with $\log g$	EW dec and line width rises with $\log g$	EW inc with T_{eff}
Ca 1	1615.7364	EW dec with $\log g$	EW dec and line width rises with $\log g$	Line width dec with T_{eff}
OH 1	1619.0121	EW dec with $\log g$	EW dec with $\log g$	EW conserved, continuum rises with T_{eff}
FeH	1619.264	EW dec with $\log g$	EW dec with $\log g$	EW conserved, continuum rises with T_{eff}
Ca 1	1619.7075	EW dec with $\log g$	EW dec and line width rises with $\log g$	EW inc with T_{eff}
Fe 1	1620.4255	EW dec with $\log g$	EW dec with $\log g$	Line width dec with T_{eff}
Fe 1	1620.7557	EW dec with $\log g$	EW dec with $\log g$	Line width dec with T_{eff}
Fe 1	1622.5618	EW dec with $\log g$	EW dec with $\log g$	EW conserved, continuum rises with T_{eff}
OH 1	1623.0235	EW dec with $\log g$	EW dec with $\log g$	EW conserved, continuum rises with T_{eff}
Si 1	1624.1833	EW dec with $\log g$	EW dec with $\log g$	EW conserved, continuum rises with T_{eff}
Fe 1	1624.6462	EW dec with $\log g$	EW dec with $\log g$	EW conserved, continuum rises with T_{eff}
FeH	1624.81	EW dec with $\log g$	EW dec with $\log g$	EW conserved, continuum rises with T_{eff}
Fe 1	1625.207	EW dec with $\log g$	EW dec with $\log g$	EW conserved, continuum rises with T_{eff}
FeH	1625.482	EW dec with $\log g$	EW dec with $\log g$	EW conserved, continuum rises with T_{eff}

Element	Wavelength (nm)	$\log g$ effect ($T_{\rm eff}$ = 3800 K)	$\log g$ effect ($T_{\rm eff}$ = 4200 K)	$T_{\rm eff}$ effect ($\log g$ = 4.5 dex)
CN 1	1626.0387	EW dec with $\log g$	EW dec with $\log g$	EW conserved, continuum rises with $T_{\rm eff}$
FeH	1626.507	EW dec with $\log g$	EW dec with $\log g$	EW conserved, continuum rises with $T_{\rm eff}$
FeH	1631.142	EW dec with $\log g$	EW dec with $\log g$	EW conserved, continuum rises with $T_{\rm eff}$
OH 1	1631.2493	EW dec with $\log g$	EW dec with $\log g$	EW conserved, continuum rises with $T_{\rm eff}$
Fe 1	1631.6323	EW dec with $\log g$	EW dec with $\log g$	EW inc with higher $T_{\rm eff}$
FeH	1635.213	EW dec with $\log g$	EW dec with $\log g$	EW conserved, continuum rises with $T_{\rm eff}$
Co 1	1635.4835	EW dec with $\log g$	EW dec with $\log g$	EW conserved, continuum rises with $T_{\rm eff}$
OH 1	1635.5742	EW dec with $\log g$	EW dec with $\log g$	EW conserved, continuum rises with $T_{\rm eff}$
Mg 1	1636.4748	EW dec with $\log g$	EW dec with $\log g$	EW conserved, continuum rises with $T_{\rm eff}$
Cr 1	1636.7546	EW dec with $\log g$	EW dec with $\log g$	EW conserved, continuum rises with $T_{\rm eff}$
Fe 1	1647.1756	EW dec with $\log g$	EW dec with $\log g$	Line width dec with $T_{\rm eff}$
FeH	1647.249	EW dec with $\log g$	EW dec with $\log g$	Line width dec with $T_{\rm eff}$
Fe 1	1648.6669	EW dec with $\log g$	EW dec and line width rises with $\log g$	EW inc with $T_{\rm eff}$
Fe 1	1652.3849	EW dec with $\log g$	EW dec with $\log g$	EW inc with $T_{\rm eff}$
OH 1	1652.6154	EW dec with $\log g$	EW dec with $\log g$	EW inc with lower $T_{\rm eff}$
OH 1	1653.4363	EW dec with $\log g$	EW dec with $\log g$	EW conserved, continuum rises with $T_{\rm eff}$
Fe 1	1653.8703	EW dec with $\log g$	EW dec with $\log g$	Line width dec with $T_{\rm eff}$
FeH	1654.676	EW dec with $\log g$	EW dec with $\log g$	EW conserved, continuum rises with $T_{\rm eff}$
FeH	1654.89	EW dec with $\log g$	EW dec with $\log g$	EW conserved, continuum rises with $T_{\rm eff}$
Fe 1	1658.1386	EW dec with $\log g$	EW dec with $\log g$	EW conserved, continuum rises with $T_{\rm eff}$

Element	Wavelength (nm)	$\log g$ effect (T_{eff} = 3800 K)	$\log g$ effect (T_{eff} = 4200 K)	T_{eff} effect ($\log g$ = 4.5 dex)
Fe 1	1658.1996	EW dec with $\log g$	EW dec with $\log g$	EW conserved, continuum rises with T_{eff}
Fe 1	1660.4917	EW dec with $\log g$	EW dec with $\log g$	EW conserved, continuum rises with T_{eff}
Fe 1	1660.7637	EW dec with $\log g$	EW dec with $\log g$	EW conserved, continuum rises with T_{eff}
Ca 2	1664.9877	EW dec with $\log g$	EW dec with $\log g$	Line width dec with T_{eff}
OH 1	1665.4454	EW dec with $\log g$	EW dec with $\log g$	EW conserved, continuum rises with T_{eff}
OH 1	1665.5985	EW dec with $\log g$	EW dec with $\log g$	EW conserved, continuum rises with T_{eff}
Ca 2	1666.2726	EW dec with $\log g$	EW dec with $\log g$	EW conserved, continuum rises with T_{eff}
OH 1	1670.4357	EW dec with $\log g$	EW dec with $\log g$	EW conserved, continuum rises with T_{eff}
Mn 1	1670.8001	EW dec with $\log g$	EW dec with $\log g$	EW conserved, continuum rises with T_{eff}
OH 1	1671.4361	EW dec with $\log g$	EW dec with $\log g$	EW conserved, continuum rises with T_{eff}
Al 1	1671.899	EW dec with $\log g$	EW dec and line width rises with $\log g$	EW inc with T_{eff}
Fe 1	1672.8312	EW dec with $\log g$	EW dec with $\log g$	EW conserved, continuum rises with T_{eff}
OH 1	1672.9737	EW dec with $\log g$	EW dec with $\log g$	EW conserved, continuum rises with T_{eff}
Al 1	1675.0453	Line width dec with $\log g$	EW dec and line width rises with $\log g$	EW inc with T_{eff}
Al 1	1676.3394	EW dec with $\log g$	EW dec and line width rises with $\log g$	EW inc with T_{eff}
Fe 1	1686.6427	EW dec with $\log g$	EW dec with $\log g$	EW conserved, continuum rises with T_{eff}
OH 1	1687.1895	EW dec with $\log g$	EW dec with $\log g$	EW conserved, continuum rises with T_{eff}
OH 1	1687.909	EW dec with $\log g$	EW dec with $\log g$	EW conserved, continuum rises with T_{eff}
Fe 1	1688.4812	EW dec with $\log g$	EW dec with $\log g$	EW conserved, continuum rises with T_{eff}
FeH	1688.612	EW dec with $\log g$	EW dec with $\log g$	EW conserved, continuum rises with T_{eff}

Element	Wavelength (nm)	$\log g$ effect ($T_{\rm eff}$ = 3800 K)	$\log g$ effect ($T_{\rm eff}$ = 4200 K)	$T_{\rm eff}$ effect ($\log g$ = 4.5 dex)
Fe 1	1689.5184	EW dec with $\log g$	EW dec with $\log g$	EW conserved, continuum rises with $T_{\rm eff}$
Fe 1	1689.8886	EW dec with $\log g$	EW dec with $\log g$	EW conserved, continuum rises with $T_{\rm eff}$
OH 1	1690.2734	EW dec with $\log g$	EW dec with $\log g$	EW conserved, continuum rises with $T_{\rm eff}$
OH 1	1690.4224	EW dec with $\log g$	EW dec with $\log g$	EW conserved, continuum rises with $T_{\rm eff}$
OH 1	1690.5632	EW dec with $\log g$	EW dec with $\log g$	EW conserved, continuum rises with $T_{\rm eff}$
OH 1	1690.9286	EW dec with $\log g$	EW dec with $\log g$	EW conserved, continuum rises with $T_{\rm eff}$

Appendix B

Results

B.1 Full FGK sample results

Table B.1: Full list of derived parameters for FGK stellar sample. Uncertainties in derived parameters are estimated by *iSpec*. *iSpec* output parameters indicated by letter O. Literature parameters indicated by letter L.

APOGEE_ID	$T_{\rm eff} \pm \Delta T_{\rm eff}$	$\log g \pm \Delta \log g$	$\log g_{cor}$	$[\rm M/H] \pm \Delta[\rm M/H]$	$[Fe/H] \pm \Delta[\rm Fe/H]$	$\rm v_{mic}$	$\rm v_{mac}$	$v \sin i$	χ^2
2M00012723+8520108	5973 ± 66	4.24 ± 0.07	4.15	0.16 ± 0.03	0.11 ± 0.1	0.74	5	10.11	1.4
2M00015324+5634361	6164 ± 143	4.15 ± 0.2	4.01	-0.15 ± 0.06	-0.23 ± 0.1	0.64	6.54	8.57	0.54
2M00072254+2627025	4741 ± 83	3.18 ± 0.11	3.18	-0.03 ± 0.04	-0.15 ± 0.1	0.88	3.67	9.97	1.02
2M00095611-0002296	6196 ± 139	4.47 ± 0.15	4.31	0.02 ± 0.05	-0.05 ± 0.1	0.21	6.54	8.48	1.41
2M00100176+0201021	6142 ± 115	4.26 ± 0.16	4.12	0.09 ± 0.04	0.02 ± 0.1	0.67	6.11	8.99	1.46
2M00125570-1441121	5730 ± 111	4.3 ± 0.12	4.27	0.04 ± 0.05	0 ± 0.1	0.65	4	9.3	0.44
2M00135646-1439234	5927 ± 127	4.33 ± 0.19	4.25	-0.15 ± 0.05	-0.21 ± 0.1	0.16	5.08	8.3	1.46

APOGEE_ID	$T_{\rm eff} \pm \Delta T_{\rm eff}$	$\log g \pm \Delta \log g$	$\log g_{cor}$	$[\mathrm{M/H}] \pm \Delta[\mathrm{M/H}]$	$[Fe/H] \pm \Delta[\mathrm{Fe/H}]$	$\mathrm{v_{mic}}$	$\mathrm{v_{mac}}$	$v \sin i$	χ^2
2M00153822-1516023	6181 ± 145	4.52 ± 0.15	4.37	0.09 ± 0.06	0.04 ± 0.1	0.52	6.35	10.49	1.7
2M00162970-1456483	6144 ± 122	4.36 ± 0.19	4.22	0.11 ± 0.05	0.06 ± 0.1	0.68	6.08	10.61	0.48
2M00164203-1533376	5852 ± 140	4.23 ± 0.2	4.17	-0.18 ± 0.06	-0.27 ± 0.1	0.36	4.76	8.23	0.48
2M00170412-1459180	5598 ± 106	4.27 ± 0.13	4.27	-0.01 ± 0.05	-0.04 ± 0.1	0.88	3.62	9.98	0.56
2M00170742-1405426	6169 ± 109	4.39 ± 0.16	4.24	0.21 ± 0.04	0.15 ± 0.1	0.66	6.13	10.81	1.42
2M00175716-1421576	5616 ± 116	4.32 ± 0.17	4.32	-0.09 ± 0.05	-0.13 ± 0.1	0.73	3.76	9.78	0.42
2M00182549+4401376	4022 ± 18	2.22 ± 0.08	2.22	-0.84 ± 0.03	-1.39 ± 0.1	0.25	4.73	10.04	3.33
2M00183985-1501183	5914 ± 126	4.25 ± 0.18	4.18	-0.06 ± 0.05	-0.11 ± 0.1	0.61	4.93	8	1.46
2M00184748-1409173	5724 ± 109	4.28 ± 0.12	4.25	0.1 ± 0.05	0.04 ± 0.1	0.61	3.91	10.42	1.56
2M00185341-1355444	6120 ± 98	4.47 ± 0.11	4.34	0.01 ± 0.04	-0.05 ± 0.1	0.33	6.03	9.11	1.37
2M00185841-1410382	6189 ± 123	4.38 ± 0.19	4.23	-0.09 ± 0.05	-0.17 ± 0.1	0.12	6.61	8.19	1.42
2M00191294-1319334	5773 ± 148	4.3 ± 0.18	4.26	-0.23 ± 0.06	-0.31 ± 0.1	0.13	4.45	8.27	0.48
2M00202829-1423435	5584 ± 143	4.29 ± 0.2	4.30	-0.39 ± 0.06	-0.47 ± 0.1	0.15	3.98	7.92	1.46
2M00220431-1447301	5648 ± 140	4.37 ± 0.23	4.36	-0.24 ± 0.06	-0.29 ± 0.1	0.41	4	8.93	1.41
2M00220632-1351147	5546 ± 113	4.15 ± 0.12	4.17	-0.16 ± 0.05	-0.24 ± 0.1	0.6	3.68	9.17	1.56
2M00225167-1351183	5723 ± 132	4.28 ± 0.16	4.25	-0.09 ± 0.06	-0.16 ± 0.1	0.58	4.11	9.61	1.45
2M00311026+5521179	5620 ± 105	4.2 ± 0.13	4.20	0.02 ± 0.05	-0.03 ± 0.1	0.76	3.67	10.76	0.61
2M00311352+8448490	5960 ± 113	4.17 ± 0.14	4.08	-0.05 ± 0.05	-0.11 ± 0.1	0.74	5.18	9.96	0.46
2M00360773+8534155	5751 ± 124	4.14 ± 0.12	4.11	0.12 ± 0.05	0.05 ± 0.1	0.54	4.02	9.77	1.67
2M00401827+0308383	5935 ± 103	4.21 ± 0.13	4.13	-0.01 ± 0.04	-0.09 ± 0.1	0.56	4.99	9.32	1.4

APOGEE_ID	$T_{\rm eff} \pm \Delta T_{\rm eff}$	$\log g \pm \Delta \log g$	$\log g_{cor}$	[M/H] $\pm \Delta$[M/H]	$[Fe/H] \pm \Delta$[Fe/H]	$v_{\rm mic}$	$v_{\rm mac}$	$v \sin i$	χ^2
2M00402658+0329038	5634 ± 108	3.92 ± 0.15	3.92	0.14 ± 0.05	0.11 ± 0.1	0.98	3.67	10.02	1.75
2M00410552+8448262	6096 ± 128	4.24 ± 0.17	4.12	0.04 ± 0.05	-0.01 ± 0.1	0.7	5.87	9.78	0.43
2M00412536+0205499	5614 ± 114	4.05 ± 0.12	4.05	0.02 ± 0.05	-0.02 ± 0.1	0.8	3.7	9.83	0.56
2M00414909+0218177	5662 ± 69	4.27 ± 0.09	4.26	0.07 ± 0.03	0.01 ± 0.1	0.69	3.73	9.18	1.43
2M00420349+8501088	5689 ± 98	4.16 ± 0.11	4.14	0.05 ± 0.04	0 ± 0.1	0.73	3.86	9.38	0.56
2M00420353+1702204	6153 ± 146	4.4 ± 0.25	4.26	-0.09 ± 0.06	-0.16 ± 0.1	0.21	6.36	8.71	0.39
2M00421361+0202308	5552 ± 116	4.3 ± 0.14	4.32	-0.04 ± 0.05	-0.08 ± 0.1	0.91	3.53	8.44	1.56
2M00423092+8621310	5935 ± 144	4.39 ± 0.2	4.31	0.03 ± 0.06	-0.03 ± 0.1	0.4	4.92	9.16	0.85
2M00424593+0154031	5970 ± 155	4.21 ± 0.19	4.12	-0.25 ± 0.06	-0.34 ± 0.1	0	5.43	8.04	1.46
2M00424932+0144596	5938 ± 102	4.23 ± 0.14	4.15	-0.09 ± 0.04	-0.15 ± 0.1	0.53	5.09	8.72	1.43
2M00425464+0214101	6115 ± 164	4.17 ± 0.23	4.05	-0.11 ± 0.07	-0.19 ± 0.1	0.37	6.17	8.1	0.41
2M00430702+0315296	6202 ± 144	4.4 ± 0.22	4.24	-0.06 ± 0.06	-0.14 ± 0.1	0.25	6.67	8.51	1.4
2M00433684+1809461	5995 ± 121	4.42 ± 0.14	4.32	-0.07 ± 0.05	-0.14 ± 0.1	0.35	5.36	8.85	0.4
2M00434390+0346182	5731 ± 107	4.32 ± 0.12	4.29	0.01 ± 0.04	-0.05 ± 0.1	0.74	4.03	9.43	1.45
2M00434931+8522225	5751 ± 152	4.35 ± 0.19	4.32	-0.28 ± 0.06	-0.39 ± 0.1	0.24	4.42	7.92	1.56
2M00440299+0201225	6298 ± 138	4.41 ± 0.18	4.21	0.04 ± 0.05	-0.01 ± 0.1	0.6	7.28	9.95	0.37
2M00444662+0349333	6083 ± 98	4.38 ± 0.14	4.26	0.09 ± 0.04	0.02 ± 0.1	0.54	5.71	9.14	1.37
2M00445171+0342235	5685 ± 60	4.01 ± 0.06	3.99	0.11 ± 0.03	0.06 ± 0.1	0.77	3.83	10.93	1.42
2M00445295+1823024	6220 ± 129	4.42 ± 0.16	4.25	0.14 ± 0.05	0.08 ± 0.1	0.55	6.58	10.61	1.44
2M00445469+8432126	6005 ± 120	4.24 ± 0.12	4.14	0.02 ± 0.05	-0.05 ± 0.1	0.62	5.34	9.26	1.4

APOGEE_ID	$T_{\text{eff}} \pm \Delta T_{\text{eff}}$	$\log g \pm \Delta \log g$	$\log g_{cor}$	$[\text{M/H}] \pm \Delta[\text{M/H}]$	$[Fe/H] \pm \Delta[\text{Fe/H}]$	v_{mic}	v_{mac}	$v \sin i$	χ^2
2M00455212+0313149	5901 ± 110	4.32 ± 0.17	4.25	-0.04 ± 0.05	-0.11 ± 0.1	0.46	4.83	8.88	1.38
2M00464721+0330241	6227 ± 130	4.46 ± 0.13	4.29	0.03 ± 0.05	-0.03 ± 0.1	0.29	6.75	8.11	1.35
2M00470180+0249074	5716 ± 98	4.18 ± 0.1	4.15	0.08 ± 0.04	0.04 ± 0.1	0.83	3.92	10.54	1.53
2M00470387+0244187	5885 ± 111	4.35 ± 0.18	4.28	-0.05 ± 0.05	-0.1 ± 0.1	0.47	4.76	8.25	1.43
2M00470858+0142087	5940 ± 89	4.35 ± 0.12	4.27	0.13 ± 0.04	0.09 ± 0.1	0.74	4.83	9.56	1.4
2M00474230-1137457	5623 ± 120	4.32 ± 0.16	4.32	0.02 ± 0.05	-0.01 ± 0.1	0.74	3.65	10.76	1.67
2M00474480+0134057	5903 ± 129	4.28 ± 0.18	4.21	0.02 ± 0.05	-0.07 ± 0.1	0.6	4.78	8.87	0.44
2M00474965+0208069	5924 ± 148	4.21 ± 0.21	4.13	-0.15 ± 0.06	-0.21 ± 0.1	0.53	5.08	8.43	1.41
2M00475858+8458472	5584 ± 107	4.15 ± 0.12	4.16	0.04 ± 0.05	0 ± 0.1	0.86	3.56	9.82	0.78
2M00485241+0241258	5835 ± 104	4.1 ± 0.12	4.04	0.05 ± 0.04	0.01 ± 0.1	0.78	4.47	10.29	1.39
2M00490316+0335190	5681 ± 109	4.31 ± 0.14	4.29	-0.03 ± 0.05	-0.08 ± 0.1	0.77	3.9	9.09	1.47
2M00493555+0215404	5627 ± 115	4.26 ± 0.15	4.26	-0.02 ± 0.05	-0.07 ± 0.1	0.71	3.72	10.18	1.49
2M00504016-1053409	5809 ± 121	4.07 ± 0.12	4.02	0.06 ± 0.05	-0.02 ± 0.1	0.83	4.35	9.38	1.74
2M00543120+8640410	5682 ± 103	4.29 ± 0.13	4.27	-0.02 ± 0.04	-0.09 ± 0.1	0.69	3.89	9.96	0.69
2M01095972+8412017	5990 ± 136	4.12 ± 0.14	4.03	-0.04 ± 0.06	-0.11 ± 0.1	0.76	5.34	9.25	0.6
2M01152144+8617532	5387 ± 94	4.23 ± 0.12	4.29	0.02 ± 0.04	0 ± 0.1	1.28	3.17	10.65	1.99
2M01215829+1236149	4871 ± 78	3.3 ± 0.12	3.30	0.05 ± 0.05	-0.04 ± 0.1	0.86	3.56	11.27	1.91
2M01233744+3414451	5096 ± 110	3.56 ± 0.13	3.56	-0.07 ± 0.06	-0.16 ± 0.1	0.72	3.51	11.47	0.63
2M01242904+1728169	6260 ± 99	4.53 ± 0.09	4.35	0.07 ± 0.04	0.01 ± 0.1	0.36	6.95	8.73	1.36
2M01254154+4447116	4823 ± 87	3.26 ± 0.13	3.26	0.1 ± 0.05	0.02 ± 0.1	1.02	3.51	9.77	1.08

APOGEE_ID	$T_{\rm eff} \pm \Delta T_{\rm eff}$	$\log g \pm \Delta \log g$	$\log g_{cor}$	$[\mathrm{M/H}] \pm \Delta[\mathrm{M/H}]$	$[Fe/H] \pm \Delta[\mathrm{Fe/H}]$	$\mathrm{v_{mic}}$	$\mathrm{v_{mac}}$	$v \sin i$	χ^2
2M01394238-1914422	6186 ± 129	4.45 ± 0.15	4.30	0.11 ± 0.05	0.05 ± 0.1	0.43	6.36	8.28	0.53
2M01394488-1805074	5998 ± 183	4.16 ± 0.2	4.06	-0.19 ± 0.07	-0.29 ± 0.1	0.21	5.54	7.72	1.56
2M01401969-1927033	5759 ± 134	4.22 ± 0.13	4.18	0.01 ± 0.05	-0.07 ± 0.1	0.78	4.16	9.49	0.71
2M01402732-1753108	5990 ± 149	4.34 ± 0.19	4.25	-0.1 ± 0.06	-0.17 ± 0.1	0.43	5.36	8.24	1.55
2M01413053-1740478	6227 ± 169	4.42 ± 0.22	4.25	-0.1 ± 0.07	-0.19 ± 0.1	0	6.89	9.02	0.55
2M01415953-1710445	5720 ± 73	4.24 ± 0.08	4.21	-0.02 ± 0.03	-0.08 ± 0.1	0.72	4.04	8.62	0.37
2M01431419-1852455	6172 ± 137	4.35 ± 0.21	4.20	-0.04 ± 0.05	-0.11 ± 0.1	0.42	6.44	8.62	0.43
2M01451321-1802059	6043 ± 114	4.14 ± 0.12	4.03	0.07 ± 0.04	0 ± 0.1	0.71	5.53	10.59	1.39
2M01451945-1745066	5690 ± 96	4.24 ± 0.12	4.22	-0.08 ± 0.04	-0.18 ± 0.1	0.41	4	8.95	1.43
2M01453625-1803354	5843 ± 128	4.2 ± 0.17	4.14	-0.18 ± 0.05	-0.28 ± 0.1	0.32	4.73	7.92	1.45
2M01480738-1857552	6196 ± 157	4.22 ± 0.2	4.06	0.01 ± 0.06	-0.07 ± 0.1	0.64	6.58	9.15	1.47
2M01491634-1727419	5790 ± 109	4.19 ± 0.12	4.15	0.07 ± 0.04	0.02 ± 0.1	0.75	4.22	10.37	0.47
2M01493055-0243447	5908 ± 103	4.32 ± 0.15	4.25	-0.01 ± 0.04	-0.08 ± 0.1	0.55	4.83	9.19	0.5
2M01493323-1842094	6187 ± 120	4.42 ± 0.16	4.27	0.07 ± 0.05	0.02 ± 0.1	0.47	6.42	10.29	0.37
2M01552991-0410507	6279 ± 139	4.4 ± 0.18	4.21	0.06 ± 0.05	0.02 ± 0.1	0.59	7.11	9.74	1.57
2M02035552+1302346	5971 ± 87	4.32 ± 0.1	4.23	0.15 ± 0.03	0.11 ± 0.1	0.65	4.98	9.4	1.45
2M02054117+1305267	6033 ± 76	4.39 ± 0.11	4.29	-0.16 ± 0.03	-0.24 ± 0.1	0.24	5.67	7.82	1.32
2M02135922-0502389	6006 ± 100	4.4 ± 0.11	4.30	-0.01 ± 0.04	-0.07 ± 0.1	0.41	5.35	9.18	0.37
2M02144474-0503382	5933 ± 137	4.14 ± 0.16	4.06	0.04 ± 0.05	-0.03 ± 0.1	0.64	4.94	11.28	0.4
2M02144482-0601547	5980 ± 129	4.08 ± 0.13	3.99	0.07 ± 0.05	0.04 ± 0.1	0.87	5.18	9.98	1.51

APOGEE_ID	$T_{\rm eff} \pm \Delta T_{\rm eff}$	$\log g \pm \Delta \log g$	$\log g_{cor}$	$[\rm M/H] \pm \Delta[\rm M/H]$	$[Fe/H] \pm \Delta[\rm Fe/H]$	$\rm v_{mic}$	$\rm v_{mac}$	$v \sin i$	χ^2
2M02145213-0606214	6002 ± 74	4.29 ± 0.08	4.19	0.04 ± 0.03	0 ± 0.1	0.59	5.28	9.72	1.55
2M02164258-0450245	5672 ± 77	4.43 ± 0.1	4.42	-0.11 ± 0.03	-0.16 ± 0.1	0.6	3.94	8.94	1.4
2M02172056-0602513	6167 ± 108	4.35 ± 0.16	4.20	0.17 ± 0.04	0.12 ± 0.1	0.64	6.17	9.94	0.38
2M02175786-0610283	6019 ± 141	4.38 ± 0.17	4.28	-0.01 ± 0.05	-0.07 ± 0.1	0.47	5.43	8.89	0.5
2M02181121-0407340	5758 ± 114	4.3 ± 0.12	4.26	0.14 ± 0.05	0.1 ± 0.1	0.75	3.99	10.25	0.56
2M02181396-0444080	6010 ± 145	4.27 ± 0.16	4.17	0.1 ± 0.06	0.02 ± 0.1	0.74	5.27	10.96	1.74
2M02181816-0500099	6065 ± 132	4.27 ± 0.17	4.16	-0.02 ± 0.05	-0.11 ± 0.1	0.37	5.73	9.45	1.42
2M02182578-0420041	5864 ± 70	4.31 ± 0.09	4.25	0.07 ± 0.03	0.01 ± 0.1	0.57	4.53	9.02	1.43
2M02184230-0439030	5856 ± 164	4.05 ± 0.2	3.99	-0.2 ± 0.07	-0.27 ± 0.1	0.52	4.85	6.83	1.62
2M02185808-0544306	5662 ± 128	4.25 ± 0.18	4.24	-0.07 ± 0.06	-0.12 ± 0.1	0.61	3.88	9.05	1.63
2M02193491-0609453	5920 ± 122	4.39 ± 0.2	4.31	-0.07 ± 0.05	-0.11 ± 0.1	0.52	4.95	10.05	0.41
2M02203496-0433068	6165 ± 140	4.3 ± 0.2	4.16	0.19 ± 0.06	0.15 ± 0.1	0.76	6.14	9.77	1.54
2M02210636-0609029	5704 ± 121	4.04 ± 0.12	4.02	0.08 ± 0.05	0.04 ± 0.1	0.81	3.92	9.97	0.65
2M02272221-0851328	5770 ± 79	4.33 ± 0.09	4.29	-0.03 ± 0.03	-0.09 ± 0.1	0.69	4.23	8.7	1.37
2M02272299-0856017	6159 ± 146	4.38 ± 0.25	4.24	-0.13 ± 0.06	-0.21 ± 0.1	0.3	6.44	8.33	1.38
2M02280061-0754483	5908 ± 136	4.31 ± 0.19	4.24	0.02 ± 0.05	-0.07 ± 0.1	0.56	4.8	9.34	1.45
2M02304582-0924379	6086 ± 101	4.39 ± 0.14	4.27	0 ± 0.04	-0.07 ± 0.1	0.54	5.82	8.79	1.41
2M02304958-0848271	5941 ± 145	4.46 ± 0.17	4.38	-0.2 ± 0.06	-0.27 ± 0.1	0	5.19	7.27	1.38
2M02305840-0927005	5907 ± 96	4.4 ± 0.14	4.33	0.01 ± 0.04	-0.02 ± 0.1	0.69	4.8	10.18	1.4
2M02305958-0729096	5782 ± 119	4.31 ± 0.14	4.27	0 ± 0.05	-0.07 ± 0.1	0.66	4.25	9.25	1.41

APOGEE_ID	$T_{\mathrm{eff}} \pm \Delta T_{\mathrm{eff}}$	$\log g \pm \Delta \log g$	$\log g_{cor}$	$[\mathrm{M/H}] \pm \Delta[\mathrm{M/H}]$	$[Fe/H] \pm \Delta[\mathrm{Fe/H}]$	$\mathrm{v}_{\mathrm{mic}}$	$\mathrm{v}_{\mathrm{mac}}$	$v \sin i$	χ^2
2M02312520+0946530	5947 ± 129	4.35 ± 0.19	4.27	-0.06 ± 0.05	-0.11 ± 0.1	0.46	5.08	8.1	1.52
2M02313090-1012465	5998 ± 134	4.26 ± 0.14	4.16	0.02 ± 0.05	-0.04 ± 0.1	0.5	5.29	9.57	1.4
2M02314326+1119182	5755 ± 165	4.25 ± 0.19	4.22	-0.34 ± 0.07	-0.41 ± 0.1	0.2	4.5	7.51	1.42
2M02315267-0758418	5771 ± 85	4.36 ± 0.11	4.32	-0.09 ± 0.04	-0.15 ± 0.1	0.55	4.29	9.13	1.33
2M02320580-0724118	6001 ± 113	4.34 ± 0.13	4.24	0.06 ± 0.04	0 ± 0.1	0.52	5.25	8.9	1.41
2M02322045-0742066	5972 ± 120	4.45 ± 0.12	4.36	0.11 ± 0.05	0.05 ± 0.1	0.62	5.02	10.44	1.25
2M02322239-0747342	5893 ± 79	4.35 ± 0.11	4.28	0.11 ± 0.03	0.07 ± 0.1	0.76	4.62	10.79	1.52
2M02323715-0827552	5956 ± 129	4.26 ± 0.17	4.17	-0.08 ± 0.05	-0.15 ± 0.1	0.49	5.17	8.97	1.39
2M02324396-0722447	5786 ± 100	4.16 ± 0.1	4.12	0.19 ± 0.04	0.13 ± 0.1	0.83	4.08	10.61	1.45
2M02343818+1053469	6051 ± 98	4.23 ± 0.11	4.12	0.06 ± 0.04	0 ± 0.1	0.47	5.56	10.52	0.36
2M02343905-0917378	5907 ± 111	4.24 ± 0.15	4.17	0.12 ± 0.05	0.07 ± 0.1	0.78	4.69	10.03	1.31
2M02350284+0900000	5600 ± 107	4.18 ± 0.12	4.18	0.12 ± 0.05	0.08 ± 0.1	0.76	3.51	9.48	1.74
2M02351754+0856501	6123 ± 170	4.23 ± 0.25	4.10	-0.1 ± 0.07	-0.18 ± 0.1	0.01	6.2	8.07	1.47
2M02351926-0915150	6056 ± 149	4.38 ± 0.21	4.27	-0.17 ± 0.06	-0.25 ± 0.1	0	5.82	8.05	1.36
2M02354285-0847122	5892 ± 72	4.38 ± 0.11	4.31	0.11 ± 0.03	0.09 ± 0.1	0.85	4.61	10.01	1.4
2M02363396+1135323	5759 ± 124	4.1 ± 0.11	4.06	0.06 ± 0.05	0 ± 0.1	0.59	4.13	10.61	0.63
2M02363434+1123313	5606 ± 98	4.35 ± 0.13	4.35	-0.03 ± 0.04	-0.07 ± 0.1	0.7	3.66	10.59	1.47
2M02364167+1139137	5956 ± 93	4.3 ± 0.11	4.21	0.14 ± 0.04	0.09 ± 0.1	0.7	4.92	11.15	0.4
2M02370158+1046345	5709 ± 117	4.38 ± 0.16	4.36	-0.14 ± 0.05	-0.19 ± 0.1	0.37	4.1	8.62	1.44
2M02372805-0906231	6046 ± 135	4.22 ± 0.16	4.11	0.08 ± 0.05	0.03 ± 0.1	0.76	5.51	10.36	1.48

APOGEE_ID	$T_{\rm eff} \pm \Delta T_{\rm eff}$	$\log g \pm \Delta \log g$	$\log g_{cor}$	$[\mathrm{M/H}] \pm \Delta[\mathrm{M/H}]$	$[Fe/H] \pm \Delta[\mathrm{Fe/H}]$	$\mathrm{v_{mic}}$	$\mathrm{v_{mac}}$	$v \sin i$	χ^2
2M02374405+0002418	5676 ± 148	4.28 ± 0.21	4.27	-0.24 ± 0.06	-0.33 ± 0.1	0.37	4.11	7.86	0.81
2M02381250-0016009	5821 ± 120	4.35 ± 0.17	4.30	-0.07 ± 0.05	-0.11 ± 0.1	0.61	4.48	9.97	0.43
2M02393964-0046440	5882 ± 144	4.1 ± 0.19	4.03	-0.11 ± 0.06	-0.17 ± 0.1	0.58	4.86	8.66	0.57
2M02401764+3435056	5026 ± 94	3.54 ± 0.09	3.54	-0.01 ± 0.05	-0.09 ± 0.1	0.96	3.54	9.71	1.78
2M02403099-0055282	6121 ± 137	4.37 ± 0.23	4.24	-0.27 ± 0.05	-0.34 ± 0.1	0	6.34	7.42	0.41
2M02405714-1144248	6203 ± 182	4.38 ± 0.27	4.22	-0.19 ± 0.07	-0.29 ± 0.1	0	6.82	8.51	1.39
2M02412152-0005336	5956 ± 106	4.34 ± 0.15	4.25	-0.11 ± 0.04	-0.17 ± 0.1	0.29	5.19	8.5	1.46
2M02412638-1224072	5950 ± 144	4.06 ± 0.17	3.98	-0.2 ± 0.06	-0.29 ± 0.1	0.43	5.31	8.34	0.4
2M02412780-1149488	5769 ± 96	4.26 ± 0.1	4.22	0.09 ± 0.04	0.04 ± 0.1	0.76	4.1	10.97	1.46
2M02413391-1232483	5901 ± 139	4.25 ± 0.21	4.18	-0.09 ± 0.06	-0.15 ± 0.1	0.47	4.89	8.19	0.44
2M02413551+0103159	5931 ± 136	4.25 ± 0.19	4.17	-0.05 ± 0.06	-0.12 ± 0.1	0.22	5.01	8.92	1.81
2M02415711-1128436	5524 ± 108	4.22 ± 0.11	4.24	0.11 ± 0.05	0.06 ± 0.1	0.92	3.31	10.57	1.73
2M02421582-1214094	6096 ± 66	4.31 ± 0.09	4.19	0.06 ± 0.03	-0.02 ± 0.1	0.47	5.83	9.48	1.34
2M02422208-0022115	5961 ± 141	4.28 ± 0.17	4.19	0 ± 0.06	-0.04 ± 0.1	0.64	5.1	10.26	2.9
2M02423990-1206442	5869 ± 130	4.25 ± 0.19	4.19	-0.08 ± 0.05	-0.14 ± 0.1	0.49	4.73	8.61	0.51
2M02424752-1249365	6077 ± 132	4.37 ± 0.18	4.25	0.11 ± 0.05	0.07 ± 0.1	0.68	5.64	9.91	0.44
2M02425260+0101143	5733 ± 127	4.34 ± 0.14	4.31	0.02 ± 0.05	-0.03 ± 0.1	0.68	4.03	10.58	0.66
2M02425321-0023240	5914 ± 121	4.1 ± 0.14	4.03	0.02 ± 0.05	-0.04 ± 0.1	0.73	4.88	8.93	0.48
2M02430917-1403317	6026 ± 143	4.26 ± 0.18	4.16	-0.19 ± 0.06	-0.26 ± 0.1	0.18	5.68	8.33	1.4
2M02431672-1337519	5529 ± 73	4.17 ± 0.07	4.19	0.12 ± 0.03	0.1 ± 0.1	0.95	3.32	9.66	1.64

APOGEE_ID	$T_{\rm eff} \pm \Delta T_{\rm eff}$	$\log g \pm \Delta \log g$	$\log g_{cor}$	$[\mathrm{M/H}] \pm \Delta[\mathrm{M/H}]$	$[Fe/H] \pm \Delta[\mathrm{Fe/H}]$	$\mathrm{v}_{\rm mic}$	$\mathrm{v}_{\rm mac}$	$v \sin i$	χ^2
2M02432027+0932544	6090 ± 116	4.37 ± 0.18	4.25	-0.14 ± 0.05	-0.24 ± 0.1	0.07	6	7.21	1.35
2M02432444+0056096	6063 ± 160	4.2 ± 0.18	4.09	0.09 ± 0.06	0.03 ± 0.1	0.85	5.61	9.25	1.68
2M02433697-0020403	6021 ± 78	4.36 ± 0.09	4.26	0 ± 0.03	-0.04 ± 0.1	0.04	5.43	10.3	0.58
2M02434007+0014187	6053 ± 118	4.46 ± 0.12	4.35	0.13 ± 0.05	0.08 ± 0.1	0.57	5.47	11.03	0.54
2M02435250-1209524	5575 ± 81	4.26 ± 0.09	4.27	0.05 ± 0.03	0.01 ± 0.1	0.82	3.5	10.28	0.46
2M02435354-0027158	5745 ± 120	4.28 ± 0.14	4.25	-0.18 ± 0.05	-0.25 ± 0.1	0.39	4.3	10.43	1.51
2M02440266-1124283	5998 ± 128	4.44 ± 0.14	4.34	-0.09 ± 0.05	-0.15 ± 0.1	0.33	5.39	8.87	1.36
2M02441370-0115169	5963 ± 131	4.37 ± 0.18	4.28	-0.06 ± 0.05	-0.12 ± 0.1	0.29	5.17	8.32	0.53
2M02442733-1201014	6198 ± 168	4.46 ± 0.2	4.30	-0.04 ± 0.07	-0.12 ± 0.1	0.24	6.62	9.01	1.35
2M02443098-1234044	5639 ± 113	4.13 ± 0.13	4.12	0.12 ± 0.05	0.07 ± 0.1	0.84	3.63	10.29	0.79
2M02445584-1335593	6198 ± 67	4.47 ± 0.07	4.31	0.13 ± 0.03	0.07 ± 0.1	0.53	6.42	10.21	0.32
2M02452511+0019562	5688 ± 129	4.29 ± 0.17	4.27	-0.07 ± 0.06	-0.15 ± 0.1	0.28	3.97	9.7	0.61
2M02453287-0005044	5963 ± 122	4.31 ± 0.17	4.22	-0.21 ± 0.05	-0.27 ± 0.1	0.2	5.33	7.28	0.47
2M02453607-0107521	5654 ± 114	4.01 ± 0.12	4.00	0.04 ± 0.05	-0.01 ± 0.1	0.78	3.81	9.98	0.69
2M02454862+0023161	5881 ± 124	4.21 ± 0.16	4.14	0.05 ± 0.05	-0.01 ± 0.1	0.56	4.65	11.11	1.81
2M02455690+0047488	5977 ± 152	4.37 ± 0.21	4.28	-0.13 ± 0.06	-0.2 ± 0.1	0.32	5.32	8.31	1.52
2M02460659-0050059	5515 ± 100	4.34 ± 0.11	4.37	-0.04 ± 0.04	-0.06 ± 0.1	0.87	3.43	9.61	1.52
2M02462882-1231002	5797 ± 110	4.21 ± 0.12	4.16	0.19 ± 0.05	0.14 ± 0.1	0.81	4.11	10.08	1.57
2M02464821+0920460	5923 ± 120	4.33 ± 0.16	4.25	0.04 ± 0.05	-0.03 ± 0.1	0.56	4.85	9.39	1.46
2M02472690-0012224	5163 ± 79	3.92 ± 0.11	4.03	-0.16 ± 0.04	-0.29 ± 0.1	0.85	3.36	14.98	1.81

APOGEE_ID	$T_{\rm eff} \pm \Delta T_{\rm eff}$	$\log g \pm \Delta \log g$	$\log g_{cor}$	$[\rm M/H] \pm \Delta[\rm M/H]$	$[Fe/H] \pm \Delta[\rm Fe/H]$	$\rm v_{mic}$	$\rm v_{mac}$	$v \sin i$	χ^2
2M02472849+0047375	5637 ± 129	4.39 ± 0.2	4.38	-0.14 ± 0.06	-0.19 ± 0.1	0.72	3.86	9.65	1.51
2M02473828-1316279	6099 ± 136	4.16 ± 0.18	4.04	-0.17 ± 0.06	-0.24 ± 0.1	0.36	6.13	7.86	0.38
2M02475488+0709573	6397 ± 148	4.5 ± 0.18	4.26	-0.32 ± 0.05	-0.35 ± 0.1	0	8.46	4.63	1.36
2M02480102+0733465	5739 ± 98	4.28 ± 0.11	4.25	0.17 ± 0.04	0.13 ± 0.1	0.92	3.89	9.64	1.61
2M02480665-0113123	6197 ± 140	4.32 ± 0.2	4.16	-0.08 ± 0.06	-0.17 ± 0.1	0	6.66	8.61	0.45
2M02483066-1315327	5562 ± 103	4.23 ± 0.11	4.24	0.08 ± 0.04	0.06 ± 0.1	1.02	3.44	9.58	0.64
2M02485316+0835418	5927 ± 68	4.35 ± 0.09	4.27	0.22 ± 0.03	0.17 ± 0.1	0.74	4.66	10.56	0.47
2M02485419-0006060	6096 ± 167	4.29 ± 0.25	4.17	-0.11 ± 0.07	-0.17 ± 0.1	0.35	6.01	7.71	1.58
2M02491482-0054028	5791 ± 135	4.36 ± 0.18	4.32	-0.07 ± 0.06	-0.13 ± 0.1	0.14	4.35	9.25	0.64
2M02491624+0007418	5841 ± 134	4.14 ± 0.15	4.08	0.03 ± 0.05	-0.03 ± 0.1	0.71	4.5	9	1.61
2M02491910-1307325	5848 ± 127	4.31 ± 0.19	4.25	-0.08 ± 0.05	-0.14 ± 0.1	0.44	4.62	8.97	0.4
2M02495122-1219490	5875 ± 119	4.32 ± 0.17	4.25	0.07 ± 0.05	0 ± 0.1	0.82	4.58	9.95	1.48
2M02500268-0044265	5887 ± 141	4.26 ± 0.21	4.19	-0.13 ± 0.06	-0.19 ± 0.1	0.43	4.87	8.37	1.47
2M02500502-1744546	5889 ± 107	4.37 ± 0.16	4.30	0.09 ± 0.04	0.05 ± 0.1	0.69	4.62	9.49	1.49
2M02502053-0014024	5656 ± 92	4.31 ± 0.14	4.30	-0.07 ± 0.04	-0.1 ± 0.1	0.68	3.86	8.35	0.48
2M02502428-1755330	5707 ± 119	4.1 ± 0.12	4.08	0.1 ± 0.05	0.05 ± 0.1	0.79	3.89	10.18	1.66
2M02502654-0033240	5803 ± 128	4.17 ± 0.14	4.12	0.08 ± 0.05	0.04 ± 0.1	0.85	4.27	10.84	0.74
2M02511334-1623153	5909 ± 105	4.32 ± 0.15	4.25	0.05 ± 0.04	-0.01 ± 0.1	0.53	4.78	10.86	1.39
2M02514305-1625514	5696 ± 115	4.05 ± 0.11	4.03	0.01 ± 0.05	-0.05 ± 0.1	0.77	3.97	10.97	0.5
2M02530549-1817264	5878 ± 128	4.3 ± 0.18	4.23	-0.02 ± 0.05	-0.09 ± 0.1	0.68	4.7	9.99	1.43

APOGEE_ID	$T_{\mathrm{eff}} \pm \Delta T_{\mathrm{eff}}$	$\log g \pm \Delta \log g$	$\log g_{cor}$	$[\mathrm{M/H}] \pm \Delta[\mathrm{M/H}]$	$[Fe/H] \pm \Delta[\mathrm{Fe/H}]$	$\mathrm{v}_{\mathrm{mic}}$	$\mathrm{v}_{\mathrm{mac}}$	$v \sin i$	χ^2
2M02531288-1647433	6301 ± 148	4.39 ± 0.2	4.19	0.16 ± 0.06	0.1 ± 0.1	0.65	7.17	9.76	0.59
2M02543250-1647297	5628 ± 61	4 ± 0.06	4.00	0.09 ± 0.03	0.04 ± 0.1	0.79	3.68	10.37	1.46
2M02570954-1637175	5713 ± 71	4.05 ± 0.07	4.03	0.03 ± 0.03	-0.02 ± 0.1	0.81	4.01	10.8	0.4
2M03082560+2619532	5835 ± 854	3.11 ± 0.96	3.11	-0.32 ± 0.46	-1.27 ± 0.1	0	4.15	27.32	2.97
2M03111311+0050126	5996 ± 148	4.25 ± 0.16	4.15	-0.02 ± 0.06	-0.1 ± 0.1	0.54	5.33	9.01	0.56
2M03130323+0003140	5717 ± 110	4.35 ± 0.15	4.32	-0.09 ± 0.05	-0.14 ± 0.1	0.73	4.09	9.33	1.96
2M03132446-0109066	5757 ± 96	4.36 ± 0.12	4.32	-0.1 ± 0.04	-0.16 ± 0.1	0.52	4.25	10.24	0.35
2M03134598-0103344	5710 ± 124	4.19 ± 0.13	4.17	-0.01 ± 0.05	-0.07 ± 0.1	0.75	4	8.27	1.78
2M03140549-0049230	5783 ± 114	4.12 ± 0.11	4.08	0.11 ± 0.05	0.07 ± 0.1	0.84	4.17	9.76	0.6
2M03141412+0015026	6112 ± 139	4.45 ± 0.17	4.33	0.14 ± 0.05	0.07 ± 0.1	0.56	5.83	11.2	1.54
2M03141726-0047019	5798 ± 104	4.23 ± 0.12	4.18	0.04 ± 0.04	-0.01 ± 0.1	0.6	4.28	9.64	1.51
2M03143222-0034353	5717 ± 126	4.27 ± 0.15	4.24	-0.15 ± 0.05	-0.21 ± 0.1	0.57	4.16	8.39	0.41
2M03144832+0048520	5606 ± 80	4.29 ± 0.1	4.29	-0.03 ± 0.03	-0.06 ± 0.1	0.95	3.67	9.63	0.43
2M03145001-0017172	5823 ± 123	4.3 ± 0.17	4.25	-0.09 ± 0.05	-0.14 ± 0.1	0.41	4.52	8.88	0.52
2M03153308-0058542	5953 ± 135	4.3 ± 0.17	4.22	0.01 ± 0.05	-0.04 ± 0.1	0.66	5.05	10.4	1.48
2M03165529+0021098	5844 ± 94	4.18 ± 0.11	4.12	0.03 ± 0.04	-0.04 ± 0.1	0.63	4.51	9.44	1.51
2M03172378+0032558	5747 ± 171	4.22 ± 0.19	4.19	-0.33 ± 0.07	-0.45 ± 0.1	0	4.47	8.65	1.53
2M03172515+0057028	6005 ± 151	4.27 ± 0.18	4.17	-0.18 ± 0.06	-0.27 ± 0.1	0.34	5.54	7.64	0.66
2M03174655-0127526	5789 ± 138	4.34 ± 0.16	4.30	-0.01 ± 0.06	-0.05 ± 0.1	0.71	4.28	10.05	1.85
2M03182714+1510386	5319 ± 171	3.88 ± 0.24	3.96	-0.04 ± 0.08	-0.1 ± 0.1	0.87	3.28	9.64	1.95

APOGEE_ID	$T_{\rm eff} \pm \Delta T_{\rm eff}$	$\log g \pm \Delta \log g$	$\log g_{cor}$	$[\mathrm{M/H}] \pm \Delta[\mathrm{M/H}]$	$[Fe/H] \pm \Delta[\mathrm{Fe/H}]$	v$_{\rm mic}$	v$_{\rm mac}$	$v \sin i$	χ^2
2M03184804-0028257	6078 ± 117	4.35 ± 0.16	4.23	0.02 ± 0.05	-0.05 ± 0.1	0.56	5.76	9.09	0.37
2M03185702+0218151	5970 ± 84	4.31 ± 0.11	4.22	-0.3 ± 0.03	-0.42 ± 0.1	0.05	5.46	8.13	1.34
2M03194782+0040572	5721 ± 84	4.18 ± 0.09	4.15	0.15 ± 0.04	0.1 ± 0.1	0.76	3.87	10	1.7
2M03195804-0120445	5585 ± 102	4.3 ± 0.13	4.31	-0.01 ± 0.04	-0.04 ± 0.1	0.83	3.59	9.67	1.66
2M03200143-0118126	6207 ± 171	4.33 ± 0.22	4.17	0.03 ± 0.06	-0.05 ± 0.1	0.25	6.62	8.15	0.72
2M03212362-0102477	5737 ± 135	4 ± 0.13	3.97	-0.13 ± 0.06	-0.19 ± 0.1	0.72	4.29	9.16	1.72
2M03212572+0129496	5985 ± 93	4.33 ± 0.12	4.24	-0.14 ± 0.04	-0.2 ± 0.1	0.09	5.38	9.1	1.35
2M03214465+0056213	5883 ± 121	4.27 ± 0.17	4.20	-0.03 ± 0.05	-0.1 ± 0.1	0.57	4.74	9.07	1.41
2M03225192+0110428	5876 ± 128	4.28 ± 0.19	4.21	-0.05 ± 0.05	-0.12 ± 0.1	0.48	4.72	8.55	1.66
2M03230649-0028021	5763 ± 83	4.31 ± 0.1	4.27	-0.06 ± 0.04	-0.1 ± 0.1	0.61	4.24	9.75	1.37
2M03230724-0118202	5904 ± 134	4.44 ± 0.17	4.37	0.02 ± 0.05	-0.02 ± 0.1	0.6	4.77	10.88	1.6
2M03234100-0051137	5995 ± 143	4.13 ± 0.15	4.03	-0.04 ± 0.06	-0.11 ± 0.1	0.52	5.37	8.91	1.6
2M03234557-0027448	6037 ± 117	4.38 ± 0.15	4.27	0.05 ± 0.05	-0.01 ± 0.1	0.66	5.47	8.77	0.55
2M03241515+0014407	5721 ± 52	4.12 ± 0.05	4.09	0.21 ± 0.02	0.15 ± 0.1	0.77	3.81	10.28	0.56
2M03244720+0030272	5638 ± 113	4.21 ± 0.14	4.20	0.09 ± 0.05	0.06 ± 0.1	0.91	3.65	10.2	1.78
2M03245441-0108530	5689 ± 121	4.39 ± 0.16	4.37	-0.01 ± 0.05	-0.05 ± 0.1	0.69	3.89	10.7	0.62
2M03250645-0026477	5623 ± 114	4.36 ± 0.17	4.36	-0.05 ± 0.05	-0.08 ± 0.1	0.93	3.72	8.49	1.6
2M03252653+0014128	5991 ± 139	4.32 ± 0.17	4.23	-0.04 ± 0.06	-0.12 ± 0.1	0.58	5.31	8.83	1.49
2M03252937+3141361	6062 ± 115	4.45 ± 0.12	4.34	0.07 ± 0.04	0.01 ± 0.1	0.53	5.59	9.59	1.43
2M03253362-0027424	5884 ± 98	4.11 ± 0.12	4.04	0.16 ± 0.04	0.11 ± 0.1	0.87	4.56	10.36	1.5

APOGEE_ID	$T_{\rm eff} \pm \Delta T_{\rm eff}$	$\log g \pm \Delta \log g$	$\log g_{cor}$	$[\mathrm{M/H}] \pm \Delta[\mathrm{M/H}]$	$[Fe/H] \pm \Delta[\mathrm{Fe/H}]$	$\mathrm{v}_{\rm mic}$	$\mathrm{v}_{\rm mac}$	$v \sin i$	χ^2
2M03253386-0047521	5965 ± 130	4.32 ± 0.18	4.23	-0.2 ± 0.05	-0.27 ± 0.1	0.48	5.33	8.03	1.38
2M03255186+0028462	5963 ± 154	4.16 ± 0.19	4.07	-0.18 ± 0.06	-0.26 ± 0.1	0.44	5.33	7.98	0.52
2M03255750+0107120	5860 ± 127	4.33 ± 0.17	4.27	0.1 ± 0.05	0.05 ± 0.1	0.68	4.47	10.54	1.5
2M03260197+0038089	5944 ± 160	4.32 ± 0.2	4.24	-0.01 ± 0.06	-0.08 ± 0.1	0.53	5.02	8.61	1.53
2M03260336+1858054	5676 ± 93	4.01 ± 0.09	4.00	0.07 ± 0.04	0.03 ± 0.1	0.77	3.85	9.79	0.53
2M03261887-0114158	5954 ± 77	4.23 ± 0.09	4.14	0.16 ± 0.03	0.1 ± 0.1	0.77	4.9	10.05	1.38
2M03264103-0009327	6085 ± 139	4.26 ± 0.2	4.14	-0.07 ± 0.06	-0.14 ± 0.1	0.41	5.91	9.16	1.64
2M03265275+0014019	5724 ± 143	4.38 ± 0.17	4.35	-0.04 ± 0.06	-0.09 ± 0.1	0.63	4.05	8.87	1.78
2M03270675+0028142	5928 ± 115	4.22 ± 0.16	4.14	-0.28 ± 0.05	-0.37 ± 0.1	0	5.23	7.97	0.45
2M03271176-0008243	6106 ± 155	4.42 ± 0.21	4.30	0 ± 0.06	-0.07 ± 0.1	0.42	5.95	9.56	1.48
2M03272186+0010178	5645 ± 105	4.29 ± 0.15	4.28	-0.02 ± 0.04	-0.06 ± 0.1	0.86	3.77	8.15	1.49
2M03274860+0018502	6018 ± 162	4.29 ± 0.18	4.19	-0.01 ± 0.06	-0.09 ± 0.1	0.51	5.43	9.34	1.59
2M03281682-0052418	6177 ± 128	4.26 ± 0.19	4.11	-0.18 ± 0.05	-0.26 ± 0.1	0.14	6.63	7.86	1.4
2M03282363+0052026	5946 ± 121	4.36 ± 0.16	4.28	0.03 ± 0.05	-0.02 ± 0.1	0.64	4.98	10.6	1.56
2M03284730+0006203	6197 ± 147	4.35 ± 0.2	4.19	0.07 ± 0.06	-0.02 ± 0.1	0.52	6.5	9.28	1.44
2M03284836-0040306	5627 ± 96	4.29 ± 0.13	4.29	-0.01 ± 0.04	-0.05 ± 0.1	0.76	3.7	9.97	1.47
2M03290514+0006356	6221 ± 138	4.42 ± 0.18	4.25	-0.1 ± 0.05	-0.18 ± 0.1	0.17	6.85	7.84	1.39
2M03291316-0029073	5890 ± 110	4.18 ± 0.14	4.11	0.08 ± 0.05	0.04 ± 0.1	0.68	4.67	9.99	0.55
2M03292309+0025353	6007 ± 137	4.28 ± 0.16	4.18	-0.16 ± 0.05	-0.26 ± 0.1	0	5.54	9.22	1.42
2M03292693-0103478	5759 ± 160	4.14 ± 0.17	4.10	-0.31 ± 0.07	-0.41 ± 0.1	0.48	4.51	9.12	1.56

APOGEE_ID	$T_{\mathrm{eff}} \pm \Delta T_{\mathrm{eff}}$	$\log g \pm \Delta \log g$	$\log g_{cor}$	$[\mathrm{M/H}] \pm \Delta[\mathrm{M/H}]$	$[Fe/H] \pm \Delta[\mathrm{Fe/H}]$	$\mathrm{v}_{\mathrm{mic}}$	$\mathrm{v}_{\mathrm{mac}}$	$v \sin i$	χ^2
2M03300488+0049474	5610 ± 113	4.21 ± 0.13	4.21	0.03 ± 0.05	-0.04 ± 0.1	0.57	3.62	9.61	0.7
2M03303726+0028448	5643 ± 121	4.09 ± 0.15	4.08	-0.18 ± 0.05	-0.28 ± 0.1	0.46	3.99	8.76	1.61
2M03305922-0026314	5936 ± 87	4.26 ± 0.11	4.18	0.1 ± 0.04	0.06 ± 0.1	0.7	4.86	9.34	1.57
2M03310551+0014551	5955 ± 146	4.41 ± 0.18	4.32	0.01 ± 0.06	-0.05 ± 0.1	0.5	5.04	9.7	1.96
2M03311177+0111498	5793 ± 89	4.3 ± 0.1	4.26	0.19 ± 0.04	0.13 ± 0.1	0.65	4.08	10.65	1.73
2M03312138+0024447	5804 ± 88	4.22 ± 0.1	4.17	0.19 ± 0.04	0.14 ± 0.1	0.77	4.13	10.48	1.61
2M03315971+0104319	6234 ± 160	4.39 ± 0.22	4.22	-0.09 ± 0.06	-0.17 ± 0.1	0.18	6.93	6.92	1.62
2M03330398+3034291	5888 ± 101	4.34 ± 0.15	4.27	0.04 ± 0.04	-0.02 ± 0.1	0.72	4.68	9.12	1.35
2M03334649-0015193	5758 ± 132	4.28 ± 0.14	4.24	-0.03 ± 0.05	-0.08 ± 0.1	0.42	4.19	8.38	0.61
2M03334860+0118452	5682 ± 118	4.23 ± 0.15	4.21	-0.13 ± 0.05	-0.22 ± 0.1	0.59	4.03	9.2	1.5
2M03343054-0016558	5651 ± 103	4.34 ± 0.15	4.33	-0.04 ± 0.05	-0.06 ± 0.1	0.59	3.8	9.93	1.45
2M03343356-0054540	5502 ± 117	4.3 ± 0.12	4.33	-0.01 ± 0.05	-0.04 ± 0.1	0.75	3.38	9.65	1.78
2M03350490-0115494	5740 ± 99	4.18 ± 0.1	4.15	-0.02 ± 0.04	-0.08 ± 0.1	0.6	4.13	9.38	1.35
2M03350858+0041306	5914 ± 145	4.31 ± 0.2	4.24	0.06 ± 0.06	-0.01 ± 0.1	0.32	4.79	9.57	0.72
2M03370769+0019443	5859 ± 113	4.31 ± 0.15	4.25	0.03 ± 0.05	-0.03 ± 0.1	0.57	4.55	9.38	0.44
2M03373544+0105205	5965 ± 165	4.26 ± 0.21	4.17	-0.19 ± 0.07	-0.28 ± 0.1	0	5.34	8.1	0.51
2M03374591-0029374	5830 ± 131	4.17 ± 0.15	4.12	0.03 ± 0.05	-0.02 ± 0.1	0.62	4.45	9.95	1.53
2M03381369-0056290	5531 ± 112	4.34 ± 0.14	4.36	-0.06 ± 0.05	-0.1 ± 0.1	0.73	3.5	9.94	0.69
2M03385479+3214536	5675 ± 94	4.3 ± 0.12	4.29	0.01 ± 0.04	-0.02 ± 0.1	1.34	3.83	9.37	0.51
2M03390295+3213314	6093 ± 126	4.34 ± 0.18	4.22	0.03 ± 0.05	-0.02 ± 0.1	0.57	5.84	10.32	0.35

APOGEE_ID	$T_{\rm eff} \pm \Delta T_{\rm eff}$	$\log g \pm \Delta \log g$	$\log g_{cor}$	$[{\rm M/H}] \pm \Delta[{\rm M/H}]$	$[Fe/H] \pm \Delta[{\rm Fe/H}]$	$v_{\rm mic}$	$v_{\rm mac}$	$v \sin i$	χ^2
2M03390941+0032512	5943 ± 117	4.4 ± 0.16	4.32	0.03 ± 0.05	-0.02 ± 0.1	0.45	4.96	11.15	0.45
2M03391301+0109317	5886 ± 158	4.39 ± 0.26	4.32	-0.16 ± 0.07	-0.24 ± 0.1	0.08	4.88	9.38	1.61
2M03391704+1353296	4992 ± 109	3.45 ± 0.13	3.45	-0.01 ± 0.06	-0.08 ± 0.1	1.04	3.59	9.96	1.9
2M03391750+0007118	5688 ± 134	4.3 ± 0.16	4.28	0.02 ± 0.06	-0.04 ± 0.1	0.65	3.87	10.26	1.64
2M03391875+0010507	5775 ± 121	4.24 ± 0.14	4.20	-0.09 ± 0.05	-0.17 ± 0.1	0.45	4.33	8.59	0.58
2M03391964+8059444	5670 ± 64	4.36 ± 0.1	4.35	-0.13 ± 0.03	-0.19 ± 0.1	0.67	3.96	9.27	1.24
2M03393055+3203082	5992 ± 147	4.24 ± 0.18	4.15	-0.21 ± 0.06	-0.28 ± 0.1	0.26	5.51	6.82	1.29
2M03393933+0021056	5555 ± 148	4.3 ± 0.19	4.32	-0.23 ± 0.06	-0.3 ± 0.1	0.49	3.74	9.05	0.62
2M03403175+3301217	5738 ± 90	4.21 ± 0.09	4.18	0.06 ± 0.04	0.01 ± 0.1	0.79	4.02	9.25	0.44
2M03405694+0019109	5920 ± 135	4.02 ± 0.16	3.94	-0.17 ± 0.06	-0.25 ± 0.1	0.56	5.14	8.67	1.42
2M03411234-0101340	5673 ± 114	4.24 ± 0.14	4.23	-0.03 ± 0.05	-0.07 ± 0.1	0.64	3.88	9.79	1.64
2M03412934+0028082	5697 ± 131	4.28 ± 0.16	4.26	-0.02 ± 0.05	-0.07 ± 0.1	0.79	3.95	9.4	0.54
2M03414201+3047117	5815 ± 95	4.28 ± 0.11	4.23	0.04 ± 0.04	-0.01 ± 0.1	0.7	4.34	10.41	0.37
2M03415103+3248270	5987 ± 100	4.36 ± 0.12	4.27	-0.04 ± 0.04	-0.11 ± 0.1	0.51	5.28	8.73	1.27
2M03415186+0024248	5785 ± 138	4.29 ± 0.16	4.25	0.02 ± 0.06	-0.04 ± 0.1	0.68	4.24	9.75	1.69
2M03415806+3223130	6006 ± 51	4.4 ± 0.06	4.30	0.08 ± 0.02	0.04 ± 0.1	0.63	5.24	9.35	0.33
2M03422301+3224367	6014 ± 55	4.38 ± 0.07	4.28	0.15 ± 0.02	0.09 ± 0.1	0.6	5.21	10.75	1.38
2M03423921+0028076	6205 ± 174	4.35 ± 0.25	4.19	-0.06 ± 0.07	-0.16 ± 0.1	0	6.7	8.32	0.61
2M03425169+0006456	5736 ± 107	4.08 ± 0.1	4.05	0.17 ± 0.05	0.11 ± 0.1	0.94	3.92	8.8	2.03
2M03431503+3137308	5893 ± 101	4.38 ± 0.17	4.31	-0.13 ± 0.04	-0.21 ± 0.1	0.57	4.88	8.14	1.41

APOGEE_ID	$T_{\rm eff} \pm \Delta T_{\rm eff}$	$\log g \pm \Delta \log g$	$\log g_{cor}$	$[\rm M/H] \pm \Delta[\rm M/H]$	$[Fe/H] \pm \Delta[\rm Fe/H]$	$\rm v_{mic}$	$\rm v_{mac}$	$v \sin i$	χ^2
2M03432662+2459395	4601 ± 48	4.31 ± 0.07	4.61	0.01 ± 0.02	-0.06 ± 0.1	0.96	3.79	9.61	1.83
2M03433078+0017188	5798 ± 120	4.4 ± 0.15	4.35	0.03 ± 0.05	-0.01 ± 0.1	0.61	4.27	10.4	1.47
2M03435418+3305013	5496 ± 97	4.28 ± 0.11	4.31	-0.33 ± 0.04	-0.43 ± 0.1	0.46	3.71	8.62	1.31
2M03440321-0047311	5974 ± 136	4.19 ± 0.17	4.10	-0.3 ± 0.05	-0.39 ± 0.1	0.26	5.51	8.29	1.42
2M03440484+2416318	5188 ± 96	4.28 ± 0.13	4.38	-0.02 ± 0.04	-0.08 ± 0.1	2.1	3.09	11.04	1.61
2M03441120+2322455	4981 ± 67	4.42 ± 0.08	4.59	0.21 ± 0.02	0.04 ± 0.1	1.57	3.36	13.25	1.84
2M03441365-0106332	5800 ± 129	4.07 ± 0.13	4.02	0.07 ± 0.05	0.02 ± 0.1	0.72	4.3	10.05	0.69
2M03442144-0939285	5775 ± 107	4.34 ± 0.13	4.30	-0.11 ± 0.04	-0.18 ± 0.1	0.56	4.33	8.95	1.28
2M03442594+0051548	5780 ± 114	4.16 ± 0.12	4.12	0.12 ± 0.05	0.06 ± 0.1	0.71	4.13	10.53	1.77
2M03443568+0045022	5921 ± 185	4.33 ± 0.3	4.25	-0.33 ± 0.07	-0.44 ± 0.1	0	5.23	7.63	1.48
2M03444075+2449067	6084 ± 137	4.34 ± 0.18	4.22	0.01 ± 0.05	-0.16 ± 0.1	1.07	5.81	18.21	1.27
2M03444552+3108454	5903 ± 89	4.26 ± 0.12	4.19	0.04 ± 0.04	-0.01 ± 0.1	0.74	4.76	8.84	1.34
2M03444993-0045264	5723 ± 60	4.18 ± 0.06	4.15	0.07 ± 0.03	0.02 ± 0.1	0.74	3.96	10.7	1.29
2M03450874+3258375	5524 ± 51	4.31 ± 0.06	4.33	0.03 ± 0.02	0.01 ± 0.1	1.19	3.38	11.01	1.53
2M03450953+3308400	6205 ± 90	4.29 ± 0.11	4.13	0.05 ± 0.03	-0.02 ± 0.1	0.49	6.59	8.48	1.38
2M03451232+3127222	5627 ± 77	4.15 ± 0.09	4.15	0 ± 0.03	-0.06 ± 0.1	0.9	3.72	9.73	0.47
2M03452957+2345379	4576 ± 51	4.41 ± 0.1	4.71	0.04 ± 0.02	-0.01 ± 0.1	1.42	3.81	7.74	2.2
2M03454262-1021519	5919 ± 115	4.19 ± 0.16	4.11	-0.14 ± 0.05	-0.22 ± 0.1	0.45	5.05	8.46	1.38
2M03454500-0050170	5772 ± 168	4.24 ± 0.2	4.20	-0.31 ± 0.07	-0.4 ± 0.1	0	4.54	7.42	0.76
2M03454900+3142080	5975 ± 88	4.33 ± 0.12	4.24	-0.09 ± 0.04	-0.17 ± 0.1	0.53	5.27	8.88	0.38

APOGEE_ID	$T_{\rm eff} \pm \Delta T_{\rm eff}$	$\log g \pm \Delta \log g$	$\log g_{cor}$	$[\mathrm{M/H}] \pm \Delta[\mathrm{M/H}]$	$[Fe/H] \pm \Delta[\mathrm{Fe/H}]$	$\mathrm{v}_{\rm mic}$	$\mathrm{v}_{\rm mac}$	$v \sin i$	χ^2
2M03455667+3212434	5851 ± 95	4.33 ± 0.14	4.27	-0.04 ± 0.04	-0.1 ± 0.1	0.72	4.59	9.56	0.36
2M03461268+2307428	5977 ± 56	4.34 ± 0.07	4.25	0.09 ± 0.02	0.05 ± 0.1	0.63	5.08	10.07	0.34
2M03462087-1108040	5993 ± 89	4.37 ± 0.12	4.28	-0.05 ± 0.04	-0.12 ± 0.1	0.49	5.32	8.7	1.35
2M03464499-0052508	5597 ± 84	4.29 ± 0.1	4.29	0.04 ± 0.04	0.01 ± 0.1	0.85	3.57	10.2	1.56
2M03465326+2252513	5204 ± 79	4.39 ± 0.1	4.49	-0.01 ± 0.03	-0.03 ± 0.1	1.77	3.06	10.68	0.65
2M03470204+4125397	4925 ± 218	4.21 ± 0.3	4.40	-0.91 ± 0.1	-0.99 ± 0.1	0	3.43	7.7	1.59
2M03470580+3134594	5736 ± 81	4.42 ± 0.1	4.39	-0.06 ± 0.03	-0.11 ± 0.1	0.67	4.12	10.31	1.42
2M03470879-1150359	6020 ± 122	4.36 ± 0.14	4.26	0 ± 0.05	-0.07 ± 0.1	0.47	5.43	9.17	1.39
2M03471420-0018375	6004 ± 141	4.41 ± 0.18	4.31	-0.08 ± 0.06	-0.14 ± 0.1	0.18	5.42	8.83	0.5
2M03472804+0003264	5719 ± 109	4.42 ± 0.13	4.39	-0.09 ± 0.05	-0.16 ± 0.1	0.66	4.09	8.8	1.45
2M03480118+3212120	6101 ± 131	4.39 ± 0.21	4.27	-0.2 ± 0.05	-0.29 ± 0.1	0	6.13	7.57	1.42
2M03481769+2502523	5455 ± 104	4.41 ± 0.12	4.45	0 ± 0.04	-0.09 ± 0.1	1.16	3.27	11.78	0.45
2M03482616+2402544	5926 ± 118	4.3 ± 0.17	4.22	-0.04 ± 0.05	-0.18 ± 0.1	0.74	4.96	14.93	0.23
2M03483175-0941238	5594 ± 118	4.16 ± 0.13	4.17	0.1 ± 0.05	0.06 ± 0.1	0.85	3.52	10.2	0.65
2M03483216+0021321	5669 ± 103	4.09 ± 0.11	4.08	0.04 ± 0.04	-0.01 ± 0.1	0.8	3.83	10.96	1.39
2M03484618+3132354	5889 ± 81	4.15 ± 0.12	4.08	-0.08 ± 0.03	-0.14 ± 0.1	0.61	4.85	8.78	1.4
2M03490907+0030510	5683 ± 128	4.33 ± 0.18	4.31	-0.07 ± 0.06	-0.14 ± 0.1	0.59	3.94	9.44	1.59
2M03491634+3202017	5527 ± 90	4.34 ± 0.12	4.36	-0.07 ± 0.04	-0.1 ± 0.1	1.14	3.5	9.01	0.52
2M03495035+2342202	5253 ± 90	4.44 ± 0.09	4.53	0.03 ± 0.04	0.01 ± 0.1	1.18	3.02	9.82	0.81
2M03495569-0550451	5841 ± 132	4.22 ± 0.16	4.16	0.01 ± 0.05	-0.03 ± 0.1	0.66	4.5	10.44	1.65

APOGEE_ID	$T_{\rm eff} \pm \Delta T_{\rm eff}$	$\log g \pm \Delta \log g$	$\log g_{cor}$	$[\mathrm{M/H}] \pm \Delta[\mathrm{M/H}]$	$[Fe/H] \pm \Delta[\mathrm{Fe/H}]$	$\mathrm{v_{mic}}$	$\mathrm{v_{mac}}$	$v \sin i$	χ^2
2M03500007-1034446	5860 ± 159	4.19 ± 0.23	4.13	-0.24 ± 0.07	-0.31 ± 0.1	0.37	4.87	8.24	0.51
2M03503213-1023054	5772 ± 92	4.1 ± 0.09	4.06	0.11 ± 0.04	0.06 ± 0.1	0.76	4.13	10.57	1.44
2M03511747-0620512	5716 ± 97	4.25 ± 0.11	4.22	0.03 ± 0.04	-0.02 ± 0.1	0.63	3.97	9.35	1.53
2M03512825-0918001	5894 ± 164	4.36 ± 0.28	4.29	-0.32 ± 0.07	-0.42 ± 0.1	0	5.08	8.17	1.37
2M03513344-1121094	5852 ± 77	4.33 ± 0.1	4.27	0.19 ± 0.03	0.15 ± 0.1	0.65	4.33	9.94	1.48
2M03514257-0502326	5582 ± 86	4.23 ± 0.1	4.24	0.03 ± 0.04	-0.01 ± 0.1	0.81	3.55	10.24	0.52
2M03514779-0652379	5683 ± 126	4.2 ± 0.15	4.18	-0.01 ± 0.05	-0.07 ± 0.1	0.63	3.9	10.69	0.63
2M03523664-0707180	5504 ± 122	4.38 ± 0.14	4.41	-0.05 ± 0.05	-0.07 ± 0.1	1.06	3.42	9.89	1.94
2M03523882-0601008	5648 ± 115	4.29 ± 0.15	4.28	0.03 ± 0.05	-0.01 ± 0.1	0.88	3.73	9.91	1.84
2M03532117-1126264	5542 ± 98	4.26 ± 0.1	4.28	0.03 ± 0.04	0 ± 0.1	0.95	3.44	9.62	1.41
2M03535403-0556274	5949 ± 135	4.26 ± 0.16	4.18	0.04 ± 0.05	-0.02 ± 0.1	0.61	5	9.29	2.14
2M03540920-0718503	6131 ± 148	4.36 ± 0.22	4.23	0.01 ± 0.06	-0.06 ± 0.1	0.58	6.11	10.09	1.45
2M03542337-0706045	5728 ± 84	4.62 ± 0.08	4.59	0.41 ± 0.03	0.34 ± 0.1	0.54	3.53	8.05	2.3
2M03545339-0523023	5799 ± 99	4.29 ± 0.12	4.24	0.1 ± 0.04	0.05 ± 0.1	0.71	4.21	10.24	0.5
2M03550047-0512379	5765 ± 124	4.34 ± 0.15	4.30	-0.2 ± 0.05	-0.31 ± 0.1	0.22	4.39	8.66	1.48
2M03550422-0706579	5985 ± 119	4.29 ± 0.15	4.20	-0.16 ± 0.05	-0.24 ± 0.1	0.42	5.4	8.49	0.45
2M03551612-1008023	5883 ± 97	4.22 ± 0.13	4.15	0.08 ± 0.04	0.03 ± 0.1	0.73	4.63	8.99	1.42
2M03553707+5213367	5901 ± 113	3.8 ± 0.23	3.73	-0.38 ± 0.04	-0.42 ± 0.1	0.26	5.35	6.36	1
2M03554691-0625257	5765 ± 127	4.08 ± 0.12	4.04	0 ± 0.05	-0.07 ± 0.1	0.76	4.23	8.85	0.64
2M03570643-0712498	5736 ± 104	4.27 ± 0.11	4.24	0.11 ± 0.04	0.06 ± 0.1	0.72	3.95	10.03	0.91

APOGEE_ID	$T_{\rm eff} \pm \Delta T_{\rm eff}$	$\log g \pm \Delta \log g$	$\log g_{cor}$	$[\mathrm{M/H}] \pm \Delta[\mathrm{M/H}]$	$[Fe/H] \pm \Delta[\mathrm{Fe/H}]$	$\mathrm{v}_{\rm mic}$	$\mathrm{v}_{\rm mac}$	$v \sin i$	χ^2
2M03572910-0537336	5774 ± 110	4.22 ± 0.12	4.18	0.06 ± 0.05	0.01 ± 0.1	0.77	4.17	10.84	1.56
2M03573438+1017420	5728 ± 75	4.27 ± 0.08	4.24	0.07 ± 0.03	0.02 ± 0.1	0.74	3.96	10.18	1.37
2M03574110-0512106	5788 ± 122	4.16 ± 0.13	4.12	0.11 ± 0.05	0.07 ± 0.1	0.86	4.18	10.45	0.74
2M03580832-0502576	5747 ± 112	4.02 ± 0.1	3.99	-0.02 ± 0.05	-0.08 ± 0.1	0.76	4.2	8.38	0.48
2M03581483+2537118	5827 ± 130	4.11 ± 0.14	4.06	-0.02 ± 0.05	-0.07 ± 0.1	0.69	4.51	10.97	1.77
2M03592345+1056260	5949 ± 148	4.13 ± 0.18	4.05	-0.08 ± 0.06	-0.16 ± 0.1	0.39	5.17	8.58	1.44
2M04001887+1104089	5899 ± 119	4.33 ± 0.17	4.26	0.06 ± 0.05	0.01 ± 0.1	0.78	4.71	8.87	1.42
2M04002744+2529204	5716 ± 122	4.28 ± 0.14	4.25	0 ± 0.05	-0.05 ± 0.1	0.71	3.99	10.77	1.51
2M04012896-0553006	6138 ± 132	4.31 ± 0.19	4.18	0.01 ± 0.05	-0.05 ± 0.1	0.47	6.16	9.97	0.57
2M04013342+0957423	5789 ± 121	4.35 ± 0.16	4.31	-0.1 ± 0.05	-0.14 ± 0.1	0.59	4.38	8.72	0.36
2M04014226+1124335	5506 ± 69	4.2 ± 0.07	4.23	0.13 ± 0.03	0.1 ± 0.1	0.95	3.26	10.07	1.72
2M04014487-0552031	6122 ± 140	4.3 ± 0.2	4.17	0.1 ± 0.06	0.05 ± 0.1	0.65	5.96	9.46	1.76
2M04015643-0546408	6081 ± 144	4.32 ± 0.19	4.20	0.01 ± 0.06	-0.02 ± 0.1	0.52	5.79	9.99	1.65
2M04024932+1117083	6016 ± 122	4.36 ± 0.15	4.26	0.11 ± 0.05	0.06 ± 0.1	0.55	5.28	10.35	1.46
2M04030616+1224527	5766 ± 88	4.44 ± 0.09	4.40	-0.01 ± 0.04	-0.06 ± 0.1	0.67	4.18	9.66	0.39
2M04034249+0959087	5869 ± 101	4.11 ± 0.12	4.05	0.24 ± 0.04	0.2 ± 0.1	0.86	4.4	9.84	1.58
2M04040155+1120167	5679 ± 88	4.2 ± 0.1	4.18	0.06 ± 0.04	0 ± 0.1	0.71	3.82	10.6	1.5
2M04042029-0439185	5192 ± 67	4.4 ± 0.09	4.50	-0.34 ± 0.03	-0.4 ± 0.1	0.49	3.41	8.01	1.38
2M04045470-0413016	5985 ± 158	4.4 ± 0.18	4.31	0.07 ± 0.06	-0.03 ± 0.1	0.09	5.14	9.11	2.47
2M04051346-0529478	5744 ± 146	4.25 ± 0.17	4.22	-0.06 ± 0.06	-0.13 ± 0.1	0.86	4.17	8.94	2.58

APOGEE_ID	$T_{\rm eff} \pm \Delta T_{\rm eff}$	$\log g \pm \Delta \log g$	$\log g_{cor}$	$[\rm M/H] \pm \Delta[\rm M/H]$	$[Fe/H] \pm \Delta[\rm Fe/H]$	v$_{\rm mic}$	v$_{\rm mac}$	$v \sin i$	χ^2
2M04052655-0645193	5553 ± 108	4.37 ± 0.13	4.39	-0.03 ± 0.05	-0.06 ± 0.1	0.88	3.51	9	1.99
2M04052834+1011369	6005 ± 153	4.38 ± 0.19	4.28	-0.02 ± 0.06	-0.09 ± 0.1	0.44	5.37	8.8	1.48
2M04055482-0417478	5849 ± 93	4.17 ± 0.11	4.11	0.15 ± 0.04	0.11 ± 0.1	0.91	4.39	10.27	1.52
2M04055772-0457481	5924 ± 156	4.26 ± 0.23	4.18	-0.14 ± 0.07	-0.21 ± 0.1	0.51	5.06	7.75	2.5
2M04055820-0501233	5928 ± 117	4.28 ± 0.16	4.20	-0.02 ± 0.05	-0.08 ± 0.1	0.58	4.95	10.74	0.65
2M04060562-0627351	5596 ± 122	4.31 ± 0.15	4.32	-0.02 ± 0.05	-0.06 ± 0.1	0.85	3.62	10.16	1.46
2M04062986-0612526	5928 ± 106	4.41 ± 0.16	4.33	-0.09 ± 0.04	-0.14 ± 0.1	0.44	5.01	9.21	0.69
2M04063006-0621367	5918 ± 103	4.26 ± 0.14	4.18	0.08 ± 0.04	0.02 ± 0.1	0.73	4.79	10.02	1.48
2M04064907+1041457	6009 ± 124	4.29 ± 0.14	4.19	0.12 ± 0.05	0.08 ± 0.1	0.76	5.23	9.61	0.39
2M04065802-0518334	5956 ± 139	4.35 ± 0.18	4.26	0.11 ± 0.06	0.06 ± 0.1	0.69	4.95	8.77	2.09
2M04074859-0622492	5984 ± 124	4.43 ± 0.13	4.34	0.06 ± 0.05	0.02 ± 0.1	0.61	5.14	9.9	1.63
2M04082636-0524004	6063 ± 157	4.37 ± 0.23	4.26	-0.16 ± 0.06	-0.24 ± 0.1	0	5.86	9.09	1.75
2M04083495-0531582	5702 ± 125	4.37 ± 0.17	4.35	-0.23 ± 0.05	-0.33 ± 0.1	0.35	4.18	8.37	1.59
2M04084767-0439210	6082 ± 91	4.38 ± 0.13	4.26	0.08 ± 0.04	0.01 ± 0.1	0.55	5.71	9.02	1.4
2M04085142-0644423	5730 ± 107	4.37 ± 0.13	4.34	-0.17 ± 0.05	-0.22 ± 0.1	0.58	4.22	8.48	1.47
2M04085465-0542006	5900 ± 144	4.3 ± 0.24	4.23	-0.24 ± 0.06	-0.3 ± 0.1	0.16	5.04	7.45	1.53
2M04090472-0508586	6062 ± 189	4.24 ± 0.22	4.13	-0.01 ± 0.08	-0.08 ± 0.1	0.44	5.71	9.28	1.32
2M04090611-0650049	6019 ± 103	4.35 ± 0.12	4.25	0.02 ± 0.04	-0.04 ± 0.1	0.58	5.4	9.77	1.47
2M04091940-0459524	5951 ± 172	4.22 ± 0.23	4.14	-0.27 ± 0.07	-0.37 ± 0.1	0.01	5.35	8.4	1.82
2M04092032-0606516	5619 ± 105	4.26 ± 0.13	4.26	0.06 ± 0.05	0.02 ± 0.1	0.82	3.61	9.52	0.72

APOGEE_ID	$T_{\text{eff}} \pm \Delta T_{\text{eff}}$	$\log g \pm \Delta \log g$	$\log g_{cor}$	$[\text{M/H}] \pm \Delta[\text{M/H}]$	$[Fe/H] \pm \Delta[\text{Fe/H}]$	v_{mic}	v_{mac}	$v \sin i$	χ^2
2M04100978+2412547	5958 ± 130	4.13 ± 0.14	4.04	0.05 ± 0.05	-0.02 ± 0.1	0.77	5.07	9.77	1.5
2M04103631+2240013	5635 ± 97	4.32 ± 0.14	4.32	0.45 ± 0.04	0.37 ± 0.1	0.77	3.17	8.86	1.65
2M04103658-0438452	5909 ± 127	4.13 ± 0.17	4.06	-0.09 ± 0.05	-0.18 ± 0.1	0.62	4.97	8.46	0.62
2M04104481+2335500	5620 ± 117	4.11 ± 0.13	4.11	0 ± 0.05	-0.08 ± 0.1	0.17	3.72	8.61	2.06
2M04104911+2248235	5963 ± 166	4.35 ± 0.23	4.26	-0.16 ± 0.07	-0.25 ± 0.1	0.4	5.28	8.69	0.6
2M04105673+2351004	5740 ± 123	3.97 ± 0.11	3.94	-0.01 ± 0.05	-0.07 ± 0.1	0.7	4.18	8.65	0.54
2M04111263-0436419	5950 ± 116	4.24 ± 0.14	4.16	0.07 ± 0.05	0 ± 0.1	0.69	4.97	10.19	1.52
2M04111400+2358124	5777 ± 117	4.22 ± 0.12	4.18	0.12 ± 0.05	0.07 ± 0.1	0.77	4.1	9.79	1.62
2M04111569-0505534	5963 ± 99	4.23 ± 0.12	4.14	0.11 ± 0.04	0.05 ± 0.1	0.81	5	9.33	1.48
2M04111641-0536482	6310 ± 170	4.34 ± 0.22	4.13	0.02 ± 0.07	-0.03 ± 0.1	0.61	7.4	9.72	2.02
2M04114242+2403351	5875 ± 115	4.28 ± 0.16	4.21	0.03 ± 0.05	-0.02 ± 0.1	0.62	4.63	10.35	1.51
2M04120236+2303193	5603 ± 114	4.27 ± 0.14	4.27	0.05 ± 0.05	0.02 ± 0.1	0.76	3.57	10.54	0.61
2M04120989-0521083	6157 ± 128	4.45 ± 0.16	4.31	0.11 ± 0.05	0.04 ± 0.1	0.72	6.16	9.53	1.66
2M04123805+2246148	5476 ± 100	4.29 ± 0.11	4.33	0.02 ± 0.04	0 ± 0.1	1.24	3.3	10.29	0.61
2M04144036+2401046	5666 ± 120	4.34 ± 0.16	4.33	-0.02 ± 0.05	-0.06 ± 0.1	0.76	3.83	10.86	0.66
2M04153721+2257521	5674 ± 131	3.98 ± 0.16	3.97	-0.07 ± 0.06	-0.11 ± 0.1	0.77	4.01	10.56	0.57
2M04155144+2436226	5910 ± 130	4.32 ± 0.18	4.25	0.08 ± 0.05	0.03 ± 0.1	0.77	4.74	10.28	0.64
2M04160967+2429097	5996 ± 134	4.24 ± 0.16	4.14	-0.05 ± 0.06	-0.12 ± 0.1	0.52	5.36	8.25	1.47
2M04161617+2249287	5966 ± 142	4.33 ± 0.18	4.24	-0.04 ± 0.06	-0.1 ± 0.1	0.35	5.17	9.1	1.55
2M04165021+2334140	5804 ± 125	4.25 ± 0.15	4.20	0.08 ± 0.05	0.03 ± 0.1	0.8	4.26	10.14	1.6

APOGEE_ID	$T_{\rm eff} \pm \Delta T_{\rm eff}$	$\log g \pm \Delta \log g$	$\log g_{cor}$	$[\rm M/H] \pm \Delta[\rm M/H]$	$[Fe/H] \pm \Delta[\rm Fe/H]$	$v_{\rm mic}$	$v_{\rm mac}$	$v \sin i$	χ^2
2M04174858+2330558	5856 ± 127	4.3 ± 0.17	4.24	0.05 ± 0.05	0 ± 0.1	0.58	4.51	10.46	0.6
2M04175193+2313522	5717 ± 136	4.03 ± 0.14	4.00	-0.12 ± 0.06	-0.18 ± 0.1	0.74	4.19	8.21	1.71
2M04214467+1901019	5993 ± 140	4.41 ± 0.16	4.32	0.02 ± 0.05	-0.03 ± 0.1	0.68	5.24	9.54	1.44
2M04224318+1721189	6151 ± 76	4.41 ± 0.11	4.27	0.07 ± 0.03	0.01 ± 0.1	0.51	6.17	9.32	1.4
2M04224779+1857111	6002 ± 121	4.21 ± 0.13	4.11	0.04 ± 0.05	-0.03 ± 0.1	0.48	5.31	10.58	0.45
2M04325783+0049525	5577 ± 117	4.28 ± 0.14	4.29	0.04 ± 0.05	0.01 ± 0.1	0.8	3.51	10.12	1.82
2M04331416+4641539	5957 ± 102	4.25 ± 0.14	4.16	-0.17 ± 0.04	-0.23 ± 0.1	0.48	5.27	6.88	1.42
2M04331416+4641539	5958 ± 102	4.26 ± 0.14	4.17	-0.17 ± 0.04	-0.23 ± 0.1	0.46	5.27	7.37	1.42
2M04364456+2715193	5942 ± 85	4.37 ± 0.12	4.29	-0.04 ± 0.03	-0.1 ± 0.1	0.49	5.04	8.69	0.35
2M04425018+6644089	5256 ± 129	4.17 ± 0.15	4.26	-0.34 ± 0.04	-0.43 ± 0.1	0.57	3.45	10.28	1.53
2M05073553-1359113	4980 ± 80	3.5 ± 0.08	3.50	0.07 ± 0.04	-0.02 ± 0.1	0.86	3.48	9.37	0.9
2M05100208-0704181	5511 ± 220	4.28 ± 0.25	4.31	-0.38 ± 0.09	-0.46 ± 0.1	0.32	3.78	9.02	1.63
2M05115563+2526598	5583 ± 117	4.23 ± 0.14	4.24	-0.04 ± 0.05	-0.09 ± 0.1	0.84	3.62	9.43	1.55
2M05174024-1331113	4910 ± 76	3.25 ± 0.12	3.25	-0.12 ± 0.04	-0.26 ± 0.1	0.76	3.78	9.33	1.9
2M05203047+2317457	5859 ± 51	4.37 ± 0.07	4.31	0 ± 0.02	-0.05 ± 0.1	0.75	4.58	7.87	1.35
2M05254184+0348047	6240 ± 147	4.33 ± 0.18	4.15	-0.01 ± 0.06	-0.1 ± 0.1	0.38	6.91	8.91	1.37
2M05302099+0306184	6055 ± 127	4.3 ± 0.16	4.19	0.05 ± 0.05	0 ± 0.1	0.58	5.58	8.31	1.43
2M05312734-0340356	3811 ± 26	4.57 ± 0.07	5.13	0.31 ± 0.03	0.31 ± 0.1	0	5.72	7.78	1.83
2M05324957+0311568	5672 ± 116	4.07 ± 0.13	4.06	0.2 ± 0.05	0.14 ± 0.1	0.82	3.67	10.2	2.11
2M05332945-0545260	5677 ± 178	4.34 ± 0.26	4.32	-0.07 ± 0.08	-0.1 ± 0.1	0.67	3.92	9.79	2.35

APOGEE_ID	$T_{\rm eff} \pm \Delta T_{\rm eff}$	$\log g \pm \Delta \log g$	$\log g_{cor}$	$[\rm M/H] \pm \Delta[\rm M/H]$	$[Fe/H] \pm \Delta[\rm Fe/H]$	$v_{\rm mic}$	$v_{\rm mac}$	$v \sin i$	χ^2
2M05342495-0522055	5803 ± 160	3.99 ± 0.17	3.94	-0.04 ± 0.07	-0.24 ± 0.1	1.76	4.47	19.47	0.43
2M05343150-0424539	5921 ± 129	4.05 ± 0.14	3.97	0.08 ± 0.05	0.02 ± 0.1	0.8	4.86	11.06	0.39
2M05344374-0559283	6242 ± 169	4.59 ± 0.18	4.41	-0.29 ± 0.06	-0.33 ± 0.1	0	7.2	0.13	1.38
2M05345439-0602020	5942 ± 162	3.99 ± 0.18	3.91	-0.17 ± 0.07	-0.24 ± 0.1	0.53	5.27	8.22	1.6
2M05353480-0621513	6043 ± 123	4.34 ± 0.15	4.23	0.03 ± 0.05	-0.04 ± 0.1	0.51	5.53	9.26	1.37
2M05355636-0436303	6034 ± 140	4.26 ± 0.16	4.15	-0.01 ± 0.05	-0.06 ± 0.1	0.57	5.53	10.83	1.36
2M05360603-0619388	5923 ± 110	4.2 ± 0.16	4.12	-0.06 ± 0.05	-0.19 ± 0.1	1.63	4.99	15.3	0.25
2M05365839-0155547	5560 ± 103	4.2 ± 0.11	4.21	0.07 ± 0.04	0.01 ± 0.1	0.86	3.45	10.32	1.69
2M05373344+7441194	5877 ± 178	4.19 ± 0.23	4.12	0.06 ± 0.07	0.01 ± 0.1	1.07	4.63	10.78	1.63
2M05375678+3121146	6076 ± 137	4.28 ± 0.17	4.16	0.1 ± 0.05	0.04 ± 0.1	0.82	5.67	9.21	1.49
2M05391089+3130230	6065 ± 137	4.44 ± 0.16	4.33	0.04 ± 0.05	0 ± 0.1	0.37	5.65	11.05	0.45
2M05391427-0221458	5958 ± 167	4.25 ± 0.22	4.16	-0.12 ± 0.07	-0.21 ± 0.1	0.45	5.23	7.39	2.16
2M05405571+0018227	5835 ± 128	4.34 ± 0.18	4.28	-0.04 ± 0.05	-0.1 ± 0.1	0.61	4.52	9.72	1.56
2M05405925-0000322	5948 ± 157	3.96 ± 0.19	3.88	-0.14 ± 0.07	-0.21 ± 0.1	0.48	5.28	8.13	1.48
2M05411719+0015045	5686 ± 116	4.46 ± 0.13	4.44	-0.07 ± 0.05	-0.11 ± 0.1	0.6	3.95	10.23	1.49
2M05445678-0109387	5621 ± 122	4.21 ± 0.14	4.21	0.08 ± 0.05	0.06 ± 0.1	0.82	3.6	9.59	2.2
2M05471268-0015575	5951 ± 138	4.31 ± 0.19	4.23	-0.1 ± 0.06	-0.16 ± 0.1	0.4	5.15	8.49	1.45
2M05475919-0819396	5182 ± 84	3.76 ± 0.11	3.86	0.13 ± 0.04	0.09 ± 0.1	1.13	3.12	0	2.11
2M05510695+0036587	5497 ± 103	4.33 ± 0.11	4.36	0.02 ± 0.04	-0.01 ± 0.1	1.01	3.33	10.44	1.54
2M06304711+5809453	4966 ± 78	3.36 ± 0.12	3.36	-0.01 ± 0.04	-0.11 ± 0.1	0.92	3.62	9.71	1.76

APOGEE_ID	$T_{\rm eff} \pm \Delta T_{\rm eff}$	$\log g \pm \Delta \log g$	$\log g_{cor}$	$[{\rm M/H}] \pm \Delta[{\rm M/H}]$	$[Fe/H] \pm \Delta[{\rm Fe/H}]$	$v_{\rm mic}$	$v_{\rm mac}$	$v \sin i$	χ^2
2M06331115+3516521	5855 ± 129	4.01 ± 0.14	3.95	0.07 ± 0.05	0.01 ± 0.1	0.81	4.57	10.91	1.61
2M06402989+0950104	4632 ± 66	3.94 ± 0.09	4.22	-0.01 ± 0.03	-0.04 ± 0.1	1.44	3.85	9.52	0.96
2M06405546-0112291	5647 ± 106	4.23 ± 0.14	4.22	0.03 ± 0.05	0 ± 0.1	0.86	3.74	9.87	0.58
2M06422101-0116277	5904 ± 111	4.33 ± 0.16	4.26	0.02 ± 0.04	-0.03 ± 0.1	0.68	4.78	8.74	0.57
2M06425377-0026454	5854 ± 133	4.07 ± 0.14	4.01	0.07 ± 0.05	0.01 ± 0.1	0.91	4.55	9.19	1.64
2M06433817-0030550	5648 ± 113	3.9 ± 0.18	3.89	0.04 ± 0.05	0 ± 0.1	1	3.84	9.35	0.72
2M06434459-0029028	5767 ± 125	4.27 ± 0.13	4.23	0.07 ± 0.05	0.02 ± 0.1	0.64	4.11	10.22	0.74
2M06434716+1839211	4860 ± 103	3.3 ± 0.16	3.30	0.06 ± 0.06	-0.03 ± 0.1	0.83	3.55	11.24	2.08
2M06434947-0103468	5272 ± 99	4.42 ± 0.11	4.51	0.06 ± 0.04	0.04 ± 0.1	1.3	3	0	0.9
2M06445089-0115065	5916 ± 122	4.24 ± 0.16	4.16	0.11 ± 0.05	0.06 ± 0.1	0.78	4.75	8.32	1.47
2M06563418+0109435	5600 ± 161	4.28 ± 0.2	4.28	-0.01 ± 0.07	-0.07 ± 0.1	0.59	3.63	10.98	0.54
2M06583851-0028490	5029 ± 681	2.34 ± 1.12	2.34	0.13 ± 0.68	-0.36 ± 0.1	0	4.06	31.41	29.19
2M07273995+2420118	4579 ± 40	4.42 ± 0.07	4.72	0.4 ± 0.02	0.33 ± 0.1	1.07	3.81	7.77	1.32
2M07300727+4711283	5964 ± 147	4.23 ± 0.17	4.14	0 ± 0.06	-0.08 ± 0.1	0.54	5.13	9.1	1.58
2M07303222+4640513	5782 ± 125	4.1 ± 0.13	4.06	0.13 ± 0.05	0.08 ± 0.1	0.87	4.15	10.36	2.16
2M07310593+4714504	5816 ± 123	4.09 ± 0.13	4.04	0.18 ± 0.05	0.13 ± 0.1	0.87	4.23	10.46	0.94
2M07312704+4421431	5904 ± 146	4.28 ± 0.23	4.21	-0.1 ± 0.06	-0.17 ± 0.1	0.51	4.92	8.53	1.82
2M07313990+4439424	5855 ± 96	4.25 ± 0.12	4.19	0.12 ± 0.04	0.06 ± 0.1	0.73	4.44	10.22	1.49
2M07314600+4016251	5795 ± 137	4.27 ± 0.16	4.23	-0.01 ± 0.06	-0.07 ± 0.1	0.62	4.32	8.1	1.58
2M07324861+3946162	5960 ± 155	4.35 ± 0.22	4.26	-0.15 ± 0.06	-0.23 ± 0.1	0.47	5.26	8	1.49

APOGEE_ID	$T_{\mathrm{eff}} \pm \Delta T_{\mathrm{eff}}$	$\log g \pm \Delta \log g$	$\log g_{cor}$	$[\mathrm{M/H}] \pm \Delta[\mathrm{M/H}]$	$[Fe/H] \pm \Delta[\mathrm{Fe/H}]$	$\mathrm{v_{mic}}$	$\mathrm{v_{mac}}$	$v \sin i$	χ^2
2M07325820+4050043	5605 ± 104	4.09 ± 0.11	4.09	0.14 ± 0.05	0.1 ± 0.1	0.82	3.52	9.96	1.84
2M07333413+4559516	5611 ± 114	4.38 ± 0.17	4.38	-0.07 ± 0.05	-0.1 ± 0.1	0.78	3.71	10.86	0.72
2M07335399+4340135	6091 ± 95	4.24 ± 0.12	4.12	0.1 ± 0.04	0.06 ± 0.1	0.68	5.77	9.72	0.52
2M07342799+4705135	5640 ± 118	4.32 ± 0.16	4.31	-0.02 ± 0.05	-0.06 ± 0.1	0.92	3.75	10.08	1.75
2M07351288+4604184	5815 ± 99	4.32 ± 0.12	4.27	0.07 ± 0.04	0.02 ± 0.1	0.77	4.3	10.24	1.58
2M07363818+4756103	6454 ± 146	4.61 ± 0.16	4.34	0.04 ± 0.05	-0.07 ± 0.1	0.17	8.6	7.58	0.43
2M07365614+4541018	5741 ± 93	4.07 ± 0.09	4.04	0.09 ± 0.04	0.05 ± 0.1	0.87	4.04	9.83	1.6
2M07373020+4549296	5720 ± 130	4.21 ± 0.15	4.18	-0.04 ± 0.06	-0.07 ± 0.1	0.71	4.06	9.81	2.27
2M07373653+4302350	5953 ± 158	4.39 ± 0.23	4.31	-0.14 ± 0.06	-0.21 ± 0.1	0.21	5.2	8.41	0.71
2M07380759+4439385	5627 ± 115	4.31 ± 0.15	4.31	0.02 ± 0.05	-0.02 ± 0.1	0.71	3.67	10.47	1.72
2M07382893+4633294	5705 ± 120	4.34 ± 0.16	4.32	-0.11 ± 0.05	-0.16 ± 0.1	0.48	4.06	8.18	0.6
2M07385132-0527558	5636 ± 269	4.01 ± 0.33	4.01	-0.32 ± 0.12	-0.42 ± 0.1	0.62	4.13	8.75	1.62
2M07385979+4300404	5750 ± 125	3.97 ± 0.12	3.94	-0.02 ± 0.05	-0.07 ± 0.1	0.82	4.24	8.93	1.24
2M07390361+4519246	5830 ± 105	4.16 ± 0.12	4.11	0.22 ± 0.04	0.17 ± 0.1	0.84	4.23	9.96	2.04
2M07391008+4107246	5728 ± 102	4.19 ± 0.1	4.16	0.05 ± 0.04	0 ± 0.1	0.83	4	8.87	1.34
2M07392997+4711235	5730 ± 102	4.18 ± 0.1	4.15	0 ± 0.04	-0.07 ± 0.1	0.55	4.07	9.52	1.66
2M07402848+4646458	5999 ± 164	4.41 ± 0.19	4.31	-0.03 ± 0.06	-0.11 ± 0.1	0.44	5.33	10.18	1.72
2M07403375+4615161	5817 ± 125	4.3 ± 0.15	4.25	0.11 ± 0.05	0.06 ± 0.1	0.65	4.27	10.69	0.89
2M07405367+4522460	5446 ± 105	4.27 ± 0.12	4.31	0.02 ± 0.05	0 ± 0.1	1.03	3.24	10.09	0.92
2M07410706+2200287	6031 ± 135	4.34 ± 0.16	4.24	0.06 ± 0.05	0.02 ± 0.1	0.71	5.42	10.12	1.46

APOGEE_ID	$T_{\rm eff} \pm \Delta T_{\rm eff}$	$\log g \pm \Delta \log g$	$\log g_{cor}$	$[\rm M/H] \pm \Delta[\rm M/H]$	$[Fe/H] \pm \Delta[\rm Fe/H]$	$\rm v_{mic}$	$\rm v_{mac}$	$v \sin i$	χ^2
2M07412150+4512493	5736 ± 141	4.46 ± 0.13	4.43	-0.04 ± 0.06	-0.08 ± 0.1	0.65	4.09	10.97	2.25
2M07412564+4034056	5916 ± 127	4.3 ± 0.19	4.22	-0.09 ± 0.05	-0.15 ± 0.1	0.56	4.97	8.42	0.44
2M07413038+4554460	5459 ± 94	4.23 ± 0.1	4.27	0.03 ± 0.04	0.03 ± 0.1	1.43	3.27	10.41	1.04
2M07413619+4549423	5742 ± 58	4.4 ± 0.07	4.37	0.09 ± 0.02	0.05 ± 0.1	0.72	3.98	10.62	1.56
2M07414058+4156032	5796 ± 138	4.19 ± 0.15	4.14	0.01 ± 0.06	-0.06 ± 0.1	0.8	4.32	10.26	0.51
2M07414582+4629144	6009 ± 94	4.42 ± 0.11	4.32	-0.11 ± 0.04	-0.17 ± 0.1	0.29	5.48	7.83	1.42
2M07420607+4549235	5844 ± 154	4.22 ± 0.21	4.16	-0.15 ± 0.06	-0.24 ± 0.1	0.57	4.69	9.02	1.61
2M07423842+4714488	5737 ± 128	4.28 ± 0.14	4.25	-0.01 ± 0.05	-0.07 ± 0.1	0.65	4.08	9.41	2.17
2M07430029+5043243	5655 ± 100	4.52 ± 0.1	4.51	0.41 ± 0.04	0.34 ± 0.1	0.7	3.27	8.69	2.36
2M07431938+4410389	5757 ± 125	4.42 ± 0.14	4.38	-0.09 ± 0.05	-0.14 ± 0.1	0.38	4.23	10.9	1.73
2M07432108+4530434	5838 ± 109	4.36 ± 0.14	4.30	0.06 ± 0.04	0.01 ± 0.1	0.66	4.41	10.72	1.59
2M07432933+4910077	5660 ± 112	4.14 ± 0.13	4.13	0.08 ± 0.05	0.02 ± 0.1	0.83	3.74	10.23	1.62
2M07434448+4200387	5671 ± 70	4.06 ± 0.08	4.05	0.19 ± 0.03	0.14 ± 0.1	0.89	3.68	9.46	1.55
2M07434713+4401054	5696 ± 120	4.14 ± 0.14	4.12	-0.18 ± 0.05	-0.28 ± 0.1	0.42	4.15	8.47	0.55
2M07435169+4526161	5464 ± 108	4.3 ± 0.12	4.34	0.02 ± 0.05	0.02 ± 0.1	1.55	3.27	11.34	0.96
2M07441178+4923192	5836 ± 113	4.3 ± 0.14	4.24	-0.01 ± 0.05	-0.04 ± 0.1	0.55	4.49	8.06	0.52
2M07442113+4428472	5815 ± 130	4.28 ± 0.16	4.23	0.02 ± 0.05	-0.02 ± 0.1	0.72	4.37	9.76	1.62
2M07442285+4203305	5700 ± 83	4.09 ± 0.08	4.07	0.15 ± 0.04	0.11 ± 0.1	0.82	3.81	10.36	1.93
2M07442617+4547128	5844 ± 124	4.24 ± 0.15	4.18	0.09 ± 0.05	0.02 ± 0.1	0.68	4.43	9.98	0.86
2M07444714+4946224	5673 ± 95	4.2 ± 0.11	4.19	0.09 ± 0.04	0.05 ± 0.1	0.71	3.76	9.2	0.58

APOGEE_ID	$T_{\rm eff} \pm \Delta T_{\rm eff}$	$\log g \pm \Delta \log g$	$\log g_{cor}$	$[\mathrm{M/H}] \pm \Delta[\mathrm{M/H}]$	$[Fe/H] \pm \Delta[\mathrm{Fe/H}]$	$v_{\rm mic}$	$v_{\rm mac}$	$v \sin i$	χ^2
2M07444999+4159567	5773 ± 93	4.11 ± 0.09	4.07	0.15 ± 0.04	0.11 ± 0.1	0.86	4.07	10.33	1.48
2M07445019+4435240	5972 ± 124	4.14 ± 0.13	4.05	0.11 ± 0.05	0.04 ± 0.1	0.54	5.07	9.48	1.77
2M07450287+4717491	5399 ± 112	4.28 ± 0.17	4.33	-0.05 ± 0.05	-0.06 ± 0.1	1.71	3.25	9.44	1.1
2M07450746+4515093	5550 ± 80	4.3 ± 0.09	4.32	-0.01 ± 0.03	-0.05 ± 0.1	0.75	3.49	10.37	1.61
2M07451241+4523353	5752 ± 112	4.33 ± 0.12	4.30	0.05 ± 0.05	0.01 ± 0.1	0.72	4.07	10.46	1.74
2M07451323+4506182	5970 ± 103	4.22 ± 0.13	4.13	-0.12 ± 0.04	-0.2 ± 0.1	0.36	5.3	8.37	1.47
2M07453334+4516272	5920 ± 136	4.38 ± 0.22	4.30	-0.08 ± 0.06	-0.15 ± 0.1	0.44	4.97	8.39	0.83
2M07454565+4044450	5524 ± 101	4.22 ± 0.1	4.24	0.06 ± 0.04	0.03 ± 0.1	0.84	3.37	10.02	0.81
2M07454792+4835084	5691 ± 115	4.29 ± 0.13	4.27	0.01 ± 0.05	-0.03 ± 0.1	0.67	3.89	10.31	1.74
2M07455393+4955193	5974 ± 95	4.38 ± 0.12	4.29	0.14 ± 0.04	0.1 ± 0.1	0.48	5	9.42	1.56
2M07455871+3602261	5835 ± 132	4.17 ± 0.15	4.11	0.05 ± 0.05	0 ± 0.1	0.71	4.44	10.51	1.56
2M07461183+3902193	5750 ± 138	4.27 ± 0.15	4.24	-0.05 ± 0.06	-0.14 ± 0.1	0.29	4.18	8.15	2
2M07461802+4250208	5736 ± 116	4.17 ± 0.11	4.14	0.07 ± 0.05	0.01 ± 0.1	0.71	4.01	10.68	1.04
2M07462590+4230039	5984 ± 146	4.34 ± 0.17	4.25	-0.02 ± 0.06	-0.09 ± 0.1	0.33	5.24	9.25	0.67
2M07462784+4521328	5769 ± 122	4.35 ± 0.15	4.31	-0.04 ± 0.05	-0.11 ± 0.1	0.66	4.23	9.92	1.63
2M07465358+4522406	5880 ± 148	4.25 ± 0.22	4.18	-0.18 ± 0.06	-0.27 ± 0.1	0.21	4.89	8.3	0.67
2M07465427+5018589	5728 ± 100	4.34 ± 0.11	4.31	-0.01 ± 0.04	-0.05 ± 0.1	0.8	4.04	8.41	1.63
2M07471029+4048003	5764 ± 117	4.26 ± 0.13	4.22	-0.02 ± 0.05	-0.05 ± 0.1	0.71	4.2	9.89	0.57
2M07472668+4349144	5924 ± 93	4.22 ± 0.12	4.14	0.05 ± 0.04	-0.01 ± 0.1	0.72	4.87	10.36	1.51
2M07473435+4104047	5498 ± 75	4.13 ± 0.07	4.16	0.14 ± 0.03	0.12 ± 0.1	1.04	3.24	9.42	0.81

APOGEE_ID	$T_{\rm eff} \pm \Delta T_{\rm eff}$	$\log g \pm \Delta \log g$	$\log g_{cor}$	$[\rm M/H] \pm \Delta[\rm M/H]$	$[Fe/H] \pm \Delta[\rm Fe/H]$	$\rm v_{mic}$	$\rm v_{mac}$	$v \sin i$	χ^2
2M07480647+5013328	5202 ± 73	4.25 ± 0.09	4.35	0.36 ± 0.03	0.33 ± 0.1	1.05	2.64	0	2.58
2M07481574+4039011	5761 ± 101	4.29 ± 0.11	4.25	0.09 ± 0.04	0.01 ± 0.1	0.3	4.06	8.7	0.67
2M07481625+4210478	5755 ± 108	4.29 ± 0.12	4.26	0.17 ± 0.04	0.12 ± 0.1	0.87	3.95	10.56	1.67
2M07481627+4439379	6192 ± 130	4.29 ± 0.17	4.13	0.05 ± 0.05	-0.01 ± 0.1	0.64	6.5	8.3	0.41
2M07481655+4420414	5696 ± 125	4.35 ± 0.16	4.33	0.04 ± 0.05	-0.02 ± 0.1	0.71	3.87	8.75	1.94
2M07482114+4614197	6168 ± 189	4.19 ± 0.27	4.04	-0.21 ± 0.07	-0.31 ± 0.1	0	6.63	8.34	1.61
2M07482404+3640213	6030 ± 107	4.26 ± 0.12	4.16	0.25 ± 0.04	0.19 ± 0.1	0.86	5.21	11.25	0.57
2M07482519+4548181	5586 ± 103	4.13 ± 0.11	4.14	0.12 ± 0.05	0.08 ± 0.1	0.81	3.47	10.15	1.9
2M07482820+4958586	6129 ± 164	4.33 ± 0.26	4.20	-0.1 ± 0.07	-0.18 ± 0.1	0.22	6.22	9.28	0.47
2M07484000+2310397	5791 ± 97	4.22 ± 0.11	4.18	0.19 ± 0.04	0.14 ± 0.1	0.85	4.08	11.4	1.56
2M07485790+4356177	5688 ± 108	4.35 ± 0.16	4.33	-0.24 ± 0.05	-0.31 ± 0.1	0.3	4.14	8.19	0.4
2M07485995+2309576	5478 ± 99	4.31 ± 0.11	4.34	-0.02 ± 0.04	-0.05 ± 0.1	1.54	3.34	10.52	1.54
2M07490405+4210488	5917 ± 65	4.36 ± 0.09	4.28	0.1 ± 0.03	0.06 ± 0.1	0.61	4.74	10.51	1.36
2M07491773+4415296	5943 ± 142	4.46 ± 0.16	4.38	-0.05 ± 0.06	-0.11 ± 0.1	0.54	5.05	9.75	1.63
2M07491783+4050254	6079 ± 155	4.41 ± 0.22	4.29	-0.03 ± 0.06	-0.09 ± 0.1	0.58	5.81	8.42	0.6
2M07491884+4538342	5737 ± 121	4.39 ± 0.16	4.36	-0.06 ± 0.05	-0.12 ± 0.1	0.69	4.12	9.3	1.52
2M07492411+4415478	5683 ± 92	4.29 ± 0.12	4.27	-0.02 ± 0.04	-0.08 ± 0.1	0.67	3.9	9.56	0.48
2M07492706+4157225	5755 ± 103	4.36 ± 0.11	4.33	-0.02 ± 0.04	-0.07 ± 0.1	0.72	4.16	8.91	1.61
2M07492873+5054154	5954 ± 86	4.31 ± 0.11	4.22	0.13 ± 0.03	0.08 ± 0.1	0.62	4.91	10.08	1.38
2M07495059+4606014	6170 ± 92	4.43 ± 0.13	4.28	-0.08 ± 0.04	-0.15 ± 0.1	0	6.46	7.74	0.42

APOGEE_ID	$T_{\rm eff} \pm \Delta T_{\rm eff}$	$\log g \pm \Delta \log g$	$\log g_{cor}$	$[\mathrm{M/H}] \pm \Delta[\mathrm{M/H}]$	$[Fe/H] \pm \Delta[\mathrm{Fe/H}]$	$\mathrm{v}_{\rm mic}$	$\mathrm{v}_{\rm mac}$	$v \sin i$	χ^2
2M07500138+3942443	5954 ± 123	4.37 ± 0.18	4.28	-0.06 ± 0.05	-0.12 ± 0.1	0.14	5.12	9.28	0.49
2M07501162+3426594	5701 ± 104	4.16 ± 0.11	4.14	0.04 ± 0.04	-0.01 ± 0.1	0.68	3.92	10.07	1.52
2M07502191+2216536	5575 ± 119	4.28 ± 0.14	4.29	-0.03 ± 0.05	-0.07 ± 0.1	0.79	3.58	9.94	1.56
2M07502705+4149501	5967 ± 110	4.31 ± 0.15	4.22	-0.16 ± 0.05	-0.24 ± 0.1	0.29	5.31	8.1	1.4
2M07502794+3910257	5908 ± 124	4.13 ± 0.16	4.06	-0.03 ± 0.05	-0.09 ± 0.1	0.53	4.89	9.54	1.5
2M07503111+4231258	5994 ± 118	4.21 ± 0.12	4.11	0.05 ± 0.05	-0.04 ± 0.1	0.74	5.25	10.09	1.57
2M07511675+5145450	6204 ± 128	4.46 ± 0.14	4.30	0.11 ± 0.05	0.05 ± 0.1	0.62	6.49	9.13	0.35
2M07512532+3439572	5959 ± 163	4.33 ± 0.22	4.24	-0.18 ± 0.06	-0.26 ± 0.1	0	5.28	8.6	0.41
2M07513878+3859385	5558 ± 94	4.31 ± 0.11	4.32	-0.02 ± 0.04	-0.05 ± 0.1	0.8	3.52	9.81	0.59
2M07514898+4031117	5418 ± 102	4.24 ± 0.12	4.29	0.01 ± 0.05	-0.01 ± 0.1	1.24	3.22	10.16	1.8
2M07515608+4712295	6035 ± 188	4.34 ± 0.25	4.23	-0.24 ± 0.07	-0.31 ± 0.1	0	5.77	7.62	1.79
2M07521435+4200396	5931 ± 146	4.13 ± 0.17	4.05	-0.01 ± 0.06	-0.08 ± 0.1	0.68	4.99	10	2.12
2M07522705+4219244	6154 ± 164	4.31 ± 0.26	4.17	-0.2 ± 0.07	-0.28 ± 0.1	0.05	6.49	7.63	0.59
2M07525262+4148235	5837 ± 125	4.12 ± 0.14	4.06	0.06 ± 0.05	-0.01 ± 0.1	0.8	4.46	8.66	1.91
2M07530522+4908538	5788 ± 159	4.3 ± 0.21	4.26	-0.26 ± 0.07	-0.34 ± 0.1	0.22	4.54	8.31	1.51
2M07530714+5131531	5955 ± 141	4.27 ± 0.17	4.18	-0.01 ± 0.06	-0.08 ± 0.1	0.63	5.08	9.1	1.54
2M07530826+4247461	5654 ± 125	4.29 ± 0.17	4.28	-0.01 ± 0.05	-0.07 ± 0.1	0.68	3.79	9.59	1.84
2M07531026+4237571	5930 ± 102	4.23 ± 0.13	4.15	0.06 ± 0.04	-0.03 ± 0.1	0.66	4.88	9.25	1.52
2M07531366+3956361	5559 ± 111	4.1 ± 0.11	4.11	0.17 ± 0.05	0.13 ± 0.1	0.86	3.36	10.25	2.1
2M07531909+3608344	6134 ± 146	4.19 ± 0.21	4.06	-0.19 ± 0.06	-0.3 ± 0.1	0.24	6.38	7.59	0.45

APOGEE_ID	$T_{\rm eff} \pm \Delta T_{\rm eff}$	$\log g \pm \Delta \log g$	$\log g_{cor}$	$[\mathrm{M/H}] \pm \Delta[\mathrm{M/H}]$	$[Fe/H] \pm \Delta[\mathrm{Fe/H}]$	v$_{\rm mic}$	v$_{\rm mac}$	$v \sin i$	χ^2
2M07533152+4206044	6042 ± 148	4.33 ± 0.2	4.22	-0.07 ± 0.06	-0.16 ± 0.1	0.49	5.64	8.62	1.49
2M07533373+3955560	5791 ± 120	4.3 ± 0.14	4.26	0.03 ± 0.05	-0.02 ± 0.1	0.55	4.25	10.39	1.52
2M07535671+4041477	5798 ± 122	4.21 ± 0.14	4.16	0.12 ± 0.05	0.07 ± 0.1	0.79	4.2	10.03	1.68
2M07540914+5435160	6125 ± 152	4.44 ± 0.19	4.31	0 ± 0.06	-0.07 ± 0.1	0.26	6.07	9.86	1.64
2M07540919+4548335	5712 ± 124	4.35 ± 0.16	4.33	-0.05 ± 0.05	-0.11 ± 0.1	0.43	4.02	9.31	1.75
2M07541007+4754568	5984 ± 147	4.34 ± 0.19	4.25	-0.09 ± 0.06	-0.15 ± 0.1	0.19	5.32	7.75	0.65
2M07542444+4826236	5916 ± 104	4.25 ± 0.16	4.17	-0.48 ± 0.04	-0.53 ± 0.1	0.53	5.35	9.61	1.24
2M07542444+4826236	5812 ± 102	4.26 ± 0.14	4.21	-0.35 ± 0.04	-0.53 ± 0.1	0.08	4.74	8.46	1.43
2M07544220+4245165	5741 ± 107	4.34 ± 0.13	4.31	-0.05 ± 0.04	-0.12 ± 0.1	0.67	4.13	9.52	0.42
2M07544319+3647495	5737 ± 135	4.29 ± 0.14	4.26	-0.01 ± 0.05	-0.07 ± 0.1	0.73	4.08	7.68	0.52
2M07545254+4321097	5653 ± 99	4.11 ± 0.12	4.10	0.06 ± 0.04	0.01 ± 0.1	1	3.75	10.14	1.55
2M07551082+4251481	5555 ± 137	4.33 ± 0.17	4.35	-0.14 ± 0.06	-0.2 ± 0.1	0.64	3.64	9.39	1.69
2M07552394+7933150	5996 ± 120	4.24 ± 0.13	4.14	0.03 ± 0.05	-0.05 ± 0.1	0.56	5.27	9.99	0.47
2M07553284+4503418	6073 ± 171	4.24 ± 0.23	4.12	-0.14 ± 0.07	-0.23 ± 0.1	0.34	5.92	8.45	0.61
2M07560287+4501305	5683 ± 112	4.31 ± 0.14	4.29	0.06 ± 0.05	0.03 ± 0.1	0.84	3.8	10.27	0.84
2M07561019+5032274	6024 ± 113	4.17 ± 0.14	4.07	-0.69 ± 0.05	-0.7 ± 0.1	0.76	6.15	6.2	0.19
2M07561936+4213074	6101 ± 134	4.56 ± 0.16	4.44	-0.07 ± 0.05	-0.14 ± 0.1	0.25	5.99	8.64	1.6
2M07562639+4631583	5724 ± 136	4.18 ± 0.14	4.15	-0.02 ± 0.06	-0.07 ± 0.1	0.55	4.06	10.51	1.55
2M07563425+5017572	5904 ± 116	4.29 ± 0.16	4.22	0.1 ± 0.05	0.03 ± 0.1	0.59	4.69	9.72	1.31
2M07563457+3529392	5948 ± 128	4.38 ± 0.17	4.30	0.09 ± 0.05	0.05 ± 0.1	0.68	4.92	9.83	1.54

APOGEE_ID	$T_{\rm eff} \pm \Delta T_{\rm eff}$	$\log g \pm \Delta \log g$	$\log g_{cor}$	$[\rm M/H] \pm \Delta[\rm M/H]$	$[Fe/H] \pm \Delta[\rm Fe/H]$	$\rm v_{mic}$	$\rm v_{mac}$	$v \sin i$	χ^2
2M07563897+2659077	5669 ± 88	4.12 ± 0.1	4.11	0.11 ± 0.04	0.07 ± 0.1	0.86	3.75	9.48	1.48
2M07563928+4808097	6095 ± 163	4.43 ± 0.23	4.31	-0.09 ± 0.07	-0.17 ± 0.1	0.25	5.97	7.67	0.52
2M07565678+4129107	5476 ± 101	4.26 ± 0.11	4.30	0.02 ± 0.04	0.02 ± 0.1	1.54	3.31	10.5	1.85
2M07570840+5038403	5993 ± 151	4.19 ± 0.17	4.10	-0.05 ± 0.06	-0.12 ± 0.1	0.58	5.35	9.15	0.62
2M07571171+4905497	5667 ± 131	4.46 ± 0.15	4.45	-0.04 ± 0.06	-0.09 ± 0.1	0.94	3.85	10.84	0.61
2M07571273+5214553	5742 ± 120	4.04 ± 0.1	4.01	-0.01 ± 0.05	-0.06 ± 0.1	0.77	4.17	8.43	1.59
2M07571681+4327408	5788 ± 120	4.27 ± 0.14	4.23	-0.02 ± 0.05	-0.07 ± 0.1	0.7	4.3	9.72	0.56
2M07575488+4058278	5966 ± 74	4.36 ± 0.1	4.27	-0.2 ± 0.03	-0.27 ± 0.1	0	5.33	7.26	1.37
2M07580710+5134378	5757 ± 130	4.33 ± 0.16	4.29	-0.24 ± 0.05	-0.31 ± 0.1	0.3	4.4	8.06	1.47
2M07581035+5253236	5646 ± 72	4.32 ± 0.1	4.31	0.05 ± 0.03	0.01 ± 0.1	0.7	3.7	10.06	1.65
2M07581096+4746199	5790 ± 124	4.36 ± 0.17	4.32	-0.09 ± 0.05	-0.15 ± 0.1	0.47	4.37	10.07	1.45
2M07581215+4436057	5751 ± 128	4.17 ± 0.12	4.14	0.05 ± 0.05	0 ± 0.1	0.8	4.1	10.39	1.63
2M07581478+2734067	5898 ± 118	4.09 ± 0.16	4.02	-0.11 ± 0.05	-0.18 ± 0.1	0.66	4.94	9.13	1.43
2M07581604+4144271	5766 ± 96	4.19 ± 0.1	4.15	0 ± 0.04	-0.06 ± 0.1	0.66	4.2	10.35	1.44
2M07581747+2647065	5650 ± 106	4.21 ± 0.14	4.20	0.05 ± 0.05	0.01 ± 0.1	0.74	3.72	9.56	1.63
2M07582559+4514289	6099 ± 119	4.51 ± 0.12	4.39	-0.02 ± 0.05	-0.08 ± 0.1	0.03	5.93	8.52	1.4
2M07582941+2559014	5713 ± 144	4.34 ± 0.18	4.32	-0.04 ± 0.06	-0.08 ± 0.1	0.7	4.02	8.94	0.6
2M07582966+4335507	5679 ± 113	4.36 ± 0.15	4.34	0 ± 0.05	-0.04 ± 0.1	0.66	3.85	9.93	1.59
2M07583037+4231230	5644 ± 109	4.09 ± 0.13	4.08	0.12 ± 0.05	0.08 ± 0.1	0.79	3.66	10	2.03
2M07591283+5003068	6147 ± 127	4.37 ± 0.22	4.23	-0.12 ± 0.05	-0.19 ± 0.1	0.19	6.36	6.6	0.42

APOGEE_ID	$T_{\rm eff} \pm \Delta T_{\rm eff}$	$\log g \pm \Delta \log g$	$\log g_{cor}$	$[{\rm M/H}] \pm \Delta[{\rm M/H}]$	$[Fe/H] \pm \Delta[{\rm Fe/H}]$	$v_{\rm mic}$	$v_{\rm mac}$	$v \sin i$	χ^2
2M07592068+5209168	5989 ± 114	4.25 ± 0.12	4.16	0.23 ± 0.05	0.17 ± 0.1	0.78	5	11.47	0.55
2M07592326+4941443	5945 ± 119	4.24 ± 0.15	4.16	0.05 ± 0.05	0 ± 0.1	0.79	4.97	9.71	1.46
2M07593359+5040215	5997 ± 147	4.37 ± 0.17	4.27	-0.01 ± 0.06	-0.09 ± 0.1	0.51	5.31	9.51	0.49
2M07593794+4846340	5979 ± 76	4.3 ± 0.1	4.21	-0.07 ± 0.03	-0.16 ± 0.1	0	5.28	10.32	1.41
2M07594365+4240189	5975 ± 159	4.35 ± 0.21	4.26	-0.1 ± 0.06	-0.18 ± 0.1	0.23	5.28	8.71	0.58
2M08000714+4527346	5725 ± 129	4.31 ± 0.16	4.28	-0.05 ± 0.05	-0.12 ± 0.1	0.54	4.08	9.86	0.7
2M08001693+4446268	5734 ± 129	4.4 ± 0.17	4.37	-0.11 ± 0.05	-0.16 ± 0.1	0.75	4.16	9.47	1.5
2M08001751+2716283	5568 ± 102	4.25 ± 0.12	4.26	0 ± 0.04	-0.05 ± 0.1	0.72	3.54	10.37	1.5
2M08002941+4317066	5986 ± 109	4.35 ± 0.13	4.26	0.01 ± 0.04	-0.06 ± 0.1	0.46	5.22	8.7	0.44
2M08005391+5300439	5997 ± 90	4.46 ± 0.08	4.36	0.06 ± 0.03	0.02 ± 0.1	0.59	5.21	9.27	1.43
2M08005541+4615386	6170 ± 144	4.3 ± 0.22	4.15	-0.15 ± 0.06	-0.24 ± 0.1	0	6.55	7.16	1.45
2M08010643+2710316	5953 ± 147	4.31 ± 0.21	4.23	-0.07 ± 0.06	-0.15 ± 0.1	0.57	5.13	7.67	0.61
2M08013264+4307298	6159 ± 166	4.31 ± 0.25	4.17	-0.03 ± 0.07	-0.11 ± 0.1	0.54	6.35	8.7	1.61
2M08014584+5406537	6235 ± 152	4.28 ± 0.17	4.11	0.05 ± 0.06	-0.03 ± 0.1	0.56	6.81	8.43	1.45
2M08015862+4944543	6244 ± 165	4.31 ± 0.21	4.13	-0.18 ± 0.06	-0.27 ± 0.1	0.16	7.11	8.61	0.44
2M08020289+4247532	5831 ± 102	4.14 ± 0.11	4.09	0.03 ± 0.04	-0.03 ± 0.1	0.68	4.46	10.79	0.44
2M08021242+5214589	6121 ± 109	4.34 ± 0.15	4.21	0.2 ± 0.04	0.14 ± 0.1	0.63	5.83	10.59	1.41
2M08022202+5508408	5471 ± 98	4.25 ± 0.1	4.29	0.02 ± 0.04	-0.02 ± 0.1	1	3.3	11.03	0.62
2M08022386+5014337	5923 ± 160	4.25 ± 0.23	4.17	-0.16 ± 0.07	-0.24 ± 0.1	0.35	5.08	9.01	0.49
2M08022845+5300050	5859 ± 125	4.15 ± 0.15	4.09	0.01 ± 0.05	-0.03 ± 0.1	0.59	4.6	9.94	1.49

APOGEE_ID	$T_{\rm eff} \pm \Delta T_{\rm eff}$	$\log g \pm \Delta \log g$	$\log g_{cor}$	$[\rm M/H] \pm \Delta[\rm M/H]$	$[Fe/H] \pm \Delta[\rm Fe/H]$	$\rm v_{mic}$	$\rm v_{mac}$	$v \sin i$	χ^2
2M08023867+4723100	5794 ± 125	4.13 ± 0.13	4.09	0.13 ± 0.05	0.08 ± 0.1	0.83	4.19	10.04	1.78
2M08025756+4101048	5913 ± 117	4.48 ± 0.14	4.41	-0.06 ± 0.05	-0.11 ± 0.1	0.55	4.9	9.24	1.4
2M08030716+4227506	5799 ± 136	4.4 ± 0.19	4.35	-0.1 ± 0.06	-0.17 ± 0.1	0.48	4.42	9.26	1.66
2M08030800+5408527	6153 ± 143	4.42 ± 0.2	4.28	-0.01 ± 0.05	-0.09 ± 0.1	0.35	6.27	9.63	1.39
2M08031115+4647543	5602 ± 109	4.19 ± 0.13	4.19	0.1 ± 0.05	0.05 ± 0.1	0.81	3.53	10.38	1.8
2M08031480+4606313	5772 ± 128	4.3 ± 0.14	4.26	0.05 ± 0.05	0.01 ± 0.1	0.9	4.15	10.7	2.03
2M08032654+5113470	5742 ± 123	4.35 ± 0.14	4.32	0.08 ± 0.05	0.04 ± 0.1	0.72	3.99	10.7	0.7
2M08033487+4935314	5805 ± 134	4.41 ± 0.19	4.36	-0.24 ± 0.06	-0.32 ± 0.1	0.16	4.58	8.49	1.41
2M08041780+5257096	5897 ± 125	4.1 ± 0.15	4.03	0.06 ± 0.05	0 ± 0.1	0.69	4.75	10.32	0.43
2M08042412+5419382	5865 ± 141	4.44 ± 0.19	4.38	-0.06 ± 0.06	-0.12 ± 0.1	0.33	4.66	9.43	1.56
2M08043773+5258413	5889 ± 119	4.22 ± 0.16	4.15	0.22 ± 0.05	0.17 ± 0.1	0.75	4.5	10.24	1.55
2M08043848+4526423	5753 ± 139	4.13 ± 0.13	4.10	-0.03 ± 0.06	-0.08 ± 0.1	0.83	4.21	9.71	1.75
2M08044133+5423434	5748 ± 110	4.45 ± 0.11	4.42	-0.23 ± 0.04	-0.3 ± 0.1	0.34	4.34	8.81	2.22
2M08044413+2656107	5966 ± 104	4.26 ± 0.12	4.17	0.07 ± 0.04	0.03 ± 0.1	0.68	5.06	9.85	1.33
2M08045092+4911452	5998 ± 126	4.35 ± 0.14	4.25	-0.01 ± 0.05	-0.08 ± 0.1	0.53	5.31	9.71	1.51
2M08045516+2730541	5452 ± 109	4.24 ± 0.12	4.28	0.04 ± 0.05	0.02 ± 0.1	1.14	3.24	10.41	0.86
2M08050697+5026242	5833 ± 97	4.39 ± 0.14	4.34	-0.12 ± 0.04	-0.18 ± 0.1	0.41	4.59	10.09	0.35
2M08052590+4953121	5877 ± 111	4.27 ± 0.15	4.20	0.08 ± 0.04	0.02 ± 0.1	0.53	4.59	9.07	1.55
2M08052890+5510408	5746 ± 133	4.17 ± 0.13	4.14	-0.02 ± 0.05	-0.09 ± 0.1	0.61	4.15	8.52	1.53
2M08054405+6822538	6230 ± 200	4.52 ± 0.21	4.35	-0.3 ± 0.08	-0.32 ± 0.1	0.16	7.12	10	0.32

APOGEE_ID	$T_{\rm eff} \pm \Delta T_{\rm eff}$	$\log g \pm \Delta \log g$	$\log g_{cor}$	$[\rm M/H] \pm \Delta[\rm M/H]$	$[Fe/H] \pm \Delta[\rm Fe/H]$	$\rm v_{mic}$	$\rm v_{mac}$	$v \sin i$	χ^2
2M08054979+5041016	5786 ± 102	4.23 ± 0.11	4.19	0.09 ± 0.04	0.03 ± 0.1	0.72	4.17	10.94	0.5
2M08061486+4405169	5822 ± 115	4.25 ± 0.14	4.20	0.04 ± 0.05	0 ± 0.1	0.69	4.38	10.09	0.68
2M08061781+5041536	5562 ± 139	4.28 ± 0.18	4.29	-0.32 ± 0.06	-0.41 ± 0.1	0.23	3.84	8.27	0.43
2M08063563+4524335	5717 ± 96	4.32 ± 0.12	4.29	-0.05 ± 0.04	-0.11 ± 0.1	0.73	4.05	9.41	1.59
2M08063731+4447283	6046 ± 145	4.27 ± 0.17	4.16	0.04 ± 0.06	-0.03 ± 0.1	0.59	5.55	8.93	0.7
2M08064191+5329318	5961 ± 135	4.2 ± 0.15	4.11	0.11 ± 0.05	0.05 ± 0.1	0.55	4.99	10.4	0.48
2M08065693+4916400	5997 ± 137	4.19 ± 0.14	4.09	0.07 ± 0.05	0.03 ± 0.1	0.61	5.24	9.51	1.56
2M08070320+5207416	5617 ± 124	4.38 ± 0.19	4.38	-0.07 ± 0.05	-0.1 ± 0.1	1.04	3.73	8.34	0.52
2M08070613+4840271	6207 ± 156	4.25 ± 0.2	4.09	-0.04 ± 0.06	-0.12 ± 0.1	0.04	6.7	7.56	1.41
2M08070705+4804497	5946 ± 125	4.28 ± 0.16	4.20	0.04 ± 0.05	-0.02 ± 0.1	0.61	4.97	8.98	1.42
2M08070869+5324374	5853 ± 147	4.28 ± 0.19	4.22	0.01 ± 0.06	-0.06 ± 0.1	0.58	4.55	9.09	1.52
2M08071217+4419268	5677 ± 78	4.36 ± 0.11	4.34	-0.04 ± 0.03	-0.07 ± 0.1	0.68	3.89	8.74	0.41
2M08071773+5027352	5596 ± 103	4.31 ± 0.14	4.32	-0.1 ± 0.05	-0.17 ± 0.1	0.56	3.71	10.11	0.4
2M08071886+4615525	5845 ± 111	4.31 ± 0.15	4.25	-0.04 ± 0.05	-0.09 ± 0.1	0.47	4.57	8.8	0.44
2M08072934+4451274	5852 ± 130	4.18 ± 0.16	4.12	0.04 ± 0.05	-0.02 ± 0.1	0.83	4.53	9.3	2.25
2M08073324+4504313	5732 ± 104	4.33 ± 0.12	4.30	0.05 ± 0.04	0.01 ± 0.1	0.83	3.99	10.58	0.64
2M08075421+4823068	5568 ± 87	4 ± 0.08	4.01	0.1 ± 0.04	0.07 ± 0.1	0.81	3.49	9.86	1.58
2M08080005+4439039	5832 ± 146	4.26 ± 0.21	4.21	-0.23 ± 0.06	-0.32 ± 0.1	0.39	4.71	8.87	2
2M08080785+4207065	5718 ± 111	4.3 ± 0.14	4.27	-0.17 ± 0.05	-0.22 ± 0.1	0.42	4.18	8.93	0.53
2M08081503+4508263	5741 ± 159	4.1 ± 0.16	4.07	-0.17 ± 0.07	-0.26 ± 0.1	0.58	4.31	8.82	1.37

APOGEE_ID	$T_{\rm eff} \pm \Delta T_{\rm eff}$	$\log g \pm \Delta \log g$	$\log g_{cor}$	$[\mathrm{M/H}] \pm \Delta[\mathrm{M/H}]$	$[Fe/H] \pm \Delta[\mathrm{Fe/H}]$	$v_{\rm mic}$	$v_{\rm mac}$	$v \sin i$	χ^2
2M08085333+4536004	5648 ± 114	4.33 ± 0.17	4.32	-0.09 ± 0.05	-0.13 ± 0.1	0.55	3.85	10.11	0.51
2M08085850+4219556	5824 ± 69	4.22 ± 0.08	4.17	0.14 ± 0.03	0.08 ± 0.1	0.64	4.28	10.42	1.42
2M08090697+4551591	5817 ± 100	4.31 ± 0.12	4.26	0.04 ± 0.04	-0.01 ± 0.1	0.57	4.35	10.07	1.37
2M08092263+5033210	5682 ± 116	4.22 ± 0.13	4.20	0.07 ± 0.05	0.02 ± 0.1	0.64	3.81	10.44	1.64
2M08093992+5424599	5844 ± 135	4.31 ± 0.19	4.25	-0.04 ± 0.06	-0.1 ± 0.1	0.72	4.56	9.4	0.44
2M08102717+2530268	5196 ± 119	3.61 ± 0.14	3.61	-0.04 ± 0.06	-0.11 ± 0.1	0.91	3.4	10.39	1.67
2M08104844+5508209	5810 ± 78	4.37 ± 0.11	4.32	-0.08 ± 0.03	-0.14 ± 0.1	0.46	4.44	8.87	1.37
2M08113031+4838056	5954 ± 132	4.46 ± 0.15	4.37	-0.11 ± 0.05	-0.17 ± 0.1	0.03	5.17	7.89	1.49
2M08113869+3227267	5605 ± 234	4.31 ± 0.34	4.31	-0.23 ± 0.1	-0.33 ± 0.1	0.57	3.87	7.75	1.68
2M08113960+5215061	5666 ± 123	4.01 ± 0.13	4.00	0.04 ± 0.05	-0.01 ± 0.1	0.8	3.85	9.81	1.55
2M08114461+4704377	5943 ± 101	4.28 ± 0.12	4.20	0.19 ± 0.04	0.13 ± 0.1	0.66	4.79	10.52	1.51
2M08125009+4830288	5422 ± 80	4.28 ± 0.1	4.33	0.04 ± 0.04	0.02 ± 0.1	1.12	3.18	10.01	1.67
2M08125308+2722149	6175 ± 129	4.32 ± 0.18	4.17	0.16 ± 0.05	0.11 ± 0.1	0.65	6.23	9.99	0.37
2M08130609+4909395	5748 ± 95	4.23 ± 0.1	4.20	0.2 ± 0.04	0.17 ± 0.1	0.94	3.9	9.38	1.67
2M08132910+5402419	5594 ± 135	4.35 ± 0.18	4.36	-0.04 ± 0.06	-0.06 ± 0.1	1.05	3.64	9.26	0.55
2M08133839+5028571	6109 ± 126	4.32 ± 0.18	4.20	-0.02 ± 0.05	-0.1 ± 0.1	0.41	6	9.04	0.35
2M08141577+4920335	5825 ± 131	4.28 ± 0.16	4.23	0.01 ± 0.05	-0.04 ± 0.1	0.58	4.42	10.02	1.57
2M08150507+2755420	6079 ± 184	4.16 ± 0.25	4.04	-0.25 ± 0.07	-0.34 ± 0.1	0	6.08	9.04	1.51
2M08152114+5306452	5633 ± 117	4.35 ± 0.16	4.35	0.07 ± 0.05	0.04 ± 0.1	0.95	3.63	10.09	1.58
2M08152814+2659073	5975 ± 170	4.24 ± 0.21	4.15	-0.19 ± 0.07	-0.27 ± 0.1	0.08	5.39	5.97	0.7

APOGEE_ID	$T_{\text{eff}} \pm \Delta T_{\text{eff}}$	$\log g \pm \Delta \log g$	$\log g_{cor}$	$[\text{M/H}] \pm \Delta[\text{M/H}]$	$[Fe/H] \pm \Delta[\text{Fe/H}]$	v_{mic}	v_{mac}	$v \sin i$	χ^2
2M08155054+5029185	6011 ± 155	4.45 ± 0.15	4.35	-0.02 ± 0.06	-0.08 ± 0.1	0.25	5.39	9.49	1.48
2M08162904+2413340	5847 ± 144	4.38 ± 0.22	4.32	-0.1 ± 0.06	-0.17 ± 0.1	0.4	4.63	9.18	2.78
2M08170822+2457063	5942 ± 100	4.3 ± 0.13	4.22	0.06 ± 0.04	0.01 ± 0.1	0.62	4.93	10.61	1.44
2M08172935-0359221	5678 ± 187	4.05 ± 0.23	4.03	-0.4 ± 0.08	-0.53 ± 0.1	0	4.33	7.72	0.47
2M08192516+2433039	6168 ± 96	4.5 ± 0.1	4.35	0.13 ± 0.04	0.08 ± 0.1	0.56	6.22	9.91	1.39
2M08195296+2407228	5886 ± 155	4.13 ± 0.19	4.06	0.02 ± 0.06	-0.04 ± 0.1	0.72	4.73	8.17	1.98
2M08200326+2436563	5682 ± 119	4.44 ± 0.13	4.42	-0.01 ± 0.05	-0.05 ± 0.1	0.77	3.86	10.11	3.5
2M08201585+4603341	5706 ± 112	4.26 ± 0.14	4.24	-0.1 ± 0.05	-0.16 ± 0.1	0.56	4.07	8.89	0.67
2M08202906+4629060	5887 ± 162	4.35 ± 0.27	4.28	-0.28 ± 0.07	-0.38 ± 0.1	0	5.01	10.02	1.66
2M08204430+2525148	5745 ± 154	4.39 ± 0.19	4.36	-0.32 ± 0.06	-0.43 ± 0.1	0	4.42	8.88	3.52
2M08210049+2304183	5574 ± 69	4.32 ± 0.09	4.33	-0.02 ± 0.03	-0.05 ± 0.1	0.97	3.56	8.86	0.48
2M08211020+4455532	5905 ± 134	4.27 ± 0.2	4.20	-0.1 ± 0.06	-0.15 ± 0.1	0.54	4.92	7.98	2.21
2M08211866+2408511	5703 ± 122	4.3 ± 0.14	4.28	0.03 ± 0.05	-0.01 ± 0.1	0.57	3.91	10.8	1.87
2M08214788+1840440	5581 ± 129	4.04 ± 0.12	4.05	0.04 ± 0.06	0 ± 0.1	0.95	3.59	10.39	0.8
2M08221641+1918079	5932 ± 150	4.06 ± 0.16	3.98	0 ± 0.06	-0.05 ± 0.1	0.76	5.01	10.66	1.5
2M08222222+2316410	5807 ± 123	4.42 ± 0.15	4.37	-0.03 ± 0.05	-0.1 ± 0.1	0.49	4.38	9.86	1.97
2M08230460+1752557	5797 ± 121	4.29 ± 0.15	4.24	-0.06 ± 0.05	-0.1 ± 0.1	0.62	4.37	8.98	0.42
2M08230621+2325108	5688 ± 127	4.21 ± 0.16	4.19	-0.17 ± 0.05	-0.25 ± 0.1	0.48	4.09	8.66	2.51
2M08232139+4508594	5981 ± 113	4.27 ± 0.13	4.18	-0.04 ± 0.05	-0.11 ± 0.1	0.44	5.26	9	0.65
2M08234285+4549131	5749 ± 139	4.29 ± 0.16	4.26	-0.25 ± 0.06	-0.31 ± 0.1	0.38	4.38	7.7	1.69

APOGEE_ID	$T_{\rm eff} \pm \Delta T_{\rm eff}$	$\log g \pm \Delta \log g$	$\log g_{cor}$	$[\mathrm{M/H}] \pm \Delta[\mathrm{M/H}]$	$[Fe/H] \pm \Delta[\mathrm{Fe/H}]$	$\mathrm{v_{mic}}$	$\mathrm{v_{mac}}$	$v \sin i$	χ^2
2M08240260+4716054	5998 ± 118	4.19 ± 0.12	4.09	0.16 ± 0.05	0.11 ± 0.1	0.95	5.14	9.22	0.79
2M08241584+2523527	5743 ± 145	4.2 ± 0.17	4.17	-0.28 ± 0.06	-0.39 ± 0.1	0.1	4.4	9.38	1.52
2M08242088+4641599	6038 ± 165	4.31 ± 0.21	4.20	-0.03 ± 0.07	-0.11 ± 0.1	0.32	5.57	10.25	1.03
2M08243577+4442023	5771 ± 117	4.31 ± 0.13	4.27	0.1 ± 0.05	0.06 ± 0.1	0.73	4.08	10.22	1.19
2M08244196+2510262	5824 ± 108	4.25 ± 0.13	4.20	0.15 ± 0.04	0.11 ± 0.1	0.77	4.26	10.32	1.87
2M08245209+1930301	5635 ± 107	4.01 ± 0.11	4.01	0.04 ± 0.05	-0.02 ± 0.1	0.89	3.75	9.24	1.47
2M08251315+1850203	5671 ± 128	4.29 ± 0.16	4.28	-0.01 ± 0.05	-0.07 ± 0.1	0.73	3.85	9.95	1.46
2M08253450+1833031	6010 ± 145	4.37 ± 0.19	4.27	-0.14 ± 0.06	-0.2 ± 0.1	0	5.52	8.75	1.4
2M08254878+2440212	5962 ± 162	4.21 ± 0.21	4.12	-0.1 ± 0.07	-0.18 ± 0.1	0.59	5.23	9.31	1.65
2M08255662+2318358	5980 ± 146	4.24 ± 0.18	4.15	-0.19 ± 0.06	-0.26 ± 0.1	0.35	5.42	8.75	0.79
2M08260515+1829404	5708 ± 106	4.26 ± 0.12	4.24	0.04 ± 0.04	-0.01 ± 0.1	0.69	3.92	10.22	1.47
2M08261662+2313393	5745 ± 119	4.37 ± 0.13	4.34	0.01 ± 0.05	-0.02 ± 0.1	0.69	4.08	9.76	2.09
2M08262994+1916003	5828 ± 124	4.31 ± 0.16	4.26	0.04 ± 0.05	-0.02 ± 0.1	0.58	4.4	10.32	1.46
2M08264729+2501402	6050 ± 148	4.36 ± 0.18	4.25	0.12 ± 0.06	0.07 ± 0.1	0.71	5.46	10.46	2.18
2M08270347+1738318	5803 ± 123	4.28 ± 0.14	4.23	0.08 ± 0.05	0.04 ± 0.1	0.76	4.25	9.92	1.51
2M08275170+4636291	5856 ± 98	4.1 ± 0.11	4.04	0.09 ± 0.04	0.03 ± 0.1	0.76	4.52	10.43	1.71
2M08282095+1950386	5976 ± 161	4.24 ± 0.2	4.15	-0.32 ± 0.06	-0.44 ± 0.1	0	5.53	7.77	1.38
2M08283118+4442098	5687 ± 124	4.13 ± 0.16	4.11	-0.25 ± 0.05	-0.36 ± 0.1	0.74	4.19	8.97	0.57
2M08302128+1849058	5722 ± 133	4.3 ± 0.15	4.27	0.02 ± 0.05	-0.04 ± 0.1	0.71	3.99	8.52	1.49
2M08312326+4549048	6069 ± 136	4.08 ± 0.15	3.97	-0.04 ± 0.06	-0.11 ± 0.1	0.79	5.83	9.05	0.72

APOGEE_ID	$T_{\rm eff} \pm \Delta T_{\rm eff}$	$\log g \pm \Delta \log g$	$\log g_{cor}$	$[\mathrm{M/H}] \pm \Delta[\mathrm{M/H}]$	$[Fe/H] \pm \Delta[\mathrm{Fe/H}]$	$\mathrm{v}_{\rm mic}$	$\mathrm{v}_{\rm mac}$	$v \sin i$	χ^2
2M08320373+5303595	5549 ± 98	4.22 ± 0.11	4.24	0.08 ± 0.04	0.06 ± 0.1	1	3.4	10.28	0.76
2M08323270+5224229	5759 ± 128	4.21 ± 0.13	4.17	0.02 ± 0.05	-0.01 ± 0.1	0.72	4.15	9.35	1.65
2M08335944+5236328	5862 ± 111	4.3 ± 0.15	4.24	0 ± 0.05	-0.05 ± 0.1	0.44	4.6	9.65	0.47
2M08343853+4617176	6191 ± 133	4.48 ± 0.14	4.32	0.09 ± 0.05	0.03 ± 0.1	0.59	6.43	8.79	0.67
2M08344144+5234243	6065 ± 155	4.14 ± 0.18	4.03	-0.04 ± 0.06	-0.1 ± 0.1	0.52	5.79	8.2	0.69
2M08393124+5402510	5845 ± 101	4.35 ± 0.15	4.29	-0.05 ± 0.04	-0.1 ± 0.1	0.53	4.56	9.11	0.4
2M08394924+5122512	5707 ± 126	4.27 ± 0.14	4.25	0.02 ± 0.05	-0.03 ± 0.1	0.57	3.94	10.53	0.7
2M08400927+5314314	6210 ± 146	4.36 ± 0.22	4.20	-0.31 ± 0.06	-0.33 ± 0.1	0	7	8.19	1.3
2M08403160+5438299	6019 ± 135	4.34 ± 0.18	4.24	-0.14 ± 0.05	-0.21 ± 0.1	0.23	5.58	8.69	1.5
2M08403797+5144396	5853 ± 125	4.28 ± 0.18	4.22	-0.07 ± 0.05	-0.14 ± 0.1	0.51	4.64	9.43	0.47
2M08404454+5547079	5640 ± 68	4.3 ± 0.09	4.29	0.01 ± 0.03	-0.04 ± 0.1	0.68	3.72	10.78	1.41
2M08410163+1227232	5931 ± 134	4.4 ± 0.21	4.32	-0.17 ± 0.06	-0.24 ± 0.1	0.09	5.11	8.85	1.43
2M08411562+5217510	6010 ± 111	4.32 ± 0.13	4.22	0.06 ± 0.04	0.01 ± 0.1	0.44	5.3	10.34	1.47
2M08413321+5251234	6061 ± 160	4.35 ± 0.21	4.24	0 ± 0.06	-0.07 ± 0.1	0.57	5.68	9.27	1.62
2M08413646+1205533	5619 ± 124	4.17 ± 0.14	4.17	0.09 ± 0.05	0.01 ± 0.1	0.65	3.6	10.03	2.23
2M08420123+1134534	5880 ± 106	4.39 ± 0.16	4.32	-0.01 ± 0.04	-0.05 ± 0.1	0.68	4.69	9.74	1.43
2M08421150+5442194	5877 ± 87	4.14 ± 0.11	4.07	0.22 ± 0.04	0.16 ± 0.1	0.8	4.45	10.8	1.67
2M08421786+1250557	5836 ± 138	4.4 ± 0.18	4.34	-0.01 ± 0.06	-0.07 ± 0.1	0.7	4.48	9.48	1.47
2M08421934+1050273	5629 ± 100	4.34 ± 0.14	4.34	-0.04 ± 0.04	-0.07 ± 0.1	0.89	3.74	9.58	1.45
2M08422351+1219401	5605 ± 85	4.03 ± 0.09	4.03	0.19 ± 0.04	0.13 ± 0.1	0.93	3.48	10.58	1.87

APOGEE_ID	$T_{\rm eff} \pm \Delta T_{\rm eff}$	$\log g \pm \Delta \log g$	$\log g_{cor}$	$[\rm M/H] \pm \Delta[\rm M/H]$	$[Fe/H] \pm \Delta[\rm Fe/H]$	$\rm v_{mic}$	$\rm v_{mac}$	$v \sin i$	χ^2
2M08423081+3411155	5825 ± 212	4.16 ± 0.27	4.11	-0.31 ± 0.09	-0.45 ± 0.1	0	4.79	8.44	1.48
2M08424001+5513510	5926 ± 134	4.37 ± 0.19	4.29	0.11 ± 0.05	0.06 ± 0.1	0.74	4.78	10.25	1.52
2M08424336+5532101	6027 ± 132	4.44 ± 0.14	4.34	0.05 ± 0.05	0 ± 0.1	0.66	5.4	10.76	0.41
2M08424972+5222490	6079 ± 146	4.1 ± 0.18	3.98	-0.09 ± 0.06	-0.16 ± 0.1	0.42	5.93	7.64	1.56
2M08425693+5135475	5569 ± 102	4.3 ± 0.13	4.31	-0.15 ± 0.04	-0.21 ± 0.1	0.54	3.69	9.54	1.4
2M08430226+5037030	5786 ± 121	4.29 ± 0.13	4.25	0 ± 0.05	-0.04 ± 0.1	0.71	4.27	10.18	1.73
2M08430331+5415008	5567 ± 80	4.27 ± 0.09	4.28	-0.01 ± 0.03	-0.06 ± 0.1	0.66	3.54	8.71	0.67
2M08432647+1225086	5560 ± 105	4.03 ± 0.09	4.04	-0.01 ± 0.05	-0.04 ± 0.1	0.8	3.59	10.04	1.75
2M08433247+1235079	5810 ± 122	4.16 ± 0.13	4.11	0.19 ± 0.05	0.12 ± 0.1	0.71	4.18	10.56	2.2
2M08440190+1059467	5534 ± 108	4.13 ± 0.11	4.15	0.13 ± 0.05	0.12 ± 0.1	1.02	3.34	9.48	1.32
2M08441857+5025107	5941 ± 137	4.04 ± 0.16	3.96	-0.21 ± 0.06	-0.27 ± 0.1	0.52	5.29	7.86	1.58
2M08442101+1050023	5817 ± 110	4.34 ± 0.14	4.29	0.03 ± 0.05	0 ± 0.1	0.65	4.36	10.12	1.51
2M08442336+1228108	5637 ± 97	4.26 ± 0.13	4.25	-0.02 ± 0.04	-0.08 ± 0.1	0.38	3.75	9.28	1.59
2M08442463+5250041	6292 ± 134	4.45 ± 0.15	4.25	0.22 ± 0.05	0.17 ± 0.1	0.78	7.03	10.55	1.72
2M08443123+5246216	5720 ± 136	4.51 ± 0.12	4.48	-0.06 ± 0.06	-0.13 ± 0.1	0.72	4.06	10.1	2.72
2M08444282+5408066	6224 ± 139	4.31 ± 0.19	4.14	-0.07 ± 0.06	-0.15 ± 0.1	0.22	6.85	8.28	1.43
2M08444287+5416399	6185 ± 175	4.29 ± 0.26	4.14	-0.15 ± 0.07	-0.24 ± 0.1	0	6.66	8.43	1.55
2M08445593+1212096	6098 ± 136	4.36 ± 0.21	4.24	-0.06 ± 0.06	-0.14 ± 0.1	0.18	5.97	8.72	1.52
2M08445656+1257013	5882 ± 122	4.34 ± 0.19	4.27	-0.1 ± 0.05	-0.18 ± 0.1	0.31	4.8	8.65	1.38
2M08450141+5524474	5915 ± 146	4.2 ± 0.19	4.12	0.01 ± 0.06	-0.06 ± 0.1	0.77	4.87	9.23	1.53

APOGEE_ID	$T_{\rm eff} \pm \Delta T_{\rm eff}$	$\log g \pm \Delta \log g$	$\log g_{cor}$	$[\rm M/H] \pm \Delta[\rm M/H]$	$[Fe/H] \pm \Delta[\rm Fe/H]$	$\rm v_{mic}$	$\rm v_{mac}$	$v \sin i$	χ^2
2M08450715+5154579	5879 ± 133	4.38 ± 0.19	4.31	0.05 ± 0.05	0 ± 0.1	0.61	4.62	10.52	1.63
2M08452656+1151009	5553 ± 92	4.23 ± 0.1	4.25	0.06 ± 0.04	0.02 ± 0.1	0.86	3.43	9.97	0.64
2M08455783+1125101	5640 ± 62	4.27 ± 0.09	4.26	-0.07 ± 0.03	-0.11 ± 0.1	0.79	3.82	8.58	1.74
2M08460495+5348446	5937 ± 134	4.37 ± 0.18	4.29	0.03 ± 0.05	-0.02 ± 0.1	0.64	4.94	10.53	0.49
2M08464981+5741557	5698 ± 97	4.38 ± 0.14	4.36	-0.22 ± 0.04	-0.28 ± 0.1	0.47	4.15	8.82	0.38
2M08465486+5325183	5805 ± 87	4.54 ± 0.08	4.49	0.44 ± 0.04	0.35 ± 0.1	0.49	3.8	8.41	2.32
2M08475148+5801421	5632 ± 101	4.29 ± 0.13	4.29	0.03 ± 0.04	-0.01 ± 0.1	0.78	3.67	10.41	0.52
2M08475981+5016386	5765 ± 60	4.22 ± 0.06	4.18	0.1 ± 0.02	0.07 ± 0.1	0.76	4.08	10.38	0.61
2M08482506+1142272	5691 ± 113	4.31 ± 0.15	4.29	-0.03 ± 0.05	-0.07 ± 0.1	0.65	3.93	10.3	0.49
2M08482673+5522106	5569 ± 112	4.33 ± 0.13	4.34	0.02 ± 0.05	-0.01 ± 0.1	0.93	3.5	10.62	1.59
2M08483412+5144439	6017 ± 159	4.45 ± 0.15	4.35	-0.01 ± 0.06	-0.06 ± 0.1	0.42	5.41	9.8	1.71
2M08484702+5219581	5908 ± 132	4.31 ± 0.19	4.24	0.13 ± 0.05	0.09 ± 0.1	0.71	4.67	10.55	1.07
2M08490165+5106209	5949 ± 83	4.3 ± 0.1	4.22	0.03 ± 0.03	-0.02 ± 0.1	0.57	5.01	9.94	1.44
2M08490883+1122497	5844 ± 97	4.42 ± 0.13	4.36	-0.04 ± 0.04	-0.09 ± 0.1	0.51	4.55	10.06	0.34
2M08491615+5740537	6009 ± 133	4.15 ± 0.14	4.05	0.1 ± 0.05	0.04 ± 0.1	0.77	5.29	11.22	1.53
2M08492842+5335049	6177 ± 162	4.33 ± 0.23	4.18	-0.01 ± 0.06	-0.08 ± 0.1	0.41	6.45	9.34	1.57
2M08492874+5413074	5697 ± 124	4.29 ± 0.15	4.27	0.03 ± 0.05	-0.01 ± 0.1	0.76	3.89	9.94	1.61
2M08505182+1156559	6270 ± 169	4.26 ± 0.19	4.07	0.06 ± 0.06	0 ± 0.1	0.8	7.06	8.52	1.42
2M08505334+1143399	5416 ± 164	4.13 ± 0.21	4.18	-0.1 ± 0.07	-0.14 ± 0.1	1.23	3.36	8.17	2.43
2M08505460+5027469	5901 ± 145	4.46 ± 0.19	4.39	-0.11 ± 0.06	-0.16 ± 0.1	0.52	4.89	8.1	1.53

APOGEE_ID	$T_{\rm eff} \pm \Delta T_{\rm eff}$	$\log g \pm \Delta \log g$	$\log g_{cor}$	$[\rm M/H] \pm \Delta[\rm M/H]$	$[Fe/H] \pm \Delta[\rm Fe/H]$	$v_{\rm mic}$	$v_{\rm mac}$	$v \sin i$	χ^2
2M08505569+1152146	6095 ± 106	4.22 ± 0.13	4.10	0.08 ± 0.04	0.02 ± 0.1	0.61	5.82	9.73	1.38
2M08510325+1145473	5962 ± 174	4.01 ± 0.18	3.92	0.03 ± 0.07	0 ± 0.1	1.13	5.15	9.94	1.52
2M08510576+1143469	5396 ± 328	3.58 ± 0.47	3.58	-0.24 ± 0.15	-0.5 ± 0.1	2.96	3.76	21.54	2.21
2M08511854+1149214	6018 ± 159	4.04 ± 0.16	3.94	0.02 ± 0.06	-0.01 ± 0.1	1.1	5.46	10.01	2.41
2M08512122+1145526	6019 ± 188	4.1 ± 0.19	4.00	0.01 ± 0.07	-0.06 ± 0.1	1.29	5.46	10.58	1.5
2M08512176+1144050	5449 ± 210	3.98 ± 0.25	4.02	-0.1 ± 0.1	-0.16 ± 0.1	1.63	3.46	9.43	2.34
2M08512205+1146409	6109 ± 226	4.19 ± 0.29	4.07	0.03 ± 0.09	-0.01 ± 0.1	1.05	5.97	9.45	2.6
2M08512788+1155409	5901 ± 201	4.19 ± 0.27	4.12	0 ± 0.08	-0.1 ± 0.1	1.03	4.81	11.47	1.42
2M08512996+1151090	6003 ± 154	4.38 ± 0.18	4.28	0.04 ± 0.06	-0.02 ± 0.1	0.65	5.29	8.98	1.62
2M08513322+1148513	6020 ± 209	4.01 ± 0.2	3.91	-0.01 ± 0.08	-0.06 ± 0.1	1.22	5.52	7.7	2.03
2M08513904+1147553	5781 ± 262	4.33 ± 0.33	4.29	-0.05 ± 0.11	-0.11 ± 0.1	0.64	4.3	11.95	4.38
2M08514122+1154290	6196 ± 175	4.19 ± 0.21	4.03	0.04 ± 0.07	-0.05 ± 0.1	0.79	6.55	10.23	1.41
2M08514401+1146245	5579 ± 138	3.87 ± 0.2	3.88	0.09 ± 0.06	0.04 ± 0.1	0.88	3.6	10.28	0.8
2M08514994+1149311	6135 ± 158	4.15 ± 0.2	4.02	0.04 ± 0.06	-0.02 ± 0.1	0.78	6.14	10.5	1.36
2M08514994+1149311	6113 ± 160	4.21 ± 0.21	4.09	0.07 ± 0.06	-0.02 ± 0.1	0.64	5.95	8.93	1.45
2M08520741+1150221	6106 ± 158	4.29 ± 0.22	4.17	0.08 ± 0.06	0.01 ± 0.1	0.67	5.87	9.22	1.58
2M08522396+1314005	4898 ± 74	3.61 ± 0.09	3.61	0.35 ± 0.04	0.26 ± 0.1	0.89	3.73	9.38	2.21
2M08523440+5525444	5968 ± 126	4.25 ± 0.15	4.16	-0.02 ± 0.05	-0.09 ± 0.1	0.53	5.17	8.65	1.42
2M08523485+5234498	5899 ± 138	4.08 ± 0.18	4.01	-0.1 ± 0.06	-0.18 ± 0.1	0.58	4.94	7.65	1.52
2M08524420+5450349	5956 ± 87	4.3 ± 0.11	4.21	0.07 ± 0.04	0.04 ± 0.1	0.68	4.99	9.34	0.44

APOGEE_ID	$T_{\rm eff} \pm \Delta T_{\rm eff}$	$\log g \pm \Delta \log g$	$\log g_{cor}$	$[\mathrm{M/H}] \pm \Delta[\mathrm{M/H}]$	$[Fe/H] \pm \Delta[\mathrm{Fe/H}]$	$v_{\rm mic}$	$v_{\rm mac}$	$v \sin i$	χ^2
2M08530006+5057270	5969 ± 130	4.39 ± 0.18	4.30	-0.04 ± 0.05	-0.09 ± 0.1	0.4	5.18	10.17	0.55
2M08541290+5838271	5925 ± 134	4.39 ± 0.19	4.31	0.08 ± 0.05	0.02 ± 0.1	0.62	4.81	10.55	0.48
2M08543569+5531167	6066 ± 132	4.48 ± 0.12	4.37	-0.12 ± 0.09	-0.2 ± 0.1	0	5.83	7.87	1.42
2M08553291+5123181	5822 ± 127	4.04 ± 0.13	3.99	-0.03 ± 0.05	-0.1 ± 0.1	0.67	4.52	8.8	0.48
2M08554709+4107078	5788 ± 144	4.25 ± 0.17	4.21	-0.09 ± 0.06	-0.17 ± 0.1	0.6	4.38	9.33	1.78
2M08562344+5529403	5590 ± 94	3.97 ± 0.1	3.98	0.07 ± 0.04	0.02 ± 0.1	0.79	3.61	10.67	1.78
2M08564599+1728530	4926 ± 139	3.45 ± 0.17	3.45	-0.01 ± 0.07	-0.15 ± 0.1	0.7	3.57	10.13	1.21
2M08571095+4108281	6099 ± 146	4.29 ± 0.22	4.17	-0.09 ± 0.06	-0.18 ± 0.1	0.2	6.01	7.97	1.79
2M08575600+4048231	5843 ± 82	4.44 ± 0.11	4.38	-0.05 ± 0.03	-0.1 ± 0.1	0.63	4.56	8.96	1.46
2M08575784+4139197	5927 ± 88	4.19 ± 0.11	4.11	0.01 ± 0.03	-0.05 ± 0.1	0.56	4.94	8.87	1.4
2M08583601+4005342	5897 ± 128	4.4 ± 0.2	4.33	-0.02 ± 0.05	-0.08 ± 0.1	0.56	4.78	8.93	1.65
2M08592639+4127392	5926 ± 129	4.18 ± 0.18	4.10	-0.1 ± 0.05	-0.16 ± 0.1	0.32	5.05	8.68	1.46
2M08594070+5704131	6013 ± 137	3.97 ± 0.14	3.87	-0.21 ± 0.06	-0.3 ± 0.1	0.25	5.71	7.88	0.41
2M09000443+2753235	5949 ± 131	4.24 ± 0.16	4.16	0.06 ± 0.05	0 ± 0.1	0.66	4.98	9.21	1.6
2M09000693+2802390	5856 ± 131	4.36 ± 0.18	4.30	0.03 ± 0.05	-0.01 ± 0.1	0.67	4.53	8.54	1.66
2M09000774+5407344	6082 ± 136	4.36 ± 0.19	4.24	0.09 ± 0.05	0.03 ± 0.1	0.37	5.7	9.69	0.77
2M09004071+4134562	6077 ± 110	4.48 ± 0.11	4.36	0.23 ± 0.04	0.18 ± 0.1	0.74	5.5	10.65	1.59
2M09004131+2736384	5770 ± 108	4.08 ± 0.11	4.04	-0.04 ± 0.05	-0.09 ± 0.1	0.67	4.3	10.39	1.49
2M09005019+4243012	5823 ± 107	4.42 ± 0.13	4.37	-0.02 ± 0.04	-0.07 ± 0.1	0.49	4.43	10.76	1.44
2M09005080+4211379	5724 ± 81	4.25 ± 0.09	4.22	-0.1 ± 0.03	-0.16 ± 0.1	0.61	4.14	10	0.39

APOGEE_ID	$T_{\rm eff} \pm \Delta T_{\rm eff}$	$\log g \pm \Delta \log g$	$\log g_{cor}$	$[\mathrm{M/H}] \pm \Delta[\mathrm{M/H}]$	$[Fe/H] \pm \Delta[\mathrm{Fe/H}]$	$\mathrm{v}_{\rm mic}$	$\mathrm{v}_{\rm mac}$	$v \sin i$	χ^2
2M09010306+5649167	5607 ± 110	4.17 ± 0.12	4.17	0.05 ± 0.05	0.03 ± 0.1	0.78	3.61	9.34	0.57
2M09010527+5627197	5742 ± 112	4.27 ± 0.12	4.24	0.17 ± 0.05	0.13 ± 0.1	0.79	3.9	9.81	0.71
2M09011116+4052420	5518 ± 93	4.2 ± 0.09	4.22	0.06 ± 0.04	0.04 ± 0.1	0.93	3.36	9.13	0.68
2M09013252+4104111	5546 ± 107	4.34 ± 0.12	4.36	0.03 ± 0.04	-0.01 ± 0.1	0.73	3.44	10.06	1.69
2M09014363+5840569	5856 ± 103	4.34 ± 0.14	4.28	0.19 ± 0.04	0.11 ± 0.1	0.71	4.35	11.52	0.51
2M09014885+4002416	5896 ± 143	4.29 ± 0.21	4.22	-0.04 ± 0.06	-0.1 ± 0.1	0.24	4.81	9.43	0.6
2M09015063+5516027	6212 ± 136	4.31 ± 0.19	4.15	-0.1 ± 0.05	-0.19 ± 0.1	0.05	6.8	7.31	1.6
2M09015845+2832121	5675 ± 98	4.31 ± 0.13	4.30	0.09 ± 0.04	0.05 ± 0.1	0.69	3.74	10.42	1.58
2M09020879+4059354	5799 ± 90	4.29 ± 0.11	4.24	0.2 ± 0.04	0.14 ± 0.1	0.6	4.09	9.69	1.59
2M09023603+5743026	5897 ± 167	4.32 ± 0.27	4.25	-0.21 ± 0.07	-0.3 ± 0.1	0.25	4.99	8.3	0.47
2M09025006+4201109	5636 ± 123	4.28 ± 0.16	4.28	0.03 ± 0.05	-0.01 ± 0.1	0.62	3.69	10.34	1.78
2M09025724+4305408	5712 ± 91	4.1 ± 0.09	4.08	0.01 ± 0.04	-0.03 ± 0.1	0.84	4.02	10.5	0.4
2M09033299+3953148	5497 ± 86	4.3 ± 0.09	4.33	0.01 ± 0.04	-0.02 ± 0.1	0.85	3.36	9.97	1.61
2M09035802+2758343	6034 ± 143	4.33 ± 0.19	4.22	-0.08 ± 0.06	-0.16 ± 0.1	0.19	5.6	6.47	1.64
2M09041565+4032382	5470 ± 53	4.22 ± 0.05	4.26	0.01 ± 0.02	-0.01 ± 0.1	0.78	3.31	9.34	0.66
2M09042805+4035508	5438 ± 69	4.35 ± 0.09	4.40	-0.17 ± 0.03	-0.2 ± 0.1	0	3.43	9.94	1.45
2M09044209+4032086	5594 ± 136	4.09 ± 0.16	4.10	-0.19 ± 0.06	-0.26 ± 0.1	0.35	3.85	9.98	0.65
2M09044845+2911332	5763 ± 96	4.18 ± 0.1	4.14	-0.08 ± 0.04	-0.19 ± 0.1	0.37	4.29	9.45	1.45
2M09044874+4517393	5707 ± 146	4.25 ± 0.18	4.23	-0.14 ± 0.06	-0.22 ± 0.1	0.62	4.12	8.57	1.78
2M09051340+5612016	5562 ± 115	4.19 ± 0.12	4.20	0.01 ± 0.05	-0.05 ± 0.1	0.67	3.52	10.21	0.68

APOGEE_ID	$T_{\rm eff} \pm \Delta T_{\rm eff}$	$\log g \pm \Delta \log g$	$\log g_{cor}$	$[\rm M/H] \pm \Delta[\rm M/H]$	$[Fe/H] \pm \Delta[\rm Fe/H]$	$\rm v_{mic}$	$\rm v_{mac}$	$v \sin i$	χ^2
2M09051893+5441423	5961 ± 132	4.26 ± 0.16	4.17	0.04 ± 0.05	-0.02 ± 0.1	0.52	5.07	9.24	1.63
2M09060716+2837063	6145 ± 175	4.3 ± 0.28	4.16	-0.21 ± 0.07	-0.29 ± 0.1	0	6.44	7.42	1.5
2M09061057+2639541	5965 ± 77	4.36 ± 0.1	4.27	0.04 ± 0.03	0.01 ± 0.1	0.55	5.06	9.68	1.39
2M09063106+2759095	5729 ± 96	4.13 ± 0.09	4.10	-0.01 ± 0.04	-0.09 ± 0.1	0.41	4.09	9.37	0.49
2M09063546+5726304	5650 ± 124	4.39 ± 0.2	4.38	-0.14 ± 0.05	-0.17 ± 0.1	0.54	3.9	10.19	0.44
2M09063638+4424589	5730 ± 122	4.17 ± 0.12	4.14	0.17 ± 0.05	0.14 ± 0.1	0.94	3.87	9.99	2.38
2M09063745+2834570	5792 ± 118	4.08 ± 0.12	4.04	0.04 ± 0.05	-0.01 ± 0.1	0.69	4.3	10.69	1.49
2M09065912+3841418	6320 ± 68	4.4 ± 0.09	4.19	0.18 ± 0.03	0.14 ± 0.1	0.68	7.28	10.73	0.34
2M09071435+2811417	5600 ± 94	4.35 ± 0.13	4.35	-0.04 ± 0.04	-0.08 ± 0.1	0.78	3.65	8.99	1.46
2M09071573+4027578	5757 ± 122	4.43 ± 0.13	4.39	-0.09 ± 0.05	-0.12 ± 0.1	0.52	4.23	8.4	1.44
2M09072612+5852301	4670 ± 85	3.22 ± 0.11	3.22	0 ± 0.04	-0.15 ± 0.1	0.69	3.6	9.51	2.02
2M09072850+2759137	6203 ± 182	4.31 ± 0.26	4.15	-0.15 ± 0.07	-0.24 ± 0.1	0	6.79	7.77	0.51
2M09073829+2728314	5836 ± 88	4.23 ± 0.11	4.17	0.08 ± 0.04	0.04 ± 0.1	0.67	4.4	9.58	0.5
2M09074216+3553544	6052 ± 167	4.34 ± 0.25	4.23	-0.41 ± 0.07	-0.46 ± 0.1	0.37	6.04	7.05	0.23
2M09074258+2757290	5744 ± 78	4.27 ± 0.08	4.24	0.09 ± 0.03	0.03 ± 0.1	0.57	4	10.5	1.47
2M09074266+4315105	5749 ± 147	4.24 ± 0.17	4.21	-0.23 ± 0.06	-0.33 ± 0.1	0.4	4.37	8.26	1.49
2M09074642+4006140	5581 ± 125	4.41 ± 0.17	4.42	-0.06 ± 0.05	-0.08 ± 0.1	0.58	3.62	10.03	0.71
2M09080753+4350456	5713 ± 101	4.35 ± 0.12	4.33	0.04 ± 0.04	0 ± 0.1	0.81	3.93	10.42	1.48
2M09081248+2849146	5623 ± 103	4.26 ± 0.13	4.26	0.08 ± 0.04	0.05 ± 0.1	0.79	3.6	10.49	1.62
2M09081391+4414378	5927 ± 155	4.23 ± 0.22	4.15	-0.11 ± 0.07	-0.18 ± 0.1	0.55	5.05	9.11	1.73

APOGEE_ID	$T_{\rm eff} \pm \Delta T_{\rm eff}$	$\log g \pm \Delta \log g$	$\log g_{cor}$	$[\mathrm{M/H}] \pm \Delta[\mathrm{M/H}]$	$[Fe/H] \pm \Delta[\mathrm{Fe/H}]$	$\mathrm{v}_{\rm mic}$	$\mathrm{v}_{\rm mac}$	$v \sin i$	χ^2
2M09082486+5445139	5636 ± 117	4.08 ± 0.14	4.08	-0.19 ± 0.05	-0.27 ± 0.1	0.5	3.98	8.42	0.57
2M09082525+2829065	6107 ± 165	4.14 ± 0.22	4.02	-0.08 ± 0.07	-0.17 ± 0.1	0.42	6.09	8.51	1.57
2M09083771+4349482	6082 ± 110	4.31 ± 0.14	4.19	0.05 ± 0.04	-0.02 ± 0.1	0.54	5.75	9.25	0.44
2M09090787+2631137	6047 ± 132	4.31 ± 0.16	4.20	0.11 ± 0.05	0.06 ± 0.1	0.53	5.47	10.51	1.59
2M09091401+4422256	5513 ± 74	4.25 ± 0.08	4.28	0.04 ± 0.03	0 ± 0.1	0.9	3.37	9.99	1.55
2M09095271+2647223	5821 ± 132	4.35 ± 0.17	4.30	0.08 ± 0.05	0.03 ± 0.1	0.33	4.32	8.5	2.14
2M09100626+4528060	6006 ± 143	4.34 ± 0.18	4.24	-0.07 ± 0.06	-0.15 ± 0.1	0.49	5.42	8.78	0.58
2M09101544+2754188	5918 ± 91	4.35 ± 0.13	4.27	0.1 ± 0.04	0.05 ± 0.1	0.62	4.75	10.39	1.4
2M09102708+2709083	5566 ± 134	4.27 ± 0.16	4.28	-0.19 ± 0.06	-0.25 ± 0.1	0.75	3.73	10.17	1.64
2M09103429+2736560	5834 ± 122	4.17 ± 0.14	4.12	0.17 ± 0.05	0.12 ± 0.1	0.75	4.31	10.08	1.81
2M09105119+4229232	5698 ± 126	4.37 ± 0.17	4.35	-0.21 ± 0.05	-0.25 ± 0.1	0.23	4.14	9.04	0.43
2M09110881+4240166	5539 ± 79	4.28 ± 0.09	4.30	0.02 ± 0.03	0 ± 0.1	1.07	3.44	10.96	0.64
2M09111880+4355265	6215 ± 147	4.38 ± 0.19	4.21	0.12 ± 0.06	0.07 ± 0.1	0.48	6.57	10.56	0.69
2M09115462+2718316	5807 ± 154	4.18 ± 0.19	4.13	-0.33 ± 0.06	-0.43 ± 0.1	0.29	4.72	8.08	1.47
2M09121481+4201500	5993 ± 118	4.37 ± 0.14	4.28	0.08 ± 0.05	0.03 ± 0.1	0.55	5.18	10.5	1.58
2M09121645+2242181	5533 ± 61	4.14 ± 0.06	4.16	0.15 ± 0.03	0.13 ± 0.1	0.94	3.3	9.92	1.67
2M09122447+2307145	5663 ± 118	4.37 ± 0.16	4.36	0 ± 0.05	-0.05 ± 0.1	0.5	3.8	10.49	1.62
2M09123655+4303528	5922 ± 123	4.38 ± 0.2	4.30	-0.13 ± 0.05	-0.18 ± 0.1	0.48	5.03	8.28	1.51
2M09124334+4510033	5611 ± 100	4.17 ± 0.12	4.17	0.1 ± 0.04	0.07 ± 0.1	0.74	3.56	9.61	1.79
2M09124345+4556040	5856 ± 93	4.31 ± 0.12	4.25	0.06 ± 0.04	0 ± 0.1	0.71	4.51	9.08	1.47

APOGEE_ID	$T_{\text{eff}} \pm \Delta T_{\text{eff}}$	$\log g \pm \Delta \log g$	$\log g_{cor}$	$[\text{M/H}] \pm \Delta[\text{M/H}]$	$[Fe/H] \pm \Delta[\text{Fe/H}]$	v_{mic}	v_{mac}	$v \sin i$	χ^2
2M09130846+4633351	6116 ± 129	4.4 ± 0.19	4.28	0.23 ± 0.05	0.19 ± 0.1	0.93	5.74	10.66	0.95
2M09142789+4603112	5983 ± 100	4.28 ± 0.13	4.19	-0.08 ± 0.04	-0.15 ± 0.1	0.51	5.31	9.51	1.42
2M09145872+4605167	5748 ± 124	4.16 ± 0.12	4.13	0 ± 0.05	-0.04 ± 0.1	0.74	4.13	10.63	1.62
2M09151444+4509274	5659 ± 111	4.06 ± 0.12	4.05	0.09 ± 0.05	0.06 ± 0.1	1.02	3.75	9.74	2.47
2M09151903+4155450	6150 ± 150	4.4 ± 0.26	4.26	-0.07 ± 0.06	-0.14 ± 0.1	0.24	6.32	8.24	0.47
2M09161145+4604439	5961 ± 164	4.29 ± 0.22	4.20	-0.09 ± 0.07	-0.17 ± 0.1	0.49	5.19	9.08	2
2M09163197+2103297	6046 ± 52	4.26 ± 0.06	4.15	0.15 ± 0.02	0.11 ± 0.1	0.7	5.43	9.57	1.34
2M09163583+2058306	6175 ± 130	4.41 ± 0.18	4.26	0.03 ± 0.05	-0.04 ± 0.1	0.48	6.38	8.88	1.42
2M09164964+2231331	5685 ± 109	4.11 ± 0.12	4.09	0.04 ± 0.05	0 ± 0.1	0.66	3.88	10.32	1.55
2M09165526+4426036	5594 ± 112	4.16 ± 0.13	4.17	0.16 ± 0.05	0.12 ± 0.1	0.94	3.45	10.48	1.87
2M09181645+4445336	5860 ± 138	4.13 ± 0.16	4.07	0.07 ± 0.06	0.02 ± 0.1	0.79	4.55	10.12	1.98
2M09190886+4225183	5835 ± 119	4.35 ± 0.16	4.29	-0.01 ± 0.05	-0.05 ± 0.1	0.47	4.48	10.37	0.58
2M09194776+4357011	5743 ± 149	4.26 ± 0.17	4.23	-0.3 ± 0.06	-0.41 ± 0.1	0	4.41	8.56	1.45
2M09205910+4329515	5809 ± 109	4.19 ± 0.12	4.14	0.1 ± 0.04	0.05 ± 0.1	0.63	4.26	10.45	0.72
2M09212217+4239347	5734 ± 132	4.28 ± 0.15	4.25	-0.04 ± 0.06	-0.1 ± 0.1	0.59	4.1	8.4	0.71
2M09224391+4224123	6008 ± 141	4.26 ± 0.15	4.16	0.08 ± 0.06	0.03 ± 0.1	0.7	5.28	10.16	0.69
2M09224927+4212082	6235 ± 91	4.36 ± 0.12	4.19	-0.14 ± 0.04	-0.22 ± 0.1	0	6.99	8.4	0.34
2M09230492+4314449	5668 ± 122	4.21 ± 0.15	4.20	0.1 ± 0.05	0.05 ± 0.1	0.78	3.73	10.18	1.78
2M09230710+4340406	6093 ± 134	4.41 ± 0.18	4.29	0.04 ± 0.05	-0.02 ± 0.1	0.29	5.82	9.61	0.41
2M09232013+4321327	6065 ± 113	4.29 ± 0.14	4.18	0.1 ± 0.04	0.04 ± 0.1	0.69	5.59	9.32	0.43

APOGEE_ID	$T_{\rm eff} \pm \Delta T_{\rm eff}$	$\log g \pm \Delta \log g$	$\log g_{cor}$	$[\mathrm{M/H}] \pm \Delta[\mathrm{M/H}]$	$[Fe/H] \pm \Delta[\mathrm{Fe/H}]$	v$_{\rm mic}$	v$_{\rm mac}$	$v \sin i$	χ^2
2M09240381+2718203	6041 ± 116	4.3 ± 0.15	4.19	-0.18 ± 0.05	-0.26 ± 0.1	0	5.75	7.53	1.39
2M09252120+4320307	5804 ± 120	4.4 ± 0.17	4.35	-0.08 ± 0.05	-0.13 ± 0.1	0.44	4.41	9.21	0.48
2M09255023+4923441	5897 ± 125	4.31 ± 0.18	4.24	0.1 ± 0.05	0.06 ± 0.1	0.61	4.65	9.55	1.77
2M09265211+4953117	5777 ± 89	4.35 ± 0.1	4.31	0.08 ± 0.04	0.04 ± 0.1	0.8	4.13	10.59	1.8
2M09270642+5051368	5690 ± 79	4.17 ± 0.1	4.15	-0.08 ± 0.03	-0.18 ± 0.1	0.53	4.02	9.48	0.37
2M09271662+4917035	5940 ± 134	4.37 ± 0.2	4.29	-0.08 ± 0.06	-0.14 ± 0.1	0.3	5.07	9.29	0.59
2M09291027+5015425	5769 ± 126	3.95 ± 0.13	3.91	0.03 ± 0.05	-0.03 ± 0.1	0.75	4.26	11.15	1.54
2M09303736+3731214	5939 ± 152	4.31 ± 0.22	4.23	-0.11 ± 0.06	-0.18 ± 0.1	0.5	5.11	8.51	1.44
2M09303989+4855002	5699 ± 102	4.18 ± 0.12	4.16	-0.06 ± 0.04	-0.13 ± 0.1	0.57	4.02	10.14	0.45
2M09315505+5103462	6012 ± 160	4.34 ± 0.21	4.24	-0.24 ± 0.06	-0.33 ± 0.1	0	5.64	7.38	2.69
2M09322129+4809536	5806 ± 112	4.18 ± 0.12	4.13	0.02 ± 0.05	-0.05 ± 0.1	0.62	4.35	8.35	0.53
2M09324101+3819508	6072 ± 123	4.26 ± 0.15	4.15	0.06 ± 0.05	-0.01 ± 0.1	0.61	5.69	9.9	0.38
2M09330006+3756483	5728 ± 112	4.36 ± 0.13	4.33	-0.01 ± 0.05	-0.07 ± 0.1	0.62	4.04	9.97	0.46
2M09334543+5603337	6108 ± 149	4.41 ± 0.22	4.29	-0.04 ± 0.06	-0.11 ± 0.1	0.35	6	9.16	0.67
2M09335804+4907508	6212 ± 167	4.4 ± 0.25	4.24	-0.2 ± 0.06	-0.29 ± 0.1	0	6.89	8.28	0.46
2M09341366+5111367	6235 ± 174	4.36 ± 0.23	4.19	-0.05 ± 0.07	-0.13 ± 0.1	0.29	6.9	8.75	1.94
2M09341949+4842168	6177 ± 133	4.34 ± 0.21	4.19	-0.14 ± 0.05	-0.22 ± 0.1	0.23	6.58	8.12	0.46
2M09342184+4704063	6082 ± 125	4.27 ± 0.18	4.15	-0.2 ± 0.05	-0.26 ± 0.1	0	6.03	7.66	1.49
2M09342525+4900582	5905 ± 129	4.33 ± 0.19	4.26	0.04 ± 0.05	0 ± 0.1	0.51	4.75	9.91	0.67
2M09342966+4329453	5627 ± 119	4.01 ± 0.12	4.01	0.1 ± 0.05	0.05 ± 0.1	0.77	3.66	10.3	1.27

APOGEE_ID	$T_{\rm eff} \pm \Delta T_{\rm eff}$	$\log g \pm \Delta \log g$	$\log g_{cor}$	$[\mathrm{M/H}] \pm \Delta[\mathrm{M/H}]$	$[Fe/H] \pm \Delta[\mathrm{Fe/H}]$	$v_{\rm mic}$	$v_{\rm mac}$	$v \sin i$	χ^2
2M09343196+3813533	5693 ± 105	4.26 ± 0.12	4.24	0.02 ± 0.04	-0.03 ± 0.1	0.89	3.89	9.76	0.41
2M09351525+3709543	5729 ± 95	4.23 ± 0.1	4.20	0.09 ± 0.04	0.04 ± 0.1	0.72	3.95	10.28	0.48
2M09352103+4944530	5751 ± 109	4.04 ± 0.1	4.01	0.08 ± 0.05	0.03 ± 0.1	0.92	4.1	10.28	0.53
2M09354612+5120144	5591 ± 105	4.31 ± 0.13	4.32	-0.02 ± 0.04	-0.06 ± 0.1	0.6	3.61	10.45	1.77
2M09354750+4912157	5945 ± 158	4.12 ± 0.18	4.04	-0.01 ± 0.06	-0.07 ± 0.1	0.85	5.07	8.98	2.45
2M09355924+4824429	6065 ± 80	4.24 ± 0.1	4.13	0.24 ± 0.03	0.2 ± 0.1	0.88	5.44	10.19	0.46
2M09360891+4258001	5897 ± 80	4.34 ± 0.12	4.27	0.09 ± 0.03	0.06 ± 0.1	0.77	4.66	9.67	1.46
2M09361296+5610398	6149 ± 70	4.34 ± 0.11	4.20	0.17 ± 0.03	0.12 ± 0.1	0.66	6.05	10.18	1.35
2M09362073+4818088	5672 ± 125	4.26 ± 0.17	4.25	-0.06 ± 0.05	-0.12 ± 0.1	0.6	3.91	10.6	0.68
2M09370477+3624309	5922 ± 150	4.29 ± 0.22	4.21	-0.18 ± 0.06	-0.27 ± 0.1	0	5.09	8.21	1.66
2M09371140+3642251	5701 ± 110	4.32 ± 0.15	4.30	-0.08 ± 0.05	-0.14 ± 0.1	0.71	4.02	9.5	0.38
2M09372858+4401167	5943 ± 137	4.39 ± 0.21	4.31	-0.05 ± 0.06	-0.12 ± 0.1	0.55	5.05	8.15	0.74
2M09373012+4903332	5992 ± 122	4.2 ± 0.14	4.11	-0.11 ± 0.05	-0.21 ± 0.1	0.37	5.41	9.57	2.27
2M09373268+4353380	5795 ± 89	4.29 ± 0.1	4.25	0.05 ± 0.04	0.01 ± 0.1	0.7	4.24	10.23	0.49
2M09374669+4629103	5939 ± 152	4.38 ± 0.23	4.30	-0.11 ± 0.06	-0.17 ± 0.1	0.49	5.09	8.51	0.71
2M09374745+4348104	6240 ± 171	4.23 ± 0.21	4.05	-0.07 ± 0.07	-0.16 ± 0.1	0.39	6.98	7.94	1.98
2M09375123+3620421	5750 ± 98	4.29 ± 0.1	4.26	0 ± 0.04	-0.04 ± 0.1	0.74	4.12	9.43	0.38
2M09375148+4426270	5609 ± 115	4.24 ± 0.14	4.24	-0.01 ± 0.05	-0.06 ± 0.1	0.8	3.66	11.07	2.1
2M09384298+3720595	5931 ± 147	4.26 ± 0.21	4.18	-0.17 ± 0.06	-0.25 ± 0.1	0.58	5.13	7.38	1.4
2M09385252+5047211	6007 ± 99	4.14 ± 0.11	4.04	-0.09 ± 0.04	-0.17 ± 0.1	0.5	5.49	9.03	1.43

APOGEE_ID	$T_{\text{eff}} \pm \Delta T_{\text{eff}}$	$\log g \pm \Delta \log g$	$\log g_{cor}$	$[\text{M/H}] \pm \Delta[\text{M/H}]$	$[Fe/H] \pm \Delta[\text{Fe/H}]$	v_{mic}	v_{mac}	$v \sin i$	χ^2
2M09390293+4948136	5753 ± 73	4.22 ± 0.07	4.19	-0.03 ± 0.03	-0.08 ± 0.1	0.67	4.17	9.63	0.34
2M09392146+4347360	5818 ± 127	4.39 ± 0.17	4.34	-0.04 ± 0.05	-0.1 ± 0.1	0.53	4.43	9.33	0.62
2M09392640+4812578	6074 ± 121	4.37 ± 0.17	4.25	0.03 ± 0.05	-0.03 ± 0.1	0.57	5.72	10.74	0.4
2M09392742+4217093	5918 ± 83	4.28 ± 0.12	4.20	-0.04 ± 0.03	-0.09 ± 0.1	0.8	4.92	9.54	1.34
2M09395023+4931120	5719 ± 114	4.17 ± 0.12	4.14	0.09 ± 0.05	0.04 ± 0.1	0.75	3.93	9.66	0.68
2M09395907+5329491	5222 ± 147	3.53 ± 0.15	3.53	0.08 ± 0.07	-0.03 ± 0.1	0.98	3.32	9.21	3.25
2M09400733+4648003	5672 ± 106	4.49 ± 0.11	4.48	-0.14 ± 0.05	-0.17 ± 0.1	0.61	3.97	10.42	1.54
2M09401495+4817021	5715 ± 124	4.32 ± 0.14	4.30	0.1 ± 0.05	0.06 ± 0.1	0.87	3.87	10.18	1.91
2M09401712+4839306	5677 ± 126	4.32 ± 0.16	4.30	0.05 ± 0.05	0.01 ± 0.1	0.76	3.8	10.51	1.68
2M09401889+3617048	5530 ± 112	4.25 ± 0.12	4.27	0.05 ± 0.05	0.02 ± 0.1	0.86	3.38	9.6	0.71
2M09405739+3730371	5730 ± 85	4.23 ± 0.09	4.20	0.02 ± 0.04	-0.02 ± 0.1	0.7	4.03	10.56	1.38
2M09410791+4327542	5807 ± 86	4.16 ± 0.09	4.11	0.16 ± 0.04	0.1 ± 0.1	0.74	4.2	10.51	1.62
2M09411906+4625139	5697 ± 88	4.15 ± 0.1	4.13	-0.04 ± 0.04	-0.08 ± 0.1	0.84	4	8.98	0.45
2M09412515+5040069	5915 ± 130	4.37 ± 0.21	4.29	-0.15 ± 0.05	-0.22 ± 0.1	0.24	5.01	8.32	1.5
2M09413460+4743250	5747 ± 146	4.14 ± 0.15	4.11	-0.25 ± 0.06	-0.33 ± 0.1	0.43	4.4	7.83	0.74
2M09421216-0746137	5903 ± 179	4.44 ± 0.26	4.37	-0.22 ± 0.07	-0.35 ± 0.1	0	5.03	8.14	1.59
2M09421343+4520418	5891 ± 100	4.41 ± 0.15	4.34	-0.04 ± 0.04	-0.08 ± 0.1	0.47	4.77	10.09	1.44
2M09425097+4407229	5824 ± 119	4.22 ± 0.14	4.17	0.05 ± 0.05	-0.03 ± 0.1	0.43	4.39	9.4	1.54
2M09425847+4350050	6011 ± 95	4.38 ± 0.11	4.28	-0.02 ± 0.04	-0.09 ± 0.1	0.47	5.4	8.58	0.38
2M09425902+4600399	5707 ± 120	4.45 ± 0.12	4.43	-0.04 ± 0.05	-0.09 ± 0.1	0.59	3.99	10.76	0.54

APOGEE_ID	$T_{\rm eff} \pm \Delta T_{\rm eff}$	$\log g \pm \Delta \log g$	$\log g_{cor}$	$[\mathrm{M/H}] \pm \Delta[\mathrm{M/H}]$	$[Fe/H] \pm \Delta[\mathrm{Fe/H}]$	$\mathrm{v_{mic}}$	$\mathrm{v_{mac}}$	$v \sin i$	χ^2
2M09430210+4326579	5677 ± 129	4.11 ± 0.16	4.09	-0.19 ± 0.06	-0.28 ± 0.1	0.61	4.1	8.65	1.74
2M09431066+4644524	6020 ± 120	4.39 ± 0.15	4.29	0.13 ± 0.05	0.08 ± 0.1	0.69	5.27	10.57	1.53
2M09431231+3611311	5890 ± 127	4.19 ± 0.17	4.12	0.12 ± 0.05	0.08 ± 0.1	0.97	4.62	9.71	1.57
2M09431969+4612370	5692 ± 85	4.22 ± 0.1	4.20	0.13 ± 0.04	0.08 ± 0.1	0.72	3.78	9.91	1.74
2M09432389+4455089	6140 ± 190	4.2 ± 0.28	4.07	-0.21 ± 0.08	-0.3 ± 0.1	0.1	6.43	7.6	0.71
2M09435415+4633581	5670 ± 133	3.9 ± 0.21	3.89	-0.2 ± 0.06	-0.29 ± 0.1	0.62	4.17	8.68	0.61
2M09435656+4319117	5605 ± 115	4.13 ± 0.13	4.13	0.14 ± 0.05	0.1 ± 0.1	0.87	3.51	10	2.07
2M09440739+4220284	6001 ± 144	4.19 ± 0.15	4.09	-0.01 ± 0.06	-0.08 ± 0.1	0.58	5.35	8.75	1.68
2M09441116+4553550	6050 ± 135	4.29 ± 0.17	4.18	-0.01 ± 0.05	-0.08 ± 0.1	0.62	5.63	8.87	0.47
2M09441852+4859263	6068 ± 153	4.32 ± 0.19	4.21	0.05 ± 0.06	-0.03 ± 0.1	0.58	5.66	9.19	0.64
2M09442369+4403016	5755 ± 91	4.27 ± 0.1	4.24	0.12 ± 0.04	0.07 ± 0.1	0.78	4.01	10.42	1.39
2M09444033+3842470	6211 ± 93	4.42 ± 0.12	4.26	-0.15 ± 0.04	-0.24 ± 0.1	0	6.83	7.46	1.37
2M09444208+3753218	5831 ± 137	4.24 ± 0.19	4.19	-0.16 ± 0.06	-0.24 ± 0.1	0.46	4.64	9.2	0.53
2M09444458+4442240	5748 ± 112	4.26 ± 0.11	4.23	0.06 ± 0.05	0.03 ± 0.1	0.77	4.05	10.4	1.7
2M09445587+4851449	5910 ± 145	4.18 ± 0.2	4.11	-0.06 ± 0.06	-0.15 ± 0.1	0.48	4.92	8.93	0.6
2M09450956+4322578	5753 ± 106	4.32 ± 0.11	4.29	0 ± 0.04	-0.04 ± 0.1	0.76	4.13	9.06	1.44
2M09452421+4322319	5947 ± 132	4.35 ± 0.17	4.27	0.06 ± 0.05	0 ± 0.1	0.63	4.95	9.51	1.67
2M09453102+4405313	5704 ± 119	4.29 ± 0.15	4.27	-0.14 ± 0.05	-0.21 ± 0.1	0.51	4.1	9.03	1.6
2M09460050+3729098	5697 ± 120	4.28 ± 0.15	4.26	-0.04 ± 0.05	-0.11 ± 0.1	0.66	3.97	9.07	0.5
2M09460303+4418468	5828 ± 143	4.11 ± 0.17	4.06	-0.04 ± 0.06	-0.09 ± 0.1	0.71	4.53	9.3	1.69

APOGEE_ID	$T_{\rm eff} \pm \Delta T_{\rm eff}$	$\log g \pm \Delta \log g$	$\log g_{cor}$	$[\mathrm{M/H}] \pm \Delta[\mathrm{M/H}]$	$[Fe/H] \pm \Delta[\mathrm{Fe/H}]$	$\mathrm{v_{mic}}$	$\mathrm{v_{mac}}$	$v \sin i$	χ^2
2M09461332+4225479	5814 ± 143	4.31 ± 0.19	4.26	-0.1 ± 0.06	-0.17 ± 0.1	0.58	4.49	8.58	1.76
2M09462167+4445306	6100 ± 151	4.37 ± 0.22	4.25	0.01 ± 0.06	-0.06 ± 0.1	0.49	5.9	9.66	0.77
2M09462425+4618542	6215 ± 138	4.27 ± 0.18	4.10	-0.08 ± 0.06	-0.18 ± 0.1	0.37	6.8	8.5	1.55
2M09464248+4506518	4896 ± 85	3.35 ± 0.14	3.35	0.01 ± 0.05	-0.08 ± 0.1	0.83	3.59	10.14	1.9
2M09464578+4759370	5766 ± 149	4.44 ± 0.16	4.40	-0.21 ± 0.06	-0.3 ± 0.1	0.25	4.39	8.46	0.42
2M09464587+4404237	5790 ± 82	4.16 ± 0.09	4.12	0.21 ± 0.03	0.16 ± 0.1	0.9	4.07	10.4	0.65
2M09471354+4717241	5799 ± 75	4.32 ± 0.09	4.27	0.17 ± 0.03	0.13 ± 0.1	0.83	4.12	10.16	0.55
2M09473216+4532254	5819 ± 123	4.31 ± 0.15	4.26	0.12 ± 0.05	0.07 ± 0.1	0.74	4.27	10.41	2.24
2M09492439+4658407	5851 ± 101	4.12 ± 0.12	4.06	0.1 ± 0.04	0.05 ± 0.1	0.84	4.48	11.07	1.64
2M09492595+4448268	5774 ± 120	4.15 ± 0.12	4.11	0.11 ± 0.05	0.08 ± 0.1	0.82	4.12	9.77	0.87
2M09493337+4335407	5938 ± 123	4.23 ± 0.15	4.15	0.05 ± 0.05	-0.02 ± 0.1	0.65	4.94	9.47	1.54
2M09493856+4515162	5754 ± 125	4.28 ± 0.13	4.25	-0.03 ± 0.05	-0.07 ± 0.1	0.57	4.17	9.83	0.55
2M09494036+4245546	5790 ± 140	4.24 ± 0.17	4.20	-0.18 ± 0.06	-0.24 ± 0.1	0.5	4.49	10.08	1.52
2M09494283+4317560	6014 ± 126	4.31 ± 0.16	4.21	-0.08 ± 0.05	-0.16 ± 0.1	0.48	5.49	8.6	1.46
2M09495714+3902272	5795 ± 60	4.32 ± 0.07	4.28	0.05 ± 0.02	-0.02 ± 0.1	0.57	4.24	10.33	1.33
2M09500239+4442391	5966 ± 131	4.24 ± 0.15	4.15	-0.03 ± 0.05	-0.11 ± 0.1	0.58	5.18	8.93	2.98
2M09500348+3816597	6243 ± 92	4.49 ± 0.09	4.31	-0.05 ± 0.04	-0.13 ± 0.1	0	6.96	8.26	0.35
2M09502973+4322234	5947 ± 135	4.44 ± 0.18	4.36	-0.14 ± 0.06	-0.21 ± 0.1	0.24	5.16	8.39	1.41
2M09503350+4538526	5944 ± 90	4.31 ± 0.13	4.23	-0.27 ± 0.04	-0.38 ± 0.1	0	5.29	7.77	1.38
2M09504852+4642025	5881 ± 139	4.17 ± 0.2	4.10	-0.24 ± 0.06	-0.34 ± 0.1	0.25	4.98	8.07	1.46

APOGEE_ID	$T_{\rm eff} \pm \Delta T_{\rm eff}$	$\log g \pm \Delta \log g$	$\log g_{cor}$	$[\rm M/H] \pm \Delta[\rm M/H]$	$[Fe/H] \pm \Delta[\rm Fe/H]$	$\rm v_{mic}$	$\rm v_{mac}$	$v \sin i$	χ^2
2M09505527+3834426	6094 ± 91	4.21 ± 0.11	4.09	0.05 ± 0.04	-0.03 ± 0.1	0.58	5.85	9.7	1.35
2M09511992+4319386	6157 ± 115	4.4 ± 0.19	4.26	-0.17 ± 0.05	-0.26 ± 0.1	0.05	6.47	7.99	1.38
2M09512383+4520084	5807 ± 86	4.34 ± 0.11	4.29	-0.01 ± 0.04	-0.07 ± 0.1	0.8	4.36	9.6	0.39
2M09513116+4627587	6121 ± 123	4.49 ± 0.13	4.36	0 ± 0.05	-0.08 ± 0.1	0.3	6.05	9.59	0.38
2M09513212+4240328	5671 ± 116	4.17 ± 0.13	4.16	0.04 ± 0.05	0 ± 0.1	0.74	3.82	10.12	2.01
2M09520922+4233083	5566 ± 84	4.07 ± 0.08	4.08	0.14 ± 0.04	0.12 ± 0.1	0.86	3.41	9.21	1.7
2M09522322+3725286	5869 ± 61	4.3 ± 0.08	4.24	0.19 ± 0.03	0.14 ± 0.1	0.79	4.42	9.55	1.45
2M09534992+4248107	5706 ± 106	4.03 ± 0.1	4.01	0.04 ± 0.04	0 ± 0.1	0.9	3.98	9.95	0.53
2M09544620+4355053	6015 ± 140	4.28 ± 0.18	4.18	-0.09 ± 0.06	-0.17 ± 0.1	0.52	5.51	8.72	0.53
2M09551443+4216019	5944 ± 110	4.3 ± 0.14	4.22	0.02 ± 0.04	-0.04 ± 0.1	0.61	4.98	8.87	1.43
2M09555615+4413016	5735 ± 150	4.23 ± 0.17	4.20	-0.34 ± 0.06	-0.43 ± 0.1	0	4.43	6.91	0.52
2M09560581+4603447	5925 ± 113	4.21 ± 0.14	4.13	0.14 ± 0.05	0.08 ± 0.1	0.54	4.77	11.06	1.68
2M09561351+4323273	5819 ± 124	4.36 ± 0.18	4.31	-0.09 ± 0.05	-0.15 ± 0.1	0.27	4.49	8.32	0.71
2M09571529+4341442	5607 ± 106	4.19 ± 0.13	4.19	0.08 ± 0.05	0.02 ± 0.1	0.78	3.57	11.02	1.74
2M09580142+4357169	5981 ± 114	4.09 ± 0.12	4.00	-0.17 ± 0.05	-0.27 ± 0.1	0.4	5.44	8.18	1.37
2M09580818+4356142	5850 ± 100	4.06 ± 0.11	4.00	-0.02 ± 0.04	-0.07 ± 0.1	0.83	4.63	9.4	0.41
2M10000478+4230592	6022 ± 90	4.27 ± 0.1	4.17	0.07 ± 0.04	0.01 ± 0.1	0.59	5.37	10.53	0.33
2M10003732+4226273	6135 ± 112	4.47 ± 0.13	4.34	0.14 ± 0.04	0.09 ± 0.1	0.55	5.98	10.2	0.38
2M10004468+4219203	5822 ± 108	4.17 ± 0.12	4.12	0.18 ± 0.05	0.13 ± 0.1	0.84	4.23	9.42	1.79
2M10005698+4503537	5905 ± 143	4.28 ± 0.22	4.21	-0.09 ± 0.06	-0.13 ± 0.1	0.55	4.91	8.9	1.62

APOGEE_ID	$T_{\rm eff} \pm \Delta T_{\rm eff}$	$\log g \pm \Delta \log g$	$\log g_{cor}$	$[\mathrm{M/H}] \pm \Delta[\mathrm{M/H}]$	$[Fe/H] \pm \Delta[\mathrm{Fe/H}]$	v$_{\rm mic}$	v$_{\rm mac}$	$v \sin i$	χ^2
2M10015967+4312296	5965 ± 115	4.41 ± 0.16	4.32	-0.09 ± 0.05	-0.16 ± 0.1	0.46	5.21	8.99	1.43
2M10020571+4641378	5905 ± 118	4.3 ± 0.17	4.23	0.04 ± 0.05	-0.02 ± 0.1	0.62	4.77	10.89	1.58
2M10023643+4651115	5969 ± 122	4.28 ± 0.15	4.19	0.1 ± 0.05	0.04 ± 0.1	0.71	5.04	9.75	0.53
2M10034340+4536019	5996 ± 103	4.34 ± 0.12	4.24	0.1 ± 0.04	0.04 ± 0.1	0.54	5.17	10.82	0.56
2M10040066+4749217	5640 ± 127	4.33 ± 0.17	4.32	0.01 ± 0.05	-0.01 ± 0.1	0.82	3.72	10.61	1.77
2M10040683+4651111	5590 ± 123	4.24 ± 0.14	4.25	0.02 ± 0.05	-0.03 ± 0.1	0.81	3.57	10.5	0.65
2M10044286+4725153	5716 ± 150	4.34 ± 0.21	4.31	-0.25 ± 0.06	-0.33 ± 0.1	0.39	4.25	8.39	1.58
2M10054169+4759413	6005 ± 118	4.32 ± 0.13	4.22	0.02 ± 0.05	-0.05 ± 0.1	0.51	5.32	9.28	1.45
2M10060891+4638124	5946 ± 171	4.27 ± 0.23	4.19	-0.21 ± 0.07	-0.3 ± 0.1	0.05	5.24	8.61	1.8
2M10063090+4824346	6062 ± 123	4.36 ± 0.16	4.25	0.06 ± 0.05	0 ± 0.1	0.75	5.6	9.88	1.42
2M10065301+4553008	5474 ± 69	4.28 ± 0.08	4.32	-0.01 ± 0.03	-0.03 ± 0.1	1.25	3.33	11.68	1.56
2M10073439+4516273	5731 ± 123	4.28 ± 0.14	4.25	-0.15 ± 0.05	-0.2 ± 0.1	0.52	4.21	10.3	1.46
2M10085412+4556333	5668 ± 129	4.41 ± 0.19	4.40	-0.14 ± 0.06	-0.19 ± 0.1	0.59	3.96	9.06	0.52
2M10085810+4459442	5808 ± 131	4.3 ± 0.16	4.25	-0.01 ± 0.05	-0.06 ± 0.1	0.82	4.37	10.15	0.49
2M10090079+4808482	5726 ± 82	4.21 ± 0.09	4.18	0.21 ± 0.03	0.17 ± 0.1	0.77	3.8	9.84	1.65
2M10091425+4617023	5711 ± 66	4.38 ± 0.09	4.36	-0.14 ± 0.03	-0.19 ± 0.1	0.51	4.11	8.73	0.39
2M10095422+4848189	5752 ± 119	4.39 ± 0.13	4.36	0.02 ± 0.05	-0.05 ± 0.1	0.5	4.09	10.48	1.36
2M10100601+4615489	5918 ± 157	4.3 ± 0.24	4.22	-0.23 ± 0.06	-0.3 ± 0.1	0.24	5.12	8.48	0.47
2M10103042+4741238	5724 ± 164	4.14 ± 0.18	4.11	-0.27 ± 0.07	-0.38 ± 0.1	0	4.34	8.39	0.61
2M10103443+4805306	5658 ± 96	4.4 ± 0.14	4.39	0 ± 0.04	-0.04 ± 0.1	0.83	3.78	11.32	1.45

APOGEE_ID	$T_{\rm eff} \pm \Delta T_{\rm eff}$	$\log g \pm \Delta \log g$	$\log g_{cor}$	$[\rm M/H] \pm \Delta[\rm M/H]$	$[Fe/H] \pm \Delta[\rm Fe/H]$	$v_{\rm mic}$	$v_{\rm mac}$	$v \sin i$	χ^2
2M10110022+4817437	5772 ± 115	4.41 ± 0.14	4.37	-0.11 ± 0.05	-0.17 ± 0.1	0.6	4.31	8.94	1.45
2M10113220+4717187	5593 ± 121	4.17 ± 0.15	4.18	-0.1 ± 0.05	-0.16 ± 0.1	0.68	3.73	9.75	1.97
2M10113816+4634598	6075 ± 147	4.34 ± 0.2	4.22	0.05 ± 0.06	-0.03 ± 0.1	0.5	5.71	9.31	1.59
2M10120305+4611361	5855 ± 146	4.18 ± 0.2	4.12	-0.17 ± 0.06	-0.27 ± 0.1	0.13	4.78	8.75	1.71
2M10121899+4624165	6217 ± 108	4.41 ± 0.14	4.24	0.11 ± 0.04	0.06 ± 0.1	0.61	6.59	9.81	1.38
2M10124972+4601163	5645 ± 89	4.3 ± 0.12	4.29	0.02 ± 0.04	0 ± 0.1	0.84	3.72	9.66	1.52
2M10133956+4434578	5834 ± 130	4.1 ± 0.16	4.05	-0.11 ± 0.06	-0.18 ± 0.1	0.44	4.64	8.8	0.63
2M10135105+4704110	5817 ± 100	3.95 ± 0.11	3.90	0.11 ± 0.04	0.07 ± 0.1	0.98	4.37	9.51	0.49
2M10142377+4703585	5798 ± 96	4.2 ± 0.11	4.15	0.06 ± 0.04	0.02 ± 0.1	0.75	4.27	9.64	1.5
2M10151439+4532013	6202 ± 175	4.46 ± 0.19	4.30	-0.02 ± 0.06	-0.09 ± 0.1	0	6.62	8.34	0.57
2M10154443+4556170	5560 ± 108	4.12 ± 0.11	4.13	0.17 ± 0.05	0.12 ± 0.1	0.65	3.35	9.99	3.13
2M10155462+4600332	5701 ± 123	4.21 ± 0.15	4.19	-0.07 ± 0.05	-0.15 ± 0.1	0.47	4.03	8.92	1.01
2M10160955+4402426	5594 ± 60	4.07 ± 0.06	4.08	0.15 ± 0.03	0.12 ± 0.1	0.9	3.48	9.51	0.69
2M10161441+4601226	5991 ± 170	4.32 ± 0.22	4.23	-0.23 ± 0.07	-0.31 ± 0.1	0	5.5	8.5	1.64
2M10161803+3739286	5842 ± 128	4.02 ± 0.15	3.96	-0.08 ± 0.06	-0.15 ± 0.1	0.71	4.67	9.13	0.52
2M10163858+4642577	5814 ± 129	4.14 ± 0.14	4.09	0.07 ± 0.05	0.03 ± 0.1	0.92	4.33	10.91	2.21
2M10171742+4731025	5607 ± 88	4.12 ± 0.1	4.12	0.12 ± 0.04	0.09 ± 0.1	0.88	3.54	9.92	1.76
2M10172551+3752537	6185 ± 127	4.16 ± 0.16	4.01	-0.21 ± 0.05	-0.33 ± 0.1	0	6.75	7.85	0.38
2M10173362+4746599	6084 ± 117	4.21 ± 0.16	4.09	-0.09 ± 0.05	-0.19 ± 0.1	0.35	5.94	8.64	1.34
2M10174573+4543574	5696 ± 85	4.44 ± 0.1	4.42	-0.07 ± 0.04	-0.12 ± 0.1	0.5	3.98	10.65	1.4

APOGEE_ID	$T_{\rm eff} \pm \Delta T_{\rm eff}$	$\log g \pm \Delta \log g$	$\log g_{cor}$	$[\rm M/H] \pm \Delta[\rm M/H]$	$[Fe/H] \pm \Delta[\rm Fe/H]$	v$_{\rm mic}$	v$_{\rm mac}$	$v \sin i$	χ^2
2M10180069+3738059	5755 ± 100	4.13 ± 0.1	4.10	0.02 ± 0.04	-0.02 ± 0.1	0.74	4.16	10.17	1.34
2M10181551+3752465	5847 ± 143	4.31 ± 0.21	4.25	-0.14 ± 0.06	-0.2 ± 0.1	0.47	4.68	8.96	0.47
2M10182639+4039132	6023 ± 142	4.41 ± 0.19	4.31	-0.05 ± 0.06	-0.12 ± 0.1	0.37	5.5	8.82	1.14
2M10192960+3631273	5959 ± 134	4.31 ± 0.16	4.22	0.03 ± 0.05	-0.02 ± 0.1	0.73	5.05	10.26	1.73
2M10193287+4358466	6000 ± 142	4.35 ± 0.15	4.25	0.04 ± 0.06	-0.01 ± 0.1	0.57	5.27	9.32	1.56
2M10193808+3810388	5994 ± 108	4.35 ± 0.13	4.25	-0.02 ± 0.04	-0.09 ± 0.1	0.54	5.3	9.7	0.39
2M10200326+4028445	5915 ± 82	4.33 ± 0.11	4.25	0.08 ± 0.03	0.04 ± 0.1	0.58	4.76	10.34	0.37
2M10203033+3634133	5865 ± 141	4.22 ± 0.18	4.16	0.05 ± 0.06	-0.02 ± 0.1	0.58	4.57	9.71	1.68
2M10204832+3456444	5840 ± 119	4.25 ± 0.15	4.19	0 ± 0.05	-0.05 ± 0.1	0.55	4.51	10.37	0.54
2M10205432+3731428	5927 ± 136	4.28 ± 0.2	4.20	-0.1 ± 0.06	-0.18 ± 0.1	0.45	5.03	9.35	2.11
2M10210511+3720336	6056 ± 123	4.47 ± 0.13	4.36	-0.03 ± 0.05	-0.06 ± 0.1	0.37	5.67	9.92	0.4
2M10211316+4433271	5884 ± 137	4.36 ± 0.22	4.29	-0.14 ± 0.06	-0.2 ± 0.1	0.2	4.85	8.13	0.68
2M10212371+3721307	5716 ± 122	4.34 ± 0.16	4.31	-0.07 ± 0.05	-0.11 ± 0.1	0.66	4.06	9.17	2.33
2M10213021+3733426	5608 ± 108	4.15 ± 0.12	4.15	0.13 ± 0.05	0.1 ± 0.1	1.01	3.52	10.16	0.9
2M10215874+4743077	5812 ± 134	4.14 ± 0.15	4.09	0.06 ± 0.05	0.01 ± 0.1	0.75	4.34	10.47	1.68
2M10222220+3853078	5723 ± 102	4.3 ± 0.11	4.27	-0.02 ± 0.04	-0.06 ± 0.1	0.62	4.04	10.7	0.44
2M10222566+4637273	5990 ± 106	4.29 ± 0.12	4.20	0.14 ± 0.04	0.11 ± 0.1	0.8	5.1	9.61	0.46
2M10222609+4736486	5707 ± 115	4.32 ± 0.14	4.30	-0.01 ± 0.05	-0.05 ± 0.1	0.62	3.97	10.39	0.65
2M10222616+3634163	5789 ± 137	4.05 ± 0.13	4.01	0.04 ± 0.06	-0.04 ± 0.1	0.68	4.3	11.54	0.67
2M10223143+4749112	5970 ± 109	4.41 ± 0.13	4.32	0 ± 0.04	-0.06 ± 0.1	0.56	5.14	8.94	1.37

APOGEE_ID	$T_{\rm eff} \pm \Delta T_{\rm eff}$	$\log g \pm \Delta \log g$	$\log g_{cor}$	$[\rm M/H] \pm \Delta[\rm M/H]$	$[Fe/H] \pm \Delta[\rm Fe/H]$	$\rm v_{mic}$	$\rm v_{mac}$	$v \sin i$	χ^2
2M10223614+4721151	5884 ± 155	4.26 ± 0.24	4.19	-0.23 ± 0.06	-0.31 ± 0.1	0.13	4.96	8.37	0.5
2M10224363+4021478	5831 ± 111	4.34 ± 0.14	4.29	0.12 ± 0.05	0.08 ± 0.1	0.46	4.31	10.52	1.28
2M10225329+3834413	5892 ± 146	4.39 ± 0.25	4.32	-0.17 ± 0.06	-0.25 ± 0.1	0.28	4.92	8.91	0.53
2M10230886+1444136	5980 ± 86	4.36 ± 0.11	4.27	-0.2 ± 0.03	-0.28 ± 0.1	0.02	5.41	7.72	1.37
2M10230983+1634298	5664 ± 103	3.94 ± 0.14	3.93	0 ± 0.04	-0.05 ± 0.1	0.81	3.92	9.72	0.38
2M10231221+1603260	5952 ± 62	4.35 ± 0.09	4.27	-0.07 ± 0.03	-0.14 ± 0.1	0.37	5.12	8.8	1.32
2M10231452+3814343	6200 ± 145	4.31 ± 0.19	4.15	0.06 ± 0.06	0 ± 0.1	0.48	6.53	10.73	0.52
2M10233123+3859074	5805 ± 164	4.4 ± 0.24	4.35	-0.22 ± 0.07	-0.3 ± 0.1	0.5	4.57	9.65	0.57
2M10233613+4716494	5606 ± 117	4.29 ± 0.15	4.29	0.04 ± 0.05	-0.01 ± 0.1	0.83	3.59	10.26	0.85
2M10235400+3758011	5757 ± 91	4.29 ± 0.09	4.25	0.05 ± 0.04	-0.02 ± 0.1	0.57	4.09	10.11	0.43
2M10235859+4607003	5658 ± 108	4.31 ± 0.15	4.30	-0.02 ± 0.05	-0.06 ± 0.1	0.7	3.81	9.58	0.54
2M10235903+4506594	5709 ± 130	4.32 ± 0.15	4.30	0.01 ± 0.05	-0.06 ± 0.1	0.57	3.95	10.77	0.68
2M10240279+3842205	5835 ± 131	4.03 ± 0.15	3.97	-0.09 ± 0.06	-0.16 ± 0.1	0.78	4.64	8.91	1.53
2M10240740+3753310	6074 ± 139	4.34 ± 0.18	4.22	0.02 ± 0.05	-0.04 ± 0.1	0.52	5.73	9.18	0.64
2M10240767+3612244	5592 ± 104	4.27 ± 0.12	4.28	0.03 ± 0.04	0.01 ± 0.1	0.97	3.56	9.72	1.49
2M10241042+3431119	5694 ± 94	4.11 ± 0.1	4.09	0.08 ± 0.04	0.04 ± 0.1	0.83	3.87	9.91	1.56
2M10242406+3523529	5989 ± 100	4.12 ± 0.1	4.03	0.09 ± 0.04	0.04 ± 0.1	0.83	5.19	10.06	1.6
2M10243330+4040287	5854 ± 93	4.14 ± 0.12	4.08	-0.07 ± 0.04	-0.13 ± 0.1	0.52	4.68	10.47	1.42
2M10243392+4819073	6132 ± 166	4.33 ± 0.25	4.20	0.03 ± 0.06	-0.03 ± 0.1	0.64	6.09	9.24	1.56
2M10243431+3643522	5774 ± 101	4.41 ± 0.13	4.37	-0.07 ± 0.04	-0.12 ± 0.1	0.73	4.28	8.58	0.49

APOGEE_ID	$T_{\rm eff} \pm \Delta T_{\rm eff}$	$\log g \pm \Delta \log g$	$\log g_{cor}$	$[{\rm M/H}] \pm \Delta[{\rm M/H}]$	$[Fe/H] \pm \Delta[{\rm Fe/H}]$	$v_{\rm mic}$	$v_{\rm mac}$	$v \sin i$	χ^2
2M10244479+4806233	5830 ± 121	4.08 ± 0.13	4.03	0.05 ± 0.05	-0.01 ± 0.1	0.83	4.45	9.46	0.61
2M10245150+3849371	5811 ± 111	4.34 ± 0.15	4.29	-0.12 ± 0.05	-0.19 ± 0.1	0.45	4.49	8.3	0.41
2M10250155+4050267	5602 ± 110	4.29 ± 0.13	4.29	0.04 ± 0.05	-0.02 ± 0.1	0.67	3.58	10.1	0.68
2M10250468+3734466	6050 ± 113	4.37 ± 0.15	4.26	0.03 ± 0.04	-0.04 ± 0.1	0.44	5.57	9.15	1.43
2M10251909+3440365	5704 ± 112	4.38 ± 0.16	4.36	-0.09 ± 0.05	-0.13 ± 0.1	0.69	4.04	8.49	0.45
2M10251918+3605543	6269 ± 147	4.46 ± 0.17	4.27	-0.29 ± 0.06	-0.32 ± 0.1	0.13	7.4	5.85	1.31
2M10253940+4054266	5990 ± 149	4.27 ± 0.16	4.18	0.01 ± 0.06	-0.08 ± 0.1	0.04	5.26	9.32	0.62
2M10255321+3836078	5666 ± 108	4.24 ± 0.13	4.23	0.05 ± 0.05	-0.01 ± 0.1	0.73	3.77	10.65	1.4
2M10255864+3435494	5862 ± 127	4.21 ± 0.16	4.15	-0.01 ± 0.05	-0.08 ± 0.1	0.65	4.63	9.53	0.62
2M10260789+3650331	5930 ± 110	4.27 ± 0.14	4.19	0.2 ± 0.05	0.15 ± 0.1	0.7	4.71	10.19	1.67
2M10261141+3806336	6061 ± 146	4.32 ± 0.19	4.21	0.04 ± 0.06	-0.02 ± 0.1	0.74	5.63	9.32	0.52
2M10263853+3504269	5622 ± 79	4.35 ± 0.12	4.35	-0.05 ± 0.03	-0.09 ± 0.1	0.71	3.73	10.13	1.46
2M10263903+3429356	5778 ± 113	4.1 ± 0.11	4.06	0.08 ± 0.05	0.03 ± 0.1	0.79	4.19	9.76	1.65
2M10264513+1752522	5749 ± 137	4.34 ± 0.16	4.31	-0.1 ± 0.06	-0.2 ± 0.1	0.4	4.22	9.33	1.4
2M10265710+4330024	6007 ± 154	4.27 ± 0.19	4.17	-0.08 ± 0.06	-0.14 ± 0.1	0.5	5.45	9.32	1.47
2M10265734+4149117	5714 ± 89	4.08 ± 0.09	4.06	-0.03 ± 0.04	-0.09 ± 0.1	0.67	4.07	8.82	0.52
2M10270044+1736036	5781 ± 109	4.1 ± 0.11	4.06	-0.04 ± 0.05	-0.11 ± 0.1	0.7	4.33	9.9	0.35
2M10270236+4656132	5636 ± 58	4.09 ± 0.06	4.09	0.11 ± 0.03	0.07 ± 0.1	0.84	3.65	9.55	1.58
2M10271902+1651190	5960 ± 146	4.36 ± 0.2	4.27	-0.14 ± 0.06	-0.22 ± 0.1	0	5.24	8.45	0.54
2M10271912+4810298	5949 ± 151	4.41 ± 0.22	4.33	-0.09 ± 0.06	-0.15 ± 0.1	0.52	5.12	9.37	0.56

APOGEE_ID	$T_{\rm eff} \pm \Delta T_{\rm eff}$	$\log g \pm \Delta \log g$	$\log g_{cor}$	$[\mathrm{M/H}] \pm \Delta[\mathrm{M/H}]$	$[Fe/H] \pm \Delta[\mathrm{Fe/H}]$	$\mathrm{v}_{\rm mic}$	$\mathrm{v}_{\rm mac}$	$v \sin i$	χ^2
2M10272110+3423277	5563 ± 75	4.31 ± 0.09	4.32	0.01 ± 0.03	-0.01 ± 0.1	0.8	3.5	9.61	1.49
2M10272848+3506063	5848 ± 121	4.34 ± 0.18	4.28	-0.1 ± 0.05	-0.17 ± 0.1	0.52	4.64	8.81	0.54
2M10273259+4710359	5883 ± 137	4.24 ± 0.18	4.17	0.1 ± 0.06	0.04 ± 0.1	0.69	4.6	10.73	1.75
2M10273587+3427483	5735 ± 118	4.4 ± 0.15	4.37	-0.17 ± 0.05	-0.23 ± 0.1	0.5	4.23	8.7	1.52
2M10273766+4550443	5829 ± 120	4.19 ± 0.16	4.14	-0.3 ± 0.05	-0.4 ± 0.1	0.12	4.78	8.03	1.43
2M10273936+4705061	5698 ± 133	4.31 ± 0.16	4.29	-0.01 ± 0.06	-0.06 ± 0.1	0.75	3.94	9.16	0.73
2M10274103+3524514	5565 ± 101	4.1 ± 0.1	4.11	0.17 ± 0.04	0.14 ± 0.1	1.06	3.38	9.52	1.98
2M10274212+1705182	5519 ± 125	4.29 ± 0.14	4.31	-0.18 ± 0.05	-0.25 ± 0.1	0.53	3.61	8.98	1.51
2M10274352+1621055	5974 ± 99	4.11 ± 0.1	4.02	0.02 ± 0.04	-0.05 ± 0.1	0.77	5.19	8.42	0.38
2M10274427+4629489	5811 ± 106	4.04 ± 0.11	3.99	0.12 ± 0.04	0.07 ± 0.1	0.89	4.3	10.26	1.46
2M10274749+1546248	5919 ± 148	4.28 ± 0.23	4.20	-0.29 ± 0.06	-0.4 ± 0.1	0.01	5.19	8.59	1.39
2M10275097+4629218	5896 ± 125	4.32 ± 0.18	4.25	0.07 ± 0.05	0 ± 0.1	0.55	4.68	9.67	1.51
2M10275231+4753032	5992 ± 103	4.23 ± 0.11	4.14	-0.03 ± 0.04	-0.11 ± 0.1	0.43	5.32	8.91	1.37
2M10280209+4332082	5730 ± 109	4.36 ± 0.13	4.33	-0.18 ± 0.05	-0.24 ± 0.1	0.31	4.22	8.58	0.49
2M10280724+3625361	5721 ± 124	4.35 ± 0.16	4.32	-0.18 ± 0.05	-0.26 ± 0.1	0.34	4.2	8.37	1.45
2M10281473+1554332	5831 ± 115	4.2 ± 0.14	4.15	-0.02 ± 0.05	-0.07 ± 0.1	0.7	4.5	10.05	1.44
2M10282001+4635563	5614 ± 80	4.14 ± 0.09	4.14	0.13 ± 0.04	0.09 ± 0.1	0.86	3.54	9.52	1.57
2M10282084+4012380	6161 ± 101	4.35 ± 0.16	4.21	-0.05 ± 0.04	-0.12 ± 0.1	0.05	6.37	7.64	0.35
2M10285127+3923546	5848 ± 118	4.32 ± 0.15	4.26	0.2 ± 0.05	0.16 ± 0.1	0.62	4.3	9.83	1.01
2M10285555+0050275	3943 ± 33	2.43 ± 0.11	2.43	-0.46 ± 0.03	-1.01 ± 0.1	0.01	4.22	9.08	4.93

APOGEE_ID	$T_{\rm eff} \pm \Delta T_{\rm eff}$	$\log g \pm \Delta \log g$	$\log g_{cor}$	$[\rm M/H] \pm \Delta[\rm M/H]$	$[Fe/H] \pm \Delta[\rm Fe/H]$	$\rm v_{mic}$	$\rm v_{mac}$	$v \sin i$	χ^2
2M10285878+4245585	5794 ± 122	4.32 ± 0.16	4.28	-0.07 ± 0.05	-0.14 ± 0.1	0.57	4.37	8.45	0.65
2M10290474+4159482	6084 ± 117	4.18 ± 0.14	4.06	-0.01 ± 0.04	-0.09 ± 0.1	0.58	5.86	8.83	0.42
2M10290765+4208500	5741 ± 131	4.35 ± 0.16	4.32	-0.21 ± 0.06	-0.28 ± 0.1	0.37	4.3	10.18	1.51
2M10291548+3945006	5712 ± 88	4.17 ± 0.09	4.15	-0.01 ± 0.04	-0.06 ± 0.1	0.64	4.02	8.74	0.5
2M10292064+3625109	5864 ± 105	4.36 ± 0.15	4.30	0.15 ± 0.04	0.11 ± 0.1	0.73	4.43	9.96	1.65
2M10293863+1651296	6093 ± 166	4.27 ± 0.24	4.15	-0.2 ± 0.07	-0.28 ± 0.1	0	6.09	8.39	0.44
2M10295837+3006524	6183 ± 105	4.4 ± 0.17	4.25	-0.1 ± 0.04	-0.19 ± 0.1	0.05	6.58	7.53	0.33
2M10300160+4334598	5854 ± 114	4.36 ± 0.17	4.30	-0.08 ± 0.05	-0.15 ± 0.1	0.54	4.64	8.27	0.5
2M10300573+1722400	6128 ± 133	4.29 ± 0.19	4.16	-0.01 ± 0.05	-0.11 ± 0.1	0.37	6.12	8.59	1.37
2M10300604+3543528	5593 ± 105	4.28 ± 0.14	4.29	-0.22 ± 0.05	-0.31 ± 0.1	0.58	3.84	9.17	0.38
2M10301114+1655138	5834 ± 112	4.07 ± 0.12	4.02	0.02 ± 0.05	-0.06 ± 0.1	0.74	4.5	9.81	0.48
2M10302693+4258577	5617 ± 102	4.34 ± 0.15	4.34	-0.15 ± 0.04	-0.2 ± 0.1	0.58	3.82	8.81	0.43
2M10302773+1500110	5838 ± 60	4.41 ± 0.08	4.35	-0.04 ± 0.02	-0.08 ± 0.1	0.61	4.52	9.57	1.34
2M10303492+3930586	5717 ± 80	4.11 ± 0.08	4.08	0.07 ± 0.03	0.02 ± 0.1	0.63	3.96	10.03	1.44
2M10303904+3607088	5872 ± 72	4.3 ± 0.1	4.24	0.21 ± 0.03	0.17 ± 0.1	0.77	4.4	9.73	0.57
2M10303923+4627251	5712 ± 129	4.36 ± 0.17	4.34	-0.18 ± 0.05	-0.23 ± 0.1	0.38	4.16	9.12	0.46
2M10304773+3613103	5783 ± 136	4.28 ± 0.15	4.24	0.02 ± 0.06	-0.03 ± 0.1	0.75	4.23	10.62	0.69
2M10311143+3613342	5745 ± 91	4.41 ± 0.1	4.38	0.04 ± 0.04	0 ± 0.1	0.77	4.05	10.52	1.39
2M10314054+4734009	5585 ± 93	4.08 ± 0.1	4.09	0.14 ± 0.04	0.1 ± 0.1	0.82	3.46	10.21	1.82
2M10321342+3610421	5854 ± 158	4.35 ± 0.25	4.29	-0.21 ± 0.07	-0.3 ± 0.1	0.28	4.78	8.28	1.47

APOGEE_ID	$T_{\rm eff} \pm \Delta T_{\rm eff}$	$\log g \pm \Delta \log g$	$\log g_{cor}$	$[\mathrm{M/H}] \pm \Delta[\mathrm{M/H}]$	$[Fe/H] \pm \Delta[\mathrm{Fe/H}]$	$\mathrm{v}_{\rm mic}$	$\mathrm{v}_{\rm mac}$	$v \sin i$	χ^2
2M10323843+3959348	5912 ± 118	4.33 ± 0.17	4.26	0.1 ± 0.05	0.06 ± 0.1	0.77	4.72	9.46	1.6
2M10324783+4317594	5826 ± 152	4.4 ± 0.22	4.35	-0.22 ± 0.06	-0.31 ± 0.1	0	4.66	8.11	1.66
2M10325508+1600213	5654 ± 111	4.39 ± 0.18	4.38	-0.17 ± 0.05	-0.21 ± 0.1	0.57	3.95	10.47	0.33
2M10330063+4405273	5695 ± 99	4.35 ± 0.13	4.33	-0.04 ± 0.04	-0.09 ± 0.1	0.65	3.95	10.02	0.44
2M10331723+4402297	5823 ± 100	4.2 ± 0.11	4.15	0.03 ± 0.04	-0.03 ± 0.1	0.72	4.4	8.19	0.58
2M10340011+4033396	6254 ± 103	4.37 ± 0.12	4.19	0.04 ± 0.04	-0.03 ± 0.1	0.53	6.95	9.84	1.34
2M10340765+4327531	6203 ± 90	4.32 ± 0.13	4.16	-0.06 ± 0.04	-0.16 ± 0.1	0.36	6.69	8.41	0.35
2M10344137+4318352	6151 ± 148	4.46 ± 0.19	4.32	-0.02 ± 0.06	-0.09 ± 0.1	0.43	6.26	9.26	0.79
2M10351978+4141118	5584 ± 95	4 ± 0.09	4.01	0.04 ± 0.04	-0.01 ± 0.1	0.82	3.61	9.77	1.63
2M10362334+4313302	5963 ± 131	4.2 ± 0.15	4.11	0.11 ± 0.05	0.05 ± 0.1	0.72	5.01	9.59	0.69
2M10364069+3339041	5883 ± 118	4.26 ± 0.16	4.19	0.12 ± 0.05	0.07 ± 0.1	0.73	4.57	10.26	1.59
2M10364963+4126093	6058 ± 155	4.19 ± 0.2	4.08	-0.06 ± 0.06	-0.14 ± 0.1	0.42	5.75	8.93	1.56
2M10370323+2405492	5914 ± 90	4.33 ± 0.13	4.26	0.03 ± 0.04	-0.02 ± 0.1	0.63	4.82	9.69	1.35
2M10371845+2337182	6082 ± 155	4.32 ± 0.23	4.20	-0.1 ± 0.06	-0.17 ± 0.1	0.48	5.91	7.95	1.39
2M10372552+2855416	4606 ± 29	4.4 ± 0.06	4.69	-0.29 ± 0.01	-0.33 ± 0.1	0.58	3.77	8.86	0.59
2M10372605+3542504	6037 ± 143	4.26 ± 0.19	4.15	-0.05 ± 0.06	-0.13 ± 0.1	0.44	5.59	10.34	1.54
2M10372821+4216278	5944 ± 125	4.38 ± 0.19	4.30	-0.07 ± 0.05	-0.13 ± 0.1	0.57	5.08	8.03	1.63
2M10373501+4244424	5787 ± 96	4.36 ± 0.13	4.32	-0.19 ± 0.04	-0.24 ± 0.1	0.3	4.46	8.75	0.4
2M10373678+1820584	5824 ± 127	4.18 ± 0.14	4.13	0.12 ± 0.05	0.07 ± 0.1	0.77	4.31	10.94	1.49
2M10380533+2459104	6166 ± 84	4.43 ± 0.12	4.28	-0.1 ± 0.03	-0.18 ± 0.1	0	6.46	7.87	0.31

APOGEE_ID	$T_{\rm eff} \pm \Delta T_{\rm eff}$	$\log g \pm \Delta \log g$	$\log g_{cor}$	$[\rm M/H] \pm \Delta[\rm M/H]$	$[Fe/H] \pm \Delta[\rm Fe/H]$	$v_{\rm mic}$	$v_{\rm mac}$	$v \sin i$	χ^2
2M10382956+2821403	6036 ± 119	4.38 ± 0.15	4.27	0.09 ± 0.05	0.03 ± 0.1	0.6	5.42	10.27	1.6
2M10383605+4045283	6205 ± 112	4.51 ± 0.11	4.35	0 ± 0.04	-0.07 ± 0.1	0	6.62	9.17	1.34
2M10390002+3458490	5969 ± 153	4.37 ± 0.22	4.28	-0.22 ± 0.06	-0.3 ± 0.1	0.11	5.37	8.64	1.44
2M10390051+3903246	6041 ± 128	4.13 ± 0.15	4.02	-0.17 ± 0.05	-0.26 ± 0.1	0.45	5.78	7.38	1.46
2M10390747+4147366	5839 ± 98	4.16 ± 0.11	4.10	0.1 ± 0.04	0.06 ± 0.1	0.79	4.42	9.84	0.6
2M10392411+4157446	5646 ± 97	4.21 ± 0.13	4.20	-0.05 ± 0.04	-0.11 ± 0.1	0.56	3.82	9.72	1.51
2M10394344+4204144	5888 ± 151	4.36 ± 0.25	4.29	-0.14 ± 0.06	-0.19 ± 0.1	0.3	4.87	7.99	1.45
2M10395048+4209052	5999 ± 565	4.23 ± 0.67	4.13	-0.97 ± 0.22	-0.93 ± 0.1	0	6.21	8.44	3.87
2M10395058+3750204	4878 ± 78	3.29 ± 0.12	3.29	0.08 ± 0.05	0 ± 0.1	0.9	3.53	11.14	2.02
2M10395292+3027516	5935 ± 110	4.29 ± 0.14	4.21	0.13 ± 0.04	0.09 ± 0.1	0.83	4.82	10.69	1.44
2M10404293+3941236	5963 ± 140	4.32 ± 0.17	4.23	0.02 ± 0.06	-0.05 ± 0.1	0.57	5.09	9.75	0.52
2M10405479-1130212	6144 ± 118	4.29 ± 0.17	4.15	0.04 ± 0.05	-0.05 ± 0.1	0.42	6.17	9.44	0.35
2M10405568+3012047	6163 ± 69	4.39 ± 0.1	4.25	0.01 ± 0.03	-0.07 ± 0.1	0.36	6.32	9.11	1.34
2M10405723+2938257	6106 ± 90	4.41 ± 0.13	4.29	0.07 ± 0.04	0.02 ± 0.1	0.49	5.88	9.5	1.37
2M10413012+3833447	6166 ± 147	4.24 ± 0.22	4.09	-0.17 ± 0.06	-0.26 ± 0.1	0.36	6.56	7.93	0.41
2M10414370+4014257	5936 ± 148	4.24 ± 0.19	4.16	0.03 ± 0.06	-0.05 ± 0.1	0.75	4.94	10.06	0.54
2M10414970+3839055	6078 ± 122	4.32 ± 0.18	4.20	-0.09 ± 0.05	-0.16 ± 0.1	0.35	5.88	8.23	0.34
2M10422007+2416225	5875 ± 117	4.32 ± 0.17	4.25	0.01 ± 0.05	-0.04 ± 0.1	0.73	4.64	9.6	1.42
2M10432764+2005134	6104 ± 115	4.31 ± 0.16	4.19	0.04 ± 0.04	-0.04 ± 0.1	0.48	5.9	9.16	0.41
2M10452758-1103250	6205 ± 165	4.34 ± 0.24	4.18	-0.13 ± 0.07	-0.22 ± 0.1	0.12	6.77	8.44	0.37

APOGEE_ID	$T_{\rm eff} \pm \Delta T_{\rm eff}$	$\log g \pm \Delta \log g$	$\log g_{cor}$	$[\mathrm{M/H}] \pm \Delta[\mathrm{M/H}]$	$[Fe/H] \pm \Delta[\mathrm{Fe/H}]$	$\mathrm{v_{mic}}$	$\mathrm{v_{mac}}$	$v \sin i$	χ^2
2M10453805+1942555	6014 ± 137	4.31 ± 0.16	4.21	0.05 ± 0.05	-0.01 ± 0.1	0.56	5.34	9.25	0.54
2M10462126+4439179	5997 ± 152	4.25 ± 0.18	4.15	-0.17 ± 0.06	-0.26 ± 0.1	0.3	5.5	8.29	1.38
2M10471913+2047124	5788 ± 66	4.41 ± 0.08	4.37	-0.03 ± 0.03	-0.09 ± 0.1	0.89	4.29	9.31	0.31
2M10483652+1534167	5628 ± 101	4.23 ± 0.13	4.23	0.1 ± 0.04	0.05 ± 0.1	0.86	3.6	10.78	1.69
2M10484541+2024105	6077 ± 156	4.31 ± 0.22	4.19	-0.04 ± 0.06	-0.11 ± 0.1	0.42	5.82	9.37	0.54
2M10484765-0215451	5558 ± 124	4.38 ± 0.15	4.39	-0.01 ± 0.05	-0.05 ± 0.1	1.23	3.5	9.44	1.74
2M10485175+4308040	5879 ± 149	4.25 ± 0.23	4.18	-0.24 ± 0.06	-0.34 ± 0.1	0.31	4.94	8.53	1.4
2M10491547+4411318	5939 ± 107	4.5 ± 0.11	4.42	-0.09 ± 0.04	-0.14 ± 0.1	0.14	5.07	8.94	1.5
2M10492661+4528377	5460 ± 81	4.31 ± 0.09	4.35	0.03 ± 0.03	0 ± 0.1	1.17	3.25	11	1.72
2M10493262+4438345	5791 ± 136	4.23 ± 0.15	4.19	0.02 ± 0.06	-0.04 ± 0.1	0.48	4.28	10.48	0.69
2M10494357+1527559	5879 ± 107	4.37 ± 0.15	4.30	0.12 ± 0.04	0.1 ± 0.1	0.85	4.54	9.27	1.53
2M10502613+4528386	5770 ± 129	4.35 ± 0.16	4.31	-0.19 ± 0.05	-0.26 ± 0.1	0	4.39	10.11	0.4
2M10502718+4330480	6204 ± 150	4.37 ± 0.2	4.21	-0.02 ± 0.06	-0.09 ± 0.1	0.12	6.64	8.51	0.41
2M10511672+4432041	5641 ± 100	4.24 ± 0.13	4.23	0.05 ± 0.04	0.02 ± 0.1	0.76	3.7	9.47	0.55
2M10512983+0005046	5916 ± 136	4.34 ± 0.22	4.26	-0.05 ± 0.06	-0.12 ± 0.1	0.54	4.91	9.82	0.72
2M10521407+4454034	5538 ± 87	4.25 ± 0.09	4.27	0.02 ± 0.04	-0.02 ± 0.1	0.83	3.44	10.35	1.6
2M10522557+4312252	6193 ± 175	4.26 ± 0.25	4.10	-0.12 ± 0.07	-0.2 ± 0.1	0.24	6.69	8.85	0.45
2M10523515+4330310	5780 ± 106	4.27 ± 0.12	4.23	0.19 ± 0.04	0.14 ± 0.1	0.6	4.03	9.62	1.71
2M10524011-0034333	6035 ± 130	4.25 ± 0.16	4.14	-0.03 ± 0.05	-0.11 ± 0.1	0.51	5.56	9.08	0.59
2M10530070+4452296	5722 ± 131	4.27 ± 0.14	4.24	0.05 ± 0.05	-0.03 ± 0.1	0.64	3.96	10.34	0.69

APOGEE_ID	$T_{\rm eff} \pm \Delta T_{\rm eff}$	$\log g \pm \Delta \log g$	$\log g_{cor}$	$[{\rm M/H}] \pm \Delta[{\rm M/H}]$	$[Fe/H] \pm \Delta[{\rm Fe/H}]$	$v_{\rm mic}$	$v_{\rm mac}$	$v \sin i$	χ^2
2M10533147+4426016	5815 ± 118	4.41 ± 0.16	4.36	-0.08 ± 0.05	-0.12 ± 0.1	0.33	4.46	9.9	0.56
2M10534362+0041564	5662 ± 101	4.19 ± 0.12	4.18	0 ± 0.04	-0.06 ± 0.1	0.86	3.82	9.98	0.52
2M10535047+0003072	5971 ± 171	4.27 ± 0.23	4.18	-0.23 ± 0.07	-0.35 ± 0.1	0.53	5.41	7.23	1.7
2M10542795+4232420	6181 ± 91	4.5 ± 0.09	4.35	0.19 ± 0.04	0.14 ± 0.1	0.5	6.23	10.01	1.4
2M10544803+0100056	5781 ± 142	4.21 ± 0.16	4.17	-0.04 ± 0.06	-0.11 ± 0.1	0.62	4.3	9.53	0.7
2M10544811-0035230	6166 ± 102	4.37 ± 0.17	4.22	-0.06 ± 0.04	-0.13 ± 0.1	0.25	6.42	8.26	0.42
2M10545053-0009534	5879 ± 151	4.24 ± 0.22	4.17	-0.03 ± 0.06	-0.11 ± 0.1	0.64	4.72	9.37	0.86
2M10552061+4444190	5798 ± 65	4.25 ± 0.07	4.20	0.25 ± 0.03	0.19 ± 0.1	0.66	4.03	10.21	1.74
2M10552298+4127346	5921 ± 68	4.34 ± 0.09	4.26	0.03 ± 0.03	-0.02 ± 0.1	0.55	4.85	9.06	0.38
2M10552537-0048469	6104 ± 72	4.35 ± 0.1	4.23	0.06 ± 0.03	-0.01 ± 0.1	0.71	5.87	7.84	1.37
2M10553470+4403515	5880 ± 124	4.3 ± 0.17	4.23	0.04 ± 0.05	0 ± 0.1	0.69	4.64	10.22	0.53
2M10555134+4508004	5742 ± 105	4.1 ± 0.11	4.07	-0.07 ± 0.05	-0.14 ± 0.1	0.64	4.21	9.17	1.43
2M10555738-0100081	6211 ± 73	4.33 ± 0.1	4.17	-0.17 ± 0.03	-0.27 ± 0.1	0	6.86	7.11	0.37
2M10560954+4325534	5758 ± 68	4.17 ± 0.07	4.13	0.11 ± 0.03	0.08 ± 0.1	0.79	4.05	9.4	1.52
2M10561124+4417040	5542 ± 124	4.33 ± 0.15	4.35	-0.14 ± 0.05	-0.21 ± 0.1	0.58	3.61	10.3	1.7
2M10563378-0110409	5767 ± 114	4.23 ± 0.14	4.19	-0.25 ± 0.05	-0.35 ± 0.1	0.39	4.46	8.13	0.59
2M10563417-0138448	6039 ± 102	4.44 ± 0.11	4.33	0.1 ± 0.04	0.05 ± 0.1	0.62	5.42	10.78	0.53
2M10564105+4406080	6232 ± 146	4.36 ± 0.18	4.19	-0.01 ± 0.05	-0.07 ± 0.1	0.38	6.83	8.29	1.38
2M10570874+4342114	5656 ± 94	4.1 ± 0.11	4.09	0.15 ± 0.04	0.12 ± 0.1	0.78	3.66	9.5	1.72
2M10570923+6516412	5717 ± 116	4.2 ± 0.13	4.17	0.26 ± 0.05	0.19 ± 0.1	0.79	3.72	11.61	1.67

APOGEE_ID	$T_{\mathrm{eff}} \pm \Delta T_{\mathrm{eff}}$	$\log g \pm \Delta \log g$	$\log g_{cor}$	$[\mathrm{M/H}] \pm \Delta[\mathrm{M/H}]$	$[Fe/H] \pm \Delta[\mathrm{Fe/H}]$	v_{mic}	v_{mac}	$v \sin i$	χ^2
2M10570923+6516412	5673 ± 119	4.12 ± 0.13	4.11	0.16 ± 0.05	0.19 ± 0.1	0.84	3.7	11.16	1.68
2M10571914+4519062	5835 ± 151	4.26 ± 0.2	4.20	-0.13 ± 0.06	-0.21 ± 0.1	0.3	4.63	8.04	1.6
2M10572060+1537578	6015 ± 112	4.25 ± 0.12	4.15	0.06 ± 0.04	-0.02 ± 0.1	0.62	5.35	9.77	0.4
2M10572333+4145438	5946 ± 136	4.23 ± 0.17	4.15	-0.02 ± 0.06	-0.08 ± 0.1	0.57	5.05	9.05	1.6
2M10573061+4354013	5941 ± 115	4.42 ± 0.16	4.34	-0.11 ± 0.05	-0.16 ± 0.1	0.34	5.1	7.21	1.43
2M10573640+2244120	6100 ± 134	4.36 ± 0.2	4.24	-0.03 ± 0.05	-0.1 ± 0.1	0.53	5.95	9.21	1.41
2M10573815+4421489	5860 ± 78	4.1 ± 0.09	4.04	0.05 ± 0.03	0 ± 0.1	0.76	4.58	10.33	1.35
2M10574086+2239331	5758 ± 119	4.15 ± 0.11	4.11	0.01 ± 0.05	-0.06 ± 0.1	0.55	4.17	9.32	1.53
2M10575237+4341110	5618 ± 103	4.38 ± 0.16	4.38	-0.08 ± 0.04	-0.11 ± 0.1	0.65	3.74	8.65	1.6
2M10575304+4527210	5704 ± 129	4.42 ± 0.16	4.40	-0.11 ± 0.06	-0.16 ± 0.1	0.54	4.05	10.96	1.54
2M10580678+4419052	5847 ± 89	4.07 ± 0.1	4.01	-0.02 ± 0.04	-0.08 ± 0.1	0.6	4.61	10.06	0.38
2M10580748+4126026	6196 ± 149	4.36 ± 0.2	4.20	0.08 ± 0.06	0.01 ± 0.1	0.63	6.48	8.37	1.48
2M10580813+4219443	5643 ± 131	4.11 ± 0.17	4.10	-0.21 ± 0.06	-0.31 ± 0.1	0.55	4.01	8.61	0.56
2M10580952+4306295	5639 ± 123	4.37 ± 0.19	4.36	-0.19 ± 0.05	-0.24 ± 0.1	0.51	3.93	9.27	1.47
2M10582443-0105271	6205 ± 170	4.3 ± 0.24	4.14	-0.11 ± 0.07	-0.19 ± 0.1	0.32	6.75	7.88	0.63
2M10582590+4458400	5900 ± 131	4.29 ± 0.19	4.22	0.03 ± 0.05	-0.03 ± 0.1	0.64	4.75	9.79	1.5
2M10585107+2159515	6120 ± 127	4.31 ± 0.2	4.18	-0.16 ± 0.05	-0.25 ± 0.1	0.17	6.22	8.1	1.41
2M10590561+4541180	5701 ± 75	4.21 ± 0.08	4.19	0.1 ± 0.03	0.05 ± 0.1	0.76	3.84	10.19	0.45
2M10590946+4509138	5922 ± 142	4.12 ± 0.17	4.04	0.05 ± 0.06	-0.01 ± 0.1	0.69	4.88	11.12	1.52
2M10591629+4349039	6008 ± 105	4.18 ± 0.12	4.08	-0.12 ± 0.04	-0.18 ± 0.1	0.22	5.52	6.21	1.43

APOGEE_ID	$T_{\rm eff} \pm \Delta T_{\rm eff}$	$\log g \pm \Delta \log g$	$\log g_{cor}$	$[\rm M/H] \pm \Delta[\rm M/H]$	$[Fe/H] \pm \Delta[\rm Fe/H]$	$\rm v_{mic}$	$\rm v_{mac}$	$v \sin i$	χ^2
2M10591734+4339102	5776 ± 124	4.38 ± 0.14	4.34	0.01 ± 0.05	-0.02 ± 0.1	0.51	4.19	9.67	0.54
2M10591827+4515392	5768 ± 118	4.28 ± 0.13	4.24	0.06 ± 0.05	0.03 ± 0.1	0.76	4.13	10.25	0.73
2M10591974+4758574	5961 ± 146	4.31 ± 0.18	4.22	-0.01 ± 0.06	-0.08 ± 0.1	0.63	5.11	8.81	1.28
2M10592720+2121352	5947 ± 138	4.36 ± 0.19	4.28	-0.02 ± 0.06	-0.06 ± 0.1	0.54	5.04	9.85	0.43
2M10594029+4209239	5835 ± 66	4.4 ± 0.09	4.34	-0.01 ± 0.03	-0.05 ± 0.1	0.57	4.48	9.97	1.42
2M10594046+5010239	5793 ± 147	4.27 ± 0.18	4.23	-0.21 ± 0.06	-0.29 ± 0.1	0	4.52	7.93	0.55
2M10594700+4534075	5597 ± 74	4.05 ± 0.08	4.05	0.18 ± 0.03	0.13 ± 0.1	0.88	3.47	9.64	1.64
2M10594852+4225497	5688 ± 119	4.28 ± 0.14	4.26	0.04 ± 0.05	0 ± 0.1	0.69	3.85	10.29	0.64
2M10594959+4509175	5715 ± 142	4.24 ± 0.18	4.22	-0.3 ± 0.06	-0.37 ± 0.1	0	4.31	7.19	0.56
2M10595749+4446439	4887 ± 196	2.26 ± 0.43	2.26	-1.69 ± 0.1	-1.66 ± 0.1	0	5.51	8.12	1.25
2M10595793+2105218	6171 ± 128	4.43 ± 0.17	4.28	0.12 ± 0.05	0.07 ± 0.1	0.74	6.25	10.17	0.38
2M11000340-0016339	6150 ± 115	4.31 ± 0.19	4.17	-0.09 ± 0.05	-0.16 ± 0.1	0.31	6.35	8.02	0.45
2M11000625+4350110	5757 ± 115	4.29 ± 0.12	4.25	0.15 ± 0.05	0.1 ± 0.1	0.71	3.98	10.37	2.23
2M11001654+0005024	5796 ± 102	4.26 ± 0.12	4.21	0.07 ± 0.04	-0.01 ± 0.1	0.52	4.23	10.27	1.52
2M11002057+4558316	6136 ± 162	4.43 ± 0.22	4.30	-0.01 ± 0.06	-0.1 ± 0.1	0.29	6.16	8.22	0.61
2M11002992+4153109	5553 ± 92	4.28 ± 0.11	4.30	-0.03 ± 0.04	-0.07 ± 0.1	0.8	3.53	9.6	0.45
2M11004670+4156580	6126 ± 122	4.37 ± 0.18	4.24	0.11 ± 0.05	0.06 ± 0.1	0.61	5.96	10.31	1.52
2M11004924+4336599	6036 ± 162	4.44 ± 0.18	4.33	-0.01 ± 0.06	-0.07 ± 0.1	0.55	5.52	10.08	0.76
2M11005447+4217173	6183 ± 149	4.18 ± 0.2	4.03	-0.04 ± 0.06	-0.12 ± 0.1	0.51	6.55	8.56	1.55
2M11010315+4432556	5657 ± 88	4.3 ± 0.12	4.29	-0.02 ± 0.04	-0.07 ± 0.1	0.7	3.81	10.16	0.4

APOGEE_ID	$T_{\rm eff} \pm \Delta T_{\rm eff}$	$\log g \pm \Delta \log g$	$\log g_{cor}$	$[\mathrm{M/H}] \pm \Delta[\mathrm{M/H}]$	$[Fe/H] \pm \Delta[\mathrm{Fe/H}]$	$\mathrm{v}_{\rm mic}$	$\mathrm{v}_{\rm mac}$	$v \sin i$	χ^2
2M11011451+4928416	6107 ± 89	4.23 ± 0.13	4.11	-0.09 ± 0.04	-0.17 ± 0.1	0.3	6.07	9.29	0.31
2M11012375+4540147	5785 ± 81	4.35 ± 0.1	4.31	-0.02 ± 0.03	-0.08 ± 0.1	0.75	4.27	9.39	1.39
2M11013201+2234497	5906 ± 118	4.38 ± 0.18	4.31	-0.02 ± 0.05	-0.08 ± 0.1	0.52	4.83	9.76	1.51
2M11013207+4213481	5994 ± 129	4.35 ± 0.17	4.25	-0.06 ± 0.05	-0.13 ± 0.1	0.29	5.35	9.73	0.63
2M11014585+4052317	5783 ± 115	4.02 ± 0.12	3.98	-0.17 ± 0.05	-0.23 ± 0.1	0.65	4.51	8.73	1.5
2M11014882+4259295	6074 ± 159	4.34 ± 0.24	4.22	-0.11 ± 0.06	-0.19 ± 0.1	0.49	5.87	8.97	1.69
2M11015499+4421500	6003 ± 67	4.38 ± 0.09	4.28	-0.16 ± 0.03	-0.22 ± 0.1	0.28	5.49	8.32	1.33
2M11015513+2059227	5942 ± 142	4.22 ± 0.19	4.14	-0.14 ± 0.06	-0.2 ± 0.1	0.5	5.16	10.46	0.45
2M11020093+4208206	5922 ± 115	4.35 ± 0.16	4.27	0.11 ± 0.05	0.06 ± 0.1	0.7	4.76	10.49	0.7
2M11021726+4246517	5773 ± 116	4.3 ± 0.14	4.26	-0.06 ± 0.05	-0.12 ± 0.1	0.58	4.27	9.51	1.49
2M11021820+4328594	6138 ± 87	4.38 ± 0.13	4.25	0.1 ± 0.03	0.04 ± 0.1	0.62	6.06	9.3	0.37
2M11022299+4527199	5588 ± 83	4.26 ± 0.1	4.27	0.06 ± 0.04	0.02 ± 0.1	0.89	3.52	10.32	0.56
2M11022388+2204433	5715 ± 117	4.34 ± 0.14	4.32	0.08 ± 0.05	0.03 ± 0.1	0.66	3.9	10.36	1.52
2M11022773+4318073	5999 ± 109	4.4 ± 0.13	4.30	0.08 ± 0.04	0.04 ± 0.1	0.61	5.21	9.39	0.45
2M11023427-1125245	6087 ± 126	4.25 ± 0.16	4.13	0.13 ± 0.05	0.07 ± 0.1	0.68	5.7	11.02	0.43
2M11023625+4618567	5597 ± 87	3.99 ± 0.09	3.99	0.03 ± 0.04	-0.03 ± 0.1	0.86	3.66	11.02	0.5
2M11023673+4236179	5566 ± 117	4.31 ± 0.15	4.32	-0.09 ± 0.05	-0.15 ± 0.1	0.79	3.62	9.8	1.62
2M11024211+4253281	6251 ± 150	4.34 ± 0.17	4.16	0.02 ± 0.06	-0.07 ± 0.1	0.43	6.95	8.05	0.54
2M11024926+4310018	6215 ± 127	4.31 ± 0.16	4.14	0.06 ± 0.05	-0.01 ± 0.1	0.41	6.64	8.31	0.59
2M11025619+5014085	5878 ± 86	4.26 ± 0.12	4.19	0.15 ± 0.04	0.09 ± 0.1	0.71	4.51	10.02	0.43

APOGEE_ID	$T_{\rm eff} \pm \Delta T_{\rm eff}$	$\log g \pm \Delta \log g$	$\log g_{cor}$	$[{\rm M/H}] \pm \Delta[{\rm M/H}]$	$[Fe/H] \pm \Delta[{\rm Fe/H}]$	$v_{\rm mic}$	$v_{\rm mac}$	$v \sin i$	χ^2
2M11030450+4648456	6136 ± 120	4.48 ± 0.13	4.35	0.21 ± 0.05	0.16 ± 0.1	0.71	5.9	10.83	0.6
2M11031120+2142247	5800 ± 114	4.24 ± 0.13	4.19	0.06 ± 0.05	0.03 ± 0.1	0.79	4.27	9.89	0.43
2M11031145+2200259	4667 ± 48	4.34 ± 0.07	4.61	0.12 ± 0.02	0.05 ± 0.1	0.65	3.69	8.98	1.8
2M11031904+2322367	5692 ± 74	4.07 ± 0.09	4.05	-0.06 ± 0.03	-0.11 ± 0.1	0.65	4.03	10.77	1.36
2M11032795+4124350	6299 ± 99	4.51 ± 0.1	4.31	0.19 ± 0.04	0.16 ± 0.1	0.94	7.11	8.86	1.41
2M11033894+2309335	6168 ± 134	4.38 ± 0.19	4.23	0.04 ± 0.05	-0.03 ± 0.1	0.52	6.32	8.44	1.4
2M11035321+4139208	5741 ± 110	4.25 ± 0.11	4.22	0.02 ± 0.05	-0.03 ± 0.1	0.68	4.07	9.7	1.33
2M11041309+4615122	6030 ± 141	4.36 ± 0.19	4.26	-0.11 ± 0.06	-0.18 ± 0.1	0	5.6	7.81	1.54
2M11041486+5045134	5771 ± 138	4.29 ± 0.15	4.25	-0.02 ± 0.06	-0.1 ± 0.1	0.4	4.23	10.92	0.53
2M11041963+4119301	5598 ± 63	4.02 ± 0.06	4.02	0.15 ± 0.03	0.1 ± 0.1	0.87	3.51	9.76	0.65
2M11042502+4244242	5851 ± 106	4.2 ± 0.13	4.14	0.08 ± 0.04	0.02 ± 0.1	0.75	4.48	8.92	1.5
2M11042566+2148114	5877 ± 135	4.38 ± 0.2	4.31	0.06 ± 0.06	-0.01 ± 0.1	0.61	4.59	10.37	1.66
2M11042819+2052565	5774 ± 106	4.21 ± 0.11	4.17	0 ± 0.04	-0.06 ± 0.1	0.54	4.23	9.02	1.47
2M11044005+4337367	6152 ± 166	4.3 ± 0.27	4.16	-0.12 ± 0.07	-0.19 ± 0.1	0.24	6.39	7.78	0.57
2M11044455+4055547	5827 ± 134	4.13 ± 0.17	4.08	-0.08 ± 0.06	-0.14 ± 0.1	0.64	4.57	8.32	1.7
2M11044684+4745113	5665 ± 96	4.31 ± 0.13	4.30	0.04 ± 0.04	0.02 ± 0.1	0.89	3.76	10.26	0.44
2M11045265+4134226	5842 ± 123	4.32 ± 0.16	4.26	0.01 ± 0.05	-0.04 ± 0.1	0.67	4.5	9.96	1.61
2M11045941+4339171	6123 ± 125	4.29 ± 0.19	4.16	-0.04 ± 0.05	-0.09 ± 0.1	0.36	6.12	10.07	1.41
2M11051428+4308303	5822 ± 89	4.13 ± 0.11	4.08	-0.04 ± 0.04	-0.09 ± 0.1	0.68	4.5	9.75	1.43
2M11051545+2512070	5951 ± 181	4.16 ± 0.22	4.08	-0.17 ± 0.07	-0.26 ± 0.1	0.37	5.26	8.56	0.42

APOGEE_ID	$T_{\rm eff} \pm \Delta T_{\rm eff}$	$\log g \pm \Delta \log g$	$\log g_{cor}$	$[\mathrm{M/H}] \pm \Delta[\mathrm{M/H}]$	$[Fe/H] \pm \Delta[\mathrm{Fe/H}]$	$v_{\rm mic}$	$v_{\rm mac}$	$v \sin i$	χ^2
2M11051641+4654442	5636 ± 114	4.06 ± 0.13	4.06	0.11 ± 0.05	0.06 ± 0.1	0.78	3.65	10.75	1.02
2M11054521+4517012	5552 ± 133	3.96 ± 0.13	3.98	-0.02 ± 0.06	-0.12 ± 0.1	0.29	3.61	9.29	1.78
2M11054988+4229452	5815 ± 109	4.21 ± 0.12	4.16	0.12 ± 0.04	0.07 ± 0.1	0.78	4.27	10.33	0.58
2M11060707+4137326	5864 ± 90	4.34 ± 0.14	4.28	-0.09 ± 0.04	-0.14 ± 0.1	0.48	4.7	9.85	1.42
2M11063336+4304296	5915 ± 148	4.41 ± 0.22	4.33	-0.04 ± 0.06	-0.09 ± 0.1	0.5	4.89	9.31	1.59
2M11065006+4436412	5785 ± 132	4.24 ± 0.16	4.20	-0.09 ± 0.06	-0.15 ± 0.1	0.5	4.37	8.47	0.75
2M11065359+5015523	5734 ± 107	4.14 ± 0.11	4.11	0.13 ± 0.04	0.09 ± 0.1	0.78	3.94	9.66	1.71
2M11065590+4240242	5763 ± 133	4.38 ± 0.17	4.34	-0.06 ± 0.06	-0.14 ± 0.1	0.59	4.23	9.36	0.53
2M11070162+2128357	5881 ± 136	4.18 ± 0.17	4.11	0.06 ± 0.06	0.01 ± 0.1	0.63	4.65	9.56	0.49
2M11070301+4440193	5785 ± 118	4.27 ± 0.13	4.23	0.02 ± 0.05	-0.03 ± 0.1	0.65	4.24	10.49	0.57
2M11070586+4547128	5949 ± 91	4.31 ± 0.11	4.23	0.02 ± 0.04	-0.05 ± 0.1	0.51	5.01	9.21	0.41
2M11071531-1133257	6199 ± 166	4.42 ± 0.21	4.26	-0.02 ± 0.06	-0.09 ± 0.1	0.39	6.6	8.58	0.4
2M11072348+4202107	5871 ± 78	4.21 ± 0.1	4.15	0.2 ± 0.03	0.16 ± 0.1	0.8	4.42	9.64	1.51
2M11072791+4207244	5978 ± 147	4.3 ± 0.19	4.21	-0.13 ± 0.06	-0.22 ± 0.1	0.31	5.33	8.74	0.48
2M11073690+4329326	5594 ± 103	4.23 ± 0.12	4.24	0.01 ± 0.04	-0.03 ± 0.1	0.92	3.61	9.98	0.77
2M11073936+4256129	5907 ± 144	4.3 ± 0.22	4.23	-0.03 ± 0.06	-0.11 ± 0.1	0.56	4.86	9.87	1.51
2M11074117+4348378	5663 ± 128	4.41 ± 0.18	4.40	-0.08 ± 0.06	-0.11 ± 0.1	0.66	3.88	10.55	0.58
2M11075093+4501392	5764 ± 101	4.39 ± 0.13	4.35	-0.06 ± 0.04	-0.11 ± 0.1	0.64	4.23	10.43	1.53
2M11075990-0646510	5932 ± 107	4.37 ± 0.17	4.29	-0.14 ± 0.04	-0.21 ± 0.1	0.33	5.09	8.68	0.39
2M11080676+4410428	5344 ± 67	3.63 ± 0.09	3.63	-0.36 ± 0.03	-0.41 ± 0.1	0.76	3.78	10.23	1.4

APOGEE_ID	$T_{\mathrm{eff}} \pm \Delta T_{\mathrm{eff}}$	$\log g \pm \Delta \log g$	$\log g_{cor}$	$[\mathrm{M/H}] \pm \Delta[\mathrm{M/H}]$	$[Fe/H] \pm \Delta[\mathrm{Fe/H}]$	$\mathrm{v}_{\mathrm{mic}}$	$\mathrm{v}_{\mathrm{mac}}$	$v \sin i$	χ^2
2M11081574+4127326	6164 ± 151	4.27 ± 0.21	4.13	0.06 ± 0.06	0 ± 0.1	0.61	6.29	8.76	0.61
2M11082267+4644137	5727 ± 133	4.4 ± 0.17	4.37	-0.18 ± 0.06	-0.23 ± 0.1	0.51	4.21	9.58	0.5
2M11083381-0442411	6188 ± 138	4.28 ± 0.2	4.13	-0.2 ± 0.05	-0.31 ± 0.1	0.13	6.73	7.79	0.37
2M11085822+4441419	5953 ± 140	4.35 ± 0.18	4.27	-0.02 ± 0.05	-0.08 ± 0.1	0.52	5.08	8.67	0.57
2M11093314+4600583	5621 ± 124	4.25 ± 0.15	4.25	0 ± 0.05	-0.04 ± 0.1	0.81	3.68	10.37	1.66
2M11094090+4323000	5821 ± 120	4.33 ± 0.17	4.28	-0.23 ± 0.05	-0.32 ± 0.1	0.45	4.65	8.01	1.45
2M11094496+4239015	6049 ± 126	4.37 ± 0.16	4.26	0.04 ± 0.05	-0.01 ± 0.1	0.6	5.55	9.97	1.71
2M11101609+4513337	6035 ± 135	4.39 ± 0.17	4.28	0.02 ± 0.05	-0.04 ± 0.1	0.4	5.49	10.09	0.56
2M11101733+5023408	5862 ± 124	4.12 ± 0.14	4.06	0.03 ± 0.05	-0.05 ± 0.1	0.66	4.61	9.38	0.5
2M11101993+4436011	5776 ± 131	4.03 ± 0.13	3.99	-0.04 ± 0.06	-0.09 ± 0.1	0.75	4.34	10.18	0.75
2M11102500+4857451	5958 ± 100	4.18 ± 0.11	4.09	0.1 ± 0.04	0.06 ± 0.1	0.71	4.99	9.83	1.53
2M11102897+4957172	5732 ± 95	4.08 ± 0.09	4.05	0.01 ± 0.04	-0.05 ± 0.1	0.65	4.09	8.91	1.54
2M11104506+4641504	5972 ± 143	4.34 ± 0.18	4.25	-0.02 ± 0.06	-0.09 ± 0.1	0.44	5.18	8.95	0.51
2M11105803+4610377	6161 ± 120	4.41 ± 0.19	4.27	-0.04 ± 0.05	-0.12 ± 0.1	0.31	6.36	8.23	1.38
2M11110760+4646132	6032 ± 119	4.32 ± 0.14	4.22	0.01 ± 0.05	-0.07 ± 0.1	0.58	5.49	8.72	0.49
2M11112736+2330479	5795 ± 137	4.08 ± 0.14	4.04	-0.04 ± 0.06	-0.11 ± 0.1	0.57	4.4	8.78	1.57
2M11113688+4549517	5842 ± 161	4.24 ± 0.22	4.18	-0.18 ± 0.07	-0.26 ± 0.1	0.47	4.71	8.33	0.59
2M11115866+2250111	5734 ± 97	4.27 ± 0.1	4.24	0.04 ± 0.04	0 ± 0.1	0.72	4.01	10.36	1.49
2M11122448+5032584	6186 ± 194	4.17 ± 0.26	4.02	-0.18 ± 0.08	-0.3 ± 0.1	0.29	6.73	8.58	0.43
2M11125204+4903508	5881 ± 129	4.34 ± 0.2	4.27	-0.13 ± 0.05	-0.18 ± 0.1	0.39	4.82	8.56	0.43

APOGEE_ID	$T_{\rm eff} \pm \Delta T_{\rm eff}$	$\log g \pm \Delta \log g$	$\log g_{cor}$	$[\rm M/H] \pm \Delta[\rm M/H]$	$[Fe/H] \pm \Delta[\rm Fe/H]$	$v_{\rm mic}$	$v_{\rm mac}$	$v \sin i$	χ^2
2M11130592+4626267	5777 ± 121	4.27 ± 0.13	4.23	0.04 ± 0.05	-0.03 ± 0.1	0.6	4.19	10.37	1.51
2M11131300+4535130	5968 ± 112	4.34 ± 0.14	4.25	0.04 ± 0.04	-0.01 ± 0.1	0.57	5.1	10.49	1.68
2M11131737+4622362	5648 ± 130	4.22 ± 0.17	4.21	-0.01 ± 0.06	-0.07 ± 0.1	0.78	3.79	9.58	0.8
2M11132173+4658147	5772 ± 102	3.99 ± 0.1	3.95	-0.15 ± 0.04	-0.21 ± 0.1	0.63	4.45	8.68	0.41
2M11132366+4446369	5936 ± 127	4.24 ± 0.16	4.16	0.06 ± 0.05	-0.01 ± 0.1	0.65	4.91	9.67	0.56
2M11134522+4846414	5671 ± 126	4.35 ± 0.18	4.34	-0.04 ± 0.05	-0.09 ± 0.1	0.62	3.87	10.33	0.5
2M11140997+5040341	5889 ± 153	4.5 ± 0.17	4.43	-0.04 ± 0.06	-0.1 ± 0.1	0.62	4.76	9.33	1.54
2M11141031+4746337	6090 ± 153	4.4 ± 0.22	4.28	0.06 ± 0.06	-0.02 ± 0.1	0.49	5.79	9.27	0.73
2M11143137+4931568	5807 ± 117	4.26 ± 0.15	4.21	-0.15 ± 0.05	-0.22 ± 0.1	0.5	4.52	8.49	1.56
2M11143340+5256487	4993 ± 100	3.45 ± 0.12	3.45	-0.01 ± 0.05	-0.1 ± 0.1	1.1	3.59	9.26	1.75
2M11143730+4617102	5892 ± 135	4.39 ± 0.23	4.32	-0.06 ± 0.06	-0.13 ± 0.1	0.54	4.8	9.15	0.59
2M11144368+4548021	5540 ± 62	4.29 ± 0.07	4.31	0.1 ± 0.03	0.09 ± 0.1	1.24	3.35	10.42	1.75
2M11144469+4635133	6055 ± 112	4.28 ± 0.14	4.17	-0.04 ± 0.04	-0.12 ± 0.1	0.3	5.69	8.56	1.45
2M11144654+2306311	5761 ± 140	4.3 ± 0.17	4.26	-0.07 ± 0.06	-0.13 ± 0.1	0.62	4.24	9.26	1.63
2M11145633+4912138	5757 ± 121	4.06 ± 0.11	4.02	0.11 ± 0.05	0.06 ± 0.1	0.87	4.08	10.11	1.77
2M11145732+5025154	6010 ± 126	4.34 ± 0.15	4.24	0.07 ± 0.05	0.01 ± 0.1	0.63	5.3	10.66	1.48
2M11150547+5036405	5618 ± 97	4.23 ± 0.12	4.23	0.12 ± 0.04	0.08 ± 0.1	0.91	3.54	10.13	1.63
2M11151340+0702089	5987 ± 75	4.23 ± 0.08	4.14	0.1 ± 0.03	0.05 ± 0.1	0.78	5.15	9.94	0.4
2M11151674+2330380	5569 ± 119	4.2 ± 0.13	4.21	-0.02 ± 0.05	-0.08 ± 0.1	0.78	3.57	9.69	1.73
2M11155218+5034289	6042 ± 162	4.38 ± 0.23	4.27	-0.07 ± 0.06	-0.15 ± 0.1	0.33	5.63	9.31	1.56

APOGEE_ID	$T_{\rm eff} \pm \Delta T_{\rm eff}$	$\log g \pm \Delta \log g$	$\log g_{cor}$	$[\mathrm{M/H}] \pm \Delta[\mathrm{M/H}]$	$[Fe/H] \pm \Delta[\mathrm{Fe/H}]$	$\mathrm{v_{mic}}$	$\mathrm{v_{mac}}$	$v \sin i$	χ^2
2M11160258+2236120	5486 ± 91	4.24 ± 0.09	4.27	0.02 ± 0.04	-0.01 ± 0.1	0.81	3.32	10.84	1.67
2M11163656+5259368	6101 ± 147	4.33 ± 0.21	4.21	-0.03 ± 0.06	-0.1 ± 0.1	0.4	5.96	8.4	0.39
2M11164594+0743538	6043 ± 117	4.36 ± 0.15	4.25	0.18 ± 0.05	0.13 ± 0.1	0.73	5.35	10.82	1.46
2M11184001+4622598	5658 ± 100	4 ± 0.11	3.99	0.07 ± 0.04	0.02 ± 0.1	0.75	3.79	10.57	1.64
2M11184506+2303085	5613 ± 113	4.26 ± 0.16	4.26	-0.11 ± 0.05	-0.16 ± 0.1	0.79	3.78	9.45	1.29
2M11185766+2245329	5852 ± 117	4.02 ± 0.13	3.96	0.05 ± 0.05	-0.01 ± 0.1	0.93	4.57	9.53	0.51
2M11190121+4738597	5751 ± 100	4.31 ± 0.1	4.28	0.06 ± 0.04	-0.01 ± 0.1	0.51	4.06	10.24	1.61
2M11190318+2221185	5836 ± 146	4.23 ± 0.2	4.17	-0.15 ± 0.06	-0.23 ± 0.1	0.46	4.65	8.72	0.76
2M11190710+0724433	6086 ± 121	4.28 ± 0.17	4.16	-0.13 ± 0.05	-0.22 ± 0.1	0	5.97	8.84	0.39
2M11190711+5033344	5705 ± 122	4.15 ± 0.13	4.13	0.1 ± 0.05	0.05 ± 0.1	0.8	3.87	10.05	1.63
2M11191986+4717559	5672 ± 116	4.13 ± 0.13	4.12	0.03 ± 0.05	-0.01 ± 0.1	0.75	3.83	9.75	0.56
2M11193288+5126120	6158 ± 118	4.37 ± 0.2	4.23	-0.22 ± 0.05	-0.31 ± 0.1	0	6.53	6.95	1.32
2M11194218+5024542	5650 ± 121	4.34 ± 0.18	4.33	-0.04 ± 0.05	-0.08 ± 0.1	0.64	3.8	10.4	0.59
2M11195476+2144266	5712 ± 125	4.15 ± 0.13	4.13	0.04 ± 0.05	0 ± 0.1	0.71	3.97	9.4	1.58
2M11195492+0810153	5742 ± 126	4.19 ± 0.13	4.16	0.11 ± 0.05	0.04 ± 0.1	0.82	3.99	9.64	0.64
2M11201546+4502324	5707 ± 94	4.06 ± 0.09	4.04	-0.01 ± 0.04	-0.06 ± 0.1	0.75	4.03	9.63	1.5
2M11202536+2137276	6016 ± 167	4.26 ± 0.2	4.16	-0.22 ± 0.07	-0.29 ± 0.1	0	5.65	7.95	0.57
2M11203105+2302355	5520 ± 99	4.25 ± 0.1	4.27	0.01 ± 0.04	-0.03 ± 0.1	0.82	3.41	10.35	0.64
2M11203687+4809433	5859 ± 135	4.35 ± 0.19	4.29	0.08 ± 0.05	0.05 ± 0.1	0.88	4.49	9.83	0.8
2M11203792+2246541	6023 ± 119	4.36 ± 0.15	4.26	0.02 ± 0.05	-0.05 ± 0.1	0.34	5.42	9.35	1.46

APOGEE_ID	$T_{\rm eff} \pm \Delta T_{\rm eff}$	$\log g \pm \Delta \log g$	$\log g_{cor}$	$[\rm M/H] \pm \Delta[\rm M/H]$	$[Fe/H] \pm \Delta[\rm Fe/H]$	v$_{\rm mic}$	v$_{\rm mac}$	$v \sin i$	χ^2
2M11211980+5003461	5771 ± 132	4.31 ± 0.15	4.27	0.02 ± 0.05	-0.03 ± 0.1	0.7	4.18	11.19	1.58
2M11215202+4940178	5537 ± 69	3.95 ± 0.07	3.97	0.04 ± 0.03	0.01 ± 0.1	0.98	3.51	9.46	0.52
2M11220655+2317405	5638 ± 110	4.16 ± 0.13	4.15	0.09 ± 0.05	0.02 ± 0.1	0.58	3.65	10.48	1.81
2M11220936+2139284	5952 ± 117	4.32 ± 0.15	4.24	-0.02 ± 0.05	-0.07 ± 0.1	0.35	5.06	9.76	1.61
2M11222346+5051553	6006 ± 169	4.14 ± 0.19	4.04	-0.12 ± 0.07	-0.23 ± 0.1	0.6	5.52	9.33	1.75
2M11223617+2117458	5947 ± 117	4.2 ± 0.14	4.12	0.12 ± 0.05	0.06 ± 0.1	0.61	4.91	9.26	0.72
2M11224566+4419028	5718 ± 82	4.31 ± 0.1	4.28	-0.14 ± 0.04	-0.21 ± 0.1	0.41	4.15	8.68	1.43
2M11224697+2239469	5919 ± 117	4.37 ± 0.16	4.29	0.07 ± 0.05	0.03 ± 0.1	0.66	4.79	10.77	0.65
2M11225070+2230338	5892 ± 108	4.34 ± 0.16	4.27	0.03 ± 0.04	-0.02 ± 0.1	0.5	4.7	8.67	0.43
2M11225078+4505460	5710 ± 123	4.38 ± 0.15	4.36	-0.03 ± 0.05	-0.07 ± 0.1	0.72	3.99	10.31	0.54
2M11225969+4422432	5948 ± 92	4.16 ± 0.1	4.08	0.02 ± 0.04	-0.04 ± 0.1	0.39	5.05	10.6	1.57
2M11230464+2135599	5722 ± 113	4.37 ± 0.14	4.34	-0.15 ± 0.05	-0.21 ± 0.1	0.57	4.17	9.74	1.58
2M11231659+4550058	6160 ± 102	4.42 ± 0.15	4.28	-0.04 ± 0.04	-0.12 ± 0.1	0.02	6.36	7.91	1.37
2M11233358+4713077	5817 ± 90	4.29 ± 0.11	4.24	-0.01 ± 0.04	-0.06 ± 0.1	0.58	4.4	10.11	0.33
2M11234684+2239571	5765 ± 99	4.09 ± 0.09	4.05	0.06 ± 0.04	0 ± 0.1	0.68	4.16	10.82	0.45
2M11235993+4532342	4315 ± 25	4.57 ± 0.06	4.96	-0.92 ± 0.03	-0.92 ± 0.1	0	4.31	5.92	1.54
2M11241090+2144250	5904 ± 136	4.15 ± 0.17	4.08	0.1 ± 0.06	0.06 ± 0.1	0.85	4.73	10.15	0.84
2M11245687+4457246	5675 ± 84	4.26 ± 0.1	4.25	0.12 ± 0.04	0.09 ± 0.1	0.8	3.72	9.45	0.57
2M11250844+2238568	6191 ± 116	4.53 ± 0.11	4.37	0.11 ± 0.05	0.06 ± 0.1	0.37	6.4	11.2	0.53
2M11252610+2124486	5701 ± 130	4.34 ± 0.17	4.32	-0.04 ± 0.06	-0.08 ± 0.1	0.74	3.97	8.22	0.61

APOGEE_ID	$T_{\mathrm{eff}} \pm \Delta T_{\mathrm{eff}}$	$\log g \pm \Delta \log g$	$\log g_{cor}$	$[\mathrm{M/H}] \pm \Delta[\mathrm{M/H}]$	$[Fe/H] \pm \Delta[\mathrm{Fe/H}]$	$\mathrm{v}_{\mathrm{mic}}$	$\mathrm{v}_{\mathrm{mac}}$	$v \sin i$	χ^2
2M11254577+4938397	5733 ± 132	4.18 ± 0.13	4.15	0 ± 0.06	-0.06 ± 0.1	0.59	4.08	9.46	0.69
2M11261056+2142447	5922 ± 142	4.39 ± 0.21	4.31	-0.04 ± 0.06	-0.08 ± 0.1	0.44	4.92	10.2	0.72
2M11262481+5326592	6235 ± 165	4.48 ± 0.16	4.31	0.03 ± 0.06	-0.05 ± 0.1	0.37	6.81	9.3	0.41
2M11262679+0410239	6145 ± 121	4.4 ± 0.19	4.26	0.04 ± 0.05	-0.05 ± 0.1	0.49	6.17	8.6	0.38
2M11262740+4701496	5776 ± 129	4.36 ± 0.16	4.32	-0.06 ± 0.05	-0.12 ± 0.1	0.58	4.28	8.3	1.51
2M11263429+2102102	6237 ± 109	4.43 ± 0.12	4.25	0.08 ± 0.04	0.03 ± 0.1	0.48	6.77	10.31	0.37
2M11263617+4913000	6021 ± 120	4.21 ± 0.13	4.11	0.08 ± 0.05	0.03 ± 0.1	0.78	5.37	10.25	0.54
2M11264502+5026511	6017 ± 117	4.38 ± 0.14	4.28	0.13 ± 0.05	0.08 ± 0.1	0.7	5.26	10.71	1.52
2M11265633+4709383	5805 ± 133	4.25 ± 0.17	4.20	-0.09 ± 0.06	-0.16 ± 0.1	0.5	4.45	9.79	0.54
2M11271093+2141457	5658 ± 128	4.29 ± 0.19	4.28	-0.11 ± 0.06	-0.15 ± 0.1	0.55	3.91	8.4	0.64
2M11271238+2204202	5772 ± 129	4.19 ± 0.14	4.15	-0.21 ± 0.05	-0.3 ± 0.1	0.39	4.45	8.2	0.46
2M11272749+4701292	5690 ± 137	4.32 ± 0.19	4.30	-0.13 ± 0.06	-0.16 ± 0.1	0.76	4.04	9.56	0.52
2M11272844+2330292	5995 ± 121	4.41 ± 0.14	4.31	-0.01 ± 0.05	-0.07 ± 0.1	0.41	5.29	9.25	0.45
2M11272905+5030245	5982 ± 181	4.27 ± 0.23	4.18	-0.23 ± 0.07	-0.32 ± 0.1	0.05	5.46	6.77	2
2M11272992+4806077	5791 ± 103	4.35 ± 0.12	4.31	0.07 ± 0.04	0.03 ± 0.1	0.75	4.2	10.22	1.48
2M11273044+2333508	5773 ± 99	4.15 ± 0.1	4.11	0.04 ± 0.04	-0.01 ± 0.1	0.78	4.2	11.06	1.37
2M11280551+2230287	5940 ± 145	4.13 ± 0.18	4.05	-0.16 ± 0.06	-0.22 ± 0.1	0.37	5.2	8.12	0.55
2M11282341+5318257	6047 ± 125	4.29 ± 0.16	4.18	-0.02 ± 0.05	-0.09 ± 0.1	0.44	5.62	8.8	0.37
2M11282698+2205009	5534 ± 92	4.05 ± 0.09	4.07	0.17 ± 0.04	0.14 ± 0.1	0.99	3.32	9.34	1.08
2M11284492+2253322	5872 ± 133	4.33 ± 0.21	4.27	-0.1 ± 0.06	-0.17 ± 0.1	0.26	4.75	8.1	0.56

APOGEE_ID	$T_{\text{eff}} \pm \Delta T_{\text{eff}}$	$\log g \pm \Delta \log g$	$\log g_{cor}$	$[\text{M/H}] \pm \Delta[\text{M/H}]$	$[Fe/H] \pm \Delta[\text{Fe/H}]$	v_{mic}	v_{mac}	$v \sin i$	χ^2
2M11284793+4749092	6129 ± 135	4.22 ± 0.2	4.09	-0.1 ± 0.06	-0.18 ± 0.1	0.63	6.24	7.32	0.44
2M11290743+4920358	5866 ± 110	4.26 ± 0.14	4.20	0.09 ± 0.05	0.05 ± 0.1	0.77	4.53	9.51	0.54
2M11291006+4822523	5498 ± 95	4.3 ± 0.1	4.33	0.01 ± 0.04	-0.02 ± 0.1	1.16	3.36	10.9	0.55
2M11291853+4602524	5758 ± 105	4.28 ± 0.11	4.24	0.2 ± 0.04	0.15 ± 0.1	0.8	3.92	10.3	0.76
2M11293435+4643238	5978 ± 127	4.37 ± 0.16	4.28	0.07 ± 0.05	0.02 ± 0.1	0.55	5.11	9.32	1.77
2M11294206+4935178	5876 ± 157	4.35 ± 0.25	4.28	-0.21 ± 0.07	-0.29 ± 0.1	0.32	4.89	7.59	1.62
2M11294322+2110576	6158 ± 128	4.22 ± 0.19	4.08	-0.12 ± 0.05	-0.2 ± 0.1	0	6.46	8.32	0.4
2M11294966+4819529	5624 ± 73	4.02 ± 0.08	4.02	0.18 ± 0.03	0.12 ± 0.1	0.84	3.56	10.67	1.71
2M11295343+4607224	5730 ± 118	4.32 ± 0.14	4.29	-0.13 ± 0.05	-0.2 ± 0.1	0.65	4.18	8.59	1.45
2M11301840+0303497	5970 ± 130	4.18 ± 0.14	4.09	0.1 ± 0.05	0.04 ± 0.1	0.79	5.06	10.68	0.44
2M11303803+4627592	5872 ± 92	4.27 ± 0.12	4.21	0.19 ± 0.04	0.15 ± 0.1	0.75	4.43	9.74	1.63
2M11303805+2127520	5719 ± 91	4.29 ± 0.11	4.26	-0.09 ± 0.04	-0.13 ± 0.1	0.6	4.1	8.56	0.39
2M11312339+5254540	6058 ± 157	4.28 ± 0.2	4.17	-0.03 ± 0.06	-0.11 ± 0.1	0.53	5.7	8.37	1.42
2M11312516+4635467	5951 ± 123	4.4 ± 0.18	4.32	-0.11 ± 0.05	-0.17 ± 0.1	0.39	5.16	9.09	1.51
2M11313430+2315472	6011 ± 118	4.48 ± 0.11	4.38	-0.15 ± 0.05	-0.23 ± 0.1	0	5.53	7.95	1.39
2M11314655+0325261	5989 ± 136	4.17 ± 0.14	4.08	0 ± 0.05	-0.07 ± 0.1	0.72	5.29	8.89	0.4
2M11315793+4543384	5705 ± 110	4.25 ± 0.12	4.23	0.05 ± 0.05	0 ± 0.1	0.85	3.9	10.04	0.58
2M11322439+0438403	6136 ± 117	4.24 ± 0.16	4.11	0.04 ± 0.04	-0.03 ± 0.1	0.48	6.12	8.97	1.35
2M11331575+0302368	6181 ± 105	4.39 ± 0.17	4.24	-0.09 ± 0.04	-0.15 ± 0.1	0.29	6.55	8.56	1.35
2M11334550+2257487	6033 ± 114	4.44 ± 0.12	4.34	0.22 ± 0.05	0.17 ± 0.1	0.51	5.24	10.57	0.6

APOGEE_ID	$T_{\text{eff}} \pm \Delta T_{\text{eff}}$	$\log g \pm \Delta \log g$	$\log g_{cor}$	$[\text{M/H}] \pm \Delta[\text{M/H}]$	$[Fe/H] \pm \Delta[\text{Fe/H}]$	v_{mic}	v_{mac}	$v \sin i$	χ^2
2M11340265+2337408	6166 ± 174	4.37 ± 0.28	4.22	-0.12 ± 0.07	-0.22 ± 0.1	0	6.49	7.27	1.4
2M11351120+4815011	5925 ± 149	4.28 ± 0.22	4.20	-0.22 ± 0.06	-0.33 ± 0.1	0.3	5.15	8.32	0.45
2M11355126+4621016	5622 ± 125	4.41 ± 0.18	4.41	-0.09 ± 0.05	-0.12 ± 0.1	0.89	3.76	10.92	1.71
2M11363621+4645040	5856 ± 113	4.33 ± 0.15	4.27	0.03 ± 0.05	-0.02 ± 0.1	0.66	4.54	9.8	1.62
2M11370740+4806146	5713 ± 116	4.39 ± 0.16	4.37	-0.11 ± 0.05	-0.16 ± 0.1	0.7	4.09	9.15	1.43
2M11371718+4636143	6140 ± 185	4.28 ± 0.29	4.15	-0.16 ± 0.07	-0.22 ± 0.1	0.39	6.36	7.87	0.58
2M11371829+4821521	6169 ± 121	4.32 ± 0.19	4.17	-0.08 ± 0.05	-0.17 ± 0.1	0.1	6.47	8.5	0.41
2M11381696+4640255	6270 ± 86	4.54 ± 0.08	4.35	0.18 ± 0.03	0.13 ± 0.1	0.62	6.9	9.82	1.38
2M11403804+4744410	5776 ± 143	4.3 ± 0.18	4.26	-0.2 ± 0.06	-0.29 ± 0.1	0.49	4.44	8.52	1.55
2M11404635+4637317	6018 ± 97	4.28 ± 0.12	4.18	-0.08 ± 0.04	-0.15 ± 0.1	0.32	5.51	8.52	0.37
2M11404794+0035451	5937 ± 101	4.39 ± 0.14	4.31	0.07 ± 0.04	0.03 ± 0.1	0.65	4.88	10.74	0.34
2M11405243+4716343	5800 ± 105	4.34 ± 0.13	4.29	0.03 ± 0.04	-0.03 ± 0.1	0.69	4.29	10.32	1.43
2M11412311+4655500	6051 ± 114	4.26 ± 0.15	4.15	-0.06 ± 0.05	-0.11 ± 0.1	0.55	5.69	10.01	0.44
2M11415871+2716055	6054 ± 148	4.28 ± 0.19	4.17	-0.02 ± 0.06	-0.1 ± 0.1	0.39	5.66	9.39	0.42
2M11421792-0006235	5778 ± 106	4.19 ± 0.11	4.15	0.04 ± 0.04	0 ± 0.1	0.76	4.21	9.54	0.53
2M11424631+0041088	5516 ± 115	4.19 ± 0.11	4.22	-0.01 ± 0.05	-0.05 ± 0.1	1.14	3.44	9.85	0.58
2M11424963-0019139	5983 ± 110	4.23 ± 0.12	4.14	0.08 ± 0.04	0.03 ± 0.1	0.66	5.14	10.33	1.4
2M11434234-0006041	5975 ± 154	4.24 ± 0.2	4.15	-0.25 ± 0.06	-0.32 ± 0.1	0.15	5.45	7.6	0.42
2M11440736+3502450	6079 ± 80	4.44 ± 0.1	4.32	-0.1 ± 0.03	-0.17 ± 0.1	0.17	5.89	8.34	0.32
2M11442949+0030234	5964 ± 124	4.22 ± 0.15	4.13	-0.04 ± 0.05	-0.11 ± 0.1	0.48	5.18	9.02	0.37

APOGEE_ID	$T_{\rm eff} \pm \Delta T_{\rm eff}$	$\log g \pm \Delta \log g$	$\log g_{cor}$	$[\rm M/H] \pm \Delta[\rm M/H]$	$[Fe/H] \pm \Delta[\rm Fe/H]$	$\rm v_{mic}$	$\rm v_{mac}$	$v \sin i$	χ^2
2M11443649+0143546	5674 ± 115	4.25 ± 0.14	4.24	0.04 ± 0.05	-0.02 ± 0.1	0.67	3.81	11.23	1.47
2M11444680+0152375	5847 ± 86	4.22 ± 0.11	4.16	0.18 ± 0.04	0.12 ± 0.1	0.73	4.34	10.29	1.5
2M11445837+2724259	6213 ± 70	4.31 ± 0.1	4.14	-0.27 ± 0.03	-0.3 ± 0.1	0.38	6.98	8.24	0.18
2M11445837+2724259	6154 ± 66	4.33 ± 0.11	4.19	-0.11 ± 0.03	-0.3 ± 0.1	0	6.4	6.95	0.35
2M11445876-0048558	5901 ± 84	4.33 ± 0.14	4.26	-0.29 ± 0.03	-0.4 ± 0.1	0	5.09	7.79	1.27
2M11450660+2634015	5940 ± 166	4.05 ± 0.2	3.97	-0.24 ± 0.07	-0.34 ± 0.1	0	5.31	7.65	1.53
2M11452382+0122510	5713 ± 126	4.24 ± 0.15	4.22	-0.06 ± 0.05	-0.15 ± 0.1	0.64	4.05	9.44	1.42
2M11452973+0159347	6099 ± 138	4.39 ± 0.2	4.27	-0.02 ± 0.05	-0.09 ± 0.1	0.43	5.93	8.93	0.38
2M11453211-0140392	5794 ± 119	4.28 ± 0.14	4.24	0.05 ± 0.05	-0.02 ± 0.1	0.68	4.25	10.02	1.88
2M11453376-0046276	5963 ± 127	4.29 ± 0.15	4.20	0.05 ± 0.05	-0.01 ± 0.1	0.6	5.06	8.93	0.56
2M11460234+3505279	5902 ± 146	4.33 ± 0.21	4.26	0.03 ± 0.06	-0.03 ± 0.1	0.59	4.76	9.5	1.38
2M11461692+0052372	5706 ± 141	4.27 ± 0.18	4.25	-0.19 ± 0.06	-0.28 ± 0.1	0.47	4.16	9.2	0.51
2M11462634+0001154	5736 ± 134	4.14 ± 0.14	4.11	-0.04 ± 0.06	-0.1 ± 0.1	0.77	4.14	9.36	0.58
2M11463198+3441046	5963 ± 92	4.21 ± 0.12	4.12	-0.14 ± 0.04	-0.22 ± 0.1	0.47	5.28	8.33	0.33
2M11463973-0018062	5608 ± 96	4.12 ± 0.11	4.12	0.09 ± 0.04	0.05 ± 0.1	0.88	3.57	10.61	0.69
2M11464736+3424349	6067 ± 121	4.34 ± 0.18	4.23	-0.19 ± 0.05	-0.27 ± 0.1	0.15	5.92	7.28	1.39
2M11465082-0057152	5998 ± 149	4.03 ± 0.14	3.93	-0.18 ± 0.06	-0.26 ± 0.1	0.52	5.57	8.35	0.39
2M11471592-0009325	6005 ± 77	4.18 ± 0.08	4.08	0.01 ± 0.03	-0.07 ± 0.1	0.62	5.36	9.44	1.3
2M11471634-0002578	6225 ± 136	4.42 ± 0.18	4.25	-0.11 ± 0.05	-0.21 ± 0.1	0.02	6.89	6.85	1.41
2M11471890+0004158	5839 ± 113	4.36 ± 0.16	4.30	-0.02 ± 0.05	-0.07 ± 0.1	0.64	4.51	10.47	1.33

APOGEE_ID	$T_{\text{eff}} \pm \Delta T_{\text{eff}}$	$\log g \pm \Delta \log g$	$\log g_{cor}$	$[\text{M/H}] \pm \Delta[\text{M/H}]$	$[Fe/H] \pm \Delta[\text{Fe/H}]$	v_{mic}	v_{mac}	$v \sin i$	χ^2
2M11474314+0032484	5659 ± 78	4.26 ± 0.1	4.25	0.05 ± 0.03	0.01 ± 0.1	0.87	3.74	9.85	0.43
2M11474992+0113288	6010 ± 141	4.24 ± 0.17	4.14	-0.22 ± 0.06	-0.32 ± 0.1	0.02	5.63	8.43	0.37
2M11475863-0027268	5944 ± 95	4.26 ± 0.12	4.18	-0.04 ± 0.04	-0.1 ± 0.1	0.48	5.05	9.3	1.24
2M11480228+3519333	6019 ± 70	4.43 ± 0.08	4.33	0.13 ± 0.03	0.08 ± 0.1	0.58	5.26	10.5	1.33
2M11480818+0138132	5815 ± 97	4.41 ± 0.12	4.36	0.1 ± 0.04	0.05 ± 0.1	0.67	4.26	10.81	1.41
2M11481421+0010525	5998 ± 136	4.31 ± 0.17	4.21	-0.05 ± 0.06	-0.12 ± 0.1	0.5	5.36	8.66	0.63
2M11483823+0040080	5820 ± 88	4.35 ± 0.13	4.30	-0.1 ± 0.04	-0.16 ± 0.1	0.62	4.51	8.56	1.36
2M11484542+0236344	6376 ± 116	4.52 ± 0.13	4.29	-0.01 ± 0.04	-0.09 ± 0.1	0.17	7.96	6.23	1.35
2M11485475-0025071	5962 ± 121	4.23 ± 0.14	4.14	0.05 ± 0.05	-0.01 ± 0.1	0.76	5.06	9.57	1.45
2M11491769+3523551	6102 ± 99	4.43 ± 0.12	4.31	0.1 ± 0.04	0.03 ± 0.1	0.58	5.81	9.56	1.38
2M11492279+1947144	5954 ± 70	4.56 ± 0.08	4.47	-0.09 ± 0.03	-0.16 ± 0.1	0.34	5.15	8.57	0.29
2M11493068+2731054	6044 ± 154	4.31 ± 0.21	4.20	-0.16 ± 0.06	-0.25 ± 0.1	0.19	5.75	9.12	0.39
2M11493255-0208094	6088 ± 122	4.38 ± 0.17	4.26	0.06 ± 0.05	0 ± 0.1	0.56	5.77	9.62	1.4
2M11494668-0011285	5951 ± 97	4.31 ± 0.12	4.23	0.02 ± 0.04	-0.04 ± 0.1	0.63	5.02	8.94	0.34
2M11495283-0213410	5666 ± 87	4.06 ± 0.09	4.05	0.03 ± 0.04	-0.03 ± 0.1	0.72	3.85	10.13	1.47
2M11495598+0043355	5716 ± 117	4.23 ± 0.13	4.20	0.07 ± 0.05	0.03 ± 0.1	0.76	3.92	9.86	1.65
2M11502683-0016103	5939 ± 106	4.32 ± 0.16	4.24	-0.16 ± 0.04	-0.23 ± 0.1	0.28	5.15	8.46	1.36
2M11503973+2015126	6011 ± 152	4.3 ± 0.19	4.20	-0.1 ± 0.06	-0.18 ± 0.1	0.4	5.49	8.48	0.44
2M11504739-0039163	5995 ± 108	4.29 ± 0.12	4.19	0.11 ± 0.04	0.06 ± 0.1	0.69	5.17	11.12	0.51
2M11505560+4506225	6199 ± 73	4.42 ± 0.09	4.26	0.11 ± 0.03	0.06 ± 0.1	0.58	6.46	10.31	0.37

APOGEE_ID	$T_{\rm eff} \pm \Delta T_{\rm eff}$	$\log g \pm \Delta \log g$	$\log g_{cor}$	$[\mathrm{M/H}] \pm \Delta[\mathrm{M/H}]$	$[Fe/H] \pm \Delta[\mathrm{Fe/H}]$	$\mathrm{v}_{\rm mic}$	$\mathrm{v}_{\rm mac}$	$v \sin i$	χ^2
2M11505634+0224170	5966 ± 80	4.44 ± 0.1	4.35	-0.05 ± 0.03	-0.11 ± 0.1	0.41	5.17	9.14	1.34
2M11505634-0103363	5800 ± 99	4.24 ± 0.13	4.19	-0.03 ± 0.04	-0.1 ± 0.1	0.66	4.37	8.45	1.32
2M11510409+3509470	5842 ± 53	4.32 ± 0.07	4.26	0.05 ± 0.02	0 ± 0.1	0.69	4.45	10.19	1.37
2M11511138+0134308	6165 ± 127	4.42 ± 0.2	4.28	-0.15 ± 0.05	-0.24 ± 0.1	0	6.51	8.33	0.35
2M11511204+4409328	5869 ± 133	4.21 ± 0.19	4.15	-0.13 ± 0.06	-0.2 ± 0.1	0.43	4.79	8.8	0.61
2M11511422+4404497	5708 ± 78	4.1 ± 0.08	4.08	0.06 ± 0.03	0.02 ± 0.1	0.81	3.94	9.58	1.45
2M11511475+0013149	6051 ± 96	4.44 ± 0.12	4.33	-0.05 ± 0.04	-0.11 ± 0.1	0.32	5.66	10.02	1.24
2M11511769+4507045	5935 ± 126	4.37 ± 0.17	4.29	0.06 ± 0.05	0.01 ± 0.1	0.67	4.88	10.26	0.53
2M11512479+0019503	6247 ± 129	4.39 ± 0.16	4.21	0.09 ± 0.05	0.03 ± 0.1	0.54	6.83	10.46	0.36
2M11513024+0047443	6190 ± 114	4.28 ± 0.16	4.12	-0.12 ± 0.05	-0.22 ± 0.1	0.27	6.66	7.85	1.41
2M11514231+0019426	5910 ± 133	4.37 ± 0.22	4.30	-0.05 ± 0.06	-0.11 ± 0.1	0.52	4.88	8.77	1.39
2M11515392+4335280	5702 ± 93	4.34 ± 0.12	4.32	-0.04 ± 0.04	-0.09 ± 0.1	0.61	3.98	9.85	0.43
2M11521190+5341200	6213 ± 93	4.33 ± 0.13	4.16	-0.1 ± 0.04	-0.17 ± 0.1	0.19	6.8	7.87	0.36
2M11522587+3416222	5840 ± 85	4.27 ± 0.11	4.21	0.08 ± 0.04	0.04 ± 0.1	0.71	4.42	9.63	0.39
2M11522780+4523167	5958 ± 115	4.31 ± 0.16	4.22	-0.11 ± 0.05	-0.19 ± 0.1	0.4	5.21	8.11	1.37
2M11523863+4432089	5737 ± 111	4.13 ± 0.1	4.10	0.04 ± 0.05	-0.02 ± 0.1	0.72	4.06	10.35	0.54
2M11524517+4442068	5735 ± 104	4.4 ± 0.13	4.37	-0.19 ± 0.04	-0.24 ± 0.1	0.49	4.25	9	1.39
2M11524695+5533555	5904 ± 77	4.32 ± 0.11	4.25	0.09 ± 0.03	0.02 ± 0.1	0.75	4.71	9.49	1.42
2M11531008+5345517	6087 ± 135	4.37 ± 0.19	4.25	-0.02 ± 0.05	-0.09 ± 0.1	0.57	5.85	9.17	1.54
2M11531825+4314378	5684 ± 117	4.32 ± 0.15	4.30	-0.01 ± 0.05	-0.07 ± 0.1	0.6	3.89	10.7	0.57

APOGEE_ID	$T_{\rm eff} \pm \Delta T_{\rm eff}$	$\log g \pm \Delta \log g$	$\log g_{cor}$	$[\mathrm{M/H}] \pm \Delta[\mathrm{M/H}]$	$[Fe/H] \pm \Delta[\mathrm{Fe/H}]$	$\mathrm{v_{mic}}$	$\mathrm{v_{mac}}$	$v \sin i$	χ^2
2M11532084+1902442	5905 ± 116	4.3 ± 0.19	4.23	-0.12 ± 0.05	-0.18 ± 0.1	0.59	4.94	7.75	0.42
2M11532736+0118563	5668 ± 76	4.22 ± 0.1	4.21	-0.07 ± 0.03	-0.17 ± 0.1	0.44	3.92	8.92	1.4
2M11532936+4340591	5719 ± 98	4.2 ± 0.1	4.17	0.14 ± 0.04	0.1 ± 0.1	0.9	3.86	9.55	0.72
2M11535370-1250592	6164 ± 140	4.27 ± 0.2	4.13	0.13 ± 0.06	0.07 ± 0.1	0.7	6.2	9.05	1.66
2M11540402+4519175	5626 ± 102	4.2 ± 0.12	4.20	0.03 ± 0.04	-0.02 ± 0.1	0.79	3.68	9.5	0.55
2M11540687+3400219	6119 ± 83	4.41 ± 0.12	4.28	0.01 ± 0.03	-0.07 ± 0.1	0.39	6.03	9.23	0.32
2M11540818+3542156	6089 ± 139	4.24 ± 0.19	4.12	-0.04 ± 0.06	-0.12 ± 0.1	0.55	5.91	8.99	0.35
2M11543807-1703424	6082 ± 91	4.37 ± 0.12	4.25	0.01 ± 0.03	-0.07 ± 0.1	0.41	5.79	9.05	0.32
2M11550501+3407397	5956 ± 92	4.35 ± 0.12	4.26	0.1 ± 0.04	0.06 ± 0.1	0.66	4.95	9.75	1.41
2M11550793+3322238	6111 ± 125	4.42 ± 0.19	4.30	-0.05 ± 0.05	-0.12 ± 0.1	0.31	6.04	8.17	0.31
2M11551005+2004152	5981 ± 130	4.36 ± 0.17	4.27	-0.11 ± 0.05	-0.19 ± 0.1	0.31	5.33	9.16	0.34
2M11552767-1050414	6120 ± 172	4.27 ± 0.26	4.14	-0.17 ± 0.07	-0.27 ± 0.1	0	6.24	8.03	0.49
2M11553800+3520110	6113 ± 115	4.36 ± 0.18	4.24	-0.05 ± 0.05	-0.13 ± 0.1	0.35	6.06	8	1.29
2M11554703+1809444	6171 ± 97	4.34 ± 0.15	4.19	-0.05 ± 0.04	-0.13 ± 0.1	0.42	6.45	8.46	1.36
2M11554732+3524354	5779 ± 115	4.11 ± 0.11	4.07	0 ± 0.05	-0.06 ± 0.1	0.76	4.28	8.74	1.38
2M11561419+2044466	6186 ± 75	4.42 ± 0.1	4.27	0.13 ± 0.03	0.06 ± 0.1	0.6	6.34	9.55	1.37
2M11561818+4301435	5545 ± 69	4.07 ± 0.07	4.09	0.13 ± 0.03	0.09 ± 0.1	0.88	3.37	9.62	0.58
2M11562645+4502438	6109 ± 116	4.31 ± 0.16	4.19	0.01 ± 0.04	-0.07 ± 0.1	0.35	5.97	8.75	0.38
2M11564031+2037081	6228 ± 124	4.39 ± 0.16	4.22	0.05 ± 0.05	-0.03 ± 0.1	0.43	6.74	9.49	0.34
2M11564066+3459474	6058 ± 134	4.3 ± 0.19	4.19	-0.09 ± 0.05	-0.15 ± 0.1	0.44	5.75	8.15	1.36

APOGEE_ID	$T_{\rm eff} \pm \Delta T_{\rm eff}$	$\log g \pm \Delta \log g$	$\log g_{cor}$	$[\rm M/H] \pm \Delta[\rm M/H]$	$[Fe/H] \pm \Delta[\rm Fe/H]$	$\rm v_{mic}$	$\rm v_{mac}$	$v \sin i$	χ^2
2M11565275+4300475	6075 ± 143	4.37 ± 0.19	4.25	0.11 ± 0.06	0.05 ± 0.1	0.63	5.63	9.19	1.71
2M11572262+4507393	5686 ± 123	4.11 ± 0.13	4.09	0.04 ± 0.05	0 ± 0.1	0.75	3.89	10.52	1.57
2M11572334+4545593	5849 ± 65	4.31 ± 0.09	4.25	0.1 ± 0.03	0.05 ± 0.1	0.66	4.42	10.37	0.35
2M11574498+4324530	5994 ± 138	4.3 ± 0.15	4.20	0.01 ± 0.05	-0.05 ± 0.1	0.5	5.28	8.88	0.57
2M11581818+4546271	5942 ± 142	4.22 ± 0.2	4.14	-0.07 ± 0.06	-0.14 ± 0.1	0.58	5.09	8.74	1.55
2M11591454+4316592	5999 ± 143	4.2 ± 0.16	4.10	-0.09 ± 0.06	-0.16 ± 0.1	0.49	5.43	8.23	1.53
2M11592942+4314104	5656 ± 103	4.27 ± 0.14	4.26	0.07 ± 0.04	0.03 ± 0.1	0.87	3.71	9.84	0.66
2M11594702+1753198	6032 ± 116	4.34 ± 0.14	4.24	0.12 ± 0.05	0.05 ± 0.1	0.7	5.35	10.2	0.43
2M11595753+1719307	5616 ± 69	4.23 ± 0.08	4.23	0.02 ± 0.03	-0.03 ± 0.1	0.77	3.65	11.19	0.36
2M12004018+1707463	5952 ± 134	4.31 ± 0.17	4.23	0.06 ± 0.05	0 ± 0.1	0.72	4.98	9.93	0.47
2M12005016+4411350	5541 ± 121	4.34 ± 0.15	4.36	-0.07 ± 0.05	-0.09 ± 0.1	0.98	3.54	7.32	0.71
2M12005253+4331389	5919 ± 93	4.18 ± 0.12	4.10	-0.02 ± 0.04	-0.08 ± 0.1	0.58	4.93	9.98	0.35
2M12005812+1923416	5872 ± 85	4.35 ± 0.12	4.29	-0.02 ± 0.03	-0.07 ± 0.1	0.55	4.66	9.55	1.38
2M12005964+4507479	6188 ± 156	4.42 ± 0.21	4.27	-0.01 ± 0.06	-0.1 ± 0.1	0.3	6.52	8.54	0.52
2M12010170+1800509	6051 ± 136	4.5 ± 0.14	4.39	-0.05 ± 0.05	-0.12 ± 0.1	0	5.66	8.71	0.38
2M12011883+1844092	6167 ± 124	4.24 ± 0.17	4.09	0.02 ± 0.05	-0.06 ± 0.1	0.59	6.36	8.72	0.4
2M12012174+1859066	5873 ± 139	4.24 ± 0.19	4.18	-0.03 ± 0.06	-0.1 ± 0.1	0.57	4.69	8.85	1.35
2M12013978+1924349	6021 ± 133	4.32 ± 0.15	4.22	0.05 ± 0.05	-0.02 ± 0.1	0.48	5.38	9.37	0.5
2M12014131+1810180	5728 ± 93	4.27 ± 0.1	4.24	0.15 ± 0.04	0.13 ± 0.1	1.05	3.87	9.26	2.32
2M12015892+1837285	5580 ± 101	4.49 ± 0.09	4.50	0.04 ± 0.04	-0.02 ± 0.1	0.67	3.5	8.65	1.62

APOGEE_ID	$T_{\rm eff} \pm \Delta T_{\rm eff}$	$\log g \pm \Delta \log g$	$\log g_{cor}$	$[\rm M/H] \pm \Delta[\rm M/H]$	$[Fe/H] \pm \Delta[\rm Fe/H]$	$v_{\rm mic}$	$v_{\rm mac}$	$v \sin i$	χ^2
2M12020436+1543069	6122 ± 136	4.37 ± 0.2	4.24	0.1 ± 0.05	0.05 ± 0.1	0.69	5.95	10.18	0.37
2M12021184+4407354	5867 ± 114	4.24 ± 0.16	4.18	-0.04 ± 0.05	-0.09 ± 0.1	0.65	4.68	9.25	0.4
2M12021975+1934167	5991 ± 89	4.33 ± 0.1	4.24	0.08 ± 0.03	0.01 ± 0.1	0.66	5.17	9.61	1.36
2M12024442+1604247	5991 ± 129	4.38 ± 0.17	4.29	-0.05 ± 0.05	-0.11 ± 0.1	0.46	5.31	8.84	0.41
2M12033187+4605385	5953 ± 113	4.25 ± 0.13	4.17	0.03 ± 0.04	-0.04 ± 0.1	0.49	5.03	9.85	0.44
2M12034364+0022317	5769 ± 99	4.28 ± 0.11	4.24	0.09 ± 0.04	0.04 ± 0.1	0.88	4.09	10.13	1.53
2M12034682+1633473	6074 ± 167	4.26 ± 0.23	4.14	-0.17 ± 0.07	-0.26 ± 0.1	0.19	5.95	8.23	0.43
2M12045603+1916573	5887 ± 107	4.33 ± 0.17	4.26	-0.09 ± 0.04	-0.16 ± 0.1	0.46	4.81	8.45	1.42
2M12050585+1751256	5839 ± 133	4.25 ± 0.17	4.19	-0.01 ± 0.05	-0.08 ± 0.1	0.6	4.51	8.73	1.61
2M12051313+4615148	6179 ± 189	4.18 ± 0.26	4.03	-0.14 ± 0.08	-0.24 ± 0.1	0.43	6.63	7.78	1.35
2M12052555-0004049	5952 ± 152	4.32 ± 0.19	4.24	-0.02 ± 0.06	-0.09 ± 0.1	0.57	5.07	8.97	0.55
2M12054242+1908264	5837 ± 124	4.23 ± 0.15	4.17	0.01 ± 0.05	-0.05 ± 0.1	0.7	4.49	9.38	0.61
2M12054271+4603527	6034 ± 163	4.35 ± 0.22	4.24	-0.04 ± 0.07	-0.11 ± 0.1	0.56	5.55	9.44	1.55
2M12054534+1903143	5580 ± 111	4.06 ± 0.11	4.07	0.1 ± 0.05	0.06 ± 0.1	0.82	3.51	10.65	0.83
2M12054534+1954527	5739 ± 97	4.26 ± 0.1	4.23	0.04 ± 0.04	-0.02 ± 0.1	0.69	4.03	11.07	1.39
2M12055940+1841418	5790 ± 93	4.27 ± 0.1	4.23	-0.01 ± 0.04	-0.08 ± 0.1	0.63	4.3	9.23	0.47
2M12061035+4553373	5917 ± 113	4.35 ± 0.18	4.27	-0.06 ± 0.05	-0.14 ± 0.1	0.55	4.93	9.05	0.41
2M12063416+1800323	5838 ± 90	4.36 ± 0.12	4.30	0.06 ± 0.04	0.02 ± 0.1	0.73	4.41	10.15	0.43
2M12064055+3646535	5989 ± 85	4.37 ± 0.09	4.28	0.09 ± 0.03	0.03 ± 0.1	0.59	5.14	9.81	0.38
2M12065080-0056113	5889 ± 99	4.2 ± 0.13	4.13	0.08 ± 0.04	0.04 ± 0.1	0.81	4.66	9.76	0.38

APOGEE_ID	$T_{\mathrm{eff}} \pm \Delta T_{\mathrm{eff}}$	$\log g \pm \Delta \log g$	$\log g_{cor}$	$[\mathrm{M/H}] \pm \Delta[\mathrm{M/H}]$	$[Fe/H] \pm \Delta[\mathrm{Fe/H}]$	$\mathrm{v}_{\mathrm{mic}}$	$\mathrm{v}_{\mathrm{mac}}$	$v \sin i$	χ^2
2M12065988+1903181	5611 ± 77	4.2 ± 0.09	4.20	0.11 ± 0.03	0.07 ± 0.1	0.89	3.54	10.22	0.64
2M12070650+1934581	6134 ± 94	4.41 ± 0.15	4.28	-0.16 ± 0.04	-0.25 ± 0.1	0	6.31	7.4	1.28
2M12070957+4653559	5709 ± 115	4.37 ± 0.15	4.35	-0.13 ± 0.05	-0.2 ± 0.1	0.29	4.1	9.21	1.54
2M12071506-0001557	6106 ± 162	4.34 ± 0.23	4.22	-0.01 ± 0.06	-0.08 ± 0.1	0.42	5.96	9.09	0.54
2M12073380+1915040	5701 ± 124	4.23 ± 0.14	4.21	0.02 ± 0.05	-0.03 ± 0.1	0.67	3.93	10.91	1.61
2M12074066+4636461	5761 ± 118	4.12 ± 0.11	4.08	0.07 ± 0.05	0.01 ± 0.1	0.83	4.13	9.51	0.68
2M12074506+3626543	5851 ± 140	4.17 ± 0.17	4.11	-0.02 ± 0.06	-0.08 ± 0.1	0.65	4.6	10.5	1.55
2M12080177+1848566	6086 ± 161	4.27 ± 0.24	4.15	-0.14 ± 0.06	-0.22 ± 0.1	0.44	5.99	8.49	1.37
2M12080864+1833213	5643 ± 122	4.21 ± 0.15	4.20	0.02 ± 0.05	-0.05 ± 0.1	0.75	3.74	9.25	0.76
2M12081974+4643265	6246 ± 173	4.48 ± 0.17	4.30	-0.15 ± 0.06	-0.22 ± 0.1	0	7.08	8.57	0.52
2M12082136+1854047	6172 ± 162	4.27 ± 0.24	4.12	-0.1 ± 0.07	-0.19 ± 0.1	0.35	6.52	7.8	1.41
2M12082409+3639242	5634 ± 133	4.45 ± 0.17	4.45	-0.06 ± 0.06	-0.14 ± 0.1	0.37	3.76	8.5	1.78
2M12090226+4011010	6201 ± 124	4.45 ± 0.14	4.29	0.15 ± 0.05	0.1 ± 0.1	0.66	6.42	10.08	0.41
2M12090787+1745429	6078 ± 106	4.36 ± 0.15	4.24	0.11 ± 0.04	0.04 ± 0.1	0.62	5.66	9.28	1.54
2M12091269+1904154	5937 ± 116	4.21 ± 0.14	4.13	-0.01 ± 0.05	-0.08 ± 0.1	0.73	5	9.29	0.54
2M12091378+3500248	6055 ± 118	4.4 ± 0.16	4.29	0 ± 0.05	-0.06 ± 0.1	0.51	5.63	9.24	1.41
2M12091906+4645222	5871 ± 120	4.35 ± 0.17	4.29	0.04 ± 0.05	-0.02 ± 0.1	0.55	4.59	11.06	0.47
2M12092847+1857183	5879 ± 145	4.33 ± 0.23	4.26	-0.14 ± 0.06	-0.21 ± 0.1	0.46	4.83	8.54	0.45
2M12093352-0006083	6055 ± 122	4.33 ± 0.17	4.22	-0.05 ± 0.05	-0.12 ± 0.1	0.54	5.7	8.56	0.34
2M12095216+4438065	5892 ± 111	4.32 ± 0.18	4.25	-0.08 ± 0.05	-0.14 ± 0.1	0.58	4.83	8.15	1.42

APOGEE_ID	$T_{\rm eff} \pm \Delta T_{\rm eff}$	$\log g \pm \Delta \log g$	$\log g_{cor}$	$[\rm M/H] \pm \Delta[\rm M/H]$	$[Fe/H] \pm \Delta[\rm Fe/H]$	$\rm v_{mic}$	$\rm v_{mac}$	$v \sin i$	χ^2
2M12100003+4653139	5946 ± 149	4.33 ± 0.2	4.25	-0.04 ± 0.06	-0.1 ± 0.1	0.31	5.06	9.08	1.56
2M12101039+4508055	5651 ± 91	4.29 ± 0.12	4.28	0.06 ± 0.04	0.04 ± 0.1	0.93	3.7	9.62	1.55
2M12104276+0436357	6031 ± 111	4.36 ± 0.15	4.26	-0.05 ± 0.04	-0.11 ± 0.1	0.45	5.55	8.28	0.35
2M12104285+3622507	5783 ± 137	4.23 ± 0.15	4.19	0 ± 0.06	-0.08 ± 0.1	0.61	4.27	9.15	0.54
2M12104407+4510297	6038 ± 71	4.21 ± 0.08	4.10	0.09 ± 0.03	0.04 ± 0.1	0.7	5.46	10.28	1.35
2M12104827-0923499	4873 ± 92	3.27 ± 0.14	3.27	0.01 ± 0.05	-0.07 ± 0.1	0.96	3.63	11.21	1.86
2M12112789+4544463	6226 ± 152	4.53 ± 0.14	4.36	0.1 ± 0.06	0.05 ± 0.1	0.31	6.66	11	1.71
2M12114039-0028301	5995 ± 156	4.41 ± 0.18	4.31	-0.03 ± 0.06	-0.09 ± 0.1	0.6	5.31	9.59	0.45
2M12114456+4536551	5836 ± 153	4.35 ± 0.23	4.29	-0.19 ± 0.06	-0.25 ± 0.1	0.39	4.68	8.49	1.9
2M12115664+4622258	6040 ± 136	4.35 ± 0.17	4.24	-0.03 ± 0.05	-0.1 ± 0.1	0.42	5.57	8.35	0.55
2M12121040+1359037	5839 ± 113	4.32 ± 0.15	4.26	0.1 ± 0.05	0.07 ± 0.1	0.75	4.38	9.78	0.53
2M12121442+4559378	5708 ± 152	4.04 ± 0.16	4.02	-0.24 ± 0.07	-0.32 ± 0.1	0.45	4.29	7.89	0.88
2M12121995+4618243	6153 ± 131	4.39 ± 0.2	4.25	0.05 ± 0.05	-0.03 ± 0.1	0.35	6.21	9.49	0.49
2M12130517+1510315	6153 ± 89	4.38 ± 0.14	4.24	-0.03 ± 0.04	-0.11 ± 0.1	0.29	6.3	8.92	0.34
2M12130627+3710063	5758 ± 131	4.31 ± 0.14	4.27	-0.01 ± 0.05	-0.06 ± 0.1	0.64	4.16	10.73	1.52
2M12131188+0540579	5984 ± 92	4.3 ± 0.11	4.21	0.04 ± 0.04	-0.03 ± 0.1	0.58	5.18	9.61	0.39
2M12131232+0548337	6008 ± 127	4.37 ± 0.16	4.27	-0.1 ± 0.05	-0.19 ± 0.1	0.26	5.47	8.66	0.35
2M12131358+3507038	6095 ± 185	4.28 ± 0.27	4.16	-0.2 ± 0.07	-0.3 ± 0.1	0.06	6.11	8.05	0.44
2M12133768+3550064	5722 ± 135	4.29 ± 0.17	4.26	-0.14 ± 0.06	-0.23 ± 0.1	0.4	4.17	8.5	1.73
2M12134495+4415002	5765 ± 84	4.25 ± 0.09	4.21	0.2 ± 0.03	0.15 ± 0.1	0.8	3.96	9.78	0.67

APOGEE_ID	$T_{\rm eff} \pm \Delta T_{\rm eff}$	$\log g \pm \Delta \log g$	$\log g_{cor}$	$[\rm M/H] \pm \Delta[\rm M/H]$	$[Fe/H] \pm \Delta[\rm Fe/H]$	$v_{\rm mic}$	$v_{\rm mac}$	$v \sin i$	χ^2
2M12140792+3708445	6129 ± 153	4.31 ± 0.24	4.18	-0.05 ± 0.06	-0.13 ± 0.1	0.36	6.17	8.4	0.41
2M12142336+1441111	5983 ± 76	4.37 ± 0.09	4.28	-0.01 ± 0.03	-0.08 ± 0.1	0.45	5.22	8.98	0.33
2M12143042+4518112	5917 ± 113	4.34 ± 0.16	4.26	0.06 ± 0.05	0.02 ± 0.1	0.78	4.8	9.88	0.46
2M12143112+4100509	6007 ± 122	4.35 ± 0.14	4.25	-0.02 ± 0.05	-0.1 ± 0.1	0.47	5.37	8.28	0.37
2M12150595+0611588	5812 ± 126	4.21 ± 0.14	4.16	0.09 ± 0.05	0.03 ± 0.1	0.74	4.29	10.69	1.5
2M12151117+3651212	5789 ± 130	4.26 ± 0.15	4.22	0.04 ± 0.05	-0.03 ± 0.1	0.5	4.24	10.25	1.63
2M12151345+4520010	6131 ± 137	4.33 ± 0.22	4.20	-0.06 ± 0.06	-0.12 ± 0.1	0.34	6.19	8.69	0.5
2M12153457+1454099	6241 ± 101	4.39 ± 0.14	4.21	-0.09 ± 0.04	-0.18 ± 0.1	0	6.99	8.56	0.39
2M12154596+3605059	5740 ± 136	4.38 ± 0.16	4.35	-0.03 ± 0.06	-0.08 ± 0.1	0.68	4.1	9.15	1.51
2M12160114+4606393	5917 ± 125	4.25 ± 0.16	4.17	0.09 ± 0.05	0.02 ± 0.1	0.59	4.78	9.3	1.51
2M12160193+3701282	5709 ± 121	4.15 ± 0.14	4.13	-0.06 ± 0.05	-0.12 ± 0.1	0.64	4.06	10.52	1.41
2M12160902+3706018	5682 ± 134	4.18 ± 0.17	4.16	-0.08 ± 0.06	-0.16 ± 0.1	0.58	3.98	10.53	1.52
2M12161795+3917484	6156 ± 88	4.34 ± 0.13	4.20	0.08 ± 0.03	0.02 ± 0.1	0.61	6.2	9.1	1.34
2M12161969+4030265	5821 ± 132	4.31 ± 0.17	4.26	-0.04 ± 0.05	-0.1 ± 0.1	0.47	4.45	9.9	0.41
2M12163408+3545506	6135 ± 147	4.34 ± 0.23	4.21	-0.03 ± 0.06	-0.1 ± 0.1	0.4	6.18	8.63	1.43
2M12163576+0008359	5698 ± 112	4.22 ± 0.13	4.20	0.09 ± 0.05	0.02 ± 0.1	0.66	3.84	9.97	1.59
2M12164266+4305064	5959 ± 97	4.33 ± 0.12	4.24	-0.01 ± 0.04	-0.07 ± 0.1	0.62	5.1	9.04	0.36
2M12170470+1411345	5792 ± 100	3.99 ± 0.1	3.95	0.05 ± 0.04	0.01 ± 0.1	0.9	4.32	9.99	0.48
2M12171237+0523021	6185 ± 132	4.42 ± 0.18	4.27	0.06 ± 0.05	-0.01 ± 0.1	0.55	6.42	9.13	0.36
2M12171654+4603401	5734 ± 117	4.16 ± 0.12	4.13	0.09 ± 0.05	0.04 ± 0.1	0.79	3.99	10.18	0.68

APOGEE_ID	$T_{\rm eff} \pm \Delta T_{\rm eff}$	$\log g \pm \Delta \log g$	$\log g_{cor}$	$[{\rm M/H}] \pm \Delta[{\rm M/H}]$	$[Fe/H] \pm \Delta[{\rm Fe/H}]$	v$_{\rm mic}$	v$_{\rm mac}$	$v \sin i$	χ^2
2M12172810+4622129	5678 ± 117	3.97 ± 0.14	3.95	-0.17 ± 0.05	-0.25 ± 0.1	0.75	4.13	8.83	0.46
2M12173529+4510070	5662 ± 82	4.28 ± 0.1	4.27	0.02 ± 0.03	-0.04 ± 0.1	0.71	3.79	10.87	0.36
2M12173618+4443157	5915 ± 77	4.37 ± 0.11	4.29	0.19 ± 0.03	0.14 ± 0.1	0.7	4.63	9.87	1.51
2M12173749+4622208	5747 ± 114	4.3 ± 0.12	4.27	0.05 ± 0.05	-0.02 ± 0.1	0.71	4.05	9.84	1.58
2M12174577+1256141	6208 ± 106	4.39 ± 0.15	4.23	-0.17 ± 0.04	-0.24 ± 0.1	0	6.83	7.2	0.37
2M12181340+4643199	6001 ± 133	4.37 ± 0.16	4.27	-0.03 ± 0.05	-0.1 ± 0.1	0.49	5.35	9.11	0.41
2M12181425+4420324	5887 ± 120	4.4 ± 0.19	4.33	-0.04 ± 0.05	-0.08 ± 0.1	0.56	4.75	8.63	0.46
2M12183868+0521384	6099 ± 128	4.39 ± 0.19	4.27	0.03 ± 0.05	-0.04 ± 0.1	0.47	5.87	9.65	0.34
2M12184812-0124201	5999 ± 97	4.41 ± 0.12	4.31	-0.05 ± 0.04	-0.13 ± 0.1	0.38	5.35	8.87	0.31
2M12185469+0438432	5900 ± 78	4.17 ± 0.1	4.10	0.08 ± 0.03	0.02 ± 0.1	0.72	4.71	10.64	0.34
2M12192484+3937289	5771 ± 55	4.26 ± 0.06	4.22	0.22 ± 0.02	0.16 ± 0.1	0.75	3.95	9.75	0.61
2M12192484+3937289	5768 ± 55	4.25 ± 0.06	4.21	0.22 ± 0.02	0.16 ± 0.1	0.74	3.94	9.71	0.61
2M12192513+4313080	5971 ± 126	4.33 ± 0.17	4.24	-0.13 ± 0.05	-0.2 ± 0.1	0.31	5.29	8.15	1.32
2M12193016+2636459	6042 ± 105	4.35 ± 0.13	4.24	0.03 ± 0.04	-0.04 ± 0.1	0.44	5.53	8.97	1.46
2M12193261+4524460	6103 ± 154	4.33 ± 0.24	4.21	-0.14 ± 0.06	-0.21 ± 0.1	0.17	6.08	7.98	1.5
2M12193795+3553397	6179 ± 158	4.47 ± 0.2	4.32	-0.08 ± 0.06	-0.14 ± 0.1	0.19	6.53	8.17	1.46
2M12194438+4743465	5805 ± 128	4.25 ± 0.15	4.20	-0.02 ± 0.05	-0.09 ± 0.1	0.58	4.38	9.25	1.45
2M12200976+2559065	5929 ± 101	4.3 ± 0.15	4.22	-0.13 ± 0.04	-0.18 ± 0.1	0.47	5.07	8.04	0.44
2M12201000+2611509	5847 ± 97	4.35 ± 0.15	4.29	-0.19 ± 0.04	-0.27 ± 0.1	0.41	4.73	8.58	1.35
2M12201265+4540478	6036 ± 132	4.41 ± 0.17	4.30	0.08 ± 0.05	0.03 ± 0.1	0.54	5.43	11.2	1.48

APOGEE_ID	$T_{\rm eff} \pm \Delta T_{\rm eff}$	$\log g \pm \Delta \log g$	$\log g_{cor}$	$[\mathrm{M/H}] \pm \Delta[\mathrm{M/H}]$	$[Fe/H] \pm \Delta[\mathrm{Fe/H}]$	$\mathrm{v}_{\rm mic}$	$\mathrm{v}_{\rm mac}$	$v \sin i$	χ^2
2M12201709+2542599	5961 ± 132	4.33 ± 0.19	4.24	-0.06 ± 0.05	-0.12 ± 0.1	0.46	5.16	7.75	0.49
2M12201823+4701069	6000 ± 130	4.22 ± 0.13	4.12	0.03 ± 0.05	-0.02 ± 0.1	0.63	5.3	10.79	0.41
2M12202357+2602467	5706 ± 110	4.04 ± 0.11	4.02	0.12 ± 0.05	0.09 ± 0.1	0.99	3.89	9.47	0.52
2M12202982+4319585	5618 ± 103	4.26 ± 0.13	4.26	0.01 ± 0.04	-0.03 ± 0.1	0.91	3.67	9.94	0.51
2M12203036-0048330	6108 ± 124	4.31 ± 0.17	4.19	0.02 ± 0.05	-0.04 ± 0.1	0.51	5.95	8.42	0.34
2M12203182+1536584	6105 ± 65	4.34 ± 0.09	4.22	0.18 ± 0.03	0.11 ± 0.1	0.71	5.75	11.22	0.33
2M12203573+4339021	5856 ± 121	4.3 ± 0.16	4.24	0.05 ± 0.05	0.01 ± 0.1	0.73	4.52	9.66	1.54
2M12204491+4259465	5755 ± 113	4.23 ± 0.12	4.20	0.17 ± 0.05	0.13 ± 0.1	0.86	3.95	9.51	0.77
2M12204557+2545572	5902 ± 66	4.2 ± 0.09	4.13	-0.02 ± 0.03	-0.08 ± 0.1	1.21	4.84	10.79	0.25
2M12204931+1331430	5657 ± 94	4.32 ± 0.13	4.31	0.01 ± 0.04	-0.02 ± 0.1	0.81	3.77	10.09	1.46
2M12210006-0138348	6084 ± 131	4.4 ± 0.18	4.28	0.01 ± 0.05	-0.07 ± 0.1	0.45	5.8	8.96	0.36
2M12210509-0200195	6125 ± 111	4.4 ± 0.17	4.27	0.09 ± 0.04	0.03 ± 0.1	0.51	5.97	9.79	1.43
2M12211101+4616413	5870 ± 124	4.19 ± 0.16	4.13	0.08 ± 0.05	0.04 ± 0.1	0.75	4.57	9.98	0.56
2M12211115+1414130	6228 ± 117	4.21 ± 0.14	4.04	-0.21 ± 0.04	-0.3 ± 0.1	0	7.05	6.91	1.42
2M12212223+2555498	5952 ± 104	4.35 ± 0.13	4.27	0.02 ± 0.04	-0.02 ± 0.1	0.63	5.02	9.88	0.37
2M12212925+4511157	5638 ± 137	4.35 ± 0.2	4.34	-0.04 ± 0.06	-0.07 ± 0.1	0.96	3.76	8.68	0.64
2M12213705+4647518	5684 ± 119	4.09 ± 0.13	4.07	0.15 ± 0.05	0.1 ± 0.1	0.87	3.76	10.07	0.73
2M12213743+2647295	5659 ± 92	4.35 ± 0.13	4.34	-0.02 ± 0.04	-0.07 ± 0.1	0.89	3.81	9.57	0.44
2M12214228+2602244	5841 ± 165	4.19 ± 0.23	4.13	-0.3 ± 0.07	-0.42 ± 0.1	0.15	4.84	8.7	0.42
2M12215247-0030105	5963 ± 113	4.37 ± 0.14	4.28	0.01 ± 0.04	-0.05 ± 0.1	0.56	5.1	9.85	1.32

APOGEE_ID	$T_{\rm eff} \pm \Delta T_{\rm eff}$	$\log g \pm \Delta \log g$	$\log g_{cor}$	$[{\rm M/H}] \pm \Delta[{\rm M/H}]$	$[Fe/H] \pm \Delta[{\rm Fe/H}]$	$\mathsf{v}_{\rm mic}$	$\mathsf{v}_{\rm mac}$	$v \sin i$	χ^2
2M12215632+0033342	6172 ± 112	4.41 ± 0.17	4.26	-0.04 ± 0.04	-0.13 ± 0.1	0.19	6.44	9.09	1.35
2M12215682-0000372	6027 ± 96	4.4 ± 0.12	4.30	0 ± 0.04	-0.06 ± 0.1	0.44	5.46	9.05	1.35
2M12215701+2607156	5762 ± 117	4.13 ± 0.11	4.09	-0.03 ± 0.05	-0.1 ± 0.1	0.61	4.24	10.66	1.39
2M12220223+4537446	5636 ± 90	4.4 ± 0.13	4.40	-0.03 ± 0.04	-0.07 ± 0.1	0.66	3.74	10.68	1.41
2M12221115+4545298	6168 ± 138	4.34 ± 0.21	4.19	-0.04 ± 0.05	-0.11 ± 0.1	0.29	6.42	9.4	0.36
2M12222451+4418567	5551 ± 111	4.32 ± 0.13	4.34	0.01 ± 0.05	-0.03 ± 0.1	0.85	3.47	10.59	0.59
2M12222853+1441562	6213 ± 84	4.49 ± 0.08	4.32	0.16 ± 0.03	0.1 ± 0.1	0.65	6.49	10.91	0.35
2M12223134-0003525	6017 ± 84	4.45 ± 0.08	4.35	0 ± 0.03	-0.08 ± 0.1	0.42	5.41	9.41	1.33
2M12223147-0206383	6123 ± 147	4.23 ± 0.2	4.10	0.05 ± 0.06	-0.03 ± 0.1	0.68	6.03	8.81	0.47
2M12224965+2447323	5802 ± 85	4.32 ± 0.1	4.27	0.04 ± 0.03	-0.03 ± 0.1	0.56	4.28	10.2	1.38
2M12225644+2703009	5985 ± 99	4.37 ± 0.12	4.28	-0.02 ± 0.04	-0.1 ± 0.1	0.37	5.25	9.3	0.38
2M12230525+2724475	5982 ± 128	4.46 ± 0.14	4.37	-0.23 ± 0.05	-0.35 ± 0.1	0	5.45	7.9	0.38
2M12231674+4440203	5907 ± 160	4.18 ± 0.22	4.11	-0.04 ± 0.07	-0.12 ± 0.1	0.53	4.89	8.85	0.4
2M12232667-0130367	5886 ± 127	4.32 ± 0.2	4.25	-0.05 ± 0.05	-0.11 ± 0.1	0.56	4.77	9.32	0.45
2M12233507+4450230	5949 ± 122	4.37 ± 0.18	4.29	-0.04 ± 0.05	-0.1 ± 0.1	0.41	5.08	8.99	0.52
2M12240465-0211333	6010 ± 139	4.38 ± 0.19	4.28	-0.08 ± 0.06	-0.15 ± 0.1	0.36	5.45	8.24	1.36
2M12240572+2607430	5296 ± 48	4.42 ± 0.05	4.50	0 ± 0.02	-0.04 ± 0.1	1.03	3.08	10.2	0.52
2M12240748+1512190	5679 ± 113	4.2 ± 0.13	4.18	0.02 ± 0.05	-0.04 ± 0.1	0.77	3.85	9.79	0.44
2M12243463+1328392	6099 ± 131	4.35 ± 0.18	4.23	0.02 ± 0.05	-0.06 ± 0.1	0.55	5.89	9.15	0.34
2M12244213+4643019	5595 ± 100	4.01 ± 0.1	4.02	0.03 ± 0.04	-0.02 ± 0.1	0.77	3.64	10.31	0.53

APOGEE_ID	$T_{\rm eff} \pm \Delta T_{\rm eff}$	$\log g \pm \Delta \log g$	$\log g_{cor}$	$[\mathrm{M/H}] \pm \Delta[\mathrm{M/H}]$	$[Fe/H] \pm \Delta[\mathrm{Fe/H}]$	$\mathrm{v}_{\rm mic}$	$\mathrm{v}_{\rm mac}$	$v \sin i$	χ^2
2M12244529+2457543	6183 ± 100	4.34 ± 0.14	4.19	0.13 ± 0.04	0.08 ± 0.1	0.71	6.33	10.05	0.44
2M12244776+2712022	5677 ± 112	4.07 ± 0.12	4.05	-0.01 ± 0.05	-0.07 ± 0.1	0.87	3.92	9.53	0.5
2M12245172+2724316	5613 ± 89	4.05 ± 0.1	4.05	-0.11 ± 0.04	-0.19 ± 0.1	0.68	3.83	9.61	1.25
2M12250109+2621005	5860 ± 70	4.31 ± 0.09	4.25	0.18 ± 0.03	0.12 ± 0.1	0.72	4.38	10.39	0.45
2M12250326+4604401	6161 ± 119	4.5 ± 0.13	4.36	0.12 ± 0.05	0.05 ± 0.1	0.56	6.17	10.26	1.47
2M12250698+4447567	5978 ± 103	4.18 ± 0.11	4.09	-0.02 ± 0.04	-0.1 ± 0.1	0.55	5.24	8.76	0.35
2M12250987+1424181	6015 ± 77	4.35 ± 0.09	4.25	0.08 ± 0.03	0.01 ± 0.1	0.54	5.31	9.23	1.35
2M12251296-0111208	5982 ± 122	4.3 ± 0.15	4.21	-0.19 ± 0.05	-0.28 ± 0.1	0	5.42	6.86	1.37
2M12251394+4547515	5864 ± 135	4.38 ± 0.19	4.32	0.07 ± 0.05	0.02 ± 0.1	0.64	4.53	10.88	1.64
2M12251788-0026421	6192 ± 134	4.43 ± 0.19	4.27	-0.2 ± 0.05	-0.22 ± 0.1	0.32	6.75	9.66	0.21
2M12252404+2659467	5900 ± 109	4.22 ± 0.15	4.15	0.07 ± 0.04	0.01 ± 0.1	0.76	4.71	9.23	1.41
2M12253313-0039284	6099 ± 98	4.38 ± 0.14	4.26	0.05 ± 0.04	-0.02 ± 0.1	0.54	5.85	9.03	1.36
2M12253368+2445270	5776 ± 80	4.24 ± 0.09	4.20	0.14 ± 0.03	0.1 ± 0.1	0.91	4.07	9.73	0.52
2M12254874+2633433	6042 ± 151	4.17 ± 0.17	4.06	-0.04 ± 0.06	-0.13 ± 0.1	0.47	5.64	8.76	1.4
2M12255895+1503282	5556 ± 89	4.18 ± 0.1	4.20	0.1 ± 0.04	0.07 ± 0.1	0.93	3.41	10.29	0.6
2M12262251+2643399	5871 ± 72	4.35 ± 0.11	4.29	-0.04 ± 0.03	-0.1 ± 0.1	0.46	4.68	9.57	0.32
2M12263000+4601024	5802 ± 142	4.23 ± 0.18	4.18	-0.13 ± 0.06	-0.2 ± 0.1	0.64	4.48	8.49	1.47
2M12264856+4725331	6164 ± 150	4.46 ± 0.18	4.32	0.09 ± 0.06	0.03 ± 0.1	0.61	6.24	9.8	1.53
2M12265233+4727114	5798 ± 91	4.29 ± 0.11	4.24	0.06 ± 0.04	0.02 ± 0.1	0.76	4.25	10.51	1.41
2M12270149-0009383	5960 ± 134	4.16 ± 0.17	4.07	-0.17 ± 0.05	-0.27 ± 0.1	0.22	5.31	8.22	1.38

APOGEE_ID	$T_{\mathrm{eff}} \pm \Delta T_{\mathrm{eff}}$	$\log g \pm \Delta \log g$	$\log g_{cor}$	$[\mathrm{M/H}] \pm \Delta[\mathrm{M/H}]$	$[Fe/H] \pm \Delta[\mathrm{Fe/H}]$	$\mathrm{v}_{\mathrm{mic}}$	$\mathrm{v}_{\mathrm{mac}}$	$v \sin i$	χ^2
2M12270627+2650445	5606 ± 52	4.31 ± 0.07	4.31	-0.02 ± 0.02	-0.07 ± 0.1	1.14	3.65	10.48	1.43
2M12271498+4415232	5819 ± 100	4.09 ± 0.11	4.04	0.1 ± 0.04	0.06 ± 0.1	0.87	4.34	9.96	0.42
2M12271972+4646124	6042 ± 147	4.34 ± 0.21	4.23	-0.09 ± 0.06	-0.17 ± 0.1	0.06	5.66	8.53	1.39
2M12275749+2624217	5626 ± 118	4.24 ± 0.15	4.24	0.07 ± 0.05	0 ± 0.1	0.64	3.62	9.39	1.73
2M12281616+2625457	5493 ± 83	4.18 ± 0.08	4.21	0.09 ± 0.04	0.07 ± 0.1	1.06	3.27	10.08	1.69
2M12283674+5713252	6070 ± 92	4.34 ± 0.12	4.23	0.06 ± 0.04	-0.03 ± 0.1	0.53	5.66	9.44	1.34
2M12285215+4523197	5855 ± 160	4.26 ± 0.23	4.20	-0.21 ± 0.07	-0.3 ± 0.1	0.43	4.8	8.4	1.51
2M12290365+4540154	5674 ± 133	4.4 ± 0.2	4.39	-0.17 ± 0.06	-0.22 ± 0.1	0.55	4.01	9.36	1.6
2M12290421+4349283	5489 ± 72	4.21 ± 0.07	4.24	0.04 ± 0.03	0 ± 0.1	0.85	3.32	10.64	0.61
2M12295739+1415148	5879 ± 135	4.26 ± 0.18	4.19	0 ± 0.05	-0.07 ± 0.1	0.8	4.69	9.82	0.41
2M12301232+2632015	6187 ± 101	4.4 ± 0.15	4.25	-0.04 ± 0.04	-0.12 ± 0.1	0.34	6.54	8.71	0.35
2M12302624+4423337	5993 ± 138	4.18 ± 0.14	4.09	0.02 ± 0.05	-0.05 ± 0.1	0.76	5.28	9.5	0.54
2M12302943+5635002	6149 ± 144	4.29 ± 0.22	4.15	-0.03 ± 0.06	-0.1 ± 0.1	0.44	6.28	8.93	1.45
2M12310447+4533395	5802 ± 151	4.27 ± 0.2	4.22	-0.15 ± 0.06	-0.22 ± 0.1	0.41	4.49	8.71	0.62
2M12310615+2640132	5992 ± 97	4.36 ± 0.12	4.27	-0.04 ± 0.04	-0.11 ± 0.1	0.57	5.31	9.22	0.29
2M12311486+4452494	5781 ± 118	4.35 ± 0.14	4.31	0.03 ± 0.05	0 ± 0.1	0.78	4.21	9.72	1.07
2M12323053+5658347	6001 ± 44	4.39 ± 0.05	4.29	0.18 ± 0.02	0.13 ± 0.1	0.66	5.11	10.58	0.4
2M12331381+4618061	5689 ± 127	4.31 ± 0.18	4.29	-0.26 ± 0.05	-0.35 ± 0.1	0.34	4.17	7.01	0.43
2M12333642+4432466	5880 ± 122	4.38 ± 0.18	4.31	0.06 ± 0.05	0.02 ± 0.1	0.59	4.61	10.36	1.52
2M12341996+4600347	5990 ± 110	4.29 ± 0.12	4.20	0.08 ± 0.04	0.03 ± 0.1	0.75	5.17	10.62	0.62

APOGEE_ID	$T_{\rm eff} \pm \Delta T_{\rm eff}$	$\log g \pm \Delta \log g$	$\log g_{cor}$	$[{\rm M/H}] \pm \Delta[{\rm M/H}]$	$[Fe/H] \pm \Delta[{\rm Fe/H}]$	$\mathsf{v}_{\rm mic}$	$\mathsf{v}_{\rm mac}$	$v \sin i$	χ^2
2M12345939+5722237	6232 ± 146	4.49 ± 0.13	4.32	0.11 ± 0.06	0.05 ± 0.1	0.59	6.69	9.47	0.46
2M12364833+4636490	5937 ± 155	4.14 ± 0.2	4.06	-0.07 ± 0.06	-0.15 ± 0.1	0.5	5.08	8.43	0.73
2M12372671+4514409	5882 ± 129	4.16 ± 0.16	4.09	0.03 ± 0.05	-0.04 ± 0.1	0.17	4.69	9.38	0.96
2M12373636+4610405	5831 ± 150	4.21 ± 0.2	4.16	-0.17 ± 0.06	-0.25 ± 0.1	0.45	4.66	8.06	1.52
2M12374122+4613284	5859 ± 87	4.4 ± 0.13	4.34	-0.09 ± 0.04	-0.16 ± 0.1	0.28	4.67	10.3	1.49
2M12385328+4425117	6103 ± 128	4.33 ± 0.18	4.21	0.04 ± 0.05	-0.02 ± 0.1	0.56	5.9	9.21	1.51
2M12391041+4611271	5778 ± 98	4.25 ± 0.11	4.21	0.09 ± 0.04	0.03 ± 0.1	0.83	4.14	9.59	0.67
2M12392897-0818281	6040 ± 116	4.11 ± 0.13	4.00	-0.2 ± 0.05	-0.28 ± 0.1	0.39	5.81	6.93	0.4
2M12395378+4605341	6030 ± 131	4.36 ± 0.16	4.26	0.06 ± 0.05	0 ± 0.1	0.63	5.42	10.68	0.72
2M12401083+4448224	5713 ± 129	4.23 ± 0.16	4.21	-0.06 ± 0.06	-0.12 ± 0.1	0.65	4.06	9.08	1.56
2M12402362+4616406	5720 ± 148	4.07 ± 0.16	4.04	-0.21 ± 0.06	-0.26 ± 0.1	0.46	4.29	10.41	0.82
2M12403140+4615523	5605 ± 81	4.18 ± 0.09	4.18	0.11 ± 0.04	0.08 ± 0.1	0.93	3.52	9.76	0.85
2M12404657+4420308	5947 ± 153	4.26 ± 0.19	4.18	-0.01 ± 0.06	-0.07 ± 0.1	0.65	5.04	8.82	1.72
2M12405736-0710571	5992 ± 59	4.35 ± 0.07	4.26	0.04 ± 0.02	-0.02 ± 0.1	0.6	5.22	9.79	0.32
2M12410384-0742279	5581 ± 103	4.22 ± 0.12	4.23	0.04 ± 0.04	-0.01 ± 0.1	0.9	3.54	10.34	0.67
2M12415688-0213442	6008 ± 87	4.35 ± 0.1	4.25	0.13 ± 0.03	0.07 ± 0.1	0.6	5.21	9.79	1.46
2M12420249+4513551	6308 ± 162	4.36 ± 0.23	4.15	-0.04 ± 0.06	-0.1 ± 0.1	0.33	7.45	8.28	0.87
2M12420465+4634413	5823 ± 141	4.29 ± 0.2	4.24	-0.09 ± 0.06	-0.17 ± 0.1	0.56	4.53	9.56	1.7
2M12420944-0856404	6064 ± 116	4.34 ± 0.17	4.23	-0.08 ± 0.05	-0.16 ± 0.1	0.25	5.78	8.19	0.36
2M12421923-0629413	5969 ± 125	4.34 ± 0.17	4.25	-0.08 ± 0.05	-0.16 ± 0.1	0.35	5.23	8.97	0.37

APOGEE_ID	$T_{\rm eff} \pm \Delta T_{\rm eff}$	$\log g \pm \Delta \log g$	$\log g_{cor}$	$[\rm M/H] \pm \Delta[\rm M/H]$	$[Fe/H] \pm \Delta[\rm Fe/H]$	$\rm v_{mic}$	$\rm v_{mac}$	$v \sin i$	χ^2
2M12422041+4614416	5697 ± 149	4.3 ± 0.2	4.28	-0.22 ± 0.06	-0.3 ± 0.1	0.5	4.16	8.4	0.62
2M12422877-0656364	5939 ± 154	4.15 ± 0.2	4.07	-0.12 ± 0.06	-0.21 ± 0.1	0.5	5.15	8.67	0.54
2M12423202+4612579	6013 ± 126	4.41 ± 0.14	4.31	0.01 ± 0.05	-0.06 ± 0.1	0.44	5.37	10.86	1.59
2M12424460-0719316	5910 ± 141	4.28 ± 0.19	4.21	0.06 ± 0.06	0 ± 0.1	0.69	4.78	9.72	1.51
2M12424491-0701206	6021 ± 103	4.35 ± 0.13	4.25	-0.15 ± 0.04	-0.23 ± 0.1	0	5.59	8.11	1.33
2M12424624+1215168	6166 ± 113	4.43 ± 0.15	4.28	0.07 ± 0.04	0 ± 0.1	0.49	6.27	8.99	0.4
2M12430337+4657115	5858 ± 138	4.07 ± 0.16	4.01	0.06 ± 0.06	0.01 ± 0.1	0.84	4.57	10.75	0.74
2M12431626-0724127	5846 ± 129	4.27 ± 0.17	4.21	0.1 ± 0.05	0.04 ± 0.1	0.67	4.42	10.98	0.7
2M12432065-0742360	5701 ± 129	4.45 ± 0.14	4.43	-0.04 ± 0.05	-0.08 ± 0.1	0.6	3.97	10.88	0.59
2M12434051+4444016	5636 ± 69	3.98 ± 0.08	3.98	0.12 ± 0.03	0.07 ± 0.1	0.96	3.67	10.12	1.6
2M12435949+1252352	6210 ± 100	4.48 ± 0.1	4.32	0.04 ± 0.04	-0.02 ± 0.1	0.34	6.61	8.94	1.37
2M12441127+4427001	5984 ± 141	4.33 ± 0.16	4.24	0.05 ± 0.06	-0.02 ± 0.1	0.58	5.17	8.97	0.71
2M12441865-0348503	6158 ± 92	4.43 ± 0.14	4.29	-0.09 ± 0.04	-0.16 ± 0.1	0.23	6.39	7.75	1.37
2M12442957+4621241	6053 ± 130	4.33 ± 0.16	4.22	0.07 ± 0.05	-0.01 ± 0.1	0.56	5.55	9.32	0.78
2M12443204-0858138	5787 ± 116	4.32 ± 0.14	4.28	-0.02 ± 0.05	-0.08 ± 0.1	0.64	4.28	9.09	0.43
2M12450436+4630359	5694 ± 138	4.19 ± 0.18	4.17	-0.26 ± 0.06	-0.39 ± 0.1	0.4	4.21	8.61	0.5
2M12452192-0341195	5959 ± 145	4.41 ± 0.2	4.32	-0.2 ± 0.06	-0.29 ± 0.1	0.18	5.29	8.37	0.51
2M12452811+4528122	6210 ± 122	4.52 ± 0.12	4.36	0.01 ± 0.05	-0.04 ± 0.1	0.34	6.65	10.28	0.5
2M12453464-0217085	5767 ± 117	4.3 ± 0.13	4.26	0.01 ± 0.05	-0.06 ± 0.1	0.72	4.18	9.71	1.66
2M12454608-0634093	6036 ± 110	4.4 ± 0.14	4.29	0.03 ± 0.04	-0.05 ± 0.1	0.56	5.48	9.63	1.38

APOGEE_ID	$T_{\rm eff} \pm \Delta T_{\rm eff}$	$\log g \pm \Delta \log g$	$\log g_{cor}$	$[\rm M/H] \pm \Delta[\rm M/H]$	$[Fe/H] \pm \Delta[\rm Fe/H]$	$\rm v_{mic}$	$\rm v_{mac}$	$v \sin i$	χ^2
2M12461723-0153587	6124 ± 154	4.15 ± 0.21	4.02	-0.18 ± 0.06	-0.28 ± 0.1	0.28	6.31	8.02	1.51
2M12463435+4519584	5576 ± 108	4.27 ± 0.13	4.28	0.04 ± 0.05	0.01 ± 0.1	0.97	3.51	9.98	1.91
2M12464853-0240002	5963 ± 110	4.35 ± 0.14	4.26	-0.03 ± 0.04	-0.1 ± 0.1	0.52	5.14	8.53	1.32
2M12465330+4439489	5697 ± 132	4.34 ± 0.18	4.32	-0.14 ± 0.06	-0.2 ± 0.1	0.58	4.07	8.95	1.61
2M12465933+4345539	5859 ± 132	4.33 ± 0.18	4.27	-0.02 ± 0.06	-0.07 ± 0.1	0.64	4.6	9.06	0.67
2M12470347+1314561	6056 ± 119	4.42 ± 0.16	4.31	-0.11 ± 0.05	-0.2 ± 0.1	0.25	5.75	8.3	1.36
2M12470691+4543349	5918 ± 142	4.31 ± 0.21	4.23	-0.04 ± 0.06	-0.09 ± 0.1	0.76	4.92	8.74	1.68
2M12470848+4559324	5773 ± 152	4.28 ± 0.19	4.24	-0.23 ± 0.06	-0.33 ± 0.1	0.4	4.46	7.97	1.91
2M12470890+1324464	6113 ± 126	4.35 ± 0.18	4.23	0.01 ± 0.05	-0.08 ± 0.1	0.4	6	9.2	0.32
2M12472191+4513023	6005 ± 156	4.27 ± 0.17	4.17	-0.01 ± 0.06	-0.09 ± 0.1	0.57	5.36	9.33	1.74
2M12472580-0735521	6137 ± 106	4.38 ± 0.16	4.25	0.01 ± 0.04	-0.06 ± 0.1	0.55	6.14	9.29	1.29
2M12473669+2724336	6061 ± 58	4.3 ± 0.07	4.19	0.09 ± 0.02	0.02 ± 0.1	0.61	5.58	9.66	0.35
2M12481268+1158032	6133 ± 77	4.33 ± 0.12	4.20	-0.07 ± 0.03	-0.15 ± 0.1	0.28	6.21	8.2	1.37
2M12482140+1040113	6118 ± 122	4.4 ± 0.19	4.28	-0.02 ± 0.05	-0.09 ± 0.1	0.41	6.06	8.69	1.35
2M12482452-0722104	5815 ± 135	4.38 ± 0.19	4.33	-0.13 ± 0.06	-0.18 ± 0.1	0.62	4.51	8.77	0.45
2M12482565+1128422	5972 ± 136	4.39 ± 0.19	4.30	-0.15 ± 0.05	-0.21 ± 0.1	0.47	5.31	7.84	0.35
2M12483409+2635493	5933 ± 82	4.28 ± 0.11	4.20	-0.04 ± 0.03	-0.1 ± 0.1	0.51	5	8.35	1.34
2M12485710+2711388	5887 ± 136	4.38 ± 0.2	4.31	0.09 ± 0.06	0.04 ± 0.1	0.7	4.61	10.69	0.67
2M12491737+4149206	6066 ± 110	4.22 ± 0.13	4.11	0.03 ± 0.04	-0.01 ± 0.1	0.67	5.69	9.67	0.37
2M12492500+2611509	6182 ± 163	4.24 ± 0.23	4.09	-0.17 ± 0.06	-0.26 ± 0.1	0.14	6.67	8.1	0.39

APOGEE_ID	$T_{\rm eff} \pm \Delta T_{\rm eff}$	$\log g \pm \Delta \log g$	$\log g_{cor}$	$[\rm M/H] \pm \Delta[\rm M/H]$	$[Fe/H] \pm \Delta[\rm Fe/H]$	$v_{\rm mic}$	$v_{\rm mac}$	$v \sin i$	χ^2
2M12493519+4610167	5568 ± 90	4.32 ± 0.11	4.33	-0.02 ± 0.04	-0.05 ± 0.1	1.35	3.55	9.66	0.54
2M12494025+4420290	6128 ± 157	4.14 ± 0.22	4.01	-0.2 ± 0.06	-0.31 ± 0.1	0.33	6.36	6.96	0.73
2M12494576+1313015	6057 ± 122	4.41 ± 0.16	4.30	-0.01 ± 0.05	-0.07 ± 0.1	0.49	5.65	9.33	1.39
2M12494683+2700492	5897 ± 136	4.2 ± 0.19	4.13	-0.03 ± 0.06	-0.08 ± 0.1	0.75	4.82	9.75	0.5
2M12495030+4354196	5633 ± 128	4.27 ± 0.16	4.27	0 ± 0.05	-0.05 ± 0.1	0.8	3.72	9.32	0.78
2M12501681+2801259	6130 ± 158	4.39 ± 0.26	4.26	-0.09 ± 0.06	-0.16 ± 0.1	0	6.2	8.05	0.52
2M12502292+2744285	6006 ± 128	4.29 ± 0.14	4.19	0.08 ± 0.05	0.05 ± 0.1	0.78	5.27	9.51	0.62
2M12502467+2722508	5711 ± 113	4.28 ± 0.13	4.26	0.02 ± 0.05	-0.01 ± 0.1	0.51	3.95	9.46	0.75
2M12502847+2613140	6010 ± 120	4.16 ± 0.13	4.06	-0.04 ± 0.05	-0.09 ± 0.1	0.43	5.45	10.13	0.44
2M12503566+2636160	5938 ± 108	4.27 ± 0.14	4.19	0.03 ± 0.04	-0.02 ± 0.1	0.71	4.95	9.85	1.41
2M12504239+4329115	6277 ± 111	4.5 ± 0.1	4.31	0.11 ± 0.04	0.06 ± 0.1	0.55	7.04	10.53	0.4
2M12511345+4217527	6052 ± 126	4.38 ± 0.17	4.27	0.02 ± 0.05	-0.04 ± 0.1	0.43	5.59	10.2	1.45
2M12513244+2830094	6127 ± 138	4.72 ± 0.18	4.59	0.02 ± 0.05	-0.08 ± 0.1	0.27	6.09	7.87	1.44
2M12513371+4232441	5988 ± 140	4.36 ± 0.18	4.27	-0.06 ± 0.06	-0.12 ± 0.1	0.5	5.3	9.24	1.52
2M12515392+4214134	5902 ± 165	4.2 ± 0.25	4.13	-0.22 ± 0.07	-0.3 ± 0.1	0.12	5.05	8.46	0.5
2M12515647+2806516	5987 ± 95	4.14 ± 0.1	4.05	0.01 ± 0.04	-0.06 ± 0.1	0.58	5.27	10.49	0.34
2M12521684+2536009	5597 ± 120	4.29 ± 0.15	4.29	-0.01 ± 0.05	-0.04 ± 0.1	0.75	3.62	9.92	1.67
2M12524945+4256321	6055 ± 157	4.34 ± 0.22	4.23	-0.13 ± 0.06	-0.21 ± 0.1	0.28	5.78	8.78	0.36
2M12530256+2532164	5947 ± 114	4.28 ± 0.16	4.20	-0.08 ± 0.05	-0.15 ± 0.1	0.38	5.12	8.81	1.55
2M12533014+4249218	6045 ± 89	4.43 ± 0.1	4.32	0 ± 0.03	-0.07 ± 0.1	0.3	5.57	9.03	0.37

APOGEE_ID	$T_{\mathrm{eff}} \pm \Delta T_{\mathrm{eff}}$	$\log g \pm \Delta \log g$	$\log g_{cor}$	$[\mathrm{M/H}] \pm \Delta[\mathrm{M/H}]$	$[Fe/H] \pm \Delta[\mathrm{Fe/H}]$	$\mathrm{v}_{\mathrm{mic}}$	$\mathrm{v}_{\mathrm{mac}}$	$v \sin i$	χ^2
2M12533211+4409583	5953 ± 112	4.28 ± 0.14	4.20	0.07 ± 0.04	0 ± 0.1	0.66	4.99	9.33	1.44
2M12533531+2737033	6136 ± 144	4.49 ± 0.17	4.36	-0.04 ± 0.06	-0.09 ± 0.1	0.36	6.19	10.66	0.52
2M12533569+1131115	6162 ± 119	4.34 ± 0.19	4.20	-0.11 ± 0.05	-0.2 ± 0.1	0.21	6.45	7.79	0.34
2M12534991+2742331	5839 ± 115	4.35 ± 0.15	4.29	-0.01 ± 0.05	-0.04 ± 0.1	0.7	4.49	9.67	0.64
2M12541709+4500449	5797 ± 141	4.25 ± 0.16	4.20	0.01 ± 0.06	-0.06 ± 0.1	0.65	4.31	9.37	1.13
2M12542404+4250378	6184 ± 137	4.34 ± 0.19	4.19	0.03 ± 0.05	-0.05 ± 0.1	0.6	6.46	8.9	0.48
2M12542802+4044325	5889 ± 129	4.27 ± 0.18	4.20	0.03 ± 0.05	-0.02 ± 0.1	0.81	4.7	8.61	1.47
2M12544036+2858051	5418 ± 72	4.25 ± 0.09	4.30	0.04 ± 0.03	0.03 ± 0.1	1.38	3.19	11.25	0.76
2M12545897+4406407	5735 ± 115	4.4 ± 0.15	4.37	-0.09 ± 0.05	-0.15 ± 0.1	0.57	4.15	8.35	1.57
2M12550201+4236246	6158 ± 67	4.48 ± 0.07	4.34	0.17 ± 0.03	0.11 ± 0.1	0.55	6.1	10.85	1.36
2M12550668+2859346	5695 ± 107	4.45 ± 0.12	4.43	-0.04 ± 0.04	-0.09 ± 0.1	0.72	3.94	9.07	0.52
2M12550857+4423134	5688 ± 107	4.16 ± 0.13	4.14	-0.1 ± 0.05	-0.18 ± 0.1	0.57	4.03	9.12	1.46
2M12552460+2903443	5995 ± 123	4.29 ± 0.14	4.19	0.1 ± 0.05	0.03 ± 0.1	0.63	5.17	9.66	1.69
2M12553048+4222522	5953 ± 102	4.23 ± 0.13	4.15	-0.08 ± 0.04	-0.15 ± 0.1	0.54	5.16	8.3	0.41
2M12553134+4304038	6123 ± 108	4.36 ± 0.17	4.23	-0.05 ± 0.04	-0.14 ± 0.1	0.22	6.12	8.21	0.43
2M12554312+2657108	5584 ± 91	4.29 ± 0.11	4.30	0.01 ± 0.04	-0.03 ± 0.1	0.81	3.56	10.36	1.46
2M12560693+2757400	5601 ± 131	4.43 ± 0.17	4.43	-0.09 ± 0.06	-0.14 ± 0.1	0.81	3.71	10.78	1.66
2M12561360+2903057	5994 ± 132	4.26 ± 0.14	4.16	0.1 ± 0.05	0.04 ± 0.1	0.7	5.18	10.92	0.55
2M12563106+4209417	5684 ± 100	4.45 ± 0.11	4.43	-0.14 ± 0.04	-0.18 ± 0.1	0.65	4.01	10.17	0.38
2M12563793+2721062	5721 ± 124	4.41 ± 0.15	4.38	-0.21 ± 0.05	-0.29 ± 0.1	0	4.21	8.99	1.48

APOGEE_ID	$T_{\rm eff} \pm \Delta T_{\rm eff}$	$\log g \pm \Delta \log g$	$\log g_{cor}$	$[\rm M/H] \pm \Delta[\rm M/H]$	$[Fe/H] \pm \Delta[\rm Fe/H]$	$\rm v_{mic}$	$\rm v_{mac}$	$v \sin i$	χ^2
2M12564033+4356336	5991 ± 168	4.26 ± 0.2	4.17	-0.2 ± 0.07	-0.28 ± 0.1	0.33	5.48	7.98	0.51
2M12565196+2748091	5892 ± 85	4.35 ± 0.12	4.28	-0.01 ± 0.03	-0.06 ± 0.1	0.47	4.75	9.01	0.44
2M12570260+4252216	5777 ± 88	4.34 ± 0.11	4.30	-0.17 ± 0.04	-0.24 ± 0.1	0.41	4.4	8.48	0.44
2M12571945+2527010	5863 ± 119	4.27 ± 0.16	4.21	0.13 ± 0.05	0.09 ± 0.1	0.65	4.46	9.75	1.65
2M12572368+2625280	5847 ± 123	4.03 ± 0.14	3.97	-0.09 ± 0.05	-0.15 ± 0.1	0.71	4.69	8.96	0.45
2M12574552+4322094	5999 ± 139	4.24 ± 0.14	4.14	0.01 ± 0.05	-0.07 ± 0.1	0.61	5.31	9.02	0.45
2M12575815+2853389	5536 ± 96	4.25 ± 0.11	4.27	-0.04 ± 0.04	-0.09 ± 0.1	0.77	3.5	11.15	0.41
2M12580405+2651228	5667 ± 127	4.44 ± 0.16	4.43	-0.07 ± 0.05	-0.11 ± 0.1	0.58	3.88	10.59	1.73
2M12580583+4106047	6214 ± 62	4.45 ± 0.07	4.28	-0.14 ± 0.02	-0.22 ± 0.1	0	6.84	7.73	0.37
2M12583271+2725086	5842 ± 138	4.22 ± 0.17	4.16	-0.01 ± 0.06	-0.08 ± 0.1	0.63	4.53	8.63	0.69
2M12583664+4343352	5853 ± 138	4.34 ± 0.21	4.28	-0.1 ± 0.06	-0.16 ± 0.1	0.53	4.65	9.11	1.2
2M12584270+2626187	5633 ± 113	4.31 ± 0.15	4.31	0 ± 0.05	-0.02 ± 0.1	0.85	3.71	9.82	0.61
2M12584789+2713514	5977 ± 133	4.38 ± 0.17	4.29	0.01 ± 0.05	-0.04 ± 0.1	0.6	5.17	10.69	1.51
2M12584793+2622523	5613 ± 103	4.12 ± 0.12	4.12	0.16 ± 0.05	0.12 ± 0.1	0.84	3.5	9.89	1.88
2M12585388+2630367	6002 ± 170	4.12 ± 0.18	4.02	-0.2 ± 0.07	-0.29 ± 0.1	0.45	5.59	7.61	0.5
2M12585471+2851335	5889 ± 130	4.45 ± 0.17	4.38	-0.06 ± 0.05	-0.11 ± 0.1	0.35	4.77	8.46	1.59
2M12592241+2707354	5796 ± 114	4.3 ± 0.13	4.25	-0.02 ± 0.05	-0.07 ± 0.1	0.5	4.33	8.79	0.43
2M12592429+4316110	5874 ± 88	4.14 ± 0.11	4.08	0.07 ± 0.04	0 ± 0.1	0.76	4.62	9.29	0.4
2M12594639+2708246	5919 ± 129	4.35 ± 0.18	4.27	0 ± 0.05	-0.06 ± 0.1	0.47	4.88	9.13	1.51
2M12595831+2700142	5944 ± 137	4.27 ± 0.17	4.19	0.03 ± 0.05	-0.04 ± 0.1	0.7	4.98	8.8	0.69

APOGEE_ID	$T_{\rm eff} \pm \Delta T_{\rm eff}$	$\log g \pm \Delta \log g$	$\log g_{cor}$	$[\mathrm{M/H}] \pm \Delta[\mathrm{M/H}]$	$[Fe/H] \pm \Delta[\mathrm{Fe/H}]$	$\mathrm{v}_{\rm mic}$	$\mathrm{v}_{\rm mac}$	$v \sin i$	χ^2
2M13000218+2831208	5764 ± 117	4.35 ± 0.14	4.31	-0.04 ± 0.05	-0.09 ± 0.1	0.69	4.21	9.25	1.45
2M13001431+4323412	5719 ± 100	4.17 ± 0.11	4.14	0.16 ± 0.04	0.13 ± 0.1	0.93	3.85	9.76	0.67
2M13001585+2838280	6211 ± 166	4.25 ± 0.22	4.09	-0.24 ± 0.06	-0.34 ± 0.1	0	6.94	7.36	1.45
2M13001597+2841130	5872 ± 131	4.27 ± 0.18	4.21	-0.01 ± 0.05	-0.07 ± 0.1	0.52	4.66	9.71	0.59
2M13002174+2646026	5940 ± 131	4.16 ± 0.15	4.08	0.02 ± 0.05	-0.05 ± 0.1	0.57	4.99	9.59	0.44
2M13003584+2814327	5936 ± 138	4.37 ± 0.19	4.29	0.09 ± 0.06	0.04 ± 0.1	0.66	4.86	10.23	1.75
2M13003715+2559046	5832 ± 101	4.15 ± 0.12	4.10	0.27 ± 0.04	0.22 ± 0.1	0.81	4.18	9.34	1.76
2M13004165+2750391	5734 ± 104	4.23 ± 0.11	4.20	0.06 ± 0.04	0 ± 0.1	0.69	4.01	10.31	0.63
2M13011084+2728012	5912 ± 123	4.21 ± 0.18	4.14	-0.09 ± 0.05	-0.15 ± 0.1	0.25	4.96	8.77	0.55
2M13012601+4311420	6176 ± 144	4.35 ± 0.23	4.20	-0.2 ± 0.06	-0.28 ± 0.1	0	6.64	8.06	1.7
2M13015152+2720148	5817 ± 112	4.26 ± 0.13	4.21	-0.01 ± 0.05	-0.07 ± 0.1	0.5	4.41	8.72	0.59
2M13020215+5653436	6069 ± 94	4.35 ± 0.13	4.24	0.02 ± 0.04	-0.02 ± 0.1	0.69	5.69	9.47	1.27
2M13020445+4327389	6293 ± 109	4.35 ± 0.14	4.15	0.01 ± 0.04	-0.06 ± 0.1	0.26	7.28	8.69	0.37
2M13020995+2748510	5857 ± 129	4.27 ± 0.17	4.21	0.02 ± 0.05	-0.05 ± 0.1	0.65	4.56	9.49	0.55
2M13021138+2640024	5737 ± 124	4.32 ± 0.14	4.29	-0.02 ± 0.05	-0.07 ± 0.1	0.68	4.09	8.37	1.6
2M13021783+2807321	5519 ± 123	4.37 ± 0.14	4.39	-0.04 ± 0.05	-0.07 ± 0.1	1.03	3.44	10.96	0.8
2M13023402+2629554	5832 ± 111	4.31 ± 0.14	4.26	0.06 ± 0.05	0.02 ± 0.1	0.74	4.39	9.98	0.58
2M13024999+2721409	5787 ± 126	4.3 ± 0.14	4.26	0.02 ± 0.05	-0.01 ± 0.1	0.75	4.25	10.09	0.85
2M13025067+2650004	6096 ± 149	4.43 ± 0.19	4.31	0.01 ± 0.06	-0.05 ± 0.1	0.55	5.88	8.73	1.59
2M13025088+2838470	5776 ± 147	4.32 ± 0.19	4.28	-0.29 ± 0.06	-0.36 ± 0.1	0.38	4.52	8.3	0.48

APOGEE_ID	$T_{\rm eff} \pm \Delta T_{\rm eff}$	$\log g \pm \Delta \log g$	$\log g_{cor}$	$[\mathrm{M/H}] \pm \Delta[\mathrm{M/H}]$	$[Fe/H] \pm \Delta[\mathrm{Fe/H}]$	$\mathrm{v}_{\rm mic}$	$\mathrm{v}_{\rm mac}$	$v \sin i$	χ^2
2M13025250+2749475	5952 ± 152	4.16 ± 0.17	4.08	-0.02 ± 0.06	-0.1 ± 0.1	0.6	5.1	9.34	1.56
2M13025569+2745588	5511 ± 99	4.32 ± 0.11	4.35	-0.04 ± 0.04	-0.07 ± 0.1	0.95	3.44	8.73	0.59
2M13031487+2836254	5743 ± 102	4.36 ± 0.12	4.33	-0.11 ± 0.04	-0.17 ± 0.1	0.54	4.2	8.85	0.34
2M13033830+4637016	6168 ± 145	4.45 ± 0.2	4.30	-0.05 ± 0.06	-0.13 ± 0.1	0.26	6.42	8.35	0.47
2M13035212+4720248	6242 ± 153	4.39 ± 0.19	4.21	0.01 ± 0.06	-0.07 ± 0.1	0.42	6.89	9.72	0.41
2M13035312+4849441	5871 ± 146	4.35 ± 0.23	4.29	-0.15 ± 0.06	-0.23 ± 0.1	0	4.8	8.31	0.64
2M13040077+4550067	5950 ± 146	4.48 ± 0.16	4.40	-0.14 ± 0.06	-0.19 ± 0.1	0.19	5.17	9.05	1.5
2M13040988+4647176	5568 ± 119	4.3 ± 0.14	4.31	0 ± 0.05	-0.04 ± 0.1	1.03	3.53	10.57	1.59
2M13042925+2836127	5800 ± 122	4.17 ± 0.13	4.12	0.11 ± 0.05	0.06 ± 0.1	0.78	4.23	10.51	0.79
2M13042978+4840349	5980 ± 131	4.35 ± 0.16	4.26	0.07 ± 0.05	0.02 ± 0.1	0.61	5.12	10.86	0.48
2M13043479+2647486	5995 ± 154	4.23 ± 0.18	4.13	-0.11 ± 0.06	-0.18 ± 0.1	0.38	5.42	8.97	0.56
2M13045542+2706511	5472 ± 121	4.26 ± 0.14	4.30	-0.04 ± 0.05	-0.05 ± 0.1	1.43	3.36	8.36	0.83
2M13050387+5724349	6187 ± 115	4.32 ± 0.17	4.17	-0.11 ± 0.05	-0.21 ± 0.1	0.13	6.63	8.22	1.39
2M13050722+2902535	6159 ± 159	4.36 ± 0.24	4.22	0.02 ± 0.06	-0.07 ± 0.1	0.49	6.29	9.78	1.53
2M13051217+2804175	5709 ± 126	4.33 ± 0.16	4.31	-0.06 ± 0.05	-0.11 ± 0.1	0.63	4.02	9.29	0.66
2M13051398+2823365	5736 ± 80	4.25 ± 0.09	4.22	0.09 ± 0.03	0.04 ± 0.1	0.77	3.97	10.63	1.51
2M13053577+4853298	5619 ± 116	4.16 ± 0.13	4.16	0.08 ± 0.05	0.03 ± 0.1	0.64	3.61	10.27	1.8
2M13054722+2725274	5929 ± 126	4.25 ± 0.18	4.17	-0.3 ± 0.05	-0.39 ± 0.1	0	5.26	7.8	1.39
2M13055203+4753107	5912 ± 108	4.34 ± 0.15	4.27	0.09 ± 0.04	0.07 ± 0.1	0.8	4.74	9.27	0.55
2M13060240+2815525	5758 ± 71	4.37 ± 0.08	4.33	-0.03 ± 0.03	-0.08 ± 0.1	0.6	4.17	10.71	1.36

APOGEE_ID	$T_{\rm eff} \pm \Delta T_{\rm eff}$	$\log g \pm \Delta \log g$	$\log g_{cor}$	$[\mathrm{M/H}] \pm \Delta[\mathrm{M/H}]$	$[Fe/H] \pm \Delta[\mathrm{Fe/H}]$	$\mathrm{v}_{\rm mic}$	$\mathrm{v}_{\rm mac}$	$v \sin i$	χ^2
2M13063051+5743411	6196 ± 93	4.46 ± 0.1	4.30	0.03 ± 0.03	-0.05 ± 0.1	0.44	6.52	8.79	0.34
2M13064697+2712007	5846 ± 65	4.26 ± 0.08	4.20	0.21 ± 0.03	0.15 ± 0.1	0.71	4.29	9.61	1.56
2M13065070+2835480	5950 ± 132	4.27 ± 0.18	4.19	-0.07 ± 0.05	-0.14 ± 0.1	0.49	5.13	8.35	0.52
2M13071094+2719319	5731 ± 88	4.14 ± 0.09	4.11	0.11 ± 0.04	0.06 ± 0.1	0.79	3.96	9.94	0.5
2M13071105-0323162	6049 ± 130	4.31 ± 0.16	4.20	-0.01 ± 0.05	-0.09 ± 0.1	0.52	5.62	8.95	0.41
2M13073542+5556110	6217 ± 172	4.35 ± 0.24	4.18	-0.13 ± 0.07	-0.23 ± 0.1	0.33	6.86	7.89	0.43
2M13075767+4625310	6172 ± 179	4.26 ± 0.26	4.11	-0.15 ± 0.07	-0.25 ± 0.1	0	6.58	8.13	0.51
2M13081189+4627225	5598 ± 140	4.35 ± 0.21	4.35	-0.24 ± 0.06	-0.29 ± 0.1	0.5	3.85	9.17	0.55
2M13083342+4452073	5594 ± 112	4.28 ± 0.14	4.29	0.05 ± 0.05	0.03 ± 0.1	1.01	3.54	9.73	0.6
2M13083736+1726243	5753 ± 77	4.29 ± 0.09	4.26	-0.06 ± 0.03	-0.11 ± 0.1	0.65	4.19	9.07	0.36
2M13083821+1732059	5781 ± 119	4.18 ± 0.12	4.14	0.04 ± 0.05	-0.02 ± 0.1	0.68	4.22	10.47	1.46
2M13085878+4804152	6053 ± 119	4.33 ± 0.17	4.22	-0.06 ± 0.05	-0.12 ± 0.1	0.42	5.69	8.44	1.48
2M13090271+1707061	6179 ± 63	4.29 ± 0.09	4.14	-0.2 ± 0.02	-0.3 ± 0.1	0	6.67	7.36	0.39
2M13091594+4607120	6191 ± 126	4.39 ± 0.18	4.23	0.05 ± 0.05	0 ± 0.1	0.47	6.47	9.71	0.44
2M13091835+4521464	6060 ± 147	4.32 ± 0.19	4.21	0.03 ± 0.06	-0.04 ± 0.1	0.62	5.64	9.14	0.44
2M13093050-0225069	6065 ± 105	4.46 ± 0.11	4.35	0.17 ± 0.04	0.12 ± 0.1	0.77	5.49	10.4	1.51
2M13094382+4851320	5894 ± 126	4.33 ± 0.18	4.26	-0.02 ± 0.05	-0.1 ± 0.1	0.14	4.77	9.18	0.58
2M13095189+1656588	5995 ± 104	4.15 ± 0.12	4.05	-0.24 ± 0.04	-0.32 ± 0.1	0.2	5.57	7.99	0.35
2M13095244+4702529	5620 ± 107	4.26 ± 0.14	4.26	-0.02 ± 0.05	-0.06 ± 0.1	0.65	3.7	10.47	0.59
2M13095268+1725294	5749 ± 135	4.2 ± 0.14	4.17	-0.13 ± 0.06	-0.22 ± 0.1	0.55	4.28	8.97	1.45

APOGEE_ID	$T_{\rm eff} \pm \Delta T_{\rm eff}$	$\log g \pm \Delta \log g$	$\log g_{cor}$	$[\mathrm{M/H}] \pm \Delta[\mathrm{M/H}]$	$[Fe/H] \pm \Delta[\mathrm{Fe/H}]$	$\mathrm{v}_{\rm mic}$	$\mathrm{v}_{\rm mac}$	$v \sin i$	χ^2
2M13105262+4910524	5935 ± 130	4.33 ± 0.17	4.25	0.11 ± 0.05	0.05 ± 0.1	0.47	4.83	9.56	0.66
2M13110387+4636434	5907 ± 102	4.36 ± 0.15	4.29	0.06 ± 0.04	0.01 ± 0.1	0.63	4.75	10.65	0.35
2M13110965+1733171	5705 ± 120	4.14 ± 0.13	4.12	0.1 ± 0.05	0.05 ± 0.1	0.8	3.87	10.46	1.54
2M13111953+1812427	5990 ± 135	4.26 ± 0.16	4.17	-0.2 ± 0.05	-0.3 ± 0.1	0.11	5.48	7.9	1.36
2M13112117+4848184	5984 ± 148	4.34 ± 0.18	4.25	-0.03 ± 0.06	-0.11 ± 0.1	0	5.26	9.44	0.76
2M13112997+1543190	6094 ± 71	4.39 ± 0.11	4.27	-0.1 ± 0.03	-0.17 ± 0.1	0.25	5.98	7.3	0.33
2M13114072+1721144	5629 ± 99	4.03 ± 0.11	4.03	0.05 ± 0.04	-0.01 ± 0.1	0.73	3.72	10.5	1.53
2M13114473+4903307	5951 ± 131	4.37 ± 0.19	4.29	-0.14 ± 0.05	-0.22 ± 0.1	0.33	5.19	8.67	1.4
2M13114936+1818373	5704 ± 79	4.07 ± 0.08	4.05	0.21 ± 0.03	0.15 ± 0.1	0.85	3.76	11.01	0.63
2M13115466+1805389	5761 ± 133	4.13 ± 0.14	4.09	-0.16 ± 0.06	-0.25 ± 0.1	0.53	4.37	9.2	0.38
2M13120798+1719088	5805 ± 132	4.26 ± 0.16	4.21	-0.03 ± 0.06	-0.09 ± 0.1	0.63	4.38	9.31	0.45
2M13121982+1731016	5974 ± 199	4.13 ± 0.23	4.04	-0.36 ± 0.08	-0.5 ± 0.1	0	5.58	7.26	1.35
2M13123854+1629421	5944 ± 143	4.33 ± 0.22	4.25	-0.29 ± 0.06	-0.35 ± 0.1	0	5.3	8.13	0.36
2M13124638+4718479	5750 ± 79	4.32 ± 0.08	4.29	-0.02 ± 0.03	-0.07 ± 0.1	0.64	4.14	8.18	0.42
2M13130749+1730459	5703 ± 94	4.57 ± 0.09	4.55	0.42 ± 0.04	0.33 ± 0.1	0.64	3.43	8.56	2.18
2M13131521+1758588	5839 ± 73	4.33 ± 0.1	4.27	0.11 ± 0.03	0.07 ± 0.1	0.74	4.36	10.91	0.39
2M13133870+1756496	5699 ± 134	4.24 ± 0.15	4.22	0 ± 0.06	-0.08 ± 0.1	0.65	3.94	9.48	0.53
2M13134102+4628344	5860 ± 68	4.43 ± 0.09	4.37	-0.06 ± 0.03	-0.12 ± 0.1	0.4	4.64	10.1	1.4
2M13134484+4654239	6119 ± 151	4.42 ± 0.21	4.29	0 ± 0.06	-0.07 ± 0.1	0.44	6.03	9.43	1.38
2M13134492+1757588	5987 ± 108	4.24 ± 0.12	4.15	0.09 ± 0.04	0.02 ± 0.1	0.77	5.16	10.06	1.38

APOGEE_ID	$T_{\rm eff} \pm \Delta T_{\rm eff}$	$\log g \pm \Delta \log g$	$\log g_{cor}$	$[\mathrm{M/H}] \pm \Delta[\mathrm{M/H}]$	$[Fe/H] \pm \Delta[\mathrm{Fe/H}]$	$\mathrm{v_{mic}}$	$\mathrm{v_{mac}}$	$v \sin i$	χ^2
2M13135409+1552590	5954 ± 70	4.36 ± 0.09	4.27	0.17 ± 0.03	0.12 ± 0.1	0.75	4.86	10.42	0.38
2M13141526+1615475	6054 ± 85	4.4 ± 0.11	4.29	0.1 ± 0.03	0.05 ± 0.1	0.62	5.52	10.83	1.33
2M13143793+4633291	5651 ± 116	4.15 ± 0.14	4.14	0.05 ± 0.05	0.02 ± 0.1	0.91	3.75	10.24	1.62
2M13145072+1520159	6076 ± 112	4.24 ± 0.14	4.12	0.1 ± 0.04	0.03 ± 0.1	0.7	5.67	9.75	0.37
2M13150727+1635230	6074 ± 86	4.38 ± 0.13	4.26	-0.05 ± 0.03	-0.13 ± 0.1	0.48	5.81	7.9	0.33
2M13151371+4606214	6023 ± 139	4.31 ± 0.18	4.21	-0.15 ± 0.06	-0.22 ± 0.1	0.18	5.62	8.39	0.45
2M13152852+1733170	5769 ± 112	4.07 ± 0.11	4.03	-0.06 ± 0.05	-0.14 ± 0.1	0.69	4.32	8.92	1.42
2M13154452+1619414	5995 ± 125	4.31 ± 0.15	4.21	-0.2 ± 0.05	-0.28 ± 0.1	0	5.5	8.13	1.37
2M13161458+4828598	5647 ± 79	4.05 ± 0.09	4.04	0.07 ± 0.03	0.03 ± 0.1	0.88	3.74	9.8	1.62
2M13162600+1611200	6004 ± 93	4.43 ± 0.1	4.33	-0.02 ± 0.04	-0.08 ± 0.1	0.47	5.35	8.63	0.38
2M13164008+1745080	5708 ± 114	4.11 ± 0.11	4.09	0.12 ± 0.05	0.05 ± 0.1	0.63	3.87	10.74	0.55
2M13164498+1644391	5808 ± 77	4.43 ± 0.09	4.38	-0.04 ± 0.03	-0.09 ± 0.1	0.54	4.39	10.14	0.3
2M13165338+1444150	5821 ± 106	4.29 ± 0.13	4.24	0.04 ± 0.04	-0.01 ± 0.1	0.77	4.37	9.67	1.38
2M13165551+4853515	6022 ± 159	4.33 ± 0.21	4.23	-0.08 ± 0.07	-0.16 ± 0.1	0.49	5.52	8.89	0.68
2M13172407+4811146	6102 ± 119	4.31 ± 0.18	4.19	-0.13 ± 0.05	-0.2 ± 0.1	0.18	6.08	7.56	0.44
2M13173534+4844442	5782 ± 135	4.39 ± 0.18	4.35	-0.09 ± 0.06	-0.15 ± 0.1	0.63	4.33	9.22	0.78
2M13173920+1324100	5720 ± 134	4 ± 0.14	3.97	-0.28 ± 0.06	-0.38 ± 0.1	0.67	4.38	7.05	1.54
2M13175035+1358057	5832 ± 137	4.17 ± 0.17	4.12	-0.04 ± 0.06	-0.11 ± 0.1	0.67	4.53	9.42	0.5
2M13180342+1714401	5956 ± 147	4.36 ± 0.2	4.27	-0.04 ± 0.06	-0.11 ± 0.1	0.43	5.11	9.53	1.4
2M13180348+4845137	5806 ± 141	4.24 ± 0.18	4.19	-0.09 ± 0.06	-0.16 ± 0.1	0.5	4.46	9.43	0.86

APOGEE_ID	$T_{\rm eff} \pm \Delta T_{\rm eff}$	$\log g \pm \Delta \log g$	$\log g_{cor}$	$[\rm M/H] \pm \Delta[\rm M/H]$	$[Fe/H] \pm \Delta[\rm Fe/H]$	$\rm v_{mic}$	$\rm v_{mac}$	$v \sin i$	χ^2
2M13181344+4806507	5612 ± 93	4.09 ± 0.11	4.09	0.21 ± 0.04	0.16 ± 0.1	0.86	3.46	9.46	1.95
2M13182452+4854200	5577 ± 51	4.19 ± 0.06	4.20	0.13 ± 0.02	0.1 ± 0.1	0.93	3.42	10.01	0.64
2M13184407+1642037	6212 ± 125	4.23 ± 0.16	4.07	-0.09 ± 0.05	-0.16 ± 0.1	0.38	6.8	7.76	0.36
2M13184676+1726324	5915 ± 82	4.41 ± 0.12	4.33	-0.04 ± 0.03	-0.09 ± 0.1	0.51	4.89	9.08	0.35
2M13185895+1224151	5998 ± 105	4.34 ± 0.12	4.24	0.21 ± 0.04	0.15 ± 0.1	0.71	5.06	10.38	1.28
2M13193776+4740338	5632 ± 100	4.11 ± 0.12	4.11	0.16 ± 0.04	0.12 ± 0.1	0.88	3.57	9.67	1.83
2M13193876+1438267	6035 ± 161	4.24 ± 0.19	4.13	-0.04 ± 0.06	-0.12 ± 0.1	0.47	5.58	8.57	0.42
2M13195863+4938008	5642 ± 126	4.23 ± 0.16	4.22	0.03 ± 0.05	-0.01 ± 0.1	0.78	3.71	11.07	1.74
2M13200499+1456395	5709 ± 108	4.26 ± 0.12	4.24	0.09 ± 0.04	0.04 ± 0.1	0.83	3.87	10.86	1.41
2M13201174-0103572	5967 ± 138	4.17 ± 0.15	4.08	0.08 ± 0.06	0.03 ± 0.1	0.84	5.07	11.26	0.47
2M13202503+1303279	5789 ± 118	4.32 ± 0.14	4.28	0 ± 0.05	-0.05 ± 0.1	0.59	4.27	10.24	1.38
2M13202943+4750146	5783 ± 81	4.27 ± 0.09	4.23	0.09 ± 0.03	0.04 ± 0.1	0.7	4.16	9.63	1.52
2M13204832+7058126	5976 ± 169	4.2 ± 0.2	4.11	-0.22 ± 0.07	-0.31 ± 0.1	0	5.44	7.46	0.44
2M13211567+4800332	5937 ± 112	4.38 ± 0.15	4.30	0.02 ± 0.05	-0.02 ± 0.1	0.66	4.94	10.39	0.64
2M13215476-0205266	6270 ± 122	4.51 ± 0.11	4.32	0.28 ± 0.05	0.24 ± 0.1	0.83	6.78	8.89	0.47
2M13221236+4819339	5613 ± 95	4.24 ± 0.12	4.24	0.01 ± 0.04	-0.03 ± 0.1	0.81	3.65	9.56	0.6
2M13221974-0049489	5794 ± 114	4.25 ± 0.13	4.21	0.06 ± 0.05	0.01 ± 0.1	0.83	4.24	9.55	0.46
2M13222976+1408416	6310 ± 144	4.5 ± 0.16	4.29	-0.22 ± 0.06	-0.25 ± 0.1	0.19	7.65	9.64	0.21
2M13224618+1351585	6009 ± 84	4.23 ± 0.09	4.13	-0.04 ± 0.03	-0.12 ± 0.1	0.52	5.43	9.21	1.31
2M13225914-0246459	6083 ± 140	4.32 ± 0.2	4.20	-0.03 ± 0.06	-0.11 ± 0.1	0.62	5.85	8.94	0.44

APOGEE_ID	$T_{\rm eff} \pm \Delta T_{\rm eff}$	$\log g \pm \Delta \log g$	$\log g_{cor}$	$[\mathrm{M/H}] \pm \Delta[\mathrm{M/H}]$	$[Fe/H] \pm \Delta[\mathrm{Fe/H}]$	$\mathrm{v_{mic}}$	$\mathrm{v_{mac}}$	$v \sin i$	χ^2
2M13231541+3712355	6052 ± 176	4.19 ± 0.23	4.08	-0.26 ± 0.07	-0.35 ± 0.1	0	5.91	8.37	0.57
2M13232296+3702294	6171 ± 153	4.37 ± 0.22	4.22	0.02 ± 0.06	-0.04 ± 0.1	0.56	6.37	8.88	0.55
2M13232312+4839237	5723 ± 126	4.18 ± 0.13	4.15	0.03 ± 0.05	-0.03 ± 0.1	0.66	4.01	10.6	1.22
2M13233815+4903558	5746 ± 140	4.3 ± 0.17	4.27	-0.09 ± 0.06	-0.15 ± 0.1	0.64	4.2	9.15	0.65
2M13234347+4815018	5729 ± 125	4.31 ± 0.14	4.28	-0.04 ± 0.05	-0.08 ± 0.1	0.78	4.08	8.78	0.58
2M13240265-0237071	6145 ± 155	4.46 ± 0.19	4.32	0 ± 0.06	-0.07 ± 0.1	0.48	6.21	9.79	0.44
2M13242473+2651368	6101 ± 139	4.36 ± 0.21	4.24	-0.04 ± 0.06	-0.12 ± 0.1	0.24	5.97	8.89	1.51
2M13245987-0108545	6317 ± 148	4.47 ± 0.18	4.26	-0.27 ± 0.06	-0.32 ± 0.1	0.03	7.76	7.74	0.22
2M13250013+2656587	5806 ± 125	4.13 ± 0.13	4.08	0.12 ± 0.05	0.06 ± 0.1	0.8	4.25	10.41	1.73
2M13250699+2647473	5984 ± 143	4.38 ± 0.19	4.29	-0.07 ± 0.06	-0.14 ± 0.1	0.42	5.29	9.46	1.72
2M13250862+4841269	5751 ± 154	4.26 ± 0.18	4.23	-0.34 ± 0.06	-0.45 ± 0.1	0	4.48	8.99	0.7
2M13253297+3816392	6261 ± 167	4.52 ± 0.16	4.33	-0.04 ± 0.06	-0.1 ± 0.1	0.21	7.08	7.95	0.41
2M13260201+4945154	5553 ± 120	4.24 ± 0.13	4.26	0.02 ± 0.05	-0.02 ± 0.1	0.8	3.48	10.3	1.94
2M13261814-0132407	5866 ± 141	4.23 ± 0.18	4.17	-0.01 ± 0.06	-0.07 ± 0.1	0.66	4.64	9.7	1.46
2M13262435+7214415	5954 ± 61	4.31 ± 0.08	4.22	-0.03 ± 0.02	-0.1 ± 0.1	0.58	5.1	9.04	0.32
2M13263247+2619048	5965 ± 136	4.29 ± 0.16	4.20	0.05 ± 0.05	0 ± 0.1	0.57	5.07	10.53	0.64
2M13263538+4823579	6058 ± 127	4.41 ± 0.16	4.30	0.05 ± 0.05	0 ± 0.1	0.48	5.59	10.45	1.57
2M13264150+2735206	6169 ± 131	4.46 ± 0.16	4.31	0.11 ± 0.05	0.06 ± 0.1	0.48	6.25	10.32	1.68
2M13264699+3955311	6230 ± 91	4.5 ± 0.08	4.33	0.14 ± 0.04	0.07 ± 0.1	0.48	6.65	9.58	0.38
2M13265697+2701478	5812 ± 140	4.38 ± 0.2	4.33	-0.15 ± 0.06	-0.22 ± 0.1	0.47	4.53	8.7	1.59

APOGEE_ID	$T_{\rm eff} \pm \Delta T_{\rm eff}$	$\log g \pm \Delta \log g$	$\log g_{cor}$	$[\mathrm{M/H}] \pm \Delta[\mathrm{M/H}]$	$[Fe/H] \pm \Delta[\mathrm{Fe/H}]$	$\mathrm{v}_{\rm mic}$	$\mathrm{v}_{\rm mac}$	$v \sin i$	χ^2
2M13270417+2540549	6006 ± 151	4.22 ± 0.17	4.12	-0.23 ± 0.06	-0.31 ± 0.1	0	5.61	8.05	1.49
2M13272998+4738573	5558 ± 110	4.26 ± 0.12	4.27	-0.01 ± 0.05	-0.05 ± 0.1	0.8	3.52	10.02	1.73
2M13273775-0246056	5985 ± 126	4.31 ± 0.16	4.22	-0.09 ± 0.05	-0.16 ± 0.1	0.45	5.33	9.18	0.41
2M13281791+2606297	5566 ± 110	4.28 ± 0.13	4.29	0 ± 0.05	-0.02 ± 0.1	0.89	3.52	9.45	0.59
2M13282809+2542398	5631 ± 71	4.05 ± 0.08	4.05	0.14 ± 0.03	0.11 ± 0.1	0.88	3.61	9.52	1.6
2M13283478+2651174	5734 ± 132	4.39 ± 0.17	4.36	-0.07 ± 0.06	-0.13 ± 0.1	0.55	4.12	9.96	0.61
2M13283531+2648147	5983 ± 97	4.43 ± 0.1	4.34	0.13 ± 0.04	0.1 ± 0.1	0.74	5.06	9.66	0.62
2M13284507+2755209	5726 ± 95	4.41 ± 0.12	4.38	-0.09 ± 0.04	-0.14 ± 0.1	0.57	4.11	9.29	1.39
2M13284799+2637345	5733 ± 133	4.29 ± 0.16	4.26	-0.23 ± 0.06	-0.29 ± 0.1	0.27	4.3	8.03	0.56
2M13285602+2659479	5704 ± 74	4.32 ± 0.09	4.30	0.05 ± 0.03	-0.01 ± 0.1	0.6	3.89	10.02	0.42
2M13290417+2652017	5721 ± 123	4.23 ± 0.13	4.20	0.06 ± 0.05	0.01 ± 0.1	0.7	3.95	10.36	1.75
2M13292013+3906422	5664 ± 121	4.02 ± 0.13	4.01	0.02 ± 0.05	-0.03 ± 0.1	0.8	3.86	9.9	0.52
2M13294198+3819074	6196 ± 154	4.34 ± 0.23	4.18	-0.12 ± 0.06	-0.2 ± 0.1	0.24	6.7	7.33	0.48
2M13300661+3618534	5808 ± 74	4.31 ± 0.09	4.26	0.01 ± 0.03	-0.03 ± 0.1	0.73	4.35	10.21	0.31
2M13303039+2634431	5642 ± 111	4.13 ± 0.13	4.12	0.11 ± 0.05	0.06 ± 0.1	0.73	3.66	9.77	0.71
2M13303120+4830066	6216 ± 165	4.43 ± 0.22	4.26	-0.07 ± 0.06	-0.15 ± 0.1	0	6.78	8.14	1.82
2M13305650+4016545	6202 ± 107	4.4 ± 0.16	4.24	-0.1 ± 0.04	-0.2 ± 0.1	0	6.71	8.25	0.36
2M13312517+4015289	6166 ± 114	4.37 ± 0.18	4.22	-0.04 ± 0.04	-0.12 ± 0.1	0.4	6.4	8.5	0.35
2M13320168+7143012	6014 ± 57	4.39 ± 0.08	4.29	-0.11 ± 0.02	-0.18 ± 0.1	0.3	5.5	8.39	0.33
2M13320342+2612115	5716 ± 124	4.16 ± 0.13	4.13	-0.01 ± 0.05	-0.07 ± 0.1	0.72	4.03	9.37	1.62

APOGEE_ID	$T_{\rm eff} \pm \Delta T_{\rm eff}$	$\log g \pm \Delta \log g$	$\log g_{cor}$	$[\rm M/H] \pm \Delta[\rm M/H]$	$[Fe/H] \pm \Delta[\rm Fe/H]$	$\rm v_{mic}$	$\rm v_{mac}$	$v \sin i$	χ^2
2M13320470+3955552	5820 ± 99	4.24 ± 0.12	4.19	0.06 ± 0.04	-0.02 ± 0.1	0.69	4.35	9.06	0.5
2M13321387+2635246	5989 ± 139	4.12 ± 0.14	4.03	-0.02 ± 0.05	-0.09 ± 0.1	0.64	5.32	9.44	0.5
2M13323094+3602069	5927 ± 67	4.2 ± 0.1	4.12	-0.28 ± 0.03	-0.37 ± 0.1	0.19	5.23	7.25	0.37
2M13323094+3602069	5930 ± 67	4.2 ± 0.09	4.12	-0.27 ± 0.03	-0.37 ± 0.1	0.18	5.24	7.79	0.37
2M13324187+2757296	5891 ± 90	4.29 ± 0.13	4.22	0 ± 0.04	-0.08 ± 0.1	0.53	4.74	9.42	1.35
2M13330856+2725349	5584 ± 138	4.08 ± 0.16	4.09	-0.18 ± 0.06	-0.26 ± 0.1	0.69	3.82	9.18	0.46
2M13333252+3646343	6056 ± 136	4.07 ± 0.16	3.96	-0.08 ± 0.06	-0.16 ± 0.1	0.6	5.79	7.39	1.46
2M13334365+3754543	5845 ± 114	4.34 ± 0.15	4.28	-0.01 ± 0.05	-0.07 ± 0.1	0.69	4.53	9.36	0.43
2M13335371+2707060	5889 ± 109	4.28 ± 0.15	4.21	0.06 ± 0.04	0 ± 0.1	0.64	4.67	9.4	1.43
2M13345738+4148279	5686 ± 123	4.44 ± 0.15	4.42	-0.27 ± 0.05	-0.31 ± 0.1	0	4.15	9.26	0.52
2M13354060+2755554	5779 ± 98	4.38 ± 0.13	4.34	-0.05 ± 0.04	-0.12 ± 0.1	0.57	4.28	8.58	0.37
2M13354175+4326046	5927 ± 152	4.24 ± 0.2	4.16	-0.01 ± 0.06	-0.08 ± 0.1	0.56	4.94	9.26	0.67
2M13354596+4207091	5450 ± 98	4.21 ± 0.1	4.25	0.01 ± 0.04	-0.01 ± 0.1	0.87	3.28	9.61	0.85
2M13363600-1558188	5952 ± 143	4.4 ± 0.19	4.32	0.01 ± 0.06	-0.05 ± 0.1	0.54	5.02	8.96	0.57
2M13370278+4031053	5810 ± 84	4.18 ± 0.09	4.13	0.1 ± 0.03	0.04 ± 0.1	0.83	4.28	10.04	0.44
2M13371610+5614345	6030 ± 181	4.39 ± 0.26	4.29	-0.25 ± 0.07	-0.32 ± 0.1	0	5.75	8.62	0.54
2M13373166+3819414	5919 ± 119	4.2 ± 0.15	4.12	0.05 ± 0.05	0 ± 0.1	0.77	4.84	8.62	0.43
2M13373485+4126056	6407 ± 94	4.56 ± 0.12	4.31	-0.28 ± 0.04	-0.29 ± 0.1	0	8.51	7.95	1.18
2M13373485+4126056	6236 ± 91	4.37 ± 0.12	4.20	-0.15 ± 0.04	-0.29 ± 0.1	0	7.02	7.52	1.36
2M13373916+4141367	5658 ± 92	3.91 ± 0.14	3.90	-0.03 ± 0.04	-0.06 ± 0.1	0.83	3.94	9.57	0.47

APOGEE_ID	$T_{\rm eff} \pm \Delta T_{\rm eff}$	$\log g \pm \Delta \log g$	$\log g_{cor}$	$[\mathrm{M/H}] \pm \Delta[\mathrm{M/H}]$	$[Fe/H] \pm \Delta[\mathrm{Fe/H}]$	$\mathrm{v}_{\rm mic}$	$\mathrm{v}_{\rm mac}$	$v \sin i$	χ^2
2M13382089+1802284	6186 ± 91	4.26 ± 0.13	4.11	-0.06 ± 0.04	-0.14 ± 0.1	0.46	6.58	8.5	0.42
2M13382165+1824403	5928 ± 84	4.28 ± 0.11	4.20	0.09 ± 0.03	0.04 ± 0.1	0.69	4.82	10.52	0.35
2M13382492+4306131	5997 ± 101	4.44 ± 0.11	4.34	-0.11 ± 0.04	-0.17 ± 0.1	0	5.4	8.44	1.4
2M13383109+4247421	5912 ± 128	4.44 ± 0.18	4.37	-0.06 ± 0.05	-0.12 ± 0.1	0.19	4.9	8.75	1.44
2M13383305+4128275	6049 ± 95	4.45 ± 0.11	4.34	-0.12 ± 0.04	-0.18 ± 0.1	0.26	5.72	8.53	0.37
2M13383585+4132570	5632 ± 107	4.08 ± 0.12	4.08	0.11 ± 0.05	0.07 ± 0.1	0.79	3.64	9.56	0.74
2M13384526+2257328	5603 ± 118	4.29 ± 0.15	4.29	-0.02 ± 0.05	-0.06 ± 0.1	0.92	3.65	8.81	0.64
2M13385108-0046182	5994 ± 131	4.13 ± 0.14	4.03	-0.2 ± 0.05	-0.29 ± 0.1	0.17	5.54	8.26	1.41
2M13394189+2319494	6439 ± 144	4.55 ± 0.17	4.29	-0.34 ± 0.05	-0.38 ± 0.1	0	8.85	5.53	1.23
2M13394695+2208362	5648 ± 114	4.22 ± 0.15	4.21	0.17 ± 0.05	0.12 ± 0.1	0.8	3.58	9.71	1.16
2M13395184+2717343	5734 ± 136	4.44 ± 0.13	4.41	-0.04 ± 0.06	-0.09 ± 0.1	0.66	4.09	7.93	1.56
2M13395937+4210565	6053 ± 147	4.37 ± 0.2	4.26	-0.04 ± 0.06	-0.1 ± 0.1	0.27	5.67	9.11	0.52
2M13401598+2137476	6203 ± 119	4.35 ± 0.17	4.19	-0.12 ± 0.05	-0.2 ± 0.1	0.25	6.75	7.83	1.37
2M13401828+2607191	6128 ± 149	4.39 ± 0.25	4.26	-0.06 ± 0.06	-0.11 ± 0.1	0.3	6.16	8.31	1.46
2M13402921+2550596	6089 ± 102	4.29 ± 0.13	4.17	0.06 ± 0.04	0.01 ± 0.1	0.61	5.78	8.82	0.42
2M13403957+0102114	5746 ± 119	4.31 ± 0.13	4.28	-0.04 ± 0.05	-0.11 ± 0.1	0.67	4.15	9.33	1.4
2M13405487+4144198	6161 ± 139	4.26 ± 0.21	4.12	-0.1 ± 0.06	-0.17 ± 0.1	0.42	6.44	7.5	0.43
2M13410311+2645182	6052 ± 90	4.42 ± 0.11	4.31	0.01 ± 0.03	-0.03 ± 0.1	0.54	5.6	10.47	0.31
2M13410476-0106062	6064 ± 122	4.26 ± 0.16	4.15	-0.03 ± 0.05	-0.11 ± 0.1	0.52	5.73	8.86	1.39
2M13411996+1708586	6240 ± 124	4.43 ± 0.15	4.25	-0.34 ± 0.05	-0.39 ± 0.1	0	7.23	8.04	0.18

APOGEE_ID	$T_{\rm eff} \pm \Delta T_{\rm eff}$	$\log g \pm \Delta \log g$	$\log g_{cor}$	$[\rm M/H] \pm \Delta[\rm M/H]$	$[Fe/H] \pm \Delta[\rm Fe/H]$	$v_{\rm mic}$	$v_{\rm mac}$	$v \sin i$	χ^2
2M13413321+5707294	6136 ± 119	4.3 ± 0.17	4.17	0.1 ± 0.05	0.02 ± 0.1	0.68	6.05	9.52	1.44
2M13413439+4216398	6028 ± 133	4.2 ± 0.15	4.10	0.07 ± 0.05	0.03 ± 0.1	0.59	5.42	10.02	0.64
2M13413894+2556207	5972 ± 146	4.19 ± 0.16	4.10	0.05 ± 0.06	-0.01 ± 0.1	0.6	5.13	8.87	0.69
2M13414203+2658285	5933 ± 72	4.28 ± 0.09	4.20	0.09 ± 0.03	0.04 ± 0.1	0.64	4.85	10.66	0.37
2M13414903-0007410	6191 ± 77	4.32 ± 0.11	4.16	-0.01 ± 0.03	-0.08 ± 0.1	0.52	6.55	8.54	0.31
2M13415360+4334085	5644 ± 109	4.1 ± 0.13	4.09	0.1 ± 0.05	0.06 ± 0.1	0.79	3.68	10.76	0.81
2M13415557+2405456	5640 ± 126	4.3 ± 0.17	4.29	-0.02 ± 0.05	-0.06 ± 0.1	0.87	3.76	9.47	1.55
2M13420081+4212400	5762 ± 63	4.17 ± 0.06	4.13	-0.01 ± 0.03	-0.06 ± 0.1	0.6	4.2	9.61	0.41
2M13420167+1917117	6074 ± 84	4.27 ± 0.12	4.15	-0.05 ± 0.03	-0.13 ± 0.1	0.45	5.82	9.67	0.27
2M13421177+4007083	5909 ± 135	4.36 ± 0.2	4.29	0.03 ± 0.05	-0.02 ± 0.1	0.7	4.79	9.95	0.6
2M13421474+0119119	5867 ± 121	4.35 ± 0.19	4.29	-0.09 ± 0.05	-0.16 ± 0.1	0.37	4.72	8.78	0.4
2M13422193+2135549	6055 ± 89	4.38 ± 0.12	4.27	0.07 ± 0.03	0.03 ± 0.1	0.66	5.55	9.86	1.29
2M13422646+2647281	5762 ± 123	4.19 ± 0.12	4.15	0.05 ± 0.05	0 ± 0.1	0.77	4.14	10.06	0.38
2M13422985+0019307	6191 ± 142	4.38 ± 0.22	4.22	-0.05 ± 0.06	-0.14 ± 0.1	0.24	6.58	9.31	0.47
2M13423295+2330149	6232 ± 157	4.4 ± 0.2	4.23	0.04 ± 0.06	-0.02 ± 0.1	0.46	6.77	9.51	1.51
2M13424071+2559161	5854 ± 102	4.35 ± 0.14	4.29	-0.01 ± 0.04	-0.06 ± 0.1	0.61	4.57	8.21	0.44
2M13424874-0058539	6090 ± 101	4.48 ± 0.11	4.36	0.01 ± 0.04	-0.04 ± 0.1	0.44	5.83	10.39	0.35
2M13425281+4353487	5665 ± 137	4.39 ± 0.21	4.38	-0.21 ± 0.06	-0.27 ± 0.1	0.5	4.03	8.05	0.49
2M13425638+2818089	5694 ± 111	4.24 ± 0.13	4.22	0 ± 0.05	-0.08 ± 0.1	0.6	3.92	9.66	1.5
2M13431819+1813185	6239 ± 110	4.46 ± 0.11	4.28	0 ± 0.04	-0.08 ± 0.1	0.26	6.87	8.78	0.34

APOGEE_ID	$T_{\rm eff} \pm \Delta T_{\rm eff}$	$\log g \pm \Delta \log g$	$\log g_{cor}$	$[\mathrm{M/H}] \pm \Delta[\mathrm{M/H}]$	$[Fe/H] \pm \Delta[\mathrm{Fe/H}]$	$\mathrm{v_{mic}}$	$\mathrm{v_{mac}}$	$v \sin i$	χ^2
2M13432770+2849572	5935 ± 71	4.14 ± 0.08	4.06	-0.02 ± 0.03	-0.09 ± 0.1	0.68	5.01	9.37	1.3
2M13432931+2142418	5832 ± 87	4.4 ± 0.13	4.35	-0.07 ± 0.04	-0.12 ± 0.1	0.62	4.53	9.09	0.39
2M13433083+1833274	6169 ± 112	4.38 ± 0.17	4.23	-0.03 ± 0.04	-0.11 ± 0.1	0.37	6.41	8.61	0.37
2M13433110+5613240	5956 ± 116	4.28 ± 0.14	4.19	0.12 ± 0.05	0.06 ± 0.1	0.74	4.95	8.97	1.52
2M13434539+2647556	5676 ± 115	4.39 ± 0.17	4.38	-0.05 ± 0.05	-0.08 ± 0.1	0.65	3.89	9.59	0.6
2M13435546+1751199	5720 ± 107	4.13 ± 0.11	4.10	0 ± 0.04	-0.03 ± 0.1	0.89	4.04	10.09	1.16
2M13435941-1602449	5948 ± 153	4.33 ± 0.22	4.25	-0.14 ± 0.06	-0.22 ± 0.1	0.65	5.18	8.3	0.49
2M13440429+0122225	6408 ± 113	4.33 ± 0.17	4.08	-0.14 ± 0.04	-0.25 ± 0.1	0	8.39	7.09	0.39
2M13440620+2718088	5984 ± 92	4.43 ± 0.11	4.34	-0.05 ± 0.04	-0.1 ± 0.1	0.47	5.27	8.22	0.37
2M13440713+2321319	5925 ± 76	4.39 ± 0.11	4.31	0.06 ± 0.03	0 ± 0.1	0.51	4.83	9.74	1.38
2M13442031+3847519	5736 ± 63	4.16 ± 0.06	4.13	0.03 ± 0.03	-0.03 ± 0.1	0.69	4.06	9.44	1.44
2M13442357+2618379	5769 ± 102	4.18 ± 0.1	4.14	0.02 ± 0.04	-0.03 ± 0.1	0.68	4.19	10.07	0.42
2M13443187+2800039	5715 ± 108	4.26 ± 0.12	4.24	0.11 ± 0.05	0.05 ± 0.1	0.71	3.87	10.22	0.73
2M13443371+3818127	5826 ± 117	4.29 ± 0.15	4.24	-0.03 ± 0.05	-0.09 ± 0.1	0.49	4.47	8.87	0.45
2M13443844+0104548	6226 ± 119	4.5 ± 0.12	4.33	-0.08 ± 0.05	-0.16 ± 0.1	0	6.86	8.34	1.4
2M13444134+4319406	6160 ± 173	4.31 ± 0.25	4.17	-0.01 ± 0.07	-0.1 ± 0.1	0.4	6.33	8.6	0.51
2M13444208-0003397	6165 ± 93	4.39 ± 0.16	4.25	-0.07 ± 0.04	-0.14 ± 0.1	0.25	6.42	7.65	0.36
2M13450505+2652228	6165 ± 115	4.43 ± 0.15	4.29	0.18 ± 0.05	0.14 ± 0.1	0.7	6.14	10.49	0.43
2M13450790+1853373	5530 ± 78	4.23 ± 0.08	4.25	0.01 ± 0.03	-0.03 ± 0.1	0.86	3.44	10.55	0.46
2M13451043-0043583	6222 ± 105	4.46 ± 0.11	4.29	0.04 ± 0.04	-0.03 ± 0.1	0.49	6.7	8.13	0.37

APOGEE_ID	$T_{\mathrm{eff}} \pm \Delta T_{\mathrm{eff}}$	$\log g \pm \Delta \log g$	$\log g_{cor}$	$[\mathrm{M/H}] \pm \Delta[\mathrm{M/H}]$	$[Fe/H] \pm \Delta[\mathrm{Fe/H}]$	$\mathrm{v_{mic}}$	$\mathrm{v_{mac}}$	$v \sin i$	χ^2
2M13451270+2716441	5572 ± 101	4.2 ± 0.11	4.21	0.1 ± 0.04	0.06 ± 0.1	0.71	3.45	10.33	1.75
2M13452854+1936413	5962 ± 77	4.33 ± 0.09	4.24	0.09 ± 0.03	0.03 ± 0.1	0.65	5	9.6	0.38
2M13453208+3929388	6001 ± 88	4.46 ± 0.08	4.36	0.16 ± 0.03	0.12 ± 0.1	0.75	5.12	9.64	0.53
2M13453536+2128359	5561 ± 112	4 ± 0.1	4.01	0.02 ± 0.05	-0.01 ± 0.1	1	3.57	9.71	0.62
2M13453966+0108561	6173 ± 96	4.29 ± 0.15	4.14	-0.05 ± 0.04	-0.12 ± 0.1	0.46	6.47	8.26	0.31
2M13454057+4312080	6176 ± 142	4.37 ± 0.21	4.22	-0.03 ± 0.06	-0.11 ± 0.1	0.29	6.45	8.47	1.43
2M13454354+1453317	3623 ± 38	4.31 ± 0.1	4.93	-0.07 ± 0.05	-0.07 ± 0.1	1.5	6.42	8.14	1.44
2M13454809+2650005	5777 ± 157	4.24 ± 0.19	4.20	-0.27 ± 0.06	-0.37 ± 0.1	0.43	4.52	7.31	0.4
2M13455500+0110279	5957 ± 134	4.35 ± 0.2	4.26	-0.27 ± 0.05	-0.37 ± 0.1	0.01	5.35	8.02	1.31
2M13455774+2615352	5770 ± 76	4.25 ± 0.08	4.21	0.08 ± 0.03	0.04 ± 0.1	0.75	4.11	10.02	1.4
2M13461435-0035546	6210 ± 125	4.42 ± 0.15	4.26	0 ± 0.05	-0.06 ± 0.1	0.43	6.66	7.79	0.35
2M13461695+1732231	6056 ± 100	4.39 ± 0.14	4.28	-0.02 ± 0.04	-0.08 ± 0.1	0.44	5.66	9.02	0.35
2M13461754+4123476	5786 ± 115	4.17 ± 0.12	4.13	0 ± 0.05	-0.05 ± 0.1	0.77	4.29	8.2	0.48
2M13461873+2754339	5958 ± 145	4.34 ± 0.18	4.25	0.01 ± 0.06	-0.06 ± 0.1	0.46	5.07	9.02	0.45
2M13461892+2322153	6209 ± 162	4.46 ± 0.18	4.30	-0.02 ± 0.06	-0.1 ± 0.1	0.41	6.68	9.05	0.45
2M13462140+2631519	5875 ± 132	4.3 ± 0.2	4.23	-0.07 ± 0.06	-0.13 ± 0.1	0.62	4.74	9.07	0.43
2M13463004+2826306	5697 ± 56	4.28 ± 0.07	4.26	0 ± 0.02	-0.06 ± 0.1	0.75	3.93	9.07	0.38
2M13464454+1910377	5969 ± 82	4.37 ± 0.11	4.28	-0.03 ± 0.03	-0.1 ± 0.1	0.53	5.17	8.41	0.33
2M13465378+4134135	5650 ± 119	4.43 ± 0.16	4.42	-0.06 ± 0.05	-0.09 ± 0.1	0.66	3.82	10.31	0.51
2M13465468+3831548	6040 ± 81	4.37 ± 0.1	4.26	-0.01 ± 0.03	-0.07 ± 0.1	0.53	5.56	9.57	0.35

APOGEE_ID	$T_{\rm eff} \pm \Delta T_{\rm eff}$	$\log g \pm \Delta \log g$	$\log g_{cor}$	$[\mathrm{M/H}] \pm \Delta[\mathrm{M/H}]$	$[Fe/H] \pm \Delta[\mathrm{Fe/H}]$	$\mathrm{v_{mic}}$	$\mathrm{v_{mac}}$	$v \sin i$	χ^2
2M13470529+2623552	5606 ± 58	4.28 ± 0.07	4.28	-0.01 ± 0.02	-0.05 ± 0.1	1.14	3.65	9.46	0.42
2M13471401+3958452	5988 ± 146	4.15 ± 0.16	4.06	-0.04 ± 0.06	-0.12 ± 0.1	0.48	5.33	9.56	0.51
2M13472695+4028323	5957 ± 114	4.15 ± 0.12	4.06	0.08 ± 0.05	0.01 ± 0.1	0.69	5.02	9.16	0.5
2M13472821+2823340	5787 ± 80	4.21 ± 0.09	4.17	0.13 ± 0.03	0.08 ± 0.1	0.79	4.14	10.3	0.44
2M13474272+4030266	5657 ± 97	4.35 ± 0.14	4.34	-0.04 ± 0.04	-0.09 ± 0.1	0.71	3.82	9.76	1.47
2M13480894+3952381	5777 ± 125	4.26 ± 0.14	4.22	0.09 ± 0.05	0.04 ± 0.1	0.73	4.13	10.32	2.41
2M13483629+1733155	5711 ± 55	4.34 ± 0.07	4.32	0.01 ± 0.02	-0.02 ± 0.1	0.74	3.96	10.13	1.38
2M13483993+0045281	6171 ± 126	4.37 ± 0.19	4.22	-0.01 ± 0.05	-0.09 ± 0.1	0.39	6.4	8.88	0.4
2M13485213+2740093	6201 ± 202	4.18 ± 0.28	4.02	-0.79 ± 0.08	-0.77 ± 0.1	0	7.38	0.02	1.2
2M13485538+2242484	5784 ± 92	4.25 ± 0.1	4.21	0.05 ± 0.04	0 ± 0.1	0.59	4.21	9.42	1.43
2M13485793+2837070	5582 ± 115	4.21 ± 0.13	4.22	0.07 ± 0.05	0.02 ± 0.1	0.84	3.5	10.22	0.54
2M13485833+2808552	5934 ± 99	4.36 ± 0.15	4.28	-0.12 ± 0.04	-0.19 ± 0.1	0.32	5.08	8.96	1.36
2M13485867+2753101	5993 ± 114	4.33 ± 0.14	4.24	-0.16 ± 0.05	-0.24 ± 0.1	0	5.45	8.22	1.39
2M13485887+4055436	5894 ± 81	4.28 ± 0.11	4.21	0.14 ± 0.03	0.09 ± 0.1	0.64	4.6	10.42	0.42
2M13485972+2757459	6194 ± 60	4.48 ± 0.06	4.32	0.09 ± 0.02	0.02 ± 0.1	0.52	6.44	8.9	0.33
2M13490867+2747100	5882 ± 74	4.37 ± 0.11	4.30	0.08 ± 0.03	0.04 ± 0.1	0.74	4.6	10.14	0.35
2M13491022+3901184	6042 ± 158	4.27 ± 0.21	4.16	-0.24 ± 0.06	-0.32 ± 0.1	0	5.82	7.17	0.59
2M13493900+2653205	5935 ± 75	4.3 ± 0.11	4.22	-0.07 ± 0.03	-0.14 ± 0.1	0.48	5.04	8.51	1.33
2M13500708+2836507	5845 ± 92	4.38 ± 0.14	4.32	-0.15 ± 0.04	-0.21 ± 0.1	0.46	4.67	8.32	0.36
2M13500861+3249553	6132 ± 89	4.41 ± 0.13	4.28	0.16 ± 0.04	0.12 ± 0.1	0.63	5.94	9.22	1.85

APOGEE_ID	$T_{\mathrm{eff}} \pm \Delta T_{\mathrm{eff}}$	$\log g \pm \Delta \log g$	$\log g_{cor}$	$[\mathrm{M/H}] \pm \Delta[\mathrm{M/H}]$	$[Fe/H] \pm \Delta[\mathrm{Fe/H}]$	$\mathrm{v}_{\mathrm{mic}}$	$\mathrm{v}_{\mathrm{mac}}$	$v \sin i$	χ^2
2M13501384+2726073	6143 ± 76	4.42 ± 0.11	4.28	0.13 ± 0.03	0.07 ± 0.1	0.65	6.05	10.34	1.36
2M13503715+2658289	6159 ± 90	4.38 ± 0.15	4.24	-0.1 ± 0.04	-0.17 ± 0.1	0.03	6.42	7.43	0.35
2M13504823+4025058	5578 ± 115	4.15 ± 0.12	4.16	0.08 ± 0.05	0.04 ± 0.1	0.81	3.5	10.58	0.9
2M13505084+3349069	6041 ± 104	4.29 ± 0.13	4.18	0.13 ± 0.04	0.06 ± 0.1	0.8	5.41	9.78	0.42
2M13514729+4318432	6211 ± 148	4.51 ± 0.14	4.35	0.06 ± 0.06	-0.02 ± 0.1	0.25	6.6	8.42	1.33
2M13520639+3956266	5713 ± 90	4.06 ± 0.09	4.04	0.11 ± 0.04	0.06 ± 0.1	0.89	3.92	10.23	1.55
2M13521871+3251250	6056 ± 81	4.29 ± 0.1	4.18	0.15 ± 0.03	0.1 ± 0.1	0.66	5.48	10.29	0.37
2M13522393+2546210	6107 ± 141	4.24 ± 0.19	4.12	0.07 ± 0.05	0 ± 0.1	0.71	5.9	9.03	1.37
2M13522416+3327487	6160 ± 141	4.3 ± 0.2	4.16	0.12 ± 0.05	0.06 ± 0.1	0.72	6.18	9.22	0.43
2M13531321+4423231	5880 ± 141	4.34 ± 0.21	4.27	-0.04 ± 0.06	-0.11 ± 0.1	0.54	4.73	8.94	0.51
2M13540516+3249353	6083 ± 86	4.25 ± 0.12	4.13	-0.22 ± 0.03	-0.3 ± 0.1	0.03	6.06	7.45	0.47
2M13542538+2512211	5942 ± 87	4.22 ± 0.11	4.14	-0.04 ± 0.04	-0.1 ± 0.1	0.72	5.06	8.54	1.42
2M13542652+2431274	5997 ± 134	4.35 ± 0.15	4.25	0.04 ± 0.05	-0.01 ± 0.1	0.63	5.25	10.12	0.44
2M13542807+4013426	5854 ± 113	4.31 ± 0.15	4.25	0.05 ± 0.05	-0.01 ± 0.1	0.62	4.51	10.03	1.5
2M13543709+2428223	6178 ± 88	4.43 ± 0.11	4.28	0.17 ± 0.03	0.11 ± 0.1	0.62	6.25	10.37	0.32
2M13555788+3151529	6170 ± 73	4.34 ± 0.11	4.19	-0.02 ± 0.03	-0.09 ± 0.1	0.25	6.4	8.11	0.37
2M13564094+2617139	5994 ± 142	4.3 ± 0.17	4.20	-0.12 ± 0.06	-0.2 ± 0.1	0.34	5.42	9.11	1.45
2M13570919+4735254	5756 ± 118	4.27 ± 0.12	4.23	0.08 ± 0.05	0 ± 0.1	0.56	4.06	9.45	0.68
2M13575453+2537446	5927 ± 127	4.12 ± 0.16	4.04	-0.18 ± 0.05	-0.26 ± 0.1	0.31	5.15	8.25	1.32
2M13581116+2631531	5813 ± 141	4.08 ± 0.15	4.03	0.02 ± 0.06	-0.04 ± 0.1	0.85	4.41	9.84	1.65

APOGEE_ID	$T_{\text{eff}} \pm \Delta T_{\text{eff}}$	$\log g \pm \Delta \log g$	$\log g_{cor}$	$[\text{M/H}] \pm \Delta[\text{M/H}]$	$[Fe/H] \pm \Delta[\text{Fe/H}]$	v_{mic}	v_{mac}	$v \sin i$	χ^2
2M13582209+3149182	5869 ± 105	4.28 ± 0.14	4.22	-0.01 ± 0.04	-0.07 ± 0.1	0.66	4.65	9.38	0.38
2M13582807+3411363	6166 ± 103	4.49 ± 0.11	4.34	0.22 ± 0.04	0.17 ± 0.1	0.79	6.09	11.08	0.38
2M13583112+4610561	5685 ± 110	4.3 ± 0.15	4.28	-0.05 ± 0.05	-0.09 ± 0.1	0.72	3.94	10.25	0.56
2M13584354+0252106	6041 ± 117	4.2 ± 0.13	4.09	0.03 ± 0.05	-0.05 ± 0.1	0.61	5.55	9.52	1.36
2M13594047+2425556	6045 ± 139	4.33 ± 0.2	4.22	-0.09 ± 0.06	-0.16 ± 0.1	0.54	5.67	8.91	0.37
2M13595587+2519336	6022 ± 99	4.38 ± 0.13	4.28	0.12 ± 0.04	0.09 ± 0.1	0.7	5.3	10.16	0.35
2M14003309+0300249	6205 ± 172	4.28 ± 0.23	4.12	-0.04 ± 0.07	-0.13 ± 0.1	0.5	6.68	8.32	1.4
2M14004541+2556112	6079 ± 100	4.37 ± 0.15	4.25	-0.15 ± 0.04	-0.22 ± 0.1	0.12	5.94	7.64	0.34
2M14004821+3232343	6006 ± 123	4.21 ± 0.13	4.11	0.16 ± 0.05	0.12 ± 0.1	0.78	5.18	10.65	1.49
2M14013776+4542286	5737 ± 130	4.3 ± 0.14	4.27	0 ± 0.05	-0.04 ± 0.1	0.53	4.06	10.62	0.67
2M14015661+2859037	5913 ± 106	4.21 ± 0.14	4.14	0.11 ± 0.04	0.04 ± 0.1	0.69	4.74	10.14	0.46
2M14015683+4334049	6008 ± 131	4.29 ± 0.15	4.19	0.13 ± 0.05	0.07 ± 0.1	0.71	5.22	10.76	0.49
2M14020450+2912227	5699 ± 110	4.22 ± 0.12	4.20	0.06 ± 0.05	0.01 ± 0.1	0.77	3.88	10.52	0.43
2M14020682+2422075	6073 ± 119	4.26 ± 0.17	4.14	-0.06 ± 0.05	-0.13 ± 0.1	0.44	5.83	8.53	1.32
2M14022004+5240338	6098 ± 123	4.5 ± 0.12	4.38	0.34 ± 0.05	0.27 ± 0.1	0.93	5.5	8.82	0.77
2M14024081+2930330	6083 ± 152	4.34 ± 0.21	4.22	0.03 ± 0.06	-0.05 ± 0.1	0.64	5.78	8.63	0.49
2M14033212+5314543	5750 ± 141	4.37 ± 0.17	4.34	-0.11 ± 0.06	-0.17 ± 0.1	0.58	4.23	8.91	0.73
2M14034560+4620461	5864 ± 128	4.39 ± 0.2	4.33	-0.06 ± 0.05	-0.12 ± 0.1	0.3	4.66	9.33	0.52
2M14035436+2905225	6323 ± 88	4.45 ± 0.1	4.24	0.13 ± 0.03	0.07 ± 0.1	0.55	7.37	10.35	0.31
2M14040873+5259147	5916 ± 152	4.23 ± 0.23	4.15	-0.27 ± 0.06	-0.34 ± 0.1	0.13	5.16	8.51	0.65

APOGEE_ID	$T_{\rm eff} \pm \Delta T_{\rm eff}$	$\log g \pm \Delta \log g$	$\log g_{cor}$	$[\mathrm{M/H}] \pm \Delta[\mathrm{M/H}]$	$[Fe/H] \pm \Delta[\mathrm{Fe/H}]$	$\mathrm{v}_{\rm mic}$	$\mathrm{v}_{\rm mac}$	$v \sin i$	χ^2
2M14045555+4523070	5744 ± 117	4.29 ± 0.12	4.26	0.03 ± 0.05	-0.02 ± 0.1	0.65	4.07	10.23	0.82
2M14045686+2942378	5707 ± 132	4.26 ± 0.16	4.24	-0.03 ± 0.06	-0.13 ± 0.1	0.6	4	9.1	1.46
2M14053761+5418418	6157 ± 97	4.38 ± 0.15	4.24	0.11 ± 0.04	0.04 ± 0.1	0.66	6.17	9.69	0.33
2M14054598+4551037	5681 ± 89	4.23 ± 0.11	4.21	0.09 ± 0.04	0.05 ± 0.1	0.76	3.78	9.73	1.53
2M14061458+2858454	5985 ± 124	4.22 ± 0.15	4.13	-0.17 ± 0.05	-0.27 ± 0.1	0.26	5.43	8.17	0.39
2M14064792+0240329	5709 ± 90	4.24 ± 0.1	4.22	0.13 ± 0.04	0.09 ± 0.1	0.83	3.82	10.36	1.32
2M14064826+5207312	6160 ± 136	4.4 ± 0.21	4.26	0.09 ± 0.05	0.03 ± 0.1	0.57	6.21	9.51	0.45
2M14065259+4743551	5575 ± 126	4.27 ± 0.14	4.28	0 ± 0.05	-0.03 ± 0.1	0.91	3.55	11.27	0.67
2M14071036+2859283	6019 ± 116	4.22 ± 0.13	4.12	-0.01 ± 0.04	-0.08 ± 0.1	0.61	5.46	9.28	0.34
2M14072065+3005327	5940 ± 167	4.22 ± 0.24	4.14	-0.28 ± 0.07	-0.41 ± 0.1	0.19	5.3	8.43	1.44
2M14072134+2806155	5748 ± 124	4.35 ± 0.14	4.32	-0.03 ± 0.05	-0.08 ± 0.1	0.66	4.14	10.16	0.39
2M14072343+2721092	5676 ± 116	4.25 ± 0.14	4.24	0.03 ± 0.05	-0.01 ± 0.1	0.79	3.83	10.09	1.52
2M14073375+2726474	5630 ± 122	4.4 ± 0.19	4.40	-0.06 ± 0.05	-0.1 ± 0.1	0.68	3.76	10.23	1.51
2M14080213+4554261	6081 ± 152	4.26 ± 0.21	4.14	-0.11 ± 0.06	-0.19 ± 0.1	0.29	5.93	7.11	0.48
2M14082083+2934147	5709 ± 129	4.13 ± 0.13	4.11	-0.01 ± 0.05	-0.07 ± 0.1	0.69	4.01	10.82	0.4
2M14083919+2946280	6080 ± 126	4.34 ± 0.19	4.22	-0.09 ± 0.05	-0.16 ± 0.1	0.33	5.88	7.98	0.38
2M14091277+2759107	5673 ± 117	4.07 ± 0.13	4.06	0.07 ± 0.05	0.03 ± 0.1	0.83	3.82	10.31	0.49
2M14091607+4607587	5791 ± 136	4.38 ± 0.19	4.34	-0.07 ± 0.06	-0.12 ± 0.1	0.75	4.35	9.73	0.66
2M14101201+5205502	5899 ± 77	4.38 ± 0.12	4.31	-0.01 ± 0.03	-0.06 ± 0.1	0.58	4.78	10.64	0.36
2M14101201+5205502	5850 ± 79	4.32 ± 0.1	4.26	0 ± 0.03	-0.06 ± 0.1	0.63	4.54	8.78	0.42

APOGEE_ID	$T_{\rm eff} \pm \Delta T_{\rm eff}$	$\log g \pm \Delta \log g$	$\log g_{cor}$	$[\rm M/H] \pm \Delta[\rm M/H]$	$[Fe/H] \pm \Delta[\rm Fe/H]$	$\rm v_{mic}$	$\rm v_{mac}$	$v \sin i$	χ^2
2M14102228+5458052	6071 ± 156	4.15 ± 0.18	4.04	-0.01 ± 0.06	-0.08 ± 0.1	0.64	5.78	9	0.52
2M14102395+4742423	6015 ± 144	4.41 ± 0.17	4.31	-0.01 ± 0.06	-0.07 ± 0.1	0.16	5.4	9.13	0.49
2M14110562+5419511	5747 ± 161	4.25 ± 0.18	4.22	-0.33 ± 0.06	-0.45 ± 0.1	0	4.46	7.89	1.44
2M14110967+4553441	5794 ± 136	4.18 ± 0.14	4.14	0 ± 0.06	-0.06 ± 0.1	0.74	4.32	9.58	0.67
2M14111162+2800208	6213 ± 96	4.34 ± 0.12	4.17	0.03 ± 0.04	-0.04 ± 0.1	0.5	6.66	8.26	1.37
2M14113364+2802119	6148 ± 83	4.38 ± 0.14	4.24	-0.08 ± 0.03	-0.16 ± 0.1	0.25	6.32	7.29	0.33
2M14114811+2919585	5557 ± 126	4.36 ± 0.17	4.38	-0.05 ± 0.05	-0.09 ± 0.1	1.05	3.55	10.92	0.49
2M14115262+4421407	5973 ± 152	4.11 ± 0.17	4.02	-0.08 ± 0.06	-0.15 ± 0.1	0.73	5.29	8.81	3.12
2M14123347+4605181	6017 ± 95	4.17 ± 0.1	4.07	0.03 ± 0.04	-0.05 ± 0.1	0.61	5.41	9.51	1.43
2M14123923+4246423	5680 ± 123	4.31 ± 0.17	4.29	-0.04 ± 0.05	-0.09 ± 0.1	0.83	3.91	8.64	0.57
2M14124803+5224374	5937 ± 124	4.1 ± 0.15	4.02	-0.15 ± 0.05	-0.21 ± 0.1	0.54	5.18	8.71	1.72
2M14134394+4615222	5864 ± 112	4.34 ± 0.17	4.28	-0.05 ± 0.05	-0.09 ± 0.1	0.45	4.66	9.88	1.55
2M14134803+4526089	5926 ± 118	4.09 ± 0.13	4.01	0.03 ± 0.05	-0.04 ± 0.1	0.68	4.93	9.36	0.54
2M14135887+4530031	5893 ± 108	4.28 ± 0.15	4.21	0.02 ± 0.04	-0.05 ± 0.1	0.55	4.73	8.86	0.49
2M14140518+1257338	6259 ± 187	4.28 ± 0.22	4.10	0.14 ± 0.07	0.08 ± 0.1	0.93	6.88	11.35	1.2
2M14141664+4522153	6157 ± 166	4.38 ± 0.28	4.24	-0.08 ± 0.07	-0.17 ± 0.1	0	6.38	8.07	1.65
2M14144227+4351238	5729 ± 129	4.27 ± 0.15	4.24	-0.14 ± 0.05	-0.19 ± 0.1	0.72	4.2	8.63	0.96
2M14150723+4505497	6004 ± 105	4.3 ± 0.12	4.20	0 ± 0.04	-0.07 ± 0.1	0.51	5.34	8.94	0.39
2M14152134+4323138	5690 ± 121	4.2 ± 0.14	4.18	0.12 ± 0.05	0.07 ± 0.1	0.87	3.78	10.6	0.72
2M14152421+5328029	6132 ± 141	4.22 ± 0.21	4.09	-0.09 ± 0.06	-0.18 ± 0.1	0.39	6.24	7.93	0.52

APOGEE_ID	$T_{\rm eff} \pm \Delta T_{\rm eff}$	$\log g \pm \Delta \log g$	$\log g_{cor}$	$[{\rm M/H}] \pm \Delta[{\rm M/H}]$	$[Fe/H] \pm \Delta[{\rm Fe/H}]$	$v_{\rm mic}$	$v_{\rm mac}$	$v \sin i$	χ^2
2M14152523+4554490	6251 ± 82	4.37 ± 0.1	4.19	0.22 ± 0.03	0.18 ± 0.1	0.78	6.72	9.26	1.45
2M14153017+4311109	5469 ± 86	4.26 ± 0.09	4.30	0.03 ± 0.04	0.01 ± 0.1	1.27	3.28	10.9	0.58
2M14155194+4529042	5929 ± 130	4.39 ± 0.2	4.31	-0.13 ± 0.05	-0.22 ± 0.1	0.17	5.06	10.11	1.96
2M14160763+4658548	5555 ± 87	4.14 ± 0.09	4.16	0.15 ± 0.04	0.12 ± 0.1	0.97	3.36	10	1.8
2M14161404+4148548	6103 ± 161	4.37 ± 0.23	4.25	0.01 ± 0.06	-0.05 ± 0.1	0.54	5.93	9.51	0.47
2M14162176+5152239	5629 ± 118	4.31 ± 0.15	4.31	0.02 ± 0.05	-0.05 ± 0.1	0.65	3.68	9.75	1.78
2M14163869+4310148	6167 ± 145	4.51 ± 0.15	4.36	0.13 ± 0.06	0.08 ± 0.1	0.55	6.21	10.61	0.73
2M14164351+4607254	5942 ± 179	4.29 ± 0.26	4.21	-0.27 ± 0.07	-0.36 ± 0.1	0	5.29	8.41	1.99
2M14164386+5424505	6169 ± 119	4.25 ± 0.16	4.10	0 ± 0.05	-0.08 ± 0.1	0.31	6.4	8.74	0.37
2M14165590+5208043	5768 ± 112	4.16 ± 0.13	4.12	-0.31 ± 0.05	-0.41 ± 0.1	0.32	4.55	7.32	1.38
2M14165640+5429341	5947 ± 87	4.24 ± 0.1	4.16	0.07 ± 0.03	0.01 ± 0.1	0.69	4.96	11.03	0.38
2M14165901+4610373	5531 ± 131	4.28 ± 0.16	4.30	-0.29 ± 0.05	-0.35 ± 0.1	0.5	3.74	8.93	0.54
2M14170635+4705599	5732 ± 177	4.25 ± 0.21	4.22	-0.33 ± 0.07	-0.41 ± 0.1	0.31	4.4	7.95	0.49
2M14171198+4203351	5995 ± 119	4.36 ± 0.14	4.26	-0.02 ± 0.05	-0.1 ± 0.1	0.5	5.3	8.28	0.36
2M14172033+4554196	5626 ± 109	4.16 ± 0.13	4.16	0.11 ± 0.05	0.09 ± 0.1	1.01	3.6	9.26	1.89
2M14172544+4145135	5973 ± 78	4.25 ± 0.09	4.16	0.15 ± 0.03	0.11 ± 0.1	0.84	5	9.26	1.44
2M14172563+4737455	5934 ± 144	4.34 ± 0.21	4.26	-0.11 ± 0.06	-0.2 ± 0.1	0.18	5.07	9.49	1.49
2M14181687+4150563	6246 ± 150	4.26 ± 0.18	4.08	-0.09 ± 0.06	-0.18 ± 0.1	0.36	7.05	8.46	0.43
2M14182146+4214319	5828 ± 96	4.32 ± 0.14	4.27	-0.07 ± 0.04	-0.12 ± 0.1	0.48	4.52	8.92	0.46
2M14183564+4731221	6118 ± 140	4.3 ± 0.21	4.18	-0.04 ± 0.06	-0.12 ± 0.1	0.43	6.09	8.79	1.52

APOGEE_ID	$T_{\rm eff} \pm \Delta T_{\rm eff}$	$\log g \pm \Delta \log g$	$\log g_{cor}$	$[\mathrm{M/H}] \pm \Delta[\mathrm{M/H}]$	$[Fe/H] \pm \Delta[\mathrm{Fe/H}]$	$\mathrm{v}_{\rm mic}$	$\mathrm{v}_{\rm mac}$	$v \sin i$	χ^2
2M14190933+4654103	5929 ± 138	4.24 ± 0.2	4.16	-0.22 ± 0.06	-0.32 ± 0.1	0.54	5.18	7.42	0.79
2M14191361+4223191	5825 ± 101	4.18 ± 0.12	4.13	0.05 ± 0.04	-0.03 ± 0.1	0.43	4.4	8.97	0.66
2M14191404+4740301	5811 ± 106	4.08 ± 0.12	4.03	-0.11 ± 0.04	-0.2 ± 0.1	0.51	4.54	8.96	0.44
2M14192928+0550096	6023 ± 140	4.32 ± 0.18	4.22	-0.06 ± 0.06	-0.14 ± 0.1	0.04	5.51	9.25	1.67
2M14200467+4522252	5893 ± 138	4.18 ± 0.18	4.11	0.03 ± 0.06	-0.03 ± 0.1	0.48	4.74	9	0.73
2M14203638+4226051	6061 ± 98	4.38 ± 0.13	4.27	0.1 ± 0.04	0.05 ± 0.1	0.67	5.56	9.37	0.4
2M14204306+4238006	5673 ± 131	4.36 ± 0.19	4.35	-0.12 ± 0.06	-0.15 ± 0.1	0.66	3.96	10.03	0.49
2M14205368+4123269	5869 ± 87	4.21 ± 0.11	4.15	0.03 ± 0.04	-0.01 ± 0.1	0.67	4.62	10.02	0.37
2M14205438+4403178	5733 ± 115	4.19 ± 0.12	4.16	0.05 ± 0.05	0 ± 0.1	0.74	4.02	10.59	1.48
2M14205521+5409491	5744 ± 132	4.15 ± 0.12	4.12	0 ± 0.05	-0.06 ± 0.1	0.77	4.13	9.39	0.6
2M14205839+4259049	6115 ± 145	4.47 ± 0.18	4.35	0.01 ± 0.03	-0.07 ± 0.1	0.56	5.99	8.86	0.44
2M14210753+4305483	5972 ± 154	4.35 ± 0.21	4.26	-0.19 ± 0.06	-0.27 ± 0.1	0.41	5.36	8.57	1.4
2M14211202+4752109	5758 ± 121	4.37 ± 0.15	4.33	-0.07 ± 0.05	-0.12 ± 0.1	0.75	4.22	9.12	0.54
2M14213861+4321376	5971 ± 133	4.25 ± 0.16	4.16	-0.03 ± 0.05	-0.1 ± 0.1	0.43	5.2	9.52	0.53
2M14223241+4328296	5663 ± 114	4.35 ± 0.15	4.34	-0.01 ± 0.05	-0.05 ± 0.1	0.68	3.81	10.59	0.5
2M14225733+5322384	5751 ± 117	4.25 ± 0.12	4.22	0.05 ± 0.05	0.01 ± 0.1	0.69	4.07	10.35	0.63
2M14225996+4132241	5861 ± 125	4.35 ± 0.19	4.29	-0.08 ± 0.05	-0.13 ± 0.1	0.59	4.68	8.39	0.48
2M14230455+4313017	6011 ± 144	4.33 ± 0.17	4.23	0.11 ± 0.06	0.06 ± 0.1	0.58	5.25	11.03	1.64
2M14233696+4139035	5509 ± 102	4.26 ± 0.11	4.29	0.08 ± 0.04	0.06 ± 0.1	1.2	3.3	9.89	0.71
2M14233987+5405447	5936 ± 135	4.45 ± 0.17	4.37	-0.06 ± 0.06	-0.13 ± 0.1	0	5.02	8.87	0.52

APOGEE_ID	$T_{\rm eff} \pm \Delta T_{\rm eff}$	$\log g \pm \Delta \log g$	$\log g_{cor}$	$[\rm M/H] \pm \Delta[\rm M/H]$	$[Fe/H] \pm \Delta[\rm Fe/H]$	$\rm v_{mic}$	$\rm v_{mac}$	$v \sin i$	χ^2
2M14234048+4608235	5599 ± 136	4.27 ± 0.18	4.27	-0.19 ± 0.06	-0.27 ± 0.1	0.45	3.82	8.72	0.93
2M14235813+5240176	5937 ± 123	4.45 ± 0.14	4.37	-0.04 ± 0.05	-0.08 ± 0.1	0.3	5	10.26	0.6
2M14240803+5406049	5888 ± 134	4.11 ± 0.16	4.04	0.01 ± 0.05	-0.06 ± 0.1	0.64	4.76	9.18	0.59
2M14241107+4331477	5927 ± 103	4.16 ± 0.12	4.08	0.05 ± 0.04	-0.03 ± 0.1	0.6	4.9	9.49	0.41
2M14243816+5408533	5780 ± 152	4.36 ± 0.2	4.32	-0.17 ± 0.06	-0.23 ± 0.1	0.28	4.42	8.67	0.54
2M14244393+4138051	5984 ± 126	4.36 ± 0.15	4.27	0.13 ± 0.05	0.09 ± 0.1	0.63	5.07	9.87	0.49
2M14245965+5821383	5750 ± 124	4.36 ± 0.14	4.33	0.03 ± 0.05	-0.03 ± 0.1	0.64	4.08	10.33	1.84
2M14250399+4253374	5744 ± 96	4.22 ± 0.1	4.19	0.08 ± 0.04	0.05 ± 0.1	0.73	4.02	9.52	1.75
2M14250643+3912427	5870 ± 130	3.91 ± 0.2	3.85	-0.05 ± 0.06	-0.1 ± 0.1	0.58	4.81	9.19	2.36
2M14252363+5018542	6228 ± 78	4.33 ± 0.09	4.16	0.05 ± 0.03	-0.03 ± 0.1	0.49	6.74	8.41	0.33
2M14253012+2035244	5820 ± 197	4.16 ± 0.25	4.11	-0.34 ± 0.08	-0.47 ± 0.1	0	4.79	7.92	1.43
2M14253077-0635128	5951 ± 96	4.23 ± 0.11	4.15	0.09 ± 0.04	0.04 ± 0.1	0.89	4.95	9.12	0.43
2M14260237+4213049	5692 ± 73	4.3 ± 0.09	4.28	0.02 ± 0.03	-0.02 ± 0.1	0.78	3.88	10.37	0.39
2M14261569+5103389	5853 ± 126	4.3 ± 0.17	4.24	0.06 ± 0.05	0.01 ± 0.1	0.63	4.49	10.77	0.51
2M14262376+4048090	5975 ± 145	3.99 ± 0.13	3.90	-0.01 ± 0.06	-0.08 ± 0.1	0.57	5.27	9.52	2.3
2M14263022+4033557	5687 ± 121	3.67 ± 0.15	3.67	0.04 ± 0.05	0.02 ± 0.1	0.95	4.09	10.65	2.79
2M14263726+5304584	5658 ± 150	4.31 ± 0.24	4.30	-0.39 ± 0.07	-0.47 ± 0.1	0	4.19	7.94	1.77
2M14264827-0510400	5355 ± 28	4.12 ± 0.03	4.19	0.42 ± 0.01	0.33 ± 0.1	0.71	2.68	9.58	1.08
2M14264995+4013386	5696 ± 131	3.73 ± 0.16	3.73	0 ± 0.05	-0.03 ± 0.1	0.76	4.14	11.01	1.75
2M14270161+5357596	6298 ± 143	4.41 ± 0.18	4.21	0.17 ± 0.06	0.13 ± 0.1	0.64	7.12	7.7	0.68

APOGEE_ID	$T_{\rm eff} \pm \Delta T_{\rm eff}$	$\log g \pm \Delta \log g$	$\log g_{cor}$	$[{\rm M/H}] \pm \Delta[{\rm M/H}]$	$[Fe/H] \pm \Delta[{\rm Fe/H}]$	$v_{\rm mic}$	$v_{\rm mac}$	$v \sin i$	χ^2
2M14270373+4720087	5969 ± 130	4.27 ± 0.15	4.18	0.07 ± 0.05	0 ± 0.1	0.7	5.08	10.33	1.52
2M14271006+5246059	5891 ± 96	4.19 ± 0.12	4.12	0.2 ± 0.04	0.17 ± 0.1	0.81	4.52	9.26	0.69
2M14280006+0851041	6206 ± 107	4.5 ± 0.1	4.34	0.08 ± 0.04	0.02 ± 0.1	0.47	6.54	9.32	1.39
2M14284725+5349199	5798 ± 126	4.4 ± 0.17	4.35	-0.1 ± 0.05	-0.15 ± 0.1	0.54	4.41	8.85	0.67
2M14285128+5734255	5628 ± 103	4.17 ± 0.12	4.17	0 ± 0.04	-0.05 ± 0.1	0.74	3.73	10.73	1.54
2M14285271+4015518	5973 ± 88	4.08 ± 0.09	3.99	-0.04 ± 0.04	-0.11 ± 0.1	0.52	5.27	8.59	1.11
2M14291144-0531309	5738 ± 134	4.11 ± 0.14	4.08	-0.58 ± 0.05	-0.71 ± 0.1	0	4.69	8.07	0.39
2M14292668+4007282	6121 ± 143	3.98 ± 0.16	3.85	0 ± 0.05	-0.06 ± 0.1	0.48	6.15	9.2	1.1
2M14294698+5341474	5450 ± 129	4.21 ± 0.15	4.25	-0.36 ± 0.06	-0.46 ± 0.1	0.46	3.66	8.45	2.05
2M14294761+5332571	5751 ± 92	4.05 ± 0.08	4.02	0.11 ± 0.04	0.06 ± 0.1	0.73	4.06	10.7	1.77
2M14295448+0736464	6118 ± 139	4.36 ± 0.22	4.24	-0.18 ± 0.05	-0.26 ± 0.1	0	6.23	8.29	0.38
2M14303105+5824183	6105 ± 59	4.31 ± 0.08	4.19	0.13 ± 0.02	0.07 ± 0.1	0.65	5.81	10.72	0.32
2M14303934-0619588	6227 ± 76	4.4 ± 0.1	4.23	0.17 ± 0.03	0.13 ± 0.1	0.72	6.59	9.36	0.34
2M14304238+5828233	5824 ± 139	4.2 ± 0.18	4.15	-0.17 ± 0.06	-0.25 ± 0.1	0.47	4.63	8.16	0.52
2M14305945+0837133	6139 ± 110	4.44 ± 0.15	4.31	0.14 ± 0.04	0.1 ± 0.1	0.72	6.01	9.66	0.41
2M14314672+4006166	5934 ± 106	4 ± 0.11	3.92	-0.02 ± 0.04	-0.08 ± 0.1	0	5.06	9.47	1.32
2M14320517+5842248	5705 ± 137	4.32 ± 0.18	4.30	-0.12 ± 0.06	-0.18 ± 0.1	0.58	4.08	8.84	0.68
2M14320808+5321514	6071 ± 78	4.28 ± 0.1	4.17	0.37 ± 0.03	0.3 ± 0.1	0.9	5.31	9.34	0.74
2M14333899+5729489	5752 ± 104	4.24 ± 0.11	4.21	0.15 ± 0.04	0.1 ± 0.1	0.87	3.97	10.13	0.89
2M14341396+5001325	5930 ± 77	4.3 ± 0.11	4.22	-0.04 ± 0.03	-0.1 ± 0.1	0.52	4.98	9.96	0.38

APOGEE_ID	$T_{\rm eff} \pm \Delta T_{\rm eff}$	$\log g \pm \Delta \log g$	$\log g_{cor}$	$[{\rm M/H}] \pm \Delta[{\rm M/H}]$	$[Fe/H] \pm \Delta[{\rm Fe/H}]$	$v_{\rm mic}$	$v_{\rm mac}$	$v \sin i$	χ^2
2M14341863+5229248	5724 ± 133	4.15 ± 0.15	4.12	-0.28 ± 0.06	-0.38 ± 0.1	0.34	4.35	7.45	0.51
2M14341888+5217575	5524 ± 85	4.2 ± 0.09	4.22	0.11 ± 0.04	0.08 ± 0.1	0.83	3.31	9.85	0.81
2M14341957+0738263	6197 ± 131	4.31 ± 0.17	4.15	0.02 ± 0.05	-0.05 ± 0.1	0.45	6.56	9.14	1.42
2M14342958+5402045	6002 ± 143	4.21 ± 0.15	4.11	-0.01 ± 0.06	-0.1 ± 0.1	0.33	5.36	8.73	0.64
2M14345442+5426335	5781 ± 84	4.16 ± 0.09	4.12	0.13 ± 0.03	0.07 ± 0.1	0.76	4.13	10.53	0.48
2M14345444+5355590	5915 ± 125	4.45 ± 0.15	4.37	-0.03 ± 0.05	-0.1 ± 0.1	0.41	4.88	8.86	0.42
2M14351196+5144362	5976 ± 112	4.28 ± 0.13	4.19	0.08 ± 0.04	0.02 ± 0.1	0.67	5.09	9.69	0.51
2M14355030+5156240	6159 ± 142	4.37 ± 0.21	4.23	0.13 ± 0.06	0.07 ± 0.1	0.58	6.16	10.37	0.57
2M14355242+5031262	5857 ± 96	4.33 ± 0.14	4.27	-0.04 ± 0.04	-0.09 ± 0.1	0.66	4.62	9.13	0.47
2M14355909+4900295	5987 ± 99	4.34 ± 0.12	4.25	0.08 ± 0.04	0.03 ± 0.1	0.7	5.15	9.97	1.56
2M14365571+5019425	5881 ± 89	4.34 ± 0.13	4.27	0.13 ± 0.04	0.09 ± 0.1	0.72	4.53	9.97	0.46
2M14380071+5223005	5853 ± 143	4.26 ± 0.19	4.20	-0.02 ± 0.06	-0.06 ± 0.1	0.57	4.59	10.45	1.67
2M14380710+5100434	5931 ± 120	4.22 ± 0.15	4.14	0.1 ± 0.05	0.05 ± 0.1	0.84	4.84	9.07	1.54
2M14381701+4945508	5552 ± 108	4.22 ± 0.12	4.24	0.08 ± 0.05	0.06 ± 0.1	1.05	3.41	9.73	0.71
2M14384119+5151496	5931 ± 129	4.33 ± 0.17	4.25	0.09 ± 0.05	0.04 ± 0.1	0.78	4.84	10.37	0.8
2M14392504+5025063	5922 ± 107	4.31 ± 0.15	4.23	0.05 ± 0.04	0 ± 0.1	0.54	4.84	9.84	0.41
2M14400169+1302249	5750 ± 120	4.28 ± 0.13	4.25	0.1 ± 0.05	0.06 ± 0.1	0.74	4.01	10.55	1.51
2M14404091+5325320	5728 ± 133	4.4 ± 0.17	4.37	-0.07 ± 0.06	-0.13 ± 0.1	0.61	4.1	9.25	0.7
2M14412878+1336052	5814 ± 150	4.23 ± 0.19	4.18	-0.05 ± 0.06	-0.14 ± 0.1	0.51	4.45	9.44	1.5
2M14412878+1336052	5872 ± 62	4.26 ± 0.09	4.20	-0.04 ± 0.03	-0.14 ± 0.1	0.46	4.69	9.02	1.34

APOGEE_ID	$T_{\rm eff} \pm \Delta T_{\rm eff}$	$\log g \pm \Delta \log g$	$\log g_{cor}$	$[\rm M/H] \pm \Delta[\rm M/H]$	$[Fe/H] \pm \Delta[\rm Fe/H]$	$\rm v_{mic}$	$\rm v_{mac}$	$v \sin i$	χ^2
2M14413156+1321098	5998 ± 141	4.35 ± 0.16	4.25	0.03 ± 0.05	-0.04 ± 0.1	0.62	5.27	9.59	0.44
2M14423283+5223053	5789 ± 102	4.17 ± 0.11	4.13	0.23 ± 0.04	0.19 ± 0.1	0.92	4.04	10.11	1.95
2M14434987+5107149	6025 ± 138	4.22 ± 0.17	4.12	-0.05 ± 0.06	-0.13 ± 0.1	0.38	5.54	9.6	1.53
2M14435238+1308510	5865 ± 98	4.21 ± 0.12	4.15	0.04 ± 0.04	-0.02 ± 0.1	0.67	4.58	9.23	1.39
2M14435586+5247046	5847 ± 135	4 ± 0.15	3.94	-0.09 ± 0.06	-0.15 ± 0.1	0.73	4.71	8.35	1.62
2M14440171+4659131	5955 ± 120	4.32 ± 0.15	4.23	0.06 ± 0.05	-0.01 ± 0.1	0.63	5	9.94	0.41
2M14443038+5025588	6028 ± 109	4.33 ± 0.13	4.23	0.04 ± 0.04	-0.01 ± 0.1	0.53	5.42	10.41	0.45
2M14445880+5204446	5828 ± 106	4.26 ± 0.13	4.21	0.11 ± 0.04	0.04 ± 0.1	0.82	4.33	9.81	0.59
2M14451172+5302128	5835 ± 118	4.25 ± 0.14	4.19	0.21 ± 0.05	0.15 ± 0.1	0.64	4.24	10.85	0.63
2M14454519+5313131	5775 ± 124	4.35 ± 0.14	4.31	0.03 ± 0.05	0 ± 0.1	0.7	4.18	10.67	1.81
2M14455682+4639248	6161 ± 92	4.44 ± 0.12	4.30	0.05 ± 0.04	-0.02 ± 0.1	0.48	6.26	9.1	0.32
2M14460128+5238586	5735 ± 125	4.36 ± 0.16	4.33	-0.05 ± 0.05	-0.1 ± 0.1	0.58	4.11	9.91	0.56
2M14460490+1159015	5915 ± 113	4.3 ± 0.16	4.22	0.15 ± 0.05	0.1 ± 0.1	0.72	4.68	10.37	0.46
2M14462179+5326508	5617 ± 123	4.04 ± 0.13	4.04	0.01 ± 0.05	-0.03 ± 0.1	0.8	3.72	11.02	0.76
2M14463425+1344593	6064 ± 94	4.29 ± 0.12	4.18	0.07 ± 0.04	0 ± 0.1	0.67	5.62	9.49	0.32
2M14464930+1222243	6065 ± 93	4.24 ± 0.11	4.13	0.1 ± 0.04	0.05 ± 0.1	0.74	5.6	9.87	1.36
2M14465374+5254430	5992 ± 98	4.36 ± 0.12	4.27	0.15 ± 0.04	0.12 ± 0.1	0.77	5.09	9.62	0.52
2M14471892+5156299	5754 ± 141	4.3 ± 0.16	4.27	-0.11 ± 0.06	-0.17 ± 0.1	0.65	4.25	8.49	1.63
2M14473358+5230201	5666 ± 93	4.22 ± 0.11	4.21	0.01 ± 0.04	-0.02 ± 0.1	0.76	3.82	10.2	1.51
2M14473566+5204197	5524 ± 102	4.41 ± 0.11	4.43	0.12 ± 0.04	0.08 ± 0.1	0.72	3.27	10.4	0.96

APOGEE_ID	$T_{\rm eff} \pm \Delta T_{\rm eff}$	$\log g \pm \Delta \log g$	$\log g_{cor}$	$[\rm M/H] \pm \Delta[\rm M/H]$	$[Fe/H] \pm \Delta[\rm Fe/H]$	$\rm v_{mic}$	$\rm v_{mac}$	$v \sin i$	χ^2
2M14480750+4724140	5962 ± 119	4.38 ± 0.17	4.29	-0.15 ± 0.05	-0.24 ± 0.1	0	5.26	8.42	1.22
2M14482736+5126309	6114 ± 87	4.41 ± 0.12	4.29	0 ± 0.03	-0.05 ± 0.1	0.59	6	8.58	0.36
2M14484160+5327037	5916 ± 147	4.29 ± 0.22	4.21	-0.2 ± 0.06	-0.28 ± 0.1	0.21	5.08	8.31	0.51
2M14491193+5254564	6088 ± 168	4.33 ± 0.25	4.21	-0.1 ± 0.07	-0.18 ± 0.1	0.27	5.95	8.34	0.72
2M14491773+4532148	6097 ± 124	4.05 ± 0.15	3.93	-0.13 ± 0.05	-0.21 ± 0.1	0.59	6.11	7.71	1.4
2M14493279+5148403	5605 ± 97	4.33 ± 0.13	4.33	0.14 ± 0.04	0.08 ± 0.1	0.7	3.47	7.85	1.87
2M14495097-0722087	6215 ± 113	4.33 ± 0.15	4.16	-0.1 ± 0.03	-0.18 ± 0.1	0.27	6.81	8.2	0.37
2M14495957+4508380	6015 ± 137	4.35 ± 0.18	4.25	-0.12 ± 0.06	-0.2 ± 0.1	0.41	5.53	8.29	0.43
2M14501934+5351154	5748 ± 129	4.31 ± 0.15	4.28	-0.1 ± 0.05	-0.18 ± 0.1	0.49	4.22	9.04	0.52
2M14502642+3058327	5670 ± 114	4.28 ± 0.15	4.27	0 ± 0.05	-0.05 ± 0.1	0.69	3.84	9.39	1.52
2M14510260-0817109	6157 ± 144	4.3 ± 0.23	4.16	-0.21 ± 0.06	-0.29 ± 0.1	0	6.52	7.33	0.36
2M14512160+3033398	5675 ± 127	4.33 ± 0.16	4.32	-0.01 ± 0.05	-0.04 ± 0.1	0.86	3.85	10.16	1.64
2M14512268+3205385	6191 ± 131	4.26 ± 0.18	4.10	-0.17 ± 0.05	-0.26 ± 0.1	0	6.73	7.43	0.42
2M14513997+5359198	6017 ± 97	4.24 ± 0.11	4.14	0.2 ± 0.04	0.14 ± 0.1	0.76	5.2	10.54	1.54
2M14514734-0626168	5981 ± 93	4.3 ± 0.11	4.21	0.13 ± 0.04	0.08 ± 0.1	0.75	5.06	9.17	0.42
2M14515224+3756433	6139 ± 185	4.25 ± 0.28	4.12	-0.2 ± 0.07	-0.3 ± 0.1	0	6.4	8.13	1.53
2M14515515+4151322	5681 ± 118	4.21 ± 0.15	4.19	-0.15 ± 0.05	-0.21 ± 0.1	0.54	4.04	9.79	1.55
2M14521428+1724423	5982 ± 107	4.43 ± 0.12	4.34	-0.02 ± 0.04	-0.08 ± 0.1	0.5	5.23	9.35	0.36
2M14522031+1753233	6200 ± 132	4.45 ± 0.15	4.29	0.07 ± 0.05	0.01 ± 0.1	0.47	6.5	8.92	0.33
2M14524099+3153557	5873 ± 131	4.22 ± 0.17	4.16	0.18 ± 0.05	0.12 ± 0.1	0.63	4.46	10.51	0.68

APOGEE_ID	$T_{\rm eff} \pm \Delta T_{\rm eff}$	$\log g \pm \Delta \log g$	$\log g_{cor}$	$[{\rm M/H}] \pm \Delta[{\rm M/H}]$	$[Fe/H] \pm \Delta[{\rm Fe/H}]$	$v_{\rm mic}$	$v_{\rm mac}$	$v \sin i$	χ^2
2M14525129+4847266	5739 ± 110	4.36 ± 0.13	4.33	-0.06 ± 0.05	-0.12 ± 0.1	0.4	4.13	9.12	0.58
2M14525848+4854164	5846 ± 110	4.17 ± 0.13	4.11	0.03 ± 0.04	-0.03 ± 0.1	0.72	4.52	9.42	0.47
2M14531191+2830295	5109 ± 103	3.76 ± 0.13	3.88	-0.01 ± 0.05	-0.1 ± 0.1	0.87	3.3	10.09	1.78
2M14532303+1814074	4849 ± 104	3.3 ± 0.16	3.30	0.08 ± 0.06	0 ± 0.1	0.97	3.52	10.89	2.1
2M14535993+3739387	6057 ± 105	4.35 ± 0.14	4.24	0.08 ± 0.04	0.01 ± 0.1	0.64	5.55	10.09	0.38
2M14541770+1737167	6057 ± 127	4.19 ± 0.16	4.08	-0.2 ± 0.05	-0.31 ± 0.1	0.05	5.89	8.26	1.38
2M14543066+3619326	6045 ± 119	4.36 ± 0.15	4.25	0.08 ± 0.05	0.04 ± 0.1	0.73	5.48	9.92	0.46
2M14544687+5203477	5989 ± 122	4.3 ± 0.14	4.21	0.16 ± 0.05	0.11 ± 0.1	0.73	5.07	10	1.66
2M14545028+5301392	5793 ± 134	4.16 ± 0.16	4.12	-0.08 ± 0.06	-0.16 ± 0.1	0.56	4.41	9.09	1.48
2M14551680+3150184	5716 ± 72	4.27 ± 0.08	4.24	0.09 ± 0.03	0.04 ± 0.1	0.73	3.89	10.53	0.48
2M14552739+3240203	5653 ± 97	4.35 ± 0.15	4.34	-0.09 ± 0.04	-0.15 ± 0.1	0.68	3.87	9.31	0.38
2M14553149+4253196	5738 ± 117	4.07 ± 0.11	4.04	0.18 ± 0.05	0.14 ± 0.1	0.91	3.93	10.19	2.01
2M14553990+1635089	5888 ± 114	4.31 ± 0.16	4.24	-0.01 ± 0.05	-0.07 ± 0.1	0.6	4.74	8.61	1.37
2M14554354+4817323	5691 ± 108	3.89 ± 0.15	3.87	0.06 ± 0.05	0.03 ± 0.1	0.89	3.96	9.66	0.48
2M14554695+3156416	6185 ± 139	4.33 ± 0.21	4.18	-0.12 ± 0.05	-0.21 ± 0.1	0.12	6.62	8.11	1.29
2M14555018+4258545	5734 ± 113	4.31 ± 0.12	4.28	0.03 ± 0.05	-0.02 ± 0.1	0.54	4.02	10.41	1.71
2M14555166+4858012	5720 ± 117	4.23 ± 0.13	4.20	0.13 ± 0.05	0.08 ± 0.1	0.81	3.87	10.84	1.73
2M14560684+3140526	6024 ± 143	4.36 ± 0.19	4.26	-0.05 ± 0.06	-0.13 ± 0.1	0.37	5.51	8.53	0.54
2M14560893+1805142	6121 ± 170	4.31 ± 0.27	4.18	-0.2 ± 0.07	-0.31 ± 0.1	0.11	6.27	8.94	1.32
2M14560980+4732142	5997 ± 138	4.4 ± 0.16	4.30	0 ± 0.05	-0.06 ± 0.1	0.49	5.29	9.82	0.45

APOGEE_ID	$T_{\rm eff} \pm \Delta T_{\rm eff}$	$\log g \pm \Delta \log g$	$\log g_{cor}$	$[\mathrm{M/H}] \pm \Delta[\mathrm{M/H}]$	$[Fe/H] \pm \Delta[\mathrm{Fe/H}]$	$\mathrm{v_{mic}}$	$\mathrm{v_{mac}}$	$v \sin i$	χ^2
2M14561194+5218295	6190 ± 133	4.42 ± 0.18	4.26	0.06 ± 0.05	0.02 ± 0.1	0.51	6.45	9.75	0.6
2M14564807+4750113	5937 ± 148	4.28 ± 0.21	4.20	-0.14 ± 0.06	-0.2 ± 0.1	0.4	5.12	8.25	0.51
2M14570205+3116277	6034 ± 128	4.36 ± 0.16	4.25	0.12 ± 0.05	0.07 ± 0.1	0.64	5.37	10.33	1.62
2M14570252+2957518	6200 ± 155	4.39 ± 0.24	4.23	-0.09 ± 0.06	-0.17 ± 0.1	0.07	6.69	8.2	0.45
2M14570260+4057572	5625 ± 120	4.18 ± 0.14	4.18	0.07 ± 0.05	0.04 ± 0.1	0.66	3.63	9.81	0.74
2M14571292+4331358	5691 ± 163	4.28 ± 0.22	4.26	-0.36 ± 0.07	-0.48 ± 0.1	0	4.28	8.68	1.89
2M14572420+3717409	6089 ± 153	4.14 ± 0.2	4.02	-0.15 ± 0.06	-0.25 ± 0.1	0.46	6.05	8.16	0.45
2M14573769+4336313	5793 ± 152	4.49 ± 0.15	4.45	-0.22 ± 0.06	-0.27 ± 0.1	0.35	4.51	8.22	0.67
2M14573855+2202139	6143 ± 76	4.3 ± 0.11	4.16	-0.01 ± 0.03	-0.09 ± 0.1	0.48	6.22	8.88	1.31
2M14574591+1813330	5916 ± 146	4.35 ± 0.22	4.27	-0.04 ± 0.06	-0.12 ± 0.1	0.51	4.9	8.56	0.37
2M14575161+4216134	6002 ± 135	4.31 ± 0.16	4.21	-0.03 ± 0.05	-0.11 ± 0.1	0.5	5.36	8.96	0.5
2M14580279+4151078	5926 ± 96	4.22 ± 0.12	4.14	0 ± 0.04	-0.04 ± 0.1	0.68	4.93	9.82	1.5
2M14580750+4049450	5880 ± 79	4.26 ± 0.11	4.19	0.08 ± 0.03	0.04 ± 0.1	0.61	4.61	9.91	1.44
2M14581187+4220409	5887 ± 116	4.28 ± 0.16	4.21	0.01 ± 0.05	-0.06 ± 0.1	0.65	4.71	10.36	0.37
2M14583962+3712229	5976 ± 112	4.31 ± 0.13	4.22	0.03 ± 0.04	-0.03 ± 0.1	0.66	5.15	9.47	0.37
2M14585684+3216131	5714 ± 152	4.32 ± 0.2	4.30	-0.22 ± 0.06	-0.31 ± 0.1	0.3	4.22	7.97	1.48
2M14585820+1719372	5959 ± 54	4.3 ± 0.07	4.21	0.23 ± 0.02	0.18 ± 0.1	0.67	4.82	10.02	0.53
2M14590997+4247543	6024 ± 137	4.37 ± 0.18	4.27	-0.05 ± 0.06	-0.11 ± 0.1	0	5.5	8.78	0.64
2M14592919+4943325	6289 ± 159	4.4 ± 0.23	4.20	-0.04 ± 0.06	-0.12 ± 0.1	0.26	7.3	7.51	0.37
2M14595483+3232435	5789 ± 108	4.39 ± 0.14	4.35	-0.03 ± 0.04	-0.09 ± 0.1	0.63	4.29	9.75	0.39

APOGEE_ID	$T_{\rm eff} \pm \Delta T_{\rm eff}$	$\log g \pm \Delta \log g$	$\log g_{cor}$	$[\rm M/H] \pm \Delta[\rm M/H]$	$[Fe/H] \pm \Delta[\rm Fe/H]$	$\mathsf{v}_{\rm mic}$	$\mathsf{v}_{\rm mac}$	$v \sin i$	χ^2
2M15000839+4832269	5795 ± 134	4.21 ± 0.16	4.17	-0.1 ± 0.06	-0.17 ± 0.1	0.55	4.43	8.48	0.51
2M15001664+3138026	5860 ± 141	4.21 ± 0.18	4.15	0.06 ± 0.06	-0.01 ± 0.1	0.61	4.54	9.28	1.57
2M15001828+3727218	5943 ± 118	4.31 ± 0.15	4.23	0.12 ± 0.05	0.07 ± 0.1	0.71	4.87	10.69	1.33
2M15002610+3136545	5948 ± 59	4.11 ± 0.06	4.03	0.01 ± 0.02	-0.06 ± 0.1	0.63	5.06	9.27	1.41
2M15011292+3807579	6058 ± 132	4.34 ± 0.17	4.23	0.14 ± 0.05	0.09 ± 0.1	0.71	5.5	10.77	0.48
2M15014911+3645186	6210 ± 152	4.16 ± 0.18	4.00	-0.02 ± 0.06	-0.11 ± 0.1	0.59	6.73	7.91	1.48
2M15014952+4816341	5749 ± 99	4.29 ± 0.1	4.26	0.1 ± 0.04	0.08 ± 0.1	0.9	4.01	9.51	0.5
2M15015096+4946411	5777 ± 138	4.35 ± 0.16	4.31	-0.02 ± 0.06	-0.08 ± 0.1	0.8	4.24	7.84	0.57
2M15020047+4308174	5660 ± 121	4.29 ± 0.16	4.28	0.04 ± 0.05	-0.01 ± 0.1	0.67	3.75	10.5	1.61
2M15022289+3620298	6019 ± 131	4.32 ± 0.15	4.22	0.02 ± 0.05	-0.04 ± 0.1	0.68	5.4	9.41	0.46
2M15022799+4134140	5984 ± 93	4.4 ± 0.11	4.31	0.05 ± 0.04	0 ± 0.1	0.45	5.16	9.74	1.33
2M15022899+2653425	5732 ± 115	4.29 ± 0.12	4.26	0.05 ± 0.05	0 ± 0.1	0.72	4	10.79	0.52
2M15023467+4228030	5600 ± 101	4.25 ± 0.12	4.25	0.09 ± 0.04	0.07 ± 0.1	0.88	3.52	9.16	1.87
2M15025022+4010297	6047 ± 72	4.2 ± 0.08	4.09	0.04 ± 0.03	-0.01 ± 0.1	0.59	5.57	10.43	0.34
2M15025998+3741490	5805 ± 124	4.18 ± 0.13	4.13	0.02 ± 0.05	-0.04 ± 0.1	0.74	4.34	8.7	0.57
2M15033040+4230066	5956 ± 119	4.17 ± 0.15	4.08	-0.08 ± 0.05	-0.16 ± 0.1	0.41	5.19	8.31	0.5
2M15035513+4136269	5693 ± 154	4.27 ± 0.21	4.25	-0.25 ± 0.07	-0.33 ± 0.1	0.42	4.18	7.43	1.95
2M15035905+2746272	5973 ± 146	4.4 ± 0.2	4.31	-0.08 ± 0.06	-0.16 ± 0.1	0.37	5.24	9.17	1.35
2M15043228+3600170	6121 ± 133	4.39 ± 0.2	4.26	0 ± 0.05	-0.06 ± 0.1	0.59	6.05	8.25	1.46
2M15043637+2614069	6037 ± 125	4.35 ± 0.17	4.24	-0.04 ± 0.05	-0.12 ± 0.1	0.55	5.58	8.19	0.38

APOGEE_ID	$T_{\rm eff} \pm \Delta T_{\rm eff}$	$\log g \pm \Delta \log g$	$\log g_{cor}$	$[{\rm M/H}] \pm \Delta[{\rm M/H}]$	$[Fe/H] \pm \Delta[{\rm Fe/H}]$	$v_{\rm mic}$	$v_{\rm mac}$	$v \sin i$	χ^2
2M15043936+2748325	5922 ± 135	4.33 ± 0.2	4.25	-0.18 ± 0.05	-0.25 ± 0.1	0	5.08	8.63	0.36
2M15044241+2650201	5794 ± 118	4.32 ± 0.14	4.28	0.02 ± 0.05	-0.04 ± 0.1	0.59	4.27	9.58	0.55
2M15044485+2155196	5887 ± 119	4.32 ± 0.2	4.25	-0.31 ± 0.05	-0.42 ± 0.1	0	5.04	7.74	1.28
2M15051038+3554447	6200 ± 138	4.25 ± 0.18	4.09	-0.02 ± 0.05	-0.1 ± 0.1	0.54	6.64	8.24	1.33
2M15051398+4223217	6127 ± 109	4.43 ± 0.14	4.30	0.11 ± 0.04	0.07 ± 0.1	0.48	5.96	10.2	0.43
2M15051544+4046358	6165 ± 140	4.35 ± 0.21	4.21	0.11 ± 0.06	0.06 ± 0.1	0.59	6.23	10.29	1.55
2M15052233+2547217	5932 ± 91	4.27 ± 0.12	4.19	0.18 ± 0.04	0.14 ± 0.1	0.84	4.74	9.86	0.46
2M15052969+4330294	5693 ± 97	4.28 ± 0.13	4.26	-0.37 ± 0.04	-0.46 ± 0.1	0.17	4.29	7.14	1.43
2M15053763+3226167	5793 ± 128	4.3 ± 0.15	4.26	0 ± 0.05	-0.05 ± 0.1	0.84	4.29	9.12	1.54
2M15053835+4151333	6035 ± 130	4.34 ± 0.16	4.23	0.1 ± 0.05	0.05 ± 0.1	0.69	5.4	10.26	0.64
2M15053955+4933173	6004 ± 158	4.31 ± 0.19	4.21	-0.04 ± 0.06	-0.11 ± 0.1	0.53	5.38	8.09	0.53
2M15055488+2745096	5952 ± 94	4.1 ± 0.1	4.02	0.01 ± 0.04	-0.07 ± 0.1	0.68	5.09	9.46	0.34
2M15062547+2543422	5756 ± 88	4.42 ± 0.1	4.38	-0.19 ± 0.04	-0.23 ± 0.1	0.51	4.33	8.41	1.28
2M15063429+2742319	6024 ± 144	4.39 ± 0.2	4.29	-0.1 ± 0.06	-0.19 ± 0.1	0.22	5.55	7.91	0.35
2M15065583+3528335	6115 ± 87	4.28 ± 0.13	4.16	-0.14 ± 0.03	-0.22 ± 0.1	0.37	6.17	8.02	0.35
2M15072331+3704316	5938 ± 151	4.31 ± 0.22	4.23	-0.19 ± 0.06	-0.3 ± 0.1	0.11	5.18	8.32	0.56
2M15074648+0852472	5811 ± 220	4.09 ± 0.26	4.04	-0.43 ± 0.09	-0.57 ± 0.1	0	4.86	8.78	1.43
2M15081096+2746554	5853 ± 119	4.28 ± 0.15	4.22	0.05 ± 0.05	0 ± 0.1	0.79	4.5	8.58	0.5
2M15082742+3759248	6194 ± 122	4.35 ± 0.16	4.19	0.04 ± 0.05	-0.04 ± 0.1	0.48	6.5	9.33	1.3
2M15085831+4330416	5691 ± 97	4.08 ± 0.1	4.06	0.01 ± 0.04	-0.02 ± 0.1	0.74	3.94	9.52	1.46

APOGEE_ID	$T_{\rm eff} \pm \Delta T_{\rm eff}$	$\log g \pm \Delta \log g$	$\log g_{cor}$	$[\rm M/H] \pm \Delta[\rm M/H]$	$[Fe/H] \pm \Delta[\rm Fe/H]$	$v_{\rm mic}$	$v_{\rm mac}$	$v \sin i$	χ^2
2M15090979+6712516	6214 ± 61	4.53 ± 0.06	4.36	0.13 ± 0.02	0.08 ± 0.1	0.49	6.55	10.29	1.34
2M15092746+4514120	5847 ± 117	4.29 ± 0.15	4.23	0 ± 0.05	-0.06 ± 0.1	0.53	4.53	9.72	0.5
2M15094039+2544056	5866 ± 85	4.27 ± 0.11	4.21	0.2 ± 0.04	0.14 ± 0.1	0.78	4.4	10.38	1.45
2M15100066+4509495	5888 ± 113	4.27 ± 0.15	4.20	0.12 ± 0.05	0.05 ± 0.1	0.53	4.6	10.35	0.51
2M15100070+4507176	6034 ± 91	4.37 ± 0.11	4.26	0.1 ± 0.04	0.04 ± 0.1	0.59	5.39	9.33	0.4
2M15105974+2713151	5809 ± 122	4.3 ± 0.15	4.25	0.07 ± 0.05	0.01 ± 0.1	0.71	4.29	10.66	0.43
2M15110770+3228224	5835 ± 138	4.31 ± 0.2	4.25	-0.22 ± 0.06	-0.3 ± 0.1	0.31	4.71	8.07	0.34
2M15110785+6823011	5935 ± 85	4.35 ± 0.11	4.27	0.04 ± 0.03	-0.02 ± 0.1	0.65	4.91	9.22	0.59
2M15111524+3650058	6094 ± 148	4.29 ± 0.2	4.17	0.04 ± 0.06	-0.03 ± 0.1	0.64	5.84	9.04	1.37
2M15113243-0053425	5997 ± 124	4.36 ± 0.14	4.26	-0.02 ± 0.05	-0.09 ± 0.1	0.52	5.32	9.6	0.39
2M15115878+0045357	6113 ± 76	4.32 ± 0.11	4.20	0.17 ± 0.03	0.12 ± 0.1	0.71	5.81	9.69	0.36
2M15120615+6826579	6172 ± 78	4.44 ± 0.1	4.29	-0.03 ± 0.03	-0.11 ± 0.1	0.33	6.42	8.42	0.33
2M15124763-0109577	5043 ± 56	4.19 ± 0.06	4.34	-0.56 ± 0.02	-0.62 ± 0.1	0.32	3.74	8.73	1.37
2M15124774+2755356	5839 ± 169	4.22 ± 0.21	4.16	-0.03 ± 0.07	-0.1 ± 0.1	0.61	4.55	7.18	1.46
2M15130258+0134212	6103 ± 133	4.26 ± 0.2	4.14	-0.15 ± 0.05	-0.25 ± 0.1	0.1	6.12	8.13	1.32
2M15140318+6610212	6232 ± 85	4.53 ± 0.08	4.36	-0.01 ± 0.03	-0.07 ± 0.1	0.16	6.83	8.75	1.44
2M15140919+3638054	6111 ± 134	4.42 ± 0.19	4.30	-0.01 ± 0.05	-0.08 ± 0.1	0.4	5.99	9.66	0.34
2M15145975+0005386	6185 ± 60	4.45 ± 0.08	4.30	-0.08 ± 0.02	-0.14 ± 0.1	0.11	6.57	7.63	0.38
2M15150174-0057385	5910 ± 123	4.38 ± 0.18	4.31	0.02 ± 0.05	-0.05 ± 0.1	0.52	4.81	9.33	1.47
2M15150970+3307371	5958 ± 119	4.52 ± 0.12	4.43	-0.05 ± 0.05	-0.09 ± 0.1	0.36	5.13	10.08	0.55

APOGEE_ID	$T_{\rm eff} \pm \Delta T_{\rm eff}$	$\log g \pm \Delta \log g$	$\log g_{cor}$	$[\rm M/H] \pm \Delta[\rm M/H]$	$[Fe/H] \pm \Delta[\rm Fe/H]$	$\rm v_{mic}$	$\rm v_{mac}$	$v \sin i$	χ^2
2M15151258+3407369	5868 ± 103	4.36 ± 0.16	4.30	-0.15 ± 0.04	-0.23 ± 0.1	0.26	4.78	7.93	0.41
2M15153365+4432236	5521 ± 109	4.3 ± 0.12	4.32	0 ± 0.05	-0.02 ± 0.1	1.19	3.42	11.15	1.76
2M15153554+3423223	5873 ± 130	4.3 ± 0.2	4.24	-0.19 ± 0.05	-0.28 ± 0.1	0.33	4.86	8.63	1.35
2M15154292+3357434	5979 ± 150	4.44 ± 0.18	4.35	-0.05 ± 0.06	-0.12 ± 0.1	0.27	5.24	9.2	1.65
2M15154316+3403325	5822 ± 117	4.3 ± 0.14	4.25	0.04 ± 0.05	-0.04 ± 0.1	0.5	4.37	10.07	1.6
2M15155519+0219089	6002 ± 106	4.4 ± 0.13	4.30	-0.04 ± 0.04	-0.1 ± 0.1	0.31	5.36	9.19	0.38
2M15160832+3341553	5816 ± 128	4.31 ± 0.16	4.26	0.04 ± 0.05	-0.01 ± 0.1	0.76	4.34	10.51	1.91
2M15164498+4348295	5925 ± 148	4.21 ± 0.19	4.13	-0.01 ± 0.06	-0.08 ± 0.1	0.36	4.94	8.91	0.55
2M15170783+3340514	6036 ± 97	4.46 ± 0.1	4.35	-0.06 ± 0.04	-0.12 ± 0.1	0	5.58	8.86	0.38
2M15172278+6827039	6016 ± 78	4.4 ± 0.11	4.30	-0.1 ± 0.03	-0.18 ± 0.1	0.19	5.51	8.6	1.41
2M15180688+4349407	5959 ± 129	4.36 ± 0.18	4.27	-0.18 ± 0.05	-0.24 ± 0.1	0	5.27	7.95	0.93
2M15181149+6803109	6208 ± 101	4.31 ± 0.14	4.15	-0.2 ± 0.04	-0.29 ± 0.1	0	6.87	7.58	0.44
2M15182284+3219135	5859 ± 124	4.36 ± 0.19	4.30	-0.05 ± 0.05	-0.11 ± 0.1	0.59	4.64	9.95	1.58
2M15182376+0228135	6129 ± 106	4.22 ± 0.15	4.09	-0.07 ± 0.04	-0.16 ± 0.1	0.25	6.2	8.89	0.34
2M15182514+3249495	5962 ± 133	4.24 ± 0.16	4.15	0.02 ± 0.05	-0.03 ± 0.1	0.66	5.1	9.93	0.56
2M15184757+3218249	6040 ± 129	4.4 ± 0.19	4.29	-0.06 ± 0.05	-0.12 ± 0.1	0.53	5.61	8.48	0.53
2M15185547+3340126	5687 ± 130	4.37 ± 0.18	4.35	-0.09 ± 0.06	-0.15 ± 0.1	0.59	3.98	7.49	1.75
2M15190055+3305407	5712 ± 104	4.34 ± 0.12	4.32	-0.03 ± 0.04	-0.06 ± 0.1	0.64	4	9.58	0.59
2M15193012+3201432	5908 ± 161	4.15 ± 0.22	4.08	-0.15 ± 0.07	-0.24 ± 0.1	0.54	5.02	8.25	0.64
2M15210604+3331548	5495 ± 74	4.14 ± 0.07	4.17	0.12 ± 0.03	0.1 ± 0.1	1.05	3.26	9.91	1.49

APOGEE_ID	$T_{\rm eff} \pm \Delta T_{\rm eff}$	$\log g \pm \Delta \log g$	$\log g_{cor}$	$[\mathrm{M/H}] \pm \Delta[\mathrm{M/H}]$	$[Fe/H] \pm \Delta[\mathrm{Fe/H}]$	$\mathrm{v_{mic}}$	$\mathrm{v_{mac}}$	$v \sin i$	χ^2
2M15213251+3307314	5677 ± 103	4.29 ± 0.13	4.27	0.02 ± 0.04	-0.01 ± 0.1	0.89	3.84	10.07	0.52
2M15213493+3317289	5920 ± 119	4.19 ± 0.15	4.11	0.06 ± 0.05	0.01 ± 0.1	0.78	4.84	10.09	1.48
2M15213748+0157306	6166 ± 115	4.31 ± 0.16	4.16	0.05 ± 0.04	0 ± 0.1	0.63	6.31	10.07	0.45
2M15215324+3302329	6025 ± 97	4.37 ± 0.13	4.27	-0.08 ± 0.04	-0.14 ± 0.1	0.52	5.53	7.97	0.35
2M15223357+3343419	5847 ± 103	4.28 ± 0.14	4.22	-0.04 ± 0.04	-0.08 ± 0.1	0.75	4.57	9.35	0.47
2M15224198+3247072	5833 ± 129	4.28 ± 0.17	4.23	-0.03 ± 0.05	-0.07 ± 0.1	0.63	4.5	10.22	0.64
2M15231672+3628365	6227 ± 155	4.33 ± 0.19	4.16	0.03 ± 0.06	-0.06 ± 0.1	0.47	6.76	8.81	1.4
2M15232610+3452091	5922 ± 75	4.16 ± 0.09	4.08	0.07 ± 0.03	0.02 ± 0.1	0.73	4.84	8.32	0.41
2M15240716+3304074	5657 ± 77	4.34 ± 0.12	4.33	-0.09 ± 0.03	-0.15 ± 0.1	0.77	3.88	9.24	0.43
2M15241850+3811157	4761 ± 94	3.2 ± 0.12	3.20	-0.12 ± 0.05	-0.24 ± 0.1	0.83	3.76	10.04	1.85
2M15253713+3827497	6022 ± 107	4.46 ± 0.1	4.36	0.28 ± 0.04	0.22 ± 0.1	0.75	5.1	10.93	1.42
2M15273071+4602159	5717 ± 142	4.31 ± 0.17	4.28	-0.04 ± 0.06	-0.09 ± 0.1	0.5	4.04	9.04	0.8
2M15280701+4612075	5716 ± 121	4.31 ± 0.15	4.28	-0.08 ± 0.05	-0.13 ± 0.1	0.71	4.08	8.93	0.68
2M15281332+4507158	5922 ± 138	4.37 ± 0.21	4.29	-0.04 ± 0.06	-0.09 ± 0.1	0.38	4.93	9.97	1.51
2M15292006+4518145	5448 ± 116	4.26 ± 0.14	4.30	-0.04 ± 0.05	-0.05 ± 0.1	1.14	3.32	10.84	1.98
2M15292512+4441325	6064 ± 171	4.19 ± 0.22	4.08	-0.2 ± 0.07	-0.3 ± 0.1	0.21	5.94	8.21	1.49
2M15295856+4847578	5724 ± 92	4.43 ± 0.1	4.40	0.4 ± 0.04	0.32 ± 0.1	0.57	3.53	8.9	1.34
2M15301469+4812119	5898 ± 108	4.05 ± 0.14	3.98	-0.1 ± 0.05	-0.17 ± 0.1	0.64	4.95	9.36	0.43
2M15302217+5707156	5766 ± 133	4.3 ± 0.14	4.26	0.02 ± 0.05	-0.05 ± 0.1	0.52	4.16	8.96	0.79
2M15302327+4924058	5951 ± 157	4.42 ± 0.21	4.34	-0.2 ± 0.06	-0.27 ± 0.1	0	5.25	9.05	0.43

APOGEE_ID	$T_{\rm eff} \pm \Delta T_{\rm eff}$	$\log g \pm \Delta \log g$	$\log g_{cor}$	$[\mathrm{M/H}] \pm \Delta[\mathrm{M/H}]$	$[Fe/H] \pm \Delta[\mathrm{Fe/H}]$	$\mathrm{v}_{\rm mic}$	$\mathrm{v}_{\rm mac}$	$v \sin i$	χ^2
2M15303561+4438293	6131 ± 100	4.42 ± 0.14	4.29	0.03 ± 0.04	-0.02 ± 0.1	0.35	6.08	8.48	1.49
2M15304761+2804447	5937 ± 86	4.39 ± 0.13	4.31	-0.07 ± 0.04	-0.13 ± 0.1	0.49	5.04	8.97	1.39
2M15304972+4335587	6014 ± 157	4.18 ± 0.18	4.08	-0.25 ± 0.06	-0.37 ± 0.1	0	5.69	8.76	1.36
2M15305382+4442104	5522 ± 96	4.19 ± 0.09	4.21	0.01 ± 0.04	-0.01 ± 0.1	0.96	3.43	9.26	0.71
2M15310293+4241320	6045 ± 134	4.22 ± 0.16	4.11	0.13 ± 0.05	0.09 ± 0.1	0.79	5.46	9.62	1.52
2M15312010+4936520	5716 ± 136	4.3 ± 0.15	4.27	-0.01 ± 0.06	-0.07 ± 0.1	0.47	4	10.51	0.62
2M15312629+3714520	6223 ± 136	4.35 ± 0.19	4.18	-0.1 ± 0.05	-0.17 ± 0.1	0.15	6.87	7.48	0.41
2M15321482+5531557	5731 ± 141	4.43 ± 0.17	4.40	-0.25 ± 0.06	-0.31 ± 0.1	0.22	4.3	7.71	0.42
2M15321526+8514275	6066 ± 70	4.3 ± 0.09	4.19	0.07 ± 0.03	0.02 ± 0.1	0.64	5.64	9.22	0.36
2M15323595+4627598	5852 ± 109	4.23 ± 0.14	4.17	0.08 ± 0.04	0.02 ± 0.1	0.53	4.48	10.69	1.45
2M15325225+4452174	6135 ± 137	4.51 ± 0.15	4.38	0.01 ± 0.05	-0.04 ± 0.1	0.39	6.13	11	0.46
2M15325255+5756266	5816 ± 113	4.27 ± 0.14	4.22	0.15 ± 0.05	0.08 ± 0.1	0.55	4.22	10.81	0.61
2M15330531+2730428	5617 ± 65	4.13 ± 0.07	4.13	0.15 ± 0.03	0.11 ± 0.1	0.88	3.54	9.32	1.66
2M15331037+4240418	6210 ± 123	4.38 ± 0.17	4.22	0.12 ± 0.05	0.08 ± 0.1	0.68	6.53	9.74	1.41
2M15335320+2734036	5806 ± 111	4.24 ± 0.13	4.19	0.01 ± 0.05	-0.02 ± 0.1	0.76	4.34	9.79	1.54
2M15341517+4902421	5965 ± 158	4.48 ± 0.16	4.39	-0.12 ± 0.06	-0.2 ± 0.1	0	5.24	8.49	1.59
2M15343847+4957343	5748 ± 96	4.42 ± 0.11	4.39	-0.24 ± 0.04	-0.3 ± 0.1	0.41	4.35	7.45	0.35
2M15344318+4552578	6208 ± 121	4.32 ± 0.16	4.16	0.14 ± 0.05	0.09 ± 0.1	0.52	6.49	9.72	0.54
2M15353561+5655482	5828 ± 115	4.26 ± 0.14	4.21	0.06 ± 0.05	0.01 ± 0.1	0.72	4.39	10.44	0.54
2M15355113+5737026	5880 ± 104	4.41 ± 0.15	4.34	-0.02 ± 0.04	-0.07 ± 0.1	0.45	4.7	9.3	0.37

APOGEE_ID	$T_{\rm eff} \pm \Delta T_{\rm eff}$	$\log g \pm \Delta \log g$	$\log g_{cor}$	$[\rm M/H] \pm \Delta[\rm M/H]$	$[Fe/H] \pm \Delta[\rm Fe/H]$	$\rm v_{mic}$	$\rm v_{mac}$	$v \sin i$	χ^2
2M15355726+4553459	6088 ± 140	4.44 ± 0.18	4.32	-0.04 ± 0.06	-0.12 ± 0.1	0.09	5.88	9.47	0.49
2M15361978+4506552	6059 ± 117	4.28 ± 0.14	4.17	0.15 ± 0.05	0.11 ± 0.1	0.76	5.5	9.52	0.63
2M15362382+5753264	5732 ± 143	4.33 ± 0.16	4.30	-0.02 ± 0.06	-0.07 ± 0.1	0.52	4.06	9.21	0.73
2M15363471+2736376	5918 ± 133	4.05 ± 0.15	3.97	0.11 ± 0.05	0.08 ± 0.1	1	4.81	10.64	0.59
2M15370521+5549345	5712 ± 111	4.21 ± 0.12	4.19	0.01 ± 0.05	-0.06 ± 0.1	0.72	3.98	9.02	0.54
2M15371038+4407025	6109 ± 159	4.24 ± 0.21	4.12	0 ± 0.06	-0.06 ± 0.1	0.56	5.99	9.23	0.52
2M15373525+2818335	5789 ± 75	4.23 ± 0.08	4.19	0.03 ± 0.03	-0.02 ± 0.1	0.59	4.26	10.39	0.41
2M15373828+4637097	5835 ± 133	4.33 ± 0.18	4.27	-0.03 ± 0.06	-0.1 ± 0.1	0.55	4.5	8.94	0.49
2M15374316+4356169	5781 ± 97	4.18 ± 0.1	4.14	0.04 ± 0.04	-0.01 ± 0.1	0.71	4.22	8.2	0.48
2M15374972+4405289	5781 ± 121	4.3 ± 0.14	4.26	0.13 ± 0.05	0.1 ± 0.1	0.85	4.09	9.84	1.83
2M15382932+4445092	5722 ± 120	4.33 ± 0.16	4.30	-0.25 ± 0.05	-0.33 ± 0.1	0.1	4.27	8.7	0.5
2M15385403+4430167	5777 ± 125	4.24 ± 0.13	4.20	0.11 ± 0.05	0.05 ± 0.1	0.49	4.11	9.7	0.88
2M15390597+4522294	6086 ± 118	4.39 ± 0.17	4.27	-0.01 ± 0.04	-0.09 ± 0.1	0.39	5.83	8.18	0.48
2M15391044+5709198	6088 ± 135	4.31 ± 0.18	4.19	0.05 ± 0.05	-0.02 ± 0.1	0.35	5.79	8.46	0.64
2M15393633+2855383	5759 ± 116	4.05 ± 0.1	4.01	-0.02 ± 0.05	-0.09 ± 0.1	0.73	4.24	9.15	0.5
2M15394973+4425017	5376 ± 108	4.28 ± 0.14	4.34	-0.04 ± 0.05	-0.04 ± 0.1	1.24	3.21	9.89	1.02
2M15395061+4842552	5900 ± 150	4.28 ± 0.22	4.21	-0.04 ± 0.06	-0.1 ± 0.1	0.51	4.83	8.54	0.59
2M15402533+4542131	5815 ± 96	4.22 ± 0.11	4.17	0.04 ± 0.04	-0.03 ± 0.1	0.52	4.35	8.92	1.46
2M15404283+4825453	6125 ± 155	4.38 ± 0.24	4.25	-0.04 ± 0.06	-0.1 ± 0.1	0.29	6.11	8.24	0.46
2M15404328+3033295	5747 ± 133	4.32 ± 0.16	4.29	-0.1 ± 0.06	-0.15 ± 0.1	0.67	4.22	9.2	1.74

APOGEE_ID	$T_{\text{eff}} \pm \Delta T_{\text{eff}}$	$\log g \pm \Delta \log g$	$\log g_{cor}$	$[\text{M/H}] \pm \Delta[\text{M/H}]$	$[Fe/H] \pm \Delta[\text{Fe/H}]$	v_{mic}	v_{mac}	$v \sin i$	χ^2
2M15404419+4751177	6030 ± 98	4.25 ± 0.11	4.15	0.08 ± 0.04	0.03 ± 0.1	0.63	5.41	9.6	0.38
2M15404804+4547471	5902 ± 121	4.17 ± 0.16	4.10	0.1 ± 0.05	0.04 ± 0.1	0.68	4.71	10.71	0.48
2M15405094+4855180	5952 ± 116	4.32 ± 0.14	4.24	0.08 ± 0.05	0.03 ± 0.1	0.64	4.96	10.26	1.46
2M15405692+2830454	5771 ± 92	4.1 ± 0.09	4.06	0 ± 0.04	-0.05 ± 0.1	0.7	4.25	10.06	1.33
2M15410475+5540460	5679 ± 99	4.29 ± 0.12	4.27	-0.01 ± 0.04	-0.04 ± 0.1	0.79	3.87	7.15	0.45
2M15411011+4513293	6113 ± 141	4.26 ± 0.21	4.14	-0.06 ± 0.06	-0.15 ± 0.1	0.33	6.08	7.98	0.63
2M15411271+4512185	6116 ± 160	4.39 ± 0.26	4.27	-0.05 ± 0.06	-0.13 ± 0.1	0	6.07	8.23	0.9
2M15412475+2836198	5965 ± 106	4.26 ± 0.12	4.17	0.1 ± 0.04	0.05 ± 0.1	0.67	5.02	9.76	1.38
2M15414272+4533348	5666 ± 135	4.2 ± 0.18	4.19	-0.16 ± 0.06	-0.24 ± 0.1	0.55	4.01	8.86	0.56
2M15415428+3059122	6012 ± 122	4.44 ± 0.13	4.34	-0.17 ± 0.05	-0.26 ± 0.1	0	5.55	8.4	0.32
2M15421560+3031163	6373 ± 99	4.54 ± 0.11	4.31	0.11 ± 0.04	0.05 ± 0.1	0.28	7.81	9.23	0.35
2M15422194+4740449	6190 ± 130	4.33 ± 0.18	4.17	0.16 ± 0.05	0.12 ± 0.1	0.7	6.35	9.82	0.45
2M15423419+3033160	5852 ± 98	4.16 ± 0.12	4.10	0.13 ± 0.04	0.07 ± 0.1	0.79	4.44	11.65	0.48
2M15423848+2929104	5644 ± 65	4.22 ± 0.08	4.21	0.11 ± 0.03	0.07 ± 0.1	0.85	3.64	10.05	0.52
2M15430668+4326065	5669 ± 100	4.6 ± 0.1	4.59	0.43 ± 0.04	0.37 ± 0.1	0.61	3.29	8.11	1.54
2M15431523+4530119	5996 ± 121	4.2 ± 0.13	4.10	-0.02 ± 0.05	-0.1 ± 0.1	0.53	5.34	9.3	1.42
2M15431531+3051436	6233 ± 98	4.43 ± 0.11	4.26	0.03 ± 0.04	-0.05 ± 0.1	0.52	6.8	8.49	0.37
2M15431974+5702469	6074 ± 131	4.35 ± 0.18	4.23	-0.04 ± 0.05	-0.11 ± 0.1	0.35	5.8	8.15	0.56
2M15435228+5718553	5893 ± 108	4.36 ± 0.16	4.29	0.03 ± 0.04	-0.01 ± 0.1	0.56	4.7	10.27	1.45
2M15443759+2911502	5657 ± 76	4.23 ± 0.1	4.22	0.12 ± 0.03	0.09 ± 0.1	0.89	3.67	9.6	0.53

APOGEE_ID	$T_{\mathrm{eff}} \pm \Delta T_{\mathrm{eff}}$	$\log g \pm \Delta \log g$	$\log g_{cor}$	$[\mathrm{M/H}] \pm \Delta[\mathrm{M/H}]$	$[Fe/H] \pm \Delta[\mathrm{Fe/H}]$	$\mathrm{v}_{\mathrm{mic}}$	$\mathrm{v}_{\mathrm{mac}}$	$v \sin i$	χ^2
2M15443801+4901415	5807 ± 89	4.36 ± 0.11	4.31	-0.01 ± 0.04	-0.06 ± 0.1	0.54	4.35	10.49	0.36
2M15444243+2826271	5840 ± 122	4.1 ± 0.14	4.04	0.12 ± 0.05	0.07 ± 0.1	0.81	4.41	9.89	1.67
2M15450246+4345477	6156 ± 104	4.34 ± 0.17	4.20	-0.06 ± 0.04	-0.12 ± 0.1	0.42	6.35	8.16	1.37
2M15451874+4401218	5840 ± 109	4.24 ± 0.13	4.18	0.01 ± 0.04	-0.04 ± 0.1	0.72	4.5	8.86	0.63
2M15452533+5433568	5859 ± 118	4.16 ± 0.14	4.10	0.18 ± 0.05	0.15 ± 0.1	0.84	4.41	9.13	1.68
2M15465844+4436154	6140 ± 84	4.48 ± 0.09	4.35	0.03 ± 0.03	-0.02 ± 0.1	0.45	6.14	7.9	1.46
2M15471370+4603543	5982 ± 127	4.11 ± 0.14	4.02	-0.07 ± 0.05	-0.15 ± 0.1	0.59	5.34	9.38	0.44
2M15472421+4446021	5953 ± 120	4.33 ± 0.17	4.25	-0.23 ± 0.05	-0.31 ± 0.1	0	5.3	7.78	1.42
2M15472521+4605184	5802 ± 128	4.28 ± 0.15	4.23	0 ± 0.05	-0.07 ± 0.1	0.69	4.34	9.39	0.52
2M15472718+4506299	5947 ± 99	4.49 ± 0.11	4.41	-0.16 ± 0.04	-0.25 ± 0.1	0.14	5.18	8.39	1.43
2M15480150+4805255	5854 ± 126	4.28 ± 0.16	4.22	0.03 ± 0.05	-0.03 ± 0.1	0.67	4.53	8.9	1.42
2M15480449+4530564	5634 ± 102	4.21 ± 0.13	4.21	-0.01 ± 0.04	-0.07 ± 0.1	0.83	3.74	8.83	0.66
2M15480589+4348005	5986 ± 141	4.14 ± 0.16	4.05	-0.24 ± 0.06	-0.33 ± 0.1	0.12	5.53	7.52	1.64
2M15480627+3000512	5746 ± 76	4.23 ± 0.08	4.20	0.14 ± 0.03	0.08 ± 0.1	0.75	3.96	10.28	0.47
2M15484147+5340510	6304 ± 102	4.49 ± 0.1	4.29	0.09 ± 0.04	0.05 ± 0.1	0.37	7.27	9.36	0.38
2M15485857+4547372	5697 ± 72	4.34 ± 0.1	4.32	-0.17 ± 0.03	-0.25 ± 0.1	0.39	4.1	8.65	0.36
2M15485857+4547372	5699 ± 72	4.35 ± 0.1	4.33	-0.16 ± 0.03	-0.25 ± 0.1	0.39	4.1	8.67	0.36
2M15490760+4332356	6079 ± 160	4.32 ± 0.23	4.20	-0.14 ± 0.06	-0.21 ± 0.1	0.08	5.94	7.89	0.55
2M15493252+4504197	5979 ± 143	4.35 ± 0.17	4.26	0.03 ± 0.06	-0.04 ± 0.1	0.53	5.16	8.88	1.63
2M15494283+4345268	5645 ± 93	4.14 ± 0.11	4.13	0.11 ± 0.04	0.05 ± 0.1	0.77	3.66	9.51	1.76

APOGEE_ID	$T_{\rm eff} \pm \Delta T_{\rm eff}$	$\log g \pm \Delta \log g$	$\log g_{cor}$	$[\rm M/H] \pm \Delta[\rm M/H]$	$[Fe/H] \pm \Delta[\rm Fe/H]$	$\rm v_{mic}$	$\rm v_{mac}$	$v \sin i$	χ^2
2M15494809+5603083	6208 ± 158	4.48 ± 0.17	4.32	-0.07 ± 0.06	-0.13 ± 0.1	0	6.72	8.79	1.47
2M15502909+4752340	6307 ± 165	4.36 ± 0.22	4.16	0.03 ± 0.06	-0.05 ± 0.1	0.36	7.37	8.43	0.46
2M15503898+4500374	5981 ± 91	4.13 ± 0.1	4.04	-0.14 ± 0.04	-0.21 ± 0.1	0.43	5.39	8.24	0.38
2M15505564+5559268	5590 ± 114	4.32 ± 0.15	4.33	-0.04 ± 0.05	-0.09 ± 0.1	0.59	3.63	10.56	0.45
2M15513578+4315341	5670 ± 106	4.38 ± 0.15	4.37	-0.02 ± 0.04	-0.07 ± 0.1	0.86	3.84	11.57	1.46
2M15521764+5605287	6210 ± 144	4.44 ± 0.16	4.28	0.06 ± 0.05	-0.02 ± 0.1	0.19	6.6	7.88	0.46
2M15524685+4321018	5984 ± 162	4.19 ± 0.19	4.10	-0.12 ± 0.07	-0.19 ± 0.1	0.58	5.38	8.92	0.63
2M15524864+5359187	5596 ± 111	4.28 ± 0.14	4.29	-0.04 ± 0.05	-0.07 ± 0.1	0.94	3.65	7.95	1.71
2M15530029+4830182	5685 ± 100	4.35 ± 0.14	4.33	-0.11 ± 0.04	-0.17 ± 0.1	0.59	3.99	9.21	0.35
2M15540538+4231170	6252 ± 72	4.35 ± 0.09	4.17	0.26 ± 0.03	0.22 ± 0.1	1.01	6.67	9.4	0.43
2M15540897+4845566	5798 ± 107	4.13 ± 0.11	4.08	0.06 ± 0.04	0 ± 0.1	0.83	4.29	10.51	1.44
2M15545955+4403287	5830 ± 108	4.33 ± 0.14	4.28	0.02 ± 0.04	-0.04 ± 0.1	0.54	4.43	10.29	1.45
2M15550822+4437517	5783 ± 125	4.28 ± 0.14	4.24	-0.01 ± 0.05	-0.06 ± 0.1	0.74	4.27	8.64	0.56
2M15554496+4413518	5738 ± 99	4.37 ± 0.12	4.34	-0.09 ± 0.04	-0.13 ± 0.1	0.52	4.16	9.75	1.38
2M15554908+5405025	5959 ± 123	4.2 ± 0.15	4.11	-0.11 ± 0.05	-0.19 ± 0.1	0.25	5.23	7.3	0.67
2M15554969+4332060	5504 ± 101	4.27 ± 0.1	4.30	-0.18 ± 0.04	-0.25 ± 0.1	0.6	3.58	8.91	0.44
2M15560547+4215068	5941 ± 110	4.32 ± 0.14	4.24	0.15 ± 0.04	0.1 ± 0.1	0.8	4.82	10.19	0.66
2M15562703+5517460	5981 ± 153	4.17 ± 0.17	4.08	-0.05 ± 0.06	-0.14 ± 0.1	0	5.29	8.81	0.64
2M15572707+5335301	5773 ± 139	4.19 ± 0.16	4.15	-0.1 ± 0.06	-0.15 ± 0.1	0.48	4.34	8.54	0.48
2M15580357+4402099	5807 ± 100	4.24 ± 0.11	4.19	0.03 ± 0.04	-0.03 ± 0.1	0.6	4.33	9.32	1.55

APOGEE_ID	$T_{\rm eff} \pm \Delta T_{\rm eff}$	$\log g \pm \Delta \log g$	$\log g_{cor}$	$[\mathrm{M/H}] \pm \Delta[\mathrm{M/H}]$	$[Fe/H] \pm \Delta[\mathrm{Fe/H}]$	$\mathrm{v_{mic}}$	$\mathrm{v_{mac}}$	$v \sin i$	χ^2
2M15581034+4325194	5723 ± 88	4.29 ± 0.1	4.26	0.13 ± 0.04	0.09 ± 0.1	0.86	3.87	10.23	0.63
2M15582488+4546240	5880 ± 112	4.26 ± 0.15	4.19	0.08 ± 0.05	0.03 ± 0.1	0.66	4.6	9.44	0.5
2M15582562+0620330	6040 ± 118	4.32 ± 0.14	4.21	0.06 ± 0.05	-0.01 ± 0.1	0.47	5.48	9.94	1.46
2M15590029+4536424	6048 ± 89	4.54 ± 0.08	4.43	0.31 ± 0.04	0.25 ± 0.1	0.81	5.22	8.69	0.64
2M15591791+5357291	5739 ± 119	4.41 ± 0.13	4.38	0.12 ± 0.05	0.04 ± 0.1	0.38	3.93	8.95	1.71
2M15593737+2851116	6165 ± 172	4.46 ± 0.21	4.32	-0.01 ± 0.06	-0.09 ± 0.1	0.36	6.35	8.69	0.37
2M15594993+4234021	5973 ± 120	4.2 ± 0.15	4.11	-0.1 ± 0.05	-0.18 ± 0.1	0.43	5.3	8.56	0.44
2M15595158+4306066	5877 ± 82	4.05 ± 0.09	3.98	0.01 ± 0.03	-0.05 ± 0.1	0.72	4.72	9.89	0.35
2M16003962+4222595	5930 ± 118	4.25 ± 0.17	4.17	-0.05 ± 0.05	-0.12 ± 0.1	0.37	5	9.89	0.43
2M16005853+0537220	5736 ± 59	4.3 ± 0.06	4.27	0 ± 0.02	-0.04 ± 0.1	0.66	4.07	10.07	0.4
2M16010957+2723116	5978 ± 93	4.32 ± 0.11	4.23	0.07 ± 0.04	0.02 ± 0.1	0.67	5.11	9.52	1.35
2M16011348+4149493	5651 ± 108	4.24 ± 0.14	4.23	0.01 ± 0.05	-0.03 ± 0.1	0.65	3.77	10.46	0.48
2M16012954+4319396	5729 ± 128	4.33 ± 0.14	4.30	-0.02 ± 0.05	-0.06 ± 0.1	0.58	4.05	10.44	0.58
2M16014984+5429337	5788 ± 129	4.24 ± 0.14	4.20	-0.01 ± 0.05	-0.05 ± 0.1	0.62	4.29	9.75	1.44
2M16015043+4243003	5797 ± 89	4.34 ± 0.12	4.29	-0.07 ± 0.04	-0.13 ± 0.1	0.49	4.38	9.51	0.43
2M16021417+4440176	5633 ± 109	4.19 ± 0.13	4.19	0.11 ± 0.05	0.06 ± 0.1	0.85	3.61	10.51	1.91
2M16022599+4119182	5951 ± 101	4.38 ± 0.15	4.30	-0.05 ± 0.04	-0.12 ± 0.1	0.51	5.1	9.39	1.43
2M16023579+4354284	5688 ± 138	4.36 ± 0.19	4.34	-0.17 ± 0.06	-0.23 ± 0.1	0.47	4.06	8.72	1.53
2M16031160+2746308	5999 ± 135	4.19 ± 0.14	4.09	0.06 ± 0.05	0.02 ± 0.1	0.69	5.27	10.31	0.41
2M16031329+4214466	6412 ± 392	4.45 ± 0.52	4.20	-1.26 ± 0.13	-1.2 ± 0.1	0.19	9.33	6.23	1.13

APOGEE_ID	$T_{\mathrm{eff}} \pm \Delta T_{\mathrm{eff}}$	$\log g \pm \Delta \log g$	$\log g_{cor}$	$[\mathrm{M/H}] \pm \Delta[\mathrm{M/H}]$	$[Fe/H] \pm \Delta[\mathrm{Fe/H}]$	$\mathrm{v}_{\mathrm{mic}}$	$\mathrm{v}_{\mathrm{mac}}$	$v \sin i$	χ^2
2M16035292+4124427	6158 ± 114	4.25 ± 0.16	4.11	0.13 ± 0.05	0.07 ± 0.1	0.65	6.17	10.6	0.45
2M16041269+4045007	5834 ± 78	4.05 ± 0.08	4.00	-0.01 ± 0.03	-0.05 ± 0.1	0.93	4.55	10	0.48
2M16042629+4030585	5877 ± 118	4.29 ± 0.16	4.22	0.21 ± 0.05	0.18 ± 0.1	1.01	4.43	9.41	1.03
2M16043444+4319017	5929 ± 95	4.17 ± 0.11	4.09	0.06 ± 0.04	0.01 ± 0.1	0.7	4.9	10.49	0.49
2M16044110+4423285	5721 ± 108	4.16 ± 0.11	4.13	0.16 ± 0.05	0.13 ± 0.1	0.89	3.85	9.48	1.66
2M16050304+4122540	5620 ± 107	4.37 ± 0.15	4.37	-0.04 ± 0.05	-0.06 ± 0.1	0.86	3.7	9.45	1.36
2M16052196+4143059	6199 ± 122	4.34 ± 0.16	4.18	0 ± 0.05	-0.07 ± 0.1	0.48	6.59	9.15	0.39
2M16053258+4335428	6239 ± 168	4.23 ± 0.19	4.05	0.01 ± 0.06	-0.07 ± 0.1	0.5	6.89	9.44	1.56
2M16054291+4134262	6186 ± 166	4.45 ± 0.22	4.30	-0.05 ± 0.07	-0.13 ± 0.1	0	6.54	9.04	1.67
2M16055844+4329012	5900 ± 149	4.08 ± 0.2	4.01	-0.08 ± 0.06	-0.16 ± 0.1	0.61	4.93	8.67	0.52
2M16060202+4123117	5802 ± 125	4.18 ± 0.14	4.13	0.15 ± 0.05	0.1 ± 0.1	0.74	4.19	10.46	0.91
2M16063131+2253008	6020 ± 81	4.41 ± 0.09	4.31	0.06 ± 0.03	0.03 ± 0.1	0.37	5.35	9.28	0.84
2M16063947+4557374	6120 ± 139	4.33 ± 0.2	4.20	-0.02 ± 0.05	-0.1 ± 0.1	0.44	6.07	8.51	0.41
2M16064411+4009117	5664 ± 129	4.32 ± 0.2	4.31	-0.16 ± 0.06	-0.21 ± 0.1	0.85	3.98	9.21	1.79
2M16065535+4435279	5854 ± 132	4.32 ± 0.17	4.26	0.02 ± 0.05	-0.02 ± 0.1	0.61	4.54	9.85	0.58
2M16070443-1110109	5936 ± 92	4.25 ± 0.11	4.17	0 ± 0.04	-0.07 ± 0.1	0.59	4.97	9.03	0.34
2M16070878+4501287	5607 ± 70	4.26 ± 0.08	4.26	0.02 ± 0.03	-0.03 ± 0.1	0.71	3.62	10.39	0.42
2M16072532+4533388	5734 ± 116	4.32 ± 0.13	4.29	0.02 ± 0.05	-0.02 ± 0.1	0.55	4.03	10.31	0.53
2M16073913+4418002	5700 ± 120	4.15 ± 0.13	4.13	0.09 ± 0.05	0.06 ± 0.1	0.83	3.86	9.59	0.62
2M16075788+4613021	5935 ± 143	4.37 ± 0.22	4.29	-0.17 ± 0.06	-0.23 ± 0.1	0.23	5.14	7.69	0.48

APOGEE_ID	$T_{\mathrm{eff}} \pm \Delta T_{\mathrm{eff}}$	$\log g \pm \Delta \log g$	$\log g_{cor}$	$[\mathrm{M/H}] \pm \Delta[\mathrm{M/H}]$	$[Fe/H] \pm \Delta[\mathrm{Fe/H}]$	$\mathrm{v}_{\mathrm{mic}}$	$\mathrm{v}_{\mathrm{mac}}$	$v \sin i$	χ^2
2M16080324+2303254	6225 ± 124	4.38 ± 0.16	4.21	0.03 ± 0.05	-0.04 ± 0.1	0.4	6.75	8.79	1.33
2M16080926+4538527	6281 ± 175	4.31 ± 0.23	4.12	-0.19 ± 0.07	-0.3 ± 0.1	0	7.41	5.76	1.38
2M16081389+4900049	5922 ± 114	4.17 ± 0.14	4.09	0.14 ± 0.05	0.09 ± 0.1	0.75	4.77	9.72	0.53
2M16081430+4512574	5966 ± 89	4.42 ± 0.11	4.33	-0.02 ± 0.03	-0.07 ± 0.1	0.55	5.14	9.78	0.42
2M16082171+2315416	6118 ± 137	4.27 ± 0.21	4.15	-0.14 ± 0.06	-0.22 ± 0.1	0.18	6.2	7.25	0.41
2M16082345+4951233	5689 ± 93	4.34 ± 0.12	4.32	-0.04 ± 0.04	-0.09 ± 0.1	0.65	3.93	10.52	1.38
2M16083345+4628135	6198 ± 154	4.38 ± 0.23	4.22	-0.1 ± 0.06	-0.19 ± 0.1	0	6.69	8.22	0.48
2M16083565+4619352	5747 ± 82	4.34 ± 0.1	4.31	-0.1 ± 0.03	-0.15 ± 0.1	0.43	4.21	10.26	1.5
2M16083882+4725319	5719 ± 100	4.39 ± 0.13	4.36	-0.16 ± 0.04	-0.21 ± 0.1	0.57	4.16	9.27	0.56
2M16083937+2238568	6092 ± 70	4.38 ± 0.11	4.26	-0.16 ± 0.03	-0.24 ± 0.1	0	6.04	8.14	0.35
2M16084443+4713251	6017 ± 162	4.22 ± 0.18	4.12	-0.03 ± 0.07	-0.11 ± 0.1	0.62	5.46	8.95	0.88
2M16084761+4410092	6058 ± 145	4.38 ± 0.22	4.27	-0.3 ± 0.06	-0.31 ± 0.1	0.16	5.96	8.94	0.35
2M16084839+3010142	5947 ± 154	4.25 ± 0.21	4.17	-0.24 ± 0.06	-0.33 ± 0.1	0	5.29	7.65	0.59
2M16085394+4922023	5580 ± 84	4.22 ± 0.1	4.23	0.1 ± 0.04	0.07 ± 0.1	0.88	3.46	9.94	0.65
2M16090056+4600235	5963 ± 144	4.33 ± 0.18	4.24	-0.02 ± 0.06	-0.09 ± 0.1	0.5	5.13	8.84	0.56
2M16092048+4041100	5764 ± 133	4.16 ± 0.14	4.12	-0.12 ± 0.06	-0.19 ± 0.1	0.58	4.33	8.98	1.49
2M16100301+4958231	5984 ± 152	4.23 ± 0.18	4.14	-0.07 ± 0.06	-0.15 ± 0.1	0.45	5.32	8.79	0.49
2M16102869+5033500	5568 ± 114	4.26 ± 0.14	4.27	-0.06 ± 0.05	-0.14 ± 0.1	0.64	3.6	10.82	1.33
2M16103022+4839513	6179 ± 149	4.3 ± 0.22	4.15	-0.04 ± 0.06	-0.1 ± 0.1	0.54	6.5	8.21	0.43
2M16104379+4057599	5914 ± 97	4.19 ± 0.12	4.12	0.02 ± 0.04	-0.03 ± 0.1	0.87	4.85	8.66	0.42

APOGEE_ID	$T_{\mathrm{eff}} \pm \Delta T_{\mathrm{eff}}$	$\log g \pm \Delta \log g$	$\log g_{cor}$	$[\mathrm{M/H}] \pm \Delta[\mathrm{M/H}]$	$[Fe/H] \pm \Delta[\mathrm{Fe/H}]$	$\mathrm{v}_{\mathrm{mic}}$	$\mathrm{v}_{\mathrm{mac}}$	$v \sin i$	χ^2
2M16111301+4203392	5718 ± 128	4.2 ± 0.13	4.17	0.09 ± 0.05	0.02 ± 0.1	0.5	3.92	9.91	0.76
2M16120676+4719119	5736 ± 146	4.13 ± 0.15	4.10	-0.16 ± 0.06	-0.24 ± 0.1	0.73	4.27	8.52	1.23
2M16122190+2359267	6174 ± 165	4.41 ± 0.24	4.26	0.01 ± 0.06	-0.06 ± 0.1	0.37	6.4	9.31	1.57
2M16122462+4316541	5903 ± 94	4.24 ± 0.13	4.17	0.11 ± 0.04	0.03 ± 0.1	0.63	4.68	9.08	0.48
2M16123913+5012384	5529 ± 115	4.38 ± 0.14	4.40	-0.09 ± 0.05	-0.11 ± 0.1	0.91	3.51	11.41	0.54
2M16125040+4952112	6141 ± 140	4.39 ± 0.22	4.26	0.05 ± 0.05	-0.02 ± 0.1	0.43	6.13	9.28	0.46
2M16130343+4103160	5984 ± 145	4.26 ± 0.16	4.17	-0.01 ± 0.06	-0.09 ± 0.1	0.46	5.25	9.01	0.5
2M16131191+4244166	6202 ± 114	4.43 ± 0.15	4.27	-0.15 ± 0.04	-0.25 ± 0.1	0	6.76	6.5	1.31
2M16131254+4124489	5641 ± 111	4.03 ± 0.12	4.02	0.06 ± 0.05	0.04 ± 0.1	0.86	3.73	9.57	0.66
2M16131508+4259191	5670 ± 136	4.02 ± 0.14	4.01	0 ± 0.06	-0.05 ± 0.1	0.93	3.9	10.62	0.69
2M16131765+5046517	6267 ± 58	4.51 ± 0.05	4.32	0 ± 0.02	-0.07 ± 0.1	0.28	7.08	7.88	0.36
2M16131791+2858476	5603 ± 103	4.3 ± 0.13	4.30	0.04 ± 0.04	0.01 ± 0.1	0.94	3.58	10.02	1.64
2M16133052+4854367	5697 ± 119	4.32 ± 0.16	4.30	-0.14 ± 0.05	-0.17 ± 0.1	0.59	4.06	9.29	0.4
2M16134727+4814362	5498 ± 93	4.23 ± 0.09	4.26	0.02 ± 0.04	-0.01 ± 0.1	0.95	3.36	9.71	0.49
2M16135145+4020559	4865 ± 136	3.26 ± 0.21	3.26	0.07 ± 0.08	-0.01 ± 0.1	1.13	3.56	9.89	1.52
2M16135962+2445542	5987 ± 106	4.37 ± 0.13	4.28	0.06 ± 0.04	0 ± 0.1	0.57	5.17	10.77	0.38
2M16140394+4158598	5664 ± 93	4.41 ± 0.14	4.40	-0.09 ± 0.04	-0.13 ± 0.1	0.57	3.89	10.13	0.39
2M16140865+2916206	5560 ± 90	4.01 ± 0.09	4.02	0.09 ± 0.04	0.05 ± 0.1	0.98	3.48	9.85	1.68
2M16141970+4822242	5694 ± 83	4.4 ± 0.11	4.38	0.43 ± 0.04	0.35 ± 0.1	0.69	3.38	8.18	2.12
2M16142492+4614508	5724 ± 110	4.27 ± 0.12	4.24	0.04 ± 0.05	0 ± 0.1	0.75	3.97	10.29	2.27

APOGEE_ID	$T_{\rm eff} \pm \Delta T_{\rm eff}$	$\log g \pm \Delta \log g$	$\log g_{cor}$	$[\rm M/H] \pm \Delta[\rm M/H]$	$[Fe/H] \pm \Delta[\rm Fe/H]$	$\rm v_{mic}$	$\rm v_{mac}$	$v \sin i$	χ^2
2M16143700+3014403	5994 ± 136	4.16 ± 0.15	4.06	-0.16 ± 0.06	-0.25 ± 0.1	0.25	5.48	8.55	1.43
2M16150685+4705095	5842 ± 141	4.03 ± 0.17	3.97	-0.18 ± 0.06	-0.25 ± 0.1	0.58	4.77	8.3	0.49
2M16150727+4745469	5651 ± 150	4.26 ± 0.23	4.25	-0.21 ± 0.07	-0.28 ± 0.1	0.71	4	9.09	1.78
2M16151289+3017306	5790 ± 111	4.26 ± 0.13	4.22	0.13 ± 0.05	0.08 ± 0.1	0.69	4.14	10.27	0.61
2M16151470+4839510	5751 ± 131	4.25 ± 0.13	4.22	-0.02 ± 0.05	-0.07 ± 0.1	0.65	4.15	8.51	1.76
2M16151619+2434011	6192 ± 124	4.44 ± 0.16	4.28	-0.11 ± 0.05	-0.19 ± 0.1	0	6.65	8.4	1.39
2M16155077+4937181	5747 ± 119	4.2 ± 0.12	4.17	-0.04 ± 0.05	-0.12 ± 0.1	0.59	4.17	9	0.43
2M16155134+4230136	5658 ± 132	4.36 ± 0.22	4.35	-0.32 ± 0.06	-0.41 ± 0.1	0.24	4.12	7.57	1.44
2M16155150+4427236	5920 ± 135	4.33 ± 0.18	4.25	0 ± 0.05	-0.05 ± 0.1	0.59	4.88	9.22	1.55
2M16155310+4205319	5762 ± 115	4.26 ± 0.12	4.22	0.03 ± 0.05	-0.06 ± 0.1	0.24	4.14	8.8	1.42
2M16155594+4702176	6058 ± 157	4.3 ± 0.22	4.19	-0.19 ± 0.06	-0.26 ± 0.1	0.11	5.87	6.97	1.63
2M16160351+5013520	5908 ± 110	4.31 ± 0.15	4.24	0.23 ± 0.05	0.2 ± 0.1	0.82	4.56	9.67	1.76
2M16160877+4506026	5637 ± 91	4.15 ± 0.11	4.14	0.14 ± 0.04	0.11 ± 0.1	0.91	3.59	9.48	1.46
2M16160918+4757320	5826 ± 91	4.02 ± 0.09	3.97	0.01 ± 0.04	-0.05 ± 0.1	0.83	4.5	10.66	0.35
2M16161594+4439452	6103 ± 98	4.38 ± 0.14	4.26	0.04 ± 0.04	-0.04 ± 0.1	0.52	5.89	9.61	0.35
2M16161718+2218412	5747 ± 96	4.08 ± 0.09	4.05	0.11 ± 0.04	0.08 ± 0.1	0.87	4.03	9.3	1.61
2M16162065+3022461	5600 ± 109	4.32 ± 0.15	4.32	-0.06 ± 0.05	-0.11 ± 0.1	0.68	3.68	8.3	0.54
2M16162331+2835493	6321 ± 134	4.42 ± 0.17	4.21	0.1 ± 0.05	0.04 ± 0.1	0.7	7.39	10.38	1.41
2M16162705+2159318	5911 ± 110	4.23 ± 0.15	4.16	0.09 ± 0.04	0.03 ± 0.1	0.62	4.75	10.32	1.58
2M16163843+4803415	6023 ± 131	4.35 ± 0.17	4.25	-0.14 ± 0.05	-0.22 ± 0.1	0	5.6	8.7	0.44

APOGEE_ID	$T_{\rm eff} \pm \Delta T_{\rm eff}$	$\log g \pm \Delta \log g$	$\log g_{cor}$	$[\mathrm{M/H}] \pm \Delta[\mathrm{M/H}]$	$[Fe/H] \pm \Delta[\mathrm{Fe/H}]$	$v_{\rm mic}$	$v_{\rm mac}$	$v \sin i$	χ^2
2M16164452+2829447	5638 ± 71	4.3 ± 0.09	4.29	0.01 ± 0.03	-0.02 ± 0.1	0.85	3.72	10.17	1.46
2M16165968+4647276	6260 ± 97	4.33 ± 0.12	4.15	0.16 ± 0.04	0.1 ± 0.1	0.68	6.86	10.29	0.35
2M16165970+4900542	5868 ± 84	4.22 ± 0.11	4.16	0.25 ± 0.04	0.19 ± 0.1	0.78	4.36	9.66	1.61
2M16171589+4450219	5827 ± 131	4.19 ± 0.15	4.14	0.07 ± 0.05	0.01 ± 0.1	0.78	4.38	9.46	1.63
2M16171839+4933274	5788 ± 111	4.15 ± 0.12	4.11	0.1 ± 0.05	0.06 ± 0.1	0.85	4.19	10.32	1.3
2M16172959+3006461	6008 ± 119	4.34 ± 0.14	4.24	-0.04 ± 0.05	-0.12 ± 0.1	0.55	5.4	8.83	0.39
2M16173515+4300277	6077 ± 174	4.13 ± 0.22	4.01	-0.2 ± 0.07	-0.3 ± 0.1	0.31	6.03	8.24	0.46
2M16173572+2219208	5775 ± 123	4.31 ± 0.14	4.27	-0.04 ± 0.05	-0.09 ± 0.1	0.53	4.26	7.37	1.7
2M16173645+4706491	6160 ± 153	4.3 ± 0.22	4.16	0.08 ± 0.06	0.01 ± 0.1	0.62	6.23	9.73	1.15
2M16174790+2931523	5838 ± 117	4.41 ± 0.17	4.35	-0.04 ± 0.05	-0.08 ± 0.1	0.55	4.52	10.19	1.44
2M16180347+4141007	6236 ± 116	4.32 ± 0.14	4.15	0.03 ± 0.04	-0.03 ± 0.1	0.4	6.83	7.96	0.44
2M16181907+4415141	6170 ± 175	4.43 ± 0.27	4.28	-0.35 ± 0.07	-0.38 ± 0.1	0	6.74	6.25	0.33
2M16182274+4000298	5761 ± 124	4.31 ± 0.13	4.27	0 ± 0.05	-0.05 ± 0.1	0.53	4.16	9.56	0.58
2M16183110+4510339	5556 ± 81	4.18 ± 0.09	4.20	0.07 ± 0.04	0.04 ± 0.1	1.59	3.44	10.21	1.71
2M16183517+2938517	5889 ± 141	4.35 ± 0.24	4.28	-0.31 ± 0.06	-0.36 ± 0.1	0	5.04	7.35	1.5
2M16183535+4908538	5874 ± 146	4.17 ± 0.18	4.11	0.07 ± 0.06	0.01 ± 0.1	0.72	4.6	8.91	1.5
2M16184273+4119012	5982 ± 161	4.25 ± 0.21	4.16	-0.25 ± 0.06	-0.34 ± 0.1	0.27	5.49	7.3	1.4
2M16184836+4917553	5645 ± 146	4.35 ± 0.23	4.34	-0.19 ± 0.06	-0.25 ± 0.1	0.7	3.95	9.18	0.5
2M16184983+4036065	5623 ± 91	4.08 ± 0.1	4.08	0.11 ± 0.04	0.07 ± 0.1	0.86	3.62	9.43	1.42
2M16190905+3221403	5879 ± 105	4.35 ± 0.15	4.28	0.11 ± 0.04	0.06 ± 0.1	0.75	4.55	10.52	0.52

APOGEE_ID	$T_{\rm eff} \pm \Delta T_{\rm eff}$	$\log g \pm \Delta \log g$	$\log g_{cor}$	$[\rm M/H] \pm \Delta[\rm M/H]$	$[Fe/H] \pm \Delta[\rm Fe/H]$	$\rm v_{mic}$	$\rm v_{mac}$	$v \sin i$	χ^2
2M16192929+5221035	6219 ± 62	4.45 ± 0.07	4.28	-0.16 ± 0.02	-0.24 ± 0.1	0	6.89	7.94	1.37
2M16193293+2151493	6093 ± 153	4.47 ± 0.19	4.35	-0.11 ± 0.06	-0.17 ± 0.1	0	5.98	8.26	0.69
2M16193995+4916552	5976 ± 142	4.3 ± 0.17	4.21	0.05 ± 0.06	-0.01 ± 0.1	0.76	5.13	9.38	0.49
2M16194528+4126549	5595 ± 115	4.24 ± 0.14	4.25	0.03 ± 0.05	0 ± 0.1	0.93	3.58	9.73	1.75
2M16195114+4416128	6210 ± 128	4.28 ± 0.16	4.12	0.01 ± 0.05	-0.05 ± 0.1	0.57	6.67	10.27	0.31
2M16200751+4854343	5792 ± 88	4.1 ± 0.09	4.06	0.09 ± 0.04	0.05 ± 0.1	0.87	4.23	9.75	0.42
2M16202778+4405268	5941 ± 90	4.33 ± 0.13	4.25	-0.16 ± 0.04	-0.23 ± 0.1	0.19	5.16	9.45	0.37
2M16202859+4906287	6054 ± 152	4.29 ± 0.18	4.18	0 ± 0.06	-0.08 ± 0.1	0.38	5.64	9.7	1.48
2M16203172+4007341	5781 ± 114	4.24 ± 0.14	4.20	-0.09 ± 0.05	-0.14 ± 0.1	0.57	4.35	7.95	1.48
2M16204167+4947305	5922 ± 70	4.23 ± 0.09	4.15	0.05 ± 0.03	-0.01 ± 0.1	0.61	4.85	9.16	1.38
2M16204248+4900561	5648 ± 133	4.13 ± 0.18	4.12	-0.19 ± 0.06	-0.26 ± 0.1	0.61	4	8.29	1.55
2M16204361+2214107	5784 ± 124	4.19 ± 0.14	4.15	-0.09 ± 0.05	-0.14 ± 0.1	0.59	4.38	10.38	0.91
2M16204954+4950257	5673 ± 88	4.39 ± 0.12	4.38	0 ± 0.04	-0.07 ± 0.1	0.59	3.83	10.13	0.38
2M16205173+4122377	5573 ± 115	4.15 ± 0.12	4.16	0.11 ± 0.05	0.07 ± 0.1	0.95	3.45	9.77	1.68
2M16205818+4116446	5950 ± 135	4.31 ± 0.17	4.23	0.08 ± 0.05	0.02 ± 0.1	0.59	4.95	10.19	0.58
2M16210000+4936338	5781 ± 121	4.15 ± 0.12	4.11	0.15 ± 0.05	0.11 ± 0.1	0.77	4.1	10.06	0.73
2M16210244+4712224	5935 ± 118	4.36 ± 0.16	4.28	-0.01 ± 0.05	-0.08 ± 0.1	0.44	4.96	9.64	0.36
2M16211558+2722320	5878 ± 77	4.26 ± 0.11	4.19	-0.12 ± 0.03	-0.21 ± 0.1	0.29	4.81	9.16	1.36
2M16212929+2343510	5641 ± 99	4.32 ± 0.13	4.31	0.13 ± 0.04	0.09 ± 0.1	1.01	3.59	10.96	0.9
2M16214309+4903574	5679 ± 94	4.18 ± 0.11	4.16	0.06 ± 0.04	0.01 ± 0.1	0.71	3.82	9.35	0.41

APOGEE_ID	$T_{\rm eff} \pm \Delta T_{\rm eff}$	$\log g \pm \Delta \log g$	$\log g_{cor}$	$[\mathrm{M/H}] \pm \Delta[\mathrm{M/H}]$	$[Fe/H] \pm \Delta[\mathrm{Fe/H}]$	$\mathrm{v_{mic}}$	$\mathrm{v_{mac}}$	$v \sin i$	χ^2
2M16214722+4743497	5831 ± 103	4.3 ± 0.13	4.25	0.05 ± 0.04	-0.01 ± 0.1	0.71	4.4	9.15	0.48
2M16214980+4225000	5763 ± 117	4.16 ± 0.12	4.12	0.19 ± 0.05	0.16 ± 0.1	0.9	3.98	9.5	1.85
2M16215041+3032471	5952 ± 109	4.37 ± 0.14	4.29	0 ± 0.04	-0.06 ± 0.1	0.47	5.05	8.79	1.43
2M16215095+3233444	5665 ± 103	4.19 ± 0.12	4.18	0.04 ± 0.04	-0.02 ± 0.1	0.73	3.79	11.23	1.61
2M16220212+4214461	6159 ± 167	4.39 ± 0.28	4.25	-0.12 ± 0.07	-0.19 ± 0.1	0	6.43	7.8	1.55
2M16220731+4151044	5693 ± 130	4.24 ± 0.15	4.22	-0.01 ± 0.05	-0.06 ± 0.1	0.71	3.93	9.26	0.68
2M16221211+4526575	5576 ± 119	4.09 ± 0.13	4.10	-0.18 ± 0.05	-0.27 ± 0.1	0.63	3.79	9.4	0.55
2M16221535+2533557	6060 ± 161	4.14 ± 0.19	4.03	-0.04 ± 0.07	-0.1 ± 0.1	0.54	5.75	8.1	1.52
2M16221795+4029342	5854 ± 149	4.05 ± 0.18	3.99	-0.23 ± 0.06	-0.31 ± 0.1	0.34	4.87	8.2	0.48
2M16221901+4449581	6225 ± 148	4.43 ± 0.19	4.26	-0.1 ± 0.06	-0.17 ± 0.1	0	6.88	7.56	0.43
2M16222025+4235312	5838 ± 148	4.37 ± 0.22	4.31	-0.2 ± 0.06	-0.29 ± 0.1	0.42	4.7	8.28	1.47
2M16224259+4912345	5850 ± 126	4.26 ± 0.16	4.20	0.11 ± 0.05	0.06 ± 0.1	0.76	4.42	9.16	0.64
2M16224263+4320425	6195 ± 133	4.33 ± 0.18	4.17	0.04 ± 0.05	-0.02 ± 0.1	0.56	6.51	8.4	0.53
2M16225595+2359196	5703 ± 107	4.25 ± 0.12	4.23	0.08 ± 0.04	0.03 ± 0.1	0.61	3.86	10.42	0.76
2M16230614+3208221	4969 ± 63	4.52 ± 0.06	4.69	-0.16 ± 0.02	-0.21 ± 0.1	0.51	3.37	10.54	1.57
2M16231106+3201063	5732 ± 86	4.4 ± 0.1	4.37	-0.03 ± 0.04	-0.08 ± 0.1	0.66	4.07	10.52	0.33
2M16231464+4429450	6143 ± 140	4.53 ± 0.15	4.39	0.11 ± 0.06	0.06 ± 0.1	0.52	6.07	10.91	1.55
2M16232664+2738569	5893 ± 136	4.31 ± 0.19	4.24	0.04 ± 0.06	-0.01 ± 0.1	0.88	4.71	8.85	1.6
2M16233325+2328477	5786 ± 101	4.14 ± 0.1	4.10	0.1 ± 0.04	0.04 ± 0.1	0.54	4.18	10.52	0.69
2M16233378+3744471	5931 ± 113	4.38 ± 0.16	4.30	0.01 ± 0.05	-0.03 ± 0.1	0.65	4.93	10.93	1.32

APOGEE_ID	$T_{\rm eff} \pm \Delta T_{\rm eff}$	$\log g \pm \Delta \log g$	$\log g_{cor}$	$[\rm M/H] \pm \Delta[\rm M/H]$	$[Fe/H] \pm \Delta[\rm Fe/H]$	$\rm v_{mic}$	$\rm v_{mac}$	$v \sin i$	χ^2
2M16233645+4650284	5897 ± 107	4.36 ± 0.18	4.29	-0.27 ± 0.04	-0.32 ± 0.1	0	5.04	8.06	0.38
2M16233762+2438152	5715 ± 144	4.27 ± 0.19	4.25	-0.35 ± 0.06	-0.44 ± 0.1	0.27	4.35	8	1.47
2M16234255+3740283	5881 ± 164	4.33 ± 0.27	4.26	-0.27 ± 0.07	-0.37 ± 0.1	0.25	4.97	7.6	1.43
2M16234310+3850137	6170 ± 197	4.26 ± 0.29	4.11	-0.2 ± 0.08	-0.29 ± 0.1	0	6.61	7.42	0.5
2M16235746+3036500	6077 ± 86	4.42 ± 0.11	4.30	0.04 ± 0.03	0 ± 0.1	0.53	5.72	9.68	0.44
2M16241027+2222095	5884 ± 88	4.33 ± 0.14	4.26	-0.24 ± 0.04	-0.31 ± 0.1	0	4.96	6.9	1.41
2M16241481+2956205	5663 ± 120	4.3 ± 0.15	4.29	0 ± 0.05	-0.04 ± 0.1	0.88	3.81	10.48	0.63
2M16242371+3046210	5754 ± 123	4.33 ± 0.13	4.30	-0.03 ± 0.05	-0.07 ± 0.1	0.63	4.16	9.95	0.64
2M16243047+4808037	5931 ± 136	4.22 ± 0.17	4.14	0.03 ± 0.05	-0.03 ± 0.1	0.7	4.92	8.71	1.49
2M16243312+4656210	5793 ± 113	4.26 ± 0.14	4.22	-0.08 ± 0.05	-0.16 ± 0.1	0.52	4.39	8.02	0.46
2M16243355+3847553	5837 ± 122	4.3 ± 0.15	4.24	0.01 ± 0.05	-0.04 ± 0.1	0.61	4.47	9.74	0.49
2M16243505+2803560	5749 ± 118	4.27 ± 0.12	4.24	0.03 ± 0.05	-0.02 ± 0.1	0.84	4.08	9.28	1.68
2M16243875+3159432	5749 ± 109	4.34 ± 0.12	4.31	0.01 ± 0.04	-0.04 ± 0.1	0.65	4.1	10.59	0.52
2M16244786+2153039	5688 ± 120	4.21 ± 0.14	4.19	-0.02 ± 0.05	-0.06 ± 0.1	0.5	3.93	9.79	1.52
2M16244956+3925199	6058 ± 84	4.29 ± 0.11	4.18	-0.14 ± 0.03	-0.22 ± 0.1	0	5.82	8.26	1.39
2M16245660+4905058	5767 ± 125	4.26 ± 0.13	4.22	0.03 ± 0.05	-0.04 ± 0.1	0.81	4.16	9.85	1.66
2M16250386+2253391	5581 ± 126	4.23 ± 0.16	4.24	-0.12 ± 0.06	-0.19 ± 0.1	0.67	3.71	8.93	0.61
2M16251417+4652068	5976 ± 86	4.33 ± 0.11	4.24	-0.09 ± 0.03	-0.14 ± 0.1	0.4	5.28	8.4	1.31
2M16251678+2906446	5892 ± 112	4.33 ± 0.17	4.26	-0.02 ± 0.05	-0.09 ± 0.1	0.49	4.76	9.01	0.69
2M16252438+2247575	5733 ± 113	4.26 ± 0.12	4.23	0.19 ± 0.05	0.14 ± 0.1	0.76	3.84	9.86	0.89

APOGEE_ID	$T_{\rm eff} \pm \Delta T_{\rm eff}$	$\log g \pm \Delta \log g$	$\log g_{cor}$	$[\rm M/H] \pm \Delta[\rm M/H]$	$[Fe/H] \pm \Delta[\rm Fe/H]$	$\rm v_{mic}$	$\rm v_{mac}$	$v \sin i$	χ^2
2M16253645+4922326	5943 ± 108	4.38 ± 0.14	4.30	0.21 ± 0.04	0.15 ± 0.1	0.73	4.75	9.33	1.6
2M16254841+3015545	5606 ± 57	4.06 ± 0.06	4.06	0.17 ± 0.03	0.12 ± 0.1	0.93	3.5	0.52	1.68
2M16261959+3057523	5636 ± 99	4.23 ± 0.13	4.23	0.15 ± 0.04	0.11 ± 0.1	0.92	3.57	9.92	0.64
2M16264739+2847517	5988 ± 117	4.35 ± 0.13	4.26	0 ± 0.05	-0.05 ± 0.1	0.49	5.25	9.92	0.45
2M16264742+2555285	5666 ± 91	4.15 ± 0.11	4.14	0.15 ± 0.04	0.1 ± 0.1	0.81	3.68	10.07	0.58
2M16264960+4434544	5972 ± 150	4.32 ± 0.18	4.23	0 ± 0.06	-0.07 ± 0.1	0.64	5.16	8.81	0.53
2M16270358+4653432	5976 ± 158	4.45 ± 0.17	4.36	-0.04 ± 0.06	-0.13 ± 0.1	0.51	5.21	9.13	0.57
2M16270389+2907247	5991 ± 133	4.36 ± 0.16	4.27	0.15 ± 0.05	0.1 ± 0.1	0.73	5.09	10.52	1.59
2M16270775+4232584	5954 ± 134	4.27 ± 0.18	4.18	-0.1 ± 0.06	-0.17 ± 0.1	0.51	5.18	8.49	1.44
2M16270833+3936205	5931 ± 157	4.38 ± 0.24	4.30	-0.13 ± 0.06	-0.21 ± 0.1	0.13	5.07	8.09	0.56
2M16271095+3807252	5676 ± 94	4.25 ± 0.11	4.24	0.06 ± 0.04	0.01 ± 0.1	0.58	3.79	10.09	0.54
2M16271397+4912078	5683 ± 98	4.21 ± 0.11	4.19	0.01 ± 0.04	-0.07 ± 0.1	0.71	3.88	9.65	1.39
2M16271423+3156028	5841 ± 112	4.28 ± 0.16	4.22	-0.25 ± 0.05	-0.33 ± 0.1	0.07	4.77	7.85	0.34
2M16272024+4426529	5582 ± 94	4.28 ± 0.11	4.29	0 ± 0.04	-0.04 ± 0.1	0.83	3.57	9.74	0.43
2M16272664+2958186	5708 ± 114	4.23 ± 0.13	4.21	0.12 ± 0.05	0.07 ± 0.1	0.83	3.84	10.41	0.65
2M16273042+2531464	5860 ± 128	4.18 ± 0.16	4.12	0.04 ± 0.05	-0.02 ± 0.1	0.64	4.57	8.36	1.59
2M16273786+3231501	5767 ± 133	4.06 ± 0.13	4.02	-0.1 ± 0.06	-0.17 ± 0.1	0.73	4.35	8.78	1.56
2M16273795+3203596	5789 ± 126	4.32 ± 0.15	4.28	0.03 ± 0.05	-0.02 ± 0.1	0.69	4.24	9.28	0.59
2M16274153+2442117	5989 ± 163	4.1 ± 0.17	4.01	-0.07 ± 0.07	-0.15 ± 0.1	0.51	5.37	8.8	0.48
2M16274657+2933315	5669 ± 96	4.19 ± 0.11	4.18	0.03 ± 0.04	-0.02 ± 0.1	0.8	3.81	10.73	0.51

APOGEE_ID	$T_{\rm eff} \pm \Delta T_{\rm eff}$	$\log g \pm \Delta \log g$	$\log g_{cor}$	$[\rm M/H] \pm \Delta[\rm M/H]$	$[Fe/H] \pm \Delta[\rm Fe/H]$	$\rm v_{mic}$	$\rm v_{mac}$	$v \sin i$	χ^2
2M16275168+3152366	5759 ± 97	4.02 ± 0.09	3.98	-0.02 ± 0.04	-0.09 ± 0.1	0.84	4.25	9.12	1.4
2M16275294+3956192	5476 ± 111	4.28 ± 0.12	4.32	0.01 ± 0.05	0 ± 0.1	1.21	3.31	9.91	0.91
2M16275937+3755470	5610 ± 126	4.31 ± 0.17	4.31	-0.02 ± 0.05	-0.06 ± 0.1	0.86	3.66	8.21	1.82
2M16280224+4837424	5839 ± 122	4.33 ± 0.17	4.27	-0.04 ± 0.05	-0.1 ± 0.1	0.71	4.53	9.16	0.4
2M16280735+3140513	5968 ± 119	4.32 ± 0.14	4.23	0.13 ± 0.05	0.08 ± 0.1	0.61	4.99	10.67	1.55
2M16280996+3932132	5551 ± 117	4.34 ± 0.14	4.36	-0.01 ± 0.05	-0.03 ± 0.1	1.21	3.49	10.95	1.55
2M16281558+3910045	5967 ± 144	4.32 ± 0.19	4.23	-0.07 ± 0.06	-0.15 ± 0.1	0.26	5.21	9.09	0.51
2M16281594+2411340	5814 ± 83	4.21 ± 0.1	4.16	0.21 ± 0.03	0.17 ± 0.1	0.86	4.15	9.76	1.65
2M16282824+2622332	6068 ± 178	4.2 ± 0.23	4.09	-0.1 ± 0.07	-0.2 ± 0.1	0.24	5.85	8.66	1.66
2M16283124+2827110	6057 ± 117	4.27 ± 0.14	4.16	0.09 ± 0.05	0.04 ± 0.1	0.67	5.55	9.67	0.43
2M16283223+3928132	5918 ± 140	4.28 ± 0.19	4.20	0.04 ± 0.06	-0.02 ± 0.1	0.47	4.83	9.89	0.7
2M16283294+2423216	5737 ± 101	4.21 ± 0.1	4.18	0.14 ± 0.04	0.1 ± 0.1	0.9	3.93	9.86	0.6
2M16283621+4044594	5944 ± 129	4.3 ± 0.16	4.22	-0.01 ± 0.05	-0.08 ± 0.1	0.47	5.02	9.11	1.42
2M16283808+2525148	5778 ± 126	4.23 ± 0.13	4.19	-0.01 ± 0.05	-0.08 ± 0.1	0.56	4.26	9.2	0.52
2M16284437+3807091	5494 ± 107	4.35 ± 0.12	4.38	-0.11 ± 0.05	-0.15 ± 0.1	0.7	3.47	10.1	0.58
2M16285587+2522473	5688 ± 152	4.25 ± 0.2	4.23	-0.2 ± 0.06	-0.29 ± 0.1	0.38	4.11	9.29	1.51
2M16290597+4047103	5618 ± 132	4.36 ± 0.18	4.36	-0.02 ± 0.06	-0.06 ± 0.1	0.82	3.68	9.14	0.69
2M16290621+4015574	6101 ± 141	4.37 ± 0.2	4.25	0.06 ± 0.05	-0.03 ± 0.1	0.48	5.86	9.53	1.41
2M16291105+4407119	6113 ± 118	4.22 ± 0.16	4.10	0.02 ± 0.05	-0.05 ± 0.1	0.6	6	8.95	0.41
2M16291841+4022568	5988 ± 122	4.28 ± 0.15	4.19	-0.09 ± 0.05	-0.14 ± 0.1	0.42	5.35	8.31	0.45

APOGEE_ID	$T_{\rm eff} \pm \Delta T_{\rm eff}$	$\log g \pm \Delta \log g$	$\log g_{cor}$	$[\rm M/H] \pm \Delta[\rm M/H]$	$[Fe/H] \pm \Delta[\rm Fe/H]$	$\rm v_{mic}$	$\rm v_{mac}$	$v \sin i$	χ^2
2M16292027+4156398	5725 ± 105	4.13 ± 0.1	4.10	0.04 ± 0.04	0 ± 0.1	0.74	4.02	9.74	1.68
2M16292102+2400155	5807 ± 127	4.14 ± 0.14	4.09	-0.04 ± 0.05	-0.1 ± 0.1	0.79	4.43	8.99	0.42
2M16292209+4136238	5930 ± 123	4.29 ± 0.18	4.21	-0.06 ± 0.05	-0.12 ± 0.1	0.52	5	8.68	1.44
2M16292796+4602531	5722 ± 124	4.21 ± 0.14	4.18	-0.18 ± 0.05	-0.28 ± 0.1	0.56	4.22	9.4	1.46
2M16294988+2440332	5873 ± 118	4.28 ± 0.16	4.22	0.07 ± 0.05	0.03 ± 0.1	0.74	4.57	9.99	0.59
2M16295553+3914554	5586 ± 101	4.4 ± 0.14	4.41	-0.03 ± 0.04	-0.05 ± 0.1	0.92	3.6	10.37	0.46
2M16300220-0048025	6038 ± 53	4.21 ± 0.06	4.10	0.08 ± 0.02	0.01 ± 0.1	0.65	5.47	9.34	0.34
2M16300784+4452156	5878 ± 77	4.33 ± 0.12	4.26	-0.05 ± 0.03	-0.1 ± 0.1	0.46	4.73	8.23	1.47
2M16301638-1256081	6030 ± 127	4.43 ± 0.14	4.33	0.05 ± 0.05	-0.02 ± 0.1	0.54	5.42	9.13	0.44
2M16301821+2729111	5655 ± 133	4.39 ± 0.21	4.38	-0.08 ± 0.06	-0.13 ± 0.1	0.87	3.86	9.69	1.55
2M16302844+0410411	6200 ± 245	4.44 ± 0.34	4.28	-0.63 ± 0.1	-0.66 ± 0.1	0	7.2	9.38	1.24
2M16303752+4406051	5594 ± 106	4.31 ± 0.14	4.32	-0.03 ± 0.05	-0.08 ± 0.1	0.71	3.63	9.69	0.5
2M16304529+3740405	5647 ± 108	4 ± 0.12	3.99	-0.03 ± 0.05	-0.08 ± 0.1	0.8	3.87	10.12	1.4
2M16304882+4317056	5789 ± 108	4.18 ± 0.11	4.14	0.13 ± 0.04	0.07 ± 0.1	0.68	4.16	10.25	1.6
2M16305638+2502156	5735 ± 148	4.18 ± 0.15	4.15	-0.04 ± 0.06	-0.11 ± 0.1	0.7	4.13	9.11	0.56
2M16310077+3945082	5962 ± 170	4.34 ± 0.24	4.25	-0.22 ± 0.07	-0.31 ± 0.1	0	5.34	9.69	1.9
2M16311216+4423575	5894 ± 127	4.31 ± 0.21	4.24	-0.31 ± 0.05	-0.42 ± 0.1	0.04	5.08	7.75	1.48
2M16313431+2606107	5746 ± 128	4.32 ± 0.15	4.29	-0.1 ± 0.05	-0.15 ± 0.1	0.44	4.21	10.16	0.52
2M16314147-1356364	5766 ± 113	4.05 ± 0.11	4.01	-0.07 ± 0.05	-0.13 ± 0.1	0.8	4.32	9.02	1.41
2M16314662+4223580	5911 ± 116	4.33 ± 0.16	4.26	0.05 ± 0.05	0.01 ± 0.1	0.61	4.78	9.76	0.42

APOGEE_ID	$T_{\rm eff} \pm \Delta T_{\rm eff}$	$\log g \pm \Delta \log g$	$\log g_{cor}$	$[\rm M/H] \pm \Delta[\rm M/H]$	$[Fe/H] \pm \Delta[\rm Fe/H]$	$v_{\rm mic}$	$v_{\rm mac}$	$v \sin i$	χ^2
2M16315282+3849032	5939 ± 126	4.32 ± 0.17	4.24	0.1 ± 0.05	0.05 ± 0.1	0.67	4.87	10.22	0.4
2M16315327+4318480	5941 ± 137	4.33 ± 0.19	4.25	-0.04 ± 0.06	-0.11 ± 0.1	0.47	5.03	9.2	0.54
2M16315952+4359008	5898 ± 123	4.29 ± 0.18	4.22	0.08 ± 0.05	0.04 ± 0.1	0.56	4.69	9.37	1.6
2M16320114+4018205	5609 ± 115	4.3 ± 0.15	4.30	0.03 ± 0.05	0 ± 0.1	0.79	3.6	10.4	0.56
2M16320319+4858503	5662 ± 98	4.29 ± 0.14	4.28	-0.1 ± 0.04	-0.18 ± 0.1	0.72	3.92	9.57	0.33
2M16320645+4102470	5916 ± 139	4.22 ± 0.2	4.14	-0.06 ± 0.06	-0.13 ± 0.1	0.5	4.95	8.29	0.51
2M16322521+2439030	6025 ± 87	4.42 ± 0.11	4.32	-0.09 ± 0.03	-0.15 ± 0.1	0	5.55	8.65	0.4
2M16324698+4449110	5997 ± 148	4.44 ± 0.15	4.34	-0.02 ± 0.06	-0.09 ± 0.1	0.45	5.31	8.53	0.5
2M16324760+4449113	5910 ± 140	4.33 ± 0.22	4.26	-0.04 ± 0.06	-0.1 ± 0.1	0.57	4.88	8.49	0.47
2M16325360+4229162	6026 ± 116	4.36 ± 0.14	4.26	0.02 ± 0.05	-0.04 ± 0.1	0.49	5.44	10.6	0.36
2M16325767+3843382	5877 ± 141	4.25 ± 0.19	4.18	-0.02 ± 0.06	-0.1 ± 0.1	0.62	4.71	8.78	0.44
2M16330153+4527273	6185 ± 165	4.14 ± 0.21	3.99	-0.2 ± 0.07	-0.31 ± 0.1	0.25	6.74	8.4	0.44
2M16332548+4426270	5860 ± 140	4.23 ± 0.17	4.17	0.04 ± 0.06	-0.02 ± 0.1	0.62	4.56	9.04	0.69
2M16333176+3810425	5972 ± 130	4.23 ± 0.15	4.14	-0.01 ± 0.05	-0.07 ± 0.1	0.5	5.18	8.99	1.47
2M16333381+4142307	5598 ± 108	4.03 ± 0.11	4.03	0.11 ± 0.05	0.08 ± 0.1	0.93	3.55	9.97	0.7
2M16333441+4252369	5760 ± 110	4.35 ± 0.13	4.31	-0.08 ± 0.05	-0.13 ± 0.1	0.57	4.24	8.94	0.38
2M16334276+3926405	5899 ± 150	4.29 ± 0.22	4.22	-0.01 ± 0.06	-0.08 ± 0.1	0.58	4.79	8.96	1.58
2M16334548+3929573	5915 ± 125	4.3 ± 0.17	4.22	0.08 ± 0.05	0.03 ± 0.1	0.76	4.77	10.18	0.65
2M16335320+4447102	5787 ± 99	4.17 ± 0.11	4.13	0.14 ± 0.04	0.09 ± 0.1	0.81	4.13	9.86	1.35
2M16340039+3914024	5718 ± 145	4.15 ± 0.16	4.12	-0.11 ± 0.06	-0.2 ± 0.1	0.65	4.15	8.94	1.58

APOGEE_ID	$T_{\mathrm{eff}} \pm \Delta T_{\mathrm{eff}}$	$\log g \pm \Delta \log g$	$\log g_{cor}$	$[\mathrm{M/H}] \pm \Delta[\mathrm{M/H}]$	$[Fe/H] \pm \Delta[\mathrm{Fe/H}]$	$\mathrm{v}_{\mathrm{mic}}$	$\mathrm{v}_{\mathrm{mac}}$	$v \sin i$	χ^2
2M16340187+2550099	5998 ± 135	4.26 ± 0.16	4.16	-0.07 ± 0.06	-0.15 ± 0.1	0.59	5.39	9.91	0.5
2M16343162+4042520	5850 ± 154	4.2 ± 0.21	4.14	-0.12 ± 0.07	-0.21 ± 0.1	0.33	4.69	8.98	1.66
2M16344383+4415084	5605 ± 110	4.37 ± 0.15	4.37	-0.02 ± 0.05	-0.06 ± 0.1	1.12	3.64	9.12	0.62
2M16344700+4413191	5986 ± 116	4.31 ± 0.13	4.22	0.12 ± 0.05	0.06 ± 0.1	0.7	5.1	9.28	0.82
2M16345641+4451286	5729 ± 125	4.36 ± 0.14	4.33	-0.01 ± 0.05	-0.06 ± 0.1	0.67	4.04	10.59	1.71
2M16350777+3946033	5925 ± 126	4.23 ± 0.16	4.15	0.09 ± 0.05	0.05 ± 0.1	0.6	4.82	9.73	1.25
2M16351462+3701197	5795 ± 44	4.18 ± 0.05	4.14	0.13 ± 0.02	0.07 ± 0.1	0.64	4.18	10.76	0.4
2M16351462+3701197	5795 ± 44	4.18 ± 0.05	4.14	0.13 ± 0.02	0.07 ± 0.1	0.64	4.18	10.76	0.4
2M16351556+4539126	5978 ± 133	4.43 ± 0.16	4.34	-0.1 ± 0.05	-0.16 ± 0.1	0.3	5.29	9.19	1.42
2M16352641+4316002	5602 ± 109	4.25 ± 0.13	4.25	0.01 ± 0.05	-0.04 ± 0.1	0.89	3.62	10.64	0.48
2M16354246+4008408	6029 ± 93	4.33 ± 0.12	4.23	-0.15 ± 0.04	-0.25 ± 0.1	0.2	5.65	8.61	0.35
2M16354524+4029288	5757 ± 132	4.24 ± 0.14	4.20	-0.04 ± 0.05	-0.09 ± 0.1	0.51	4.2	8.48	1.03
2M16354870+3946515	5858 ± 144	4.33 ± 0.22	4.27	-0.05 ± 0.06	-0.11 ± 0.1	0.55	4.64	9.61	0.82
2M16355525+4353392	6035 ± 100	4.33 ± 0.12	4.22	0 ± 0.04	-0.05 ± 0.1	0.58	5.51	9.86	0.4
2M16355912+4527277	6223 ± 141	4.22 ± 0.17	4.05	-0.11 ± 0.06	-0.21 ± 0.1	0.43	6.9	8.31	0.38
2M16360385+4008029	5590 ± 126	4.34 ± 0.18	4.35	-0.05 ± 0.05	-0.07 ± 0.1	0.91	3.64	8.84	1.05
2M16360577+4449368	6042 ± 104	4.33 ± 0.14	4.22	-0.05 ± 0.04	-0.12 ± 0.1	0.43	5.62	8.97	1.37
2M16365075+4220592	5830 ± 109	4.21 ± 0.13	4.16	0.13 ± 0.05	0.09 ± 0.1	0.85	4.32	9.45	0.48
2M16370192+4323364	5519 ± 71	4.32 ± 0.08	4.34	-0.02 ± 0.03	-0.04 ± 0.1	1.03	3.43	9.97	1.37
2M16373007+4447368	5635 ± 115	4.4 ± 0.18	4.40	-0.05 ± 0.05	-0.09 ± 0.1	0.78	3.76	10.11	1.7

APOGEE_ID	$T_{\text{eff}} \pm \Delta T_{\text{eff}}$	$\log g \pm \Delta \log g$	$\log g_{cor}$	$[\text{M/H}] \pm \Delta[\text{M/H}]$	$[Fe/H] \pm \Delta[\text{Fe/H}]$	v_{mic}	v_{mac}	$v \sin i$	χ^2
2M16373226+4308064	5698 ± 136	4.33 ± 0.18	4.31	-0.18 ± 0.06	-0.25 ± 0.1	0.2	4.11	9.12	1.46
2M16374458+4056394	5943 ± 107	4.31 ± 0.15	4.23	-0.16 ± 0.04	-0.23 ± 0.1	0.51	5.17	9.13	0.35
2M16375899+4029212	6190 ± 147	4.36 ± 0.21	4.20	0.11 ± 0.06	0.07 ± 0.1	0.88	6.4	10.09	0.93
2M16380746+4257375	5635 ± 126	4.26 ± 0.16	4.26	0 ± 0.05	-0.05 ± 0.1	0.85	3.72	9.12	0.56
2M16382002+4131199	6112 ± 156	4.34 ± 0.22	4.22	0.02 ± 0.06	-0.05 ± 0.1	0	5.98	8.82	1.7
2M16382460+4208524	5763 ± 141	4.17 ± 0.16	4.13	-0.24 ± 0.06	-0.34 ± 0.1	0.48	4.45	8.92	0.42
2M16384248+3809125	6009 ± 127	4.43 ± 0.14	4.33	-0.03 ± 0.05	-0.08 ± 0.1	0.56	5.39	10.06	1.32
2M16384896+4049326	5925 ± 132	4.4 ± 0.19	4.32	0.03 ± 0.05	-0.01 ± 0.1	0.61	4.86	10.09	0.55
2M16385340+3947432	5940 ± 165	4.32 ± 0.25	4.24	-0.31 ± 0.07	-0.42 ± 0.1	0	5.31	8.47	1.44
2M16385922+4535228	5721 ± 79	4.31 ± 0.09	4.28	-0.03 ± 0.03	-0.08 ± 0.1	0.8	4.04	8.6	0.37
2M16385922+4535228	5725 ± 78	4.32 ± 0.09	4.29	-0.03 ± 0.03	-0.08 ± 0.1	0.77	4.05	9.46	0.37
2M16390283+4517403	5483 ± 109	4.32 ± 0.12	4.35	-0.02 ± 0.05	-0.04 ± 0.1	1.3	3.36	9.41	0.9
2M16390433+4324265	6127 ± 102	4.44 ± 0.14	4.31	-0.02 ± 0.04	-0.08 ± 0.1	0.46	6.11	8.53	0.36
2M16394554+4347291	5868 ± 149	4.3 ± 0.23	4.24	-0.2 ± 0.06	-0.28 ± 0.1	0.15	4.85	7.94	1.51
2M16402611+4504052	6091 ± 125	4.34 ± 0.17	4.22	0.12 ± 0.05	0.07 ± 0.1	0.6	5.72	10.69	0.49
2M16403740+4151204	5813 ± 146	4.21 ± 0.17	4.16	-0.04 ± 0.06	-0.12 ± 0.1	0.53	4.44	8.21	0.67
2M16410456+4210035	6020 ± 164	4.1 ± 0.18	4.00	-0.16 ± 0.07	-0.24 ± 0.1	0.41	5.65	7.82	0.49
2M16410822-0251258	5542 ± 201	4.17 ± 0.23	4.19	-0.26 ± 0.09	-0.36 ± 0.1	0.4	3.77	9.34	1.46
2M16410836+4021238	5746 ± 126	4.12 ± 0.13	4.09	-0.26 ± 0.05	-0.34 ± 0.1	0.25	4.42	8.09	1.5
2M16410941+4530133	5707 ± 119	4.03 ± 0.13	4.01	-0.09 ± 0.05	-0.15 ± 0.1	0.82	4.12	9.24	0.52

APOGEE_ID	$T_{\rm eff} \pm \Delta T_{\rm eff}$	$\log g \pm \Delta \log g$	$\log g_{cor}$	$[\mathrm{M/H}] \pm \Delta[\mathrm{M/H}]$	$[Fe/H] \pm \Delta[\mathrm{Fe/H}]$	$\mathrm{v_{mic}}$	$\mathrm{v_{mac}}$	$v \sin i$	χ^2
2M16412294+4414338	5717 ± 125	4.3 ± 0.15	4.27	-0.04 ± 0.05	-0.1 ± 0.1	0.69	4.04	8.55	0.78
2M16414098+4802367	5845 ± 120	4.36 ± 0.17	4.30	-0.02 ± 0.05	-0.08 ± 0.1	0.59	4.53	8.96	0.49
2M16415022+1308556	5574 ± 145	4.17 ± 0.15	4.18	0.03 ± 0.06	-0.02 ± 0.1	0.71	3.54	10.95	1.69
2M16415467+4513171	5485 ± 93	4.27 ± 0.1	4.30	0.03 ± 0.04	0.02 ± 0.1	1.24	3.31	10.5	2.03
2M16420492+4823271	6025 ± 120	4.31 ± 0.15	4.21	-0.2 ± 0.05	-0.29 ± 0.1	0	5.67	8.49	0.45
2M16421802+3951197	6148 ± 164	4.17 ± 0.24	4.03	-0.12 ± 0.07	-0.21 ± 0.1	0.03	6.4	8.25	1.81
2M16421882+3954433	6227 ± 156	4.44 ± 0.17	4.27	-0.04 ± 0.06	-0.11 ± 0.1	0	6.82	8.09	0.51
2M16422953+4008293	5831 ± 131	4.3 ± 0.16	4.25	0.01 ± 0.05	-0.04 ± 0.1	0.62	4.45	10.3	0.67
2M16423829+4503109	5816 ± 123	4.17 ± 0.14	4.12	0.18 ± 0.05	0.13 ± 0.1	0.86	4.22	10.8	0.93
2M16425135+4015340	5782 ± 85	4.43 ± 0.09	4.39	-0.01 ± 0.03	-0.06 ± 0.1	0.58	4.24	10.97	0.33
2M16425819+4354402	5916 ± 66	4.19 ± 0.08	4.11	0.14 ± 0.03	0.1 ± 0.1	0.8	4.72	10.34	0.42
2M16430032+3803165	5826 ± 126	4.16 ± 0.14	4.11	0 ± 0.05	-0.07 ± 0.1	0.63	4.47	8.92	0.45
2M16430263+4040498	5906 ± 129	4.25 ± 0.2	4.18	-0.09 ± 0.05	-0.15 ± 0.1	0.7	4.91	8.73	0.65
2M16432193+4013014	5712 ± 139	4.27 ± 0.16	4.25	-0.02 ± 0.06	-0.09 ± 0.1	0.67	4	8.94	1.53
2M16433962+3833267	5651 ± 101	4.19 ± 0.13	4.18	0.08 ± 0.04	0.03 ± 0.1	0.73	3.7	9.33	1.51
2M16434357+4458140	5702 ± 130	4.43 ± 0.15	4.41	-0.02 ± 0.05	-0.06 ± 0.1	0.81	3.95	10.99	0.63
2M16434909+4122183	5730 ± 122	4.33 ± 0.14	4.30	-0.02 ± 0.05	-0.05 ± 0.1	0.77	4.06	9.94	1.54
2M16440168+4241578	5781 ± 73	4.31 ± 0.08	4.27	0.03 ± 0.03	-0.04 ± 0.1	0.48	4.21	10.47	1.35
2M16440830+4121294	5634 ± 116	4.01 ± 0.12	4.01	0.08 ± 0.05	0.02 ± 0.1	0.66	3.71	10.18	1.8
2M16442598+4346008	5915 ± 136	4.31 ± 0.21	4.23	-0.05 ± 0.06	-0.1 ± 0.1	0.38	4.91	10.11	0.56

APOGEE_ID	$T_{\rm eff} \pm \Delta T_{\rm eff}$	$\log g \pm \Delta \log g$	$\log g_{cor}$	$[\mathrm{M/H}] \pm \Delta[\mathrm{M/H}]$	$[Fe/H] \pm \Delta[\mathrm{Fe/H}]$	$v_{\rm mic}$	$v_{\rm mac}$	$v \sin i$	χ^2
2M16442607+3750558	5610 ± 125	3.94 ± 0.16	3.94	-0.01 ± 0.05	-0.06 ± 0.1	0.98	3.76	9.71	0.57
2M16444715+3708433	6162 ± 113	4.35 ± 0.18	4.21	-0.17 ± 0.04	-0.27 ± 0.1	0	6.52	7.64	1.36
2M16445997+0605172	5064 ± 135	3.59 ± 0.16	3.59	-0.24 ± 0.06	-0.31 ± 0.1	0.87	3.7	11.03	1.43
2M16450493+4652338	5612 ± 94	4.23 ± 0.11	4.23	0.06 ± 0.04	0.02 ± 0.1	0.78	3.6	9.47	1.3
2M16454646-0045543	6168 ± 97	4.3 ± 0.15	4.15	-0.24 ± 0.04	-0.33 ± 0.1	0	6.62	8.03	1.41
2M16462283+4217465	5959 ± 147	4.19 ± 0.16	4.10	0 ± 0.06	-0.08 ± 0.1	0.51	5.11	10.13	1.46
2M16463433+4758423	5620 ± 82	4.33 ± 0.11	4.33	-0.02 ± 0.03	-0.07 ± 0.1	0.94	3.69	9.08	1.38
2M16470588+3851005	5628 ± 109	4.17 ± 0.13	4.17	0.04 ± 0.05	-0.01 ± 0.1	0.68	3.68	9.97	0.57
2M16472416+4623103	5918 ± 129	4.35 ± 0.18	4.27	0.04 ± 0.05	-0.01 ± 0.1	0.7	4.82	10.82	0.5
2M16472499+4614520	5914 ± 77	4.32 ± 0.12	4.25	-0.09 ± 0.03	-0.16 ± 0.1	0.51	4.95	8.68	0.33
2M16480533-0316347	6217 ± 112	4.51 ± 0.1	4.34	0.14 ± 0.04	0.09 ± 0.1	0.44	6.55	9.83	1.45
2M16485004+4825011	5817 ± 85	4.23 ± 0.1	4.18	0 ± 0.03	-0.06 ± 0.1	0.69	4.41	9.84	1.41
2M16490138-1936275	6048 ± 116	4.28 ± 0.15	4.17	-0.18 ± 0.05	-0.27 ± 0.1	0	5.79	7.19	1.34
2M16490725+4740066	5959 ± 137	4.42 ± 0.19	4.33	-0.11 ± 0.06	-0.18 ± 0.1	0.12	5.2	8.6	1.45
2M16491706+4632130	5693 ± 139	4.36 ± 0.2	4.34	-0.23 ± 0.06	-0.29 ± 0.1	0.55	4.15	8.34	0.42
2M16504386-0120106	6189 ± 151	4.37 ± 0.23	4.22	-0.12 ± 0.06	-0.21 ± 0.1	0	6.65	8.08	0.42
2M16510908+4748169	5795 ± 107	4.38 ± 0.15	4.34	-0.23 ± 0.04	-0.33 ± 0.1	0.21	4.54	7.85	1.35
2M16511294-1946063	5609 ± 108	4.35 ± 0.16	4.35	-0.04 ± 0.05	-0.08 ± 0.1	1.21	3.68	8.85	1.46
2M16512954+4736262	5563 ± 97	4.26 ± 0.11	4.27	0.06 ± 0.04	0.03 ± 0.1	1.28	3.45	11.46	1.73
2M16524862+3627597	6151 ± 109	4.39 ± 0.19	4.25	-0.12 ± 0.04	-0.2 ± 0.1	0	6.38	7.65	0.39

APOGEE_ID	$T_{\rm eff} \pm \Delta T_{\rm eff}$	$\log g \pm \Delta \log g$	$\log g_{cor}$	$[\rm M/H] \pm \Delta[\rm M/H]$	$[Fe/H] \pm \Delta[\rm Fe/H]$	$\rm v_{mic}$	$\rm v_{mac}$	$v \sin i$	χ^2
2M16525687+3713349	6010 ± 143	4.49 ± 0.12	4.39	-0.02 ± 0.05	-0.07 ± 0.1	0.52	5.38	7.93	1.48
2M16530387+3812482	5791 ± 119	4.09 ± 0.12	4.05	0.1 ± 0.05	0.06 ± 0.1	0.84	4.21	9.57	1.65
2M16531727+3439022	5745 ± 109	4.09 ± 0.1	4.06	-0.03 ± 0.05	-0.1 ± 0.1	0.67	4.18	8.65	0.43
2M16532292+3849250	5701 ± 97	4.19 ± 0.11	4.17	0.16 ± 0.04	0.1 ± 0.1	0.71	3.78	10.59	0.61
2M16533707+4725162	5720 ± 118	4.31 ± 0.14	4.28	-0.02 ± 0.05	-0.07 ± 0.1	0.85	4.02	8.07	0.42
2M16534497+3745063	5737 ± 114	4.2 ± 0.12	4.17	0.05 ± 0.05	0 ± 0.1	0.7	4.03	9.34	1.71
2M16561211+3948241	5899 ± 99	4.09 ± 0.13	4.02	-0.04 ± 0.04	-0.11 ± 0.1	0.73	4.87	9.61	0.37
2M16562027+3912275	5589 ± 113	4.21 ± 0.13	4.22	0.04 ± 0.05	-0.01 ± 0.1	0.8	3.56	10.43	1.58
2M16563399+3855442	5811 ± 104	4.39 ± 0.13	4.34	0.02 ± 0.04	-0.02 ± 0.1	0.61	4.34	10.65	1.41
2M16563947+3935154	5819 ± 154	4.33 ± 0.22	4.28	-0.16 ± 0.06	-0.26 ± 0.1	0.52	4.57	9.39	0.52
2M16564128+3500270	5789 ± 115	4.27 ± 0.13	4.23	0.02 ± 0.05	-0.02 ± 0.1	0.77	4.26	9.31	0.51
2M16571566+6244185	5535 ± 88	4.13 ± 0.09	4.15	0.11 ± 0.04	0.09 ± 0.1	1.02	3.36	9.11	2.05
2M16571699+3547119	5962 ± 146	4.22 ± 0.17	4.13	0.05 ± 0.06	-0.01 ± 0.1	0.76	5.07	9.45	0.71
2M16572858+6349011	5610 ± 89	4.12 ± 0.1	4.12	0.14 ± 0.04	0.1 ± 0.1	0.84	3.52	10.14	1.66
2M16574935+3625109	6226 ± 141	4.26 ± 0.17	4.09	-0.02 ± 0.06	-0.08 ± 0.1	0.45	6.82	8.21	0.44
2M16580047+3755436	5918 ± 100	4.34 ± 0.14	4.26	0.11 ± 0.04	0.05 ± 0.1	0.75	4.74	10.16	1.53
2M16580107+3810235	5952 ± 107	4.24 ± 0.13	4.16	0.07 ± 0.04	0.01 ± 0.1	0.57	4.98	10.97	0.4
2M16590813+3819088	6171 ± 108	4.23 ± 0.15	4.08	-0.03 ± 0.04	-0.1 ± 0.1	0.45	6.44	8.18	1.34
2M16591042-2253578	5994 ± 145	4.13 ± 0.16	4.03	-0.25 ± 0.06	-0.35 ± 0.1	0.17	5.59	8.17	1.4
2M16591534+3931465	5972 ± 125	4.34 ± 0.15	4.25	0.01 ± 0.05	-0.06 ± 0.1	0.46	5.15	9.82	0.37

APOGEE_ID	$T_{\rm eff} \pm \Delta T_{\rm eff}$	$\log g \pm \Delta \log g$	$\log g_{cor}$	$[\mathrm{M/H}] \pm \Delta[\mathrm{M/H}]$	$[Fe/H] \pm \Delta[\mathrm{Fe/H}]$	$\mathrm{v_{mic}}$	$\mathrm{v_{mac}}$	$v \sin i$	χ^2
2M16594003+3606419	5804 ± 120	4.26 ± 0.15	4.21	-0.09 ± 0.05	-0.17 ± 0.1	0.3	4.44	8.96	0.39
2M16594833+6328379	5945 ± 145	4.24 ± 0.18	4.16	-0.01 ± 0.06	-0.08 ± 0.1	0.48	5.03	9.64	0.58
2M17001718+6208206	5780 ± 126	4.28 ± 0.14	4.24	0.07 ± 0.05	0.02 ± 0.1	0.73	4.16	10.18	0.8
2M17001874+3427145	5819 ± 114	4.2 ± 0.14	4.15	-0.04 ± 0.05	-0.08 ± 0.1	0.66	4.47	9.94	0.39
2M17003786+3635532	5781 ± 112	4.3 ± 0.12	4.26	0 ± 0.05	-0.06 ± 0.1	0.52	4.25	9.88	0.44
2M17005252+3852055	5740 ± 135	4.36 ± 0.16	4.33	-0.04 ± 0.06	-0.09 ± 0.1	0.67	4.11	9.16	1.48
2M17014328+3642090	5757 ± 117	4.28 ± 0.13	4.24	-0.21 ± 0.05	-0.28 ± 0.1	0.3	4.38	7.59	1.56
2M17023209+3537465	6075 ± 164	4.25 ± 0.23	4.13	-0.07 ± 0.07	-0.15 ± 0.1	0.33	5.85	8.75	1.47
2M17024128+3617193	5976 ± 142	4.28 ± 0.16	4.19	0.03 ± 0.06	-0.04 ± 0.1	0.65	5.15	9.2	1.55
2M17025276+3505373	5939 ± 96	4.45 ± 0.12	4.37	-0.06 ± 0.04	-0.11 ± 0.1	0.38	5.03	9.28	0.35
2M17030676+3602554	5763 ± 133	4.37 ± 0.15	4.33	-0.02 ± 0.05	-0.07 ± 0.1	0.61	4.18	9.06	0.52
2M17032386+3457577	5812 ± 123	4.21 ± 0.14	4.16	0.15 ± 0.05	0.1 ± 0.1	0.69	4.22	10.75	1.45
2M17033750+3540419	5792 ± 128	4.2 ± 0.14	4.16	-0.03 ± 0.05	-0.1 ± 0.1	0.71	4.34	9.39	0.46
2M17035684+6212263	5945 ± 91	4.39 ± 0.14	4.31	-0.24 ± 0.04	-0.31 ± 0.1	0	5.25	8.85	0.38
2M17042567-2238044	6230 ± 107	4.48 ± 0.1	4.31	0.06 ± 0.04	0 ± 0.1	0.47	6.74	9.61	1.33
2M17044578+3337193	5983 ± 138	4.39 ± 0.17	4.30	0.07 ± 0.05	0.01 ± 0.1	0.62	5.13	10.68	1.58
2M17052315+3300450	4818 ± 74	4.47 ± 0.08	4.69	0.16 ± 0.02	0.14 ± 0.1	0.82	3.49	9.92	2.4
2M17054157+3353112	5692 ± 88	4.3 ± 0.11	4.28	-0.03 ± 0.04	-0.08 ± 0.1	0.8	3.94	8.41	0.43
2M17062973+6334094	5989 ± 168	4.14 ± 0.18	4.05	-0.16 ± 0.07	-0.26 ± 0.1	0.33	5.47	8.35	1.46
2M17064935+3455400	5838 ± 131	4.15 ± 0.15	4.09	0.12 ± 0.05	0.07 ± 0.1	0.83	4.39	10.05	1.58

APOGEE_ID	$T_{\rm eff} \pm \Delta T_{\rm eff}$	$\log g \pm \Delta \log g$	$\log g_{cor}$	$[\rm M/H] \pm \Delta[\rm M/H]$	$[Fe/H] \pm \Delta[\rm Fe/H]$	$v_{\rm mic}$	$v_{\rm mac}$	$v \sin i$	χ^2
2M17064990+3356004	5799 ± 118	4.11 ± 0.14	4.06	-0.26 ± 0.05	-0.36 ± 0.1	0.35	4.64	8.29	1.58
2M17072012+3405369	6070 ± 139	4.35 ± 0.18	4.24	0.07 ± 0.05	-0.01 ± 0.1	0.42	5.65	9.34	0.71
2M17072058+3632469	5544 ± 92	4.33 ± 0.11	4.35	-0.02 ± 0.04	-0.06 ± 0.1	0.93	3.48	10.5	0.4
2M17073037+3405368	5780 ± 116	4.18 ± 0.12	4.14	0.03 ± 0.05	-0.01 ± 0.1	0.77	4.23	10.26	0.96
2M17082566+3228342	5724 ± 92	4.24 ± 0.1	4.21	0.09 ± 0.04	0.05 ± 0.1	0.97	3.93	10.15	1.64
2M17082644+4319291	6024 ± 91	4.44 ± 0.09	4.34	0.06 ± 0.04	0 ± 0.1	0.58	5.37	9.49	1.44
2M17085516+3422316	5804 ± 118	4.2 ± 0.13	4.15	0 ± 0.05	-0.08 ± 0.1	0.44	4.36	9.84	1.53
2M17092554+3545593	5770 ± 125	4.26 ± 0.13	4.22	0.12 ± 0.05	0.08 ± 0.1	0.76	4.07	10.03	1.57
2M17092940+6400463	5947 ± 133	4.13 ± 0.16	4.05	-0.05 ± 0.06	-0.15 ± 0.1	0.57	5.12	9.16	1.41
2M17095026+3248572	5731 ± 148	4.3 ± 0.18	4.27	-0.2 ± 0.06	-0.26 ± 0.1	0.54	4.26	8.98	0.57
2M17101682+6228057	6219 ± 137	4.35 ± 0.18	4.18	0.15 ± 0.05	0.11 ± 0.1	0.73	6.56	9.25	0.43
2M17102459+3441496	5999 ± 168	4.06 ± 0.16	3.96	-0.2 ± 0.07	-0.28 ± 0.1	0.53	5.59	9.7	1.5
2M17102728+3249105	5756 ± 103	4.35 ± 0.12	4.31	0.05 ± 0.04	0.03 ± 0.1	0.82	4.08	9.5	0.57
2M17103670+6329314	5616 ± 92	4.34 ± 0.13	4.34	-0.04 ± 0.04	-0.08 ± 0.1	0.91	3.7	9.07	0.41
2M17103837+5711079	5787 ± 154	4.29 ± 0.2	4.25	-0.23 ± 0.06	-0.34 ± 0.1	0	4.51	7.87	1.97
2M17104728+3259593	6025 ± 132	4.29 ± 0.17	4.19	-0.06 ± 0.05	-0.12 ± 0.1	0.31	5.53	8.26	1.62
2M17111915+3557289	5851 ± 107	4.26 ± 0.14	4.20	0.11 ± 0.04	0.05 ± 0.1	0.76	4.43	10.31	1.44
2M17112436+6402017	5731 ± 123	4.35 ± 0.14	4.32	0.06 ± 0.05	0.03 ± 0.1	0.93	3.97	10.46	0.61
2M17115461+3157469	5585 ± 108	4.3 ± 0.13	4.31	-0.01 ± 0.05	-0.05 ± 0.1	1.05	3.58	9.21	0.54
2M17122569+2802151	5638 ± 79	4.21 ± 0.1	4.20	0.06 ± 0.03	0.01 ± 0.1	0.74	3.67	10.13	0.48

APOGEE_ID	$T_{\rm eff} \pm \Delta T_{\rm eff}$	$\log g \pm \Delta \log g$	$\log g_{cor}$	$[\mathrm{M/H}] \pm \Delta[\mathrm{M/H}]$	$[Fe/H] \pm \Delta[\mathrm{Fe/H}]$	$\mathrm{v}_{\rm mic}$	$\mathrm{v}_{\rm mac}$	$v \sin i$	χ^2
2M17123936+3225546	5836 ± 124	4.11 ± 0.14	4.05	0.15 ± 0.05	0.1 ± 0.1	1.04	4.36	11.04	0.65
2M17124121+5705159	6039 ± 128	4.33 ± 0.16	4.22	0.07 ± 0.05	-0.01 ± 0.1	0.61	5.47	9.68	0.54
2M17124997+3501258	5812 ± 118	4.28 ± 0.14	4.23	0.06 ± 0.05	0.01 ± 0.1	0.75	4.31	9.88	1.49
2M17125124+3306356	5996 ± 160	4.11 ± 0.17	4.01	-0.16 ± 0.07	-0.24 ± 0.1	0.45	5.51	8.31	1.59
2M17125257+3334435	5838 ± 96	4.29 ± 0.12	4.23	0.11 ± 0.04	0.08 ± 0.1	0.7	4.36	9.61	0.52
2M17133003+2734515	5583 ± 103	4.09 ± 0.11	4.10	0.14 ± 0.05	0.11 ± 0.1	0.9	3.46	9.43	1.89
2M17134758+3359269	5929 ± 121	4.16 ± 0.15	4.08	-0.02 ± 0.05	-0.09 ± 0.1	0.65	4.98	9.75	0.45
2M17140148+3523355	5941 ± 130	4.31 ± 0.17	4.23	-0.02 ± 0.05	-0.08 ± 0.1	0.57	5.02	7.41	1.55
2M17140430+3338198	5929 ± 124	4.43 ± 0.17	4.35	-0.14 ± 0.05	-0.19 ± 0.1	0.29	5.06	9.28	0.51
2M17143245+6154048	5760 ± 96	4.2 ± 0.1	4.16	0.09 ± 0.04	0.04 ± 0.1	0.73	4.07	9.16	1.65
2M17150138+3220509	5936 ± 125	4.22 ± 0.15	4.14	0.19 ± 0.05	0.14 ± 0.1	0.7	4.77	9.81	1.7
2M17150712+4436262	5948 ± 80	4.22 ± 0.1	4.14	-0.11 ± 0.03	-0.2 ± 0.1	0.37	5.17	8.42	0.32
2M17152246+3356037	5923 ± 138	4.22 ± 0.2	4.14	-0.06 ± 0.06	-0.13 ± 0.1	0.67	4.98	8.55	1.53
2M17152938+2807234	5737 ± 87	4.21 ± 0.09	4.18	0.12 ± 0.04	0.07 ± 0.1	0.72	3.94	10.23	0.62
2M17153786+3301303	6246 ± 152	4.46 ± 0.16	4.28	-0.05 ± 0.06	-0.12 ± 0.1	0.22	6.98	8.45	0.52
2M17155310-2510260	5962 ± 100	4.33 ± 0.12	4.24	0.04 ± 0.04	-0.01 ± 0.1	0.6	5.05	9.04	1.4
2M17160393+2722291	5996 ± 149	4.26 ± 0.16	4.16	0 ± 0.06	-0.05 ± 0.1	0.27	5.3	9.96	0.64
2M17161967+2837415	5660 ± 127	4.37 ± 0.17	4.36	0.01 ± 0.05	-0.03 ± 0.1	0.63	3.78	10.71	1.67
2M17163318+1440263	5629 ± 125	4.11 ± 0.14	4.11	0.1 ± 0.05	0.04 ± 0.1	0.78	3.63	11.53	1.7
2M17165255+3039159	5545 ± 83	4.15 ± 0.09	4.17	0.13 ± 0.04	0.09 ± 0.1	0.96	3.36	9.7	0.65

APOGEE_ID	$T_{\mathrm{eff}} \pm \Delta T_{\mathrm{eff}}$	$\log g \pm \Delta \log g$	$\log g_{cor}$	$[\mathrm{M/H}] \pm \Delta[\mathrm{M/H}]$	$[Fe/H] \pm \Delta[\mathrm{Fe/H}]$	$\mathrm{v_{mic}}$	$\mathrm{v_{mac}}$	$v \sin i$	χ^2
2M17170079+2601240	5729 ± 108	4.11 ± 0.11	4.08	-0.2 ± 0.05	-0.29 ± 0.1	0.67	4.3	8.52	0.45
2M17170876+2754368	6106 ± 151	4.37 ± 0.22	4.25	-0.03 ± 0.06	-0.1 ± 0.1	0	5.99	7.32	0.57
2M17171520+6056560	5959 ± 137	4.36 ± 0.18	4.27	0.03 ± 0.05	-0.02 ± 0.1	0.54	5.04	9.86	0.57
2M17171896+5635460	5549 ± 106	3.94 ± 0.12	3.96	0.03 ± 0.05	-0.01 ± 0.1	0.84	3.55	9.61	1.68
2M17172738+2601206	5883 ± 149	4.3 ± 0.21	4.23	-0.01 ± 0.06	-0.05 ± 0.1	0.69	4.71	9.28	1.55
2M17175913+5757098	6249 ± 138	4.38 ± 0.18	4.20	-0.05 ± 0.05	-0.12 ± 0.1	0	7	8.42	0.47
2M17183113+5903162	5990 ± 125	4.34 ± 0.15	4.25	0 ± 0.05	-0.05 ± 0.1	0.53	5.25	8.41	1.51
2M17184132+2632290	5777 ± 114	4.25 ± 0.12	4.21	0.09 ± 0.05	0.03 ± 0.1	0.71	4.13	9.21	0.65
2M17190036+3059061	5702 ± 126	4.36 ± 0.15	4.34	0 ± 0.05	-0.03 ± 0.1	0.7	3.94	10.13	0.53
2M17190378+6103030	5767 ± 127	4.24 ± 0.15	4.20	-0.07 ± 0.05	-0.16 ± 0.1	0.72	4.28	9.45	0.66
2M17192087+6107028	5802 ± 114	4.19 ± 0.14	4.14	-0.32 ± 0.05	-0.43 ± 0.1	0	4.68	8.19	1.36
2M17194638+0633135	5403 ± 171	3.95 ± 0.24	4.00	-0.24 ± 0.08	-0.3 ± 0.1	0.71	3.55	10.72	1.59
2M17194742+5637151	5748 ± 84	4.18 ± 0.08	4.15	0.09 ± 0.03	0.03 ± 0.1	0.74	4.03	9.35	1.54
2M17200014-0801231	5616 ± 203	4.18 ± 0.27	4.18	-0.21 ± 0.09	-0.31 ± 0.1	0.59	3.91	9.68	1.56
2M17200170+5939381	6056 ± 112	4.34 ± 0.15	4.23	0.1 ± 0.04	0.04 ± 0.1	0.65	5.53	10.36	1.56
2M17200760+5553177	5933 ± 106	4.3 ± 0.14	4.22	0.02 ± 0.04	-0.03 ± 0.1	0.61	4.93	10.27	0.46
2M17203955+3228056	5714 ± 200	4.24 ± 0.24	4.22	-0.08 ± 0.09	-0.21 ± 0.1	0.01	4.08	7.18	5.61
2M17211195+3222193	5934 ± 142	4.26 ± 0.2	4.18	-0.08 ± 0.06	-0.14 ± 0.1	0.48	5.05	8.91	1.44
2M17212728+2656360	5800 ± 67	4.19 ± 0.07	4.14	0.01 ± 0.03	-0.05 ± 0.1	0.54	4.33	9.73	1.49
2M17213207+2822561	5713 ± 111	4.18 ± 0.12	4.16	0.14 ± 0.05	0.09 ± 0.1	0.75	3.84	10.34	1.52

APOGEE_ID	$T_{\rm eff} \pm \Delta T_{\rm eff}$	$\log g \pm \Delta \log g$	$\log g_{cor}$	$[\rm M/H] \pm \Delta[\rm M/H]$	$[Fe/H] \pm \Delta[\rm Fe/H]$	$\rm v_{mic}$	$\rm v_{mac}$	$v \sin i$	χ^2
2M17214034+3147556	5897 ± 129	4.03 ± 0.15	3.96	0.07 ± 0.05	0.02 ± 0.1	0.92	4.76	10.4	0.41
2M17215621+2640260	5882 ± 103	4.18 ± 0.13	4.11	0.17 ± 0.04	0.12 ± 0.1	0.79	4.53	9.55	0.57
2M17220566+5827227	5975 ± 151	4.15 ± 0.18	4.06	-0.09 ± 0.06	-0.18 ± 0.1	0.56	5.31	8.08	0.58
2M17222719+2724012	5898 ± 138	4.23 ± 0.19	4.16	0.01 ± 0.06	-0.03 ± 0.1	0.69	4.77	9.93	0.58
2M17224415+2807395	5564 ± 99	4.21 ± 0.11	4.22	0.01 ± 0.04	-0.03 ± 0.1	0.77	3.52	11	1.53
2M17224713+6017065	5899 ± 113	4.16 ± 0.15	4.09	0.08 ± 0.05	0.05 ± 0.1	0.79	4.72	10.01	1.71
2M17231323+5948363	5728 ± 139	4.38 ± 0.18	4.35	-0.13 ± 0.06	-0.19 ± 0.1	0.49	4.16	9.4	0.57
2M17240743+6041540	5691 ± 136	4.08 ± 0.16	4.06	-0.28 ± 0.06	-0.37 ± 0.1	0.49	4.25	7.3	0.67
2M17241676+2707195	5725 ± 114	4.18 ± 0.12	4.15	0.11 ± 0.05	0.07 ± 0.1	0.75	3.93	9.64	1.78
2M17241852+6221028	5940 ± 130	4.4 ± 0.18	4.32	-0.02 ± 0.05	-0.09 ± 0.1	0.49	5	9.91	1.5
2M17241955+6013348	6071 ± 152	4.43 ± 0.18	4.32	0.01 ± 0.06	-0.07 ± 0.1	0.44	5.72	10.15	1.53
2M17242804+6225480	5803 ± 99	4.36 ± 0.12	4.31	0.02 ± 0.04	-0.05 ± 0.1	0.61	4.3	8.71	1.43
2M17243667+5704407	5884 ± 135	4.24 ± 0.2	4.17	-0.05 ± 0.06	-0.13 ± 0.1	0.57	4.77	8.01	0.64
2M17251533+5835085	5680 ± 120	4.26 ± 0.14	4.24	0.04 ± 0.05	-0.02 ± 0.1	0.58	3.82	9.66	0.77
2M17253297+5658354	5496 ± 118	4.42 ± 0.12	4.45	-0.02 ± 0.05	-0.03 ± 0.1	1.54	3.37	6.81	0.74
2M17253510+6033050	6038 ± 137	4.27 ± 0.18	4.16	-0.09 ± 0.06	-0.16 ± 0.1	0.48	5.64	8.92	0.62
2M17270288+6044532	5704 ± 85	4.03 ± 0.08	4.01	0.03 ± 0.04	0 ± 0.1	0.86	3.98	9.95	0.45
2M17271950+6056173	5948 ± 115	4.13 ± 0.14	4.05	-0.17 ± 0.05	-0.25 ± 0.1	0.35	5.25	8	1.51
2M17272235+5947125	5984 ± 116	4.05 ± 0.12	3.96	-0.19 ± 0.05	-0.27 ± 0.1	0.54	5.49	7.67	0.44
2M17273105+5611057	5736 ± 121	4.12 ± 0.13	4.09	-0.07 ± 0.05	-0.12 ± 0.1	0.56	4.18	9.99	1.35

APOGEE_ID	$T_{\rm eff} \pm \Delta T_{\rm eff}$	$\log g \pm \Delta \log g$	$\log g_{cor}$	$[\rm M/H] \pm \Delta[\rm M/H]$	$[Fe/H] \pm \Delta[\rm Fe/H]$	$\rm v_{mic}$	$\rm v_{mac}$	$v \sin i$	χ^2
2M17275642+5650548	5981 ± 159	4.31 ± 0.21	4.22	-0.11 ± 0.06	-0.18 ± 0.1	0.42	5.33	8.69	0.56
2M17283135+5714249	5755 ± 104	4.22 ± 0.1	4.19	0.03 ± 0.04	-0.01 ± 0.1	0.74	4.12	10.54	0.45
2M17284162+5649339	5781 ± 130	4.11 ± 0.13	4.07	-0.03 ± 0.05	-0.09 ± 0.1	0.79	4.31	8.83	0.78
2M17284365+5655308	5885 ± 94	4.18 ± 0.12	4.11	0.13 ± 0.04	0.08 ± 0.1	0.76	4.59	10.18	1.45
2M17284995-2643469	5895 ± 60	4.2 ± 0.08	4.13	0.16 ± 0.02	0.1 ± 0.1	0.62	4.59	10.57	1.36
2M17291306+5955202	5832 ± 72	4.15 ± 0.08	4.10	0.19 ± 0.03	0.14 ± 0.1	0.83	4.27	9.68	0.54
2M17295429+5540400	5870 ± 104	4.27 ± 0.14	4.21	0.2 ± 0.04	0.16 ± 0.1	0.84	4.41	9.56	1.62
2M17301639+4724078	5426 ± 173	4.43 ± 0.23	4.48	-0.31 ± 0.07	-0.38 ± 0.1	0.7	3.54	8.82	1.47
2M17310734+6145012	5912 ± 125	4.06 ± 0.15	3.99	0.04 ± 0.05	0 ± 0.1	0.99	4.86	11.03	0.53
2M17312022-2603207	5666 ± 96	4.42 ± 0.13	4.41	-0.08 ± 0.04	-0.13 ± 0.1	0.57	3.89	9.7	1.36
2M17323969-2427453	5533 ± 107	3.93 ± 0.12	3.95	0.04 ± 0.05	0.01 ± 0.1	0.86	3.5	10.1	1.89
2M17332914-2404177	5741 ± 75	4.21 ± 0.08	4.18	-0.16 ± 0.03	-0.24 ± 0.1	0.35	4.28	8.39	1.43
2M17333076+5805168	5866 ± 141	4.35 ± 0.22	4.29	-0.21 ± 0.06	-0.29 ± 0.1	0.25	4.84	8.9	0.52
2M17333838+5713306	5747 ± 127	4.01 ± 0.11	3.98	0.02 ± 0.05	-0.03 ± 0.1	0.79	4.16	9.22	0.71
2M17352178-2317502	5639 ± 104	4.31 ± 0.14	4.30	0.04 ± 0.04	0 ± 0.1	0.93	3.68	10.28	0.63
2M17352320+5645525	5691 ± 118	4.06 ± 0.12	4.04	0.06 ± 0.05	0.02 ± 0.1	0.9	3.89	9.83	0.68
2M17355861+5636516	5825 ± 122	4.27 ± 0.15	4.22	0.05 ± 0.05	0 ± 0.1	0.52	4.38	9.72	1.48
2M17371386+5618421	5684 ± 121	4.01 ± 0.12	3.99	-0.04 ± 0.05	-0.09 ± 0.1	0.7	4	9.51	1.65
2M17371612-2435356	6018 ± 77	4.36 ± 0.1	4.26	-0.06 ± 0.03	-0.13 ± 0.1	0.42	5.48	9.76	0.37
2M17373753+5654037	5675 ± 110	4.11 ± 0.12	4.10	0.14 ± 0.05	0.1 ± 0.1	0.84	3.73	9.5	0.76

APOGEE_ID	$T_{\rm eff} \pm \Delta T_{\rm eff}$	$\log g \pm \Delta \log g$	$\log g_{cor}$	$[\rm M/H] \pm \Delta[\rm M/H]$	$[Fe/H] \pm \Delta[\rm Fe/H]$	$v_{\rm mic}$	$v_{\rm mac}$	$v \sin i$	χ^2
2M17391670+5715273	5746 ± 135	4.16 ± 0.13	4.13	0 ± 0.05	-0.07 ± 0.1	0.71	4.13	9.34	1.67
2M17394822-0628445	6071 ± 69	4.37 ± 0.09	4.26	0.06 ± 0.03	0 ± 0.1	0.56	5.66	9.17	0.34
2M17400077+5711407	5831 ± 121	4.17 ± 0.14	4.12	0.14 ± 0.05	0.1 ± 0.1	1.05	4.33	10.26	0.8
2M17422861-2546393	5993 ± 104	4.33 ± 0.12	4.24	0.07 ± 0.04	0.01 ± 0.1	0.68	5.2	8.94	0.5
2M17452041-2207124	5714 ± 96	4.25 ± 0.11	4.23	-0.02 ± 0.04	-0.07 ± 0.1	0.74	4.01	9.51	1.27
2M17454448-0543381	5959 ± 79	4.29 ± 0.1	4.20	-0.03 ± 0.03	-0.09 ± 0.1	0.55	5.12	9.08	0.39
2M17475035-0553029	5779 ± 82	4.38 ± 0.1	4.34	0.01 ± 0.03	-0.02 ± 0.1	0.67	4.21	10.19	1.39
2M17490139-2300435	5844 ± 131	3.99 ± 0.14	3.93	-0.02 ± 0.05	-0.08 ± 0.1	0.69	4.62	9.64	1.39
2M17534729+7309326	5802 ± 133	4.07 ± 0.15	4.02	-0.13 ± 0.06	-0.21 ± 0.1	0.56	4.53	8.38	1.35
2M17541836-2557434	5974 ± 77	4.32 ± 0.1	4.23	-0.09 ± 0.03	-0.17 ± 0.1	0.49	5.27	8.84	0.36
2M17553796-2510469	5823 ± 88	4.24 ± 0.11	4.19	0.1 ± 0.04	0.05 ± 0.1	0.76	4.31	8.86	1.52
2M17554007-2520348	6091 ± 156	4.33 ± 0.24	4.21	-0.05 ± 0.06	-0.15 ± 0.1	0.36	5.92	8.49	0.5
2M18050591-0917375	6192 ± 70	4.46 ± 0.08	4.30	0.08 ± 0.03	0.03 ± 0.1	0.52	6.44	8.65	0.34
2M18060522-0803271	5665 ± 53	4.34 ± 0.07	4.33	0.03 ± 0.02	0 ± 0.1	0.85	3.77	10.95	0.39
2M18134289-2707380	5898 ± 120	4.23 ± 0.16	4.16	0.03 ± 0.05	-0.04 ± 0.1	0.51	4.75	9.25	0.54
2M18212638-0816575	5806 ± 95	4.24 ± 0.11	4.19	-0.01 ± 0.04	-0.08 ± 0.1	0.5	4.37	9.67	1.37
2M18242517-0806376	6069 ± 123	4.33 ± 0.16	4.22	0.09 ± 0.05	0.04 ± 0.1	0.72	5.63	9.83	1.39
2M18254965-0338180	5924 ± 92	4.38 ± 0.13	4.30	0.04 ± 0.04	0.01 ± 0.1	0.79	4.85	9.95	1.47
2M18255215-0412080	6044 ± 92	4.26 ± 0.11	4.15	0.06 ± 0.04	0.01 ± 0.1	0.73	5.52	10.16	1.28
2M18263773+4605014	5804 ± 185	4.22 ± 0.23	4.17	-0.21 ± 0.08	-0.31 ± 0.1	0.3	4.58	8.59	1.54

APOGEE_ID	$T_{\text{eff}} \pm \Delta T_{\text{eff}}$	$\log g \pm \Delta \log g$	$\log g_{cor}$	$[\text{M/H}] \pm \Delta[\text{M/H}]$	$[Fe/H] \pm \Delta[\text{Fe/H}]$	v_{mic}	v_{mac}	$v \sin i$	χ^2
2M18264183-0309278	5805 ± 89	4.26 ± 0.1	4.21	0 ± 0.04	-0.06 ± 0.1	0.69	4.35	9.48	0.38
2M18273796-0356132	5923 ± 63	4.23 ± 0.08	4.15	0.16 ± 0.03	0.12 ± 0.1	0.91	4.73	9.71	1.44
2M18282635-0235474	5985 ± 116	4.29 ± 0.15	4.20	-0.06 ± 0.05	-0.14 ± 0.1	0.47	5.3	8.96	1.34
2M18301883-0850133	6134 ± 136	4.31 ± 0.22	4.18	-0.12 ± 0.05	-0.21 ± 0.1	0.18	6.27	7.82	1.4
2M18302365-0236454	6040 ± 91	4.28 ± 0.12	4.17	-0.15 ± 0.04	-0.23 ± 0.1	0.35	5.72	7.84	1.34
2M18311544-0313388	5802 ± 125	4.29 ± 0.15	4.24	-0.02 ± 0.05	-0.08 ± 0.1	0.71	4.35	8.23	0.52
2M18314974-0925516	5928 ± 133	4.37 ± 0.18	4.29	0.05 ± 0.05	-0.01 ± 0.1	0.48	4.86	10.48	1.47
2M18420034+4749499	6162 ± 150	4.41 ± 0.22	4.27	0.01 ± 0.06	-0.05 ± 0.1	0.44	6.31	9.31	0.36
2M18430881+0612150	5605 ± 159	4.33 ± 0.21	4.33	-0.02 ± 0.07	-0.07 ± 0.1	0.89	3.65	8.3	1.67
2M18431321+4739461	6178 ± 139	4.32 ± 0.19	4.17	0.09 ± 0.05	0.03 ± 0.1	0.73	6.34	10.98	0.41
2M18434242+4756159	6182 ± 96	4.55 ± 0.1	4.40	0.16 ± 0.04	0.12 ± 0.1	0.76	6.28	9.93	1.51
2M18434242+4756159	6198 ± 94	4.57 ± 0.1	4.41	0.19 ± 0.04	0.12 ± 0.1	0.72	6.36	10.12	1.53
2M18441281+4332024	4886 ± 33	3.6 ± 0.04	3.60	0.36 ± 0.02	0.26 ± 0.1	0.75	3.75	9.36	2.37
2M18441761+4427271	5569 ± 118	4.27 ± 0.14	4.28	-0.03 ± 0.05	-0.07 ± 0.1	1.14	3.57	9.91	0.55
2M18443906+4756189	5639 ± 115	4.26 ± 0.15	4.25	0.11 ± 0.05	0.08 ± 0.1	0.84	3.61	10.07	1.72
2M18444161+4743513	6045 ± 136	4.24 ± 0.16	4.13	0.17 ± 0.05	0.11 ± 0.1	0.78	5.4	11.09	1.73
2M18444581+4357493	5998 ± 113	4.11 ± 0.12	4.01	-0.16 ± 0.05	-0.25 ± 0.1	0.23	5.52	8.48	1.41
2M18444674+4729496	4700 ± 68	4.51 ± 0.08	4.77	0.43 ± 0.02	0.38 ± 0.1	1.2	3.63	8.19	2.18
2M18450550+4746278	5957 ± 144	4.4 ± 0.2	4.31	-0.04 ± 0.06	-0.1 ± 0.1	0.36	5.11	10.53	0.42
2M18450550+4746278	5962 ± 135	4.4 ± 0.19	4.31	-0.03 ± 0.06	-0.1 ± 0.1	0.36	5.13	10.51	0.42

APOGEE_ID	$T_{\rm eff} \pm \Delta T_{\rm eff}$	$\log g \pm \Delta \log g$	$\log g_{cor}$	$[\rm M/H] \pm \Delta[\rm M/H]$	$[Fe/H] \pm \Delta[\rm Fe/H]$	$\rm v_{mic}$	$\rm v_{mac}$	$v \sin i$	χ^2
2M18450571+4746278	5903 ± 157	4.2 ± 0.22	4.13	-0.02 ± 0.07	-0.09 ± 0.1	0.64	4.84	9.68	0.39
2M18451180+4353502	5640 ± 104	3.95 ± 0.13	3.94	0.12 ± 0.04	0.07 ± 0.1	0.86	3.7	10.46	1.65
2M18451745+4320226	5739 ± 141	4.35 ± 0.16	4.32	-0.04 ± 0.06	-0.09 ± 0.1	0.56	4.11	9.63	0.68
2M18454750+4804570	6647 ± 167	4.43 ± 0.22	4.08	0.04 ± 0.06	-0.04 ± 0.1	1.04	10.46	9.49	0.19
2M18455585+4712289	4839 ± 101	4.38 ± 0.15	4.60	0.06 ± 0.04	0.05 ± 0.1	1.35	3.48	9.44	1.95
2M18470215+4659058	5738 ± 108	4.28 ± 0.11	4.25	0.1 ± 0.04	0.05 ± 0.1	0.71	3.97	9.12	0.59
2M18471337+4734341	5956 ± 139	4.05 ± 0.14	3.96	0.02 ± 0.05	-0.06 ± 0.1	0.76	5.12	8.94	0.52
2M18472606+4404271	5725 ± 138	4.35 ± 0.17	4.32	-0.06 ± 0.06	-0.13 ± 0.1	0.54	4.09	9.91	0.53
2M18474359+4736256	5804 ± 125	4.29 ± 0.15	4.24	0.1 ± 0.05	0.05 ± 0.1	0.84	4.23	10.05	0.66
2M18480170+4221121	5722 ± 98	4.2 ± 0.11	4.17	0.12 ± 0.04	0.08 ± 0.1	0.82	3.89	9.99	1.6
2M18480343+4351395	5623 ± 96	4.14 ± 0.11	4.14	0.08 ± 0.04	0.04 ± 0.1	0.79	3.63	9.86	1.5
2M18482606+4347402	5734 ± 132	4.36 ± 0.16	4.33	-0.07 ± 0.06	-0.13 ± 0.1	0.44	4.12	8.52	0.54
2M18484675+4631224	5981 ± 90	4.43 ± 0.1	4.34	0.02 ± 0.04	-0.02 ± 0.1	0.59	5.17	10.64	1.2
2M18485085+4734372	5868 ± 130	4.14 ± 0.16	4.08	0.15 ± 0.05	0.1 ± 0.1	0.8	4.49	9.94	1.32
2M18490196+4359119	5554 ± 98	4.22 ± 0.11	4.24	0.1 ± 0.04	0.07 ± 0.1	0.85	3.39	10.1	1.76
2M18491057+4443175	5657 ± 107	4.29 ± 0.14	4.28	0.05 ± 0.05	0.01 ± 0.1	0.69	3.73	10.53	0.46
2M18493364+4742398	6001 ± 169	4.22 ± 0.18	4.12	-0.01 ± 0.07	-0.09 ± 0.1	0.83	5.35	9.44	0.37
2M18495099+4607438	5771 ± 117	4.15 ± 0.12	4.11	0.16 ± 0.05	0.12 ± 0.1	0.9	4.05	9.87	1.7
2M18495813+4358487	6128 ± 155	4.19 ± 0.2	4.06	0 ± 0.06	-0.08 ± 0.1	0.68	6.13	8.93	0.32
2M18503104+4335103	5678 ± 81	4.31 ± 0.1	4.29	0.05 ± 0.03	0.02 ± 0.1	0.71	3.8	10.78	1.48

APOGEE_ID	$T_{\text{eff}} \pm \Delta T_{\text{eff}}$	$\log g \pm \Delta \log g$	$\log g_{cor}$	$[\text{M/H}] \pm \Delta[\text{M/H}]$	$[Fe/H] \pm \Delta[\text{Fe/H}]$	v_{mic}	v_{mac}	$v \sin i$	χ^2
2M18503111+4619240	5837 ± 172	4.29 ± 0.22	4.23	0.14 ± 0.07	0.1 ± 0.1	0.79	4.33	9.79	0.87
2M18503522+4603190	5654 ± 103	4.28 ± 0.14	4.27	0.02 ± 0.04	-0.02 ± 0.1	0.76	3.76	9.83	0.45
2M18504673+4716036	5648 ± 112	4.3 ± 0.16	4.29	-0.02 ± 0.05	-0.07 ± 0.1	0.78	3.78	9.35	1.56
2M18504878+4629527	5669 ± 124	4.37 ± 0.19	4.36	-0.07 ± 0.05	-0.12 ± 0.1	0.63	3.9	8.91	0.45
2M18513961+4338099	5282 ± 67	4.16 ± 0.07	4.24	-0.18 ± 0.03	-0.28 ± 0.1	0.62	3.3	9.12	1.58
2M18514438+4323297	6344 ± 139	4.4 ± 0.19	4.18	0.18 ± 0.05	0.08 ± 0.1	1.05	7.49	11.09	1.26
2M18522007+4832098	5780 ± 100	4.07 ± 0.1	4.03	-0.03 ± 0.04	-0.09 ± 0.1	0.77	4.32	9.18	1.36
2M18523616+4508233	6313 ± 164	4.2 ± 0.2	3.99	0 ± 0.06	-0.1 ± 0.1	1.49	7.48	12.22	1.17
2M18524681+4640335	5942 ± 149	4.16 ± 0.19	4.08	-0.09 ± 0.06	-0.15 ± 0.1	0.56	5.12	8.16	1.46
2M18525653+4636364	6043 ± 147	4.42 ± 0.17	4.31	0.02 ± 0.06	-0.02 ± 0.1	0.51	5.53	10.35	1.58
2M18534999-3025169	5875 ± 129	4.37 ± 0.19	4.30	0.08 ± 0.05	0.03 ± 0.1	0.62	4.56	10.98	1.49
2M18535093+4353217	5804 ± 118	4.13 ± 0.12	4.08	0.13 ± 0.05	0.08 ± 0.1	0.64	4.23	10.48	1.58
2M18535961+4716186	6190 ± 141	4.42 ± 0.18	4.26	0.13 ± 0.06	0.08 ± 0.1	0.51	6.38	10.48	0.41
2M18540460+4541515	6248 ± 99	4.41 ± 0.12	4.23	0.21 ± 0.04	0.16 ± 0.1	0.67	6.7	10.3	0.44
2M18544828+4913408	6085 ± 126	4.28 ± 0.16	4.16	0.16 ± 0.05	0.1 ± 0.1	0.66	5.64	10.57	0.49
2M18545124+4436562	5548 ± 104	4.37 ± 0.13	4.39	-0.09 ± 0.04	-0.15 ± 0.1	0.48	3.57	8.75	0.53
2M18545124+4436562	5583 ± 108	4.33 ± 0.15	4.34	-0.15 ± 0.05	-0.15 ± 0.1	0.6	3.73	8.98	0.45
2M18545324+4029307	5688 ± 91	4.19 ± 0.1	4.17	0.15 ± 0.04	0.1 ± 0.1	0.76	3.74	10.08	0.88
2M18545588+4046311	5807 ± 92	4.17 ± 0.1	4.12	0.08 ± 0.04	0.03 ± 0.1	0.68	4.29	9.86	0.47
2M18545588+4046311	5807 ± 92	4.17 ± 0.1	4.12	0.08 ± 0.04	0.03 ± 0.1	0.69	4.29	9.88	0.47

APOGEE_ID	$T_{\rm eff} \pm \Delta T_{\rm eff}$	$\log g \pm \Delta \log g$	$\log g_{cor}$	$[\mathrm{M/H}] \pm \Delta[\mathrm{M/H}]$	$[Fe/H] \pm \Delta[\mathrm{Fe/H}]$	v$_{\rm mic}$	v$_{\rm mac}$	$v \sin i$	χ^2
2M18561431+4431052	5476 ± 92	4.43 ± 0.1	4.47	-0.25 ± 0.04	-0.28 ± 0.1	0.7	3.57	10.42	1.3
2M18562126+4530531	6011 ± 82	4.27 ± 0.09	4.17	0.07 ± 0.03	0.01 ± 0.1	0.9	5.31	9.68	1.34
2M18562126+4530531	6037 ± 80	4.39 ± 0.1	4.28	0.1 ± 0.03	0.01 ± 0.1	0.63	5.41	9.8	1.36
2M18562213+4530252	6448 ± 72	4.34 ± 0.1	4.08	0.11 ± 0.03	0.07 ± 0.1	1.02	8.46	9.57	1.19
2M18563059-3053422	5772 ± 68	4.17 ± 0.08	4.13	-0.15 ± 0.03	-0.22 ± 0.1	0.68	4.4	8.5	1.37
2M18563663+4739230	5977 ± 97	4.23 ± 0.11	4.14	-0.01 ± 0.04	-0.07 ± 0.1	0.95	5.22	10.57	1.35
2M18565615+4047403	5967 ± 130	4.28 ± 0.16	4.19	0.01 ± 0.05	-0.06 ± 0.1	0.46	5.13	10.68	1.36
2M18572332+4611030	5929 ± 93	4.12 ± 0.12	4.04	-0.09 ± 0.04	-0.18 ± 0.1	0.49	5.06	9.26	0.29
2M18572332+4611030	5929 ± 93	4.12 ± 0.12	4.04	-0.09 ± 0.04	-0.18 ± 0.1	0.49	5.07	9.17	0.29
2M18572932+4526522	6246 ± 142	4.29 ± 0.16	4.11	0.08 ± 0.05	0.01 ± 0.1	0.67	6.85	8.68	1.44
2M18574324+4435558	4898 ± 119	3.44 ± 0.17	3.44	-0.16 ± 0.06	-0.26 ± 0.1	1.13	3.73	14.73	1.73
2M18575331+3954425	5596 ± 114	4.26 ± 0.14	4.27	0.05 ± 0.05	0.03 ± 0.1	0.71	3.56	9.62	0.58
2M18575331+3954425	5593 ± 114	4.26 ± 0.14	4.27	0.05 ± 0.05	0.03 ± 0.1	0.71	3.55	9.61	0.58
2M18575579+4423529	5661 ± 131	4.16 ± 0.16	4.15	0.17 ± 0.06	0.12 ± 0.1	1.02	3.63	0.06	1.75
2M18580944+4356091	5997 ± 150	4.29 ± 0.18	4.19	-0.13 ± 0.06	-0.18 ± 0.1	0	5.44	8.82	0.5
2M18581163+4529514	5003 ± 87	3.52 ± 0.08	3.52	-0.01 ± 0.04	-0.08 ± 0.1	0.87	3.59	9.18	1.65
2M18582199+4138213	5671 ± 107	4.29 ± 0.13	4.28	0.06 ± 0.05	0.01 ± 0.1	0.69	3.77	10.11	0.43
2M18583986+4547476	5773 ± 125	4.17 ± 0.14	4.13	-0.21 ± 0.05	-0.32 ± 0.1	0.4	4.46	8.11	1.36
2M18590109+4915197	5797 ± 116	4.29 ± 0.13	4.24	0 ± 0.05	-0.06 ± 0.1	0.74	4.31	8.91	1.4
2M18590801+4540561	5720 ± 94	4.17 ± 0.11	4.14	-0.05 ± 0.04	-0.12 ± 0.1	0.65	4.09	9.81	1.25

APOGEE_ID	$T_{\rm eff} \pm \Delta T_{\rm eff}$	$\log g \pm \Delta \log g$	$\log g_{cor}$	$[\mathrm{M/H}] \pm \Delta[\mathrm{M/H}]$	$[Fe/H] \pm \Delta[\mathrm{Fe/H}]$	$\mathrm{v_{mic}}$	$\mathrm{v_{mac}}$	$v \sin i$	χ^2
2M18590868+4825236	5988 ± 98	4.06 ± 0.1	3.97	-0.11 ± 0.04	-0.18 ± 0.1	0.69	5.43	9.14	1.54
2M18590868+4825236	5988 ± 96	4.17 ± 0.11	4.08	-0.08 ± 0.04	-0.18 ± 0.1	0.42	5.37	9.02	1.63
2M18590984+4617058	5241 ± 88	3.69 ± 0.1	3.69	-0.29 ± 0.04	-0.36 ± 0.1	0.72	3.61	9.58	1.39
2M18591050+4457017	6141 ± 112	4.17 ± 0.15	4.04	0.12 ± 0.04	0.1 ± 0.1	1.08	6.09	8.97	1.33
2M18591050+4457017	6164 ± 110	4.28 ± 0.16	4.14	0.16 ± 0.04	0.1 ± 0.1	0.84	6.17	9.09	1.38
2M18591193+3859313	6015 ± 126	4.36 ± 0.16	4.26	-0.04 ± 0.05	-0.13 ± 0.1	0.24	5.45	8.54	0.37
2M18591344+4353427	5791 ± 91	4.24 ± 0.1	4.20	0.15 ± 0.04	0.11 ± 0.1	0.88	4.13	9.91	1.45
2M18595370+3903130	5714 ± 132	4 ± 0.12	3.98	0.02 ± 0.06	-0.04 ± 0.1	0.76	4.04	10.99	0.5
2M19000694+4401450	6187 ± 117	4.41 ± 0.16	4.26	0.08 ± 0.05	0.02 ± 0.1	0.62	6.41	8.78	1.26
2M19004297+3834248	6364 ± 184	4.32 ± 0.25	4.09	0.15 ± 0.07	-0.11 ± 0.1	1.09	7.7	24.34	0.26
2M19004979+4523036	5294 ± 109	4.36 ± 0.13	4.44	0.07 ± 0.05	0.03 ± 0.1	0.85	3.01	11.02	0.84
2M19005082+4601169	5684 ± 99	4.17 ± 0.11	4.15	0.16 ± 0.04	0.1 ± 0.1	0.78	3.72	10.43	1.37
2M19005237+4448030	5965 ± 159	4.26 ± 0.2	4.17	-0.17 ± 0.06	-0.23 ± 0.1	0	5.32	7.98	0.6
2M19005694+3939590	5963 ± 105	4.22 ± 0.12	4.13	0.14 ± 0.04	0.07 ± 0.1	0.77	4.97	9.99	0.48
2M19010575+4751448	5712 ± 128	4.35 ± 0.15	4.33	0.02 ± 0.05	-0.02 ± 0.1	0.74	3.95	10.33	0.51
2M19011779+4559405	5680 ± 100	4.14 ± 0.11	4.12	0.11 ± 0.04	0.06 ± 0.1	0.82	3.77	10.4	1.36
2M19012502+4823156	5779 ± 112	4.21 ± 0.12	4.17	0.22 ± 0.05	0.17 ± 0.1	0.78	3.99	10.17	1.58
2M19013056+3838212	5331 ± 116	3.89 ± 0.16	3.96	0.07 ± 0.05	0.01 ± 0.1	1.12	3.17	11.29	1.8
2M19013272+4925423	6255 ± 167	4.4 ± 0.23	4.22	-0.05 ± 0.07	-0.14 ± 0.1	0.35	7.05	8.39	0.45
2M19015856+4306084	5819 ± 139	4.06 ± 0.14	4.01	0.04 ± 0.06	-0.03 ± 0.1	0.76	4.42	9.21	1.67

APOGEE_ID	$T_{\rm eff} \pm \Delta T_{\rm eff}$	$\log g \pm \Delta \log g$	$\log g_{cor}$	$[\mathrm{M/H}] \pm \Delta[\mathrm{M/H}]$	$[Fe/H] \pm \Delta[\mathrm{Fe/H}]$	$v_{\rm mic}$	$v_{\rm mac}$	$v \sin i$	χ^2
2M19020990+4516393	5738 ± 86	4.25 ± 0.1	4.22	-0.08 ± 0.04	-0.18 ± 0.1	0.62	4.17	8.58	1.32
2M19020990+4516393	5733 ± 86	4.23 ± 0.1	4.20	-0.08 ± 0.04	-0.18 ± 0.1	0.6	4.16	9.4	1.32
2M19021130+3903478	6292 ± 118	4.4 ± 0.16	4.20	0.17 ± 0.05	0.12 ± 0.1	0.68	7.09	10.17	1.61
2M19022137+4036188	6618 ± 203	4.34 ± 0.29	4.00	-0.03 ± 0.08	-0.07 ± 0.1	0.98	10.24	9.13	0.26
2M19022736+4750165	5957 ± 116	4.2 ± 0.13	4.11	0.14 ± 0.05	0.08 ± 0.1	0.78	4.94	9	1.35
2M19022767+5008087	5784 ± 159	4.18 ± 0.17	4.14	0.1 ± 0.07	0.06 ± 0.1	0.86	4.17	10.72	1.78
2M19024182+4525407	5831 ± 134	4.29 ± 0.17	4.24	0.05 ± 0.05	0 ± 0.1	0.66	4.41	11.34	1.73
2M19024305+5014286	5704 ± 132	4.34 ± 0.18	4.32	-0.07 ± 0.06	-0.15 ± 0.1	0.7	4.01	9.78	1.42
2M19024305+5014286	5702 ± 133	4.35 ± 0.18	4.33	-0.07 ± 0.06	-0.15 ± 0.1	0.72	4.01	9.17	1.42
2M19030407+4521428	5998 ± 120	4.29 ± 0.13	4.19	0.09 ± 0.05	0.02 ± 0.1	0.48	5.21	9.66	1.62
2M19032464+4312516	5909 ± 116	4.16 ± 0.15	4.09	0.09 ± 0.05	0.02 ± 0.1	0.7	4.76	9.38	1.49
2M19033745+4917150	5767 ± 141	4.21 ± 0.14	4.17	0.02 ± 0.06	-0.06 ± 0.1	0.5	4.18	10.79	0.52
2M19034610+4939394	6082 ± 164	4.27 ± 0.23	4.15	-0.16 ± 0.07	-0.26 ± 0.1	0	5.98	8.74	1.44
2M19034959+4606581	5899 ± 161	4.36 ± 0.24	4.29	-0.01 ± 0.07	-0.07 ± 0.1	0.18	4.78	8.45	0.59
2M19040185+4758435	5934 ± 123	4.34 ± 0.18	4.26	-0.06 ± 0.05	-0.13 ± 0.1	0.43	5.02	8.59	1.46
2M19040240+3900587	5692 ± 112	4.31 ± 0.14	4.29	-0.01 ± 0.05	-0.02 ± 0.1	1.22	3.92	7.59	0.58
2M19040872+4936522	5385 ± 112	4.35 ± 0.16	4.41	0.4 ± 0.05	0.33 ± 0.1	0.8	2.69	9.05	2.34
2M19050419+4649438	6028 ± 142	4.28 ± 0.18	4.18	-0.05 ± 0.06	-0.12 ± 0.1	0.51	5.53	8.81	0.46
2M19051549+4327454	6053 ± 102	4.28 ± 0.13	4.17	0.13 ± 0.04	0.07 ± 0.1	0.83	5.49	9.18	0.44
2M19052120+4844387	5858 ± 134	4.21 ± 0.17	4.15	0.11 ± 0.06	0.07 ± 0.1	0.79	4.47	10.75	1.56

APOGEE_ID	$T_{\rm eff} \pm \Delta T_{\rm eff}$	$\log g \pm \Delta \log g$	$\log g_{cor}$	$[\rm M/H] \pm \Delta[\rm M/H]$	$[Fe/H] \pm \Delta[\rm Fe/H]$	$\rm v_{mic}$	$\rm v_{mac}$	$v \sin i$	χ^2
2M19053499+4304329	5754 ± 133	4.2 ± 0.15	4.17	-0.22 ± 0.06	-0.33 ± 0.1	0.56	4.39	8.09	1.39
2M19054526+3831225	5981 ± 90	4.22 ± 0.1	4.13	0.01 ± 0.04	-0.02 ± 0.1	1.02	5.21	9.8	0.34
2M19054526+3831225	5994 ± 89	4.35 ± 0.1	4.25	0.04 ± 0.03	-0.02 ± 0.1	0.71	5.23	9.9	0.38
2M19054670+3851153	5601 ± 94	3.96 ± 0.11	3.96	0.14 ± 0.04	0.11 ± 0.1	1.05	3.56	9.36	1.65
2M19055361+4919212	5845 ± 126	4.33 ± 0.17	4.27	0.05 ± 0.05	0.01 ± 0.1	0.59	4.46	10.59	1.47
2M19055567+3928176	5825 ± 112	4.32 ± 0.14	4.27	0 ± 0.05	-0.05 ± 0.1	0.63	4.43	8.4	1.46
2M19060566+4652511	6186 ± 184	4.29 ± 0.27	4.14	-0.16 ± 0.07	-0.25 ± 0.1	0	6.67	8.55	0.47
2M19062594+3921363	5692 ± 96	4.32 ± 0.13	4.30	-0.07 ± 0.04	-0.11 ± 0.1	0.7	3.97	9.17	0.42
2M19063321+3929164	6284 ± 142	4.2 ± 0.16	4.01	-0.03 ± 0.06	-0.11 ± 0.1	1.24	7.28	11.48	0.24
2M19063541+4812212	5728 ± 103	4.36 ± 0.13	4.33	-0.03 ± 0.04	-0.07 ± 0.1	1.09	4.06	8.98	1.43
2M19063541+4812212	5730 ± 103	4.36 ± 0.13	4.33	-0.03 ± 0.04	-0.07 ± 0.1	1.08	4.07	8.94	1.43
2M19063554+4633519	5696 ± 112	4.35 ± 0.14	4.33	-0.03 ± 0.05	-0.06 ± 0.1	0.67	3.95	9.79	0.41
2M19064518+4013593	5788 ± 123	4.24 ± 0.14	4.20	0.14 ± 0.05	0.1 ± 0.1	0.91	4.12	10.57	1.89
2M19064546+3912428	6016 ± 134	4.27 ± 0.17	4.17	-0.16 ± 0.05	-0.26 ± 0.1	0.15	5.58	8.54	1.37
2M19065595+4240192	6319 ± 116	4.17 ± 0.13	3.96	0.08 ± 0.04	0 ± 0.1	1.1	7.44	10.43	1.21
2M19065834+4226082	5816 ± 120	4.09 ± 0.13	4.04	0.04 ± 0.05	-0.01 ± 0.1	1.05	4.39	7.19	1.44
2M19065834+4226082	5879 ± 118	4.16 ± 0.15	4.09	0.06 ± 0.05	-0.01 ± 0.1	0.91	4.64	9.94	1.39
2M19071403+4918590	5754 ± 141	4.33 ± 0.16	4.30	-0.04 ± 0.06	-0.08 ± 0.1	0.76	4.17	9.31	0.5
2M19071403+4918590	5773 ± 139	4.34 ± 0.16	4.30	-0.02 ± 0.06	-0.08 ± 0.1	0.75	4.23	7.74	0.5
2M19075329+3946361	5727 ± 123	4.41 ± 0.15	4.38	-0.18 ± 0.05	-0.23 ± 0.1	0.48	4.21	8.79	0.47

APOGEE_ID	$T_{\rm eff} \pm \Delta T_{\rm eff}$	$\log g \pm \Delta \log g$	$\log g_{cor}$	$[\mathrm{M/H}] \pm \Delta[\mathrm{M/H}]$	$[Fe/H] \pm \Delta[\mathrm{Fe/H}]$	$\mathrm{v_{mic}}$	$\mathrm{v_{mac}}$	$v \sin i$	χ^2
2M19075860+4007111	5431 ± 93	4.26 ± 0.11	4.31	0.02 ± 0.04	-0.01 ± 0.1	0.96	3.23	10.65	1.65
2M19080992+4137474	5965 ± 148	4.33 ± 0.19	4.24	-0.04 ± 0.06	-0.09 ± 0.1	0.34	5.16	8.28	0.52
2M19081793+4705366	5769 ± 128	4.18 ± 0.13	4.14	0.09 ± 0.05	0.02 ± 0.1	0.85	4.11	10.05	2.16
2M19082205+4606268	6300 ± 112	4.57 ± 0.11	4.37	0.26 ± 0.04	0.24 ± 0.1	0.84	7.04	8.05	0.59
2M19082325+5012168	5753 ± 117	4.05 ± 0.11	4.02	-0.07 ± 0.05	-0.15 ± 0.1	0.69	4.27	9.84	1.47
2M19082450+4207306	5711 ± 128	4.19 ± 0.15	4.17	-0.08 ± 0.06	-0.14 ± 0.1	0.56	4.08	9.86	0.57
2M19083681+3819457	5760 ± 133	4.18 ± 0.13	4.14	0.01 ± 0.05	-0.06 ± 0.1	0.84	4.17	9.14	0.48
2M19091556+3932174	5903 ± 105	4.18 ± 0.15	4.11	-0.06 ± 0.04	-0.13 ± 0.1	0.63	4.89	8.69	0.4
2M19095484+3813438	5544 ± 94	4.19 ± 0.1	4.21	0.12 ± 0.04	0.08 ± 0.1	1	3.35	0	1.71
2M19095549+4915044	5531 ± 98	3.91 ± 0.13	3.93	0.12 ± 0.04	0.11 ± 0.1	1.36	3.42	0	0.93
2M19095725+4659267	6317 ± 91	4.38 ± 0.12	4.17	0.16 ± 0.04	0.1 ± 0.1	0.53	7.29	8.66	1.47
2M19100982+4638222	5807 ± 138	4.43 ± 0.17	4.38	-0.04 ± 0.06	-0.08 ± 0.1	0.8	4.38	9.91	0.53
2M19101043+4709381	4703 ± 42	3.42 ± 0.06	3.42	0.48 ± 0.02	0.33 ± 0.1	0.7	2.93	9.66	2.68
2M19101342+4648387	5912 ± 111	4.19 ± 0.14	4.12	0.25 ± 0.05	0.19 ± 0.1	0.86	4.58	10.34	0.74
2M19101968+4911052	5773 ± 268	4.21 ± 0.31	4.17	-0.04 ± 0.11	-0.09 ± 0.1	0.86	4.27	9.3	3.93
2M19102533+4931237	4822 ± 92	4.34 ± 0.13	4.56	0.09 ± 0.03	0.06 ± 0.1	1.45	3.5	8.73	2.23
2M19103720+3914394	5736 ± 152	4.16 ± 0.17	4.13	-0.26 ± 0.06	-0.37 ± 0.1	0.5	4.37	9.56	1.34
2M19104752+4220194	5419 ± 165	4.3 ± 0.21	4.35	0.04 ± 0.07	0.01 ± 0.1	1.18	3.17	0	2.28
2M19105255+4203201	5645 ± 105	4.11 ± 0.13	4.10	0.17 ± 0.05	0.13 ± 0.1	0.85	3.6	9.57	1.88
2M19105919+4336561	6119 ± 150	4.4 ± 0.22	4.27	0.06 ± 0.06	0.01 ± 0.1	0.31	5.97	10.37	1.61

APOGEE_ID	$T_{\mathrm{eff}} \pm \Delta T_{\mathrm{eff}}$	$\log g \pm \Delta \log g$	$\log g_{cor}$	$[\mathrm{M/H}] \pm \Delta[\mathrm{M/H}]$	$[Fe/H] \pm \Delta[\mathrm{Fe/H}]$	$\mathrm{v_{mic}}$	$\mathrm{v_{mac}}$	$v \sin i$	χ^2
2M19110616+4202436	5580 ± 108	4.09 ± 0.12	4.10	-0.19 ± 0.05	-0.28 ± 0.1	0.6	3.82	9.37	1.42
2M19110844+4406544	5661 ± 145	3.8 ± 0.22	3.79	-0.09 ± 0.06	-0.2 ± 0.1	0	4.07	7.04	1.85
2M19112760+4658537	5940 ± 151	4.36 ± 0.21	4.28	-0.04 ± 0.06	-0.1 ± 0.1	0.45	5.02	8.9	1.71
2M19113246+4348536	5871 ± 89	4.01 ± 0.1	3.95	0.13 ± 0.04	0.06 ± 0.1	0.94	4.57	11.55	0.43
2M19114027+4754568	5781 ± 125	4.11 ± 0.12	4.07	0.04 ± 0.05	-0.05 ± 0.1	0.66	4.24	9.5	1.41
2M19115818+3902135	5815 ± 114	4.02 ± 0.13	3.97	-0.13 ± 0.05	-0.21 ± 0.1	0.65	4.6	9.29	0.52
2M19120224+4240186	6014 ± 140	4.29 ± 0.19	4.19	-0.05 ± 0.06	-0.09 ± 0.1	0.92	5.46	10.17	1.57
2M19121663+3849036	6111 ± 106	4.49 ± 0.11	4.37	0.07 ± 0.04	0.03 ± 0.1	0.53	5.9	10.3	0.39
2M19123497+4157391	5661 ± 112	4.31 ± 0.15	4.30	0.03 ± 0.05	0.01 ± 0.1	0.9	3.77	9.73	1.7
2M19124093+4624012	6319 ± 123	4.37 ± 0.17	4.16	0.07 ± 0.05	0 ± 0.1	0.58	7.41	9.04	1.31
2M19124891+4207188	6115 ± 148	4.41 ± 0.21	4.29	0.02 ± 0.06	-0.04 ± 0.1	0.3	5.99	8.33	0.44
2M19130406+4312004	5850 ± 125	4.33 ± 0.19	4.27	-0.17 ± 0.05	-0.25 ± 0.1	0.47	4.72	8.65	0.38
2M19130471+4215255	6339 ± 176	4.11 ± 0.22	3.89	-0.08 ± 0.07	-0.12 ± 0.1	1.42	7.8	7.53	1.31
2M19131424+4351038	6267 ± 96	4.35 ± 0.12	4.16	0.2 ± 0.04	0.15 ± 0.1	0.71	6.86	10.23	0.35
2M19133899+4725035	5733 ± 97	4.27 ± 0.11	4.24	0.15 ± 0.04	0.1 ± 0.1	0.81	3.89	10.2	0.62
2M19134451+4745186	5554 ± 109	4.26 ± 0.13	4.28	-0.04 ± 0.05	-0.09 ± 0.1	0.91	3.54	9.44	0.47
2M19134816+4014431	5907 ± 175	4.26 ± 0.27	4.19	-0.09 ± 0.07	-0.15 ± 0.1	0.54	4.93	8.21	0.56
2M19135726+4620047	6102 ± 120	4.16 ± 0.15	4.04	0.02 ± 0.05	-0.05 ± 0.1	0.69	5.95	8.36	1.6
2M19140739+4056322	5646 ± 101	4.29 ± 0.13	4.28	0.07 ± 0.04	0.03 ± 0.1	0.83	3.67	10.62	1.64
2M19140739+4056322	5643 ± 101	4.3 ± 0.14	4.29	0.06 ± 0.04	0.03 ± 0.1	0.86	3.67	10.59	1.64

APOGEE_ID	$T_{\rm eff} \pm \Delta T_{\rm eff}$	$\log g \pm \Delta \log g$	$\log g_{cor}$	$[\mathrm{M/H}] \pm \Delta[\mathrm{M/H}]$	$[Fe/H] \pm \Delta[\mathrm{Fe/H}]$	$\mathrm{v}_{\rm mic}$	$\mathrm{v}_{\rm mac}$	$v \sin i$	χ^2
2M19141861+4238492	5009 ± 63	3.67 ± 0.07	3.67	0.1 ± 0.03	0.04 ± 0.1	1.02	3.34	11.15	1.79
2M19141972+4652319	5961 ± 176	4.3 ± 0.24	4.21	-0.19 ± 0.07	-0.29 ± 0.1	0.1	5.31	9.09	0.54
2M19143102+4313524	5726 ± 138	4.18 ± 0.15	4.15	-0.13 ± 0.06	-0.21 ± 0.1	0.5	4.19	8.78	1.52
2M19144528+4109042	6185 ± 165	4.27 ± 0.22	4.12	0.1 ± 0.06	0.02 ± 0.1	1.1	6.39	11.08	0.38
2M19144624+4440385	5888 ± 146	4.32 ± 0.21	4.25	0.01 ± 0.06	-0.05 ± 0.1	0.65	4.71	9.5	0.48
2M19145415+4741483	6199 ± 106	4.41 ± 0.14	4.25	0.13 ± 0.04	0.1 ± 0.1	0.99	6.43	10.2	0.4
2M19145415+4741483	6246 ± 102	4.56 ± 0.09	4.38	0.18 ± 0.04	0.1 ± 0.1	0.68	6.72	10.14	0.44
2M19145685+4747112	5924 ± 150	4.35 ± 0.21	4.27	-0.01 ± 0.06	-0.08 ± 0.1	0.74	4.91	9.47	0.67
2M19150807+4117554	5970 ± 130	4.31 ± 0.17	4.22	-0.1 ± 0.05	-0.17 ± 0.1	0.53	5.26	8.65	1.23
2M19151746+4806236	5611 ± 132	4.22 ± 0.17	4.22	-0.04 ± 0.06	-0.1 ± 0.1	0.88	3.7	9.48	1.7
2M19153049+4712204	6162 ± 129	4.5 ± 0.13	4.36	0.23 ± 0.05	0.19 ± 0.1	0.57	6.06	10.03	1.58
2M19153224+4745341	5043 ± 127	3.61 ± 0.13	3.61	0 ± 0.06	-0.17 ± 0.1	1.16	3.45	13.24	1.59
2M19155629+4003522	5887 ± 175	4.21 ± 0.24	4.14	0.11 ± 0.07	0.07 ± 0.1	1	4.62	9.89	1.99
2M19160641+4931371	4787 ± 64	3.63 ± 0.07	3.63	0.46 ± 0.03	0.38 ± 0.1	0.8	3.82	8.78	2.35
2M19162065+4133465	5861 ± 131	4.13 ± 0.16	4.07	0.1 ± 0.05	0.03 ± 0.1	0.81	4.52	9.8	1.58
2M19162197+4603252	6138 ± 143	4.36 ± 0.22	4.23	0.08 ± 0.06	0.01 ± 0.1	0.28	6.08	10.56	1.5
2M19163489+4002501	5864 ± 82	4.23 ± 0.11	4.17	0.12 ± 0.03	0.06 ± 0.1	0.66	4.49	10.2	1.43
2M19163489+4002501	5814 ± 83	4.18 ± 0.09	4.13	0.1 ± 0.03	0.06 ± 0.1	0.73	4.3	8.83	1.49
2M19165219+4753040	5635 ± 178	4.38 ± 0.28	4.38	-0.16 ± 0.08	-0.21 ± 0.1	0.69	3.88	8.84	0.61
2M19165316+4652436	5927 ± 120	4.32 ± 0.16	4.24	0.19 ± 0.05	0.14 ± 0.1	0.74	4.7	9.14	0.61

APOGEE_ID	$T_{\text{eff}} \pm \Delta T_{\text{eff}}$	$\log g \pm \Delta \log g$	$\log g_{cor}$	$[\text{M/H}] \pm \Delta[\text{M/H}]$	$[Fe/H] \pm \Delta[\text{Fe/H}]$	v_{mic}	v_{mac}	$v \sin i$	χ^2
2M19172334+4412307	6213 ± 205	4.09 ± 0.23	3.92	-0.12 ± 0.08	-0.22 ± 0.1	0.85	6.87	9.72	1.42
2M19172687+4653575	6182 ± 104	4.35 ± 0.15	4.20	0.09 ± 0.04	0.04 ± 0.1	0.53	6.36	10.32	0.36
2M19173428+4406066	5538 ± 132	4.28 ± 0.15	4.30	-0.19 ± 0.06	-0.24 ± 0.1	0.54	3.66	9.87	0.4
2M19174282+4659070	6042 ± 138	4.4 ± 0.18	4.29	0.05 ± 0.05	0.01 ± 0.1	0.66	5.49	10.39	0.57
2M19174520+4709467	5832 ± 149	4.08 ± 0.18	4.03	-0.2 ± 0.06	-0.27 ± 0.1	0.55	4.73	8.71	0.42
2M19174635+4124366	6048 ± 85	4.21 ± 0.11	4.10	-0.24 ± 0.03	-0.28 ± 0.1	0.61	5.87	9.01	1.2
2M19174635+4124366	6041 ± 78	4.32 ± 0.11	4.21	-0.09 ± 0.03	-0.28 ± 0.1	0.31	5.65	8.8	1.29
2M19180506+4656584	6051 ± 162	4.29 ± 0.22	4.18	-0.09 ± 0.07	-0.17 ± 0.1	0.03	5.72	8.44	1.48
2M19181244+4358466	5923 ± 118	4.31 ± 0.16	4.23	0.04 ± 0.05	-0.01 ± 0.1	0.61	4.85	9.35	1.39
2M19182595+4717282	5797 ± 102	4.14 ± 0.11	4.09	0.23 ± 0.04	0.17 ± 0.1	0.59	4.07	10.39	1.87
2M19182922+4437340	5702 ± 135	4.38 ± 0.18	4.36	-0.12 ± 0.06	-0.19 ± 0.1	0.6	4.06	9.56	0.45
2M19183320+4424161	5638 ± 149	4.29 ± 0.22	4.28	-0.08 ± 0.07	-0.12 ± 0.1	0.47	3.81	9.42	0.64
2M19184480+4135201	5721 ± 133	4.29 ± 0.15	4.26	0 ± 0.05	-0.05 ± 0.1	0.8	4.01	9.78	0.66
2M19184935+3937549	5613 ± 72	4.16 ± 0.08	4.16	0.12 ± 0.03	0.09 ± 0.1	0.92	3.55	9.79	0.58
2M19185014+3940563	5568 ± 64	4.23 ± 0.08	4.24	0.4 ± 0.03	0.31 ± 0.1	0.79	3.06	8.94	2.01
2M19185125+4656433	5434 ± 86	4.33 ± 0.11	4.38	0.06 ± 0.04	0.01 ± 0.1	0.71	3.17	9.43	1.73
2M19185411+4329468	5971 ± 99	4.04 ± 0.11	3.95	-0.1 ± 0.04	-0.18 ± 0.1	0.69	5.33	9.31	1.25
2M19185411+4329468	5978 ± 97	4.15 ± 0.11	4.06	-0.06 ± 0.04	-0.18 ± 0.1	0.45	5.29	9.15	1.32
2M19185632+4638432	5694 ± 106	4.24 ± 0.13	4.22	-0.01 ± 0.04	-0.05 ± 0.1	0.98	3.93	9.69	0.52
2M19185753+4438507	5738 ± 115	4.13 ± 0.11	4.10	0.06 ± 0.05	-0.03 ± 0.1	0.88	4.04	10.87	1.35

APOGEE_ID	$T_{\mathrm{eff}} \pm \Delta T_{\mathrm{eff}}$	$\log g \pm \Delta \log g$	$\log g_{cor}$	$[\mathrm{M/H}] \pm \Delta[\mathrm{M/H}]$	$[Fe/H] \pm \Delta[\mathrm{Fe/H}]$	$\mathrm{v}_{\mathrm{mic}}$	$\mathrm{v}_{\mathrm{mac}}$	$v \sin i$	χ^2
2M19190154+3952194	5858 ± 125	4.14 ± 0.15	4.08	0.08 ± 0.05	0.03 ± 0.1	0.82	4.53	10.38	0.45
2M19202934+4117283	5971 ± 89	4.12 ± 0.09	4.03	-0.02 ± 0.03	-0.1 ± 0.1	0.67	5.22	9.73	1.33
2M19204580+3846463	6186 ± 151	4.45 ± 0.17	4.30	0 ± 0.06	-0.07 ± 0.1	0.42	6.49	9.01	1.42
2M19204792+4409188	6168 ± 125	4.2 ± 0.17	4.05	0.01 ± 0.05	-0.04 ± 0.1	0.82	6.39	9.78	1.29
2M19204792+4409188	6185 ± 122	4.32 ± 0.17	4.17	0.04 ± 0.05	-0.04 ± 0.1	0.54	6.45	9.93	1.38
2M19211530+3840187	5317 ± 831	4.23 ± 0.98	4.31	0.15 ± 0.34	0.05 ± 0.1	0.56	2.95	0	25.15
2M19212465+4830532	5692 ± 83	4.02 ± 0.08	4.00	0.05 ± 0.03	-0.03 ± 0.1	0.69	3.92	9.68	1.46
2M19214099+3751064	5513 ± 158	4.47 ± 0.13	4.50	0.02 ± 0.06	-0.02 ± 0.1	0.81	3.36	0	1.97
2M19214120+4438528	6036 ± 137	4.22 ± 0.16	4.11	0.36 ± 0.06	0.3 ± 0.1	1.29	5.12	9.4	0.77
2M19214232+4826361	5765 ± 221	4.06 ± 0.21	4.02	0 ± 0.09	-0.02 ± 0.1	1.06	4.23	9.8	2.03
2M19214760+4646239	5853 ± 128	4.28 ± 0.17	4.22	0.06 ± 0.05	0.01 ± 0.1	0.68	4.49	10.01	1.7
2M19215162+4819560	5728 ± 189	4.33 ± 0.22	4.30	-0.02 ± 0.08	-0.06 ± 0.1	0.69	4.05	1.34	1.1
2M19215883+3847437	6007 ± 133	4.26 ± 0.14	4.16	-0.01 ± 0.05	-0.11 ± 0.1	0.46	5.38	8.77	0.43
2M19220135+3727324	6414 ± 142	4.48 ± 0.16	4.23	0.15 ± 0.05	0.11 ± 0.1	0.71	8.11	8.4	1.52
2M19220642+3808347	5536 ± 81	4.22 ± 0.09	4.24	0.09 ± 0.03	0.05 ± 0.1	0.95	3.36	10.41	0.68
2M19220913+3814317	6200 ± 151	4.23 ± 0.2	4.07	-0.05 ± 0.06	-0.15 ± 0.1	0.47	6.67	8.5	1.38
2M19221069+4837491	5996 ± 115	4.37 ± 0.15	4.27	-0.14 ± 0.05	-0.22 ± 0.1	0.3	5.44	8.24	0.33
2M19222053+4350209	5835 ± 100	4.34 ± 0.13	4.28	-0.01 ± 0.04	-0.05 ± 0.1	0.71	4.48	10.53	1.29
2M19222872+4849459	5857 ± 102	4.25 ± 0.13	4.19	0.12 ± 0.04	0.07 ± 0.1	0.79	4.45	10.84	1.51
2M19223236+4444379	5619 ± 115	4 ± 0.12	4.00	0.08 ± 0.05	0.03 ± 0.1	0.86	3.67	10.39	1.58

APOGEE_ID	$T_{\mathrm{eff}} \pm \Delta T_{\mathrm{eff}}$	$\log g \pm \Delta \log g$	$\log g_{cor}$	$[\mathrm{M/H}] \pm \Delta[\mathrm{M/H}]$	$[Fe/H] \pm \Delta[\mathrm{Fe/H}]$	$\mathrm{v}_{\mathrm{mic}}$	$\mathrm{v}_{\mathrm{mac}}$	$v \sin i$	χ^2
2M19223267+4902152	5733 ± 110	4.09 ± 0.1	4.06	0.1 ± 0.05	0.03 ± 0.1	0.64	3.99	9.97	1.61
2M19224155+3841276	5508 ± 111	4.45 ± 0.1	4.48	0.08 ± 0.05	0.03 ± 0.1	0.9	3.28	9.96	0.8
2M19224311+4555016	5944 ± 133	4.17 ± 0.15	4.09	0.15 ± 0.05	0.1 ± 0.1	0.89	4.87	10.59	0.53
2M19225238+4832272	5942 ± 111	4.3 ± 0.16	4.22	-0.11 ± 0.05	-0.2 ± 0.1	0.42	5.12	8.98	0.37
2M19231859+4036240	5244 ± 197	4.22 ± 0.23	4.31	-0.06 ± 0.08	-0.21 ± 0.1	2.3	3.15	15.05	1.7
2M19232960+4806529	6119 ± 141	4.43 ± 0.21	4.30	-0.06 ± 0.06	-0.13 ± 0.1	0	6.1	8.16	0.49
2M19233232+3803272	5675 ± 120	4.27 ± 0.15	4.26	-0.01 ± 0.05	-0.05 ± 0.1	0.75	3.86	9.87	0.63
2M19234729+3846372	5990 ± 88	4.2 ± 0.09	4.11	0.14 ± 0.04	0.08 ± 0.1	0.97	5.12	11.79	1.23
2M19235074+3840244	5463 ± 101	4.24 ± 0.11	4.28	0.12 ± 0.04	0.11 ± 0.1	1.25	3.17	10.47	1.29
2M19235640+4318525	5804 ± 116	4.19 ± 0.13	4.14	0.06 ± 0.05	0.01 ± 0.1	0.77	4.3	9.95	1.44
2M19235640+4318525	5804 ± 114	4.2 ± 0.13	4.15	0.08 ± 0.05	0.01 ± 0.1	0.73	4.27	10.14	1.44
2M19240457+3832440	5612 ± 117	4.28 ± 0.15	4.28	-0.04 ± 0.05	-0.09 ± 0.1	0.74	3.69	9.55	0.59
2M19240775+4902249	5764 ± 88	4.27 ± 0.09	4.23	0.07 ± 0.04	0.02 ± 0.1	0.59	4.1	10.41	0.55
2M19240775+4902249	5764 ± 88	4.27 ± 0.09	4.23	0.07 ± 0.04	0.02 ± 0.1	0.59	4.1	10.41	0.55
2M19241119+4203097	5490 ± 91	4.18 ± 0.1	4.21	0.18 ± 0.04	0.15 ± 0.1	1.07	3.17	0	1.86
2M19243886+4838430	5815 ± 106	4.07 ± 0.12	4.02	-0.05 ± 0.05	-0.13 ± 0.1	0.7	4.5	9.18	1.52
2M19245080+3905355	5941 ± 148	4.3 ± 0.2	4.22	-0.03 ± 0.06	-0.11 ± 0.1	0.56	5.03	9.24	1.49
2M19245704+4435152	5918 ± 118	4.06 ± 0.14	3.98	0.06 ± 0.05	0.02 ± 0.1	0.85	4.87	9.77	1.42
2M19250004+4913545	6119 ± 214	4.2 ± 0.31	4.07	-0.08 ± 0.09	-0.16 ± 0.1	0.42	6.16	9.09	0.48
2M19250201+4429508	4737 ± 54	4.12 ± 0.08	4.37	-0.1 ± 0.02	-0.35 ± 0.1	2.91	3.64	36.22	1.46

APOGEE_ID	$T_{\rm eff} \pm \Delta T_{\rm eff}$	$\log g \pm \Delta \log g$	$\log g_{cor}$	$[\rm M/H] \pm \Delta[\rm M/H]$	$[Fe/H] \pm \Delta[\rm Fe/H]$	$\rm v_{mic}$	$\rm v_{mac}$	$v \sin i$	χ^2
2M19251679+4500420	5698 ± 107	3.98 ± 0.11	3.96	0.11 ± 0.05	0.04 ± 0.1	0.86	3.89	11.28	1.47
2M19252303+3827517	6059 ± 111	4.31 ± 0.14	4.20	0.14 ± 0.04	0.08 ± 0.1	0.66	5.51	10.78	1.61
2M19253173+3807388	5926 ± 119	4.31 ± 0.18	4.23	-0.11 ± 0.05	-0.17 ± 0.1	0.49	5.03	9.2	1.49
2M19253263+4159249	5864 ± 75	4.22 ± 0.1	4.16	0.08 ± 0.03	0.01 ± 0.1	0.71	4.54	9.49	1.33
2M19253263+4159249	5904 ± 73	4.27 ± 0.1	4.20	0.09 ± 0.03	0.01 ± 0.1	0.65	4.71	10.61	1.28
2M19253585+3847159	5132 ± 162	4.43 ± 0.19	4.55	0.12 ± 0.06	0.09 ± 0.1	1.01	2.93	10.73	2.1
2M19253812+4452336	5601 ± 121	4.42 ± 0.16	4.42	-0.05 ± 0.05	-0.09 ± 0.1	0.82	3.66	11.66	0.46
2M19254039+3840204	5663 ± 81	4.31 ± 0.12	4.30	-0.09 ± 0.04	-0.15 ± 0.1	0.7	3.9	9.43	0.36
2M19254039+3840204	5681 ± 47	4.36 ± 0.07	4.34	-0.08 ± 0.02	-0.15 ± 0.1	0.56	3.95	9.44	1.33
2M19254165+3812597	5592 ± 122	4.03 ± 0.12	4.04	0.03 ± 0.05	-0.01 ± 0.1	0.79	3.63	10.27	0.83
2M19255330+5101382	4831 ± 65	3.37 ± 0.11	3.37	0.31 ± 0.04	0.23 ± 0.1	1.01	3.21	0	2.33
2M19255850+4351399	5753 ± 122	4.13 ± 0.11	4.10	0.06 ± 0.05	0 ± 0.1	0.61	4.1	10.43	1.39
2M19255933+4243425	5997 ± 69	4.13 ± 0.07	4.03	-0.02 ± 0.03	-0.1 ± 0.1	0.61	5.36	9.58	0.34
2M19260576+4721300	6232 ± 163	4.27 ± 0.19	4.10	0.02 ± 0.06	-0.06 ± 0.1	0.5	6.82	9.56	0.62
2M19260597+3827210	5293 ± 123	4.36 ± 0.15	4.44	0.09 ± 0.05	0.05 ± 0.1	0.99	2.98	11.14	1.91
2M19260620+3802366	6197 ± 179	4.12 ± 0.21	3.96	-0.03 ± 0.07	-0.14 ± 0.1	0.76	6.65	9.4	1.27
2M19261331+3726425	6050 ± 123	4.33 ± 0.15	4.22	0.11 ± 0.05	0.04 ± 0.1	0.62	5.49	9.44	1.61
2M19261781+3839214	5834 ± 90	4.39 ± 0.14	4.34	-0.08 ± 0.04	-0.14 ± 0.1	0.56	4.55	9.05	0.43
2M19261932+4152126	5734 ± 111	4.08 ± 0.11	4.05	-0.03 ± 0.05	-0.08 ± 0.1	0.7	4.14	9.73	0.41
2M19262515+3718461	5990 ± 133	4.38 ± 0.16	4.29	0.07 ± 0.05	0.02 ± 0.1	0.57	5.18	10.67	1.42

APOGEE_ID	$T_{\mathrm{eff}} \pm \Delta T_{\mathrm{eff}}$	$\log g \pm \Delta \log g$	$\log g_{cor}$	$[\mathrm{M/H}] \pm \Delta[\mathrm{M/H}]$	$[Fe/H] \pm \Delta[\mathrm{Fe/H}]$	$\mathrm{v}_{\mathrm{mic}}$	$\mathrm{v}_{\mathrm{mac}}$	$v \sin i$	χ^2
2M19262561+4202093	5775 ± 128	4.28 ± 0.14	4.24	0.05 ± 0.05	0.01 ± 0.1	0.73	4.16	10.77	2.7
2M19262571+3824374	5954 ± 156	4.29 ± 0.2	4.20	-0.03 ± 0.06	-0.1 ± 0.1	0.5	5.1	8.88	0.63
2M19262906+4842436	5490 ± 171	4 ± 0.15	4.03	-0.11 ± 0.08	-0.21 ± 0.1	0.56	3.55	10.43	1.1
2M19263602+4242028	5632 ± 207	4.13 ± 0.24	4.13	-0.01 ± 0.09	-0.1 ± 0.1	0.57	3.76	9.71	2.97
2M19263888+4455483	5697 ± 118	4.02 ± 0.13	4.00	-0.19 ± 0.05	-0.27 ± 0.1	0.61	4.2	9.31	1.39
2M19264137+4203414	6199 ± 159	4.3 ± 0.23	4.14	-0.07 ± 0.06	-0.16 ± 0.1	0.37	6.67	7.72	0.47
2M19264282+3850215	6176 ± 131	4.41 ± 0.2	4.26	-0.06 ± 0.05	-0.14 ± 0.1	0.09	6.48	8.32	1.47
2M19264400+3745057	5534 ± 84	4.49 ± 0.07	4.51	0.04 ± 0.03	0.01 ± 0.1	0.55	3.38	10.22	1.6
2M19270298+4835118	5825 ± 80	4.23 ± 0.09	4.18	0.19 ± 0.03	0.13 ± 0.1	0.44	4.23	11.01	1.6
2M19271797+3806475	5659 ± 102	4.09 ± 0.12	4.08	-0.04 ± 0.04	-0.1 ± 0.1	0.72	3.88	9.75	0.42
2M19271865+4352357	5618 ± 126	4.22 ± 0.16	4.22	-0.02 ± 0.05	-0.06 ± 0.1	0.89	3.7	9.54	0.48
2M19272048+4857121	5627 ± 96	4.05 ± 0.11	4.05	0.18 ± 0.04	0.12 ± 0.1	0.79	3.55	10.77	2.03
2M19272048+4857121	5627 ± 96	4.05 ± 0.11	4.05	0.18 ± 0.04	0.12 ± 0.1	0.8	3.55	10.77	2.03
2M19274223+3800508	5380 ± 110	4.34 ± 0.15	4.40	0.15 ± 0.05	0.14 ± 0.1	1.39	2.99	0	1.36
2M19274576+4819454	5709 ± 144	3.97 ± 0.16	3.95	-0.06 ± 0.06	-0.1 ± 0.1	0.8	4.12	9.58	1.67
2M19274981+4931045	5163 ± 55	3.17 ± 0.08	3.17	-0.09 ± 0.03	-0.2 ± 0.1	0.67	3.84	10.64	1.77
2M19280539+4924572	5732 ± 104	4.13 ± 0.1	4.10	0.11 ± 0.04	0.04 ± 0.1	0.91	3.96	9.57	1.83
2M19281984+3703353	6165 ± 96	4.17 ± 0.12	4.03	0.02 ± 0.04	-0.09 ± 0.1	0.66	6.36	10.76	1.24
2M19282449+4817149	6190 ± 124	4.28 ± 0.17	4.12	0.12 ± 0.05	0.06 ± 0.1	0.87	6.4	10.27	0.41
2M19284706+4617396	5565 ± 101	4.32 ± 0.13	4.33	-0.05 ± 0.04	-0.08 ± 0.1	0.91	3.57	8.64	1.6

APOGEE_ID	$T_{\mathrm{eff}} \pm \Delta T_{\mathrm{eff}}$	$\log g \pm \Delta \log g$	$\log g_{cor}$	$[\mathrm{M/H}] \pm \Delta[\mathrm{M/H}]$	$[Fe/H] \pm \Delta[\mathrm{Fe/H}]$	v$_{\mathrm{mic}}$	v$_{\mathrm{mac}}$	$v \sin i$	χ^2
2M19284793+4202459	5652 ± 122	4.06 ± 0.14	4.05	0.06 ± 0.05	0.02 ± 0.1	0.78	3.76	10.17	1.47
2M19285558+4938526	6181 ± 147	4.33 ± 0.21	4.18	0.05 ± 0.06	-0.03 ± 0.1	0.64	6.41	8.73	0.47
2M19285638+4254340	5919 ± 117	4.42 ± 0.17	4.34	-0.18 ± 0.05	-0.26 ± 0.1	0.24	5.06	8.56	0.42
2M19285935+4758102	6233 ± 132	4.16 ± 0.14	3.99	0.06 ± 0.05	0.01 ± 0.1	0.87	6.8	9.77	0.33
2M19290186+4951549	5819 ± 143	4.15 ± 0.17	4.10	-0.04 ± 0.06	-0.12 ± 0.1	0.47	4.48	10.18	1.49
2M19290373+3907474	5946 ± 120	4.13 ± 0.13	4.05	0.06 ± 0.05	-0.01 ± 0.1	0.79	4.99	8.96	0.52
2M19290535+4954118	6030 ± 141	4.27 ± 0.16	4.17	0.01 ± 0.05	-0.08 ± 0.1	0.6	5.48	8.64	0.36
2M19292281+4135071	6055 ± 87	4.13 ± 0.1	4.02	0.18 ± 0.04	0.15 ± 0.1	1.17	5.47	9.97	0.99
2M19293363+4742283	5878 ± 111	4.27 ± 0.15	4.20	0.04 ± 0.05	-0.01 ± 0.1	0.64	4.64	10.03	0.4
2M19294147+3815587	6041 ± 144	4.08 ± 0.15	3.97	-0.01 ± 0.06	-0.09 ± 0.1	0.88	5.62	10.18	0.37
2M19294641+4836117	5802 ± 129	4.32 ± 0.16	4.27	-0.04 ± 0.05	-0.1 ± 0.1	0.64	4.37	10	1.45
2M19295157+3854267	5354 ± 144	4.33 ± 0.2	4.40	0.36 ± 0.06	0.32 ± 0.1	1.27	2.71	9.29	3.02
2M19295514+4313372	6243 ± 154	4.33 ± 0.18	4.15	0.01 ± 0.06	-0.08 ± 0.1	0.43	6.9	8.75	0.52
2M19300891+4209142	5748 ± 135	4.03 ± 0.13	4.00	-0.17 ± 0.06	-0.25 ± 0.1	0.58	4.36	9.22	1.37
2M19301246+3725163	5707 ± 121	3.98 ± 0.12	3.96	0.02 ± 0.05	-0.02 ± 0.1	0.86	4.02	10.27	0.54
2M19302763+4245513	5653 ± 47	4.31 ± 0.06	4.30	-0.01 ± 0.02	-0.06 ± 0.1	0.98	3.78	9.37	1.42
2M19302763+4245513	5649 ± 47	4.3 ± 0.06	4.29	-0.01 ± 0.02	-0.06 ± 0.1	0.96	3.77	10	1.42
2M19302837+4409311	5786 ± 107	4.33 ± 0.13	4.29	0.12 ± 0.04	0.09 ± 0.1	0.86	4.12	9.61	1.5
2M19303351+3854503	5594 ± 97	4.01 ± 0.1	4.02	0.17 ± 0.04	0.12 ± 0.1	0.82	3.48	10.24	1.65
2M19310572+4921482	6119 ± 190	4.2 ± 0.27	4.07	-0.18 ± 0.08	-0.28 ± 0.1	0	6.26	7.63	0.43

APOGEE_ID	$T_{\rm eff} \pm \Delta T_{\rm eff}$	$\log g \pm \Delta \log g$	$\log g_{cor}$	$[\mathrm{M/H}] \pm \Delta[\mathrm{M/H}]$	$[Fe/H] \pm \Delta[\mathrm{Fe/H}]$	$\mathrm{v_{mic}}$	$\mathrm{v_{mac}}$	$v \sin i$	χ^2
2M19310830+4312575	5581 ± 101	4.29 ± 0.12	4.30	0.07 ± 0.04	0.04 ± 0.1	1.11	3.48	11.61	0.95
2M19311817+4749378	5404 ± 99	4.05 ± 0.12	4.10	-0.09 ± 0.05	-0.14 ± 0.1	0.68	3.36	8.16	1.18
2M19312934+4605559	6102 ± 117	4.42 ± 0.15	4.30	0.06 ± 0.05	-0.01 ± 0.1	0.54	5.86	9.4	1.5
2M19312941+4514461	5680 ± 84	3.98 ± 0.09	3.96	0.08 ± 0.04	0.04 ± 0.1	0.89	3.87	10.17	0.51
2M19320356+4534402	5837 ± 98	4.1 ± 0.11	4.04	0.27 ± 0.04	0.22 ± 0.1	0.89	4.22	9.66	1.95
2M19320463+4836159	6100 ± 162	4.41 ± 0.22	4.29	0 ± 0.06	-0.07 ± 0.1	0.48	5.91	9.38	0.44
2M19322044+3820302	5701 ± 82	4.28 ± 0.1	4.26	0.16 ± 0.03	0.12 ± 0.1	0.96	3.75	10.14	1.55
2M19322256+4253471	5494 ± 96	4.24 ± 0.1	4.27	0.08 ± 0.04	0.04 ± 0.1	0.96	3.28	10.74	1.01
2M19322962+4056051	5317 ± 123	4.42 ± 0.14	4.50	0.05 ± 0.05	0.01 ± 0.1	1.12	3.03	0	2.7
2M19323337+3955326	5886 ± 176	4.24 ± 0.28	4.17	-0.31 ± 0.07	-0.42 ± 0.1	0.13	5.05	8.07	1.65
2M19323685+4317115	5830 ± 120	4.14 ± 0.13	4.09	0.07 ± 0.05	0.01 ± 0.1	0.75	4.41	8.93	1.52
2M19324184+4057029	5654 ± 114	4.09 ± 0.13	4.08	0.13 ± 0.05	0.1 ± 0.1	0.96	3.68	10.04	1.26
2M19324327+4137039	5936 ± 126	4.29 ± 0.19	4.21	-0.05 ± 0.05	-0.11 ± 0.1	0.58	5.03	9.51	1.58
2M19324529+4900362	5848 ± 109	4.18 ± 0.13	4.12	0.13 ± 0.05	0.08 ± 0.1	0.81	4.41	10.14	1.3
2M19325295+4749224	5544 ± 101	4.22 ± 0.11	4.24	0.07 ± 0.04	0.04 ± 0.1	0.98	3.4	9.75	1.7
2M19330396+4123334	6101 ± 122	4.31 ± 0.18	4.19	-0.04 ± 0.05	-0.11 ± 0.1	0.47	5.97	8.15	0.35
2M19331638+4107000	5705 ± 111	4.13 ± 0.12	4.11	0.13 ± 0.05	0.09 ± 0.1	0.72	3.83	9.95	1.29
2M19331647+3800197	5649 ± 95	4.03 ± 0.11	4.02	-0.01 ± 0.04	-0.06 ± 0.1	0.79	3.84	9.69	0.42
2M19332069+4824208	5901 ± 152	4.38 ± 0.26	4.31	-0.17 ± 0.06	-0.23 ± 0.1	0.28	4.96	8.73	0.43
2M19332971+4443407	5927 ± 132	4.24 ± 0.19	4.16	-0.1 ± 0.05	-0.17 ± 0.1	0.49	5.04	8.54	1.57

APOGEE_ID	$T_{\rm eff} \pm \Delta T_{\rm eff}$	$\log g \pm \Delta \log g$	$\log g_{cor}$	$[\mathrm{M/H}] \pm \Delta[\mathrm{M/H}]$	$[Fe/H] \pm \Delta[\mathrm{Fe/H}]$	$\mathrm{v_{mic}}$	$\mathrm{v_{mac}}$	$v \sin i$	χ^2
2M19334034+4516308	5662 ± 240	3.76 ± 0.36	3.75	-0.21 ± 0.1	-0.44 ± 0.1	0.98	4.22	15.43	0.54
2M19335277+4702446	5928 ± 109	4.34 ± 0.15	4.26	0.1 ± 0.04	0.04 ± 0.1	0.74	4.81	11.29	1.34
2M19335277+4702446	5882 ± 111	4.29 ± 0.15	4.22	0.1 ± 0.05	0.04 ± 0.1	0.78	4.58	9.94	1.39
2M19340023+4650594	5775 ± 117	4.13 ± 0.13	4.09	-0.07 ± 0.05	-0.14 ± 0.1	0.6	4.33	9.17	1.28
2M19340028+4850088	5626 ± 103	3.94 ± 0.12	3.94	0.19 ± 0.04	0.14 ± 0.1	0.86	3.58	7.74	1.69
2M19341193+4521415	5673 ± 120	4.03 ± 0.13	4.02	0.02 ± 0.05	-0.02 ± 0.1	0.89	3.89	9.93	1.4
2M19341205+4752292	5914 ± 134	4.1 ± 0.16	4.03	-0.01 ± 0.05	-0.05 ± 0.1	0.79	4.91	10.23	0.38
2M19343286+4249298	4481 ± 48	4.4 ± 0.09	4.74	-0.04 ± 0.02	-0.1 ± 0.1	0.48	3.98	8.6	1.66
2M19344207+4117432	5611 ± 80	4.29 ± 0.11	4.29	-0.13 ± 0.03	-0.2 ± 0.1	0.63	3.79	8.95	1.35
2M19344300+4651099	5320 ± 66	4.2 ± 0.07	4.27	0.02 ± 0.03	-0.03 ± 0.1	1.08	3.1	10.09	1.36
2M19345420+4714493	5948 ± 156	4.31 ± 0.22	4.23	-0.22 ± 0.06	-0.32 ± 0.1	0	5.27	7.42	0.45
2M19345587+4154030	5672 ± 69	4.2 ± 0.09	4.19	-0.11 ± 0.03	-0.19 ± 0.1	0.61	3.98	9.6	1.41
2M19355058+4452498	6494 ± 195	4.51 ± 0.19	4.23	-0.34 ± 0.07	-0.38 ± 0.1	0	9.35	6.63	0.22
2M19355185+4250141	6130 ± 162	4.19 ± 0.22	4.06	-0.06 ± 0.06	-0.27 ± 0.1	0.06	6.21	12.07	1.55
2M19355791+4649016	5744 ± 112	4.21 ± 0.11	4.18	0.19 ± 0.05	0.14 ± 0.1	0.78	3.9	10.78	1.7
2M19361884+4949268	5099 ± 82	3.67 ± 0.1	3.67	-0.2 ± 0.04	-0.26 ± 0.1	0.85	3.57	0	1.65
2M19362997+4640224	5948 ± 116	4.29 ± 0.14	4.21	0.04 ± 0.05	-0.03 ± 0.1	0.62	4.99	9.89	1.6
2M19363103+4629507	5747 ± 133	4.22 ± 0.13	4.19	0.01 ± 0.05	-0.07 ± 0.1	0.62	4.11	8.11	0.54
2M19363273+4509550	5787 ± 137	4.31 ± 0.16	4.27	-0.02 ± 0.06	-0.07 ± 0.1	0.76	4.29	8.53	0.49
2M19363364+3817318	4690 ± 65	4.17 ± 0.1	4.44	-0.05 ± 0.03	-0.09 ± 0.1	2.23	3.69	10.09	1.91

APOGEE_ID	$T_{\text{eff}} \pm \Delta T_{\text{eff}}$	$\log g \pm \Delta \log g$	$\log g_{cor}$	$[\text{M/H}] \pm \Delta[\text{M/H}]$	$[Fe/H] \pm \Delta[\text{Fe/H}]$	v_{mic}	v_{mac}	$v \sin i$	χ^2
2M19363578+3948431	5953 ± 127	4.27 ± 0.16	4.19	0.03 ± 0.05	-0.03 ± 0.1	0.6	5.03	10.83	1.35
2M19363801+4441418	4912 ± 55	3.31 ± 0.09	3.31	0.07 ± 0.03	-0.03 ± 0.1	0.82	3.55	11.28	1.87
2M19364879+3842568	5637 ± 81	4.15 ± 0.1	4.14	0.16 ± 0.04	0.14 ± 0.1	1.18	3.57	0.34	0.77
2M19364879+3842568	5720 ± 73	4.54 ± 0.07	4.51	0.45 ± 0.03	0.14 ± 0.1	0.7	3.45	8.55	1.06
2M19365036+4628479	6065 ± 118	4.18 ± 0.14	4.07	0.05 ± 0.05	-0.01 ± 0.1	0.9	5.67	9.54	1.55
2M19365036+4628479	6114 ± 116	4.32 ± 0.16	4.20	0.1 ± 0.04	-0.01 ± 0.1	0.65	5.9	9.5	1.61
2M19370654+4640310	5928 ± 120	4.33 ± 0.18	4.25	-0.1 ± 0.05	-0.18 ± 0.1	0.47	5.03	8.46	0.5
2M19370743+4217274	5741 ± 189	4.11 ± 0.19	4.08	0.17 ± 0.08	0.13 ± 0.1	1.04	3.94	11.04	2.75
2M19371984+3844411	5965 ± 106	4.27 ± 0.13	4.18	0.13 ± 0.04	0.07 ± 0.1	0.81	4.99	9.37	0.45
2M19375424+5021431	4865 ± 53	3.33 ± 0.08	3.33	0.01 ± 0.03	-0.07 ± 0.1	0.92	3.59	11.23	1.92
2M19375440+4928384	6129 ± 151	4.47 ± 0.17	4.34	0 ± 0.06	-0.03 ± 0.1	0.54	6.1	10.31	1.5
2M19375456+4459048	6632 ± 1044	4.3 ± 1.64	3.96	-0.29 ± 0.44	-0.22 ± 0.1	0	10.66	0	11.93
2M19375669+4557522	6184 ± 166	4.32 ± 0.26	4.17	-0.32 ± 0.07	-0.35 ± 0.1	0.16	6.82	9.45	1.24
2M19375669+4557522	6027 ± 160	4.24 ± 0.2	4.14	-0.2 ± 0.06	-0.35 ± 0.1	0	5.71	7.76	1.4
2M19380439+4448549	5862 ± 136	4.21 ± 0.17	4.15	0.02 ± 0.05	-0.05 ± 0.1	0.61	4.59	9.2	0.52
2M19380462+4939178	5954 ± 118	4.12 ± 0.14	4.03	-0.04 ± 0.05	-0.09 ± 0.1	0.68	5.15	9.88	1.34
2M19382388+3822003	6256 ± 175	4.17 ± 0.18	3.99	0 ± 0.07	-0.09 ± 0.1	1.47	7.04	11.62	1.42
2M19385248+4618567	5628 ± 105	4.3 ± 0.14	4.30	0.09 ± 0.04	0.05 ± 0.1	1.07	3.6	10.75	1.64
2M19385272+4009136	6213 ± 127	4.21 ± 0.15	4.04	-0.01 ± 0.05	-0.1 ± 0.1	0.71	6.72	10.47	1.24
2M19390065+4654069	6432 ± 103	4.41 ± 0.16	4.15	-0.18 ± 0.04	-0.21 ± 0.1	0.38	8.63	8.88	1.16

APOGEE_ID	$T_{\mathrm{eff}} \pm \Delta T_{\mathrm{eff}}$	$\log g \pm \Delta \log g$	$\log g_{cor}$	$[\mathrm{M/H}] \pm \Delta[\mathrm{M/H}]$	$[Fe/H] \pm \Delta[\mathrm{Fe/H}]$	$\mathrm{v}_{\mathrm{mic}}$	$\mathrm{v}_{\mathrm{mac}}$	$v \sin i$	χ^2
2M19390065+4654069	6279 ± 105	4.27 ± 0.13	4.08	-0.04 ± 0.04	-0.21 ± 0.1	0.16	7.24	7.91	1.31
2M19390090-0525200	6163 ± 89	4.39 ± 0.15	4.25	-0.17 ± 0.03	-0.24 ± 0.1	0	6.52	7.17	0.35
2M19391536+4530461	5560 ± 70	4.02 ± 0.07	4.03	0.18 ± 0.03	0.15 ± 0.1	1.06	3.37	9.65	0.74
2M19391541+4714544	5713 ± 122	4.23 ± 0.13	4.21	0.02 ± 0.05	-0.04 ± 0.1	0.69	3.97	9.72	1.53
2M19391738+4704269	5806 ± 97	4.2 ± 0.11	4.15	0.07 ± 0.04	0.02 ± 0.1	0.73	4.29	10.64	0.37
2M19391944+4639345	5729 ± 116	4.17 ± 0.12	4.14	0.2 ± 0.05	0.15 ± 0.1	0.71	3.83	10.09	1.15
2M19392772+4617090	5351 ± 149	4.36 ± 0.2	4.43	0.11 ± 0.06	0.08 ± 0.1	1.46	3	0	2.35
2M19393877+4629292	5997 ± 97	4.43 ± 0.1	4.33	0.18 ± 0.04	0.13 ± 0.1	0.66	5.08	10.85	0.5
2M19395016+4402469	6132 ± 139	4.25 ± 0.19	4.12	0.1 ± 0.05	0.04 ± 0.1	0.78	6.03	9.12	0.43
2M19395217+3902516	5991 ± 150	4.24 ± 0.18	4.15	-0.15 ± 0.06	-0.23 ± 0.1	0.42	5.44	8.12	0.39
2M19395358+4700553	5774 ± 117	4.19 ± 0.12	4.15	0.11 ± 0.05	0.05 ± 0.1	0.71	4.11	10.51	0.67
2M19395364+4512492	5836 ± 146	4.37 ± 0.23	4.31	-0.26 ± 0.06	-0.33 ± 0.1	0	4.75	8.6	1.47
2M19400942+4657575	5563 ± 95	4.02 ± 0.09	4.03	0.13 ± 0.04	0.08 ± 0.1	0.79	3.44	10.24	1.58
2M19401696+5054134	5984 ± 163	4.22 ± 0.18	4.13	-0.04 ± 0.07	-0.13 ± 0.1	0.23	5.29	9.45	1.32
2M19402120+4529209	5922 ± 116	4.37 ± 0.18	4.29	-0.05 ± 0.05	-0.11 ± 0.1	0.5	4.94	9.61	1.46
2M19402120+4529209	5977 ± 121	4.47 ± 0.11	4.38	0 ± 0.05	-0.11 ± 0.1	0.4	5.17	9.69	1.5
2M19402267+4546361	6056 ± 108	4.15 ± 0.12	4.04	0.11 ± 0.04	0.06 ± 0.1	1.06	5.56	11.11	1.39
2M19404989+4852239	5154 ± 115	4.3 ± 0.15	4.41	0.34 ± 0.05	0.29 ± 0.1	0.71	2.67	10.55	2.9
2M19405136+5101517	5561 ± 142	4.32 ± 0.18	4.33	-0.15 ± 0.06	-0.21 ± 0.1	0.66	3.67	10.38	1.39
2M19405615+4553013	5854 ± 140	4.37 ± 0.22	4.31	-0.15 ± 0.06	-0.2 ± 0.1	0.52	4.72	8.53	0.39

APOGEE_ID	$T_{\rm eff} \pm \Delta T_{\rm eff}$	$\log g \pm \Delta \log g$	$\log g_{cor}$	$[\mathrm{M/H}] \pm \Delta[\mathrm{M/H}]$	$[Fe/H] \pm \Delta[\mathrm{Fe/H}]$	$\mathrm{v_{mic}}$	$\mathrm{v_{mac}}$	$v \sin i$	χ^2
2M19410030+5041414	5952 ± 141	4.24 ± 0.17	4.16	0.01 ± 0.06	-0.06 ± 0.1	0.68	5.06	9.47	1.28
2M19410064+4853095	6025 ± 118	4.37 ± 0.14	4.27	0.07 ± 0.05	0.01 ± 0.1	0.64	5.38	8.78	1.39
2M19410324+3844456	5588 ± 111	4.01 ± 0.11	4.02	0 ± 0.05	-0.04 ± 0.1	0.92	3.66	10.04	0.46
2M19411279+5033548	6246 ± 144	4.25 ± 0.16	4.07	0.1 ± 0.06	0.03 ± 0.1	0.98	6.84	9.32	1.31
2M19412225+4636081	5540 ± 190	4.3 ± 0.22	4.32	-0.02 ± 0.08	-0.05 ± 0.1	1.14	3.48	8.1	1.64
2M19413907+4615592	5427 ± 102	4.32 ± 0.14	4.37	0.36 ± 0.05	0.31 ± 0.1	1.02	2.8	9.42	1.41
2M19414552+4402209	6057 ± 108	4.15 ± 0.13	4.04	-0.05 ± 0.04	-0.11 ± 0.1	0.74	5.74	8.96	0.32
2M19414552+4402209	6026 ± 114	4.24 ± 0.13	4.14	-0.04 ± 0.05	-0.11 ± 0.1	0.53	5.52	8.27	0.38
2M19415238+2322412	5821 ± 71	4.24 ± 0.1	4.19	-0.12 ± 0.03	-0.21 ± 0.1	0.55	4.55	8.29	1.39
2M19422462+4631037	5724 ± 91	4.35 ± 0.1	4.32	0 ± 0.04	-0.05 ± 0.1	0.66	4.01	10.44	0.39
2M19424675+4619095	5636 ± 256	4.36 ± 0.4	4.36	-0.05 ± 0.11	-0.09 ± 0.1	0.64	3.76	11.37	3.53
2M19432366+5021177	5845 ± 107	4.23 ± 0.13	4.17	0.13 ± 0.04	0.08 ± 0.1	0.72	4.39	10.2	0.71
2M19432935+4252521	5699 ± 93	4.16 ± 0.1	4.14	0.16 ± 0.04	0.12 ± 0.1	0.78	3.77	9.26	0.68
2M19432935+4252521	5699 ± 93	4.16 ± 0.1	4.14	0.16 ± 0.04	0.12 ± 0.1	0.78	3.77	9.26	0.68
2M19433017+4835336	5695 ± 61	4.09 ± 0.06	4.07	0.14 ± 0.03	0.11 ± 0.1	0.88	3.8	9.88	1.3
2M19433308+4805046	5945 ± 165	4.21 ± 0.22	4.13	-0.15 ± 0.07	-0.23 ± 0.1	0.34	5.2	8.28	0.57
2M19435406+5104527	4673 ± 59	3.04 ± 0.07	3.04	0.33 ± 0.04	0.21 ± 0.1	1.15	3.31	9.3	2.34
2M19435771+4955214	5901 ± 143	4.04 ± 0.17	3.97	0.06 ± 0.06	0 ± 0.1	0.87	4.79	9.18	1.6
2M19441664+4542111	6122 ± 133	4.31 ± 0.19	4.18	0.14 ± 0.05	0.09 ± 0.1	0.54	5.9	10.44	1.42
2M19443187+4858386	5466 ± 153	4.35 ± 0.19	4.39	0.09 ± 0.06	0.04 ± 0.1	0.92	3.19	9.86	1.89

APOGEE_ID	$T_{\rm eff} \pm \Delta T_{\rm eff}$	$\log g \pm \Delta \log g$	$\log g_{cor}$	$[\mathrm{M/H}] \pm \Delta[\mathrm{M/H}]$	$[Fe/H] \pm \Delta[\mathrm{Fe/H}]$	$v_{\rm mic}$	$v_{\rm mac}$	$v \sin i$	χ^2
2M19444834+5006363	5828 ± 88	4.07 ± 0.09	4.02	0.1 ± 0.04	0.04 ± 0.1	0.78	4.39	10.96	1.39
2M19450497+5014144	5704 ± 98	4.29 ± 0.12	4.27	-0.03 ± 0.04	-0.09 ± 0.1	0.7	3.98	8.53	0.46
2M19451822+4806096	6113 ± 153	4.43 ± 0.22	4.31	-0.23 ± 0.06	-0.31 ± 0.1	0	6.23	9.02	1.51
2M19452396+4404359	6407 ± 138	4.46 ± 0.17	4.21	0.08 ± 0.05	-0.02 ± 0.1	0.55	8.13	10.13	0.31
2M19453753+4947315	5927 ± 144	4.34 ± 0.2	4.26	-0.01 ± 0.06	-0.08 ± 0.1	0.6	4.93	8.72	0.47
2M19454379+4729184	5930 ± 147	4.27 ± 0.19	4.19	-0.02 ± 0.06	-0.09 ± 0.1	0.53	4.96	8.73	0.64
2M19454595+4959188	5299 ± 80	4.33 ± 0.1	4.41	-0.06 ± 0.03	-0.11 ± 0.1	0.88	3.15	9.68	1.53
2M19455634+5004257	5794 ± 104	4.1 ± 0.1	4.06	0.06 ± 0.04	-0.01 ± 0.1	0.76	4.28	9.04	1.31
2M19461484+4059436	5279 ± 78	3.78 ± 0.09	3.87	-0.01 ± 0.04	-0.07 ± 0.1	0.88	3.28	0	1.61
2M19461782+4449395	5575 ± 85	3.92 ± 0.11	3.93	-0.05 ± 0.04	-0.11 ± 0.1	0.75	3.72	11.09	0.4
2M19463773+5101135	6655 ± 133	4.25 ± 0.18	3.90	-0.19 ± 0.05	-0.28 ± 0.1	0	10.81	0	1.23
2M19471189+4931386	6064 ± 126	4.35 ± 0.16	4.24	0.04 ± 0.05	-0.03 ± 0.1	0.62	5.65	8.95	1.39
2M19473759+4728048	5998 ± 158	4.2 ± 0.17	4.10	-0.04 ± 0.06	-0.12 ± 0.1	0.56	5.36	8.98	0.48
2M19480452+5024323	5869 ± 174	4.13 ± 0.21	4.07	0.04 ± 0.07	-0.01 ± 0.1	0.95	4.62	9.65	1.87
2M19481429+4344486	6353 ± 147	4.29 ± 0.22	4.07	-0.34 ± 0.06	-0.39 ± 0.1	0	8.13	6.95	0.32
2M19481670+4031304	5582 ± 103	4.29 ± 0.12	4.30	0 ± 0.04	-0.02 ± 0.1	1.03	3.57	2.08	1.47
2M19481670+4031304	5575 ± 99	4.29 ± 0.12	4.30	-0.01 ± 0.04	-0.02 ± 0.1	0.83	3.56	9.96	1.37
2M19482241+4914117	5632 ± 87	3.9 ± 0.14	3.90	-0.04 ± 0.04	-0.09 ± 0.1	0.91	3.87	9.42	1.47
2M19483036+4354051	5712 ± 131	4.09 ± 0.13	4.07	0.06 ± 0.05	0 ± 0.1	0.64	3.96	10.86	1.6
2M19485701+4258312	6146 ± 160	4.34 ± 0.24	4.20	-0.01 ± 0.06	-0.08 ± 0.1	0.34	6.23	9.32	0.43

APOGEE_ID	$T_{\text{eff}} \pm \Delta T_{\text{eff}}$	$\log g \pm \Delta \log g$	$\log g_{cor}$	$[\text{M/H}] \pm \Delta[\text{M/H}]$	$[Fe/H] \pm \Delta[\text{Fe/H}]$	v_{mic}	v_{mac}	$v \sin i$	χ^2
2M19491993+4153280	6150 ± 229	4.25 ± 0.33	4.11	0.06 ± 0.09	-0.03 ± 0.1	0.81	6.19	10.41	0.54
2M19492084+4829253	6161 ± 123	4.48 ± 0.14	4.34	-0.01 ± 0.05	-0.08 ± 0.1	0	6.32	8.83	1.37
2M19492496+4118001	4742 ± 56	4.4 ± 0.09	4.65	0.19 ± 0.02	0.15 ± 0.1	1.02	3.58	11.05	2.19
2M19493050+4919123	6141 ± 140	4.47 ± 0.16	4.34	0.13 ± 0.06	0.08 ± 0.1	0.62	6.03	10.82	0.61
2M19493954+4620271	5871 ± 102	4.24 ± 0.13	4.18	0.04 ± 0.04	0 ± 0.1	0.81	4.61	9.37	1.41
2M19495685+4937244	5518 ± 172	4.48 ± 0.14	4.50	-0.01 ± 0.07	-0.06 ± 0.1	0.77	3.4	8.02	2.05
2M19500038+4823061	5731 ± 109	4.32 ± 0.12	4.29	-0.01 ± 0.04	-0.05 ± 0.1	0.92	4.05	10.19	0.44
2M19500341+4003015	6087 ± 147	4.24 ± 0.19	4.12	0.03 ± 0.06	-0.01 ± 0.1	0.75	5.82	9.63	0.5
2M19500857+3954488	6505 ± 170	4.47 ± 0.15	4.18	0.21 ± 0.06	-0.14 ± 0.1	1.51	8.86	35.55	0.22
2M19501408+4811554	6113 ± 119	4.37 ± 0.17	4.25	0.11 ± 0.05	0.03 ± 0.1	0.59	5.88	9.74	0.42
2M19503244+4138307	5071 ± 103	4.45 ± 0.11	4.59	0.08 ± 0.04	0.04 ± 0.1	1	3.03	9.21	1.98
2M19503330+4822093	6207 ± 114	4.5 ± 0.11	4.34	0.1 ± 0.04	0.03 ± 0.1	0.51	6.53	11.36	0.34
2M19505021+4804508	4788 ± 29	4.58 ± 0.03	4.81	0.41 ± 0.01	0.35 ± 0.1	0.72	3.53	8.49	2.02
2M19520946+4734308	5716 ± 113	4.29 ± 0.12	4.26	0 ± 0.05	-0.05 ± 0.1	0.73	3.99	10.64	0.45
2M19521126+4139597	5745 ± 105	4.01 ± 0.1	3.98	-0.05 ± 0.05	-0.11 ± 0.1	0.75	4.23	9.63	1.4
2M19521906+4444467	5351 ± 141	4.45 ± 0.16	4.52	0.32 ± 0.06	0.27 ± 0.1	0.91	2.75	8.63	2.17
2M19525039+4756455	6046 ± 146	4.34 ± 0.18	4.23	0.01 ± 0.06	-0.05 ± 0.1	0.68	5.57	8.53	0.5
2M19532801+4829023	6083 ± 135	4.39 ± 0.19	4.27	0.14 ± 0.05	0.08 ± 0.1	0.51	5.65	10.71	1.45
2M19533900+4737462	5705 ± 130	4.35 ± 0.16	4.33	-0.02 ± 0.05	-0.06 ± 0.1	0.74	3.96	10.08	0.47
2M19534035+4747591	5916 ± 124	4.27 ± 0.17	4.19	-0.01 ± 0.05	-0.08 ± 0.1	0.53	4.88	8.62	0.47

APOGEE_ID	$T_{\text{eff}} \pm \Delta T_{\text{eff}}$	$\log g \pm \Delta \log g$	$\log g_{cor}$	$[\text{M/H}] \pm \Delta[\text{M/H}]$	$[Fe/H] \pm \Delta[\text{Fe/H}]$	v_{mic}	v_{mac}	$v \sin i$	χ^2
2M19534459+4435343	6220 ± 125	4.5 ± 0.11	4.33	0.22 ± 0.05	0.19 ± 0.1	0.58	6.47	8.66	1.54
2M19534751+4831121	6200 ± 176	4.15 ± 0.22	3.99	-0.08 ± 0.07	-0.17 ± 0.1	0.33	6.72	8.1	0.46
2M19545417+4708430	6234 ± 113	4.18 ± 0.12	4.01	0 ± 0.04	-0.07 ± 0.1	0.78	6.87	7.78	1.29
2M19554781+4506424	5954 ± 106	4.17 ± 0.12	4.08	0.03 ± 0.04	-0.04 ± 0.1	0.71	5.05	9.18	1.24
2M19554832+4639549	5711 ± 116	4.26 ± 0.13	4.24	0.03 ± 0.05	-0.01 ± 0.1	0.73	3.95	9.95	0.49
2M19555801+4008327	6087 ± 130	4.29 ± 0.17	4.17	0.11 ± 0.05	0.05 ± 0.1	0.68	5.71	9.52	0.5
2M19560369+4706004	5940 ± 158	4.2 ± 0.21	4.12	-0.13 ± 0.06	-0.2 ± 0.1	0	5.15	7.51	0.53
2M19561944+4141404	5677 ± 129	3.97 ± 0.14	3.95	0 ± 0.05	-0.05 ± 0.1	0.76	3.94	10.96	0.46
2M19561944+4141404	5679 ± 129	3.97 ± 0.14	3.95	0.01 ± 0.05	-0.05 ± 0.1	0.75	3.94	10.97	0.46
2M19562027+4453467	5672 ± 113	4.33 ± 0.16	4.32	-0.03 ± 0.05	-0.07 ± 0.1	1	3.87	8.53	0.48
2M19563851+4108374	5926 ± 120	4.19 ± 0.15	4.11	0 ± 0.05	-0.07 ± 0.1	0.67	4.94	9.43	0.39
2M19564403+4450404	5729 ± 134	4.39 ± 0.17	4.36	-0.04 ± 0.06	-0.07 ± 0.1	1.21	4.07	9.61	0.53
2M19565512+4456153	5876 ± 114	4.18 ± 0.14	4.11	0.02 ± 0.05	-0.05 ± 0.1	0.77	4.67	9.82	0.4
2M19565722+4746418	6001 ± 93	4.35 ± 0.11	4.25	0.25 ± 0.04	0.19 ± 0.1	0.83	5.03	10.9	0.54
2M19571897+4647530	5991 ± 138	4.15 ± 0.14	4.06	0.04 ± 0.05	-0.03 ± 0.1	0.59	5.25	9.78	0.52
2M19573701+4647166	5914 ± 110	4.15 ± 0.15	4.08	-0.11 ± 0.05	-0.17 ± 0.1	0.33	5	8.98	1.35
2M19580834+4028399	5828 ± 176	4.3 ± 0.22	4.25	0.13 ± 0.07	0.1 ± 0.1	0.85	4.29	9.78	0.98
2M19591476+4409484	5794 ± 124	4.22 ± 0.14	4.18	0.11 ± 0.05	0.06 ± 0.1	0.87	4.19	9.54	0.52
2M20015142+4421140	6252 ± 124	4.39 ± 0.18	4.21	-0.26 ± 0.05	-0.31 ± 0.1	0.39	7.25	10.13	1.19
2M20023331+4431589	5541 ± 95	3.99 ± 0.09	4.01	0.07 ± 0.04	0.01 ± 0.1	0.8	3.47	9.84	1.54

APOGEE_ID	$T_{\mathrm{eff}} \pm \Delta T_{\mathrm{eff}}$	$\log g \pm \Delta \log g$	$\log g_{cor}$	$[\mathrm{M/H}] \pm \Delta[\mathrm{M/H}]$	$[Fe/H] \pm \Delta[\mathrm{Fe/H}]$	$\mathrm{v}_{\mathrm{mic}}$	$\mathrm{v}_{\mathrm{mac}}$	$v \sin i$	χ^2
2M20023331+4431589	5542 ± 96	3.99 ± 0.09	4.01	0.07 ± 0.04	0.01 ± 0.1	0.79	3.47	9.84	1.54
2M20031264+4526232	5622 ± 87	4.02 ± 0.09	4.02	0.14 ± 0.04	0.09 ± 0.1	0.92	3.59	10.73	1.5
2M20032836+4507502	5964 ± 87	4.29 ± 0.1	4.20	0.12 ± 0.03	0.07 ± 0.1	0.68	4.99	10.66	0.38
2M20035806+4459470	5948 ± 124	4.05 ± 0.14	3.97	-0.04 ± 0.05	-0.1 ± 0.1	0.87	5.13	9.2	0.37
2M20041723+4438335	5925 ± 148	4.39 ± 0.23	4.31	-0.14 ± 0.06	-0.19 ± 0.1	0.41	5.05	8.71	0.42
2M20042355+3333018	5146 ± 186	3.43 ± 0.3	3.43	-0.24 ± 0.1	-0.32 ± 0.1	0.85	3.87	10.21	0.73
2M20084295+2209120	4906 ± 73	3.22 ± 0.11	3.22	0.01 ± 0.05	-0.07 ± 0.1	1.06	3.65	9.41	1.88
2M20242972+1645437	5725 ± 156	4.25 ± 0.17	4.22	0.04 ± 0.06	-0.02 ± 0.1	1.07	3.99	11.21	0.56
2M20334362+4007031	6150 ± 158	4.47 ± 0.19	4.33	-0.02 ± 0.06	-0.1 ± 0.1	0.21	6.26	9.26	1.53
2M20382092+1319530	5077 ± 101	3.58 ± 0.11	3.58	-0.01 ± 0.05	-0.1 ± 0.1	0.9	3.45	9.52	0.83
2M20390586-0455461	4775 ± 61	3.02 ± 0.08	3.02	0.08 ± 0.04	0.07 ± 0.1	1.73	3.64	9.24	2.88
2M20401610+0033197	6610 ± 189	4.27 ± 0.26	3.94	-0.51 ± 0.07	-0.67 ± 0.1	0	10.65	4.52	0.5
2M20403691+3723508	4815 ± 93	3.13 ± 0.13	3.13	-0.37 ± 0.05	-0.46 ± 0.1	0.76	4.07	10.79	1.61
2M21025161-0036351	5703 ± 130	4.24 ± 0.15	4.22	-0.02 ± 0.05	-0.07 ± 0.1	0.62	3.98	9.44	1.81
2M21031246+0003094	5674 ± 91	4.1 ± 0.1	4.09	0.03 ± 0.04	-0.03 ± 0.1	0.8	3.86	9.66	0.56
2M21054526-0008060	5804 ± 140	4.37 ± 0.18	4.32	-0.04 ± 0.06	-0.09 ± 0.1	0.65	4.38	10.19	1.53
2M21071442+1042354	6124 ± 157	4.28 ± 0.24	4.15	-0.06 ± 0.06	-0.13 ± 0.1	0	6.14	7.65	0.56
2M21072421+0002567	5684 ± 121	4.02 ± 0.12	4.00	0.1 ± 0.05	0.05 ± 0.1	0.81	3.84	10.56	0.71
2M21091067+3022353	6238 ± 64	4.35 ± 0.09	4.17	-0.18 ± 0.03	-0.21 ± 0.1	0.44	7.07	10.3	0.18
2M21091067+3022353	6160 ± 66	4.33 ± 0.1	4.19	-0.04 ± 0.03	-0.21 ± 0.1	0.26	6.36	8.35	0.33

APOGEE_ID	$T_{\rm eff} \pm \Delta T_{\rm eff}$	$\log g \pm \Delta \log g$	$\log g_{cor}$	$[{\rm M/H}] \pm \Delta[{\rm M/H}]$	$[Fe/H] \pm \Delta[{\rm Fe/H}]$	$v_{\rm mic}$	$v_{\rm mac}$	$v \sin i$	χ^2
2M21130764+1027504	5877 ± 112	4.22 ± 0.15	4.15	-0.04 ± 0.05	-0.1 ± 0.1	0.59	4.73	8.51	1.34
2M21144847+1100301	6219 ± 550	3.88 ± 0.69	3.71	-0.69 ± 0.22	-1.01 ± 0.1	0	7.54	4.98	0.51
2M21152723+4201346	5002 ± 103	3.4 ± 0.15	3.40	-0.05 ± 0.05	-0.16 ± 0.1	1.03	3.66	9.53	1.86
2M21164414+0013567	5783 ± 141	4.34 ± 0.16	4.30	-0.01 ± 0.06	-0.07 ± 0.1	0.68	4.26	9.54	0.62
2M21165893+1137346	5778 ± 124	4.32 ± 0.14	4.28	-0.02 ± 0.05	-0.07 ± 0.1	0.69	4.25	8.52	1.51
2M21205897+0022176	5755 ± 65	4.23 ± 0.07	4.20	0.05 ± 0.03	0 ± 0.1	0.62	4.09	11.18	1.38
2M21220520+5039279	5941 ± 139	4.2 ± 0.18	4.12	-0.07 ± 0.06	-0.14 ± 0.1	0.54	5.09	8.26	0.49
2M21222880+0056061	5677 ± 137	4.23 ± 0.16	4.21	0 ± 0.06	-0.07 ± 0.1	0.67	3.87	9.66	0.62
2M21230966-0006027	6115 ± 168	4.27 ± 0.23	4.15	-0.01 ± 0.06	-0.08 ± 0.1	0.67	6.04	8.95	0.51
2M21231691+0059543	5795 ± 127	4.28 ± 0.15	4.24	0.05 ± 0.05	0.01 ± 0.1	0.82	4.25	10.63	0.53
2M21241801+0027414	5828 ± 100	4.17 ± 0.12	4.12	0.1 ± 0.04	0.04 ± 0.1	0.68	4.35	10.49	1.49
2M21250192+0008371	6209 ± 123	4.5 ± 0.12	4.34	-0.04 ± 0.05	-0.1 ± 0.1	0.46	6.7	7.97	0.41
2M21254987-0042318	5945 ± 115	4.43 ± 0.14	4.35	-0.02 ± 0.05	-0.09 ± 0.1	0.47	5.02	10.15	1.38
2M21272442+0009449	5953 ± 166	4.45 ± 0.2	4.37	-0.23 ± 0.07	-0.33 ± 0.1	0	5.29	7.63	1.57
2M21272972+1208018	5574 ± 115	4.07 ± 0.12	4.08	0.07 ± 0.05	0.01 ± 0.1	0.76	3.52	10.38	0.63
2M21285852+0023158	5855 ± 137	4.35 ± 0.2	4.29	-0.03 ± 0.06	-0.08 ± 0.1	0.57	4.6	10.46	1.75
2M21294710+0008318	5958 ± 82	4.11 ± 0.1	4.02	-0.14 ± 0.03	-0.22 ± 0.1	0.46	5.28	8.04	0.37
2M21300899+0106184	6104 ± 125	4.42 ± 0.18	4.30	-0.04 ± 0.05	-0.12 ± 0.1	0.3	5.98	8.45	1.38
2M21305866+0053194	5634 ± 80	4.19 ± 0.1	4.19	0.15 ± 0.03	0.1 ± 0.1	0.91	3.57	10.64	1.67
2M21311766+0025033	5956 ± 129	4.15 ± 0.14	4.06	0.1 ± 0.05	0.05 ± 0.1	0.72	4.99	10.94	0.47

APOGEE_ID	$T_{\rm eff} \pm \Delta T_{\rm eff}$	$\log g \pm \Delta \log g$	$\log g_{cor}$	$[\mathrm{M/H}] \pm \Delta[\mathrm{M/H}]$	$[Fe/H] \pm \Delta[\mathrm{Fe/H}]$	$\mathrm{v}_{\rm mic}$	$\mathrm{v}_{\rm mac}$	$v \sin i$	χ^2
2M21312407+0025071	5721 ± 109	4.18 ± 0.12	4.15	0.23 ± 0.05	0.18 ± 0.1	0.86	3.77	9.92	1.85
2M21314137+0053088	5791 ± 118	4.14 ± 0.12	4.10	0.16 ± 0.05	0.1 ± 0.1	0.77	4.14	11.01	0.66
2M21315040-0123088	5659 ± 111	4.07 ± 0.12	4.06	0.01 ± 0.05	-0.03 ± 0.1	0.87	3.84	9.97	1.47
2M21321194+0013180	4459 ± 25	3.83 ± 0.06	4.17	-0.86 ± 0.02	-1.02 ± 0.1	0	4.19	22.6	1.73
2M21322121+0108150	5854 ± 145	4.04 ± 0.16	3.98	-0.03 ± 0.06	-0.1 ± 0.1	0.69	4.66	9.69	0.39
2M21324626+0109212	6037 ± 107	4.3 ± 0.13	4.19	0.12 ± 0.04	0.06 ± 0.1	0.66	5.4	10.6	0.43
2M21332497+0036523	5858 ± 101	4.23 ± 0.13	4.17	0.12 ± 0.04	0.06 ± 0.1	0.77	4.46	10.38	0.48
2M21332613-0111163	5737 ± 126	4.19 ± 0.14	4.16	-0.08 ± 0.05	-0.14 ± 0.1	0.64	4.18	10.22	0.44
2M21341969+0002317	5814 ± 92	4.3 ± 0.11	4.25	0.13 ± 0.04	0.08 ± 0.1	0.77	4.23	10.48	0.51
2M21350646+0030292	5760 ± 108	4.11 ± 0.1	4.07	0.01 ± 0.04	-0.05 ± 0.1	0.7	4.19	9.36	0.43
2M21351439-0040467	5800 ± 98	4.28 ± 0.12	4.23	-0.04 ± 0.04	-0.11 ± 0.1	0.58	4.37	8.78	1.42
2M21353376-0028376	5631 ± 118	4.01 ± 0.13	4.01	-0.04 ± 0.05	-0.08 ± 0.1	0.77	3.83	9.79	1.5
2M21531344+4707426	5640 ± 112	4.18 ± 0.14	4.17	0.05 ± 0.05	0.01 ± 0.1	0.78	3.7	10.17	0.78
2M21541260+4715320	5791 ± 74	4.19 ± 0.08	4.15	0.08 ± 0.03	0.02 ± 0.1	0.65	4.22	10.37	0.39
2M21570546+1641017	5841 ± 117	4.38 ± 0.18	4.32	-0.09 ± 0.05	-0.13 ± 0.1	0.55	4.59	9.75	0.36
2M21583813+1636246	6088 ± 156	4.17 ± 0.21	4.05	-0.24 ± 0.06	-0.32 ± 0.1	0	6.13	7.22	0.41
2M21585496-0422226	4813 ± 71	3.5 ± 0.07	3.50	0.06 ± 0.04	-0.05 ± 0.1	0.67	3.89	11.06	1.96
2M21592962+1744261	5581 ± 85	4.35 ± 0.11	4.36	-0.02 ± 0.04	-0.06 ± 0.1	0.94	3.58	11.11	0.41
2M21595255+1711169	5635 ± 89	4.18 ± 0.11	4.18	0.1 ± 0.04	0.06 ± 0.1	0.83	3.63	10.31	0.54
2M22001919+1702208	6072 ± 80	4.42 ± 0.1	4.31	0.09 ± 0.03	0.04 ± 0.1	0.65	5.63	10.72	0.31

APOGEE_ID	$T_{\rm eff} \pm \Delta T_{\rm eff}$	$\log g \pm \Delta \log g$	$\log g_{cor}$	$[\mathrm{M/H}] \pm \Delta[\mathrm{M/H}]$	$[Fe/H] \pm \Delta[\mathrm{Fe/H}]$	$\mathrm{v}_{\rm mic}$	$\mathrm{v}_{\rm mac}$	$v \sin i$	χ^2
2M22002265+1708028	5809 ± 107	4.28 ± 0.13	4.23	0.14 ± 0.04	0.1 ± 0.1	0.79	4.2	10.14	0.59
2M22004698+1709113	6167 ± 156	4.37 ± 0.23	4.22	0.07 ± 0.06	0 ± 0.1	0.54	6.29	9.53	1.41
2M22005669+1628518	5668 ± 118	4 ± 0.13	3.99	-0.1 ± 0.05	-0.14 ± 0.1	0.73	4.01	9.93	0.44
2M22012457+1758188	6184 ± 165	4.37 ± 0.25	4.22	-0.12 ± 0.07	-0.2 ± 0.1	0.08	6.61	8.58	0.39
2M22013547+1743298	6164 ± 82	4.31 ± 0.12	4.17	0.16 ± 0.03	0.1 ± 0.1	0.8	6.17	8.75	0.37
2M22015893+1702258	5682 ± 101	4 ± 0.11	3.98	-0.06 ± 0.05	-0.11 ± 0.1	0.8	4.02	9.13	0.4
2M22030241+1602182	6049 ± 82	4.32 ± 0.11	4.21	-0.04 ± 0.03	-0.11 ± 0.1	0.42	5.65	8.72	0.34
2M22033565+1543562	5590 ± 113	4.42 ± 0.15	4.43	-0.05 ± 0.05	-0.06 ± 0.1	0.97	3.62	9.73	1.47
2M22034728+1528439	5802 ± 93	4.23 ± 0.11	4.18	0.21 ± 0.04	0.16 ± 0.1	0.79	4.1	9.88	0.53
2M22035239+1706173	5602 ± 113	4.12 ± 0.13	4.12	0.15 ± 0.05	0.11 ± 0.1	0.94	3.49	9.88	1.76
2M22054841+1540383	5917 ± 139	4.26 ± 0.21	4.18	-0.15 ± 0.06	-0.21 ± 0.1	0.39	5.04	8.01	0.41
2M22115493+7012378	5807 ± 123	3.97 ± 0.13	3.92	0.03 ± 0.05	-0.02 ± 0.1	0.76	4.41	11.12	1.79
2M22441947+5126582	6170 ± 69	4.27 ± 0.09	4.12	0.03 ± 0.03	-0.03 ± 0.1	0.54	6.36	9.52	0.33
2M23050631+1633466	5153 ± 105	3.72 ± 0.15	3.72	0.2 ± 0.05	0.13 ± 0.1	1.06	3.07	9.58	2
2M23060482+6355339	3903 ± 13	4.71 ± 0.04	5.24	0.17 ± 0.01	0.14 ± 0.1	0	5.43	9.2	1.31
2M23124678+4308571	5601 ± 107	4.35 ± 0.15	4.35	-0.07 ± 0.05	-0.11 ± 0.1	0.9	3.69	9.55	0.46
2M23124910+4726557	5583 ± 54	4.19 ± 0.06	4.20	0.04 ± 0.02	0 ± 0.1	0.72	3.54	10.42	1.51
2M23140658+1204051	6185 ± 141	4.43 ± 0.18	4.28	0.01 ± 0.05	-0.06 ± 0.1	0.36	6.47	9.06	0.42
2M23145008+4220141	5836 ± 114	4.09 ± 0.13	4.03	0.05 ± 0.05	0.01 ± 0.1	0.82	4.47	9.57	1.53
2M23163232+1055503	6063 ± 151	4.2 ± 0.2	4.09	-0.09 ± 0.06	-0.16 ± 0.1	0.39	5.81	8.51	0.45

APOGEE_ID	$T_{\rm eff} \pm \Delta T_{\rm eff}$	$\log g \pm \Delta \log g$	$\log g_{cor}$	$[\rm M/H] \pm \Delta[\rm M/H]$	$[Fe/H] \pm \Delta[\rm Fe/H]$	$v_{\rm mic}$	$v_{\rm mac}$	$v \sin i$	χ^2
2M23163376+4332432	6248 ± 144	4.24 ± 0.17	4.06	-0.09 ± 0.06	-0.19 ± 0.1	0.47	7.07	7.46	1.45
2M23203850+4202060	5921 ± 154	4.02 ± 0.18	3.94	-0.11 ± 0.07	-0.17 ± 0.1	0.61	5.09	8.26	1.44
2M23205478+4133134	5947 ± 142	4.26 ± 0.18	4.18	-0.03 ± 0.06	-0.11 ± 0.1	0.62	5.06	8.59	0.55
2M23214099+4151384	5901 ± 92	4.31 ± 0.13	4.24	0.04 ± 0.04	-0.02 ± 0.1	0.59	4.75	9.15	0.4
2M23224149+1211477	6085 ± 78	4.37 ± 0.11	4.25	0.04 ± 0.03	-0.02 ± 0.1	0.43	5.78	9.36	0.35
2M23315208+1956142	5439 ± 230	3.32 ± 0.33	3.32	0.28 ± 0.13	-0.51 ± 0.1	0.76	3.37	42.93	5.23
2M23325959+3052418	5788 ± 115	4.18 ± 0.12	4.14	0.14 ± 0.05	0.09 ± 0.1	0.84	4.14	10.15	1.77
2M23343773+3111234	5782 ± 106	4.16 ± 0.11	4.12	0.18 ± 0.04	0.13 ± 0.1	0.83	4.07	10.55	1.74
2M23355899+3115344	5956 ± 124	4.36 ± 0.16	4.27	0.07 ± 0.05	0.02 ± 0.1	0.61	4.99	11.1	1.42
2M23372818+2859333	6167 ± 100	4.44 ± 0.13	4.29	0.21 ± 0.04	0.17 ± 0.1	0.72	6.12	9.76	0.42
2M23394687+3106477	6433 ± 83	4.59 ± 0.1	4.33	-0.2 ± 0.03	-0.23 ± 0.1	0	8.66	9.4	1.2
2M23400520+2925149	5966 ± 169	4.3 ± 0.22	4.21	-0.2 ± 0.07	-0.28 ± 0.1	0.24	5.34	7.88	1.54
2M23411706+3029293	5671 ± 101	4.11 ± 0.13	4.10	-0.27 ± 0.04	-0.37 ± 0.1	0.53	4.16	7.6	0.38
2M23422583+3058212	6073 ± 66	4.35 ± 0.09	4.23	0.12 ± 0.03	0.05 ± 0.1	0.54	5.61	10.18	1.38
2M23432248+2924547	5986 ± 141	4.27 ± 0.18	4.18	-0.07 ± 0.06	-0.14 ± 0.1	0.59	5.32	8.53	0.54
2M23434684+3043428	5906 ± 68	4.23 ± 0.09	4.16	0.04 ± 0.03	-0.02 ± 0.1	0.78	4.78	9.61	1.37
2M23454320-0012219	5571 ± 122	4.37 ± 0.16	4.38	-0.04 ± 0.05	-0.06 ± 0.1	0.98	3.57	9.89	0.62
2M23461101+0109422	6126 ± 124	4.45 ± 0.15	4.32	0.03 ± 0.05	-0.04 ± 0.1	0.43	6.04	9.63	0.33
2M23464963-0115281	5829 ± 118	4.27 ± 0.15	4.22	0.07 ± 0.05	0.02 ± 0.1	0.64	4.38	10.72	1.49
2M23474350-0035121	5389 ± 85	4.25 ± 0.11	4.31	-0.02 ± 0.04	-0.02 ± 0.1	1.59	3.21	10.5	1.7

APOGEE_ID	$T_{\rm eff} \pm \Delta T_{\rm eff}$	$\log g \pm \Delta \log g$	$\log g_{cor}$	$[\rm M/H] \pm \Delta[\rm M/H]$	$[Fe/H] \pm \Delta[\rm Fe/H]$	$\rm v_{mic}$	$\rm v_{mac}$	$v \sin i$	χ^2
2M23475682-0001597	5911 ± 106	4.31 ± 0.15	4.24	0.14 ± 0.04	0.11 ± 0.1	0.89	4.68	9.53	0.53
2M23480803-0024109	5538 ± 106	4.14 ± 0.11	4.16	0.1 ± 0.05	0.08 ± 0.1	0.95	3.37	9.24	0.76
2M23492408-0119149	5756 ± 117	4.16 ± 0.12	4.12	-0.05 ± 0.05	-0.11 ± 0.1	0.65	4.23	9.16	1.46
2M23501471-0958269	4597 ± 55	2.78 ± 0.1	2.78	0.08 ± 0.04	0 ± 0.1	1.16	3.72	11.21	2.28
2M23504167+0044455	5838 ± 120	4.41 ± 0.15	4.35	0.05 ± 0.05	0.01 ± 0.1	0.67	4.42	10.4	1.44
2M23511893+0105009	5643 ± 84	4.12 ± 0.1	4.11	0.11 ± 0.04	0.06 ± 0.1	0.77	3.65	10.22	1.62
2M23514677+5755384	5858 ± 110	4.31 ± 0.16	4.25	-0.05 ± 0.05	-0.13 ± 0.1	0.52	4.63	8.66	0.37
2M23515689-1941278	6084 ± 113	4.43 ± 0.14	4.31	0.21 ± 0.05	0.18 ± 0.1	0.7	5.56	9.87	0.52
2M23520932+0021396	5655 ± 112	4.24 ± 0.14	4.23	0.05 ± 0.05	0.02 ± 0.1	0.86	3.73	10.24	0.58
2M23523679+0003442	5971 ± 125	4.34 ± 0.17	4.25	-0.05 ± 0.05	-0.1 ± 0.1	0.56	5.2	8.8	0.43
2M23540505+0013362	5907 ± 106	4.38 ± 0.18	4.31	-0.12 ± 0.04	-0.19 ± 0.1	0.35	4.94	8.89	0.36
2M23543083-1917047	5615 ± 120	4.29 ± 0.16	4.29	-0.04 ± 0.05	-0.1 ± 0.1	0.76	3.71	9.04	0.53
2M23545294-2051223	5713 ± 118	4.09 ± 0.12	4.07	-0.01 ± 0.05	-0.06 ± 0.1	0.54	4.04	10.23	1.54
2M23551700+5526170	5709 ± 126	4.27 ± 0.16	4.25	-0.05 ± 0.05	-0.11 ± 0.1	0.63	4.03	8.84	1.66
2M23573126+5635167	5521 ± 65	4.26 ± 0.07	4.28	0.07 ± 0.03	0.02 ± 0.1	0.98	3.35	10.65	0.54
2M23574056+1654533	5630 ± 118	4.35 ± 0.17	4.35	-0.04 ± 0.05	-0.09 ± 0.1	1.11	3.74	9.54	1.47
2M23575840-2014151	6160 ± 143	4.41 ± 0.21	4.27	0.05 ± 0.06	0 ± 0.1	0.44	6.26	9.99	1.44
2M23593396-1931485	5949 ± 101	4.28 ± 0.12	4.20	0.04 ± 0.04	-0.03 ± 0.1	0.61	5	9.54	1.51
BD-00:4470	6431 ± 150	5.4 ± 0	5.14	-0.89 ± 0.12	-0.8 ± 0.1	0	9.57	2.74	1.67
BD-13:3834	6681 ± 1373	5.34 ± 5.92	4.98	-0.69 ± 0.37	-0.76 ± 0.1	0	11.79	23.11	2.59

APOGEE_ID	$T_{\rm eff} \pm \Delta T_{\rm eff}$	$\log g \pm \Delta \log g$	$\log g_{cor}$	$[\rm M/H] \pm \Delta[\rm M/H]$	$[Fe/H] \pm \Delta[\rm Fe/H]$	$\rm v_{mic}$	$\rm v_{mac}$	$v \sin i$	χ^2
G172-61	5674 ± 456	4.13 ± 0.65	4.12	-0.81 ± 0.2	-0.83 ± 0.1	0	4.64	0	2.33
HD_103890	6071 ± 443	4.2 ± 0.57	4.09	-0.02 ± 0.17	-0.07 ± 0.1	0.7	5.78	9.85	2.61
HD_104860	5873 ± 364	4.28 ± 0.58	4.22	-0.07 ± 0.16	-0.2 ± 0.1	1.44	4.73	14.41	1.86
HD_11007	6090 ± 192	4.19 ± 0.26	4.07	-0.2 ± 0.08	-0.23 ± 0.1	0.86	6.1	8.21	1.33
HD_121370	5974 ± 95	4.05 ± 0.09	3.96	0.13 ± 0.04	-0.02 ± 0.1	0.68	5.08	14.36	0.37
HD_126868	5521 ± 128	3.74 ± 0.14	3.74	0.02 ± 0.06	-0.17 ± 0.1	0.99	3.6	13.52	1.27
HD_132142	5028 ± 135	4.25 ± 0.16	4.40	-0.35 ± 0.05	-0.42 ± 0.1	0.44	3.55	9.27	1.5
HD_146233	6516 ± 395	4.85 ± 0.52	4.56	0.39 ± 0.16	0.42 ± 0.1	2	8.79	8.36	6.68
HD_151044	6072 ± 186	4.22 ± 0.23	4.11	0.01 ± 0.07	-0.03 ± 0.1	1.4	5.75	10.1	0.4
HD_16160	4729 ± 61	4.29 ± 0.08	4.54	-0.06 ± 0.02	-0.13 ± 0.1	0.76	3.61	9.24	1.77
HD_176377	5912 ± 157	4.43 ± 0.22	4.36	-0.09 ± 0.07	-0.16 ± 0.1	0	4.93	8.97	0.39
HD_185144	5366 ± 102	4.4 ± 0.15	4.46	-0.21 ± 0.04	-0.25 ± 0.1	0.72	3.36	9.6	1.52
HD_190470	4937 ± 87	4.22 ± 0.1	4.40	0.09 ± 0.03	0.05 ± 0.1	0.97	3.42	11.33	0.82
HD_22521	5980 ± 178	4.18 ± 0.2	4.09	-0.04 ± 0.07	-0.13 ± 0.1	0.41	5.28	9.33	1.44
HD_22879	5762 ± 286	4.01 ± 0.27	3.97	-0.52 ± 0.12	-0.68 ± 0.1	0	4.77	8.22	0.46
HD_49736	5928 ± 194	4.19 ± 0.25	4.11	-0.03 ± 0.08	-0.09 ± 0.1	0.84	4.97	9.4	0.48
HD_49933	6727 ± 293	4.5 ± 0.28	4.12	-0.38 ± 0.11	-0.44 ± 0.1	0	11.74	9.85	0.17
HD_6582	5647 ± 163	4.49 ± 0.2	4.48	-0.66 ± 0.07	-0.7 ± 0.1	0	4.38	6.55	1.31
HD_82885	5442 ± 106	4.55 ± 0.1	4.59	0.37 ± 0.04	0.3 ± 0.1	0.8	2.8	9.82	2.06
HD_9826	6160 ± 235	4.28 ± 0.33	4.14	0.1 ± 0.09	0.01 ± 0.1	0.86	6.22	11.95	1.58

APOGEE_ID	$T_{\rm eff} \pm \Delta T_{\rm eff}$	$\log g \pm \Delta \log g$	$\log g_{cor}$	$[\rm M/H] \pm \Delta[\rm M/H]$	$[Fe/H] \pm \Delta[\rm Fe/H]$	$\rm v_{mic}$	$\rm v_{mac}$	$v \sin i$	χ^2
HD_99491	5378 ± 107	4.46 ± 0.12	4.52	0.36 ± 0.05	0.29 ± 0.1	0.84	2.73	9.17	1.03

B.2 Full M dwarf sample results

Table B.2: Full list of derived parameters for M dwarf stellar sample. Uncertainties in derived parameters are 100 K for T_{eff}, 0.1 dex for $\log g$ and 0.1 dex for $[M/H]$. Normalization parameters denoted by letter N.

APOGEE_ID	T_{eff}	$\log g$	[M/H]	v_{mic}	v_{mac}	$v \sin i$	χ^2	$[\mathrm{M/H}]_N$	$T_{\mathrm{eff,N}}$
2M00004701+1624101	3827	4.97	0.07	0.00	5.75	6.26	19.1	0.2	3900
2M00204772+5936173	3660	4.93	-0.01	0.71	6.33	8.46	18.6	0.2	3600
2M00243855+5119224	3727	5.4	-0.34	1.38	6.33	5.22	46.5	0.1	3600
2M00244054+5511590	3726	4.57	-0.31	0.00	6.02	3.10	12.2	0.1	3600
2M00251060+6724193	3708	4.96	-0.23	1.08	6.17	3.12	25.9	0	3600
2M00262872+6747026	3841	4.88	0.02	0.62	5.68	7.65	23.9	0.2	3900
2M00274401+5330504	3465	5.02	-0.01	0.24	7.14	1.65	27.8	-0.2	3300
2M00313293+6152504	3572	4.8	-0.65	1.68	6.64	7.46	13.4	-0.1	3300
2M00334916+6712243	3784	4.84	-0.04	0.65	5.86	7.18	14.3	0.2	3800
2M00350487+5953079	3196	5.05	-0.13	1.88	8.38	0.00	41.5	0	3000
2M00363436+5537360	3989	4.88	0.07	0.30	5.21	0.00	17.9	0.2	4000
2M00372598+5133072	3876	4.66	-0.01	0.00	5.51	4.94	8.1	0.2	4000
2M00391896+5508132	3133	4.9	-0.02				18	0	3000
2M00444820+1830403	3739	5	-0.37	0.87	6.07	4.88	8.3	0.1	3600
2M01285381+1803284	3878	5.03	-0.72	2.02	5.61	5.65	13.4	-0.1	3800
2M02073745+1354497	3827	4.97	0.23	0.00	5.75	8.43	18.6	0.4	3900
2M02090912+1435362	3592	4.92	-0.02	0.53	6.59	5.22	16.3	0.2	3500
2M02122001+1249287	3650	5.21	0.2	0.59	6.50	3.51	43.3	0.4	3600
2M02362715+5528349	3576	5.39	-0.36	1.82	6.90	6.38	11.6	0.1	3400
2M02381299+5542044	3979	4.7	0.05	0.00	5.20	0.00	21.4	0.4	3800
2M02465257+5619505	3354	4.5	-0.09	0.86	7.52	7.53	16.2	0.1	3200
2M03062774+6254388	3157	4.96	-0.15				29	0.2	3000
2M03140624+5728568	3288	4.99	0.15	0.99	7.92	2.14	16.5	0.4	3200
2M03152943+5751330	3361	5.19	-0.17	1.33	7.68	0.00	11.8	0.1	3200
2M03190939+0130543	3410	5.4	-0.91	1.26	7.59	7.06	35	-0.4	3000
2M03212176+7958022	3545	4.95	-0.19	0.80	6.79	5.58	8.3	0.1	3400
2M03215239+6335088	3654	4.99	-0.06	0.48	6.37	6.09	40.9	0.2	3600

APOGEE_ID	$T_{\rm eff}$	$\log g$	[M/H]	$v_{\rm mic}$	$v_{\rm mac}$	$v \sin i$	χ^2	$[\rm M/H]_N$	$T_{\rm eff,N}$
2M03241544+0928579	3592	5.22	-0.32	1.55	6.72	4.86	14.5	0.1	3400
2M03280163+5226180	3822	4.79	-0.04	0.00	5.71	6.88	16.9	0.2	3800
2M03355099+7140275	3113	4.94	0				37	0.2	3000
2M03391302+4635276	3568	4.92	-0.48	1.15	6.69	0.07	42.3	-0.4	3200
2M03391968+3251001	3478	5.12	0.14	0.78	7.13	7.77	14.1	0.4	3400
2M03400164+4638456	3597	4.49	-0.47	0.00	6.50	4.66	41.2	-0.1	3400
2M03431519+5006558	3637	5.4	-0.03	0.75	6.66	0.00	27.2	0.3	3600
2M03441913+7126195	3635	4.99	0.15	0.13	6.45	8.40	54.5	0.3	3600
2M03443389+7125059	3722	5.34	-0.02	1.33	6.31	7.70	44.7	0.2	3800
2M03481149+3054134	3554	5.4	-0.36	1.09	6.99	3.14	18.2	0.1	3400
2M04125880+5236421	3294	5.3	-0.28	1.14	8.04	6.36	17.4	-0.2	3000
2M04244284+4537062	3709	4.51	-0.23	0.00	6.08	5.11	13.9	0	3600
2M04310001+3647548	3404	4.85	0	1.34	7.35	5.67	12.1	0.2	3300
2M04311499+4217111	3506	4.78	0.09	0.82	6.90	5.40	9.6	0.2	3400
2M04311837+3655082	3680	4.78	-0.04	0.00	6.22	5.33	7.2	0.2	3600
2M04334819+4227070	3449	5.4	-0.01	1.28	7.42	8.74	38.1	0.3	3400
2M04342248+4302148	3499	4.69	0.05	0.23	6.91	5.21	9.5	0.2	3400
2M04351236+5821100	3511	5.11	-0.54	1.56	6.99	4.73	11.9	-0.2	3200
2M04371030+4703549	3634	4.91	-0.52	1.39	6.42	5.02	8.9	-0.1	3400
2M04400301+4620167	3475	5	0	0.65	7.09	5.61	26.3	0.2	3400
2M04422854+5818015	3372	5.27	-0.27	1.65	7.67	0.00	14.7	0.1	3200
2M04443813+3857031	3490	4.6	-0.02	0.72	6.94	4.30	11.1	0.2	3400
2M04463593+5900524	3641	4.56	-0.04	0.10	6.33	2.90	10.3	0.2	3600
2M04483289+5003109	3488	5	-0.02	0.73	7.04	6.44	18.8	0.2	3400
2M04552111+5017249	3865	4.83	-0.71	1.76	5.58	5.20	13.6	-0.1	3700
2M04581599+5017278	3949	4.92	-0.19	0.00	5.34	9.48	11.5	0	3900
2M04584599+5056378	3838	4.87	-0.02	0.00	5.68	9.83	10.8	0.2	3800
2M05011792+4204125	3670	4.8	0.12	0.00	6.26	5.42	16.6	0.4	3600
2M05014512+5039319	3689	4.98	-0.18	0.74	6.24	8.47	8.7	0.2	3600

APOGEE_ID	$T_{\rm eff}$	$\log g$	[M/H]	$v_{\rm mic}$	$v_{\rm mac}$	$v \sin i$	χ^2	$[{\rm M/H}]_N$	$T_{\rm eff,N}$
2M05145032+4639432	3911	4.78	-0.23	0.00	5.42	4.97	8.1	0.1	3800
2M05172841+2531214	3330	5	-0.01	0.97	7.73	11.80	16.6	0	3200
2M05201152+2457212	3499	4.58	0.2	0.00	6.90	4.72	12.5	0.4	3400
2M05222053+3031097	3490	4.99	0.03	0.64	7.03	5.34	11.4	0.2	3400
2M05292729+2724457	3956	4.7	0.01	0.00	5.26	0.00	8.7	0.2	4000
2M05313731+4128000	3683	4.6	-0.24	0.15	6.18	2.58	12.8	0.1	3600
2M05354753+2717497	3491	4.57	-0.03	0.32	6.93	6.56	12.8	0.2	3400
2M05370749+4111165	3451	5.15	-0.21	0.74	7.26	5.78	18.5	-0.2	3200
2M05394770+2917450	3667	4.68	-0.01	0.00	6.25	5.60	9.2	0.2	3600
2M05483220+2119180	3473	5.36	-0.31	1.40	7.29	4.01	13	-0.2	3200
2M05483253+2117577	3861	4.91	-0.71	1.53	5.62	5.33	8.4	-0.5	3600
2M05571864+1708299	3427	4.58	-1.33	1.71	7.20	9.78	13.2	-0.4	3000
2M05580690+1557564	3477	4.46	-0.35	0.71	6.99	3.55	13.3	-0.2	3200
2M06025298+3129415	3421	4.45	-1.41	1.75	7.23	9.42	13.7	-0.4	3000
2M06043950+2753529	3494	4.69	0.04	0.26	6.93	5.27	11	0.2	3400
2M06070493+1403109	3223	4.97	-0.04				30	0.2	3100
2M06075349+2746207	3836	4.9	-0.01	0.11	5.70	9.00	19.2	0.2	3800
2M06102756+2759447	3796	4.86	0.01	0.00	5.82	7.05	11	0.2	3800
2M06135175+0631517	3709	4.69	-0.08	0.00	6.09	5.17	8	0.2	3600
2M06161499+2754094	3679	5.18	-0.14	1.04	6.37	8.58	36.6	0.2	3600
2M06183480+2503064	3421	4.97	0.06	0.67	7.31	5.15	13.7	0	3300
2M06183640+0806535	3723	4.5	-0.18	0.00	6.03	7.76	7.3	0	3600
2M06234645+0502411	3909	4.74	0.05	0.00	5.42	4.53	11.8	0.2	4000
2M06270211+0309473	3745	5.17	-0.36				8	0.2	3600
2M06274397+0923541	3670	4.98	-0.14	0.66	6.31	6.71	10.8	0.2	3600
2M06295663+0934185	3359	4.95	-0.16	1.16	7.58	7.18	11.9	0.1	3200
2M06320207+3431132	3465	5.4	-0.37	1.19	7.36	5.75	17	-0.2	3200
2M06362535+1830520	3478	5.4	-0.44	1.61	7.30	3.77	12.8	-0.2	3200
2M06370004+1515162	3704	4.99	-0.18	0.70	6.19	5.40	8.4	0.1	3600

APOGEE_ID	$T_{\rm eff}$	$\log g$	[M/H]	$v_{\rm mic}$	$v_{\rm mac}$	$v \sin i$	χ^2	$[\rm M/H]_N$	$T_{\rm eff,N}$
2M06375540+0858594	3379	5.4	-0.04	0.93	7.73	0.00	21.1	-0.2	3200
2M06412818+1545482	3480	4.98	0.03	0.75	7.06	6.92	12.2	0.2	3400
2M06421118+0334527	3356	4.62	-0.06	0.63	7.52	5.55	11.7	0	3200
2M06423361+0239388	3804	5.4	-0.6	1.83	6.06	6.67	21.3	-0.1	3600
2M06484673-0516193	3805	4.82	-0.03	0.00	5.78	4.46	12.3	0.2	3800
2M06505947-0910506	3377	4.8	-0.1	0.90	7.45	9.47	10.8	0	3200
2M06513673+2023264	3499	4.99	-0.12	1.18	6.99	9.28	11.4	0.3	3400
2M06543764+1708058	3397	4.5	-0.04	0.84	7.33	3.20	16.8	-0.2	3200
2M06572462+0651440	3434	5.39	-0.69	1.47	7.48	9.46	17	-0.4	3000
2M07053085+0443219	3810	4.96	-0.71	1.48	5.80	3.28	12	-0.1	3600
2M07062584+0148472	3359	4.47	-0.09	0.78	7.50	5.12	33	0	3200
2M07155314-0101135	3898	4.74	-0.18	0.00	5.45	0.00	7.2	0.2	3800
2M07235757-0833017	3496	5.11	-0.03	1.03	7.05	5.01	18.8	0.2	3400
2M07315261-0748360	3843	4.81	-0.11	0.00	5.65	5.47	6.9	0.2	3800
2M07320352-0752173	3708	4.77	-0.06	0.00	6.11	7.64	7	0.2	3600
2M07323759-0813177	3654	5	-0.02	0.85	6.38	0.00	9.9	0.2	3600
2M07404603+3758253	3437	5.29	-1.01	2.20	7.40	7.57	29.2	-0.4	3000
2M07421457+7949418	3368	5.4	-0.03	0.58	7.78	10.16	41.9	-0.2	3200
2M07431638+6642456	3514	4.94	-0.03	0.81	6.91	5.04	38.5	0	3400
2M07492701+7752423	3404	5.2	-0.08	0.77	7.49	0.00	26.5	-0.2	3200
2M07581269+4118134	3432	5.39	-0.16	1.03	7.49	4.70	13.7	-0.2	3200
2M08050361+4121251	3413	4.69	-1.32	2.14	7.28	3.48	16	-0.4	3000
2M08595755+0417552	3769	4.8	-0.1	0.00	5.90	7.68	10.6	0.2	3700
2M09005033+0514293	3394	4.51	-0.03	0.60	7.34	3.30	11.3	-0.2	3200
2M09022952+0417072	3446	4.89	-0.21	0.73	7.18	0.35	36.6	-0.2	3200
2M09301445+2630250	3354	4.67	0.12	1.12	7.53	5.46	16	0	3200
2M10330667+2837490	3499	5.4	-0.08	1.00	7.21	5.69	38.2	0.1	3400
2M10383323+3529492	3505	4.91	-0.05	0.72	6.94	6.86	9.1	0.2	3400
2M10391962+3044566	3660	4.95	-0.1	1.18	6.34	5.11	17.4	0.2	3600

APOGEE_ID	$T_{\rm eff}$	$\log g$	[M/H]	$v_{\rm mic}$	$v_{\rm mac}$	$v \sin i$	χ^2	$[\rm M/H]_N$	$T_{\rm eff,N}$
2M10401225+3510463	3552	5.03	-0.24	1.12	6.79	7.92	15.8	0.1	3400
2M10441137+4500152	3816	4.7	-0.58	1.16	5.72	4.92	7.7	-0.1	3600
2M10453795+1833111	3857	4.61	-0.01	0.00	5.57	4.10	10.6	0.2	4000
2M10463343+1906373	3899	4.91	-0.04	0.00	5.49	8.24	11.8	0	4000
2M10470720+2004362	3122	5.23	-0.12				81	0.2	3000
2M10473327+2007406	3367	4.91	-0.08	0.93	7.53	10.70	19	0	3200
2M10475231+2020315	3674	4.71	-0.04	0.00	6.22	5.97	14.3	0.2	3600
2M10482152+4451236	3472	5.24	-0.54	1.91	7.22	3.89	34.2	-0.1	3200
2M10572599+4923562	3585	4.92	0	0.42	6.62	5.97	10.8	0.2	3500
2M11021557+4941485	3482	5.4	-0.09				38	0.2	3400
2M11091225-0436249	3847	4.81	-0.07	0.00	5.63	8.36	9.6	0.2	3900
2M11152550+0003159	3491	5.18	-0.7	2.21	7.11	2.40	27.9	-0.1	3200
2M11202022+0034356	3389	4.66	-0.63	0.85	7.38	9.47	15.3	-0.2	3000
2M11294200+0405175	3410	5.4	-0.9	1.21	7.59	4.46	25.2	-0.4	3000
2M11323938+0513167	3902	4.89	-0.07	0.91	5.48	5.50	11.7	0	4000
2M11353571+0414146	3864	5.4	-0.82	1.99	5.86	0.00	12.6	-0.4	3600
2M11452712+2558113	3486	4.79	-0.36	1.00	6.98	1.89	11.5	-0.2	3200
2M11474440+0048164	3281	5.28	-0.15				15	0.4	3200
2M11511794+1829229	3475	5.16	-0.29	1.39	7.17	6.39	11.5	-0.2	3200
2M11580290+2013015	3338	4.98	-0.04	0.91	7.69	0.97	32.7	0	3200
2M12005016+1938424	3525	4.95	-0.08	0.63	6.87	2.80	11.8	0	3400
2M12081818+4027012	3941	4.85	-0.2	1.24	5.34	0.00	28.3	0	4000
2M12082601+4022490	3764	4.86	0.11	0.00	5.93	7.08	12.3	0.4	3800
2M12102152+4026185	3787	4.98	-0.61	1.48	5.89	5.66	8.7	-0.1	3600
2M12105688+4103275	3771	4.42	-0.43	0.00	5.86	5.23	6.7	0.1	3600
2M12110303+4043482	3565	5.13	-0.28	1.25	6.78	0.00	16.8	0.1	3400
2M12153222+1515555	3432	5.35	-0.19	1.08	7.47	8.85	19.3	-0.2	3200
2M12205197+4006468	3524	4.83	-0.62	1.46	6.84	0.00	21.2	-0.2	3200
2M12212146+5745089	3663	4.86	-0.01	0.70	6.30	5.54	9.1	0.2	3600

APOGEE_ID	$T_{\rm eff}$	$\log g$	[M/H]	$v_{\rm mic}$	$v_{\rm mac}$	$v \sin i$	χ^2	$[M/H]_N$	$T_{\rm eff,N}$
2M12223238+5730387	3415	4.73	-0.01	0.78	7.27	3.65	16.4	0	3300
2M12271328+5705444	3601	4.99	-0.18	0.06	6.58	3.43	8.9	-0.2	3400
2M12301148+5555229	3672	5.04	-0.85	1.91	6.33	6.15	17.3	-0.1	3400
2M12330155+5738113	3639	4.9	-0.58	1.65	6.40	4.76	16.8	-0.1	3400
2M12505082+1301468	3453	5.14	-0.22	0.82	7.25	3.28	13	-0.2	3200
2M12573249+4057012	3658	4.67	0.07	0.00	6.28	5.59	11.1	0.4	3600
2M13085124-0131075	3487	4.86	-0.01	0.88	7.00	5.49	10.6	0.2	3400
2M13202492-0139266	3714	4.96	-0.18	0.19	6.14	8.87	5.7	0	3600
2M13315838+5443452	3675	4.84	0	0.27	6.25	6.70	18.4	0.2	3600
2M13421941+1847193	3823	4.86	-0.07	0.00	5.73	6.83	25.7	0.2	3800
2M13462703+1707100	3659	4.6	-0.06	0.00	6.27	4.84	15.6	0.2	3600
2M13514938+4157445	3653	5	0.16	0.08	6.38	7.11	22.1	0.4	3600
2M13525797+3331361	3487	4.6	-0.02	0.72	6.95	4.46	19	0.2	3400
2M13552585+2556161	3987	4.55	-0.35	0.00	5.16	5.29	12.3	0.1	3900
2M13570155+2534378	3802	4.99	-0.26	0.25	5.85	10.04	6.2	0	3700
2M13572571+3400176	3438	4.93	-0.09	0.76	7.23	7.46	13.9	0	3300
2M13581901+0119475	3653	4.75	0.05	0.00	6.31	6.83	12.9	0.4	3600
2M14010995+2621429	3956	4.83	-0.17	0.00	5.29	6.75	7.3	0	4000
2M14022155+2517517	3891	4.97	-0.05	0.00	5.54	10.01	23.3	0	4000
2M14035430+3008026	3330	5.4	0.44	2.17	7.95	99.54	61.2	0.2	3200
2M14044784+5237559	3489	4.57	-0.03	0.75	6.94	2.37	22.4	0	3400
2M14130286+0506321	3324	4.95	0.16	0.83	7.74	7.41	16.9	0.2	3200
2M14173915+0624144	3590	5.4	-0.22	0.50	6.85	7.60	42.9	-0.2	3400
2M14180725+0611519	3429	5.4	-0.19	1.30	7.51	0.00	34.4	-0.2	3200
2M14385800+1327388	3672	4.63	0.08	0.00	6.22	5.10	8.7	0.4	3600
2M14431906+1120548	3513	5.01	-0.04	0.65	6.94	2.62	11.1	0	3400
2M14535251+1739448	3747	4.73	-0.32	0.53	5.96	5.97	5.7	0.1	3600
2M14540912+4135008	3484	4.61	-0.01	0.77	6.97	3.43	28.5	0.2	3400
2M14583396+4216146	3503	5.34	-0.56	1.74	7.15	11.02	38.7	-0.2	3200

APOGEE_ID	T_{eff}	$\log g$	[M/H]	$\mathrm{v}_{\mathrm{mic}}$	$\mathrm{v}_{\mathrm{mac}}$	$v \sin i$	χ^2	$[\mathrm{M/H}]_N$	$T_{\mathrm{eff,N}}$
2M15024283+3211141	3577	4.84	-0.33				11	0.1	3400
2M15090689+3254449	3477	5	0	0.92	7.09	5.29	13.8	0.2	3400
2M15281240+4340086	3477	5.4	-0.35	1.50	7.31	4.51	23	-0.2	3200
2M16340737+0038043	3482	5.27	-0.33	1.32	7.20	5.41	14.4	-0.2	3200
2M16343937+0051089	3393	5.39	-0.67	0.80	7.66	43.98	63.8	-0.4	3000
2M16383835+3700273	3428	5.4	-0.2	1.16	7.51	5.51	51.2	-0.2	3200
2M16385433+3643018	3917	4.88	-0.2	0.09	5.43	4.33	10.4	0	4000
2M16440030+3721597	3355	5.4	-0.32	0.00	7.84	12.41	75.1	-0.4	3000
2M16445239+3644423	3642	5.3	-0.55	1.93	6.58	4.95	18.8	-0.1	3400
2M16470934+3657361	3748	5.32	-0.32	1.42	6.20	4.29	13.5	0.1	3600
2M16495034+4745402	3682	4.72	0.1	0.00	6.20	6.34	11.6	0.4	3600
2M16541202+1154529	3795	4.79	-0.46	0.15	5.81	4.61	5.9	-0.1	3600
2M16565961+1133582	3343	5.4	-0.32	0.65	7.89	42.71	87.1	-0.4	3000
2M16593773+1155377	3934	4.66	-0.27	0.00	5.33	6.54	12.6	-0.2	3800
2M17014341+1119582	3531	4.93	-0.11	0.90	6.84	2.21	32.3	0	3400
2M17190292+2340254	3839	4.78	-0.02	0.00	5.66	8.74	20.6	0.2	3900
2M17331825+3402191	3971	4.89	-0.22	0.00	5.27	5.97	10.9	0	4000
2M17403275+7256146	3988	4.94	-0.14	0.16	5.23	5.17	21.2	0	4000
2M17480236+7436562	3460	5.4	-0.35	0.88	7.38	2.51	49.6	-0.2	3200
2M17491402+4823093	3882	4.88	-0.18	0.00	5.54	5.47	8.3	0.1	3800
2M17541820+4758412	3721	4.77	-0.3	1.34	6.06	3.04	7.9	0.1	3600
2M17592886+0318233	3925	4.76	-0.01	0.00	5.37	6.80	15.1	0.2	4000
2M18055545+0316213	3501	4.7	0.08	0.04	6.90	4.56	27.3	0.2	3400
2M18161819+0131277	3483	5.14	-0.33	0.93	7.12	3.99	10.4	-0.2	3200
2M18254864-0258170	3857	4.79	0.06	0.00	5.60	7.13	11.7	0.2	4000
2M18415473+0651285	3401	4.78	0	0.75	7.34	7.40	11	0.2	3300
2M18451027+0620158	3727	4.69	0.04	0.00	6.03	5.75	9.1	0.4	3700
2M18561502+0449049	3648	4.8	-0.62	1.47	6.34	6.49	13.4	-0.1	3400
2M18562628+4622532	3302	5.32	-0.34	1.68	8.02	5.60	22.1	-0.2	3000

APOGEE_ID	T_{eff}	$\log g$	[M/H]	v_{mic}	v_{mac}	$v \sin i$	χ^2	$[\mathrm{M/H}]_N$	$T_{\mathrm{eff,N}}$
2M18571939+0523084	3674	4.66	-0.11	0.00	6.22	5.82	15	0.2	3600
2M19010098+4522386	3325	4.97	0.13	1.05	7.74	4.74	19	0.2	3200
2M19121128+4316106	3503	4.71	-0.45	1.14	6.90	5.13	15.1	-0.2	3200
2M19213157+4317347	3910	4.84	-0.17				7	0.1	3800
2M19263973+1736418	3565	5.38	-0.39	1.62	6.93	5.00	16.7	-0.2	3300
2M19272432+2619292	3526	5.1	-0.09	0.57	6.93	3.09	29.9	0	3400
2M19302719+1723396	3677	4.8	-0.01	0.00	6.23	6.81	9	0.2	3600
2M19313868-0658253	3491	4.86	0	0.47	6.98	6.31	9.6	0.2	3400
2M19324633-0652178	3342	4.49	-0.03	0.52	7.58	7.40	10.7	0	3200
2M19325604+1723567	3634	4.95	-0.61	1.71	6.44	4.78	13.7	-0.1	3400
2M19341617+2553535	3499	4.81	-0.65	1.42	6.94	7.16	14	-0.1	3200
2M19383321+3230175	3481	4.99	-0.01	0.80	7.07	4.47	21.3	0.2	3400
2M19390444+2424089	3522	5.01	-0.11	0.75	6.90	4.19	12.8	0	3400
2M19395886+3950530	3688	4.97	-0.09	0.83	6.24	0.00	16.6	0.2	3600
2M19412775+3239512	3483	4.62	-0.53	1.21	6.97	11.22	17	-0.1	3200
2M19420033+4038302	3862	4.65	-0.02	0.00	5.56	8.70	26.3	0.2	4000
2M19454969+3223132	3565	4.67	-0.09	0.00	6.64	4.98	10.4	-0.2	3400
2M19482428+3250327	3492	4.82	-0.55	1.54	6.96	10.27	15.8	-0.1	3200
2M19485718+5015245	3497	5.4	-0.13	1.62	7.22	2.87	37	0.3	3400
2M19533423+0503410	3811	5.38	-0.66	1.76	6.02	1.64	8.7	-0.1	3600
2M19541829+1738289	3426	5.4	-0.76	1.66	7.52	0.00	20.6	-0.4	3000
2M19543665+4357180	3856	4.73	-0.22	0.00	5.59	7.78	30	0.2	3800
2M19585332+0522081	3806	4.94	-0.24	0.00	5.81	6.22	5.8	-0.2	3600
2M20015056+4500500	3666	5.4	-0.05	1.32	6.56	6.77	26.5	0.2	3600
2M20024041+3109447	3500	4.91	-0.04	0.93	6.96	7.05	11.2	0.2	3400
2M20053276+3039324	3729	4.47	-0.23	0.00	6.01	4.41	7.4	0	3600
2M20122244+2043113	3654	5.27	-0.6	2.12	6.52	4.93	14.8	-0.1	3400
2M20162519+5621561	3723	4.96	0.15	0.73	6.11	4.45	13.1	0.4	3800
2M20185746+2704165	3714	5.25	-0.22	1.14	6.28	3.96	22.3	0.1	3600

APOGEE_ID	$T_{\rm eff}$	$\log g$	[M/H]	$v_{\rm mic}$	$v_{\rm mac}$	$v \sin i$	χ^2	$[{\rm M/H}]_N$	$T_{\rm eff,N}$
2M20202082+2837583	3833	4.96	0.08	0.00	5.73	6.10	20.8	0.2	4000
2M20291663+4507525	3693	4.93	-0.05	0.00	6.21	6.65	8.1	0	3600
2M20331096+4553299	3612	5.08	-0.24	0.73	6.58	5.70	13.4	-0.2	3400
2M20584898+5115421	3515	4.79	-0.05	0.20	6.86	3.38	12.2	0	3400
2M21003448+5156016	3359	4.68	-0.03	0.76	7.51	10.81	26.2	0	3200
2M21013304+4046208	3490	5.15	-0.45	1.46	7.10	0.00	32.9	-0.2	3200
2M21074857+2945266	3540	4.98	-0.16	0.63	6.82	5.17	9.8	0	3400
2M21140743+4924350	3508	5.18	-0.48	1.55	7.04	6.04	12	-0.2	3200
2M21232573+6734153	3426	5.4	-0.18	0.97	7.52	7.28	63.1	-0.2	3200
2M21281491+4654126	3781	4.54	0.03	0.00	5.82	0.00	17.2	0.2	4000
2M21400112+5408179	3580	5.2	-0.31	1.57	6.76	5.19	20.7	0.1	3400
2M21402935+5400301	3477	4.98	-0.34	1.02	7.07	4.73	18.2	-0.2	3200
2M21474194+5341222	3683	4.73	-0.04	0.00	6.19	6.70	11.3	0.2	3600
2M21561443+3943468	3451	5.39	-0.23	1.19	7.41	4.24	33.9	-0.2	3200
2M21573509+5026323	3308	5.39	-0.07	1.52	8.04	0.00	33.1	0.1	3200
2M22010861+4901108	3989	4.76	-0.03	0.00	5.18	0.00	18.5	0.2	4000
2M23034347+6524293	3269	5.19	-0.14	0.92	8.10	10.72	33.7	-0.2	3000
2M23110137+4653414	3316	4.65	0.03	0.92	7.70	5.28	15.3	0.2	3200
2M23134861+1227072	3490	5.1	0.1	0.49	7.08	3.40	23.7	0.2	3400
2M23165396+6109419	3718	4.93	-0.25	1.19	6.12	4.40	30.2	0	3600
2M23171589+6110496	3559	4.71	-0.01	0.00	6.67	3.62	18.9	0.2	3500
2M23175293+6109518	3515	4.95	-0.07	0.70	6.91	5.89	35.5	0	3400
2M23200542+6356068	3738	4.81	-0.01	0.00	6.01	3.33	13.8	0.2	3700
2M23205304+1205009	3398	4.81	-0.22	1.15	7.37	0.00	11.8	0.1	3200
2M23212582+6547582	3561	5.04	-0.23				13	0.1	3400
2M23230603+6211124	3667	4.86	0	0.29	6.28	2.21	26.2	0.2	3600
2M23460112+7456172	3461	5.18	-0.23	0.97	7.23	5.96	30	-0.2	3200
2M23592772+1630288	3399	5.04	0.09	0.73	7.44	3.82	25.1	0.2	3300
2M23592810+7506017	3980	4.93	-0.04	0.00	5.25	2.56	11.9	0	4000

APOGEE_ID	$T_{\rm eff}$	$\log g$	[M/H]	$\mathrm{v}_{\rm mic}$	$\mathrm{v}_{\rm mac}$	$v \sin i$	χ^2	$[\mathrm{M/H}]_N$	$T_{\rm eff,N}$
2M23595589+1508091	3725	5.28	-0.12	1.31	6.26	5.57	39.7	0.3	3700

B.2.1 Summary of each individual M dwarf in the sample

Star 2M00004701+1624101 (UCAC4 533-000024 [1]) was characterized in Gilhool et al. (2017), giving it the following parameters: $T_{\rm eff} = 3725\,$K,$\log g = 5.0\,$dex, $[M/H] = +0.5\,$dex. The available ASPCAP parameters for this star are $T_{\rm eff} = 3735\,$K and $\log g = 4.46\,$dex, with a $[M/H] = +0.18\,$dex. The matching spectrum for the star has been obtained by normalizing the APOGEE observed one with a synthetic spectrum with $T_{\rm eff} = 3900\,$K, $\log g = 5.0\,$dex and $[M/H] = +0.2\,$dex, and the derived spectroscopical parameters for this star are $T_{\rm eff} = 3827 \pm 100\,$K,$\log g = 4.97 \pm 0.1\,$dex, $[M/H] = +0.07 \pm 0.1\,$dex.

Star 2M00204772+5936173 (GSC 03665-00665 [2]) was characterized in Gaidos et al. (2014), giving it $T_{\rm eff} = 3557\,$K and in Lépine et al. (2013), with $\log g = 4.5\,$dex and $T_{\rm eff} = 3530\,$K. The available ASPCAP parameters for this star are $T_{\rm eff} = 3666\,$K, $\log g = 4.53\,$dex, and $[M/H] = +0.10\,$dex. The matching spectrum for the star has been obtained by normalizing the APOGEE observed one with a synthetic spectrum with $T_{\rm eff} = 3600\,$K, $\log g = 5.0\,$dex and $[M/H] = +0.2\,$dex, and the derived spectroscopical parameters for this star are $T_{\rm eff} = 3660 \pm 100\,$K,$\log g = 4.93 \pm 0.1\,$dex, $[M/H] = -0.01 \pm 0.1\,$dex.

Star 2M00243855+5119224 (LP 150-1 [3]) was characterized in Gilhool et al. (2017), giving it the following parameters: $T_{\rm eff} = 3504\,$K,$\log g = 5.0\,$dex, $[M/H] = +0.0\,$dex. The available ASPCAP parameters for this star are $T_{\rm eff} = 3597\,$K and $[M/H] = -0.22\,$dex, with an $\log g = 4.53\,$dex. The matching spectrum for the star has been obtained by normalizing the APOGEE observed one with a synthetic spectrum with $T_{\rm eff} = 3600\,$K, $\log g = 5.0\,$dex and $[M/H] = +0.1\,$dex, and the derived spectroscopical parameters for this star are $T_{\rm eff} = 3727 \pm 100\,$K,$\log g = 5.4 \pm 0.1\,$dex, $[M/H] = -0.34 \pm 0.1\,$dex.

Star 2M00244054+5511590 (LSPM J0024+5511 [4]) has not been previously spectroscopically characterized in the literature. The available ASPCAP parameters for this star are $T_{\rm eff} = 3785\,$K and $[M/H] = -0.05\,$dex, and $\log g = 4.38\,$dex. The matching spectrum for the

[1] http://simbad.u-strasbg.fr/simbad/sim-id?Ident=%409627302&Name=UCAC4+533-000024
[2] http://simbad.u-strasbg.fr/simbad/sim-id?Ident=%40130462&Name=GSC+03665-00665
[3] http://simbad.u-strasbg.fr/simbad/sim-id?Ident=%4045008&Name=LP++150-1
[4] http://simbad.u-strasbg.fr/simbad/sim-id?Ident=%403990584&Name=LSPM+J0024%2B5511

star has been obtained by normalizing the APOGEE observed one with a synthetic spectrum with $T_{\text{eff}} = 3600\,$K, $\log g = 5.0\,$dex and $[M/H] = +0.1\,$dex, and the derived spectroscopical parameters for this star are $T_{\text{eff}} = 3726 \pm 100\,$K,$\log g = 4.57 \pm 0.1\,$dex, $[M/H] = -0.31 \pm 0.1\,$dex.

Star 2M00251060+6724193 (LSPM J0025+6724 [5]) has not been previously characterized in the literature, and is flagged in Simbad Wenger et al. (2000) as a double or multiple star. The available ASPCAP parameters for this star are $T_{\text{eff}} = 3615\,$K and $[M/H] = -0.08\,$dex, and $\log g = 4.32\,$dex. The matching spectrum for the star has been obtained by normalizing the APOGEE observed one with a synthetic spectrum with $T_{\text{eff}} = 3600\,$K, $\log g = 5.0\,$dex and $[M/H] = +0.0\,$dex, and the derived spectroscopical parameters for this star are $T_{\text{eff}} = 3708 \pm 100\,$K,$\log g = 4.96 \pm 0.1\,$dex, $[M/H] = -0.23 \pm 0.1\,$dex.

Star 2M00262872+6747026 (G+243-26 [6]) was characterized in Gilhool et al. (2017), giving it the following parameters: $T_{\text{eff}} = 3756\,$K,$\log g = 4.5\,$dex, $[M/H] = +0.0\,$dex. The available ASPCAP parameters for this star are $T_{\text{eff}} = 3809\,$K and $[M/H] = 0.09\,$dex, with an $\log g = 4.34\,$dex. The matching spectrum for the star has been obtained by normalizing the APOGEE observed one with a synthetic spectrum with $T_{\text{eff}} = 3900\,$K, $\log g = 5.0\,$dex and $[M/H] = +0.2\,$dex, and the derived spectroscopical parameters for this star are $T_{\text{eff}} = 3841 \pm 100\,$K,$\log g = 4.88 \pm 0.1\,$dex, $[M/H] = +0.02 \pm 0.1\,$dex.

Star 2M00274401+5330504 (2MASS J00274401+5330504 [7]) has not been previously characterized in the literature, and is flagged in Simbad Wenger et al. (2000) as a high proper-motion star. The available ASPCAP parameters for this star are $T_{\text{eff}} = 3471\,$K and $\log g = 4.78\,$dex, with a $[M/H] = 0.09\,$dex. The matching spectrum for the star has been obtained by normalizing the APOGEE observed one with a synthetic spectrum with $T_{\text{eff}} = 3300\,$K, $\log g = 5.0\,$dex and $[M/H] = -0.2\,$dex, and the derived spectroscopical parameters for this star are $T_{\text{eff}} = 3465 \pm 100\,$K,$\log g = 5.02 \pm 0.1\,$dex, $[M/H] = -0.01 \pm 0.1\,$dex.

Star 2M00313293+6152504 (G+243-26 [8]) was characterized in Gilhool et al. (2017), giving it the following parameters: $T_{\text{eff}} = 3383\,$K,$\log g = 4.5\,$dex, $[M/H] = -0.5\,$dex. The available ASPCAP parameters for this star are $T_{\text{eff}} = 3497\,$K and $\log g = 4.45\,$dex, with a $[M/H] = -0.45\,$dex. The matching spectrum for the star has been obtained by normalizing the APOGEE observed one with a synthetic spectrum with $T_{\text{eff}} = 3300\,$K, $\log g = 5.0\,$dex

[5] http://simbad.u-strasbg.fr/simbad/sim-id?Ident=%403990609&Name=LSPM+J0025%2B6724
[6] http://simbad.u-strasbg.fr/simbad/sim-id?Ident=%40222475&Name=G+243-26
[7] http://simbad.u-strasbg.fr/simbad/sim-id?Ident=2Mass+j00274401%2B5330504
[8] http://simbad.u-strasbg.fr/simbad/sim-id?Ident=%40165109&Name=G+243-29

and $[M/H] = -0.1$ dex, and the derived spectroscopical parameters for this star are $T_{\text{eff}} = 3572 \pm 100$ K,$\log g = 4.8 \pm 0.1$ dex, $[M/H] = -0.65 \pm 0.1$ dex.

Star 2M00334916+6712243 (UCAC4 787-001030 [9]) has not been previously characterized in the literature, and is flagged in Simbad Wenger et al. (2000) as a high proper-motion star. The available ASPCAP parameters for this star are $T_{\text{eff}} = 3723$ K and $\log g = 4.28$ dex and $[M/H] = -0.06$ dex. The matching spectrum for the star has been obtained by normalizing the APOGEE observed one with a synthetic spectrum with $T_{\text{eff}} = 3800$ K, $\log g = 5.0$ dex and $[M/H] = +0.2$ dex, and the derived spectroscopical parameters for this star are $T_{\text{eff}} = 3784 \pm 100$ K,$\log g = 4.84 \pm 0.1$ dex, $[M/H] = -0.04 \pm 0.1$ dex.

Star 2M00350487+5953079 (NLTT 1875 [10]) was characterized in Gilhool et al. (2017), giving it the following parameters: $T_{\text{eff}} = 3225$ K,$\log g = 5.0$ dex, $[M/H] = +0.0$ dex. The available ASPCAP parameters for this star are $T_{\text{eff}} = 3273$ K and $\log g = 4.59$ dex, with a $[M/H] = -0.15$ dex. The matching spectrum for the star has been obtained by normalizing the APOGEE observed one with a synthetic spectrum with $T_{\text{eff}} = 3000$ K, $\log g = 5.0$ dex and $[M/H] = +0.0$ dex, and the derived spectroscopical parameters for this star are $T_{\text{eff}} = 3196 \pm 100$ K,$\log g = 5.05 \pm 0.1$ dex, $[M/H] = -0.13 \pm 0.1$ dex.

Star 2M00363436+5537360 (UCAC4 729-006249 [11]) has not been previously characterized in the literature, and is flagged in Simbad Wenger et al. (2000) as a rotationally variable star. The available ASPCAP parameters for this star are $T_{\text{eff}} = 3966$ K and $\log g = 4.56$ dex, and $[M/H] = -0.14$ dex. The matching spectrum for the star has been obtained by normalizing the APOGEE observed one with a synthetic spectrum with $T_{\text{eff}} = 4000$ K, $\log g = 5.0$ dex and $[M/H] = +0.2$ dex, and the derived spectroscopical parameters for this star are $T_{\text{eff}} = 3989 \pm 100$ K,$\log g = 4.88 \pm 0.1$ dex, $[M/H] = +0.07 \pm 0.1$ dex.

Star 2M00372598+5133072 (G 172-14 [12]) was characterized in Gilhool et al. (2017), giving it the following parameters: $T_{\text{eff}} = 3862$ K,$\log g = 4.5$ dex, $[M/H] = +0.0$ dex. It is also present in Gaidos et al. (2014), with $T_{\text{eff}} = 4062$ K, and in Lépine et al. (2013), with $T_{\text{eff}} = 3650$ K and $\log g = 4.5$ dex. The available ASPCAP parameters for this star are $T_{\text{eff}} = 3905$ K and $[M/H] = +0.07$ dex, with an $\log g = 4.44$ dex. The matching spectrum for the star has been obtained by normalizing the APOGEE observed one with a synthetic spectrum with $T_{\text{eff}} =$

[9] http://simbad.u-strasbg.fr/simbad/sim-id?Ident=2Mass+j00334916%2B6712243
[10] http://simbad.u-strasbg.fr/simbad/sim-id?Ident=2Mass+j00350487%2B5953079
[11] http://simbad.u-strasbg.fr/simbad/sim-id?Ident=2Mass+j00363436%2B5537360
[12] http://simbad.u-strasbg.fr/simbad/sim-id?Ident=2Mass+j00372598%2B5133072

4000 K, $\log g = 5.0$ dex and $[M/H] = +0.2$ dex, and the derived spectroscopical parameters for this star are $T_{\text{eff}} = 3876 \pm 100$ K,$\log g = 4.66 \pm 0.1$ dex, $[M/H] = -0.01 \pm 0.1$ dex.

Star 2M00391896+5508132 (G 217-60 [13]) was characterized in Gilhool et al. (2017), giving it the following parameters: $T_{\text{eff}} = 3145$ K,$\log g = 4.5$ dex, $[M/H] = -0.5$ dex. It is also present in Terrien et al. (2015), with $T_{\text{eff}} = 3333$ K and $[M/H] = -0.32$ dex. The available ASPCAP parameters for this star are $T_{\text{eff}} = 3222$ K and $\log g = 4.11$ dex, with a $[M/H] = -0.79$ dex. The matching spectrum for the star has been obtained by normalizing the APOGEE observed one with a synthetic spectrum with $T_{\text{eff}} = 3000$ K, $\log g = 5.0$ dex and $[M/H] = +0.0$ dex, and the derived spectroscopical parameters for this star are $T_{\text{eff}} = 3133 \pm 100$ K,$\log g = 4.9 \pm 0.1$ dex, $[M/H] = -0.02 \pm 0.1$ dex.

Star 2M00444820+1830403 (LP 405-58 [14]) was characterized in Gilhool et al. (2017), giving it the following parameters: $T_{\text{eff}} = 3636$ K,$\log g = 4.5$ dex, $[M/H] = +0.0$ dex. The available ASPCAP parameters for this star are $T_{\text{eff}} = 3721$ K and $[M/H] = -0.37$ dex, with an $\log g = 4.29$ dex. The matching spectrum for the star has been obtained by normalizing the APOGEE observed one with a synthetic spectrum with $T_{\text{eff}} = 3600$ K, $\log g = 5.0$ dex and $[M/H] = +0.1$ dex, and the derived spectroscopical parameters for this star are $T_{\text{eff}} = 3739 \pm 100$ K,$\log g = 5.0 \pm 0.1$ dex, $[M/H] = -0.37 \pm 0.1$ dex.

Star 2M01285381+1803284 (LP 405-58 [15]) was characterized in Gilhool et al. (2017), giving it the following parameters: $T_{\text{eff}} = 3641$ K,$\log g = 4.5$ dex, $[M/H] = -0.5$ dex. The available ASPCAP parameters for this star are $T_{\text{eff}} = 3716$ K and $[M/H] = -0.38$ dex, with an $\log g = 4.40$ dex. The matching spectrum for the star has been obtained by normalizing the APOGEE observed one with a synthetic spectrum with $T_{\text{eff}} = 3800$ K, $\log g = 5.0$ dex and $[M/H] = -0.1$ dex, and the derived spectroscopical parameters for this star are $T_{\text{eff}} = 3878 \pm 100$ K,$\log g = 5.03 \pm 0.1$ dex, $[M/H] = -0.72 \pm 0.1$ dex.

Star 2M02073745+1354497 (G 3-40 [16]) was characterized in Gilhool et al. (2017), giving it the following parameters: $T_{\text{eff}} = 3774$ K,$\log g = 5.0$ dex, $[M/H] = +0.5$ dex. The available ASPCAP parameters for this star are $T_{\text{eff}} = 3823$ K and $[M/H] = +0.22$ dex, with an $\log g = 4.48$ dex. The matching spectrum for the star has been obtained by normalizing the APOGEE observed one with a synthetic spectrum with $T_{\text{eff}} = 3900$ K, $\log g = 5.0$ dex

[13] http://simbad.u-strasbg.fr/simbad/sim-id?Ident=2Mass+j00391896%2B5508132
[14] http://simbad.u-strasbg.fr/simbad/sim-id?Ident=2Mass+j00444820%2B1830403
[15] http://simbad.u-strasbg.fr/simbad/sim-id?Ident=2Mass+j01285381%2B1803284
[16] http://simbad.u-strasbg.fr/simbad/sim-id?Ident=2Mass+j02073745%2B1354497

and $[M/H] = +0.4$ dex, and the derived spectroscopical parameters for this star are $T_{\rm eff} = 3827 \pm 100$ K,$\log g = 4.97 \pm 0.1$ dex, $[M/H] = +0.23 \pm 0.1$ dex.

Star 2M02090912+1435362 (Ross 326 [17]) was characterized in Gilhool et al. (2017), giving it the following parameters: $T_{\rm eff} = 3608$ K,$\log g = 5.0$ dex, $[M/H] = +0.0$ dex. The available ASPCAP parameters for this star are $T_{\rm eff} = 3669$ K and $[M/H] = -0.1$ dex, with an $\log g = 4.34$ dex. The matching spectrum for the star has been obtained by normalizing the APOGEE observed one with a synthetic spectrum with $T_{\rm eff} = 3500$ K, $\log g = 5.0$ dex and $[M/H] = +0.2$ dex, and the derived spectroscopical parameters for this star are $T_{\rm eff} = 3592 \pm 100$ K,$\log g = 4.92 \pm 0.1$ dex, $[M/H] = -0.02 \pm 0.1$ dex.

Star 2M02122001+1249287 (NLTT 7300 [18]) was characterized in Gilhool et al. (2017), giving it the following parameters: $T_{\rm eff} = 3459$ K,$\log g = 5.5$ dex, $[M/H] = +0.5$ dex. The available ASPCAP parameters for this star are $T_{\rm eff} = 3571$ K and $[M/H] = +0.24$ dex, with an $\log g = 4.41$ dex. The matching spectrum for the star has been obtained by normalizing the APOGEE observed one with a synthetic spectrum with $T_{\rm eff} = 3600$ K, $\log g = 5.0$ dex and $[M/H] = +0.4$ dex, and the derived spectroscopical parameters for this star are $T_{\rm eff} = 3650 \pm 100$ K,$\log g = 5.21 \pm 0.1$ dex, $[M/H] = +0.2 \pm 0.1$ dex.

Star 2M02362715+5528349 (G 173-61 [19]) was characterized in Gilhool et al. (2017), giving it the following parameters: $T_{\rm eff} = 3382$ K,$\log g = 4.5$ dex, $[M/H] = 0.0$ dex. It is also present in Terrien et al. (2015), with $T_{\rm eff} = 3361$ K and $[M/H] = -0.15$ dex. The available ASPCAP parameters for this star are $T_{\rm eff} = 3413$ K and $\log g = 4.35$ dex, with a $[M/H] = -0.36$ dex. The matching spectrum for the star has been obtained by normalizing the APOGEE observed one with a synthetic spectrum with $T_{\rm eff} = 3400$ K, $\log g = 5.0$ dex and $[M/H] = +0.1$ dex, and the derived spectroscopical parameters for this star are $T_{\rm eff} = 3576 \pm 100$ K,$\log g = 5.39 \pm 0.1$ dex, $[M/H] = -0.36 \pm 0.1$ dex.

Star 2M02381299+5542044 (UCAC4 729-023923 [20]) has not been previously characterized in the literature, and is flagged in Simbad Wenger et al. (2000) as a high proper-motion star. The available ASPCAP parameters for this star are $T_{\rm eff} = 4030$ K, $\log g = 4.40$ dex, and $[M/H] = -0.28$ dex. The matching spectrum for the star has been obtained by normalizing the APOGEE observed one with a synthetic spectrum with $T_{\rm eff} = 3800$ K, $\log g = 5.0$ dex

[17] http://simbad.u-strasbg.fr/simbad/sim-id?Ident=2Mass+j02090912%2B1435362
[18] http://simbad.u-strasbg.fr/simbad/sim-id?Ident=2Mass+j02122001%2B1249287
[19] http://simbad.u-strasbg.fr/simbad/sim-id?Ident=2Mass+j02362715%2B5528349
[20] http://simbad.u-strasbg.fr/simbad/sim-id?Ident=2Mass+j02381299%2B5542044

and $[M/H] = +0.4$ dex, and the derived spectroscopical parameters for this star are $T_{\rm eff} = 3979 \pm 100$ K,$\log g = 4.7 \pm 0.1$ dex, $[M/H] = +0.05 \pm 0.1$ dex.

Star 2M02465257+5619505 (G 174-12 [21]) was characterized in Gilhool et al. (2017), giving it the following parameters: $T_{\rm eff} = 3378$ K,$\log g = 4.5$ dex, $[M/H] = +0.0$ dex. The available ASPCAP parameters for this star are $T_{\rm eff} = 3428$ K and $\log g = 4.44$ dex, with a $[M/H] = -0.09$ dex. The matching spectrum for the star has been obtained by normalizing the APOGEE observed one with a synthetic spectrum with $T_{\rm eff} = 3200$ K, $\log g = 5.0$ dex and $[M/H] = +0.1$ dex, and the derived spectroscopical parameters for this star are $T_{\rm eff} = 3354 \pm 100$ K,$\log g = 4.5 \pm 0.1$ dex, $[M/H] = -0.09 \pm 0.1$ dex.

Star 2M03062774+6254388 (G 246-23 [22]) was characterized in Gilhool et al. (2017), giving it the following parameters: $T_{\rm eff} = 3165$ K,$\log g = 5.0$ dex, $[M/H] = +0.0$ dex. The available ASPCAP parameters for this star are $T_{\rm eff} = 3214$ K and $\log g = 4.37$ dex, with a $[M/H] = -0.48$ dex. The matching spectrum for the star has been obtained by normalizing the APOGEE observed one with a synthetic spectrum with $T_{\rm eff} = 3000$ K, $\log g = 5.0$ dex and $[M/H] = +0.2$ dex, and the derived spectroscopical parameters for this star are $T_{\rm eff} = 3157 \pm 100$ K,$\log g = 4.96 \pm 0.1$ dex, $[M/H] = -0.15 \pm 0.1$ dex.

Star 2M03140624+5728568 (G 174-37 [23]) was characterized in Gilhool et al. (2017), giving it the following parameters: $T_{\rm eff} = 3412$ K,$\log g = 5.5$ dex, $[M/H] = +0.5$ dex. The available ASPCAP parameters for this star are $T_{\rm eff} = 3463$ K and $\log g = 4.73$ dex, with a $[M/H] = -0.09$ dex. The matching spectrum for the star has been obtained by normalizing the APOGEE observed one with a synthetic spectrum with $T_{\rm eff} = 3200$ K, $\log g = 5.0$ dex and $[M/H] = +0.4$ dex, and the derived spectroscopical parameters for this star are $T_{\rm eff} = 3288 \pm 100$ K,$\log g = 4.99 \pm 0.1$ dex, $[M/H] = +0.15 \pm 0.1$ dex.

Star 2M03152943+5751330 (G 246-30 [24]) was characterized in Gilhool et al. (2017), giving it the following parameters: $T_{\rm eff} = 3312$ K,$\log g = 5.0$ dex, $[M/H] = +0.0$ dex. The available ASPCAP parameters for this star are $T_{\rm eff} = 3356$ K and $\log g = 4.48$ dex, with a $[M/H] = -0.39$ dex. The matching spectrum for the star has been obtained by normalizing the APOGEE observed one with a synthetic spectrum with $T_{\rm eff} = 3200$ K, $\log g = 5.0$ dex and $[M/H] = +0.1$ dex, and the derived spectroscopical parameters for this star are $T_{\rm eff} =$

[21] `http://simbad.u-strasbg.fr/simbad/sim-id?Ident=2Mass+j02465257%2B5619505`

[22] `http://simbad.u-strasbg.fr/simbad/sim-id?Ident=2Mass+j03062774%2B6254388`

[23] `http://simbad.u-strasbg.fr/simbad/sim-id?Ident=2Mass+j03140624%2B5728568`

[24] `http://simbad.u-strasbg.fr/simbad/sim-id?Ident=2Mass+j03152943%2B5751330`

3361 ± 100 K,$\log g = 5.19 \pm 0.1$ dex, $[M/H] = -0.17 \pm 0.1$ dex.

Star 2M03190939+0130543 (LSPM J0319+0130 [25]) has not been previously characterized in the literature, and is flagged in Simbad Wenger et al. (2000) as a high proper-motion star. The available ASPCAP parameters for this star are $T_{\rm eff} = 3114$ K, $\log g = 4.29$ dex, and $[M/H] = +0.32$ dex. The matching spectrum for the star has been obtained by normalizing the APOGEE observed one with a synthetic spectrum with $T_{\rm eff} = 3000$ K, $\log g = 5.0$ dex and $[M/H] = -0.4$ dex, and the derived spectroscopical parameters for this star are $T_{\rm eff} = 3410 \pm 100$ K,$\log g = 5.4 \pm 0.1$ dex, $[M/H] = -0.91 \pm 0.1$ dex.

Star 2M03212176+7958022 (G 245-71 [26]) was characterized in Gilhool et al. (2017), giving it the following parameters: $T_{\rm eff} = 3586$ K,$\log g = 4.5$ dex, $[M/H] = +0.0$ dex. It was also characterized in Gaidos et al. (2014), giving it $T_{\rm eff} = 3582$ K and in Lépine et al. (2013), with $\log g = 4.5$ dex and $T_{\rm eff} = 3460$ K. The available ASPCAP parameters for this star are $T_{\rm eff} = 3646$ K, and $[M/H] = -0.21$ dex, with $\log g = 4.45$ dex. The matching spectrum for the star has been obtained by normalizing the APOGEE observed one with a synthetic spectrum with $T_{\rm eff} = 3400$ K, $\log g = 5.0$ dex and $[M/H] = +0.1$ dex, and the derived spectroscopical parameters for this star are $T_{\rm eff} = 3545 \pm 100$ K,$\log g = 4.95 \pm 0.1$ dex, $[M/H] = -0.19 \pm 0.1$ dex.

Star 2M03215239+6335088 (LSPM J0321+6335 [27]) has not been previously characterized in the literature, and is flagged in Simbad Wenger et al. (2000) as a high proper-motion star. The available ASPCAP parameters for this star are $T_{\rm eff} = 3619$ K, $\log g = 4.39$ dex, and $[M/H] = +0.03$ dex. The matching spectrum for the star has been obtained by normalizing the APOGEE observed one with a synthetic spectrum with $T_{\rm eff} = 3600$ K, $\log g = 5.0$ dex and $[M/H] = +0.2$ dex, and the derived spectroscopical parameters for this star are $T_{\rm eff} = 3654 \pm 100$ K,$\log g = 4.99 \pm 0.1$ dex, $[M/H] = -0.06 \pm 0.1$ dex.

Star 2M03241544+0928579 (LP 472-62 [28]) has not been previously characterized in the literature, and is flagged in Simbad Wenger et al. (2000) as a high proper-motion star. The available ASPCAP parameters for this star are $T_{\rm eff} = 3558$ K, and $[M/H] = +0.22$ dex, with $\log g = 4.42$ dex. The matching spectrum for the star has been obtained by normalizing the APOGEE observed one with a synthetic spectrum with $T_{\rm eff} = 3400$ K, $\log g = 5.0$ dex and $[M/H] = +0.1$ dex, and the derived spectroscopical parameters for this star are $T_{\rm eff} = 3592 \pm$

[25] http://simbad.u-strasbg.fr/simbad/sim-id?Ident=2Mass+j03190939%2B0130543
[26] http://simbad.u-strasbg.fr/simbad/sim-id?Ident=2Mass+j03212176%2B7958022
[27] http://simbad.u-strasbg.fr/simbad/sim-id?Ident=2Mass+j03215239%2B6335088
[28] http://simbad.u-strasbg.fr/simbad/sim-id?Ident=2Mass+j03241544%2B0928579

100 K,$\log g = 5.22 \pm 0.1$ dex, $[M/H] = -0.32 \pm 0.1$ dex.

Star 2M03280163+5226180 (G 174-52 [29]) was characterized in Gilhool et al. (2017), giving it the following parameters: $T_{\rm eff} = 3780$ K,$\log g = 4.5$ dex, $[M/H] = +0.0$ dex. The available ASPCAP parameters for this star are $T_{\rm eff} = 3831$ K, and $[M/H] = -0.01$ dex, with $\log g = 4.34$ dex. The matching spectrum for the star has been obtained by normalizing the APOGEE observed one with a synthetic spectrum with $T_{\rm eff} = 3800$ K, $\log g = 5.0$ dex and $[M/H] = +0.2$ dex, and the derived spectroscopical parameters for this star are $T_{\rm eff} = 3822 \pm 100$ K,$\log g = 4.79 \pm 0.1$ dex, $[M/H] = -0.04 \pm 0.1$ dex.

Star 2M03355099+7140275 (G 221-16 [30]) was characterized in Gilhool et al. (2017), giving it the following parameters: $T_{\rm eff} = 3192$ K,$\log g = 5.5$ dex, $[M/H] = +0.5$ dex. The available ASPCAP parameters for this star are $T_{\rm eff} = 3228$ K, and $\log g = 4.67$ dex, with $[M/H] = -0.22$ dex. The matching spectrum for the star has been obtained by normalizing the APOGEE observed one with a synthetic spectrum with $T_{\rm eff} = 3000$ K, $\log g = 5.0$ dex and $[M/H] = +0.2$ dex, and the derived spectroscopical parameters for this star are $T_{\rm eff} = 3113 \pm 100$ K,$\log g = 4.94 \pm 0.1$ dex, $[M/H] = +0.0 \pm 0.1$ dex.

Star 2M03391302+4635276 (LSPM J0339+4635 [31]) was characterized in Gilhool et al. (2017), giving it the following parameters: $T_{\rm eff} = 3402$ K,$\log g = 4.5$ dex, $[M/H] = +0.0$ dex. The available ASPCAP parameters for this star are $T_{\rm eff} = 3446$ K, and $\log g = 4.27$ dex, with $[M/H] = -0.24$ dex. The matching spectrum for the star has been obtained by normalizing the APOGEE observed one with a synthetic spectrum with $T_{\rm eff} = 3200$ K, $\log g = 5.0$ dex and $[M/H] = -0.4$ dex, and the derived spectroscopical parameters for this star are $T_{\rm eff} = 3568 \pm 100$ K,$\log g = 4.92 \pm 0.1$ dex, $[M/H] = -0.48 \pm 0.1$ dex.

Star 2M03391968+3251001 (LP 300-24 [32]) was characterized in Gilhool et al. (2017), giving it the following parameters: $T_{\rm eff} = 3500$ K,$\log g = 5.5$ dex, $[M/H] = +0.5$ dex. The available ASPCAP parameters for this star are $T_{\rm eff} = 3513$ K, $\log g = 4.47$ dex, and $[M/H] = -0.27$ dex. The matching spectrum for the star has been obtained by normalizing the APOGEE observed one with a synthetic spectrum with $T_{\rm eff} = 3400$ K, $\log g = 5.0$ dex and $[M/H] = +0.4$ dex, and the derived spectroscopical parameters for this star are $T_{\rm eff} = 3478 \pm 100$ K,$\log g = 5.12 \pm 0.1$ dex, $[M/H] = +0.14 \pm 0.1$ dex.

[29] `http://simbad.u-strasbg.fr/simbad/sim-id?Ident=2Mass+j03280163%2B5226180`
[30] `http://simbad.u-strasbg.fr/simbad/sim-id?Ident=2Mass+j03355099%2B7140275`
[31] `http://simbad.u-strasbg.fr/simbad/sim-id?Ident=2Mass+j03391302%2B4635276`
[32] `http://simbad.u-strasbg.fr/simbad/sim-id?Ident=2Mass+j03391968%2B3251001`

Star 2M03400164+4638456 (G 78-45 [33]) was characterized in Gilhool et al. (2017), giving it the following parameters: $T_{\text{eff}} = 3637\,$K,$\log g = 4.5\,$dex, $[M/H] = -0.5\,$dex. The available ASPCAP parameters for this star are $T_{\text{eff}} = 3712\,$K and $[M/H] = -0.45\,$dex, with $\log g = 4.33\,$dex,. The matching spectrum for the star has been obtained by normalizing the APOGEE observed one with a synthetic spectrum with $T_{\text{eff}} = 3400\,$K, $\log g = 5.0\,$dex and $[M/H] = -0.1\,$dex, and the derived spectroscopical parameters for this star are $T_{\text{eff}} = 3597 \pm 100\,$K,$\log g = 4.49 \pm 0.1\,$dex, $[M/H] = -0.47 \pm 0.1\,$dex.

Star 2M03431519+5006558 (2MASS J03431519+5006558 [34]) has not been previously characterized in the literature, and is flagged in Simbad Wenger et al. (2000) as a high proper-motion star. The available ASPCAP parameters for this star are $T_{\text{eff}} = 3457\,$K and $[M/H] = -0.23\,$dex, and $\log g = 4.85\,$dex,. The matching spectrum for the star has been obtained by normalizing the APOGEE observed one with a synthetic spectrum with $T_{\text{eff}} = 3600\,$K, $\log g = 5.0\,$dex and $[M/H] = +0.3\,$dex, and the derived spectroscopical parameters for this star are $T_{\text{eff}} = 3637 \pm 100\,$K,$\log g = 5.4 \pm 0.1\,$dex, $[M/H] = -0.03 \pm 0.1\,$dex.

Star 2M03441913+7126195 (NLTT 11595 [35]) was characterized in Gilhool et al. (2017), giving it the following parameters: $T_{\text{eff}} = 3582\,$K,$\log g = 5.0\,$dex, $[M/H] = +0.5\,$dex. The available ASPCAP parameters for this star are $T_{\text{eff}} = 3641\,$K and $[M/H] = +0.12\,$dex, with $\log g = 4.41\,$dex,. The matching spectrum for the star has been obtained by normalizing the APOGEE observed one with a synthetic spectrum with $T_{\text{eff}} = 3600\,$K, $\log g = 5.0\,$dex and $[M/H] = +0.3\,$dex, and the derived spectroscopical parameters for this star are $T_{\text{eff}} = 3635 \pm 100\,$K,$\log g = 4.99 \pm 0.1\,$dex, $[M/H] = +0.15 \pm 0.1\,$dex.

Star 2M03443389+7125059 (NLTT 11608 [36]) has not been previously characterized in the literature, and is flagged in Simbad Wenger et al. (2000) as a high proper-motion star. The available ASPCAP parameters for this star are $T_{\text{eff}} = 3521\,$K and $[M/H] = -0.1\,$dex, and $\log g = 4.42\,$dex,. The matching spectrum for the star has been obtained by normalizing the APOGEE observed one with a synthetic spectrum with $T_{\text{eff}} = 3800\,$K, $\log g = 5.0\,$dex and $[M/H] = +0.2\,$dex, and the derived spectroscopical parameters for this star are $T_{\text{eff}} = 3722 \pm 100\,$K,$\log g = 5.34 \pm 0.1\,$dex, $[M/H] = -0.02 \pm 0.1\,$dex.

Star 2M03481149+3054134 (LP 300-40 [37]) was characterized in Gilhool et al. (2017),

[33] http://simbad.u-strasbg.fr/simbad/sim-id?Ident=2Mass+j03400164%2B4638456
[34] http://simbad.u-strasbg.fr/simbad/sim-id?Ident=2Mass+j03431519%2B5006558
[35] http://simbad.u-strasbg.fr/simbad/sim-id?Ident=2Mass+j03441913%2B7126195
[36] http://simbad.u-strasbg.fr/simbad/sim-id?Ident=2Mass+j03443389%2B7125059
[37] http://simbad.u-strasbg.fr/simbad/sim-id?Ident=2Mass+j03481149%2B3054134

giving it the following parameters: $T_{\text{eff}} = 3311\,\text{K}$,$\log g = 5.0\,\text{dex}$, $[M/H] = +0.0\,\text{dex}$. The available ASPCAP parameters for this star are $T_{\text{eff}} = 3363\,\text{K}$ and $\log g = 4.41\,\text{dex}$, with $[M/H] = -0.41\,\text{dex}$. The matching spectrum for the star has been obtained by normalizing the APOGEE observed one with a synthetic spectrum with $T_{\text{eff}} = 3400\,\text{K}$, $\log g = 5.0\,\text{dex}$ and $[M/H] = +0.1\,\text{dex}$, and the derived spectroscopical parameters for this star are $T_{\text{eff}} = 3554 \pm 100\,\text{K}$,$\log g = 5.4 \pm 0.1\,\text{dex}$, $[M/H] = -0.36 \pm 0.1\,\text{dex}$.

Star 2M04125880+5236421 (Ross 28 [38]) was characterized in Gilhool et al. (2017), giving it the following parameters: $T_{\text{eff}} = 3206\,\text{K}$,$\log g = 5.0\,\text{dex}$, $[M/H] = +0.0\,\text{dex}$. It was also characterized in Gaidos et al. (2014), giving it $T_{\text{eff}} = 3087\,\text{K}$ and in Lépine et al. (2013), with $\log g = 5.0\,\text{dex}$ and $T_{\text{eff}} = 3140\,\text{K}$. The star is also present in Rojas-Ayala et al. (2012), with $T_{\text{eff}} = 3051\,\text{K}$ and $[M/H] = +0.02\,\text{dex}$. The available ASPCAP parameters for this star are $T_{\text{eff}} = 3243\,\text{K}$ and $\log g = 4.32\,\text{dex}$, with $[M/H] = -0.30\,\text{dex}$. The matching spectrum for the star has been obtained by normalizing the APOGEE observed one with a synthetic spectrum with $T_{\text{eff}} = 3000\,\text{K}$, $\log g = 5.0\,\text{dex}$ and $[M/H] = -0.2\,\text{dex}$, and the derived spectroscopical parameters for this star are $T_{\text{eff}} = 3294 \pm 100\,\text{K}$,$\log g = 5.3 \pm 0.1\,\text{dex}$, $[M/H] = -0.28 \pm 0.1\,\text{dex}$.

Star 2M04244284+4537062 (LSPM J0424+4537 [39]) has not been previously characterized in the literature, and is flagged in Simbad Wenger et al. (2000) as a high proper-motion star. The available ASPCAP parameters for this star are $T_{\text{eff}} = 3760\,\text{K}$, $\log g = 4.44\,\text{dex}$, and $[M/H] = -0.02\,\text{dex}$. The matching spectrum for the star has been obtained by normalizing the APOGEE observed one with a synthetic spectrum with $T_{\text{eff}} = 3600\,\text{K}$, $\log g = 5.0\,\text{dex}$ and $[M/H] = +0.0\,\text{dex}$, and the derived spectroscopical parameters for this star are $T_{\text{eff}} = 3709 \pm 100\,\text{K}$,$\log g = 4.51 \pm 0.1\,\text{dex}$, $[M/H] = -0.23 \pm 0.1\,\text{dex}$.

Star 2M04310001+3647548 (PM J04310+3647 [40]) was characterized in Terrien et al. (2015), giving it the following parameters: $T_{\text{eff}} = 3424\,\text{K}$, $[M/H] = +0.02\,\text{dex}$. The available ASPCAP parameters for this star are $T_{\text{eff}} = 3501\,\text{K}$,$\log g = 4.71\,\text{dex}$, and $[M/H] = +0.11\,\text{dex}$. The matching spectrum for the star has been obtained by normalizing the APOGEE observed one with a synthetic spectrum with $T_{\text{eff}} = 3300\,\text{K}$, $\log g = 5.0\,\text{dex}$ and $[M/H] = +0.2\,\text{dex}$, and the derived spectroscopical parameters for this star are $T_{\text{eff}} = 3404 \pm 100\,\text{K}$,$\log g = 4.85 \pm 0.1\,\text{dex}$, $[M/H] = +0.0 \pm 0.1\,\text{dex}$.

[38] `http://simbad.u-strasbg.fr/simbad/sim-id?Ident=2Mass+j04125880%2B5236421`
[39] `http://simbad.u-strasbg.fr/simbad/sim-id?Ident=2Mass+j04244284%2B4537062`
[40] `http://simbad.u-strasbg.fr/simbad/sim-id?Ident=2Mass+j04310001%2B3647548`

Star 2M04311499+4217111 (PM J04310+3647 [41]) was characterized in Gaidos et al. (2014), giving it $T_{\rm eff} = 3634$ K and in Lépine et al. (2013), with $\log g = 5.0$ dex and $T_{\rm eff} = 3530$ K. The available ASPCAP parameters for this star are $T_{\rm eff} = 3643$ K,$\log g = 4.63$ dex, and $[M/H] = +0.01$ dex. The matching spectrum for the star has been obtained by normalizing the APOGEE observed one with a synthetic spectrum with $T_{\rm eff} = 3400$ K, $\log g = 5.0$ dex and $[M/H] = +0.2$ dex, and the derived spectroscopical parameters for this star are $T_{\rm eff} = 3506 \pm 100$ K,$\log g = 4.78 \pm 0.1$ dex, $[M/H] = +0.09 \pm 0.1$ dex.

Star 2M04311837+3655082 (UCAC4 635-017819 [42]) has not been previously spectroscopically characterized in the literature, and is flagged in Simbad Wenger et al. (2000) as a high proper-motion star. The available ASPCAP parameters for this star are $T_{\rm eff} = 3695$ K,$\log g = 4.36$ dex, and $[M/H] = -0.10$ dex. The matching spectrum for the star has been obtained by normalizing the APOGEE observed one with a synthetic spectrum with $T_{\rm eff} = 3600$ K, $\log g = 5.0$ dex and $[M/H] = +0.2$ dex, and the derived spectroscopical parameters for this star are $T_{\rm eff} = 3680 \pm 100$ K,$\log g = 4.78 \pm 0.1$ dex, $[M/H] = -0.04 \pm 0.1$ dex.

Star 2M04334819+4227070 (LP 201-54 [43]) has not been previously spectroscopically characterized in the literature, and is flagged in Simbad Wenger et al. (2000) as a high proper-motion star. The available ASPCAP parameters for this star are $T_{\rm eff} = 3381$ K,$\log g = 4.73$ dex, and $[M/H] = -0.04$ dex. The matching spectrum for the star has been obtained by normalizing the APOGEE observed one with a synthetic spectrum with $T_{\rm eff} = 3400$ K, $\log g = 5.0$ dex and $[M/H] = +0.3$ dex, and the derived spectroscopical parameters for this star are $T_{\rm eff} = 3449 \pm 100$ K,$\log g = 5.4 \pm 0.1$ dex, $[M/H] = -0.01 \pm 0.1$ dex.

Star 2M04342248+4302148 (UCAC4 687-030746 [44]) was characterized in Terrien et al. (2015), giving it the following parameters: $T_{\rm eff} = 3473$ K, $[M/H] = +0.11$ dex. The available ASPCAP parameters for this star are $T_{\rm eff} = 3598$ K, $[M/H] = -0.01$ dex, and $\log g = 4.46$ dex. The matching spectrum for the star has been obtained by normalizing the APOGEE observed one with a synthetic spectrum with $T_{\rm eff} = 3400$ K, $\log g = 5.0$ dex and $[M/H] = +0.2$ dex, and the derived spectroscopical parameters for this star are $T_{\rm eff} = 3499 \pm 100$ K,$\log g = 4.69 \pm 0.1$ dex, $[M/H] = +0.05 \pm 0.1$ dex.

Star 2M04351236+5821100 (G 175-38 [45]) was characterized in Gilhool et al. (2017), giving

[41] http://simbad.u-strasbg.fr/simbad/sim-id?Ident=2Mass+j04311499%2B4217111
[42] http://simbad.u-strasbg.fr/simbad/sim-id?Ident=2Mass+j04311837%2B3655082
[43] http://simbad.u-strasbg.fr/simbad/sim-id?Ident=2Mass+j04334819%2B4227070
[44] http://simbad.u-strasbg.fr/simbad/sim-id?Ident=2Mass+j04342248%2B4302148
[45] http://simbad.u-strasbg.fr/simbad/sim-id?Ident=2Mass+j04351236%2B5821100

it the following parameters: $T_{\rm eff} = 3356\,$K,$\log g = 4.5\,$dex, $[M/H] = +0.0\,$dex. The available ASPCAP parameters for this star are $T_{\rm eff} = 3387\,$K, $\log g = 4.20\,$dex, and $[M/H] = -0.45\,$dex. The matching spectrum for the star has been obtained by normalizing the APOGEE observed one with a synthetic spectrum with $T_{\rm eff} = 3200\,$K, $\log g = 5.0\,$dex and $[M/H] = -0.2\,$dex, and the derived spectroscopical parameters for this star are $T_{\rm eff} = 3511 \pm 100\,$K,$\log g = 5.11 \pm 0.1\,$dex, $[M/H] = -0.54 \pm 0.1\,$dex.

Star 2M04371030+4703549 (G 81-28 [46]) was characterized in Gilhool et al. (2017), giving it the following parameters: $T_{\rm eff} = 3564\,$K,$\log g = 4.5\,$dex, $[M/H] = -0.5\,$dex. The available ASPCAP parameters for this star are $T_{\rm eff} = 3662\,$K, $[M/H] = -0.37\,$dex, and $\log g = 4.41\,$dex. The matching spectrum for the star has been obtained by normalizing the APOGEE observed one with a synthetic spectrum with $T_{\rm eff} = 3400\,$K, $\log g = 5.0\,$dex and $[M/H] = -0.1\,$dex, and the derived spectroscopical parameters for this star are $T_{\rm eff} = 3634 \pm 100\,$K,$\log g = 4.91 \pm 0.1\,$dex, $[M/H] = -0.52 \pm 0.1\,$dex.

Star 2M04400301+4620167 (LSPM J0440+4620 [47]) has not been previously spectroscopically characterized in the literature, and is flagged in Simbad Wenger et al. (2000) as a high proper-motion star. The available ASPCAP parameters for this star are $T_{\rm eff} = 3526\,$K, $[M/H] = -0.26\,$dex, and $\log g = 4.69\,$dex. The matching spectrum for the star has been obtained by normalizing the APOGEE observed one with a synthetic spectrum with $T_{\rm eff} = 3400\,$K, $\log g = 5.0\,$dex and $[M/H] = +0.2\,$dex, and the derived spectroscopical parameters for this star are $T_{\rm eff} = 3475 \pm 100\,$K,$\log g = 5.00 \pm 0.1\,$dex, $[M/H] = +0.0 \pm 0.1\,$dex.

Star 2M04422854+5818015 (LP 84-40 [48]) was characterized in Gilhool et al. (2017), giving it the following parameters: $T_{\rm eff} = 3274\,$K,$\log g = 5.0\,$dex, $[M/H] = +0.0\,$dex. The available ASPCAP parameters for this star are $T_{\rm eff} = 3332\,$K, $\log g = 4.49\,$dex, and $[M/H] = -0.49\,$dex. The matching spectrum for the star has been obtained by normalizing the APOGEE observed one with a synthetic spectrum with $T_{\rm eff} = 3200\,$K, $\log g = 5.0\,$dex and $[M/H] = +0.1\,$dex, and the derived spectroscopical parameters for this star are $T_{\rm eff} = 3372 \pm 100\,$K,$\log g = 5.27 \pm 0.1\,$dex, $[M/H] = -0.27 \pm 0.1\,$dex.

Star 2M04443813+3857031 (LSPM J0444+3857 [49]) has not been previously spectroscopically characterized in the literature, and is flagged in Simbad Wenger et al. (2000) as a

[46] http://simbad.u-strasbg.fr/simbad/sim-id?Ident=2Mass+j04371030%2B4703549
[47] http://simbad.u-strasbg.fr/simbad/sim-id?Ident=2Mass+j04400301%2B4620167
[48] http://simbad.u-strasbg.fr/simbad/sim-id?Ident=2Mass+j04422854%2B5818015
[49] http://simbad.u-strasbg.fr/simbad/sim-id?Ident=2Mass+j04443813%2B3857031

high proper-motion star. The available ASPCAP parameters for this star are $T_{\mathrm{eff}} = 3540$ K, $\log g = 4.38$ dex, and $[M/H] = +0.01$ dex. The matching spectrum for the star has been obtained by normalizing the APOGEE observed one with a synthetic spectrum with $T_{\mathrm{eff}} = 3400$ K, $\log g = 5.0$ dex and $[M/H] = +0.2$ dex, and the derived spectroscopical parameters for this star are $T_{\mathrm{eff}} = 3490 \pm 100$ K,$\log g = 4.6 \pm 0.1$ dex, $[M/H] = -0.02 \pm 0.1$ dex.

Star 2M04463593+5900524 (UCAC4 746-035662 [50]) has not been previously spectroscopically characterized in the literature, and is flagged in Simbad Wenger et al. (2000) as a high proper-motion star. The available ASPCAP parameters for this star are $T_{\mathrm{eff}} = 3676$ K, $\log g = 4.42$ dex, and $[M/H] = +0.06$ dex. The matching spectrum for the star has been obtained by normalizing the APOGEE observed one with a synthetic spectrum with $T_{\mathrm{eff}} = 3600$ K, $\log g = 5.0$ dex and $[M/H] = +0.2$ dex, and the derived spectroscopical parameters for this star are $T_{\mathrm{eff}} = 3641 \pm 100$ K,$\log g = 4.56 \pm 0.1$ dex, $[M/H] = -0.04 \pm 0.1$ dex.

Star 2M04483289+5003109 (LSPM J0448+5003 [51]) was characterized in Gilhool et al. (2017), giving it the following parameters: $T_{\mathrm{eff}} = 3436$ K,$\log g = 5.0$ dex, $[M/H] = +0.5$ dex. The available ASPCAP parameters for this star are $T_{\mathrm{eff}} = 3488$ K, $\log g = 4.60$ dex, and $[M/H] = -0.02$ dex. The matching spectrum for the star has been obtained by normalizing the APOGEE observed one with a synthetic spectrum with $T_{\mathrm{eff}} = 3400$ K, $\log g = 5.0$ dex and $[M/H] = +0.2$ dex, and the derived spectroscopical parameters for this star are $T_{\mathrm{eff}} = 3488 \pm 100$ K,$\log g = 5.0 \pm 0.1$ dex, $[M/H] = -0.02 \pm 0.1$ dex.

Star 2M04552111+5017249 (LSPM J0455+5017 [52]) has not been previously spectroscopically characterized in the literature, and is flagged in Simbad Wenger et al. (2000) as a high proper-motion star. The available ASPCAP parameters for this star are $T_{\mathrm{eff}} = 3796$ K, $\log g = 4.32$ dex, and $[M/H] = +0.09$ dex. The matching spectrum for the star has been obtained by normalizing the APOGEE observed one with a synthetic spectrum with $T_{\mathrm{eff}} = 3700$ K, $\log g = 5.0$ dex and $[M/H] = -0.1$ dex, and the derived spectroscopical parameters for this star are $T_{\mathrm{eff}} = 3865 \pm 100$ K,$\log g = 4.83 \pm 0.1$ dex, $[M/H] = -0.71 \pm 0.1$ dex.

Star 2M04581599+5017278 (LSPM J0458+5017 [53]) has not been previously spectroscopically characterized in the literature, and is flagged in Simbad Wenger et al. (2000) as a high proper-motion star. The available ASPCAP parameters for this star are $T_{\mathrm{eff}} = 3912$ K,

[50] http://simbad.u-strasbg.fr/simbad/sim-id?Ident=2Mass+j04463593%2B5900524
[51] http://simbad.u-strasbg.fr/simbad/sim-id?Ident=2Mass+j04463593%2B5900524
[52] http://simbad.u-strasbg.fr/simbad/sim-id?Ident=2Mass+j04552111%2B5017249
[53] http://simbad.u-strasbg.fr/simbad/sim-id?Ident=2Mass+j04581599%2B5017278

$[M/H] = -0.14$ dex, and $\log g = 4.36$ dex. The matching spectrum for the star has been obtained by normalizing the APOGEE observed one with a synthetic spectrum with $T_{\rm eff} = 3900$ K, $\log g = 5.0$ dex and $[M/H] = +0.0$ dex, and the derived spectroscopical parameters for this star are $T_{\rm eff} = 3949 \pm 100$ K,$\log g = 4.92 \pm 0.1$ dex, $[M/H] = -0.19 \pm 0.1$ dex.

Star 2M04584599+5056378 (G 191-15 [54]) was characterized in Gilhool et al. (2017), giving it the following parameters: $T_{\rm eff} = 3807$ K,$\log g = 4.5$ dex, $[M/H] = +0.0$ dex. It was also characterized in Gaidos et al. (2014), giving it $T_{\rm eff} = 3870$ K and in Lépine et al. (2013), with $\log g = 4.5$ dex and $T_{\rm eff} = 3560$ K. The available ASPCAP parameters for this star are $T_{\rm eff} = 3853$ K, $[M/H] = +0.00$ dex, and $\log g = 4.44$ dex. The matching spectrum for the star has been obtained by normalizing the APOGEE observed one with a synthetic spectrum with $T_{\rm eff} = 3800$ K, $\log g = 5.0$ dex and $[M/H] = +0.2$ dex, and the derived spectroscopical parameters for this star are $T_{\rm eff} = 3838 \pm 100$ K,$\log g = 4.87 \pm 0.1$ dex, $[M/H] = -0.02 \pm 0.1$ dex.

Star 2M05011792+4204125 (G 96-15 [55]) was characterized in Gilhool et al. (2017), giving it the following parameters: $T_{\rm eff} = 3656$ K,$\log g = 5.0$ dex, $[M/H] = +0.5$ dex. The available ASPCAP parameters for this star are $T_{\rm eff} = 3721$ K, $[M/H] = +0.22$ dex, and $\log g = 4.49$ dex. The matching spectrum for the star has been obtained by normalizing the APOGEE observed one with a synthetic spectrum with $T_{\rm eff} = 3600$ K, $\log g = 5.0$ dex and $[M/H] = +0.4$ dex, and the derived spectroscopical parameters for this star are $T_{\rm eff} = 3670 \pm 100$ K,$\log g = 4.8 \pm 0.1$ dex, $[M/H] = +0.12 \pm 0.1$ dex.

Star 2M05014512+5039319 (G 191-18 [56]) was characterized in Gilhool et al. (2017), giving it the following parameters: $T_{\rm eff} = 3605$ K,$\log g = 4.5$ dex, $[M/H] = +0.0$ dex. The available ASPCAP parameters for this star are $T_{\rm eff} = 3671$ K, $[M/H] = -0.20$ dex, and $\log g = 4.31$ dex. The matching spectrum for the star has been obtained by normalizing the APOGEE observed one with a synthetic spectrum with $T_{\rm eff} = 3600$ K, $\log g = 5.0$ dex and $[M/H] = +0.2$ dex, and the derived spectroscopical parameters for this star are $T_{\rm eff} = 3689 \pm 100$ K,$\log g = 4.98 \pm 0.1$ dex, $[M/H] = -0.18 \pm 0.1$ dex.

Star 2M05145032+4639432 (LSPM J0514+4639 [57]) has not been previously spectroscopically characterized in the literature, and is flagged in Simbad Wenger et al. (2000) as a high proper-motion star. The available ASPCAP parameters for this star are $T_{\rm eff} = 3897$ K,

[54] http://simbad.u-strasbg.fr/simbad/sim-id?Ident=2Mass+j04584599%2B5056378
[55] http://simbad.u-strasbg.fr/simbad/sim-id?Ident=2Mass+j05011792%2B4204125
[56] http://simbad.u-strasbg.fr/simbad/sim-id?Ident=2Mass+j05014512%2B5039319
[57] http://simbad.u-strasbg.fr/simbad/sim-id?Ident=2Mass+j05145032%2B4639432

$[M/H] = -0.23$ dex, and $\log g = 4.34$ dex. The matching spectrum for the star has been obtained by normalizing the APOGEE observed one with a synthetic spectrum with $T_{\rm eff} = 3800$ K, $\log g = 5.0$ dex and $[M/H] = +0.1$ dex, and the derived spectroscopical parameters for this star are $T_{\rm eff} = 3911 \pm 100$ K,$\log g = 4.78 \pm 0.1$ dex, $[M/H] = -0.23 \pm 0.1$ dex.

Star 2M05172841+2531214 (2MASS J05172841+2531214 [58]) has not been previously spectroscopically characterized in the literature, and is flagged in Simbad Wenger et al. (2000) as a high proper-motion star. The available ASPCAP parameters for this star are $T_{\rm eff} = 3448$ K, $[M/H] = -0.26$ dex, and $\log g = 4.76$ dex. The matching spectrum for the star has been obtained by normalizing the APOGEE observed one with a synthetic spectrum with $T_{\rm eff} = 3200$ K, $\log g = 5.0$ dex and $[M/H] = +0.0$ dex, and the derived spectroscopical parameters for this star are $T_{\rm eff} = 3330 \pm 100$ K,$\log g = 5.0 \pm 0.1$ dex, $[M/H] = -0.01 \pm 0.1$ dex.

Star 2M05201152+2457212 (UCAC4 575-015987 [59]) has not been previously spectroscopically characterized in the literature, and is flagged in Simbad Wenger et al. (2000) as a high proper-motion star. The available ASPCAP parameters for this star are $T_{\rm eff} = 3651$ K, $[M/H] = -0.06$ dex, and $\log g = 4.48$ dex. The matching spectrum for the star has been obtained by normalizing the APOGEE observed one with a synthetic spectrum with $T_{\rm eff} = 3400$ K, $\log g = 5.0$ dex and $[M/H] = +0.4$ dex, and the derived spectroscopical parameters for this star are $T_{\rm eff} = 3499 \pm 100$ K,$\log g = 4.58 \pm 0.1$ dex, $[M/H] = +0.2 \pm 0.1$ dex.

Star 2M05222053+3031097 (UCAC4 575-015987 [60]) has been characterized in (Kopytova et al. 2016), with published parameters of $T_{\rm eff} = 3815$ K and $\log g = 3.58$ dex, and in (Terrien et al. 2015), with parameters $T_{\rm eff} = 3428$ K, $[M/H] = +0.21$ dex. The available ASPCAP parameters for this star are $T_{\rm eff} = 3518$ K, $[M/H] = +0.00$ dex, and $\log g = 4.48$ dex. The matching spectrum for the star has been obtained by normalizing the APOGEE observed one with a synthetic spectrum with $T_{\rm eff} = 3400$ K, $\log g = 5.0$ dex and $[M/H] = +0.2$ dex, and the derived spectroscopical parameters for this star are $T_{\rm eff} = 3490 \pm 100$ K,$\log g = 4.99 \pm 0.1$ dex, $[M/H] = +0.03 \pm 0.1$ dex.

Star 2M05292729+2724457 (UCAC4 588-018766 [61]) was characterized in Gilhool et al. (2017), giving it the following parameters: $T_{\rm eff} = 3911$ K,$\log g = 4.5$ dex, $[M/H] = +0.0$ dex. The available ASPCAP parameters for this star are $T_{\rm eff} = 3952$ K, $[M/H] = +0.17$ dex, and

[58] http://simbad.u-strasbg.fr/simbad/sim-id?Ident=2Mass+j05172841%2B2531214
[59] http://simbad.u-strasbg.fr/simbad/sim-id?Ident=2Mass+j05201152%2B2457212
[60] http://simbad.u-strasbg.fr/simbad/sim-id?Ident=2Mass+j05222053%2B3031097
[61] http://simbad.u-strasbg.fr/simbad/sim-id?Ident=2Mass+j05292729%2B2724457

$\log g = 4.48$ dex. The matching spectrum for the star has been obtained by normalizing the APOGEE observed one with a synthetic spectrum with $T_{\text{eff}} = 4000$ K, $\log g = 5.0$ dex and $[M/H] = +0.2$ dex, and the derived spectroscopical parameters for this star are $T_{\text{eff}} = 3956 \pm 100$ K,$\log g = 4.7 \pm 0.1$ dex, $[M/H] = +0.01 \pm 0.1$ dex.

Star 2M05313731+4128000 (LSPM J0531+4127 [62]) was characterized in Gilhool et al. (2017), giving it the following parameters: $T_{\text{eff}} = 3622$ K,$\log g = 4.5$ dex, $[M/H] = -0.5$ dex. The available ASPCAP parameters for this star are $T_{\text{eff}} = 3693$ K, $[M/H] = -0.18$ dex, and $\log g = 4.44$ dex. The matching spectrum for the star has been obtained by normalizing the APOGEE observed one with a synthetic spectrum with $T_{\text{eff}} = 3600$ K, $\log g = 5.0$ dex and $[M/H] = +0.1$ dex, and the derived spectroscopical parameters for this star are $T_{\text{eff}} = 3683 \pm 100$ K,$\log g = 4.6 \pm 0.1$ dex, $[M/H] = -0.24 \pm 0.1$ dex.

Star 2M05354753+2717497 (LSPM J0535+2717 [63]) has not been previously spectroscopically characterized in the literature, and is flagged in Simbad Wenger et al. (2000) as a high proper-motion star. The available ASPCAP parameters for this star are $T_{\text{eff}} = 3597$ K, $[M/H] = -0.03$ dex, and $\log g = 4.30$ dex. The matching spectrum for the star has been obtained by normalizing the APOGEE observed one with a synthetic spectrum with $T_{\text{eff}} = 3400$ K, $\log g = 5.0$ dex and $[M/H] = +0.2$ dex, and the derived spectroscopical parameters for this star are $T_{\text{eff}} = 3491 \pm 100$ K,$\log g = 4.57 \pm 0.1$ dex, $[M/H] = -0.03 \pm 0.1$ dex.

Star 2M05370749+4111165 (LSPM J0537+4111 [64]) has not been previously spectroscopically characterized in the literature, and is flagged in Simbad Wenger et al. (2000) as a high proper-motion star. The available ASPCAP parameters for this star are $T_{\text{eff}} = 3447$ K, $[M/H] = -0.06$ dex, and $\log g = 4.38$ dex. The matching spectrum for the star has been obtained by normalizing the APOGEE observed one with a synthetic spectrum with $T_{\text{eff}} = 3200$ K, $\log g = 5.0$ dex and $[M/H] = -0.2$ dex, and the derived spectroscopical parameters for this star are $T_{\text{eff}} = 3451 \pm 100$ K,$\log g = 5.15 \pm 0.1$ dex, $[M/H] = -0.21 \pm 0.1$ dex.

Star 2M05394770+2917450 (LSPM J0539+2917 [65]) has not been previously spectroscopically characterized in the literature, and is flagged in Simbad Wenger et al. (2000) as a high proper-motion star. The available ASPCAP parameters for this star are $T_{\text{eff}} = 3681$ K, $[M/H] = -0.16$ dex, and $\log g = 4.35$ dex. The matching spectrum for the star has been ob-

[62] http://simbad.u-strasbg.fr/simbad/sim-id?Ident=2Mass+j05313731%2B4128000
[63] http://simbad.u-strasbg.fr/simbad/sim-id?Ident=2Mass+j05354753%2B2717497
[64] http://simbad.u-strasbg.fr/simbad/sim-id?Ident=2Mass+j05370749%2B4111165
[65] http://simbad.u-strasbg.fr/simbad/sim-id?Ident=2Mass+j05394770%2B2917450

tained by normalizing the APOGEE observed one with a synthetic spectrum with $T_{\rm eff} = 3600$ K, $\log g = 5.0$ dex and $[M/H] = +0.2$ dex, and the derived spectroscopical parameters for this star are $T_{\rm eff} = 3667 \pm 100$ K,$\log g = 4.68 \pm 0.1$ dex, $[M/H] = -0.01 \pm 0.1$ dex.

Star 2M05483220+2119180 (G 100-38 [66]) was characterized in Gilhool et al. (2017), giving it the following parameters: $T_{\rm eff} = 3334$ K,$\log g = 5.0$ dex, $[M/H] = +0.0$ dex. The star was also characterized in Terrien et al. (2015), giving it the following parameters: $T_{\rm eff} = 3350$ K, $[M/H] = -0.06$ dex. The available ASPCAP parameters for this star are $[M/H] = -0.29$ dex, and $T_{\rm eff} = 3383$ K and $\log g = 4.54$ dex. The matching spectrum for the star has been obtained by normalizing the APOGEE observed one with a synthetic spectrum with $T_{\rm eff} = 3200$ K, $\log g = 5.0$ dex and $[M/H] = -0.2$ dex, and the derived spectroscopical parameters for this star are $T_{\rm eff} = 3473 \pm 100$ K,$\log g = 5.36 \pm 0.1$ dex, $[M/H] = -0.31 \pm 0.1$ dex.

Star 2M05483253+2117577 (G 100-37 [67]) was characterized in Gilhool et al. (2017), giving it the following parameters: $T_{\rm eff} = 3789$ K,$\log g = 4.5$ dex, $[M/H] = -0.5$ dex. The available ASPCAP parameters for this star are $T_{\rm eff} = 3851$ K and $[M/H] = -0.49$ dex, and $\log g = 4.40$ dex. The matching spectrum for the star has been obtained by normalizing the APOGEE observed one with a synthetic spectrum with $T_{\rm eff} = 3600$ K, $\log g = 5.0$ dex and $[M/H] = -0.5$ dex, and the derived spectroscopical parameters for this star are $T_{\rm eff} = 3891 \pm 100$ K,$\log g = 4.91 \pm 0.1$ dex, $[M/H] = -0.71 \pm 0.1$ dex.

Star 2M05571864+1708299 (G 100-49 [68]) was characterized in Gilhool et al. (2017), giving it the following parameters: $T_{\rm eff} = 3180$ K,$\log g = 4.5$ dex, $[M/H] = -0.5$ dex. The available ASPCAP parameters for this star are $[M/H] = -0.57$ dex, and $T_{\rm eff} = 3210$ K and $\log g = 4.00$ dex. The matching spectrum for the star has been obtained by normalizing the APOGEE observed one with a synthetic spectrum with $T_{\rm eff} = 3000$ K, $\log g = 5.0$ dex and $[M/H] = -0.4$ dex, and the derived spectroscopical parameters for this star are $T_{\rm eff} = 3427 \pm 100$ K,$\log g = 4.58 \pm 0.1$ dex, $[M/H] = -1.33 \pm 0.1$ dex.

Star 2M05580690+1557564 (LSPM J0558+1557 [69]) was characterized in Gilhool et al. (2017), giving it the following parameters: $T_{\rm eff} = 3418$ K,$\log g = 4.5$ dex, $[M/H] = -0.5$ dex. The available ASPCAP parameters for this star are $T_{\rm eff} = 3585$ K and $[M/H] = -0.33$ dex, and $\log g = 4.28$ dex. The matching spectrum for the star has been obtained by normalizing

[66] http://simbad.u-strasbg.fr/simbad/sim-id?Ident=2Mass+j05483220%2B2119180
[67] http://simbad.u-strasbg.fr/simbad/sim-id?Ident=2Mass+j05483253%2B2117577
[68] http://simbad.u-strasbg.fr/simbad/sim-id?Ident=2Mass+j05571864%2B1708299
[69] http://simbad.u-strasbg.fr/simbad/sim-id?Ident=2Mass+j05580690%2B1557564

the APOGEE observed one with a synthetic spectrum with $T_{\text{eff}} = 3200\,$K, $\log g = 5.0\,$dex and $[M/H] = -0.2\,$dex, and the derived spectroscopical parameters for this star are $T_{\text{eff}} = 3477 \pm 100\,$K,$\log g = 4.46 \pm 0.1\,$dex, $[M/H] = -0.35 \pm 0.1\,$dex.

Star 2M06025298+3129415 (G 98-37 [70]) was characterized in Gilhool et al. (2017), giving it the following parameters: $T_{\text{eff}} = 3259\,$K,$\log g = 4.5\,$dex, $[M/H] = -0.5\,$dex. The available ASPCAP parameters for this star are $[M/H] = -0.67\,$dex, and $T_{\text{eff}} = 3373\,$K and $\log g = 4.72\,$dex. The matching spectrum for the star has been obtained by normalizing the APOGEE observed one with a synthetic spectrum with $T_{\text{eff}} = 3000\,$K, $\log g = 5.0\,$dex and $[M/H] = -0.4\,$dex, and the derived spectroscopical parameters for this star are $T_{\text{eff}} = 3421 \pm 100\,$K,$\log g = 4.45 \pm 0.1\,$dex, $[M/H] = -1.41 \pm 0.1\,$dex.

Star 2M06043950+2753529 (G 100-57 [71]) was characterized in Gilhool et al. (2017), giving it the following parameters: $T_{\text{eff}} = 3560\,$K,$\log g = 4.5\,$dex, $[M/H] = +0.0\,$dex. The available ASPCAP parameters for this star are $T_{\text{eff}} = 3615\,$K and $[M/H] = +0.07\,$dex, and $\log g = 4.44\,$dex. The matching spectrum for the star has been obtained by normalizing the APOGEE observed one with a synthetic spectrum with $T_{\text{eff}} = 3400\,$K, $\log g = 5.0\,$dex and $[M/H] = +0.2\,$dex, and the derived spectroscopical parameters for this star are $T_{\text{eff}} = 3494 \pm 100\,$K,$\log g = 4.69 \pm 0.1\,$dex, $[M/H] = +0.04 \pm 0.1\,$dex.

Star 2M06070493+1403109 (LSPM J0607+1403 [72]) was characterized in Gilhool et al. (2017), giving it the following parameters: $T_{\text{eff}} = 3246\,$K,$\log g = 5.0\,$dex, $[M/H] = +0.0\,$dex. The available ASPCAP parameters for this star are $[M/H] = -0.40\,$dex, and $T_{\text{eff}} = 3283\,$K and $\log g = 4.43\,$dex. The matching spectrum for the star has been obtained by normalizing the APOGEE observed one with a synthetic spectrum with $T_{\text{eff}} = 3100\,$K, $\log g = 5.0\,$dex and $[M/H] = +0.2\,$dex, and the derived spectroscopical parameters for this star are $T_{\text{eff}} = 3223 \pm 100\,$K,$\log g = 4.97 \pm 0.1\,$dex, $[M/H] = -0.04 \pm 0.1\,$dex.

Star 2M06075349+2746207 (G 100-59 [73]) was characterized in Gilhool et al. (2017), giving it the following parameters: $T_{\text{eff}} = 3788\,$K,$\log g = 5.0\,$dex, $[M/H] = +0.0\,$dex. The available ASPCAP parameters for this star are $T_{\text{eff}} = 3847\,$K and $[M/H] = -0.01\,$dex, and $\log g = 4.43\,$dex. The matching spectrum for the star has been obtained by normalizing the APOGEE observed one with a synthetic spectrum with $T_{\text{eff}} = 3800\,$K, $\log g = 5.0\,$dex and $[M/H] = +0.2\,$dex, and

[70] http://simbad.u-strasbg.fr/simbad/sim-id?Ident=2Mass+j06025298%2B3129415
[71] http://simbad.u-strasbg.fr/simbad/sim-id?Ident=2Mass+j06043950%2B2753529
[72] http://simbad.u-strasbg.fr/simbad/sim-id?Ident=2Mass+j06070493%2B1403109
[73] http://simbad.u-strasbg.fr/simbad/sim-id?Ident=2Mass+j06075349%2B2746207

the derived spectroscopical parameters for this star are $T_{\text{eff}} = 3836 \pm 100$ K,$\log g = 4.9 \pm 0.1$ dex, $[M/H] = -0.01 \pm 0.1$ dex.

Star 2M06102756+2759447 (G 100-59 [74]) was characterized in Gilhool et al. (2017), giving it the following parameters: $T_{\text{eff}} = 3732$ K,$\log g = 4.5$ dex, $[M/H] = +0.0$ dex. The available ASPCAP parameters for this star are $T_{\text{eff}} = 3790$ K and $[M/H] = +0.08$ dex, and $\log g = 4.42$ dex. The matching spectrum for the star has been obtained by normalizing the APOGEE observed one with a synthetic spectrum with $T_{\text{eff}} = 3800$ K, $\log g = 5.0$ dex and $[M/H] = +0.2$ dex, and the derived spectroscopical parameters for this star are $T_{\text{eff}} = 3796 \pm 100$ K,$\log g = 4.86 \pm 0.1$ dex, $[M/H] = +0.01 \pm 0.1$ dex.

Star 2M06135175+0631517 (UCAC4 483-018810 [75]) has not been previously spectroscopically characterized in the literature, and is flagged in Simbad Wenger et al. (2000) as a high proper-motion star. The available ASPCAP parameters for this star are $T_{\text{eff}} = 3784$ K and $[M/H] = -0.22$ dex, and $\log g = 4.39$ dex. The matching spectrum for the star has been obtained by normalizing the APOGEE observed one with a synthetic spectrum with $T_{\text{eff}} = 3600$ K, $\log g = 5.0$ dex and $[M/H] = +0.2$ dex, and the derived spectroscopical parameters for this star are $T_{\text{eff}} = 3709 \pm 100$ K,$\log g = 4.69 \pm 0.1$ dex, $[M/H] = -0.08 \pm 0.1$ dex.

Star 2M06161499+2754094 (UCAC4 483-018810 [76]) was characterized in Gilhool et al. (2017), giving it the following parameters: $T_{\text{eff}} = 3547$ K,$\log g = 4.5$ dex, $[M/H] = +0.0$ dex. The available ASPCAP parameters for this star are $T_{\text{eff}} = 3578$ K and $[M/H] = -0.12$ dex, and $\log g = 4.35$ dex. The matching spectrum for the star has been obtained by normalizing the APOGEE observed one with a synthetic spectrum with $T_{\text{eff}} = 3600$ K, $\log g = 5.0$ dex and $[M/H] = +0.2$ dex, and the derived spectroscopical parameters for this star are $T_{\text{eff}} = 3679 \pm 100$ K,$\log g = 5.18 \pm 0.1$ dex, $[M/H] = -0.14 \pm 0.1$ dex.

Star 2M06183480+2503064 (G 103-29 [77]) was characterized in Terrien et al. (2015), giving it the following parameters: $T_{\text{eff}} = 3339$ K and $[M/H] = +0.33$ dex. The available ASPCAP parameters for this star are $[M/H] = +0.09$ dex, and $T_{\text{eff}} = 3494$ K and $\log g = 4.69$ dex. The matching spectrum for the star has been obtained by normalizing the APOGEE observed one with a synthetic spectrum with $T_{\text{eff}} = 3300$ K, $\log g = 5.0$ dex and $[M/H] = +0.0$ dex, and the derived spectroscopical parameters for this star are $T_{\text{eff}} = 3421 \pm 100$ K,$\log g = 4.97 \pm 0.1$ dex,

[74] `http://simbad.u-strasbg.fr/simbad/sim-id?Ident=2Mass+j06102756%2B2759447`
[75] `http://simbad.u-strasbg.fr/simbad/sim-id?Ident=2Mass+j06135175%2B0631517`
[76] `http://simbad.u-strasbg.fr/simbad/sim-id?Ident=2Mass+j06161499%2B2754094`
[77] `http://simbad.u-strasbg.fr/simbad/sim-id?Ident=2Mass+j06183480%2B2503064`

$[M/H] = +0.06 \pm 0.1$ dex.

Star 2M06183640+0806535 (LSPM J0618+0806 [78]) has not been previously spectroscopically characterized in the literature, and is flagged in Simbad Wenger et al. (2000) as a high proper-motion star. The available ASPCAP parameters for this star are $[M/H] = -0.20$ dex, $T_{\rm eff} = 3782$ K and $\log g = 4.28$ dex. The matching spectrum for the star has been obtained by normalizing the APOGEE observed one with a synthetic spectrum with $T_{\rm eff} = 3600$ K, $\log g = 5.0$ dex and $[M/H] = +0.0$ dex, and the derived spectroscopical parameters for this star are $T_{\rm eff} = 3723 \pm 100$ K,$\log g = 4.5 \pm 0.1$ dex, $[M/H] = -0.18 \pm 0.1$ dex.

Star 2M06234645+0502411 (TYC 141-24-1 [79]) was characterized in Gilhool et al. (2017), giving it the following parameters: $T_{\rm eff} = 3861$ K,$\log g = 5.0$ dex, $[M/H] = +0.5$ dex. It is also present in Gaidos et al. (2014), with $T_{\rm eff} = 3798$ K and $[M/H] = +0.40$ dex, and in Lépine et al. (2013), with $T_{\rm eff} = 3700$ K and $\log g = 4.5$ dex. The available ASPCAP parameters for this star are $T_{\rm eff} = 3893$ K and $[M/H] = +0.25$ dex, as well as $\log g = 4.46$ dex. The matching spectrum for the star has been obtained by normalizing the APOGEE observed one with a synthetic spectrum with $T_{\rm eff} = 4000$ K, $\log g = 5.0$ dex and $[M/H] = +0.2$ dex, and the derived spectroscopical parameters for this star are $T_{\rm eff} = 3909 \pm 100$ K,$\log g = 4.74 \pm 0.1$ dex, $[M/H] = +0.05 \pm 0.1$ dex.

Star 2M06270211+0309473 (G 106-47 [80]) was characterized in Gilhool et al. (2017), giving it the following parameters: $T_{\rm eff} = 3642$ K,$\log g = 4.5$ dex, $[M/H] = +0.0$ dex. The available ASPCAP parameters for this star are $T_{\rm eff} = 3734$ K and $[M/H] = -0.36$ dex, as well as $\log g = 4.51$ dex. The matching spectrum for the star has been obtained by normalizing the APOGEE observed one with a synthetic spectrum with $T_{\rm eff} = 3600$ K, $\log g = 5.0$ dex and $[M/H] = +0.2$ dex, and the derived spectroscopical parameters for this star are $T_{\rm eff} = 3745 \pm 100$ K,$\log g = 5.17 \pm 0.1$ dex, $[M/H] = -0.36 \pm 0.1$ dex.

Star 2M06274397+0923541 (Ross 603 [81]) was characterized in Gilhool et al. (2017), giving it the following parameters: $T_{\rm eff} = 3611$ K,$\log g = 4.5$ dex, $[M/H] = +0.0$ dex. It is also present in Gaidos et al. (2014), with $T_{\rm eff} = 3519$ K, and in Lépine et al. (2013), with $T_{\rm eff} = 3470$ K and $\log g = 4.5$ dex. The available ASPCAP parameters for this star are $T_{\rm eff} = 3683$ K and $[M/H] = -0.16$ dex, as well as $\log g = 4.44$ dex. The matching spectrum for the star has been

[78] `http://simbad.u-strasbg.fr/simbad/sim-id?Ident=2Mass+j06183640%2B0806535`
[79] `http://simbad.u-strasbg.fr/simbad/sim-id?Ident=2Mass+j06234645%2B0502411`
[80] `http://simbad.u-strasbg.fr/simbad/sim-id?Ident=2Mass+j06270211%2B0309473`
[81] `http://simbad.u-strasbg.fr/simbad/sim-id?Ident=2Mass+j06274397%2B0923541`

obtained by normalizing the APOGEE observed one with a synthetic spectrum with $T_{\text{eff}} = 3600\,$K, $\log g = 5.0\,$dex and $[M/H] = +0.2\,$dex, and the derived spectroscopical parameters for this star are $T_{\text{eff}} = 3670 \pm 100\,$K,$\log g = 4.98 \pm 0.1\,$dex, $[M/H] = -0.14 \pm 0.1\,$dex.

Star 2M06295663+0934185 (G 105-41 [82]) was characterized in Gilhool et al. (2017), giving it the following parameters: $T_{\text{eff}} = 3312\,$K,$\log g = 5.0\,$dex, $[M/H] = +0.5\,$dex. The available ASPCAP parameters for this star are $[M/H] = -0.22\,$dex, as well as $T_{\text{eff}} = 3351\,$K and $\log g = 4.38\,$dex. The matching spectrum for the star has been obtained by normalizing the APOGEE observed one with a synthetic spectrum with $T_{\text{eff}} = 3200\,$K, $\log g = 5.0\,$dex and $[M/H] = +0.1\,$dex, and the derived spectroscopical parameters for this star are $T_{\text{eff}} = 3359 \pm 100\,$K,$\log g = 4.95 \pm 0.1\,$dex, $[M/H] = -0.16 \pm 0.1\,$dex.

Star 2M06320207+3431132 (LSPM J0632+3431S [83]) was characterized in Gilhool et al. (2017), giving it the following parameters: $T_{\text{eff}} = 3260\,$K,$\log g = 5.0\,$dex, $[M/H] = +0.5\,$dex. It was also characterized in Terrien et al. (2015), with $T_{\text{eff}} = 3313\,$K, $[M/H] = -0.09\,$dex. The available ASPCAP parameters for this star are $[M/H] = -0.41\,$dex, as well as $T_{\text{eff}} = 3296\,$K and $\log g = 4.35\,$dex. The matching spectrum for the star has been obtained by normalizing the APOGEE observed one with a synthetic spectrum with $T_{\text{eff}} = 3200\,$K, $\log g = 5.0\,$dex and $[M/H] = -0.2\,$dex, and the derived spectroscopical parameters for this star are $T_{\text{eff}} = 3465 \pm 100\,$K,$\log g = 5.4 \pm 0.1\,$dex, $[M/H] = -0.37 \pm 0.1\,$dex.

Star 2M06362535+1830520 (2MASS J06362535+1830520 [84]) was characterized in Gilhool et al. (2017), giving it the following parameters: $T_{\text{eff}} = 3283\,$K,$\log g = 5.0\,$dex, $[M/H] = +0.0\,$dex. The available ASPCAP parameters for this star are $[M/H] = -0.49\,$dex, as well as $T_{\text{eff}} = 3345\,$K and $\log g = 4.39\,$dex. The matching spectrum for the star has been obtained by normalizing the APOGEE observed one with a synthetic spectrum with $T_{\text{eff}} = 3200\,$K, $\log g = 5.0\,$dex and $[M/H] = -0.2\,$dex, and the derived spectroscopical parameters for this star are $T_{\text{eff}} = 3478 \pm 100\,$K,$\log g = 5.4 \pm 0.1\,$dex, $[M/H] = -0.44 \pm 0.1\,$dex.

Star 2M06370004+1515162 (G 105-48 [85]) was characterized in Gilhool et al. (2017), giving it the following parameters: $T_{\text{eff}} = 3647\,$K,$\log g = 4.5\,$dex, $[M/H] = +0.0\,$dex. The available ASPCAP parameters for this star are $T_{\text{eff}} = 3712\,$K and $[M/H] = -0.13\,$dex, as well as $\log g = 4.47\,$dex. The matching spectrum for the star has been obtained by normalizing

[82] `http://simbad.u-strasbg.fr/simbad/sim-id?Ident=2Mass+j06295663%2B0934185`
[83] `http://simbad.u-strasbg.fr/simbad/sim-id?Ident=2Mass+j06320207%2B3431132`
[84] `http://simbad.u-strasbg.fr/simbad/sim-id?Ident=2Mass+j06362535%2B1830520`
[85] `http://simbad.u-strasbg.fr/simbad/sim-id?Ident=2Mass+j06370004%2B1515162`

the APOGEE observed one with a synthetic spectrum with $T_{\text{eff}} = 3600$ K, $\log g = 5.0$ dex and $[M/H] = +0.1$ dex, and the derived spectroscopical parameters for this star are $T_{\text{eff}} = 3704 \pm 100$ K,$\log g = 4.99 \pm 0.1$ dex, $[M/H] = -0.18 \pm 0.1$ dex.

Star 2M06375540+0858594 (2MASS J06375540+0858594 [86]) was characterized in Gilhool et al. (2017), giving it the following parameters: $T_{\text{eff}} = 3247$ K,$\log g = 5.5$ dex, $[M/H] = +0.5$ dex. The available ASPCAP parameters for this star are $[M/H] = -0.20$ dex, as well as $T_{\text{eff}} = 3285$ K and $\log g = 4.67$ dex. The matching spectrum for the star has been obtained by normalizing the APOGEE observed one with a synthetic spectrum with $T_{\text{eff}} = 3200$ K, $\log g = 5.0$ dex and $[M/H] = -0.2$ dex, and the derived spectroscopical parameters for this star are $T_{\text{eff}} = 3379 \pm 100$ K,$\log g = 5.4 \pm 0.1$ dex, $[M/H] = -0.04 \pm 0.1$ dex.

Star 2M06412818+1545482 (Wolf 289 [87]) was characterized in Terrien et al. (2015), giving it the following parameters: $T_{\text{eff}} = 3347$ K and $[M/H] = +0.27$ dex. The available ASPCAP parameters for this star are $[M/H] = +0.1$ dex, as well as $T_{\text{eff}} = 3501$ K and $\log g = 4.72$ dex. The matching spectrum for the star has been obtained by normalizing the APOGEE observed one with a synthetic spectrum with $T_{\text{eff}} = 3400$ K, $\log g = 5.0$ dex and $[M/H] = +0.2$ dex, and the derived spectroscopical parameters for this star are $T_{\text{eff}} = 3480 \pm 100$ K,$\log g = 4.98 \pm 0.1$ dex, $[M/H] = +0.03 \pm 0.1$ dex.

Star 2M06421118+0334527 (G 108-21 [88]) was characterized in Gilhool et al. (2017), giving it the following parameters: $T_{\text{eff}} = 3437$ K, $\log g = 4.5$ dex and $[M/H] = +0.0$ dex. It is also present in Gaidos et al. (2014), with $T_{\text{eff}} = 3475$ K and $[M/H] = -0.05$ dex, and in Lépine et al. (2013), with $T_{\text{eff}} = 3300$ K and $\log g = 5.0$ dex. The available ASPCAP parameters for this star are $[M/H] = -0.14$ dex, as well as $T_{\text{eff}} = 3484$ K and $\log g = 4.46$ dex. The matching spectrum for the star has been obtained by normalizing the APOGEE observed one with a synthetic spectrum with $T_{\text{eff}} = 3200$ K, $\log g = 5.0$ dex and $[M/H] = +0.0$ dex, and the derived spectroscopical parameters for this star are $T_{\text{eff}} = 3356 \pm 100$ K,$\log g = 4.62 \pm 0.1$ dex, $[M/H] = -0.06 \pm 0.1$ dex.

Star 2M06423361+0239388 (LSPM J0642+0239 [89]) has not been previously spectroscopically characterized in the literature, and is flagged in Simbad Wenger et al. (2000) as a high proper-motion star. The available ASPCAP parameters for this star are $[M/H] = +0.09$ dex,

[86] http://simbad.u-strasbg.fr/simbad/sim-id?Ident=2Mass+j06375540%2B0858594
[87] http://simbad.u-strasbg.fr/simbad/sim-id?Ident=2Mass+j06412818%2B1545482
[88] http://simbad.u-strasbg.fr/simbad/sim-id?Ident=2Mass+j06421118%2B0334527
[89] http://simbad.u-strasbg.fr/simbad/sim-id?Ident=2Mass+j06423361%2B0239388

$T_{\mathrm{eff}} = 3601\,$K, and $\log g = 4.42\,$dex. The matching spectrum for the star has been obtained by normalizing the APOGEE observed one with a synthetic spectrum with $T_{\mathrm{eff}} = 3600\,$K, $\log g = 5.0\,$dex and $[M/H] = -0.1\,$dex, and the derived spectroscopical parameters for this star are $T_{\mathrm{eff}} = 3804 \pm 100\,$K,$\log g = 5.4 \pm 0.1\,$dex, $[M/H] = -0.6 \pm 0.1\,$dex.

Star 2M06484673-0516193 (PM J06487-0516 [90]) has not been previously spectroscopically characterized in the literature, and is flagged in Simbad Wenger et al. (2000) as a high proper-motion star. The available ASPCAP parameters for this star are $[M/H] = -0.20\,$dex, $T_{\mathrm{eff}} = 3775\,$K, and $\log g = 4.39\,$dex. The matching spectrum for the star has been obtained by normalizing the APOGEE observed one with a synthetic spectrum with $T_{\mathrm{eff}} = 3800\,$K, $\log g = 5.0\,$dex and $[M/H] = +0.2\,$dex, and the derived spectroscopical parameters for this star are $T_{\mathrm{eff}} = 3805 \pm 100\,$K,$\log g = 4.82 \pm 0.1\,$dex, $[M/H] = -0.03 \pm 0.1\,$dex.

Star 2M06505947-0910506 (L 886-20 [91]) was characterized in Gilhool et al. (2017), giving it the following parameters: $T_{\mathrm{eff}} = 3397\,$K, $\log g = 4.5\,$dex and $[M/H] = +0.0\,$dex. It is also present in Terrien et al. (2015), with $T_{\mathrm{eff}} = 3378\,$K and $[M/H] = -0.08\,$dex. The available ASPCAP parameters for this star are $[M/H] = -0.14\,$dex, as well as $T_{\mathrm{eff}} = 3425\,$K and $\log g = 4.46\,$dex. The matching spectrum for the star has been obtained by normalizing the APOGEE observed one with a synthetic spectrum with $T_{\mathrm{eff}} = 3200\,$K, $\log g = 5.0\,$dex and $[M/H] = +0.0\,$dex, and the derived spectroscopical parameters for this star are $T_{\mathrm{eff}} = 3377 \pm 100\,$K,$\log g = 4.8 \pm 0.1\,$dex, $[M/H] = -0.1 \pm 0.1\,$dex.

Star 2M06513673+2023264 (UCAC4 552-033338 [92]) was characterized in Gilhool et al. (2017), giving it the following parameters: $T_{\mathrm{eff}} = 3481\,$K, $\log g = 4.5\,$dex and $[M/H] = +0.0\,$dex. The available ASPCAP parameters for this star are $[M/H] = -0.20\,$dex, as well as $T_{\mathrm{eff}} = 3527\,$K and $\log g = 4.54\,$dex. The matching spectrum for the star has been obtained by normalizing the APOGEE observed one with a synthetic spectrum with $T_{\mathrm{eff}} = 3400\,$K, $\log g = 5.0\,$dex and $[M/H] = +0.3\,$dex, and the derived spectroscopical parameters for this star are $T_{\mathrm{eff}} = 3499 \pm 100\,$K,$\log g = 4.99 \pm 0.1\,$dex, $[M/H] = -0.12 \pm 0.1\,$dex.

Star 2M06543764+1708058 (LSPM J0654+1708S [93]) was characterized in Gilhool et al. (2017), giving it the following parameters: $T_{\mathrm{eff}} = 3408\,$K, $\log g = 4.5\,$dex and $[M/H] = -0.5\,$dex. The available ASPCAP parameters for this star are $[M/H] = -0.28\,$dex, as well

[90] `http://simbad.u-strasbg.fr/simbad/sim-id?Ident=2Mass+j06484673-0516193`
[91] `http://simbad.u-strasbg.fr/simbad/sim-id?Ident=2Mass+j06505947-0910506`
[92] `http://simbad.u-strasbg.fr/simbad/sim-id?Ident=2Mass+j06513673%2B2023264`
[93] `http://simbad.u-strasbg.fr/simbad/sim-id?Ident=2Mass+j06543764%2B1708058`

as $T_{\text{eff}} = 3437$ K and $\log g = 4.11$ dex. The matching spectrum for the star has been obtained by normalizing the APOGEE observed one with a synthetic spectrum with $T_{\text{eff}} = 3200$ K, $\log g = 5.0$ dex and $[M/H] = -0.2$ dex, and the derived spectroscopical parameters for this star are $T_{\text{eff}} = 3397 \pm 100$ K,$\log g = 4.5 \pm 0.1$ dex, $[M/H] = -0.04 \pm 0.1$ dex.

Star 2M06572462+0651440 (G 108-41 [94]) was characterized in Gilhool et al. (2017), giving it the following parameters: $T_{\text{eff}} = 3218$ K, $\log g = 5.0$ dex and $[M/H] = +0.0$ dex. The available ASPCAP parameters for this star are $[M/H] = -0.41$ dex, as well as $T_{\text{eff}} = 3253$ K and $\log g = 4.23$ dex. The matching spectrum for the star has been obtained by normalizing the APOGEE observed one with a synthetic spectrum with $T_{\text{eff}} = 3000$ K, $\log g = 5.0$ dex and $[M/H] = -0.4$ dex, and the derived spectroscopical parameters for this star are $T_{\text{eff}} = 3434 \pm 100$ K,$\log g = 5.39 \pm 0.1$ dex, $[M/H] = -0.69 \pm 0.1$ dex.

Star 2M07053085+0443219 (LSPM J0705+0443 [95]) has not been previously spectroscopically characterized in the literature, and is flagged in Simbad Wenger et al. (2000) as a high proper-motion star. The available ASPCAP parameters for this star are $T_{\text{eff}} = 3737$ K and $[M/H] = -0.04$ dex, as well as $\log g = 4.18$ dex. The matching spectrum for the star has been obtained by normalizing the APOGEE observed one with a synthetic spectrum with $T_{\text{eff}} = 3600$ K, $\log g = 5.0$ dex and $[M/H] = -0.1$ dex, and the derived spectroscopical parameters for this star are $T_{\text{eff}} = 3810 \pm 100$ K,$\log g = 4.96 \pm 0.1$ dex, $[M/H] = -0.71 \pm 0.1$ dex.

Star 2M07062584+0148472 (LSPM J0706+0148 [96]) has not been previously spectroscopically characterized in the literature, and is flagged in Simbad Wenger et al. (2000) as a high proper-motion star. The available ASPCAP parameters for this star are $T_{\text{eff}} = 3459$ K and $[M/H] = +0.12$ dex, as well as $\log g = 4.35$ dex. The matching spectrum for the star has been obtained by normalizing the APOGEE observed one with a synthetic spectrum with $T_{\text{eff}} = 3200$ K, $\log g = 5.0$ dex and $[M/H] = +0.0$ dex, and the derived spectroscopical parameters for this star are $T_{\text{eff}} = 3359 \pm 100$ K,$\log g = 4.47 \pm 0.1$ dex, $[M/H] = -0.09 \pm 0.1$ dex.

Star 2M07155314-0101135 (UCAC4 445-033109 [97]) has not been previously spectroscopically characterized in the literature, and is flagged in Simbad Wenger et al. (2000) as a high proper-motion star. The available ASPCAP parameters for this star are $T_{\text{eff}} = 3898$ K and $[M/H] = -0.21$ dex, as well as $\log g = 4.34$ dex. The matching spectrum for the star has

[94] http://simbad.u-strasbg.fr/simbad/sim-id?Ident=2Mass+j06572462%2B0651440
[95] http://simbad.u-strasbg.fr/simbad/sim-id?Ident=2Mass+j07053085%2B0443219
[96] http://simbad.u-strasbg.fr/simbad/sim-id?Ident=2Mass+j07062584%2B0148472
[97] http://simbad.u-strasbg.fr/simbad/sim-id?Ident=2Mass+j07155314-0101135

been obtained by normalizing the APOGEE observed one with a synthetic spectrum with $T_{\rm eff} = 3800$ K, $\log g = 5.0$ dex and $[M/H] = +0.2$ dex, and the derived spectroscopical parameters for this star are $T_{\rm eff} = 3898 \pm 100$ K,$\log g = 4.74 \pm 0.1$ dex, $[M/H] = -0.18 \pm 0.1$ dex.

Star 2M07235757-0833017 (PM J07239-0833 [98]) has not been previously spectroscopically characterized in the literature, and is flagged in Simbad Wenger et al. (2000) as a double or multiple star. The available ASPCAP parameters for this star are $T_{\rm eff} = 3519$ K and $[M/H] = +0.06$ dex, as well as $\log g = 4.50$ dex. The matching spectrum for the star has been obtained by normalizing the APOGEE observed one with a synthetic spectrum with $T_{\rm eff} = 3400$ K, $\log g = 5.0$ dex and $[M/H] = +0.2$ dex, and the derived spectroscopical parameters for this star are $T_{\rm eff} = 3496 \pm 100$ K,$\log g = 5.11 \pm 0.1$ dex, $[M/H] = -0.03 \pm 0.1$ dex.

Star 2M07315261-0748360 (UCAC4 411-033083 [99]) has not been previously spectroscopically characterized in the literature, and is flagged in Simbad Wenger et al. (2000) as a high proper-motion star. The available ASPCAP parameters for this star are $T_{\rm eff} = 3820$ K and $[M/H] = -0.13$ dex, as well as $\log g = 4.35$ dex. The matching spectrum for the star has been obtained by normalizing the APOGEE observed one with a synthetic spectrum with $T_{\rm eff} = 3800$ K, $\log g = 5.0$ dex and $[M/H] = +0.2$ dex, and the derived spectroscopical parameters for this star are $T_{\rm eff} = 3843 \pm 100$ K,$\log g = 4.81 \pm 0.1$ dex, $[M/H] = -0.11 \pm 0.1$ dex.

Star 2M07320352-0752173 (UCAC4 411-033155 [100]) has not been previously spectroscopically characterized in the literature, and is flagged in Simbad Wenger et al. (2000) as a high proper-motion star. The available ASPCAP parameters for this star are $T_{\rm eff} = 3754$ K and $[M/H] = -0.06$ dex, as well as $\log g = 4.39$ dex. The matching spectrum for the star has been obtained by normalizing the APOGEE observed one with a synthetic spectrum with $T_{\rm eff} = 3600$ K, $\log g = 5.0$ dex and $[M/H] = +0.2$ dex, and the derived spectroscopical parameters for this star are $T_{\rm eff} = 3708 \pm 100$ K,$\log g = 4.77 \pm 0.1$ dex, $[M/H] = -0.06 \pm 0.1$ dex.

Star 2M07323759-0813177 (UCAC4 409-033001 [101]) has not been previously spectroscopically characterized in the literature, and is flagged in Simbad Wenger et al. (2000) as a high proper-motion star. The available ASPCAP parameters for this star are $T_{\rm eff} = 3665$ K and $[M/H] = -0.07$ dex, as well as $\log g = 4.58$ dex. The matching spectrum for the star has been obtained by normalizing the APOGEE observed one with a synthetic spectrum with

[98] http://simbad.u-strasbg.fr/simbad/sim-id?Ident=2Mass+j07235757-0833017
[99] http://simbad.u-strasbg.fr/simbad/sim-id?Ident=2Mass+j07315261-0748360
[100] http://simbad.u-strasbg.fr/simbad/sim-id?Ident=2Mass+j07320352-0752173
[101] http://simbad.u-strasbg.fr/simbad/sim-id?Ident=2Mass+j07323759-0813177

$T_{\text{eff}} = 3600\,\text{K}$, $\log g = 5.0$ dex and $[M/H] = +0.2$ dex, and the derived spectroscopical parameters for this star are $T_{\text{eff}} = 3654 \pm 100\,\text{K}$,$\log g = 5.0 \pm 0.1$ dex, $[M/H] = -0.02 \pm 0.1$ dex.

Star 2M07404603+3758253 (LP 256-45 [102]) was characterized in Gilhool et al. (2017), giving it the following parameters: $T_{\text{eff}} = 3166\,\text{K}$, $\log g = 4.5$ dex and $[M/H] = +0.5$ dex. The available ASPCAP parameters for this star are $[M/H] = -0.77$ dex, as well as $T_{\text{eff}} = 3109\,\text{K}$ and $\log g = 3.59$ dex. The matching spectrum for the star has been obtained by normalizing the APOGEE observed one with a synthetic spectrum with $T_{\text{eff}} = 3000\,\text{K}$, $\log g = 5.0$ dex and $[M/H] = -0.4$ dex, and the derived spectroscopical parameters for this star are $T_{\text{eff}} = 3437 \pm 100\,\text{K}$,$\log g = 5.29 \pm 0.1$ dex, $[M/H] = -1.01 \pm 0.1$ dex.

Star 2M07421457+7949418 (LSPM J0742+7949 [103]) was characterized in Gilhool et al. (2017), giving it the following parameters: $T_{\text{eff}} = 3266\,\text{K}$, $\log g = 5.5$ dex and $[M/H] = +0.5$ dex. The available ASPCAP parameters for this star are $[M/H] = -0.15$ dex, as well as $T_{\text{eff}} = 3320\,\text{K}$ and $\log g = 4.75$ dex. The matching spectrum for the star has been obtained by normalizing the APOGEE observed one with a synthetic spectrum with $T_{\text{eff}} = 3200\,\text{K}$, $\log g = 5.0$ dex and $[M/H] = -0.2$ dex, and the derived spectroscopical parameters for this star are $T_{\text{eff}} = 3368 \pm 100\,\text{K}$,$\log g = 5.4 \pm 0.1$ dex, $[M/H] = -0.03 \pm 0.1$ dex.

Star 2M07431638+6642456 (LSPM J0743+6642 [104]) was characterized in Gilhool et al. (2017), giving it the following parameters: $T_{\text{eff}} = 3532\,\text{K}$, $\log g = 4.5$ dex and $[M/H] = +0.0$ dex. The available ASPCAP parameters for this star are $T_{\text{eff}} = 3612\,\text{K}$ and $[M/H] = -0.04$ dex, as well as $\log g = 4.45$ dex. The matching spectrum for the star has been obtained by normalizing the APOGEE observed one with a synthetic spectrum with $T_{\text{eff}} = 3400\,\text{K}$, $\log g = 5.0$ dex and $[M/H] = +0.0$ dex, and the derived spectroscopical parameters for this star are $T_{\text{eff}} = 3514 \pm 100\,\text{K}$,$\log g = 4.94 \pm 0.1$ dex, $[M/H] = -0.03 \pm 0.1$ dex.

Star 2M07492701+7752423 (G 251-46 [105]) was characterized in Gilhool et al. (2017), giving it the following parameters: $T_{\text{eff}} = 3308\,\text{K}$, $\log g = 5.5$ dex and $[M/H] = +0.5$ dex. The available ASPCAP parameters for this star are $[M/H] = -0.04$ dex, as well as $T_{\text{eff}} = 3348\,\text{K}$ and $\log g = 4.57$ dex. The matching spectrum for the star has been obtained by normalizing the APOGEE observed one with a synthetic spectrum with $T_{\text{eff}} = 3200\,\text{K}$, $\log g = 5.0$ dex and $[M/H] = -0.2$ dex, and the derived spectroscopical parameters for this star are $T_{\text{eff}} =$

[102] http://simbad.u-strasbg.fr/simbad/sim-id?Ident=2Mass+j07404603%2B3758253
[103] http://simbad.u-strasbg.fr/simbad/sim-id?Ident=2Mass+j07421457%2B7949418
[104] http://simbad.u-strasbg.fr/simbad/sim-id?Ident=2Mass+j07431638%2B6642456
[105] http://simbad.u-strasbg.fr/simbad/sim-id?Ident=2Mass+j07492701%2B7752423

3404 ± 100 K,$\log g = 5.2 \pm 0.1$ dex, $[M/H] = -0.08 \pm 0.1$ dex.

Star 2M07581269+4118134 (G 111-47 [106]) was characterized in Gaidos et al. (2014), with $T_{\text{eff}} = 3197$ K, and in Lépine et al. (2013), with $T_{\text{eff}} = 3280$ K and $\log g = 5.0$ dex. The available ASPCAP parameters for this star are $[M/H] = -0.15$ dex, as well as $T_{\text{eff}} = 3417$ K and $\log g = 4.79$ dex. The matching spectrum for the star has been obtained by normalizing the APOGEE observed one with a synthetic spectrum with $T_{\text{eff}} = 3200$ K, $\log g = 5.0$ dex and $[M/H] = -0.2$ dex, and the derived spectroscopical parameters for this star are $T_{\text{eff}} = 3432 \pm 100$ K,$\log g = 5.39 \pm 0.1$ dex, $[M/H] = -0.16 \pm 0.1$ dex.

Star 2M08050361+4121251 (G 111-52 [107]) has not been previously spectroscopically characterized in the literature, and is flagged in Simbad Wenger et al. (2000) as a high proper-motion star. The available ASPCAP parameters for this star are $[M/H] = -0.46$ dex, as well as $T_{\text{eff}} = 3215$ K and $\log g = 4.34$ dex. The matching spectrum for the star has been obtained by normalizing the APOGEE observed one with a synthetic spectrum with $T_{\text{eff}} = 3000$ K, $\log g = 5.0$ dex and $[M/H] = -0.4$ dex, and the derived spectroscopical parameters for this star are $T_{\text{eff}} = 3413 \pm 100$ K,$\log g = 4.69 \pm 0.1$ dex, $[M/H] = -1.32 \pm 0.1$ dex.

Star 2M08595755+0417552 (UCAC4 472-041130 [108]) was characterized in Gilhool et al. (2017), giving it the following parameters: $T_{\text{eff}} = 3758$ K, $\log g = 4.5$ dex and $[M/H] = +0.0$ dex. It is also present in Terrien et al. (2015), with $T_{\text{eff}} = 3823$ K and $[M/H] = -0.11$ dex. The available ASPCAP parameters for this star are $T_{\text{eff}} = 3806$ K and $[M/H] = -0.07$ dex, as well as $\log g = 4.40$ dex. The matching spectrum for the star has been obtained by normalizing the APOGEE observed one with a synthetic spectrum with $T_{\text{eff}} = 3700$ K, $\log g = 5.0$ dex and $[M/H] = +0.2$ dex, and the derived spectroscopical parameters for this star are $T_{\text{eff}} = 3769 \pm 100$ K,$\log g = 4.8 \pm 0.1$ dex, $[M/H] = -0.1 \pm 0.1$ dex.

Star 2M09005033+0514293 (Ross 687 [109]) was characterized in Gilhool et al. (2017), giving it the following parameters: $T_{\text{eff}} = 3392$ K, $\log g = 4.5$ dex and $[M/H] = +0.0$ dex. It is also present in Terrien et al. (2015), with $T_{\text{eff}} = 3367$ K and $[M/H] = -0.14$ dex, as well as in Gaidos et al. (2014), giving it $T_{\text{eff}} = 3468$ K and $[M/H] = +0.04$ dex, and in Lépine et al. (2013) with $\log g = 5.0$ dex and $T_{\text{eff}} = 3440$ K. The available ASPCAP parameters for this star are $[M/H] = -0.13$ dex, as well as $T_{\text{eff}} = 3419$ K and $\log g = 4.25$ dex. The matching

[106] `http://simbad.u-strasbg.fr/simbad/sim-id?Ident=2Mass+j07581269%2B4118134`
[107] `http://simbad.u-strasbg.fr/simbad/sim-id?Ident=2Mass+j08050361%2B4121251`
[108] `http://simbad.u-strasbg.fr/simbad/sim-id?Ident=2Mass+j08595755%2B0417552`
[109] `http://simbad.u-strasbg.fr/simbad/sim-id?Ident=2Mass+j09005033%2B0514293`

spectrum for the star has been obtained by normalizing the APOGEE observed one with a synthetic spectrum with $T_{\rm eff} = 3200$ K, $\log g = 5.0$ dex and $[M/H] = -0.2$ dex, and the derived spectroscopical parameters for this star are $T_{\rm eff} = 3394 \pm 100$ K,$\log g = 4.51 \pm 0.1$ dex, $[M/H] = -0.03 \pm 0.1$ dex.

Star 2M09022952+0417072 (LSPM J0902+0417 [110]) was characterized in Gilhool et al. (2017), giving it the following parameters: $T_{\rm eff} = 3334$ K, $\log g = 4.5$ dex and $[M/H] = +0.0$ dex. The available ASPCAP parameters for this star are $[M/H] = -0.16$ dex, as well as $T_{\rm eff} = 3366$ K and $\log g = 4.23$ dex. The matching spectrum for the star has been obtained by normalizing the APOGEE observed one with a synthetic spectrum with $T_{\rm eff} = 3200$ K, $\log g = 5.0$ dex and $[M/H] = -0.2$ dex, and the derived spectroscopical parameters for this star are $T_{\rm eff} = 3446 \pm 100$ K,$\log g = 4.89 \pm 0.1$ dex, $[M/H] = -0.21 \pm 0.1$ dex.

Star 2M09301445+2630250 (UCAC4 583-044696 [111]) was characterized in Gilhool et al. (2017), giving it the following parameters: $T_{\rm eff} = 3439$ K, $\log g = 5.0$ dex and $[M/H] = +0.5$ dex. It is also present in Terrien et al. (2015), with $T_{\rm eff} = 3359$ K and $[M/H] = +0.13$ dex, as well as in Gaidos et al. (2014), giving it $T_{\rm eff} = 3440$ K, and in Lépine et al. (2013) with $\log g = 5.0$ dex and $T_{\rm eff} = 3290$ K. The available ASPCAP parameters for this star are $[M/H] = +0.07$ dex, as well as $T_{\rm eff} = 3500$ K and $\log g = 4.55$ dex. The matching spectrum for the star has been obtained by normalizing the APOGEE observed one with a synthetic spectrum with $T_{\rm eff} = 3200$ K, $\log g = 5.0$ dex and $[M/H] = +0.0$ dex, and the derived spectroscopical parameters for this star are $T_{\rm eff} = 3354 \pm 100$ K,$\log g = 4.67 \pm 0.1$ dex, $[M/H] = +0.12 \pm 0.1$ dex.

Star 2M10330667+2837490 (LP 316-277 [112]) was characterized in Gilhool et al. (2017), giving it the following parameters: $T_{\rm eff} = 3366$ K, $\log g = 5.5$ dex and $[M/H] = +0.5$ dex. The available ASPCAP parameters for this star are $[M/H] = -0.14$ dex, as well as $T_{\rm eff} = 3413$ K and $\log g = 4.65$ dex. The matching spectrum for the star has been obtained by normalizing the APOGEE observed one with a synthetic spectrum with $T_{\rm eff} = 3400$ K, $\log g = 5.0$ dex and $[M/H] = +0.1$ dex, and the derived spectroscopical parameters for this star are $T_{\rm eff} = 3499 \pm 100$ K,$\log g = 5.4 \pm 0.1$ dex, $[M/H] = -0.08 \pm 0.1$ dex.

Star 2M10383323+3529492 (G 119-25 [113]) was characterized in Gilhool et al. (2017), giving it the following parameters: $T_{\rm eff} = 3536$ K, $\log g = 4.5$ dex and $[M/H] = +0.0$ dex. It is

[110] http://simbad.u-strasbg.fr/simbad/sim-id?Ident=2Mass+j09022952%2B0417072
[111] http://simbad.u-strasbg.fr/simbad/sim-id?Ident=2Mass+j09301445%2B2630250
[112] http://simbad.u-strasbg.fr/simbad/sim-id?Ident=2Mass+j10330667%2B2837490
[113] http://simbad.u-strasbg.fr/simbad/sim-id?Ident=2Mass+j10383323%2B3529492

also present in Terrien et al. (2015), with $T_{\rm eff} = 3495\,$K and $[M/H] = -0.05\,$dex, as well as in Gaidos et al. (2014), giving it $T_{\rm eff} = 3536\,$K, and in Lépine et al. (2013) with $\log g = 5.0\,$dex and $T_{\rm eff} = 3450\,$K. The available ASPCAP parameters for this star are $T_{\rm eff} = 3600\,$K and $[M/H] = -0.09\,$dex, as well as $\log g = 4.46\,$dex. The matching spectrum for the star has been obtained by normalizing the APOGEE observed one with a synthetic spectrum with $T_{\rm eff} = 3400\,$K, $\log g = 5.0\,$dex and $[M/H] = +0.2\,$dex, and the derived spectroscopical parameters for this star are $T_{\rm eff} = 3505 \pm 100\,$K,$\log g = 4.91 \pm 0.1\,$dex, $[M/H] = -0.05 \pm 0.1\,$dex.

Star 2M10391962+3044566 (LP 316-428 [114]) was characterized in Gilhool et al. (2017), giving it the following parameters: $T_{\rm eff} = 3545\,$K, $\log g = 4.5\,$dex and $[M/H] = +0.0\,$dex. The available ASPCAP parameters for this star are $T_{\rm eff} = 3605\,$K and $[M/H] = -0.01\,$dex, as well as $\log g = 4.35\,$dex. The matching spectrum for the star has been obtained by normalizing the APOGEE observed one with a synthetic spectrum with $T_{\rm eff} = 3600\,$K, $\log g = 5.0\,$dex and $[M/H] = +0.2\,$dex, and the derived spectroscopical parameters for this star are $T_{\rm eff} = 3660 \pm 100\,$K,$\log g = 4.95 \pm 0.1\,$dex, $[M/H] = -0.1 \pm 0.1\,$dex.

Star 2M10401225+3510463 (LP 263-11 [115]) was characterized in Gilhool et al. (2017), giving it the following parameters: $T_{\rm eff} = 3505\,$K, $\log g = 4.5\,$dex and $[M/H] = +0.0\,$dex. The available ASPCAP parameters for this star are $T_{\rm eff} = 3603\,$K and $[M/H] = -0.23\,$dex, as well as $\log g = 4.43\,$dex. The matching spectrum for the star has been obtained by normalizing the APOGEE observed one with a synthetic spectrum with $T_{\rm eff} = 3400\,$K, $\log g = 5.0\,$dex and $[M/H] = +0.1\,$dex, and the derived spectroscopical parameters for this star are $T_{\rm eff} = 3552 \pm 100\,$K,$\log g = 5.03 \pm 0.1\,$dex, $[M/H] = -0.24 \pm 0.1\,$dex.

Star 2M10441137+4500152 (LSPM J1044+4500 [116]) was characterized in Gilhool et al. (2017), giving it the following parameters: $T_{\rm eff} = 3818\,$K, $\log g = 4.5\,$dex and $[M/H] = -0.5\,$dex. The available ASPCAP parameters for this star are $T_{\rm eff} = 3876\,$K and $[M/H] = -0.51\,$dex, as well as $\log g = 4.32\,$dex. The matching spectrum for the star has been obtained by normalizing the APOGEE observed one with a synthetic spectrum with $T_{\rm eff} = 3600\,$K, $\log g = 5.0\,$dex and $[M/H] = -0.1\,$dex, and the derived spectroscopical parameters for this star are $T_{\rm eff} = 3816 \pm 100\,$K,$\log g = 4.7 \pm 0.1\,$dex, $[M/H] = -0.58 \pm 0.1\,$dex.

Star 2M10453795+1833111 (UCAC4 543-051461 [117]) was characterized in Terrien et al.

[114] http://simbad.u-strasbg.fr/simbad/sim-id?Ident=2Mass+j10391962%2B3044566
[115] http://simbad.u-strasbg.fr/simbad/sim-id?Ident=2Mass+j10401225%2B3510463
[116] http://simbad.u-strasbg.fr/simbad/sim-id?Ident=2Mass+j10441137%2B4500152
[117] http://simbad.u-strasbg.fr/simbad/sim-id?Ident=2Mass+j10453795%2B1833111

(2015), giving it the following parameters: $T_{\rm eff} = 3846$ K and $[M/H] = +0.09$ dex. The available ASPCAP parameters for this star are $T_{\rm eff} = 3886$ K and $[M/H] = +0.1$ dex, as well as $\log g = 4.40$ dex. The matching spectrum for the star has been obtained by normalizing the APOGEE observed one with a synthetic spectrum with $T_{\rm eff} = 4000$ K, $\log g = 5.0$ dex and $[M/H] = +0.2$ dex, and the derived spectroscopical parameters for this star are $T_{\rm eff} = 3857 \pm 100$ K,$\log g = 4.61 \pm 0.1$ dex, $[M/H] = -0.01 \pm 0.1$ dex.

Star 2M10463343+1906373 (2MASS J10463343+1906373 [118]) has not been previously spectroscopically characterized in the literature, and is flagged in Simbad Wenger et al. (2000) as a high proper-motion star. The available ASPCAP parameters for this star are $T_{\rm eff} = 3843$ K and $[M/H] = +0.07$ dex, as well as $\log g = 4.39$ dex. The matching spectrum for the star has been obtained by normalizing the APOGEE observed one with a synthetic spectrum with $T_{\rm eff} = 4000$ K, $\log g = 5.0$ dex and $[M/H] = +0.0$ dex, and the derived spectroscopical parameters for this star are $T_{\rm eff} = 3899 \pm 100$ K,$\log g = 4.91 \pm 0.1$ dex, $[M/H] = -0.04 \pm 0.1$ dex.

Star 2M10470720+2004362 (LP 431-12 [119]) has not been previously spectroscopically characterized in the literature, and is flagged in Simbad Wenger et al. (2000) as a high proper-motion star. The available ASPCAP parameters for this star are $T_{\rm eff} = 3084$ K and $[M/H] = +0.43$ dex, as well as $\log g = 4.57$ dex. The matching spectrum for the star has been obtained by normalizing the APOGEE observed one with a synthetic spectrum with $T_{\rm eff} = 3000$ K, $\log g = 5.0$ dex and $[M/H] = +0.2$ dex, and the derived spectroscopical parameters for this star are $T_{\rm eff} = 3122 \pm 100$ K,$\log g = 5.23 \pm 0.1$ dex, $[M/H] = -0.12 \pm 0.1$ dex.

Star 2M10473327+2007406 (G 58-18B [120]) was characterized in Gilhool et al. (2017), giving it the following parameters: $T_{\rm eff} = 3432$ K, $\log g = 5.0$ dex and $[M/H] = +0.0$ dex. The available ASPCAP parameters for this star are $[M/H] = -0.16$ dex, as well as $T_{\rm eff} = 3491$ K and $\log g = 4.59$ dex. The matching spectrum for the star has been obtained by normalizing the APOGEE observed one with a synthetic spectrum with $T_{\rm eff} = 3200$ K, $\log g = 5.0$ dex and $[M/H] = +0.0$ dex, and the derived spectroscopical parameters for this star are $T_{\rm eff} = 3367 \pm 100$ K,$\log g = 4.91 \pm 0.1$ dex, $[M/H] = -0.08 \pm 0.1$ dex.

Star 2M10475231+2020315 (G 58-19 [121]) was characterized in Gilhool et al. (2017), giving it the following parameters: $T_{\rm eff} = 3663$ K, $\log g = 4.5$ dex and $[M/H] = +0.0$ dex. The

[118] http://simbad.u-strasbg.fr/simbad/sim-id?Ident=2Mass+j10463343%2B1906373
[119] http://simbad.u-strasbg.fr/simbad/sim-id?Ident=2Mass+j10470720%2B2004362
[120] http://simbad.u-strasbg.fr/simbad/sim-id?Ident=2Mass+j10473327%2B2007406
[121] http://simbad.u-strasbg.fr/simbad/sim-id?Ident=2Mass+j10475231%2B2020315

available ASPCAP parameters for this star are $T_{\text{eff}} = 3735$ K and $[M/H] = -0.02$ dex, as well as $\log g = 4.39$ dex. The matching spectrum for the star has been obtained by normalizing the APOGEE observed one with a synthetic spectrum with $T_{\text{eff}} = 3600$ K, $\log g = 5.0$ dex and $[M/H] = +0.2$ dex, and the derived spectroscopical parameters for this star are $T_{\text{eff}} = 3674 \pm 100$ K,$\log g = 4.71 \pm 0.1$ dex, $[M/H] = -0.04 \pm 0.1$ dex.

Star 2M10482152+4451236 (LSPM J1048+4451 [122]) has not been previously spectroscopically characterized in the literature, and is flagged in Simbad Wenger et al. (2000) as a high proper-motion star. The available ASPCAP parameters for this star are $T_{\text{eff}} = 3316$ K and $[M/H] = +0.21$ dex, as well as $\log g = 4.23$ dex. The matching spectrum for the star has been obtained by normalizing the APOGEE observed one with a synthetic spectrum with $T_{\text{eff}} = 3200$ K, $\log g = 5.0$ dex and $[M/H] = -0.1$ dex, and the derived spectroscopical parameters for this star are $T_{\text{eff}} = 3472 \pm 100$ K,$\log g = 5.24 \pm 0.1$ dex, $[M/H] = -0.54 \pm 0.1$ dex.

Star 2M10572599+4923562 (LSPM J1057+4923 [123]) was characterized in Gilhool et al. (2017), giving it the following parameters: $T_{\text{eff}} = 3619$ K, $\log g = 4.5$ dex and $[M/H] = +0.0$ dex. The available ASPCAP parameters for this star are $T_{\text{eff}} = 3693$ K and $[M/H] = -0.02$ dex, as well as $\log g = 4.45$ dex. The matching spectrum for the star has been obtained by normalizing the APOGEE observed one with a synthetic spectrum with $T_{\text{eff}} = 3500$ K, $\log g = 5.0$ dex and $[M/H] = +0.2$ dex, and the derived spectroscopical parameters for this star are $T_{\text{eff}} = 3585 \pm 100$ K,$\log g = 4.92 \pm 0.1$ dex, $[M/H] = +0.0 \pm 0.1$ dex.

Star 2M11021557+4941485 (LSPM J1102+4941 [124]) has not been previously spectroscopically characterized in the literature, and is flagged in Simbad Wenger et al. (2000) as a high proper-motion star. The available ASPCAP parameters for this star are $[M/H] = -0.34$ dex, as well as $T_{\text{eff}} = 3330$ K and $\log g = 4.55$ dex. The matching spectrum for the star has been obtained by normalizing the APOGEE observed one with a synthetic spectrum with $T_{\text{eff}} = 3400$ K, $\log g = 5.0$ dex and $[M/H] = +0.2$ dex, and the derived spectroscopical parameters for this star are $T_{\text{eff}} = 3482 \pm 100$ K,$\log g = 5.4 \pm 0.1$ dex, $[M/H] = -0.09 \pm 0.1$ dex.

Star 2M11091225-0436249 (G 163-53 [125]) is present in Gaidos et al. (2014), giving it $T_{\text{eff}} = 3725$ K and $[M/H] = -0.23$ dex, and in Lépine et al. (2013) with $\log g = 5.0$ dex and $T_{\text{eff}} = 4000$ K. The available ASPCAP parameters for this star are $T_{\text{eff}} = 3856$ K and

[122] `http://simbad.u-strasbg.fr/simbad/sim-id?Ident=2Mass+j10482152%2B4451236`
[123] `http://simbad.u-strasbg.fr/simbad/sim-id?Ident=2Mass+j10572599%2B4923562`
[124] `http://simbad.u-strasbg.fr/simbad/sim-id?Ident=2Mass+j11021557%2B4941485`
[125] `http://simbad.u-strasbg.fr/simbad/sim-id?Ident=2Mass+j11091225-0436249`

$[M/H] = -0.04$ dex, as well as $\log g = 4.41$ dex. The matching spectrum for the star has been obtained by normalizing the APOGEE observed one with a synthetic spectrum with $T_{\text{eff}} = 3900$ K, $\log g = 5.0$ dex and $[M/H] = +0.2$ dex, and the derived spectroscopical parameters for this star are $T_{\text{eff}} = 3847 \pm 100$ K,$\log g = 4.81 \pm 0.1$ dex, $[M/H] = -0.07 \pm 0.1$ dex.

Star 2M11152550+0003159 (G 10-8 [126]) has not been previously spectroscopically characterized in the literature, and is flagged in Simbad Wenger et al. (2000) as a high proper-motion star. The available ASPCAP parameters for this star are $T_{\text{eff}} = 3257$ K and $[M/H] = +0.43$ dex, as well as $\log g = 3.98$ dex. The matching spectrum for the star has been obtained by normalizing the APOGEE observed one with a synthetic spectrum with $T_{\text{eff}} = 3200$ K, $\log g = 5.0$ dex and $[M/H] = -0.1$ dex, and the derived spectroscopical parameters for this star are $T_{\text{eff}} = 3491 \pm 100$ K,$\log g = 5.18 \pm 0.1$ dex, $[M/H] = -0.7 \pm 0.1$ dex.

Star 2M11202022+0034356 (Wolf 379 [127]) has not been previously spectroscopically characterized in the literature, and is flagged in Simbad Wenger et al. (2000) as a high proper-motion star. The available ASPCAP parameters for this star are $T_{\text{eff}} = 3310$ K and $[M/H] = +0.20$ dex, as well as $\log g = 4.18$ dex. The matching spectrum for the star has been obtained by normalizing the APOGEE observed one with a synthetic spectrum with $T_{\text{eff}} = 3000$ K, $\log g = 5.0$ dex and $[M/H] = -0.2$ dex, and the derived spectroscopical parameters for this star are $T_{\text{eff}} = 3389 \pm 100$ K,$\log g = 4.66 \pm 0.1$ dex, $[M/H] = -0.63 \pm 0.1$ dex.

Star 2M11294200+0405175 (NLTT 27544 [128]) has not been previously spectroscopically characterized in the literature, and is flagged in Simbad Wenger et al. (2000) as a high proper-motion star. The available ASPCAP parameters for this star are $T_{\text{eff}} = 3088$ K and $[M/H] = +0.51$ dex, as well as $\log g = 4.30$ dex. The matching spectrum for the star has been obtained by normalizing the APOGEE observed one with a synthetic spectrum with $T_{\text{eff}} = 3000$ K, $\log g = 5.0$ dex and $[M/H] = -0.4$ dex, and the derived spectroscopical parameters for this star are $T_{\text{eff}} = 3410 \pm 100$ K,$\log g = 5.4 \pm 0.1$ dex, $[M/H] = -0.9 \pm 0.1$ dex.

Star 2M11323938+0513167 (G 10-31 [129]) was characterized in Gilhool et al. (2017), giving it the following parameters: $T_{\text{eff}} = 3806$ K, $\log g = 4.5$ dex and $[M/H] = +0.0$ dex. The available ASPCAP parameters for this star are $T_{\text{eff}} = 3847$ K and $[M/H] = +0.06$ dex, as well as $\log g = 4.44$ dex. The matching spectrum for the star has been obtained by normaliz-

[126] http://simbad.u-strasbg.fr/simbad/sim-id?Ident=2Mass+j11152550%2B0003159
[127] http://simbad.u-strasbg.fr/simbad/sim-id?Ident=2Mass+j11202022%2B0034356
[128] http://simbad.u-strasbg.fr/simbad/sim-id?Ident=2Mass+j11294200%2B0405175
[129] http://simbad.u-strasbg.fr/simbad/sim-id?Ident=2Mass+j11323938%2B0513167

ing the APOGEE observed one with a synthetic spectrum with $T_{\rm eff} = 4000\,$K, $\log g = 5.0\,$dex and $[M/H] = +0.0\,$dex, and the derived spectroscopical parameters for this star are $T_{\rm eff} = 3902 \pm 100\,$K,$\log g = 4.89 \pm 0.1\,$dex, $[M/H] = -0.07 \pm 0.1\,$dex.

Star 2M11353571+0414146 (G 10-35 [130]) was characterized in Gilhool et al. (2017), giving it the following parameters: $T_{\rm eff} = 3557\,$K, $\log g = 4.5\,$dex and $[M/H] = -0.5\,$dex. The available ASPCAP parameters for this star are $T_{\rm eff} = 3672\,$K and $[M/H] = -0.53\,$dex, as well as $\log g = 4.48\,$dex. The matching spectrum for the star has been obtained by normalizing the APOGEE observed one with a synthetic spectrum with $T_{\rm eff} = 3600\,$K, $\log g = 5.0\,$dex and $[M/H] = -0.4\,$dex, and the derived spectroscopical parameters for this star are $T_{\rm eff} = 3864 \pm 100\,$K,$\log g = 5.4 \pm 0.1\,$dex, $[M/H] = -0.82 \pm 0.1\,$dex.

Star 2M11452712+2558113 (LSPM J1145+2558 [131]) has not been previously spectroscopically characterized in the literature, and is flagged in Simbad Wenger et al. (2000) as a high proper-motion star. The available ASPCAP parameters for this star are $T_{\rm eff} = 3401\,$K and $[M/H] = +0.24\,$dex, as well as $\log g = 4.14\,$dex. The matching spectrum for the star has been obtained by normalizing the APOGEE observed one with a synthetic spectrum with $T_{\rm eff} = 3200\,$K, $\log g = 5.0\,$dex and $[M/H] = -0.2\,$dex, and the derived spectroscopical parameters for this star are $T_{\rm eff} = 3486 \pm 100\,$K,$\log g = 4.79 \pm 0.1\,$dex, $[M/H] = -0.36 \pm 0.1\,$dex.

Star 2M11474440+0048164 (Ross 128 [132]) is present in Terrien et al. (2015), with $T_{\rm eff} = 3288\,$K and $[M/H] = -0.09\,$dex, as well as in Gaidos et al. (2014), giving it $T_{\rm eff} = 3145\,$K, and in Lépine et al. (2013) with $\log g = 5.0\,$dex and $T_{\rm eff} = 3130\,$K. The available ASPCAP parameters for this star are $[M/H] = -0.44\,$dex, as well as $T_{\rm eff} = 3212\,$K and $\log g = 4.45\,$dex. The matching spectrum for the star has been obtained by normalizing the APOGEE observed one with a synthetic spectrum with $T_{\rm eff} = 3200\,$K, $\log g = 5.0\,$dex and $[M/H] = +0.4\,$dex, and the derived spectroscopical parameters for this star are $T_{\rm eff} = 3281 \pm 100\,$K,$\log g = 5.28 \pm 0.1\,$dex, $[M/H] = -0.15 \pm 0.1\,$dex.

Star 2M11511794+1829229 (V* CU Leo [133]) was characterized in Gilhool et al. (2017), giving it the following parameters: $T_{\rm eff} = 3422\,$K, $\log g = 5.0\,$dex and $[M/H] = +0.0\,$dex. It is also present in Terrien et al. (2015), with $T_{\rm eff} = 3420\,$K and $[M/H] = -0.15\,$dex. The available ASPCAP parameters for this star are $[M/H] = -0.29\,$dex, as well as $T_{\rm eff} = 3452\,$K

[130] http://simbad.u-strasbg.fr/simbad/sim-id?Ident=2Mass+j11353571%2B0414146
[131] http://simbad.u-strasbg.fr/simbad/sim-id?Ident=2Mass+j11452712%2B2558113
[132] http://simbad.u-strasbg.fr/simbad/sim-id?Ident=2Mass+j11474440%2B0048164
[133] http://simbad.u-strasbg.fr/simbad/sim-id?Ident=2Mass+j11511794%2B1829229

and $\log g = 4.54$ dex. The matching spectrum for the star has been obtained by normalizing the APOGEE observed one with a synthetic spectrum with $T_{\rm eff} = 3200$ K, $\log g = 5.0$ dex and $[M/H] = -0.2$ dex, and the derived spectroscopical parameters for this star are $T_{\rm eff} = 3475 \pm 100$ K,$\log g = 5.16 \pm 0.1$ dex, $[M/H] = -0.29 \pm 0.1$ dex.

Star 2M11580290+2013015 (LP 375-67 [134]) was characterized in Gilhool et al. (2017), giving it the following parameters: $T_{\rm eff} = 3377$ K, $\log g = 5.0$ dex and $[M/H] = +0.0$ dex. The available ASPCAP parameters for this star are $[M/H] = -0.15$ dex, as well as $T_{\rm eff} = 3421$ K and $\log g = 4.66$ dex. The matching spectrum for the star has been obtained by normalizing the APOGEE observed one with a synthetic spectrum with $T_{\rm eff} = 3200$ K, $\log g = 5.0$ dex and $[M/H] = +0.0$ dex, and the derived spectroscopical parameters for this star are $T_{\rm eff} = 3338 \pm 100$ K,$\log g = 4.98 \pm 0.1$ dex, $[M/H] = -0.04 \pm 0.1$ dex.

Star 2M12005016+1938424 (LSPM J1200+1938 [135]) was characterized in Gilhool et al. (2017), giving it the following parameters: $T_{\rm eff} = 3522$ K, $\log g = 4.5$ dex and $[M/H] = +0.0$ dex. The available ASPCAP parameters for this star are $T_{\rm eff} = 3585$ K and $[M/H] = -0.15$ dex, as well as $\log g = 4.35$ dex. The matching spectrum for the star has been obtained by normalizing the APOGEE observed one with a synthetic spectrum with $T_{\rm eff} = 3400$ K, $\log g = 5.0$ dex and $[M/H] = +0.0$ dex, and the derived spectroscopical parameters for this star are $T_{\rm eff} = 3525 \pm 100$ K,$\log g = 4.95 \pm 0.1$ dex, $[M/H] = -0.08 \pm 0.1$ dex.

Star 2M12081818+4027012 (LSPM J1208+4027 [136]) was characterized in Gilhool et al. (2017), giving it the following parameters: $T_{\rm eff} = 3840$ K, $\log g = 4.5$ dex and $[M/H] = +0.0$ dex. The available ASPCAP parameters for this star are $T_{\rm eff} = 3880$ K and $[M/H] = -0.13$ dex, as well as $\log g = 4.32$ dex. The matching spectrum for the star has been obtained by normalizing the APOGEE observed one with a synthetic spectrum with $T_{\rm eff} = 4000$ K, $\log g = 5.0$ dex and $[M/H] = +0.0$ dex, and the derived spectroscopical parameters for this star are $T_{\rm eff} = 3941 \pm 100$ K,$\log g = 4.85 \pm 0.1$ dex, $[M/H] = -0.2 \pm 0.1$ dex.

Star 2M12082601+4022490 (LP 216-57 [137]) was characterized in Gilhool et al. (2017), giving it the following parameters: $T_{\rm eff} = 3747$ K, $\log g = 4.5$ dex and $[M/H] = +0.0$ dex. The available ASPCAP parameters for this star are $T_{\rm eff} = 3791$ K and $[M/H] = +0.07$ dex, as well as $\log g = 4.43$ dex. The matching spectrum for the star has been obtained by normalizing

[134] http://simbad.u-strasbg.fr/simbad/sim-id?Ident=2Mass+j11580290%2B2013015
[135] http://simbad.u-strasbg.fr/simbad/sim-id?Ident=2Mass+j12005016%2B1938424
[136] http://simbad.u-strasbg.fr/simbad/sim-id?Ident=2Mass+j12081818%2B4027012
[137] http://simbad.u-strasbg.fr/simbad/sim-id?Ident=2Mass+j12082601%2B4022490

the APOGEE observed one with a synthetic spectrum with $T_{\text{eff}} = 3800\,$K, $\log g = 5.0\,$dex and $[M/H] = +0.4\,$dex, and the derived spectroscopical parameters for this star are $T_{\text{eff}} = 3764 \pm 100\,$K,$\log g = 4.86 \pm 0.1\,$dex, $[M/H] = +0.11 \pm 0.1\,$dex.

Star 2M12102152+4026185 (G 198-26 [138]) was characterized in Gilhool et al. (2017), giving it the following parameters: $T_{\text{eff}} = 3653\,$K, $\log g = 4.5\,$dex and $[M/H] = -0.5\,$dex. The available ASPCAP parameters for this star are $T_{\text{eff}} = 3726\,$K and $[M/H] = -0.40\,$dex, as well as $\log g = 4.37\,$dex. The matching spectrum for the star has been obtained by normalizing the APOGEE observed one with a synthetic spectrum with $T_{\text{eff}} = 3600\,$K, $\log g = 5.0\,$dex and $[M/H] = -0.1\,$dex, and the derived spectroscopical parameters for this star are $T_{\text{eff}} = 3787 \pm 100\,$K,$\log g = 4.98 \pm 0.1\,$dex, $[M/H] = -0.61 \pm 0.1\,$dex.

Star 2M12105688+4103275 (G 123-8 [139]) was characterized in Gilhool et al. (2017), giving it the following parameters: $T_{\text{eff}} = 3837\,$K, $\log g = 4.5\,$dex and $[M/H] = -0.5\,$dex. It was also characterized in Gaidos et al. (2014), giving it $T_{\text{eff}} = 3864\,$K and $[M/H] = -0.4\,$dex, and in Lépine et al. (2013), with $\log g = 4.5\,$dex and $T_{\text{eff}} = 3720\,$K. The available ASPCAP parameters for this star are $T_{\text{eff}} = 3893\,$K and $[M/H] = -0.39\,$dex, as well as $\log g = 4.32\,$dex. The matching spectrum for the star has been obtained by normalizing the APOGEE observed one with a synthetic spectrum with $T_{\text{eff}} = 3600\,$K, $\log g = 5.0\,$dex and $[M/H] = +0.1\,$dex, and the derived spectroscopical parameters for this star are $T_{\text{eff}} = 3771 \pm 100\,$K,$\log g = 4.42 \pm 0.1\,$dex, $[M/H] = -0.43 \pm 0.1\,$dex.

Star 2M12110303+4043482 (G 123-10 [140]) was characterized in Gilhool et al. (2017), giving it the following parameters: $T_{\text{eff}} = 3435\,$K, $\log g = 4.5\,$dex and $[M/H] = +0.0\,$dex. The available ASPCAP parameters for this star are $[M/H] = -0.28\,$dex, as well as $T_{\text{eff}} = 3476\,$K and $\log g = 4.40\,$dex. The matching spectrum for the star has been obtained by normalizing the APOGEE observed one with a synthetic spectrum with $T_{\text{eff}} = 3400\,$K, $\log g = 5.0\,$dex and $[M/H] = +0.1\,$dex, and the derived spectroscopical parameters for this star are $T_{\text{eff}} = 3565 \pm 100\,$K,$\log g = 5.13 \pm 0.1\,$dex, $[M/H] = -0.28 \pm 0.1\,$dex.

Star 2M12153222+1515555 (LP 434-69 [141]) was characterized in Gilhool et al. (2017), giving it the following parameters: $T_{\text{eff}} = 3323\,$K, $\log g = 5.0\,$dex and $[M/H] = +0.0\,$dex. The available ASPCAP parameters for this star are $[M/H] = -0.20\,$dex, as well as $T_{\text{eff}} = 3391\,$K

[138] `http://simbad.u-strasbg.fr/simbad/sim-id?Ident=2Mass+j12102152%2B4026185`
[139] `http://simbad.u-strasbg.fr/simbad/sim-id?Ident=2Mass+j12105688%2B4103275`
[140] `http://simbad.u-strasbg.fr/simbad/sim-id?Ident=2Mass+j12110303%2B4043482`
[141] `http://simbad.u-strasbg.fr/simbad/sim-id?Ident=2Mass+j12153222%2B1515555`

and $\log g = 4.66$ dex. The matching spectrum for the star has been obtained by normalizing the APOGEE observed one with a synthetic spectrum with $T_{\text{eff}} = 3200$ K, $\log g = 5.0$ dex and $[M/H] = -0.2$ dex, and the derived spectroscopical parameters for this star are $T_{\text{eff}} = 3432 \pm 100$ K,$\log g = 5.35 \pm 0.1$ dex, $[M/H] = -0.19 \pm 0.1$ dex.

Star 2M12205197+4006468 (G 123-23 [142]) has not been previously spectroscopically characterized in the literature, and is flagged in Simbad Wenger et al. (2000) as a high proper-motion star. The available ASPCAP parameters for this star are $[M/H] = +0.25$ dex, as well as $T_{\text{eff}} = 3362$ K and $\log g = 4.07$ dex. The matching spectrum for the star has been obtained by normalizing the APOGEE observed one with a synthetic spectrum with $T_{\text{eff}} = 3200$ K, $\log g = 5.0$ dex and $[M/H] = -0.2$ dex, and the derived spectroscopical parameters for this star are $T_{\text{eff}} = 3524 \pm 100$ K,$\log g = 4.83 \pm 0.1$ dex, $[M/H] = -0.62 \pm 0.1$ dex.

Star 2M12212146+5745089 (UCAC4 739-050229 [143]) was characterized in Gilhool et al. (2017), giving it the following parameters: $T_{\text{eff}} = 3655$ K, $\log g = 4.5$ dex and $[M/H] = +0.0$ dex. It is also present in Terrien et al. (2015), with $T_{\text{eff}} = 3590$ K and $[M/H] = -0.02$ dex. The available ASPCAP parameters for this star are $T_{\text{eff}} = 3721$ K and $[M/H] = +0.02$ dex, as well as $\log g = 4.51$ dex. The matching spectrum for the star has been obtained by normalizing the APOGEE observed one with a synthetic spectrum with $T_{\text{eff}} = 3600$ K, $\log g = 5.0$ dex and $[M/H] = +0.2$ dex, and the derived spectroscopical parameters for this star are $T_{\text{eff}} = 3663 \pm 100$ K,$\log g = 4.86 \pm 0.1$ dex, $[M/H] = -0.01 \pm 0.1$ dex.

Star 2M12223238+5730387 does not have a dedicated page in Simbad. The available ASPCAP parameters for this star are $[M/H] = -0.1$ dex, as well as $T_{\text{eff}} = 3487$ K and $\log g = 4.47$ dex. The matching spectrum for the star has been obtained by normalizing the APOGEE observed one with a synthetic spectrum with $T_{\text{eff}} = 3300$ K, $\log g = 5.0$ dex and $[M/H] = +0.0$ dex, and the derived spectroscopical parameters for this star are $T_{\text{eff}} = 3415 \pm 100$ K,$\log g = 4.73 \pm 0.1$ dex, $[M/H] = -0.01 \pm 0.1$ dex.

Star 2M12271328+5705444 (LSPM J1227+5705 [144]) was characterized in Gilhool et al. (2017), giving it the following parameters: $T_{\text{eff}} = 3596$ K, $\log g = 4.5$ dex and $[M/H] = +0.0$ dex. The available ASPCAP parameters for this star are $T_{\text{eff}} = 3661$ K and $[M/H] = -0.21$ dex, as well as $\log g = 4.45$ dex. The matching spectrum for the star has been obtained by normalizing the APOGEE observed one with a synthetic spectrum with $T_{\text{eff}} = 3400$ K, $\log g = 5.0$ dex

[142] http://simbad.u-strasbg.fr/simbad/sim-id?Ident=2Mass+j12205197%2B4006468
[143] http://simbad.u-strasbg.fr/simbad/sim-id?Ident=2Mass+j12212146%2B5745089
[144] http://simbad.u-strasbg.fr/simbad/sim-id?Ident=2Mass+j12271328%2B5705444

and $[M/H] = -0.2$ dex, and the derived spectroscopical parameters for this star are $T_{\rm eff} = 3601 \pm 100$ K,$\log g = 4.99 \pm 0.1$ dex, $[M/H] = -0.18 \pm 0.1$ dex.

Star 2M12301148+5555229 (LP 131-12 [145]) was characterized in Gilhool et al. (2017), giving it the following parameters: $T_{\rm eff} = 3580$ K, $\log g = 4.5$ dex and $[M/H] = -0.5$ dex. The available ASPCAP parameters for this star are $T_{\rm eff} = 3683$ K and $[M/H] = -0.70$ dex, as well as $\log g = 4.45$ dex. The matching spectrum for the star has been obtained by normalizing the APOGEE observed one with a synthetic spectrum with $T_{\rm eff} = 3400$ K, $\log g = 5.0$ dex and $[M/H] = -0.1$ dex, and the derived spectroscopical parameters for this star are $T_{\rm eff} = 3672 \pm 100$ K,$\log g = 5.04 \pm 0.1$ dex, $[M/H] = -0.85 \pm 0.1$ dex.

Star 2M12330155+5738113 (G 199-25 [146]) was characterized in Gilhool et al. (2017), giving it the following parameters: $T_{\rm eff} = 3560$ K, $\log g = 4.5$ dex and $[M/H] = -0.5$ dex. The available ASPCAP parameters for this star are $T_{\rm eff} = 3661$ K and $[M/H] = -0.38$ dex, as well as $\log g = 4.48$ dex. The matching spectrum for the star has been obtained by normalizing the APOGEE observed one with a synthetic spectrum with $T_{\rm eff} = 3400$ K, $\log g = 5.0$ dex and $[M/H] = -0.1$ dex, and the derived spectroscopical parameters for this star are $T_{\rm eff} = 3639 \pm 100$ K,$\log g = 4.9 \pm 0.1$ dex, $[M/H] = -0.58 \pm 0.1$ dex.

Star 2M12505082+1301468 (LP 496-34 [147]) was characterized in Gilhool et al. (2017), giving it the following parameters: $T_{\rm eff} = 3393$ K, $\log g = 4.5$ dex and $[M/H] = +0.0$ dex. The available ASPCAP parameters for this star are $[M/H] = -0.23$ dex, as well as $T_{\rm eff} = 3444$ K and $\log g = 4.57$ dex. The matching spectrum for the star has been obtained by normalizing the APOGEE observed one with a synthetic spectrum with $T_{\rm eff} = 3200$ K, $\log g = 5.0$ dex and $[M/H] = -0.2$ dex, and the derived spectroscopical parameters for this star are $T_{\rm eff} = 3453 \pm 100$ K,$\log g = 5.14 \pm 0.1$ dex, $[M/H] = -0.22 \pm 0.1$ dex.

Star 2M12573249+4057012 (G 123-74 [148]) was characterized in Gilhool et al. (2017), giving it the following parameters: $T_{\rm eff} = 3644$ K, $\log g = 4.5$ dex and $[M/H] = +0.0$ dex. The available ASPCAP parameters for this star are $T_{\rm eff} = 3699$ K and $[M/H] = +0.11$ dex, as well as $\log g = 4.32$ dex. The matching spectrum for the star has been obtained by normalizing the APOGEE observed one with a synthetic spectrum with $T_{\rm eff} = 3600$ K, $\log g = 5.0$ dex and $[M/H] = +0.4$ dex, and the derived spectroscopical parameters for this star are $T_{\rm eff} =$

[145] http://simbad.u-strasbg.fr/simbad/sim-id?Ident=2Mass+j12301148%2B5555229
[146] http://simbad.u-strasbg.fr/simbad/sim-id?Ident=2Mass+j12330155%2B5738113
[147] http://simbad.u-strasbg.fr/simbad/sim-id?Ident=2Mass+j12505082%2B1301468
[148] http://simbad.u-strasbg.fr/simbad/sim-id?Ident=2Mass+j12573249%2B4057012

3658 ± 100 K,$\log g = 4.67 \pm 0.1$ dex, $[M/H] = +0.07 \pm 0.1$ dex.

Star 2M13085124-0131075 (G 14-34 [149]) was characterized in Gilhool et al. (2017), giving it the following parameters: $T_{\rm eff} = 3498$ K, $\log g = 4.5$ dex and $[M/H] = +0.0$ dex, as well as in Gaidos et al. (2014), giving it $T_{\rm eff} = 3518$ K and $[M/H] = -0.05$ dex. The available ASPCAP parameters for this star are $T_{\rm eff} = 3531$ K and $[M/H] = +0.0$ dex, as well as $\log g = 4.46$ dex. The matching spectrum for the star has been obtained by normalizing the APOGEE observed one with a synthetic spectrum with $T_{\rm eff} = 3400$ K, $\log g = 5.0$ dex and $[M/H] = +0.2$ dex, and the derived spectroscopical parameters for this star are $T_{\rm eff} = 3487 \pm 100$ K,$\log g = 4.86 \pm 0.1$ dex, $[M/H] = -0.01 \pm 0.1$ dex.

Star 2M13202492-0139266 (G 14-47 [150]) was characterized in Gilhool et al. (2017), giving it the following parameters: $T_{\rm eff} = 3680$ K, $\log g = 4.5$ dex and $[M/H] = +0.0$ dex, as well as in Gaidos et al. (2014), giving it $T_{\rm eff} = 3715$ K and $[M/H] = -0.23$ dex. The available ASPCAP parameters for this star are $T_{\rm eff} = 3765$ K and $[M/H] = -0.14$ dex, as well as $\log g = 4.47$ dex. The matching spectrum for the star has been obtained by normalizing the APOGEE observed one with a synthetic spectrum with $T_{\rm eff} = 3600$ K, $\log g = 5.0$ dex and $[M/H] = +0.0$ dex, and the derived spectroscopical parameters for this star are $T_{\rm eff} = 3714 \pm 100$ K,$\log g = 4.96 \pm 0.1$ dex, $[M/H] = -0.18 \pm 0.1$ dex.

Star 2M13315838+5443452 (UCAC4 724-051571 [151]) was characterized in Gilhool et al. (2017), giving it the following parameters: $T_{\rm eff} = 3663$ K, $\log g = 4.5$ dex and $[M/H] = +0.0$ dex, as well as in Terrien et al. (2015), giving it $T_{\rm eff} = 3617$ K and $[M/H] = +0.04$ dex. The available ASPCAP parameters for this star are $T_{\rm eff} = 3727$ K and $[M/H] = +0.02$ dex, as well as $\log g = 4.38$ dex. The matching spectrum for the star has been obtained by normalizing the APOGEE observed one with a synthetic spectrum with $T_{\rm eff} = 3600$ K, $\log g = 5.0$ dex and $[M/H] = +0.2$ dex, and the derived spectroscopical parameters for this star are $T_{\rm eff} = 3675 \pm 100$ K,$\log g = 4.84 \pm 0.1$ dex, $[M/H] = +0.0 \pm 0.1$ dex.

Star 2M13421941+1847193 (Wolf 491 [152]) was characterized in Gilhool et al. (2017), giving it the following parameters: $T_{\rm eff} = 3804$ K, $\log g = 4.5$ dex and $[M/H] = +0.0$ dex. The available ASPCAP parameters for this star are $T_{\rm eff} = 3857$ K and $[M/H] = -0.09$ dex, as well as $\log g = 4.44$ dex. The matching spectrum for the star has been obtained by normaliz-

[149] http://simbad.u-strasbg.fr/simbad/sim-id?Ident=2Mass+j13085124-0131075
[150] http://simbad.u-strasbg.fr/simbad/sim-id?Ident=2Mass+j13202492-0139266
[151] http://simbad.u-strasbg.fr/simbad/sim-id?Ident=2Mass+j13315838%2B5443452
[152] http://simbad.u-strasbg.fr/simbad/sim-id?Ident=2Mass+j13421941%2B1847193

ing the APOGEE observed one with a synthetic spectrum with $T_{\rm eff} = 3800$ K, $\log g = 5.0$ dex and $[M/H] = +0.2$ dex, and the derived spectroscopical parameters for this star are $T_{\rm eff} = 3823 \pm 100$ K,$\log g = 4.86 \pm 0.1$ dex, $[M/H] = -0.07 \pm 0.1$ dex.

Star 2M13462703+1707100 (Wolf 500 [153]) was characterized in Gilhool et al. (2017), giving it the following parameters: $T_{\rm eff} = 3662$ K, $\log g = 4.5$ dex and $[M/H] = +0.0$ dex. The available ASPCAP parameters for this star are $T_{\rm eff} = 3734$ K and $[M/H] = -0.01$ dex, as well as $\log g = 4.37$ dex. The matching spectrum for the star has been obtained by normalizing the APOGEE observed one with a synthetic spectrum with $T_{\rm eff} = 3600$ K, $\log g = 5.0$ dex and $[M/H] = +0.2$ dex, and the derived spectroscopical parameters for this star are $T_{\rm eff} = 3659 \pm 100$ K,$\log g = 4.6 \pm 0.1$ dex, $[M/H] = -0.06 \pm 0.1$ dex.

Star 2M13514938+4157445 (UCAC4 660-056582 [154]) was characterized in Terrien et al. (2015), giving it the following parameters: $T_{\rm eff} = 3499$ K and $[M/H] = +0.24$ dex. The available ASPCAP parameters for this star are $T_{\rm eff} = 3664$ K and $[M/H] = +0.14$ dex, as well as $\log g = 4.43$ dex. The matching spectrum for the star has been obtained by normalizing the APOGEE observed one with a synthetic spectrum with $T_{\rm eff} = 3600$ K, $\log g = 5.0$ dex and $[M/H] = +0.4$ dex, and the derived spectroscopical parameters for this star are $T_{\rm eff} = 3653 \pm 100$ K,$\log g = 5.0 \pm 0.1$ dex, $[M/H] = +0.16 \pm 0.1$ dex.

Star 2M13525797+3331361 (LSPM J1352+3331 [155]) was characterized in Gilhool et al. (2017), giving it the following parameters: $T_{\rm eff} = 3473$ K, $\log g = 5.0$ dex and $[M/H] = +0.5$ dex. The available ASPCAP parameters for this star are $[M/H] = -0.21$ dex, as well as $T_{\rm eff} = 3516$ K and $\log g = 4.46$ dex. The matching spectrum for the star has been obtained by normalizing the APOGEE observed one with a synthetic spectrum with $T_{\rm eff} = 3400$ K, $\log g = 5.0$ dex and $[M/H] = +0.2$ dex, and the derived spectroscopical parameters for this star are $T_{\rm eff} = 3487 \pm 100$ K,$\log g = 4.6 \pm 0.1$ dex, $[M/H] = -0.02 \pm 0.1$ dex.

Star 2M13552585+2556161 (LSPM J1355+2556 [156]) has not been previously spectroscopically characterized in the literature, but it is flagged in Simbad Wenger et al. (2000) as a high proper-motion star. The available ASPCAP parameters for this star are $T_{\rm eff} = 4048$ K and $[M/H] = -0.32$ dex, as well as $\log g = 4.32$ dex. The matching spectrum for the star has been obtained by normalizing the APOGEE observed one with a synthetic spectrum with

[153] http://simbad.u-strasbg.fr/simbad/sim-id?Ident=2Mass+j13462703%2B1707100
[154] http://simbad.u-strasbg.fr/simbad/sim-id?Ident=2Mass+j13514938%2B4157445
[155] http://simbad.u-strasbg.fr/simbad/sim-id?Ident=2Mass+j13525797%2B3331361
[156] http://simbad.u-strasbg.fr/simbad/sim-id?Ident=2Mass+j13552585%2B2556161

$T_{\rm eff} = 3900\,$K, $\log g = 5.0\,$dex and $[M/H] = +0.1\,$dex, and the derived spectroscopical parameters for this star are $T_{\rm eff} = 3987 \pm 100\,$K,$\log g = 4.55 \pm 0.1\,$dex, $[M/H] = -0.35 \pm 0.1\,$dex.

Star 2M13570155+2534378 (StKM 1-1108 [157]) was characterized in Gilhool et al. (2017), giving it the following parameters: $T_{\rm eff} = 3735\,$K, $\log g = 4.5\,$dex and $[M/H] = +0.0\,$dex. It is also present in Gaidos et al. (2014), with $T_{\rm eff} = 3742\,$K and $[M/H] = +0.0\,$dex, and in Lépine et al. (2013), with $T_{\rm eff} = 3630\,$K and $\log g = 4.5\,$dex. The available ASPCAP parameters for this star are $T_{\rm eff} = 3797\,$K and $[M/H] = -0.16\,$dex, as well as $\log g = 4.51\,$dex. The matching spectrum for the star has been obtained by normalizing the APOGEE observed one with a synthetic spectrum with $T_{\rm eff} = 3700\,$K, $\log g = 5.0\,$dex and $[M/H] = +0.0\,$dex, and the derived spectroscopical parameters for this star are $T_{\rm eff} = 3802 \pm 100\,$K,$\log g = 4.99 \pm 0.1\,$dex, $[M/H] = -0.26 \pm 0.1\,$dex.

Star 2M13572571+3400176 (LP 270-17 [158]) was characterized in Gilhool et al. (2017), giving it the following parameters: $T_{\rm eff} = 3463\,$K, $\log g = 4.5\,$dex and $[M/H] = +0.0\,$dex. The available ASPCAP parameters for this star are $[M/H] = -0.19\,$dex, as well as $T_{\rm eff} = 3503\,$K and $\log g = 4.53\,$dex. The matching spectrum for the star has been obtained by normalizing the APOGEE observed one with a synthetic spectrum with $T_{\rm eff} = 3300\,$K, $\log g = 5.0\,$dex and $[M/H] = +0.0\,$dex, and the derived spectroscopical parameters for this star are $T_{\rm eff} = 3438 \pm 100\,$K,$\log g = 4.93 \pm 0.1\,$dex, $[M/H] = -0.09 \pm 0.1\,$dex.

Star 2M13581901+0119475 (NLTT 35834 [159]) was characterized in Terrien et al. (2015), giving it the following parameters: $T_{\rm eff} = 3602\,$K and $[M/H] = +0.06\,$dex. The available ASPCAP parameters for this star are $T_{\rm eff} = 3705\,$K and $[M/H] = +0.08\,$dex, as well as $\log g = 4.39\,$dex. The matching spectrum for the star has been obtained by normalizing the APOGEE observed one with a synthetic spectrum with $T_{\rm eff} = 3600\,$K, $\log g = 5.0\,$dex and $[M/H] = +0.4\,$dex, and the derived spectroscopical parameters for this star are $T_{\rm eff} = 3653 \pm 100\,$K,$\log g = 4.75 \pm 0.1\,$dex, $[M/H] = +0.05 \pm 0.1\,$dex.

Star 2M14010995+2621429 (LP 324-48 [160]) was characterized in Gilhool et al. (2017), giving it the following parameters: $T_{\rm eff} = 3868\,$K, $\log g = 4.5\,$dex and $[M/H] = +0.0\,$dex. It was also characterized in Gaidos et al. (2014), giving it $T_{\rm eff} = 3887\,$K and $[M/H] = -0.27\,$dex, as well as in Lépine et al. (2013), with $\log g = 4.5\,$dex and $T_{\rm eff} = 3640\,$K. The available ASPCAP

[157] `http://simbad.u-strasbg.fr/simbad/sim-id?Ident=2Mass+j13570155%2B2534378`
[158] `http://simbad.u-strasbg.fr/simbad/sim-id?Ident=2Mass+j13572571%2B3400176`
[159] `http://simbad.u-strasbg.fr/simbad/sim-id?Ident=2Mass+j13581901%2B0119475`
[160] `http://simbad.u-strasbg.fr/simbad/sim-id?Ident=2Mass+j14010995%2B2621429`

parameters for this star are $T_{\rm eff} = 3909\,$K and $[M/H] = -0.01\,$dex, as well as $\log g = 4.42\,$dex. The matching spectrum for the star has been obtained by normalizing the APOGEE observed one with a synthetic spectrum with $T_{\rm eff} = 4000\,$K, $\log g = 5.0\,$dex and $[M/H] = +0.0\,$dex, and the derived spectroscopical parameters for this star are $T_{\rm eff} = 3956 \pm 100\,$K,$\log g = 4.83 \pm 0.1\,$dex, $[M/H] = -0.17 \pm 0.1\,$dex.

Star 2M14022155+2517517 (LSPM J1402+2517 [161]) was characterized in Gilhool et al. (2017), giving it the following parameters: $T_{\rm eff} = 3769\,$K, $\log g = 4.5\,$dex and $[M/H] = +0.0\,$dex. The available ASPCAP parameters for this star are $T_{\rm eff} = 3827\,$K and $[M/H] = +0.01\,$dex, as well as $\log g = 4.38\,$dex. The matching spectrum for the star has been obtained by normalizing the APOGEE observed one with a synthetic spectrum with $T_{\rm eff} = 4000\,$K, $\log g = 5.0\,$dex and $[M/H] = +0.0\,$dex, and the derived spectroscopical parameters for this star are $T_{\rm eff} = 3891 \pm 100\,$K,$\log g = 4.97 \pm 0.1\,$dex, $[M/H] = -0.05 \pm 0.1\,$dex.

Star 2M14035430+3008026 (NLTT 36152 [162]) was characterized in Gilhool et al. (2017), giving it the following parameters: $T_{\rm eff} = 3413\,$K, $\log g = 5.0\,$dex and $[M/H] = +0.0\,$dex. There are no available ASPCAP parameters for this star. The matching spectrum for the star has been obtained by normalizing the APOGEE observed one with a synthetic spectrum with $T_{\rm eff} = 3200\,$K, $\log g = 5.0\,$dex and $[M/H] = +0.2\,$dex, and the derived spectroscopical parameters for this star are $T_{\rm eff} = 3330 \pm 100\,$K,$\log g = 5.4 \pm 0.1\,$dex, $[M/H] = +0.44 \pm 0.1\,$dex.

Star 2M14044784+5237559 (LSPM J1404+5237 [163]) was characterized in Gilhool et al. (2017), giving it the following parameters: $T_{\rm eff} = 3444\,$K, $\log g = 5.0\,$dex and $[M/H] = +0.5\,$dex. The available ASPCAP parameters for this star are $[M/H] = -0.02\,$dex, as well as $T_{\rm eff} = 3477\,$K and $\log g = 4.45\,$dex. The matching spectrum for the star has been obtained by normalizing the APOGEE observed one with a synthetic spectrum with $T_{\rm eff} = 3400\,$K, $\log g = 5.0\,$dex and $[M/H] = +0.0\,$dex, and the derived spectroscopical parameters for this star are $T_{\rm eff} = 3489 \pm 100\,$K,$\log g = 4.57 \pm 0.1\,$dex, $[M/H] = -0.03 \pm 0.1\,$dex.

Star 2M14130286+0506321 (NLTT 36587 [164]) was characterized in Gilhool et al. (2017), giving it the following parameters: $T_{\rm eff} = 3395\,$K, $\log g = 5.5\,$dex and $[M/H] = +0.5\,$dex, as well as inTerrien et al. (2015), giving it the following parameters: $T_{\rm eff} = 3323\,$K and $[M/H] = +0.27\,$dex. The available ASPCAP parameters for this star are $[M/H] = +0.07\,$dex, as well as

[161] http://simbad.u-strasbg.fr/simbad/sim-id?Ident=2Mass+j14022155%2B2517517
[162] http://simbad.u-strasbg.fr/simbad/sim-id?Ident=2Mass+j14035430%2B3008026
[163] http://simbad.u-strasbg.fr/simbad/sim-id?Ident=2Mass+j14044784%2B5237559
[164] http://simbad.u-strasbg.fr/simbad/sim-id?Ident=2Mass+j14130286%2B0506321

$T_{\rm eff} = 3431$ K and $\log g = 4.66$ dex. The matching spectrum for the star has been obtained by normalizing the APOGEE observed one with a synthetic spectrum with $T_{\rm eff} = 3200$ K, $\log g = 5.0$ dex and $[M/H] = +0.2$ dex, and the derived spectroscopical parameters for this star are $T_{\rm eff} = 3324 \pm 100$ K,$\log g = 4.95 \pm 0.1$ dex, $[M/H] = +0.16 \pm 0.1$ dex.

Star 2M14173915+0624144 (LSPM J1417+0624 [165]) was characterized in Gilhool et al. (2017), giving it the following parameters: $T_{\rm eff} = 3315$ K, $\log g = 5.0$ dex and $[M/H] = +0.0$ dex. The available ASPCAP parameters for this star are $[M/H] = -0.16$ dex, as well as $T_{\rm eff} = 3366$ K and $\log g = 4.67$ dex. The matching spectrum for the star has been obtained by normalizing the APOGEE observed one with a synthetic spectrum with $T_{\rm eff} = 3400$ K, $\log g = 5.0$ dex and $[M/H] = -0.2$ dex, and the derived spectroscopical parameters for this star are $T_{\rm eff} = 3590 \pm 100$ K,$\log g = 5.4 \pm 0.1$ dex, $[M/H] = -0.22 \pm 0.1$ dex.

Star 2M14180725+0611519 (LSPM J1418+0611 [166]) has not been previously spectroscopically characterized in the literature, and is flagged in Simbad Wenger et al. (2000) as a high proper-motion star. The available ASPCAP parameters for this star are $[M/H] = -0.13$ dex, as well as $T_{\rm eff} = 3322$ K and $\log g = 4.59$ dex. The matching spectrum for the star has been obtained by normalizing the APOGEE observed one with a synthetic spectrum with $T_{\rm eff} = 3200$ K, $\log g = 5.0$ dex and $[M/H] = -0.2$ dex, and the derived spectroscopical parameters for this star are $T_{\rm eff} = 3429 \pm 100$ K,$\log g = 5.4 \pm 0.1$ dex, $[M/H] = -0.19 \pm 0.1$ dex.

Star 2M14385800+1327388 (2MASS J14385800+1327388 [167]) was characterized in Gilhool et al. (2017), giving it the following parameters: $T_{\rm eff} = 3696$ K, $\log g = 4.5$ dex and $[M/H] = +0.0$ dex. The available ASPCAP parameters for this star are $T_{\rm eff} = 3743$ K and $[M/H] = +0.19$ dex, as well as $\log g = 4.24$ dex. The matching spectrum for the star has been obtained by normalizing the APOGEE observed one with a synthetic spectrum with $T_{\rm eff} = 3600$ K, $\log g = 5.0$ dex and $[M/H] = +0.4$ dex, and the derived spectroscopical parameters for this star are $T_{\rm eff} = 3672 \pm 100$ K, $\log g = 4.63 \pm 0.1$ dex, $[M/H] = +0.08 \pm 0.1$ dex.

Star 2M14431906+1120548 (LP 500-87 [168]) was characterized in Gilhool et al. (2017), giving it the following parameters: $T_{\rm eff} = 3479$ K, $\log g = 5.0$ dex and $[M/H] = +0.0$ dex. The available ASPCAP parameters for this star are $[M/H] = -0.07$ dex, as well as $T_{\rm eff} = 3510$ K and $\log g = 4.60$ dex. The matching spectrum for the star has been obtained by normalizing

[165] http://simbad.u-strasbg.fr/simbad/sim-id?Ident=2Mass+j14173915%2B0624144
[166] http://simbad.u-strasbg.fr/simbad/sim-id?Ident=2Mass+j14180725%2B0611519
[167] http://simbad.u-strasbg.fr/simbad/sim-id?Ident=2Mass+j14385800%2B1327388
[168] http://simbad.u-strasbg.fr/simbad/sim-id?Ident=2Mass+j14431906%2B1120548

the APOGEE observed one with a synthetic spectrum with $T_{\mathrm{eff}} = 3400\,$K, $\log g = 5.0\,$dex and $[M/H] = +0.0\,$dex, and the derived spectroscopical parameters for this star are $T_{\mathrm{eff}} = 3513 \pm 100\,$K, $\log g = 5.01 \pm 0.1\,$dex, $[M/H] = -0.04 \pm 0.1\,$dex.

Star 2M14535251+1739448 (LP 441-27 [169]) was characterized in Gilhool et al. (2017), giving it the following parameters: $T_{\mathrm{eff}} = 3765\,$K, $\log g = 4.5\,$dex and $[M/H] = -0.5\,$dex. The available ASPCAP parameters for this star are $T_{\mathrm{eff}} = 3828\,$K and $[M/H] = -0.27\,$dex, as well as $\log g = 4.45\,$dex. The matching spectrum for the star has been obtained by normalizing the APOGEE observed one with a synthetic spectrum with $T_{\mathrm{eff}} = 3600\,$K, $\log g = 5.0\,$dex and $[M/H] = +0.1\,$dex, and the derived spectroscopical parameters for this star are $T_{\mathrm{eff}} = 3747 \pm 100\,$K, $\log g = 4.73 \pm 0.1\,$dex, $[M/H] = -0.32 \pm 0.1\,$dex.

Star 2M14540912+4135008 (LSPM J1454+4135 [170]) was characterized in Gilhool et al. (2017), giving it the following parameters: $T_{\mathrm{eff}} = 3513\,$K, $\log g = 4.5\,$dex and $[M/H] = +0.0\,$dex. The available ASPCAP parameters for this star are $T_{\mathrm{eff}} = 3587\,$K and $[M/H] = +0.03\,$dex, as well as $\log g = 4.37\,$dex. The matching spectrum for the star has been obtained by normalizing the APOGEE observed one with a synthetic spectrum with $T_{\mathrm{eff}} = 3400\,$K, $\log g = 5.0\,$dex and $[M/H] = +0.2\,$dex, and the derived spectroscopical parameters for this star are $T_{\mathrm{eff}} = 3484 \pm 100\,$K, $\log g = 4.61 \pm 0.1\,$dex, $[M/H] = -0.01 \pm 0.1\,$dex.

Star 2M14583396+4216146 (G 179-5 [171]) has not been previously spectroscopically characterized in the literature, and is flagged in Simbad Wenger et al. (2000) as a high proper-motion star. The available ASPCAP parameters for this star are $[M/H] = -0.69\,$dex, as well as $T_{\mathrm{eff}} = 3395\,$K and $\log g = 4.06\,$dex. The matching spectrum for the star has been obtained by normalizing the APOGEE observed one with a synthetic spectrum with $T_{\mathrm{eff}} = 3200\,$K, $\log g = 5.0\,$dex and $[M/H] = -0.2\,$dex, and the derived spectroscopical parameters for this star are $T_{\mathrm{eff}} = 3503 \pm 100\,$K, $\log g = 5.34 \pm 0.1\,$dex, $[M/H] = -0.56 \pm 0.1\,$dex.

Star 2M15024283+3211141 (G 167-13 [172]) was characterized in Gilhool et al. (2017), giving it the following parameters: $T_{\mathrm{eff}} = 3549\,$K, $\log g = 4.5\,$dex and $[M/H] = -0.5\,$dex. The available ASPCAP parameters for this star are $T_{\mathrm{eff}} = 3644\,$K and $[M/H] = -0.35\,$dex, as well as $\log g = 4.35\,$dex. The matching spectrum for the star has been obtained by normalizing the APOGEE observed one with a synthetic spectrum with $T_{\mathrm{eff}} = 3400\,$K, $\log g = 5.0\,$dex

[169] http://simbad.u-strasbg.fr/simbad/sim-id?Ident=2Mass+j14535251%2B1739448
[170] http://simbad.u-strasbg.fr/simbad/sim-id?Ident=2Mass+j14540912%2B4135008
[171] http://simbad.u-strasbg.fr/simbad/sim-id?Ident=2Mass+j14583396%2B4216146
[172] http://simbad.u-strasbg.fr/simbad/sim-id?Ident=2Mass+j15024283%2B3211141

and $[M/H] = +0.1$ dex, and the derived spectroscopical parameters for this star are $T_{\rm eff} = 3577 \pm 100$ K, $\log g = 4.84 \pm 0.1$ dex, $[M/H] = -0.33 \pm 0.1$ dex.

Star 2M15090689+3254449 (G 167-23 [173]) was characterized in Gilhool et al. (2017), giving it the following parameters: $T_{\rm eff} = 3432$ K, $\log g = 5.5$ dex and $[M/H] = +0.5$ dex. The available ASPCAP parameters for this star are $[M/H] = +0.09$ dex, as well as $T_{\rm eff} = 3478$ K and $\log g = 4.71$ dex. The matching spectrum for the star has been obtained by normalizing the APOGEE observed one with a synthetic spectrum with $T_{\rm eff} = 3400$ K, $\log g = 5.0$ dex and $[M/H] = +0.2$ dex, and the derived spectroscopical parameters for this star are $T_{\rm eff} = 3477 \pm 100$ K, $\log g = 5.0 \pm 0.1$ dex, $[M/H] = +0.0 \pm 0.1$ dex.

Star 2M15281240+4340086 (LP 223-18 [174]) was characterized in Gilhool et al. (2017), giving it the following parameters: $T_{\rm eff} = 3353$ K, $\log g = 5.0$ dex and $[M/H] = +0.0$ dex, as well as inTerrien et al. (2015), giving it the following parameters: $T_{\rm eff} = 3369$ K and $[M/H] = -0.07$ dex. The available ASPCAP parameters for this star are $[M/H] = -0.37$ dex, as well as $T_{\rm eff} = 3406$ K and $\log g = 4.53$ dex. The matching spectrum for the star has been obtained by normalizing the APOGEE observed one with a synthetic spectrum with $T_{\rm eff} = 3200$ K, $\log g = 5.0$ dex and $[M/H] = -0.2$ dex, and the derived spectroscopical parameters for this star are $T_{\rm eff} = 3477 \pm 100$ K, $\log g = 5.4 \pm 0.1$ dex, $[M/H] = -0.35 \pm 0.1$ dex.

Star 2M16340737+0038043 (Ross 1000 [175]) was characterized in Gilhool et al. (2017), giving it the following parameters: $T_{\rm eff} = 3390$ K, $\log g = 4.5$ dex and $[M/H] = +0.0$ dex. The available ASPCAP parameters for this star are $[M/H] = -0.26$ dex, as well as $T_{\rm eff} = 3433$ K and $\log g = 4.59$ dex. The matching spectrum for the star has been obtained by normalizing the APOGEE observed one with a synthetic spectrum with $T_{\rm eff} = 3200$ K, $\log g = 5.0$ dex and $[M/H] = -0.2$ dex, and the derived spectroscopical parameters for this star are $T_{\rm eff} = 3482 \pm 100$ K, $\log g = 5.27 \pm 0.1$ dex, $[M/H] = -0.33 \pm 0.1$ dex.

Star 2M16343937+0051089 (LSPM J1634+0051 [176]) has not been previously spectroscopically characterized in the literature, and is flagged in Simbad Wenger et al. (2000) as a double or multiple star. The available ASPCAP parameters for this star are $[M/H] = +0.53$ dex, as well as $T_{\rm eff} = 3213$ K and $\log g = 4.62$ dex. The matching spectrum for the star has been obtained by normalizing the APOGEE observed one with a synthetic spectrum with $T_{\rm eff} = 3000$ K,

[173] http://simbad.u-strasbg.fr/simbad/sim-id?Ident=2Mass+j15090689%2B3254449
[174] http://simbad.u-strasbg.fr/simbad/sim-id?Ident=2Mass+j15281240%2B4340086
[175] http://simbad.u-strasbg.fr/simbad/sim-id?Ident=2Mass+j16340737%2B0038043
[176] http://simbad.u-strasbg.fr/simbad/sim-id?Ident=2Mass+j16343937%2B0051089

$\log g = 5.0$ dex and $[M/H] = -0.4$ dex, and the derived spectroscopical parameters for this star are $T_{\rm eff} = 3393 \pm 100$ K, $\log g = 5.39 \pm 0.1$ dex, $[M/H] = -0.67 \pm 0.1$ dex.

Star 2M16383835+3700273 (LP 275-76 [177]) was characterized in Gilhool et al. (2017), giving it the following parameters: $T_{\rm eff} = 3288$ K, $\log g = 5.0$ dex and $[M/H] = +0.0$ dex. The available ASPCAP parameters for this star are $[M/H] = -0.21$ dex, as well as $T_{\rm eff} = 3352$ K and $\log g = 4.62$ dex. The matching spectrum for the star has been obtained by normalizing the APOGEE observed one with a synthetic spectrum with $T_{\rm eff} = 3200$ K, $\log g = 5.0$ dex and $[M/H] = -0.2$ dex, and the derived spectroscopical parameters for this star are $T_{\rm eff} = 3428 \pm 100$ K, $\log g = 5.4 \pm 0.1$ dex, $[M/H] = -0.2 \pm 0.1$ dex.

Star 2M16385433+3643018 (LP 276-2 [178]) has not been previously spectroscopically characterized in the literature, and is flagged in Simbad Wenger et al. (2000) as a high proper-motion star. There are no available ASPCAP parameters for this star. The matching spectrum for the star has been obtained by normalizing the APOGEE observed one with a synthetic spectrum with $T_{\rm eff} = 4000$ K, $\log g = 5.0$ dex and $[M/H] = +0.0$ dex, and the derived spectroscopical parameters for this star are $T_{\rm eff} = 3917 \pm 100$ K, $\log g = 4.88 \pm 0.1$ dex, $[M/H] = -0.2 \pm 0.1$ dex.

Star 2M16440030+3721597 (LP 276-14 [179]) was characterized in Gilhool et al. (2017), giving it the following parameters: $T_{\rm eff} = 3216$ K, $\log g = 5.0$ dex and $[M/H] = +0.0$ dex. The available ASPCAP parameters for this star are $[M/H] = -0.54$ dex, as well as $T_{\rm eff} = 3259$ K and $\log g = 4.58$ dex. The matching spectrum for the star has been obtained by normalizing the APOGEE observed one with a synthetic spectrum with $T_{\rm eff} = 3000$ K, $\log g = 5.0$ dex and $[M/H] = -0.4$ dex, and the derived spectroscopical parameters for this star are $T_{\rm eff} = 3355 \pm 100$ K, $\log g = 5.4 \pm 0.1$ dex, $[M/H] = -0.32 \pm 0.1$ dex.

Star 2M16445239+3644423 (LSPM J1644+3644 [180]) has not been previously spectroscopically characterized in the literature, and is flagged in Simbad Wenger et al. (2000) as a high proper-motion star. There are no available ASPCAP parameters for this star. The matching spectrum for the star has been obtained by normalizing the APOGEE observed one with a synthetic spectrum with $T_{\rm eff} = 3400$ K, $\log g = 5.0$ dex and $[M/H] = -0.1$ dex, and the derived spectroscopical parameters for this star are $T_{\rm eff} = 3642 \pm 100$ K, $\log g = 5.3 \pm 0.1$ dex,

[177] http://simbad.u-strasbg.fr/simbad/sim-id?Ident=2Mass+j16383835%2B3700273
[178] http://simbad.u-strasbg.fr/simbad/sim-id?Ident=2Mass+j16385433%2B3643018
[179] http://simbad.u-strasbg.fr/simbad/sim-id?Ident=2Mass+j16440030%2B3721597
[180] http://simbad.u-strasbg.fr/simbad/sim-id?Ident=2Mass+j16445239%2B3644423

$[M/H] = -0.55 \pm 0.1$ dex.

Star 2M16470934+3657361 (LSPM J1647+3657 [181]) has not been previously spectroscopically characterized in the literature, and is flagged in Simbad Wenger et al. (2000) as a high proper-motion star. The available ASPCAP parameters for this star are $[M/H] = +0.02$ dex, as well as $T_{\rm eff} = 3654$ K and $\log g = 4.52$ dex. The matching spectrum for the star has been obtained by normalizing the APOGEE observed one with a synthetic spectrum with $T_{\rm eff} = 3600$ K, $\log g = 5.0$ dex and $[M/H] = +0.1$ dex, and the derived spectroscopical parameters for this star are $T_{\rm eff} = 3748 \pm 100$ K, $\log g = 5.32 \pm 0.1$ dex, $[M/H] = -0.32 \pm 0.1$ dex.

Star 2M16495034+4745402 (LP 179-3 [182]) was characterized in Gilhool et al. (2017), giving it the following parameters: $T_{\rm eff} = 3719$ K, $\log g = 4.5$ dex and $[M/H] = +0.0$ dex. It is also present in Terrien et al. (2015), with $T_{\rm eff} = 3650$ K and $[M/H] = +0.09$ dex. The available ASPCAP parameters for this star are $T_{\rm eff} = 3775$ K and $[M/H] = +0.14$ dex, as well as $\log g = 4.46$ dex. The matching spectrum for the star has been obtained by normalizing the APOGEE observed one with a synthetic spectrum with $T_{\rm eff} = 3600$ K, $\log g = 5.0$ dex and $[M/H] = +0.4$ dex, and the derived spectroscopical parameters for this star are $T_{\rm eff} = 3682 \pm 100$ K, $\log g = 4.72 \pm 0.1$ dex, $[M/H] = +0.1 \pm 0.1$ dex.

Star 2M16541202+1154529 (Ross 644 [183]) was characterized in Gilhool et al. (2017), giving it the following parameters: $T_{\rm eff} = 3788$ K, $\log g = 4.5$ dex and $[M/H] = -0.5$ dex. It is also present in Gaidos et al. (2014), with $T_{\rm eff} = 3834$ K and $[M/H] = -0.53$ dex, and in Lépine et al. (2013), with $T_{\rm eff} = 3690$ K and $\log g = 4.5$ dex, as well as Mann et al. (2015) with $T_{\rm eff} = 3834$ K and $[M/H] = -0.48$ dex. The available ASPCAP parameters for this star are $T_{\rm eff} = 3849$ K and $[M/H] = -0.36$ dex, as well as $\log g = 4.43$ dex. The matching spectrum for the star has been obtained by normalizing the APOGEE observed one with a synthetic spectrum with $T_{\rm eff} = 3600$ K, $\log g = 5.0$ dex and $[M/H] = -0.1$ dex, and the derived spectroscopical parameters for this star are $T_{\rm eff} = 3795 \pm 100$ K, $\log g = 4.79 \pm 0.1$ dex, $[M/H] = -0.46 \pm 0.1$ dex.

Star 2M16565961+1133582 (LSPM J1656+1133 [184]) has not been previously spectroscopically characterized in the literature, and is flagged in Simbad Wenger et al. (2000) as a high proper-motion star. The available ASPCAP parameters for this star are $[M/H] = +0.12$ dex, as well as $T_{\rm eff} = 3173$ K and $\log g = 4.02$ dex. The matching spectrum for the star has been ob-

[181] `http://simbad.u-strasbg.fr/simbad/sim-id?Ident=2Mass+j16470934%2B3657361`
[182] `http://simbad.u-strasbg.fr/simbad/sim-id?Ident=2Mass+j16495034%2B4745402`
[183] `http://simbad.u-strasbg.fr/simbad/sim-id?Ident=2Mass+j16541202%2B1154529`
[184] `http://simbad.u-strasbg.fr/simbad/sim-id?Ident=2Mass+j16565961%2B1133582`

tained by normalizing the APOGEE observed one with a synthetic spectrum with $T_{\rm eff} = 3000\,$K, $\log g = 5.0\,$dex and $[M/H] = -0.4\,$dex, and the derived spectroscopical parameters for this star are $T_{\rm eff} = 3343 \pm 100\,$K, $\log g = 5.4 \pm 0.1\,$dex, $[M/H] = -0.32 \pm 0.1\,$dex.

Star 2M16593773+1155377 (LSPM J1659+1155 [185]) was characterized in Gilhool et al. (2017), giving it the following parameters: $T_{\rm eff} = 3889\,$K, $\log g = 4.5\,$dex and $[M/H] = +0.0\,$dex. The available ASPCAP parameters for this star are $T_{\rm eff} = 3933\,$K and $[M/H] = -0.05\,$dex, as well as $\log g = 4.35\,$dex. The matching spectrum for the star has been obtained by normalizing the APOGEE observed one with a synthetic spectrum with $T_{\rm eff} = 3800\,$K, $\log g = 5.0\,$dex and $[M/H] = -0.2\,$dex, and the derived spectroscopical parameters for this star are $T_{\rm eff} = 3934 \pm 100\,$K, $\log g = 4.66 \pm 0.1\,$dex, $[M/H] = -0.27 \pm 0.1\,$dex.

Star 2M17014341+1119582 (LSPM J1701+1119 [186]) was characterized in Gilhool et al. (2017), giving it the following parameters: $T_{\rm eff} = 3539\,$K, $\log g = 4.5\,$dex and $[M/H] = +0.0\,$dex. The available ASPCAP parameters for this star are $T_{\rm eff} = 3606\,$K and $[M/H] = -0.19\,$dex, as well as $\log g = 4.28\,$dex. The matching spectrum for the star has been obtained by normalizing the APOGEE observed one with a synthetic spectrum with $T_{\rm eff} = 3400\,$K, $\log g = 5.0\,$dex and $[M/H] = +0.0\,$dex, and the derived spectroscopical parameters for this star are $T_{\rm eff} = 3531 \pm 100\,$K, $\log g = 4.93 \pm 0.1\,$dex, $[M/H] = -0.11 \pm 0.1\,$dex.

Star 2M17190292+2340254 (LP 388-18 [187]) was characterized in Gilhool et al. (2017), giving it the following parameters: $T_{\rm eff} = 3778\,$K, $\log g = 4.5\,$dex and $[M/H] = +0.0\,$dex. The available ASPCAP parameters for this star are $T_{\rm eff} = 3825\,$K and $[M/H] = +0.01\,$dex, as well as $\log g = 4.33\,$dex. The matching spectrum for the star has been obtained by normalizing the APOGEE observed one with a synthetic spectrum with $T_{\rm eff} = 3900\,$K, $\log g = 5.0\,$dex and $[M/H] = +0.2\,$dex, and the derived spectroscopical parameters for this star are $T_{\rm eff} = 3839 \pm 100\,$K, $\log g = 4.78 \pm 0.1\,$dex, $[M/H] = -0.02 \pm 0.1\,$dex.

Star 2M17331825+3402191 (LSPM J1733+3402 [188]) was characterized in Gilhool et al. (2017), giving it the following parameters: $T_{\rm eff} = 3897\,$K, $\log g = 4.5\,$dex and $[M/H] = -0.5\,$dex. The available ASPCAP parameters for this star are $T_{\rm eff} = 3944\,$K and $[M/H] = -0.20\,$dex, as well as $\log g = 4.36\,$dex. The matching spectrum for the star has been obtained by normalizing the APOGEE observed one with a synthetic spectrum with $T_{\rm eff} = 4000\,$K, $\log g = 5.0\,$dex

[185] http://simbad.u-strasbg.fr/simbad/sim-id?Ident=2Mass+j16593773%2B1155377
[186] http://simbad.u-strasbg.fr/simbad/sim-id?Ident=2Mass+j17014341%2B1119582
[187] http://simbad.u-strasbg.fr/simbad/sim-id?Ident=2Mass+j17190292%2B2340254
[188] http://simbad.u-strasbg.fr/simbad/sim-id?Ident=2Mass+j17331825%2B3402191

and $[M/H] = +0.0$ dex, and the derived spectroscopical parameters for this star are $T_{\mathrm{eff}} = 3971 \pm 100$ K, $\log g = 4.89 \pm 0.1$ dex, $[M/H] = -0.22 \pm 0.1$ dex.

Star 2M17403275+7256146 does not have a dedicated page in Simbad Wenger et al. (2000). The available ASPCAP parameters for this star are $T_{\mathrm{eff}} = 3934$ K and $[M/H] = -0.11$ dex, as well as $\log g = 4.35$ dex. The matching spectrum for the star has been obtained by normalizing the APOGEE observed one with a synthetic spectrum with $T_{\mathrm{eff}} = 4000$ K, $\log g = 5.0$ dex and $[M/H] = +0.0$ dex, and the derived spectroscopical parameters for this star are $T_{\mathrm{eff}} = 3988 \pm 100$ K, $\log g = 4.94 \pm 0.1$ dex, $[M/H] = -0.14 \pm 0.1$ dex.

Star 2M17480236+7436562 (2MASS J17480236+7436562 [189]) has not been previously spectroscopically characterized in the literature, and is flagged in Simbad Wenger et al. (2000) as a high proper-motion star. The available ASPCAP parameters for this star are $[M/H] = -0.35$ dex, as well as $T_{\mathrm{eff}} = 3266$ K and $\log g = 4.48$ dex. The matching spectrum for the star has been obtained by normalizing the APOGEE observed one with a synthetic spectrum with $T_{\mathrm{eff}} = 3200$ K, $\log g = 5.0$ dex and $[M/H] = -0.2$ dex, and the derived spectroscopical parameters for this star are $T_{\mathrm{eff}} = 3460 \pm 100$ K, $\log g = 5.4 \pm 0.1$ dex, $[M/H] = -0.35 \pm 0.1$ dex.

Star 2M17491402+4823093 (UCAC4 692-057424 [190]) was characterized in Gilhool et al. (2017), giving it the following parameters: $T_{\mathrm{eff}} = 3824$ K, $\log g = 4.5$ dex and $[M/H] = +0.0$ dex. The available ASPCAP parameters for this star are $T_{\mathrm{eff}} = 3877$ K and $[M/H] = -0.20$ dex, as well as $\log g = 4.29$ dex. The matching spectrum for the star has been obtained by normalizing the APOGEE observed one with a synthetic spectrum with $T_{\mathrm{eff}} = 3800$ K, $\log g = 5.0$ dex and $[M/H] = +0.1$ dex, and the derived spectroscopical parameters for this star are $T_{\mathrm{eff}} = 3882 \pm 100$ K, $\log g = 4.88 \pm 0.1$ dex, $[M/H] = -0.18 \pm 0.1$ dex.

Star 2M17541820+4758412 (LP 181-1 [191]) was characterized in Gilhool et al. (2017), giving it the following parameters: $T_{\mathrm{eff}} = 3664$ K, $\log g = 4.5$ dex and $[M/H] = -0.5$ dex. The available ASPCAP parameters for this star are $T_{\mathrm{eff}} = 3743$ K and $[M/H] = -0.17$ dex, as well as $\log g = 4.47$ dex. The matching spectrum for the star has been obtained by normalizing the APOGEE observed one with a synthetic spectrum with $T_{\mathrm{eff}} = 3600$ K, $\log g = 5.0$ dex and $[M/H] = +0.1$ dex, and the derived spectroscopical parameters for this star are $T_{\mathrm{eff}} = 3721 \pm 100$ K, $\log g = 4.77 \pm 0.1$ dex, $[M/H] = -0.3 \pm 0.1$ dex.

[189] http://simbad.u-strasbg.fr/simbad/sim-id?Ident=2Mass+j17480236%2B7436562
[190] http://simbad.u-strasbg.fr/simbad/sim-id?Ident=2Mass+j17491402%2B4823093
[191] http://simbad.u-strasbg.fr/simbad/sim-id?Ident=2Mass+j17541820%2B4758412

Star 2M17592886+0318233 (UCAC4 467-067420 [192]) was characterized in Terrien et al. (2015), giving it the following parameters: $T_{\rm eff} = 3830\,$K and $[M/H] = -0.01\,$dex. The available ASPCAP parameters for this star are $T_{\rm eff} = 3900\,$K and $[M/H] = -0.15\,$dex, as well as $\log g = 4.42\,$dex. The matching spectrum for the star has been obtained by normalizing the APOGEE observed one with a synthetic spectrum with $T_{\rm eff} = 4000\,$K, $\log g = 5.0\,$dex and $[M/H] = +0.2\,$dex, and the derived spectroscopical parameters for this star are $T_{\rm eff} = 3925 \pm 100\,$K, $\log g = 4.76 \pm 0.1\,$dex, $[M/H] = -0.01 \pm 0.1\,$dex.

Star 2M18055545+0316213 (NLTT 45916 [193]) has not been previously spectroscopically characterized in the literature, and is flagged in Simbad Wenger et al. (2000) as a high proper-motion star. The available ASPCAP parameters for this star are $T_{\rm eff} = 3566\,$K and $[M/H] = -0.18\,$dex, as well as $\log g = 4.30\,$dex. The matching spectrum for the star has been obtained by normalizing the APOGEE observed one with a synthetic spectrum with $T_{\rm eff} = 3400\,$K, $\log g = 5.0\,$dex and $[M/H] = +0.2\,$dex, and the derived spectroscopical parameters for this star are $T_{\rm eff} = 3501 \pm 100\,$K, $\log g = 4.7 \pm 0.1\,$dex, $[M/H] = +0.08 \pm 0.1\,$dex.

Star 2M18161819+0131277 (G 21-7 [194]) was characterized in Gilhool et al. (2017), giving it the following parameters: $T_{\rm eff} = 3388\,$K, $\log g = 4.5\,$dex and $[M/H] = +0.0\,$dex. It is also present in Gaidos et al. (2014), with $T_{\rm eff} = 3431\,$K and $[M/H] = -0.26\,$dex, and in Lépine et al. (2013), with $T_{\rm eff} = 3370\,$K and $\log g = 5.0\,$dex, as well as Terrien et al. (2015), with $T_{\rm eff} = 3364\,$K and $[M/H] = -0.21\,$dex. The available ASPCAP parameters for this star are $[M/H] = -0.41\,$dex, as well as $T_{\rm eff} = 3437\,$K and $\log g = 4.39\,$dex. The matching spectrum for the star has been obtained by normalizing the APOGEE observed one with a synthetic spectrum with $T_{\rm eff} = 3200\,$K, $\log g = 5.0\,$dex and $[M/H] = -0.2\,$dex, and the derived spectroscopical parameters for this star are $T_{\rm eff} = 3483 \pm 100\,$K, $\log g = 5.14 \pm 0.1\,$dex, $[M/H] = -0.33 \pm 0.1\,$dex.

Star 2M18254864-0258170 (UCAC4 436-076101 [195]) has not been previously spectroscopically characterized in the literature, and is flagged in Simbad Wenger et al. (2000) as a high proper-motion star. The available ASPCAP parameters for this star are $T_{\rm eff} = 3790\,$K and $[M/H] = -0.20\,$dex, as well as $\log g = 4.46\,$dex. The matching spectrum for the star has been obtained by normalizing the APOGEE observed one with a synthetic spectrum with $T_{\rm eff} = 4000\,$K, $\log g = 5.0\,$dex and $[M/H] = +0.2\,$dex, and the derived spectroscopical param-

[192] http://simbad.u-strasbg.fr/simbad/sim-id?Ident=2Mass+j17592886%2B0318233
[193] http://simbad.u-strasbg.fr/simbad/sim-id?Ident=2Mass+j18055545%2B0316213
[194] http://simbad.u-strasbg.fr/simbad/sim-id?Ident=2Mass+j18161819%2B0131277
[195] http://simbad.u-strasbg.fr/simbad/sim-id?Ident=2Mass+j18254864-0258170

eters for this star are $T_{\rm eff} = 3857 \pm 100$ K, $\log g = 4.79 \pm 0.1$ dex, $[M/H] = +0.06 \pm 0.1$ dex.

Star 2M18415473+0651285 (G 141-28 [196]) was characterized in Gilhool et al. (2017), giving it the following parameters: $T_{\rm eff} = 3458$ K, $\log g = 5.0$ dex and $[M/H] = +0.5$ dex. The available ASPCAP parameters for this star are $[M/H] = +0.00$ dex, as well as $T_{\rm eff} = 3494$ K and $\log g = 4.62$ dex. The matching spectrum for the star has been obtained by normalizing the APOGEE observed one with a synthetic spectrum with $T_{\rm eff} = 3300$ K, $\log g = 5.0$ dex and $[M/H] = +0.2$ dex, and the derived spectroscopical parameters for this star are $T_{\rm eff} = 3401 \pm 100$ K, $\log g = 4.78 \pm 0.1$ dex, $[M/H] = +0.00 \pm 0.1$ dex.

Star 2M18451027+0620158 (TYC 460-624-1 [197]) is present in Gaidos et al. (2014), with $T_{\rm eff} = 3678$ K and $[M/H] = -0.13$ dex, and in Lépine et al. (2013), with $T_{\rm eff} = 3460$ K and $\log g = 4.5$ dex, as well as Terrien et al. (2015), with $T_{\rm eff} = 3779$ K and $[M/H] = -0.03$ dex. The available ASPCAP parameters for this star are $T_{\rm eff} = 3782$ K and $[M/H] = -0.13$ dex, as well as $\log g = 4.45$ dex. The matching spectrum for the star has been obtained by normalizing the APOGEE observed one with a synthetic spectrum with $T_{\rm eff} = 3700$ K, $\log g = 5.0$ dex and $[M/H] = +0.4$ dex, and the derived spectroscopical parameters for this star are $T_{\rm eff} = 3727 \pm 100$ K, $\log g = 4.69 \pm 0.1$ dex, $[M/H] = +0.04 \pm 0.1$ dex.

Star 2M18561502+0449049 (G 141-50 [198]) was characterized in Gilhool et al. (2017), giving it the following parameters: $T_{\rm eff} = 3613$ K, $\log g = 4.5$ dex and $[M/H] = -0.5$ dex. The available ASPCAP parameters for this star are $T_{\rm eff} = 3695$ K and $[M/H] = -0.41$ dex, as well as $\log g = 4.54$ dex. The matching spectrum for the star has been obtained by normalizing the APOGEE observed one with a synthetic spectrum with $T_{\rm eff} = 3400$ K, $\log g = 5.0$ dex and $[M/H] = -0.1$ dex, and the derived spectroscopical parameters for this star are $T_{\rm eff} = 3648 \pm 100$ K, $\log g = 4.8 \pm 0.1$ dex, $[M/H] = -0.62 \pm 0.1$ dex.

Star 2M18562628+4622532 (G 205-47 [199]) was characterized in Gilhool et al. (2017), giving it the following parameters: $T_{\rm eff} = 3247$ K, $\log g = 5.0$ dex and $[M/H] = +0.0$ dex, as well as in Terrien et al. (2015), with $T_{\rm eff} = 3307$ K and $[M/H] = -0.03$ dex. The available ASPCAP parameters for this star are $[M/H] = -0.41$ dex, as well as $T_{\rm eff} = 3287$ K and $\log g = 4.47$ dex. The matching spectrum for the star has been obtained by normalizing the APOGEE observed one with a synthetic spectrum with $T_{\rm eff} = 3000$ K, $\log g = 5.0$ dex and $[M/H] = -0.2$ dex,

[196] http://simbad.u-strasbg.fr/simbad/sim-id?Ident=2Mass+j18415473%2B0651285
[197] http://simbad.u-strasbg.fr/simbad/sim-id?Ident=2Mass+j18451027%2B0620158
[198] http://simbad.u-strasbg.fr/simbad/sim-id?Ident=2Mass+j18561502%2B0449049
[199] http://simbad.u-strasbg.fr/simbad/sim-id?Ident=2Mass+j18562628%2B4622532

and the derived spectroscopical parameters for this star are $T_{\rm eff} = 3302 \pm 100$ K, $\log g = 5.32 \pm 0.1$ dex, $[M/H] = -0.34 \pm 0.1$ dex.

Star 2M18571939+0523084 (LSPM J1857+0523 [200]) was characterized in Gilhool et al. (2017), giving it the following parameters: $T_{\rm eff} = 3668$ K, $\log g = 4.5$ dex and $[M/H] = +0.0$ dex. The available ASPCAP parameters for this star are $T_{\rm eff} = 3741$ K and $[M/H] = -0.05$ dex, as well as $\log g = 4.42$ dex. The matching spectrum for the star has been obtained by normalizing the APOGEE observed one with a synthetic spectrum with $T_{\rm eff} = 3600$ K, $\log g = 5.0$ dex and $[M/H] = +0.2$ dex, and the derived spectroscopical parameters for this star are $T_{\rm eff} = 3674 \pm 100$ K, $\log g = 4.66 \pm 0.1$ dex, $[M/H] = -0.11 \pm 0.1$ dex.

Star 2M19010098+4522386 (KIC 9006264 [201]) has not been previously spectroscopically characterized in the literature, and is flagged in Simbad Wenger et al. (2000) as a high proper-motion star. The available ASPCAP parameters for this star are $T_{\rm eff} = 3462$ K and $[M/H] = -0.23$ dex, as well as $\log g = 4.71$ dex. The matching spectrum for the star has been obtained by normalizing the APOGEE observed one with a synthetic spectrum with $T_{\rm eff} = 3200$ K, $\log g = 5.0$ dex and $[M/H] = +0.2$ dex, and the derived spectroscopical parameters for this star are $T_{\rm eff} = 3325 \pm 100$ K, $\log g = 4.97 \pm 0.1$ dex, $[M/H] = +0.13 \pm 0.1$ dex.

Star 2M19121128+4316106 (G 208-12 [202]) was characterized in Gilhool et al. (2017), giving it the following parameters: $T_{\rm eff} = 3380$ K, $\log g = 4.5$ dex and $[M/H] = -0.5$ dex. The available ASPCAP parameters for this star are $[M/H] = -0.33$ dex, as well as $T_{\rm eff} = 3413$ K and $\log g = 4.12$ dex. The matching spectrum for the star has been obtained by normalizing the APOGEE observed one with a synthetic spectrum with $T_{\rm eff} = 3200$ K, $\log g = 5.0$ dex and $[M/H] = -0.2$ dex, and the derived spectroscopical parameters for this star are $T_{\rm eff} = 3503 \pm 100$ K, $\log g = 4.71 \pm 0.1$ dex, $[M/H] = -0.45 \pm 0.1$ dex.

Star 2M19213157+4317347 (KOI-314 [203]) was characterized in Terrien et al. (2015), with $T_{\rm eff} = 4030$ K and $[M/H] = -0.16$ dex, and in Frasca et al. (2016), giving it the following parameters: $T_{\rm eff} = 4128$ K, $\log g = 4.48$ dex and $[M/H] = -0.23$ dex. It was also characterized in Muirhead et al. (2014), with $T_{\rm eff} = 3847$ K and $[M/H] = -0.25$ dex. The available ASPCAP parameters for this star are $[M/H] = -0.22$ dex, as well as $T_{\rm eff} = 3874$ K and $\log g = 4.38$ dex. The matching spectrum for the star has been obtained by normalizing the APOGEE observed

[200] http://simbad.u-strasbg.fr/simbad/sim-id?Ident=2Mass+j18571939%2B0523084
[201] http://simbad.u-strasbg.fr/simbad/sim-id?Ident=2Mass+j19010098%2B4522386
[202] http://simbad.u-strasbg.fr/simbad/sim-id?Ident=2Mass+j19121128%2B4316106
[203] http://simbad.u-strasbg.fr/simbad/sim-id?Ident=2Mass+j19213157%2B4317347

one with a synthetic spectrum with $T_{\text{eff}} = 3800\,\text{K}$, $\log g = 5.0\,\text{dex}$ and $[M/H] = +0.1\,\text{dex}$, and the derived spectroscopical parameters for this star are $T_{\text{eff}} = 3910 \pm 100\,\text{K}$, $\log g = 4.84 \pm 0.1\,\text{dex}$, $[M/H] = -0.17 \pm 0.1\,\text{dex}$.

Star 2M19263973+1736418 (LSPM J1926+1736 [204]) has not been previously spectroscopically characterized in the literature, and is flagged in Simbad Wenger et al. (2000) as a high proper-motion star. The available ASPCAP parameters for this star are $[M/H] = +0.01\,\text{dex}$, as well as $T_{\text{eff}} = 3465\,\text{K}$ and $\log g = 4.53\,\text{dex}$. The matching spectrum for the star has been obtained by normalizing the APOGEE observed one with a synthetic spectrum with $T_{\text{eff}} = 3300\,\text{K}$, $\log g = 5.0\,\text{dex}$ and $[M/H] = -0.2\,\text{dex}$, and the derived spectroscopical parameters for this star are $T_{\text{eff}} = 3565 \pm 100\,\text{K}$, $\log g = 5.38 \pm 0.1\,\text{dex}$, $[M/H] = -0.39 \pm 0.1\,\text{dex}$.

Star 2M19272432+2619292 (LSPM J1927+2619 [205]) has not been previously spectroscopically characterized in the literature, and is flagged in Simbad Wenger et al. (2000) as a high proper-motion star. The available ASPCAP parameters for this star are $[M/H] = +0.19\,\text{dex}$, as well as $T_{\text{eff}} = 3525\,\text{K}$ and $\log g = 4.43\,\text{dex}$. The matching spectrum for the star has been obtained by normalizing the APOGEE observed one with a synthetic spectrum with $T_{\text{eff}} = 3400\,\text{K}$, $\log g = 5.0\,\text{dex}$ and $[M/H] = +0.0\,\text{dex}$, and the derived spectroscopical parameters for this star are $T_{\text{eff}} = 3526 \pm 100\,\text{K}$, $\log g = 5.1 \pm 0.1\,\text{dex}$, $[M/H] = -0.09 \pm 0.1\,\text{dex}$.

Star 2M19302719+1723396 (PM J19304+1723 [206]) has not been previously spectroscopically characterized in the literature, and is flagged in Simbad Wenger et al. (2000) as a high proper-motion star. The available ASPCAP parameters for this star are $[M/H] = -0.21\,\text{dex}$, as well as $T_{\text{eff}} = 3685\,\text{K}$ and $\log g = 4.44\,\text{dex}$. The matching spectrum for the star has been obtained by normalizing the APOGEE observed one with a synthetic spectrum with $T_{\text{eff}} = 3600\,\text{K}$, $\log g = 5.0\,\text{dex}$ and $[M/H] = +0.2\,\text{dex}$, and the derived spectroscopical parameters for this star are $T_{\text{eff}} = 3677 \pm 100\,\text{K}$, $\log g = 4.8 \pm 0.1\,\text{dex}$, $[M/H] = -0.01 \pm 0.1\,\text{dex}$.

Star 2M19313868-0658253 (UCAC4 416-131506 [207]) was characterized in Gilhool et al. (2017), giving it the following parameters: $T_{\text{eff}} = 3536\,\text{K}$, $\log g = 5.0\,\text{dex}$ and $[M/H] = +0.5\,\text{dex}$, as well as in Terrien et al. (2015), with $T_{\text{eff}} = 3308\,\text{K}$ and $[M/H] = +0.14\,\text{dex}$. The available ASPCAP parameters for this star are $T_{\text{eff}} = 3592\,\text{K}$ and $[M/H] = +0.0\,\text{dex}$, as well as $\log g = 4.44\,\text{dex}$. The matching spectrum for the star has been obtained by normalizing the APOGEE

[204] `http://simbad.u-strasbg.fr/simbad/sim-id?Ident=2Mass+j19263973%2B1736418`
[205] `http://simbad.u-strasbg.fr/simbad/sim-id?Ident=2Mass+j19272432%2B2619292`
[206] `http://simbad.u-strasbg.fr/simbad/sim-id?Ident=2Mass+j19302719%2B1723396`
[207] `http://simbad.u-strasbg.fr/simbad/sim-id?Ident=2Mass+j19313868-0658253`

observed one with a synthetic spectrum with $T_{\rm eff} = 3400\,$K, $\log g = 5.0\,$dex and $[M/H] = +0.2\,$dex, and the derived spectroscopical parameters for this star are $T_{\rm eff} = 3491 \pm 100\,$K, $\log g = 4.86 \pm 0.1\,$dex, $[M/H] = +0.0 \pm 0.1\,$dex.

Star 2M19324633-0652178 (SCR J1932-0652 [208]) was characterized in Gilhool et al. (2017), giving it the following parameters: $T_{\rm eff} = 3389\,$K, $\log g = 4.5\,$dex and $[M/H] = +0.5\,$dex. The available ASPCAP parameters for this star are $[M/H] = -0.03\,$dex, as well as $T_{\rm eff} = 3420\,$K and $\log g = 4.41\,$dex. The matching spectrum for the star has been obtained by normalizing the APOGEE observed one with a synthetic spectrum with $T_{\rm eff} = 3200\,$K, $\log g = 5.0\,$dex and $[M/H] = +0.0\,$dex, and the derived spectroscopical parameters for this star are $T_{\rm eff} = 3342 \pm 100\,$K, $\log g = 4.49 \pm 0.1\,$dex, $[M/H] = -0.03 \pm 0.1\,$dex.

Star 2M19325604+1723567 (G 142-38 [209]) was characterized in Gilhool et al. (2017), giving it the following parameters: $T_{\rm eff} = 3393\,$K, $\log g = 4.5\,$dex and $[M/H] = -0.5\,$dex. The available ASPCAP parameters for this star are $T_{\rm eff} = 3583\,$K and $[M/H] = -0.36\,$dex, as well as $\log g = 4.37\,$dex. The matching spectrum for the star has been obtained by normalizing the APOGEE observed one with a synthetic spectrum with $T_{\rm eff} = 3400\,$K, $\log g = 5.0\,$dex and $[M/H] = -0.1\,$dex, and the derived spectroscopical parameters for this star are $T_{\rm eff} = 3634 \pm 100\,$K, $\log g = 4.95 \pm 0.1\,$dex, $[M/H] = -0.61 \pm 0.1\,$dex.

Star 2M19341617+2553535 (LSPM J1934+2553 [210]) was characterized in Gilhool et al. (2017), giving it the following parameters: $T_{\rm eff} = 3342\,$K, $\log g = 4.5\,$dex and $[M/H] = -0.5\,$dex. The available ASPCAP parameters for this star are $[M/H] = -0.45\,$dex, as well as $T_{\rm eff} = 3459\,$K and $\log g = 4.60\,$dex. The matching spectrum for the star has been obtained by normalizing the APOGEE observed one with a synthetic spectrum with $T_{\rm eff} = 3200\,$K, $\log g = 5.0\,$dex and $[M/H] = -0.1\,$dex, and the derived spectroscopical parameters for this star are $T_{\rm eff} = 3499 \pm 100\,$K, $\log g = 4.81 \pm 0.1\,$dex, $[M/H] = -0.65 \pm 0.1\,$dex.

Star 2M19341617+2553535 (G 125-22 [211]) has not been previously characterized in the literature, and is flagged in Simbad Wenger et al. (2000) as a double or multiple star. The available ASPCAP parameters for this star are $[M/H] = +0.00\,$dex, as well as $T_{\rm eff} = 3514\,$K and $\log g = 4.63\,$dex. The matching spectrum for the star has been obtained by normalizing the APOGEE observed one with a synthetic spectrum with $T_{\rm eff} = 3400\,$K, $\log g = 5.0\,$dex

[208] http://simbad.u-strasbg.fr/simbad/sim-id?Ident=2Mass+j19324633-0652178
[209] http://simbad.u-strasbg.fr/simbad/sim-id?Ident=2Mass+j19325604%2B1723567
[210] http://simbad.u-strasbg.fr/simbad/sim-id?Ident=2Mass+j19341617%2B2553535
[211] http://simbad.u-strasbg.fr/simbad/sim-id?Ident=2Mass+j19383321%2B3230175

and $[M/H] = +0.2$ dex, and the derived spectroscopical parameters for this star are $T_{\rm eff} = 3481 \pm 100$ K, $\log g = 4.99 \pm 0.1$ dex, $[M/H] = -0.01 \pm 0.1$ dex.

Star 2M19390444+2424089 (UCAC4 573-095540 [212]) was characterized in Gilhool et al. (2017), giving it the following parameters: $T_{\rm eff} = 3475$ K, $\log g = 4.5$ dex and $[M/H] = +0.0$ dex. It is also present in Terrien et al. (2015), with $T_{\rm eff} = 3431$ K and $[M/H] = -0.13$ dex. The available ASPCAP parameters for this star are $[M/H] = -0.16$ dex, as well as $T_{\rm eff} = 3526$ K and $\log g = 4.57$ dex. The matching spectrum for the star has been obtained by normalizing the APOGEE observed one with a synthetic spectrum with $T_{\rm eff} = 3400$ K, $\log g = 5.0$ dex and $[M/H] = +0.0$ dex, and the derived spectroscopical parameters for this star are $T_{\rm eff} = 3522 \pm 100$ K, $\log g = 5.01 \pm 0.1$ dex, $[M/H] = -0.11 \pm 0.1$ dex.

Star 2M19395886+3950530 (KIC 4758595 [213]) was characterized in Walkowicz et al. (2011), giving it the following parameters: $T_{\rm eff} = 3519$ K, $\log g = 4.41$ dex. The available ASPCAP parameters for this star are $[M/H] = -0.01$ dex, as well as $T_{\rm eff} = 3678$ K and $\log g = 4.37$ dex. The matching spectrum for the star has been obtained by normalizing the APOGEE observed one with a synthetic spectrum with $T_{\rm eff} = 3600$ K, $\log g = 5.0$ dex and $[M/H] = +0.2$ dex, and the derived spectroscopical parameters for this star are $T_{\rm eff} = 3688 \pm 100$ K, $\log g = 4.97 \pm 0.1$ dex, $[M/H] = -0.09 \pm 0.1$ dex.

Star 2M19412775+3239512 (G 125-27 [214]) was characterized in Gilhool et al. (2017), giving it the following parameters: $T_{\rm eff} = 3379$ K, $\log g = 4.5$ dex and $[M/H] = -0.5$ dex. It is also present in Terrien et al. (2015), with $T_{\rm eff} = 3403$ K and $[M/H] = -0.33$ dex. The available ASPCAP parameters for this star are $[M/H] = -0.48$ dex, as well as $T_{\rm eff} = 3461$ K and $\log g = 4.25$ dex. The matching spectrum for the star has been obtained by normalizing the APOGEE observed one with a synthetic spectrum with $T_{\rm eff} = 3200$ K, $\log g = 5.0$ dex and $[M/H] = -0.1$ dex, and the derived spectroscopical parameters for this star are $T_{\rm eff} = 3483 \pm 100$ K, $\log g = 4.62 \pm 0.1$ dex, $[M/H] = -0.53 \pm 0.1$ dex.

Star 2M19420033+4038302 (KIC 5461756 [215]) was characterized in Walkowicz et al. (2011), giving it the following parameters: $T_{\rm eff} = 3861$ K, $\log g = 4.61$ dex. The available ASPCAP parameters for this star are $[M/H] = -0.27$ dex, as well as $T_{\rm eff} = 3843$ K and $\log g = 4.35$ dex. The matching spectrum for the star has been obtained by normalizing the APOGEE observed

[212] http://simbad.u-strasbg.fr/simbad/sim-id?Ident=2Mass+j19390444%2B2424089
[213] http://simbad.u-strasbg.fr/simbad/sim-id?Ident=2Mass+j19395886%2B3950530
[214] http://simbad.u-strasbg.fr/simbad/sim-id?Ident=2Mass+j19412775%2B3239512
[215] http://simbad.u-strasbg.fr/simbad/sim-id?Ident=2Mass+j19420033%2B4038302

one with a synthetic spectrum with $T_{\text{eff}} = 4000\,$K, $\log g = 5.0\,$dex and $[M/H] = +0.2\,$dex, and the derived spectroscopical parameters for this star are $T_{\text{eff}} = 3862 \pm 100\,$K, $\log g = 4.65 \pm 0.1\,$dex, $[M/H] = -0.02 \pm 0.1\,$dex.

Star 2M19454969+3223132 (G 125-30 [216]) was characterized in Gilhool et al. (2017), giving it the following parameters: $T_{\text{eff}} = 3623\,$K, $\log g = 4.5\,$dex and $[M/H] = +0.0\,$dex. It is also present in Gaidos et al. (2014), with $T_{\text{eff}} = 3589\,$K, and in Lépine et al. (2013), with $T_{\text{eff}} = 3550\,$K and $\log g = 4.5\,$dex. The available ASPCAP parameters for this star are $T_{\text{eff}} = 3712\,$K and $[M/H] = -0.28\,$dex, as well as $\log g = 4.48\,$dex. The matching spectrum for the star has been obtained by normalizing the APOGEE observed one with a synthetic spectrum with $T_{\text{eff}} = 3400\,$K, $\log g = 5.0\,$dex and $[M/H] = -0.2\,$dex, and the derived spectroscopical parameters for this star are $T_{\text{eff}} = 3565 \pm 100\,$K, $\log g = 4.67 \pm 0.1\,$dex, $[M/H] = -0.09 \pm 0.1\,$dex.

Star 2M19482428+3250327 (G 125-33 [217]) was characterized in Gilhool et al. (2017), giving it the following parameters: $T_{\text{eff}} = 3339\,$K, $\log g = 4.5\,$dex and $[M/H] = -0.5\,$dex. The available ASPCAP parameters for this star are $[M/H] = -0.38\,$dex, as well as $T_{\text{eff}} = 3388\,$K and $\log g = 4.10\,$dex. The matching spectrum for the star has been obtained by normalizing the APOGEE observed one with a synthetic spectrum with $T_{\text{eff}} = 3200\,$K, $\log g = 5.0\,$dex and $[M/H] = -0.1\,$dex, and the derived spectroscopical parameters for this star are $T_{\text{eff}} = 3492 \pm 100\,$K, $\log g = 4.82 \pm 0.1\,$dex, $[M/H] = -0.55 \pm 0.1\,$dex.

Star 2M19485718+5015245 (2MASS J19485718+5015245 [218]) was characterized in Gilhool et al. (2017), giving it the following parameters: $T_{\text{eff}} = 3355\,$K, $\log g = 5.0\,$dex and $[M/H] = +0.0\,$dex. The available ASPCAP parameters for this star are $[M/H] = -0.22\,$dex, as well as $T_{\text{eff}} = 3425\,$K and $\log g = 4.65\,$dex. The matching spectrum for the star has been obtained by normalizing the APOGEE observed one with a synthetic spectrum with $T_{\text{eff}} = 3400\,$K, $\log g = 5.0\,$dex and $[M/H] = +0.3\,$dex, and the derived spectroscopical parameters for this star are $T_{\text{eff}} = 3497 \pm 100\,$K, $\log g = 5.4 \pm 0.1\,$dex, $[M/H] = -0.13 \pm 0.1\,$dex.

Star 2M19533423+0503410 (UCAC4 476-112194 [219]) has not been previously spectroscopically characterized in the literature, and is flagged in Simbad Wenger et al. (2000) as a high proper-motion star. The available ASPCAP parameters for this star are $[M/H] = +0.18\,$dex, as well as $T_{\text{eff}} = 3617\,$K and $\log g = 4.47\,$dex. The matching spectrum for the

[216] http://simbad.u-strasbg.fr/simbad/sim-id?Ident=2Mass+j19454969%2B3223132
[217] http://simbad.u-strasbg.fr/simbad/sim-id?Ident=2Mass+j19482428%2B3250327
[218] http://simbad.u-strasbg.fr/simbad/sim-id?Ident=2Mass+j19485718%2B5015245
[219] http://simbad.u-strasbg.fr/simbad/sim-id?Ident=2Mass+j19533423%2B0503410

star has been obtained by normalizing the APOGEE observed one with a synthetic spectrum with $T_{\rm eff} = 3600$ K, $\log g = 5.0$ dex and $[M/H] = -0.1$ dex, and the derived spectroscopical parameters for this star are $T_{\rm eff} = 3811 \pm 100$ K, $\log g = 5.38 \pm 0.1$ dex, $[M/H] = -0.66 \pm 0.1$ dex.

Star 2M19541829+1738289 (2MASS J19541829+1738289 [220]) was characterized in Gilhool et al. (2017), giving it the following parameters: $T_{\rm eff} = 3163$ K, $\log g = 4.5$ dex and $[M/H] = +0.0$ dex. The available ASPCAP parameters for this star are $[M/H] = -0.67$ dex, as well as $T_{\rm eff} = 3198$ K and $\log g = 4.08$ dex. The matching spectrum for the star has been obtained by normalizing the APOGEE observed one with a synthetic spectrum with $T_{\rm eff} = 3000$ K, $\log g = 5.0$ dex and $[M/H] = -0.4$ dex, and the derived spectroscopical parameters for this star are $T_{\rm eff} = 3426 \pm 100$ K, $\log g = 5.4 \pm 0.1$ dex, $[M/H] = -0.76 \pm 0.1$ dex.

Star 2M19543665+4357180 (KOI-571 [221]) was characterized in Steffen & Farr (2013), giving it the following parameters: $T_{\rm eff} = 4031$ K, $\log g = 4.74$ dex, as well as in Rowe et al. (2014), with $T_{\rm eff} = 4048$ K, $\log g = 4.75$ dex, and $[M/H] = -0.21$ dex. The available ASPCAP parameters for this star are $[M/H] = -0.24$ dex, as well as $T_{\rm eff} = 3890$ K and $\log g = 4.49$ dex. The matching spectrum for the star has been obtained by normalizing the APOGEE observed one with a synthetic spectrum with $T_{\rm eff} = 3800$ K, $\log g = 5.0$ dex and $[M/H] = +0.2$ dex, and the derived spectroscopical parameters for this star are $T_{\rm eff} = 3856 \pm 100$ K, $\log g = 4.73 \pm 0.1$ dex, $[M/H] = -0.22 \pm 0.1$ dex.

Star 2M19585332+0522081 (TYC 489-1364-1 [222]) was characterized in Gaidos et al. (2014), giving it $T_{\rm eff} = 3843$ K and $[M/H] = -0.29$ dex, as well as in Lépine et al. (2013), with $\log g = 4.5$ dex and $T_{\rm eff} = 3690$ K. The available ASPCAP parameters for this star are $[M/H] = -0.13$ dex, as well as $T_{\rm eff} = 3843$ K and $\log g = 4.45$ dex. The matching spectrum for the star has been obtained by normalizing the APOGEE observed one with a synthetic spectrum with $T_{\rm eff} = 3600$ K, $\log g = 5.0$ dex and $[M/H] = -0.2$ dex, and the derived spectroscopical parameters for this star are $T_{\rm eff} = 3806 \pm 100$ K, $\log g = 4.94 \pm 0.1$ dex, $[M/H] = -0.24 \pm 0.1$ dex.

Star 2M20015056+4500500 (G 209-11 [223]) was characterized in Gilhool et al. (2017), giving it the following parameters: $T_{\rm eff} = 3483$ K, $\log g = 5.5$ dex and $[M/H] = +0.5$ dex. The available ASPCAP parameters for this star are $[M/H] = +0.0$ dex, as well as $T_{\rm eff} = 3522$ K and $\log g = 4.67$ dex. The matching spectrum for the star has been obtained by normaliz-

[220] http://simbad.u-strasbg.fr/simbad/sim-id?Ident=2Mass+j19541829%2B1738289
[221] http://simbad.u-strasbg.fr/simbad/sim-id?Ident=2Mass+j19543665%2B4357180
[222] http://simbad.u-strasbg.fr/simbad/sim-id?Ident=2Mass+j19585332%2B0522081
[223] http://simbad.u-strasbg.fr/simbad/sim-id?Ident=2Mass+j20015056%2B4500500

ing the APOGEE observed one with a synthetic spectrum with $T_{\rm eff} = 3600\,$K, $\log g = 5.0\,$dex and $[M/H] = +0.2\,$dex, and the derived spectroscopical parameters for this star are $T_{\rm eff} = 3666 \pm 100\,$K, $\log g = 5.4 \pm 0.1\,$dex, $[M/H] = -0.05 \pm 0.1\,$dex.

Star 2M20024041+3109447 (G 125-54 [224]) was characterized in Gilhool et al. (2017), giving it the following parameters: $T_{\rm eff} = 3534\,$K, $\log g = 4.5\,$dex and $[M/H] = +0.0\,$dex. The available ASPCAP parameters for this star are $T_{\rm eff} = 3597\,$K and $[M/H] = -0.14\,$dex, as well as $\log g = 4.38\,$dex. The matching spectrum for the star has been obtained by normalizing the APOGEE observed one with a synthetic spectrum with $T_{\rm eff} = 3400\,$K, $\log g = 5.0\,$dex and $[M/H] = +0.2\,$dex, and the derived spectroscopical parameters for this star are $T_{\rm eff} = 3500 \pm 100\,$K, $\log g = 4.91 \pm 0.1\,$dex, $[M/H] = -0.04 \pm 0.1\,$dex.

Star 2M20053276+3039324 (LP 338-11 [225]) was characterized in Gilhool et al. (2017), giving it the following parameters: $T_{\rm eff} = 3790\,$K, $\log g = 4.5\,$dex and $[M/H] = -0.5\,$dex. The available ASPCAP parameters for this star are $T_{\rm eff} = 3847\,$K and $[M/H] = -0.16\,$dex, as well as $\log g = 4.37\,$dex. The matching spectrum for the star has been obtained by normalizing the APOGEE observed one with a synthetic spectrum with $T_{\rm eff} = 3600\,$K, $\log g = 5.0\,$dex and $[M/H] = +0.0\,$dex, and the derived spectroscopical parameters for this star are $T_{\rm eff} = 3729 \pm 100\,$K, $\log g = 4.47 \pm 0.1\,$dex, $[M/H] = -0.23 \pm 0.1\,$dex.

Star 2M20122244+2043113 (LSPM J2012+2043 [226]) was characterized in Gilhool et al. (2017), giving it the following parameters: $T_{\rm eff} = 3431\,$K, $\log g = 4.5\,$dex and $[M/H] = -0.5\,$dex. The available ASPCAP parameters for this star are $[M/H] = -0.43\,$dex, as well as $T_{\rm eff} = 3531\,$K and $\log g = 4.49\,$dex. The matching spectrum for the star has been obtained by normalizing the APOGEE observed one with a synthetic spectrum with $T_{\rm eff} = 3400\,$K, $\log g = 5.0\,$dex and $[M/H] = -0.1\,$dex, and the derived spectroscopical parameters for this star are $T_{\rm eff} = 3654 \pm 100\,$K, $\log g = 5.27 \pm 0.1\,$dex, $[M/H] = -0.6 \pm 0.1\,$dex.

Star 2M20162519+5621561 (LSPM J2016+5621 [227]) was characterized in Gilhool et al. (2017), giving it the following parameters: $T_{\rm eff} = 3629\,$K, $\log g = 4.5\,$dex and $[M/H] = +0.0\,$dex. The available ASPCAP parameters for this star are $T_{\rm eff} = 3691\,$K and $[M/H] = +0.14\,$dex, as well as $\log g = 4.43\,$dex. The matching spectrum for the star has been obtained by normalizing the APOGEE observed one with a synthetic spectrum with $T_{\rm eff} = 3800\,$K, $\log g = 5.0\,$dex

[224] http://simbad.u-strasbg.fr/simbad/sim-id?Ident=2Mass+j20024041%2B3109447
[225] http://simbad.u-strasbg.fr/simbad/sim-id?Ident=2Mass+j20053276%2B3039324
[226] http://simbad.u-strasbg.fr/simbad/sim-id?Ident=2Mass+j20053276%2B3039324
[227] http://simbad.u-strasbg.fr/simbad/sim-id?Ident=2Mass+j20162519%2B5621561

and $[M/H] = +0.4$ dex, and the derived spectroscopical parameters for this star are $T_{\rm eff} = 3723 \pm 100$ K, $\log g = 4.96 \pm 0.1$ dex, $[M/H] = +0.15 \pm 0.1$ dex.

Star 2M20185746+2704165 (LSPM J2018+2704 [228]) was characterized in Gilhool et al. (2017), giving it the following parameters: $T_{\rm eff} = 3585$ K, $\log g = 4.5$ dex and $[M/H] = +0.0$ dex. The available ASPCAP parameters for this star are $T_{\rm eff} = 3668$ K and $[M/H] = -0.19$ dex, as well as $\log g = 4.43$ dex. The matching spectrum for the star has been obtained by normalizing the APOGEE observed one with a synthetic spectrum with $T_{\rm eff} = 3600$ K, $\log g = 5.0$ dex and $[M/H] = +0.1$ dex, and the derived spectroscopical parameters for this star are $T_{\rm eff} = 3714 \pm 100$ K, $\log g = 5.25 \pm 0.1$ dex, $[M/H] = -0.22 \pm 0.1$ dex.

Star 2M20202082+2837583 (UCAC4 594-108974 [229]) has not been previously spectroscopically characterized in the literature, and is flagged in Simbad Wenger et al. (2000) as a high proper-motion star. The available ASPCAP parameters for this star are $[M/H] = -0.26$ dex, as well as $T_{\rm eff} = 3728$ K and $\log g = 4.39$ dex. The matching spectrum for the star has been obtained by normalizing the APOGEE observed one with a synthetic spectrum with $T_{\rm eff} = 4000$ K, $\log g = 5.0$ dex and $[M/H] = +0.2$ dex, and the derived spectroscopical parameters for this star are $T_{\rm eff} = 3833 \pm 100$ K, $\log g = 4.96 \pm 0.1$ dex, $[M/H] = +0.08 \pm 0.1$ dex.

Star 2M20291663+4507525 (UCAC4 676-084259 [230]) was characterized in Gilhool et al. (2017), giving it the following parameters: $T_{\rm eff} = 3673$ K, $\log g = 4.5$ dex and $[M/H] = +0.0$ dex. The available ASPCAP parameters for this star are $T_{\rm eff} = 3735$ K and $[M/H] = -0.05$ dex, as well as $\log g = 4.39$ dex. The matching spectrum for the star has been obtained by normalizing the APOGEE observed one with a synthetic spectrum with $T_{\rm eff} = 3600$ K, $\log g = 5.0$ dex and $[M/H] = +0.0$ dex, and the derived spectroscopical parameters for this star are $T_{\rm eff} = 3693 \pm 100$ K, $\log g = 4.93 \pm 0.1$ dex, $[M/H] = -0.05 \pm 0.1$ dex.

Star 2M20331096+4553299 (LSPM J2033+4553 [231]) was characterized in Gilhool et al. (2017), giving it the following parameters: $T_{\rm eff} = 3538$ K, $\log g = 4.5$ dex and $[M/H] = +0.0$ dex. The available ASPCAP parameters for this star are $T_{\rm eff} = 3591$ K and $[M/H] = -0.25$ dex, as well as $\log g = 4.27$ dex. The matching spectrum for the star has been obtained by normalizing the APOGEE observed one with a synthetic spectrum with $T_{\rm eff} = 3400$ K, $\log g = 5.0$ dex and $[M/H] = -0.2$ dex, and the derived spectroscopical parameters for this star are $T_{\rm eff} =$

[228] http://simbad.u-strasbg.fr/simbad/sim-id?Ident=2Mass+j20185746%2B2704165
[229] http://simbad.u-strasbg.fr/simbad/sim-id?Ident=2Mass+j20202082%2B2837583
[230] http://simbad.u-strasbg.fr/simbad/sim-id?Ident=2Mass+j20291663%2B4507525
[231] http://simbad.u-strasbg.fr/simbad/sim-id?Ident=2Mass+j20331096%2B4553299

3612 ± 100 K, $\log g = 5.08 \pm 0.1$ dex, $[M/H] = -0.24 \pm 0.1$ dex.

Star 2M20584898+5115421 (2MASS J20584898+5115421 [232]) was characterized in Gilhool et al. (2017), giving it the following parameters: $T_{\text{eff}} = 3543$ K, $\log g = 4.5$ dex and $[M/H] = +0.0$ dex. It is also present in Terrien et al. (2015), with $T_{\text{eff}} = 3605$ K and $[M/H] = -0.04$ dex. The available ASPCAP parameters for this star are $T_{\text{eff}} = 3620$ K and $[M/H] = -0.14$ dex, as well as $\log g = 4.44$ dex. The matching spectrum for the star has been obtained by normalizing the APOGEE observed one with a synthetic spectrum with $T_{\text{eff}} = 3400$ K, $\log g = 5.0$ dex and $[M/H] = +0.0$ dex, and the derived spectroscopical parameters for this star are $T_{\text{eff}} = 3515 \pm 100$ K, $\log g = 4.79 \pm 0.1$ dex, $[M/H] = -0.05 \pm 0.1$ dex.

Star 2M21003448+5156016 (2MASS J21003448+5156016 [233]) has not been previously spectroscopically characterized in the literature, and is flagged in Simbad Wenger et al. (2000) as a high proper-motion star. The available ASPCAP parameters for this star are $[M/H] = +0.08$ dex, as well as $T_{\text{eff}} = 3412$ K and $\log g = 4.35$ dex. The matching spectrum for the star has been obtained by normalizing the APOGEE observed one with a synthetic spectrum with $T_{\text{eff}} = 3200$ K, $\log g = 5.0$ dex and $[M/H] = +0.0$ dex, and the derived spectroscopical parameters for this star are $T_{\text{eff}} = 3359 \pm 100$ K, $\log g = 4.68 \pm 0.1$ dex, $[M/H] = -0.03 \pm 0.1$ dex.

Star 2M21013304+4046208 (G 212-16 [234]) was characterized in Gilhool et al. (2017), giving it the following parameters: $T_{\text{eff}} = 3258$ K, $\log g = 4.5$ dex and $[M/H] = +0.0$ dex. It is also present in Terrien et al. (2015), with $T_{\text{eff}} = 3303$ K and $[M/H] = -0.15$ dex. The available ASPCAP parameters for this star are $[M/H] = -0.21$ dex, as well as $T_{\text{eff}} = 3300$ K and $\log g = 4.30$ dex. The matching spectrum for the star has been obtained by normalizing the APOGEE observed one with a synthetic spectrum with $T_{\text{eff}} = 3200$ K, $\log g = 5.0$ dex and $[M/H] = -0.2$ dex, and the derived spectroscopical parameters for this star are $T_{\text{eff}} = 3490 \pm 100$ K, $\log g = 5.15 \pm 0.1$ dex, $[M/H] = -0.45 \pm 0.1$ dex.

Star 2M21074857+2945266 (BD+29 4321B [235]) was characterized in Gilhool et al. (2017), giving it the following parameters: $T_{\text{eff}} = 3517$ K, $\log g = 4.5$ dex and $[M/H] = +0.0$ dex. It is also present in Terrien et al. (2015), with $T_{\text{eff}} = 3467$ K and $[M/H] = -0.19$ dex. The available ASPCAP parameters for this star are $T_{\text{eff}} = 3598$ K and $[M/H] = -0.17$ dex, as well as $\log g = 4.50$ dex. The matching spectrum for the star has been obtained by normalizing

[232] http://simbad.u-strasbg.fr/simbad/sim-id?Ident=2Mass+j20584898%2B5115421

[233] http://simbad.u-strasbg.fr/simbad/sim-id?Ident=2Mass+j21003448%2B5156016

[234] http://simbad.u-strasbg.fr/simbad/sim-id?Ident=2Mass+j21013304%2B4046208

[235] http://simbad.u-strasbg.fr/simbad/sim-id?Ident=2Mass+j21074857%2B2945266

the APOGEE observed one with a synthetic spectrum with $T_{\text{eff}} = 3400\,$K, $\log g = 5.0\,$dex and $[M/H] = +0.0\,$dex, and the derived spectroscopical parameters for this star are $T_{\text{eff}} = 3540 \pm 100\,$K, $\log g = 4.98 \pm 0.1\,$dex, $[M/H] = -0.16 \pm 0.1\,$dex.

Star 2M21140743+4924350 (LSPM J2114+4924 [236]) has not been previously spectroscopically characterized in the literature, and is flagged in Simbad Wenger et al. (2000) as a high proper-motion star. The available ASPCAP parameters for this star are $[M/H] = +0.14\,$dex, as well as $T_{\text{eff}} = 3428\,$K and $\log g = 4.30\,$dex. The matching spectrum for the star has been obtained by normalizing the APOGEE observed one with a synthetic spectrum with $T_{\text{eff}} = 3200\,$K, $\log g = 5.0\,$dex and $[M/H] = -0.2\,$dex, and the derived spectroscopical parameters for this star are $T_{\text{eff}} = 3508 \pm 100\,$K, $\log g = 5.18 \pm 0.1\,$dex, $[M/H] = -0.48 \pm 0.1\,$dex.

Star 2M21232573+6734153 (G 262-41 [237]) was characterized in Gilhool et al. (2017), giving it the following parameters: $T_{\text{eff}} = 3287\,$K, $\log g = 5.0\,$dex and $[M/H] = +0.0\,$dex. The available ASPCAP parameters for this star are $[M/H] = -0.32\,$dex, as well as $T_{\text{eff}} = 3343\,$K and $\log g = 4.56\,$dex. The matching spectrum for the star has been obtained by normalizing the APOGEE observed one with a synthetic spectrum with $T_{\text{eff}} = 3200\,$K, $\log g = 5.0\,$dex and $[M/H] = -0.2\,$dex, and the derived spectroscopical parameters for this star are $T_{\text{eff}} = 3426 \pm 100\,$K, $\log g = 5.4 \pm 0.1\,$dex, $[M/H] = -0.18 \pm 0.1\,$dex.

Star 2M21281491+4654126 (UCAC4 685-101767 [238]) has not been previously spectroscopically characterized in the literature, and is flagged in Simbad Wenger et al. (2000) as a high proper-motion star. The available ASPCAP parameters for this star are $T_{\text{eff}} = 3871\,$K and $[M/H] = +0.21\,$dex, as well as $\log g = 4.41\,$dex. The matching spectrum for the star has been obtained by normalizing the APOGEE observed one with a synthetic spectrum with $T_{\text{eff}} = 4000\,$K, $\log g = 5.0\,$dex and $[M/H] = +0.2\,$dex, and the derived spectroscopical parameters for this star are $T_{\text{eff}} = 3781 \pm 100\,$K, $\log g = 4.54 \pm 0.1\,$dex, $[M/H] = 0.03 \pm 0.1\,$dex.

Star 2M21400112+5408179 (Ross 200 [239]) was characterized in Gilhool et al. (2017), giving it the following parameters: $T_{\text{eff}} = 3465\,$K, $\log g = 4.5\,$dex and $[M/H] = +0.0\,$dex. The available ASPCAP parameters for this star are $T_{\text{eff}} = 3579\,$K and $[M/H] = -0.27\,$dex, as well as $\log g = 4.55\,$dex. The matching spectrum for the star has been obtained by normalizing the APOGEE observed one with a synthetic spectrum with $T_{\text{eff}} = 3400\,$K, $\log g = 5.0\,$dex

[236] http://simbad.u-strasbg.fr/simbad/sim-id?Ident=2Mass+j21140743%2B4924350
[237] http://simbad.u-strasbg.fr/simbad/sim-id?Ident=2Mass+j21232573%2B6734153
[238] http://simbad.u-strasbg.fr/simbad/sim-id?Ident=2Mass+j21281491%2B4654126
[239] http://simbad.u-strasbg.fr/simbad/sim-id?Ident=2MASS+J21400112%2B5408179

and $[M/H] = +0.1$ dex, and the derived spectroscopical parameters for this star are $T_{\rm eff} = 3580 \pm 100$ K, $\log g = 5.2 \pm 0.1$ dex, $[M/H] = -0.31 \pm 0.1$ dex.

Star 2M21402935+5400301 (Ross 201 [240]) was characterized in Gilhool et al. (2017), giving it the following parameters: $T_{\rm eff} = 3318$ K, $\log g = 4.5$ dex and $[M/H] = +0.0$ dex. The available ASPCAP parameters for this star are $[M/H] = -0.30$ dex, as well as $T_{\rm eff} = 3362$ K and $\log g = 4.22$ dex. The matching spectrum for the star has been obtained by normalizing the APOGEE observed one with a synthetic spectrum with $T_{\rm eff} = 3200$ K, $\log g = 5.0$ dex and $[M/H] = -0.2$ dex, and the derived spectroscopical parameters for this star are $T_{\rm eff} = 3477 \pm 100$ K, $\log g = 4.98 \pm 0.1$ dex, $[M/H] = -0.34 \pm 0.1$ dex.

Star 2M21474194+5341222 (LSPM J2147+5341 [241]) was characterized in Gilhool et al. (2017), giving it the following parameters: $T_{\rm eff} = 3699$ K, $\log g = 4.5$ dex and $[M/H] = +0.0$ dex. The available ASPCAP parameters for this star are $T_{\rm eff} = 3755$ K and $[M/H] = +0.0$ dex, as well as $\log g = 4.42$ dex. The matching spectrum for the star has been obtained by normalizing the APOGEE observed one with a synthetic spectrum with $T_{\rm eff} = 3600$ K, $\log g = 5.0$ dex and $[M/H] = +0.2$ dex, and the derived spectroscopical parameters for this star are $T_{\rm eff} = 3683 \pm 100$ K, $\log g = 4.73 \pm 0.1$ dex, $[M/H] = -0.04 \pm 0.1$ dex.

Star 2M21561443+3943468 (G 214-3 [242]) was characterized in Gilhool et al. (2017), giving it the following parameters: $T_{\rm eff} = 3317$ K, $\log g = 5.0$ dex and $[M/H] = +0.0$ dex. The available ASPCAP parameters for this star are $[M/H] = -0.39$ dex, as well as $T_{\rm eff} = 3367$ K and $\log g = 4.46$ dex. The matching spectrum for the star has been obtained by normalizing the APOGEE observed one with a synthetic spectrum with $T_{\rm eff} = 3200$ K, $\log g = 5.0$ dex and $[M/H] = -0.2$ dex, and the derived spectroscopical parameters for this star are $T_{\rm eff} = 3451 \pm 100$ K, $\log g = 5.39 \pm 0.1$ dex, $[M/H] = -0.23 \pm 0.1$ dex.

Star 2M21573509+5026323 (G 232-42 [243]) was characterized in Gilhool et al. (2017), giving it the following parameters: $T_{\rm eff} = 3231$ K, $\log g = 5.5$ dex and $[M/H] = +0.5$ dex. The available ASPCAP parameters for this star are $[M/H] = -0.36$ dex, as well as $T_{\rm eff} = 3272$ K and $\log g = 4.53$ dex. The matching spectrum for the star has been obtained by normalizing the APOGEE observed one with a synthetic spectrum with $T_{\rm eff} = 3200$ K, $\log g = 5.0$ dex and $[M/H] = +0.1$ dex, and the derived spectroscopical parameters for this star are $T_{\rm eff} =$

[240] http://simbad.u-strasbg.fr/simbad/sim-id?Ident=2Mass+j21402935%2B5400301
[241] http://simbad.u-strasbg.fr/simbad/sim-id?Ident=2Mass+j21474194%2B5341222
[242] http://simbad.u-strasbg.fr/simbad/sim-id?Ident=2Mass+j21561443%2B3943468
[243] http://simbad.u-strasbg.fr/simbad/sim-id?Ident=2Mass+j21573509%2B5026323

3308 ± 100 K, $\log g = 5.39 \pm 0.1$ dex, $[M/H] = -0.07 \pm 0.1$ dex.

Star 2M22010861+4901108 (Wolf 966 [244]) was characterized in Gilhool et al. (2017), giving it the following parameters: $T_{\rm eff} = 3951$ K, $\log g = 4.5$ dex and $[M/H] = +0.0$ dex. It is also present in Gaidos et al. (2014), with $T_{\rm eff} = 4532$ K. The available ASPCAP parameters for this star are $T_{\rm eff} = 3992$ K and $[M/H] = -0.01$ dex, as well as $\log g = 4.35$ dex. The matching spectrum for the star has been obtained by normalizing the APOGEE observed one with a synthetic spectrum with $T_{\rm eff} = 4000$ K, $\log g = 5.0$ dex and $[M/H] = +0.2$ dex, and the derived spectroscopical parameters for this star are $T_{\rm eff} = 3989 \pm 100$ K, $\log g = 4.76 \pm 0.1$ dex, $[M/H] = -0.03 \pm 0.1$ dex.

Star 2M23034347+6524293 (LSPM J2303+6524 [245]) was characterized in Gilhool et al. (2017), giving it the following parameters: $T_{\rm eff} = 3265$ K, $\log g = 5.5$ dex and $[M/H] = +0.5$ dex. The available ASPCAP parameters for this star are $[M/H] = -0.13$ dex, as well as $T_{\rm eff} = 3338$ K and $\log g = 4.70$ dex. The matching spectrum for the star has been obtained by normalizing the APOGEE observed one with a synthetic spectrum with $T_{\rm eff} = 3000$ K, $\log g = 5.0$ dex and $[M/H] = -0.2$ dex, and the derived spectroscopical parameters for this star are $T_{\rm eff} = 3269 \pm 100$ K, $\log g = 5.19 \pm 0.1$ dex, $[M/H] = -0.14 \pm 0.1$ dex.

Star 2M23110137+4653414 (2MASS J23110137+4653414 [246]) has not been previously spectroscopically characterized in the literature, and is flagged in Simbad Wenger et al. (2000) as a high proper-motion star. The available ASPCAP parameters for this star are $[M/H] = -0.13$ dex, as well as $T_{\rm eff} = 3412$ K and $\log g = 4.41$ dex. The matching spectrum for the star has been obtained by normalizing the APOGEE observed one with a synthetic spectrum with $T_{\rm eff} = 3200$ K, $\log g = 5.0$ dex and $[M/H] = +0.2$ dex, and the derived spectroscopical parameters for this star are $T_{\rm eff} = 3316 \pm 100$ K, $\log g = 4.65 \pm 0.1$ dex, $[M/H] = +0.03 \pm 0.1$ dex.

Star 2M23134861+1227072 (LSPM J2313+1227 [247]) has not been previously spectroscopically characterized in the literature, and is flagged in Simbad Wenger et al. (2000) as a high proper-motion star. The available ASPCAP parameters for this star are $[M/H] = -0.07$ dex, as well as $T_{\rm eff} = 3504$ K and $\log g = 4.53$ dex. The matching spectrum for the star has been obtained by normalizing the APOGEE observed one with a synthetic spectrum with $T_{\rm eff} = 3400$ K, $\log g = 5.0$ dex and $[M/H] = +0.2$ dex, and the derived spectroscopical parameters for this star

[244] http://simbad.u-strasbg.fr/simbad/sim-id?Ident=2Mass+j22010861%2B4901108
[245] http://simbad.u-strasbg.fr/simbad/sim-id?Ident=2Mass+j23034347%2B6524293
[246] http://simbad.u-strasbg.fr/simbad/sim-id?Ident=2Mass+j23110137%2B4653414
[247] http://simbad.u-strasbg.fr/simbad/sim-id?Ident=2Mass+j23134861%2B1227072

are $T_{\text{eff}} = 3490 \pm 100$ K, $\log g = 5.1 \pm 0.1$ dex, $[M/H] = +0.1 \pm 0.1$ dex.

Star 2M23165396+6109419 (LSPM J2313+1227 [248]) has not been previously spectroscopically characterized in the literature, and is flagged in Simbad Wenger et al. (2000) as a high proper-motion star. The available ASPCAP parameters for this star are $T_{\text{eff}} = 3692$ K and $[M/H] = -0.13$ dex, as well as $\log g = 4.38$ dex. The matching spectrum for the star has been obtained by normalizing the APOGEE observed one with a synthetic spectrum with $T_{\text{eff}} = 3600$ K, $\log g = 5.0$ dex and $[M/H] = +0.0$ dex, and the derived spectroscopical parameters for this star are $T_{\text{eff}} = 3718 \pm 100$ K, $\log g = 4.93 \pm 0.1$ dex, $[M/H] = -0.25 \pm 0.1$ dex.

Star 2M23171589+6110496 (LSPM J2317+6110 [249]) has not been previously spectroscopically characterized in the literature, and is flagged in Simbad Wenger et al. (2000) as a high proper-motion star. The available ASPCAP parameters for this star are $T_{\text{eff}} = 3588$ K and $[M/H] = +0.09$ dex, as well as $\log g = 4.44$ dex. The matching spectrum for the star has been obtained by normalizing the APOGEE observed one with a synthetic spectrum with $T_{\text{eff}} = 3500$ K, $\log g = 5.0$ dex and $[M/H] = +0.2$ dex, and the derived spectroscopical parameters for this star are $T_{\text{eff}} = 3559 \pm 100$ K, $\log g = 4.71 \pm 0.1$ dex, $[M/H] = -0.01 \pm 0.1$ dex.

Star 2M23175293+6109518 (LSPM J2317+6109 [250]) was characterized in Gilhool et al. (2017), giving it the following parameters: $T_{\text{eff}} = 3479$ K, $\log g = 4.5$ dex and $[M/H] = +0.0$ dex. The available ASPCAP parameters for this star are $[M/H] = -0.16$ dex, as well as $T_{\text{eff}} = 3527$ K and $\log g = 4.46$ dex. The matching spectrum for the star has been obtained by normalizing the APOGEE observed one with a synthetic spectrum with $T_{\text{eff}} = 3400$ K, $\log g = 5.0$ dex and $[M/H] = +0.0$ dex, and the derived spectroscopical parameters for this star are $T_{\text{eff}} = 3515 \pm 100$ K, $\log g = 4.95 \pm 0.1$ dex, $[M/H] = -0.07 \pm 0.1$ dex.

Star 2M23200542+6356068 (G 241-51 [251]) was characterized in Gilhool et al. (2017), giving it the following parameters: $T_{\text{eff}} = 3701$ K, $\log g = 4.5$ dex and $[M/H] = +0.0$ dex. The available ASPCAP parameters for this star are $T_{\text{eff}} = 3759$ K and $[M/H] = +0.06$ dex, as well as $\log g = 4.42$ dex. The matching spectrum for the star has been obtained by normalizing the APOGEE observed one with a synthetic spectrum with $T_{\text{eff}} = 3700$ K, $\log g = 5.0$ dex and $[M/H] = +0.2$ dex, and the derived spectroscopical parameters for this star are $T_{\text{eff}} = 3738 \pm 100$ K, $\log g = 4.81 \pm 0.1$ dex, $[M/H] = -0.01 \pm 0.1$ dex.

[248] http://simbad.u-strasbg.fr/simbad/sim-id?Ident=2Mass+j23134861%2B1227072
[249] http://simbad.u-strasbg.fr/simbad/sim-id?Ident=2Mass+j23171589%2B6110496
[250] http://simbad.u-strasbg.fr/simbad/sim-id?Ident=2Mass+j23175293%2B6109518
[251] http://simbad.u-strasbg.fr/simbad/sim-id?Ident=2Mass+j23200542%2B6356068

Star 2M23205304+1205009 (LP 522-36 [252]) was characterized in Gilhool et al. (2017), giving it the following parameters: $T_{\rm eff} = 3434$ K, $\log g = 4.5$ dex and $[M/H] = +0.0$ dex. The available ASPCAP parameters for this star are $[M/H] = -0.34$ dex, as well as $T_{\rm eff} = 3480$ K and $\log g = 4.44$ dex. The matching spectrum for the star has been obtained by normalizing the APOGEE observed one with a synthetic spectrum with $T_{\rm eff} = 3200$ K, $\log g = 5.0$ dex and $[M/H] = +0.1$ dex, and the derived spectroscopical parameters for this star are $T_{\rm eff} = 3398 \pm 100$ K, $\log g = 4.81 \pm 0.1$ dex, $[M/H] = -0.22 \pm 0.1$ dex.

Star 2M23212582+6547582 (LSPM J2321+6547 [253]) has not been previously spectroscopically characterized in the literature, and is flagged in Simbad Wenger et al. (2000) as a high proper-motion star. The available ASPCAP parameters for this star are $[M/H] = +0.15$ dex, as well as $T_{\rm eff} = 3554$ K and $\log g = 4.34$ dex. The matching spectrum for the star has been obtained by normalizing the APOGEE observed one with a synthetic spectrum with $T_{\rm eff} = 3400$ K, $\log g = 5.0$ dex and $[M/H] = +0.1$ dex, and the derived spectroscopical parameters for this star are $T_{\rm eff} = 3561 \pm 100$ K, $\log g = 5.04 \pm 0.1$ dex, $[M/H] = -0.23 \pm 0.1$ dex.

Star 2M23212582+6547582 (LSPM J2323+6211 [254]) has not been previously spectroscopically characterized in the literature, and is flagged in Simbad Wenger et al. (2000) as a high proper-motion star. The available ASPCAP parameters for this star are $[M/H] = -0.03$ dex, as well as $T_{\rm eff} = 3683$ K and $\log g = 4.40$ dex. The matching spectrum for the star has been obtained by normalizing the APOGEE observed one with a synthetic spectrum with $T_{\rm eff} = 3600$ K, $\log g = 5.0$ dex and $[M/H] = +0.2$ dex, and the derived spectroscopical parameters for this star are $T_{\rm eff} = 3667 \pm 100$ K, $\log g = 4.86 \pm 0.1$ dex, $[M/H] = +0.0 \pm 0.1$ dex.

Star 2M23460112+7456172 (LSPM J2346+7456 [255]) was characterized in Gilhool et al. (2017), giving it the following parameters: $T_{\rm eff} = 3401$ K, $\log g = 5.0$ dex and $[M/H] = +0.0$ dex. The available ASPCAP parameters for this star are $[M/H] = -0.35$ dex, as well as $T_{\rm eff} = 3466$ K and $\log g = 4.48$ dex. The matching spectrum for the star has been obtained by normalizing the APOGEE observed one with a synthetic spectrum with $T_{\rm eff} = 3200$ K, $\log g = 5.0$ dex and $[M/H] = -0.2$ dex, and the derived spectroscopical parameters for this star are $T_{\rm eff} = 3461 \pm 100$ K, $\log g = 5.18 \pm 0.1$ dex, $[M/H] = -0.23 \pm 0.1$ dex.

Star 2M23592772+1630288 (LSPM J2359+1630 [256]) was characterized in Gilhool et al.

[252] `http://simbad.u-strasbg.fr/simbad/sim-id?Ident=2Mass+j23205304%2B1205009`
[253] `http://simbad.u-strasbg.fr/simbad/sim-id?Ident=2Mass+j23212582%2B6547582`
[254] `http://simbad.u-strasbg.fr/simbad/sim-id?Ident=2Mass+j23230603%2B6211124`
[255] `http://simbad.u-strasbg.fr/simbad/sim-id?Ident=2Mass+j23460112%2B7456172`
[256] `http://simbad.u-strasbg.fr/simbad/sim-id?Ident=2Mass+j23592772%2B1630288`

(2017), giving it the following parameters: $T_{\rm eff} = 3423\,$K, $\log g = 5.5\,$dex and $[M/H] = +0.5\,$dex. The available ASPCAP parameters for this star are $[M/H] = +0.08\,$dex, as well as $T_{\rm eff} = 3469\,$K and $\log g = 4.76\,$dex. The matching spectrum for the star has been obtained by normalizing the APOGEE observed one with a synthetic spectrum with $T_{\rm eff} = 3300\,$K, $\log g = 5.0\,$dex and $[M/H] = +0.2\,$dex, and the derived spectroscopical parameters for this star are $T_{\rm eff} = 3399 \pm 100\,$K, $\log g = 5.04 \pm 0.1\,$dex, $[M/H] = +0.09 \pm 0.1\,$dex.

Star 2M23200542+6356068 (LP 28-30 [257]) was characterized in Gilhool et al. (2017), giving it the following parameters: $T_{\rm eff} = 3892\,$K, $\log g = 4.5\,$dex and $[M/H] = +0.0\,$dex. The available ASPCAP parameters for this star are $T_{\rm eff} = 3933\,$K and $[M/H] = +0.03\,$dex, as well as $\log g = 4.36\,$dex. The matching spectrum for the star has been obtained by normalizing the APOGEE observed one with a synthetic spectrum with $T_{\rm eff} = 4000\,$K, $\log g = 5.0\,$dex and $[M/H] = +0.0\,$dex, and the derived spectroscopical parameters for this star are $T_{\rm eff} = 3980 \pm 100\,$K, $\log g = 4.93 \pm 0.1\,$dex, $[M/H] = -0.04 \pm 0.1\,$dex.

Star 2M23595589+1508091 (LSPM J2359+1508E [258]) was characterized in Gilhool et al. (2017), giving it the following parameters: $T_{\rm eff} = 3565\,$K, $\log g = 4.5\,$dex and $[M/H] = +0.0\,$dex. The available ASPCAP parameters for this star are $T_{\rm eff} = 3629\,$K and $[M/H] = -0.14\,$dex, as well as $\log g = 4.40\,$dex. The matching spectrum for the star has been obtained by normalizing the APOGEE observed one with a synthetic spectrum with $T_{\rm eff} = 3700\,$K, $\log g = 5.0\,$dex and $[M/H] = +0.3\,$dex, and the derived spectroscopical parameters for this star are $T_{\rm eff} = 3725 \pm 100\,$K, $\log g = 5.28 \pm 0.1\,$dex, $[M/H] = -0.12 \pm 0.1\,$dex.

[257] `http://simbad.u-strasbg.fr/simbad/sim-id?Ident=2Mass+j23592810%2B7506017`
[258] `http://simbad.u-strasbg.fr/simbad/sim-id?Ident=2Mass+j23595589%2B1508091`